CRC REVIVALS

# Engineering Economics of Alternative Energy Sources

Khalil Denno

CRC Press
Taylor & Francis Group

# Engineering Economics of Alternative Energy Sources

Author

**Khalil Denno, Ph.D.**
Distinguished Professor
Electrical Engineering
Newark College of Engineering
New Jersey Institute of Technology
Newark, New Jersey

CRC Press
Taylor & Francis Group
Boca Raton London New York

CRC Press is an imprint of the
Taylor & Francis Group, an **informa** business

First published 1990 by CRC Press
Taylor & Francis Group
6000 Broken Sound Parkway NW, Suite 300
Boca Raton, FL 33487-2742

Reissued 2018 by CRC Press



**Library of Congress Cataloging-in-Publication Data**

Denno, K.
Engineering economics of alternative energy sources / author, Khalil Denno.
p. cm.
Includes bibliographical references.
ISBN 0-8493-6641-0
1. Renewable energy sources. 2. Renewable energy sources—Economic aspects. I. Title.
TJ808.D45 1990
333.79—dc20 90-1513

A Library of Congress record exists under LC control number: 90001513

Publisher's Note
The publisher has gone to great lengths to ensure the quality of this reprint but points out that some imperfections in the original copies may be apparent.

Disclaimer
The publisher has made every effort to trace copyright holders and welcomes correspondence from those they have been unable to contact.

ISBN 13: 978-1-315-89263-4 (hbk)
ISBN 13: 978-1-351-07173-4 (ebk)

Visit the Taylor & Francis Web site at http://www.taylorandfrancis.com and the
CRC Press Web site at http://www.crcpress.com

*To my wife*

*BADIA*

Who lighted for me the path and stressed
the far reaching contributions of this book to humanity

# PREFACE

This text book presents a comprehensive picture for the economic aspects, feasibility and adaptability as well as modelling of alternative energy sources and their interconnections. The economic analysis for each mode of energy source is preceded by the introduction of the sources basic structural components and operational as well as fuel characteristics. Coverage of alternative energy sources in this book planned to be total and complete including: low temperature and high temperature fuel cells, rechargeable storage batteries (including the lead acid, Nickel-Cadmium, lithium and the Sodium-Sulphur batteries), the Redox Flow Cells energy system in compatibility with fuel cells and storage batteries, the MHD energy system using nonfossil renewable fuels, the solar energy system using direct thermal units and photovoltiac generators, the trind energy conversion system and its economic feasibility, various modes of tidal ocean wave energy converters, the geothermal energy conversion system, and finally, the ocean thermal energy converters including off-shore installation and cold water piping system.

Following the presentation of unit and system description for those modes of alternative energy sources, incremented energy costs curve or its equivalent will be presented, followed by the core introduction of the economic coordination equation for each possible system of operation of the particular mode, and by the presentation of the economic scheduling of generation. The aspect of economic scheduling of generation will be applied on several modes of system consumption such as localized dispersed system, interconnected load centers, and a totally central system.

Results of economic feasibility as well as future directions for adaptation to the nature of cyclic load demands will be presented with futuristic conclusive and indicative economic paths.

For the purpose of energy system design, a set of precalculated metrics representing linkage energy coefficients (known as the transmission loss coefficients) and the symmetric resistance elements (setting network design in the power reference frame) have been introduced in Chapters 1 and 2. To utilize those precalculated matrices as invariant frames, appropriate multiplying factors have been derived for every mode of renewable energy system throughout this book.

This book could be adopted by the following sectors:

1. Graduate students in the field of electrical engineering, mechanical engineering physics and operations research.
2. All engineering and professional societies.
3. Electric utilities worldwide.
4. Research organization worldwide.
5. Libraries worldwide.

# THE AUTHOR

**Khalil Denno, Ph.D.,** is a Distinguished Professor of Electrical Engineering at Newark College of Engineering, New Jersey Institute of Technology in Newark, New Jersey.

Dr. Denno received his B.S. degree from University of Bagdad, Iraq in 1955. He obtained his M.E.E. degree in 1959 from Rensselaer Polytechnic Institute of Troy, New York and his Ph.D. degree in 1967 from Iowa State University in Ames, Iowa. He joined the Newark College of Engineering of New Jersey Institute of Technology as Associate Professor in 1969, was promoted to the rank of Professor in 1973, and became Distinguished Professor in September 1987.

Dr. Denno is a Fellow of the Institution of Electrical Engineers (IEE), a senior member of the Institute of Electrical and Electronics Engineers (IEEE), a member of the American Nuclear Society, a member of the New York Academy of Sciences, a member of the American Society of Engineering Education, and a member of the Sigma Xi Society.

Dr. Denno has been honored in winning the 1982 Harlan Perlis Award for Excellence in Research, as well as with numerous listings in national and international honor societies and biographies.

Dr. Denno's main specialties are in the fields of Energy Conversion, Renewable Energy Sources, and Conventional Power System and Magnetohydrodynamics. He is a licensed Professional Engineer in New Jersey and Chartered Engineer in the U.K. He is the author of a book entitled *Power System Design and Applications for Alternative Energy Sources,* published by Prentice-Hall, Englewood Cliffs, New Jersey.

Dr. Denno has published 120 research papers in leading national and international journals covering the fields of magnetohydrodynamic power generation, fusion energy, lightning phenomenon, particle accelerators, conventional energy systems, characterization of cold plasma, and various modes of renewable energy sources.

# TABLE OF CONTENTS

## SPECIAL ACKNOWLEDGMENT

With special thanks and deep gratitude to Ms. Joan Delli-Santi who typed and reviewed this manuscript with patience and dedication.

# INTRODUCTION

Scope and objectives of this book are directed uniquely to deal comprehensively with the economics of various known forms of renewable energy sources, their system of operation as well as systems interconnection and their modeling. Presentation of subject matter targeted the aspects of system design using invariant basis of design which includes elements of sources linkage coefficients as well as elements of the symmetric resistance matrix which identify system design in the power flow reference frame.

Economic evaluation of system feasibility has been based on developing its incremental energy coast curve, optimal allocation of power generation, and total relative annual cost with respect to standard developed systems of centralized mode and then dispersed mode.

Renewable energy sources presented in this book includes: fuel cells, storage batteries, the redox flow cells, bioelectrochemical cells, magnetohydrodynamic generators using nonfossil fuel, solar energy converters, wind energy converters, ocean tidal energy converters, geothermal energy converters, and ocean thermal energy converters.

Besides the system design development presented, modeling of the system itself and its interconnection to other modes of renewable energy sources have been identified in every possible economic link-up.

The author would like to stress the total uniqueness of this book subject matter and its far reaching importance to the potential users in the area of selecting any mode of renewable sources of system as well as possible linkage to any other energy system or systems.

Chapter 1

# SYNTHESIS OF ENERGY SYSTEMS
## (Conventional and Renewable)

## I. POWER SYSTEM IDENTIFICATION IN THE POWER FLOW REFERENCE FRAME[2,3,5,12,15]

Electrical energy systems are generally represented in a conventional form in terms of data related to actual generating sources, loads, and impedances of the interconnecting network. This is the first reference frame as called by Kron.[10] On the other hand, engineers in a single power area and multiarea power poll usually deal with real power of the generating sources and real energy exchange at area boundaries.

In situations where prompt and decisive action is needed in comparing several energy systems of different configurations under a unified constraint, it becomes necessary that those systems be expressed and identified in an overall power equivalent reference frame. Also, the calculation of economic scheduling of generation, which relates the generating capacity of individual plants to total generation based on coordinating incremental production costs and incremental transmission losses, is carried in the power flow reference frame (the sixth reference as called by Kron).[10]

Optimization of energy systems from an economic standpoint can proceed on the basis of arbitrary interconnecting networks in the power flow reference frame subject to certain constraints such as minimum losses, specified total generation, specified plant capacity, and total received load.

Determination of the optimum energy system network in the sixth or power flow reference frame can be followed by a series of transformations aimed at representing the optimum system in the actual or first reference frame. To compare and analyze from the start, several power system alternatives in the actual first reference frame require excessive computer time as well as large memory capacity to absorb all the data.

The foregoing points out the necessity to develop a criterion by which power system optimization in the power flow reference frame can be carried out using the [B] matrix, power source outputs within their maximum ranges, and fuel cost data. Such a criterion was developed earlier and treated successfully on small power systems.

Based on the solution obtained for the optimum [B] matrix, coupled with data from load flow calculations, a new path for designing the power network in the sixth or power flow reference frame will be developed and tested in this chapter.

## II. OBJECTIVES OF SYSTEM SYNTHESIS[1,9,10]

Given several optimum energy system configurations to be established in a single area or multiarea mode, each system follows the conditions:

1. The system contains n equivalent generating renewable energy sources such as fuel cells, solar cells, OTEC plant, etc., as well as electromechanical plants, each has its own fuel cost curve as shown in Figure 1.1.
2. Each system operates optimally according to the coordination criteria relating incremental generation costs and incremental transmission losses costs, as expressed by Equation 1.1.

$$\frac{\partial F_i}{\partial P_i} + \lambda \frac{\partial P_L}{\partial P_i} = \lambda \tag{1.1}$$

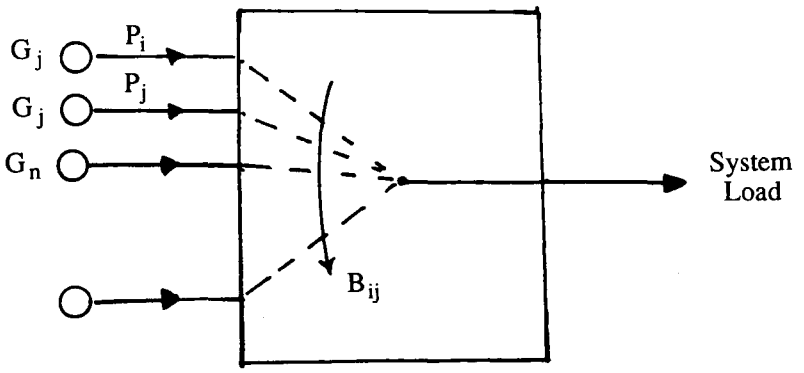


FIGURE 1.1 Power flow reference frame. (From Kron, G., Tensorial analysis of integrated transmission system, *IEEE*, 70, 1239—1246, 1951. With permission.)

where $\lambda$ = incremental cost of received power in dollars per megawatt hour, known as Lagrange multiplier; $P_i$ = capacity of plant i in megawatts (MW); and $F_i$ = fuel cost of plant i in dollars per hour.

3. The [B] matrix for an optimum energy system[1,2,8,9] follows a solution expressed in terms of source output constrained by maximum range or capacity and fuel cost data as indicated in Equation 1.4. The latter is obtained from Equation 1.1, subject to the following constraint equations:

$$\phi\left(P_1, P_2 — P_n\right) = \sum_{i=1}^{N} P_i - P_r - P_L = 0 \tag{1.2}$$

$$P_L \simeq \sum_{i=1}^{N}\sum_{j=1}^{M} P_i B_{ij} P_j \tag{1.3}$$

where $P_L$ = total transmission losses in megawatts and $P_r$ = given received power (load) in megawatts.

$$B_{ij} = \left[-F_{ii}F_{jj}P_iP_j = \lambda\left(F_{ii} - F_{ii}f_j\right)P_i + \left(\lambda F_{jj} - F_{jj}f_i\right)P_j + f_i + f_j - f_i - f_j - \lambda^2\right]$$

$$\Big/\left[2\lambda F_{jj}P_j^2 + 2\lambda F_{ii}P_i\left(2\lambda f_i - 2^2\right)P_i + \left(2\lambda f_j - 2\lambda^2\right)P\right] \tag{1.4}$$

4. The [B] matrix expressed above is an implicit function of all power sources as indicated in Equations 1.5 and 1.6.

$$P_j = f\left(P_i\right) \tag{1.5}$$

$$B_{ij} = g\left(P_i\right) \tag{1.6}$$

The problem centers on obtaining the optimum energy system representation in the power flow reference frame in terms of the symmetrical resistance matrix. The solution will be verified on two systems, namely:

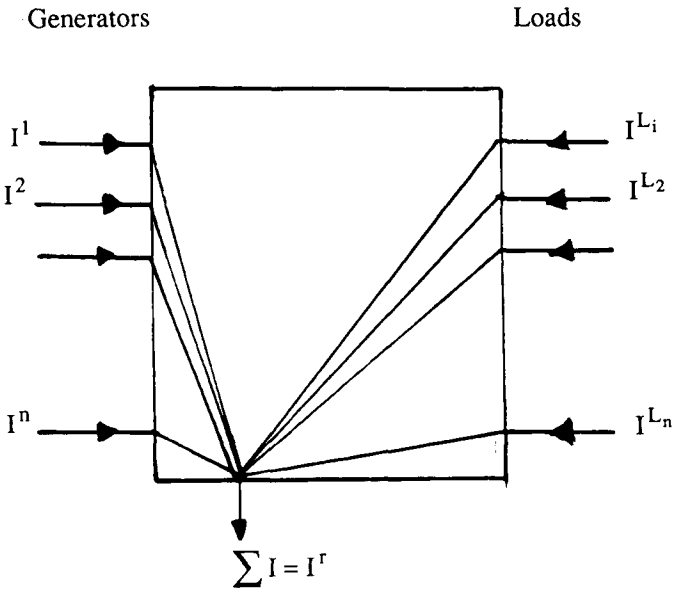


FIGURE 1.2 Measurement reference frame. (From Kron, G., Tensorial analysis of integrated transmission system, *IEEE*, 70, 1239—1246, 1951. With permission.)

1. A totally centralized system with electromechanical and electrochemical energy sources
2. A mixed dispersed-centralized system with electrochemical and electromechanical energy generating units

## III. THE SIX BASIC REFERENCE FRAMES[1,8-10]

Energy system representation could be established in any of the following reference frames introduced by Kron.[10] Although the ultimate goal is the sixth frame in which the entire system is expressed in terms of power sources and power exchanges, a review of the preceding five references is presented below.

1. "Measurement" Reference Frame 1: system is expressed in terms of generating and load currents as shown in Figure 1.2
2. "Leakage" Reference Frame 2:[9] all individual load currents are replaced by a unified hypothetical load current as shown in Figure 1.3
3. "Through" Reference Frame 3:[9] the unified load current is replaced by an equivalent generator current as shown in Figure 1.4
4. "Time" Reference Frame 4: frame 3 is converted to a new time reference frame where each current possesses two components, one along its own generator terminal voltage $I^D$ and the other at right angles to it $I^Q$. See Figure 1.5 where d, q, D, Q are the old and new time reference axes.
5. "Real" Power reference frame 5: derived from the new time reference frame, the real power of each generator is

$$P = I^D \left| E_o \right| \tag{1.7}$$

where $I^D$ = generator real current in the new time reference frame and $E_o$ = generator terminal voltage.

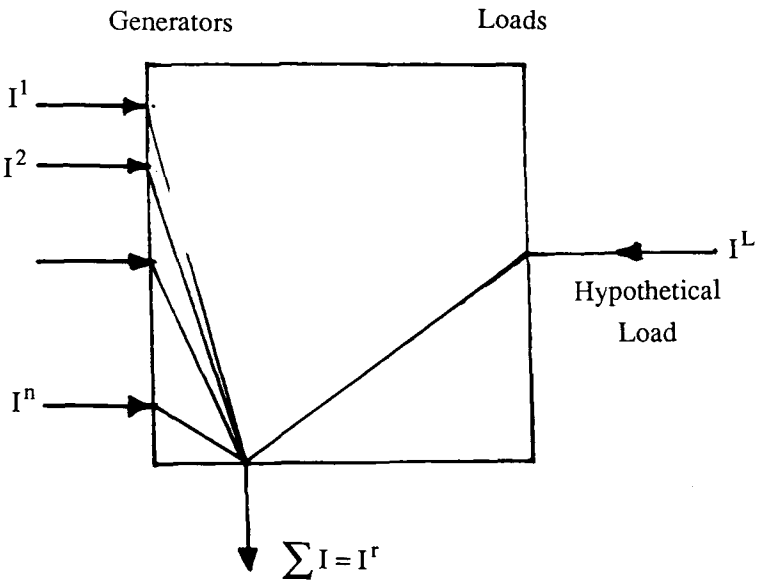


FIGURE 1.3 Leakage reference frame. (From Kron, G., Tensorial analysis of integrated transmission system, *IEEE*, 70, 1239—1246, 1951. With permission.)

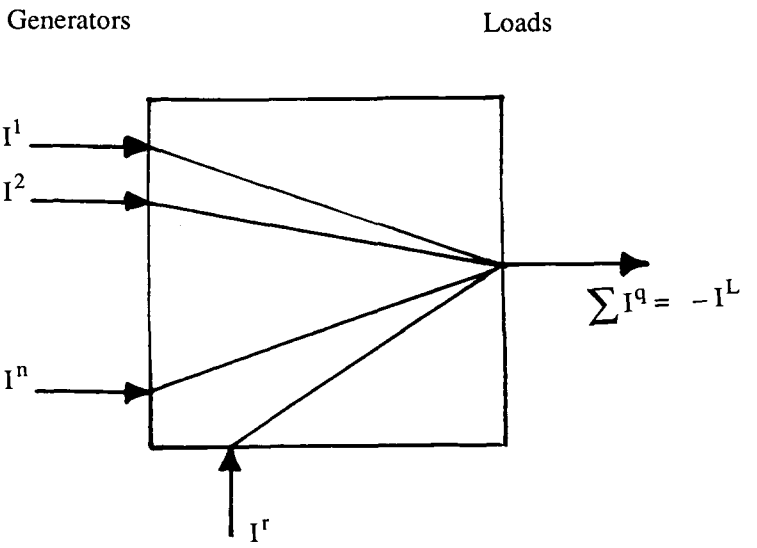


FIGURE 1.4 Through reference frame. (From Kron, G., Tensorial analysis of integrated transmission system, *IEEE*, 70, 1239—1246, 1951. With permission.)

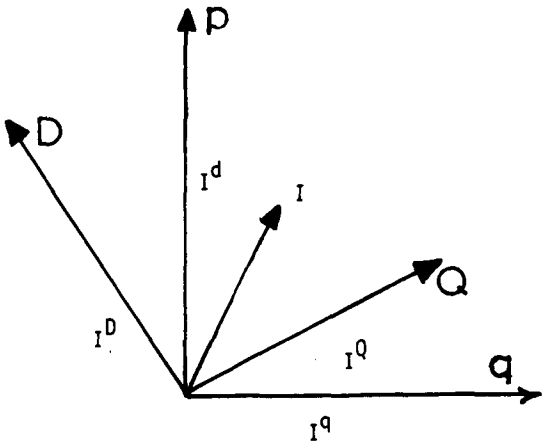


FIGURE 1.5 Time reference frame. (From Kron, G., Tensorial analysis of integrated transmission system, *IEEE*, 70, 1239—1246, 1951. With permission.)

$$\therefore I^D = \frac{1}{|E_o|} P \tag{1.8}$$

This reference frame is expressed in terms of the following diagonal matrix:

$$|C| = D\frac{1}{|E_o|} \tag{1.9}$$

6. "Power Flow" reference frame 6: all real powers are expressed in a frame involving power exchange among various equivalent generating sources as shown in Figure 1.1. The matrix of transformation to the power flow or sixth reference frame is known as the loss matrix with the following general terms:

$$B_{ij} = K_{ij}R_{ij} - H_{ij}\left(f_i - f_j\right) \tag{1.10}$$

Then the total transmission loss $P_L$ is expressed as

$$P_L = \sum_{ij} P_i K_{ij} R_{ij} P_j - P_j H_{ij}\left(f_i - f_j\right) P_i \tag{1.11}$$

where

$$K_{ij} = \frac{1}{V_i V_j}\left(1 + S_i S_j\right)\cos\phi_{ij}\left(S_i - S_j\right)\sin\phi_{ij} \tag{1.12}$$

$$H_{ij} = \frac{1}{V_i V_j}\left(1 + S_i S_j\right)\sin\phi_{ij}\left(S_i - S_j\right)\cos\phi_{ij} \tag{1.13}$$

$$f_i = R_{Gi-Lk} I_k \tag{1.14}$$

$$f_j = R_{Gj-Lk} I_k \tag{1.15}$$

$$I_k = i_{LK} / i_L \tag{1.16}$$

and where $l_k$ = the ratio of load current at bus k to total load current; $R_{Gi\text{-}Lk}$ = resistance between generator i and load k; $R_{Gj\text{-}Lk}$ = resistance between generator j and load k; $R_{ij}$ = symmetric resistance in the sixth frame; $H_{ij}(f_i - f_j)$ could be neglected in a power system where $\phi_{ij}$ and $(S_i - S_j)$ are small, respectively. $S_i$ = ratio of reactive to real power at bus i and $\phi_{ij}$ = phase angle between buses i and j, respectively. Equation 1.11 becomes:

$$P_L \approx \sum_i \sum_j P_i K_{ij} R_{ij} P_j \tag{1.17}$$

or

$$B_{ij} = K_{ij} R_{ij} \tag{1.18}$$

$$R_{ij} = K_{ij}^{-1} B_{ij} \tag{1.19}$$

## IV. BASIS FOR ENERGY SYSTEM DESIGN IN THE POWER FLOW FRAME[1-15] *

The design criterion for an optimum energy system of an arbitrary interconnecting network subject to the constraints of minimum transmission losses, specified total received load, and specified plant capacity, is one of the objectives of this paper. Such a criterion is based on the calculation of the symmetrical resistance matrix in the power flow reference frame.

Also a knowledge of the resistance matrices of more than one interconnecting network could serve as the basis for identifying the nature and type of the power system, i.e., whether it be a centralized system, a dispersed system, or a mixed centralized-dispersed system as far as the locations of the power generating sources are concerned.

The solution of the [B] matrix in terms of energy generating sources within their capacity and fuel cost data was obtained and restated in equation 1.4 with the [K] matrix given in Equation 1.12.

Equation 1.18 can be expanded in matrix form and written as follows:

$$\begin{bmatrix} B_{11} & B_{12} & \cdots & B_{1n} \\ B_{21} & B_{22} & \cdots & B_{2n} \\ \vdots & & & \vdots \\ B_{n1} & B_{n2} & \cdots & B_{nn} \end{bmatrix} = \begin{bmatrix} (K_{11}R_{11}) & (K_{12}R_{12}) & \cdots & (K_{1n}R_{1n}) \\ (K_{21}R_{21}) & (K_{22}R_{22}) & \cdots & (K_{2n}R_{2n}) \\ \vdots & & & \vdots \\ (K_{n1}R_{n1}) & (K_{n2}R_{n2}) & \cdots & (K_{nn}R_{nn}) \end{bmatrix} \tag{1.20}$$

Therefore,

$$R_{11} = \frac{B_{11}}{K_{11}}$$

$$R_{12} = \frac{B_{12}}{B_{12}} \quad \text{and so on}$$

$$R_{nn} = \frac{B_{nn}}{K_{nn}} \tag{1.21}$$

* © IEEE, 1978. Reprinted with permission from Denno, K., Power system identification in the power flow reference frame in the presence of tie flows, Control of Power Systems Conference and Exposition, Oklahoma City, No. 78 CH-1282-3, REG5, IEEE, 1978, 90—95.

## V. USING THE DIAGONAL [R] MATRICES IN COMPARISON OF ENERGY SYSTEM ALTERNATIVES[1-4,11] *

The overall [R] matrix can be expressed as below:

$$[R] = \begin{bmatrix} B_{11}/K_{11} & \cdots & B_{1n}/K_{1n} \\ B_{21}/K_{21} & \cdots & B_{2n}/K_{2n} \\ \vdots & & \vdots \\ B_{1n}/K_{1n} & & B_{nn}/K_{nn} \end{bmatrix} \tag{1.22}$$

The elements in the matrix of Equation 1.22 are the self-symmetrical resistances of the individual energy sources from a reference point and mutual symmetrical resistances among the individual sources, all represented in the energy flow frame. $R_{11}$, $R_{22}$ — $R_{nn}$ = the self-symmetrical resistances of energy source number 1 with respect to a reference point. $R_{12}$, $R_{13}$ — $R_{1n}$ = the mutual symmetrical resistances between source number 1 with respect to power source number 2.

Calculation of the [R] matrix elements requires the following procedure:

1. Load flow calculations to secure information for the [K] matrix, namely, voltage magnitude, phase angle, and real and reactive power of each bus-bar.
2. Complete establishment of the [B] matrices under all loadings for the presumed energy system.
3. Application of Equation 1.22 together with the procedure of calculating the [R] symmetric matrix which reflects an optimum energy system design in the energy flow reference frame and which was demonstrated for the two systems in the following section.

## VI. CASE STUDY 1[1-15]

A. A centralized system of 32 equivalent power energy bus-bars with total peak received load of 23,000 MW.
B. A dispersed-centralized system of 123 equivalent bus-bars having the same total peak received load of 23,000 MW.

For the above two presumed systems, load flow calculations were carried on all loadings based on the Gauss-Seidel method on a program developed by the Public Service Electric and Gas Company (PSE&G) of New Jersey.

Also the [B] matrices for all loadings were obtained for the above mentioned two systems according to Equation 1.4.

By compiling elements from the [K] matrices with those of the [B] matrices for the two systems, elements of the [R] matrices are obtained by a simple computer program according to Equation 1.22, run on the RCA 70 machine, the capacity of which was quite adequate even for the large number of 123 bus-bars.

However, since the number of bus-bars in the centralized-dispersed system is 123, compared to 32 to the centralized system, a unified basis for comparison is obtained from extracting the diagonal elements from the full matrix and forming a new diagonal matrix.

As explained earlier, the elements of the new diagonal matrix have a great significance since

they represent the symmetrical resistance of each energy source with respect to the system centroid or reference point, and hence can serve as a justified basis for comparing more than one optimum power network in the sixth reference frame.

## A. LOAD FLOW CALCULATIONS[1-15]

Basic systematic procedure for the load flow calculations involves these steps:

1. Designating the slack or swing bus which is characterized as a large generating bus with a relatively high moment of inertia. For the swing bus, selected values for the voltage magnitude and phase angle are assumed, leaving real and reactive powers variables. Voltage controlled buses will have fixed voltage magnitude and real power while load buses will be assigned constant real and reactive powers.
2. Assignment of fixed tolerance and accelerating factors to insure rapid convergence of any change in voltage magnitude. Typical values for tolerance and accelerating factors are 0.001 and 1.6, respectively.
3. Through iteration technique, a set of voltage magnitudes and phase angles for voltage controlled buses and load buses are secured, according to the following equation. The process is repeated until the limit of tolerance is met.

$$E_p(\text{modified}) = \frac{1}{Y_{pp}}\left(\frac{P_p - jQ_p}{E_{p-\text{old}}} - \sum_{\substack{q=1 \\ P=q}}^{n} Y_{pq}E_q\right) \tag{1.23}$$

where $E_p$ (modified) = the modified value for bus voltage; $E_p^*$ (old) = the conjugate value for old bus voltage; $Y_{pp}$ = the self bus admittance for bus p; $P_p$-$jQ_p$ = the power at bus p; and $Y_{pq}E_q$ = the line admittance and bus voltage.

4. The bus phase angle is calculated according to the following equation:

$$\delta = \frac{\text{Im}\left(E_p\right)}{\text{Real}\left(E_p\right)} \tag{1.24}$$

where $E_p$ = the bus voltage obtained earlier; and $\delta_p$ = the phase angle of bus p voltage where slack bus phase angle is the reference.

5. The reactive power for each bus is calculated as:

$$Q_p = -\,\text{Im}\left[Y_{pq}V_p + \sum_{\substack{q=1 \\ P=q}}^{n} V_{pq}V_qV_p^*\right] \tag{1.25}$$

where $Q_p$ = the reactive power at bus p; $V_p$ = the bus voltage; $V_p^*$ = the conjugate of bus voltage; $V_{pq}$ = the line voltage; $Y_{pp}$ = the bus admittance and bus p; and $Y_{pq}$ = the line admittance for line pq.

6. The bus current can be calculated from:

$$I_p = \frac{P_p - jQ_p}{E_q^*} \tag{1.26}$$

where $I_p$ = the current at bus p; $P_p$ - $jQ_p$ = the power at bus p; $E_p^*$ = the conjugate value of

voltage at bus P; $P_p = jQ_p$ = the power at bus p; and $Y_{pq}$, $E_q$ = the line admittance and bus voltage.

7. The transmission line loss can be calculated as:

$$P + jQ = \sum_{\substack{p=1 \\ p=q}}^{n} \sum_{\substack{q=1 \\ q=p}}^{n} \frac{I_{pq}^2}{Y_{pq}} \tag{1.27}$$

where P + jQ = the real and reactive power of line; $I_{pq}$ = the line current for line $p_q$; and $Y_{pq}$ = the line admittance for line $p_q$.

8. The line current can be calculated as:

$$I_{pq} = \left(E_p - E_q\right) Y_{pq} \tag{1.28}$$

where $I_{pq}$ = the line current for line $p_q$; $E_p$, $E_q$ = the bus voltage for bus p and q; and $Y_{pq}$ = the line admittance for line $p_q$.

Load flow calculations were carried out using Gauss-Seidel method that is being used by most utility companies including PSE&G of New Jersey whose power grid system is used in this example. Also, we have to mention that Gauss-Seidel method is somehow preferred over Newton Raphson method, because it is characterized with fewer operations to complete any iteration process.

Handling capability of PSE&G load flow calculations program is basically Fortran IV. This Fortran IV computer program is written in the SAP language for the IBM-704 by the American Electric Power Corporation. The general features of the load flow program is described as follows.

This program can handle network assembly limit of 800 buses and 1200 lines. Within the 800 buses, all of the buses are either static capacitors or shunt reactors, and up to 300 buses can have voltage regulation. With a total of 1200 lines, up to 300 lines can be transformers with either the fixed taps or the tap changing under the load condition.

All input data will be reprinted as part of the final results. The load flow output also includes important summaries, such as the Area Power Interchange Summary which gives the actual iteration count of the solution, the tolerances and the acceleration factors, the total load and loss, the line charging, the generation, and the mismatch, all in megawatt (MW) and megavar (Mvar) units. Other summaries are the Tap-changing Summary, the Generator Summary, the Line over Load Summary, and the Summary of High and Low Voltage (above 1.05 per unit and below 0.95 per unit).

Load flow information secured by using the program of PSE&G of New Jersey conducted with respect to a peak load of around 23,000 MW on a PSE&G power grid system increasing over several stages by about 10,000 MW. Two modes of systems are considered in the calculation, one remaining centralized and the other is centralized-dispersed whereby the new additional generator bus-bars taking the bulk of the 10,000 MW increase to be supplied by on site assembly of fuel-cells electrochemical generators.

Description of generation expansion on a centralized mode is shown in Table 1.1.

Results of load flow calculations have been obtained for several levels of loadings from 60 to 100%. Shown in Tables 1.2 and 1.3 are those for centralized system, while Tables 1.4 and 1.5 are for mixed centralized-dispersed systems.

## B. CALCULATION OF THE [B] MATRIX[1-15]

Elements of the transmission loss coefficient matrix under several levels of loadings were

**TABLE 1.1**
**Generation Expansion Program**

| Year | Bus no. | Capacity (MW) | Type | Generation cost ($/kW) | Transmission cost ($/kW) |
|---|---|---|---|---|---|
| $\Delta G_1$ | 450 | 533 | N | 250 | 65 |
| | 343 | 200 | GT | 100 | 10 |
| | 359 | 200 | GT | 100 | 10 |
| | 301 | 40 | F4 | 160 | 30 |
| | 711 | 22 | GT | 100 | 10 |
| | 182 | 216 | GT | 100 | 10 |
| | 157 | 190 | GT | 100 | 10 |
| $\Delta G_2$ | 450 | 532 | N | 250 | 65 |
| | 391 | 200 | GT | 100 | 10 |
| | 285 | 270 | F | 160 | 20 |
| | 427 | 545 | N | 250 | 65 |
| | 693 | 60 | F | 180 | 10 |
| | 687 | 160 | F | 180 | 20 |
| | 157 | 126 | F | 180 | 20 |
| $\Delta G_3$ | 427 | 558 | N | 250 | 65 |
| | 391 | 400 | F | 160 | 30 |
| | 391 | 400 | F | 160 | 30 |
| $\Delta G_4$ | 183 | 400 | F | 160 | 20 |
| $\Delta G_5$ | 435 | 400 | GT | 100 | 10 |
| | 439 | 100 | GT | 100 | 10 |
| $\Delta G_6$ | 430 | 1100 | N | 300 | 20 |
| | 439 | 100 | GT | 100 | 10 |
| | 439 | 400 | F | 160 | 20 |
| | 195 | 1190 | N | 300 | 50 |
| $\Delta G_7$ | 430 | 1100 | N | 300 | 20 |
| $\Delta G_8$ | 438 | 1100 | N | 330 | 65 |
| | 439 | 400 | F | 160 | 20 |
| $\Delta G_9$ | 438 | 1100 | N | 330 | 65 |
| | 197 | 1200 | N | 300 | 40 |
| | 198 | 1300 | PH | | |

*Note:* N = nuclear powerplant; GT = gas-turbine powerplant; F = steam-fossil powerplant; and PH = pumped-hydro powerplant.

Reprinted from Energy Utilization of PSE&G for the Middle Atlantic Power Research Committee, Newark, NJ, 1976. With permission.

## TABLE 1.2
## New Off-Nominal Setting(s) for TCUL Transformers (70%)

| Bus no. from | Bus no. to | PBI | Transformer tap |
|---|---|---|---|
| 2 | 295 | 0 | 0.912000 |
| 179 | 180 | 0 | 0.975000 |
| 283 | 282 | 0 | 0.975000 |
| 286 | 288 | 0 | 0.944000 |
| 287 | 288 | 0 | 0.937000 |
| 298 | 299 | 0 | 0.975000 |
| 304 | 305 | 0 | 1.025000 |
| 309 | 336 | 0 | 1.019000 |
| 327 | 332 | 0 | 1.019000 |
| 328 | 332 | 0 | 1.006000 |
| 339 | 365 | 0 | 0.925000 |
| 378 | 426 | 0 | 0.981000 |
| 385 | 386 | 0 | 0.937000 |
| 390 | 391 | 0 | 1.019000 |
| 416 | 425 | 0 | 0.956000 |
| 701 | 702 | 0 | 1.025000 |

*Note:* Load flow calculations 70% loading for centralized system.

## Table of Generator Data Sorted by Node Number

| Node no. | Name | Generator voltage | Generator angle | Generator P (MW) | Generator Q (Mvar) |
|---|---|---|---|---|---|
| 1 | G001 | 1.0000 | 0.0000 | 427.8999 | –461.3999 |
| 150 | G150 | 1.0340 | –1.7000 | 560.0000 | 0.0000 |
| 156 | G156 | 1.0200 | –18.5000 | 59.0000 | 38.7000 |
| 157 | G157 | 1.0300 | –3.4000 | 126.0000 | 0.5000 |
| 161 | G161 | 1.0270 | –5.6000 | 0.0000 | 0.0000 |
| 164 | G164 | 1.0300 | –5.7000 | 330.0000 | –11.1000 |
| 172 | G172 | 1.0300 | 4.5000 | 623.0000 | 2.0000 |
| 174 | G174 | 1.0300 | –3.7000 | 342.0000 | –32.3000 |
| 182 | G182 | 1.0350 | –2.9000 | 0.0000 | 0.0000 |
| 183 | G183 | 1.0360 | –2.6000 | 335.0000 | –300.0000 |
| 285 | G285 | 1.0300 | –6.8000 | 270.0000 | –37.2000 |
| 291 | G291 | 1.0300 | –7.7000 | 580.0000 | 168.3000 |
| 301 | G301 | 1.0000 | –11.9000 | 40.0000 | 59.0000 |
| 315 | G315 | 1.0080 | –6.5000 | 0.0000 | 0.0000 |
| 316 | G316 | 1.0090 | –6.6000 | 0.0000 | 0.0000 |
| 327 | G327 | 1.0290 | –8.0000 | 27.0000 | 100.0000 |
| 332 | G332 | 1.0140 | –7.0000 | 0.0000 | 0.0000 |
| 336 | G336 | 0.9820 | –8.5000 | 0.0000 | 0.0000 |
| 339 | G339 | 1.0160 | –5.7000 | 976.0000 | 400.0000 |
| 343 | G343 | 1.0340 | –7.6000 | 0.0000 | 0.0000 |
| 357 | G357 | 1.0130 | –6.3000 | 535.0000 | 300.0000 |
| 359 | G359 | 1.0320 | –5.3000 | 0.0000 | 0.0000 |
| 365 | G365 | 1.0360 | –7.4000 | 61.0000 | –80.0000 |
| 371 | G371 | 1.0300 | –2.4000 | 638.0000 | 128.2000 |
| 372 | G372 | 1.0050 | –6.2000 | 0.0000 | 0.0000 |
| 390 | G390 | 1.0300 | –5.8000 | 454.0000 | 181.0000 |
| 391 | G391 | 1.0350 | –4.1000 | 670.0000 | 320.0000 |
| 427 | G427 | 1.0300 | 2.1000 | 1103.0000 | 31.0000 |
| 450 | G450 | 1.0300 | 4.2000 | 1065.0000 | –153.7000 |
| 685 | G685 | 1.0000 | –46.1000 | 131.0000 | 169.1000 |
| 687 | G687 | 1.0000 | –53.5000 | 160.0000 | 207.9000 |
| 693 | G693 | 0.9540 | –52.4000 | 0.0000 | 0.0000 |

**TABLE 1.2 (continued)**
**Table of Load Data Sorted by Node Number**

| Node no. | Name | Load bus voltage | Load bus angle | Load P (MW) | Load Q (Mvar) | Sync. cond. Q (Mvar) |
|---|---|---|---|---|---|---|
| 1 | L001 | 1.0000 | 0.0000 | 0.0000 | 0.0000 | 0.000 |
| 2 | L002 | 1.0110 | –2.9000 | 0.0000 | 0.0000 | 0.000 |
| 16 | L016 | 1.0220 | –0.7000 | 0.0000 | 0.0000 | 0.000 |
| 96 | L096 | 1.0170 | –18.6000 | 0.0000 | 0.0000 | 0.000 |
| 125 | L125 | 1.0080 | –18.8000 | 0.0000 | 0.0000 | 0.000 |
| 126 | L126 | 1.0290 | –6.2000 | 0.0000 | 0.0000 | 0.000 |
| 150 | L150 | 1.0340 | –1.7000 | 163.0000 | 4.1000 | 0.000 |
| 151 | L151 | 1.0040 | –18.8000 | 22.4000 | 2.7000 | 0.000 |
| 152 | L152 | 1.0030 | –17.5000 | 14.3000 | 1.1000 | 0.000 |
| 153 | L153 | 1.0120 | –3.6000 | 47.0000 | –8.1000 | 0.000 |
| 155 | L155 | 1.0360 | –2.6000 | 91.0000 | 13.8000 | 0.000 |
| 156 | L156 | 1.0200 | –18.5000 | 48.0000 | 7.6000 | 0.000 |
| 157 | L157 | 1.0300 | –3.4000 | 0.0000 | 0.0000 | 0.000 |
| 158 | L158 | 1.0240 | –7.1000 | 84.0000 | 12.9000 | 0.000 |
| 160 | L160 | 1.0120 | –18.1000 | 2.1000 | 0.4000 | 0.000 |
| 161 | L161 | 1.0270 | –5.6000 | 71.0000 | 3.5000 | 0.000 |
| 162 | L162 | 1.0240 | –8.5000 | 87.5000 | 15.0000 | 0.000 |
| 164 | L164 | 1.0300 | –5.7000 | 14.5000 | –1.2000 | 0.000 |
| 167 | L167 | 1.0260 | –0.8000 | 12.4000 | 14.5000 | 0.000 |
| 168 | L168 | 1.0260 | 1.9000 | 134.0000 | 18.6000 | 0.000 |
| 170 | L170 | 1.0200 | –9.2000 | 143.0000 | 33.2000 | 0.000 |
| 171 | L171 | 1.0070 | –18.9000 | 17.0000 | 11.8000 | 0.000 |
| 172 | L172 | 1.0300 | 4.5000 | 26.0000 | –2.7000 | 0.000 |
| 174 | L174 | 1.0300 | –3.7000 | 273.0000 | 48.1000 | 0.000 |
| 175 | L175 | 1.0230 | –7.9000 | 157.0000 | 35.6000 | 0.000 |
| 177 | L177 | 0.9990 | –16.6000 | 46.1000 | 2.0000 | 0.000 |
| 178 | L178 | 1.0240 | –8.5000 | 36.9000 | 1.9000 | 0.000 |
| 179 | L179 | 1.0000 | –11.1000 | 0.0000 | 0.0000 | 0.000 |
| 180 | L180 | 1.0240 | –8.6000 | 169.0000 | 44.5000 | 0.000 |
| 181 | L181 | 1.0320 | –3.3000 | 21.0000 | 12.6000 | 0.000 |
| 182 | L182 | 1.0350 | –2.9000 | 0.0000 | 0.0000 | 0.000 |
| 183 | L183 | 1.0360 | –2.6000 | 0.0000 | 0.0000 | 0.000 |
| 184 | L184 | 1.0370 | –2.5000 | 83.5000 | 4.8000 | 0.000 |
| 185 | L185 | 1.0370 | –2.4000 | 104.0000 | 32.2000 | 0.000 |
| 186 | L186 | 1.0340 | –1.9000 | 52.2000 | 8.4000 | 0.000 |
| 187 | L187 | 1.0240 | –3.3000 | 64.4000 | 7.4000 | 0.000 |
| 188 | L188 | 1.0260 | –7.4000 | 36.2000 | –4.1000 | 0.000 |
| 189 | L189 | 1.0270 | –7.6000 | 36.6000 | –1.5000 | 0.000 |
| 190 | L190 | 1.0430 | –4.3000 | 43.3000 | 9.1000 | 0.000 |
| 191 | L191 | 1.0250 | –8.4000 | 14.8000 | 3.3000 | 0.000 |
| 192 | L192 | 0.9980 | –17.5000 | 18.0000 | 4.6000 | 0.000 |
| 202 | L202 | 1.0300 | –5.7000 | 0.0000 | 0.0000 | 0.000 |
| 227 | L227 | 1.0150 | –1.3000 | 0.0000 | 0.0000 | 0.000 |
| 231 | L231 | 1.0150 | –7.0000 | 0.0000 | 0.0000 | 0.000 |
| 280 | L280 | 1.0210 | –5.0000 | 37.1000 | 11.8000 | 0.000 |
| 281 | L281 | 1.0170 | –6.8000 | 159.0000 | 26.3000 | 0.000 |
| 282 | L282 | 1.0180 | –9.5000 | 62.3000 | 23.1000 | 0.000 |
| 283 | L283 | 1.0000 | –10.7000 | 149.0000 | 51.5000 | 0.000 |
| 285 | L285 | 1.0300 | –6.8000 | 106.0000 | 42.0000 | 0.000 |
| 286 | L286 | 1.0030 | –6.9000 | 63.6000 | 59.0000 | 0.000 |
| 287 | L287 | 1.0020 | –6.3000 | 63.6000 | 59.0000 | 0.000 |
| 288 | L288 | 1.0370 | –5.6000 | 0.0000 | 0.0000 | 0.000 |
| 289 | L289 | 0.9830 | –8.2000 | 40.5000 | 7.4000 | 0.000 |
| 290 | L290 | 1.0100 | –9.7000 | 117.0000 | 90.3000 | 0.000 |
| 291 | L291 | 1.0300 | –7.7000 | 229.0000 | 74.2000 | 0.000 |

**TABLE 1.2 (continued)**
**Table of Load Data Sorted by Node Number**

| Node no. | Name | Load bus voltage | Load bus angle | Load P (MW) | Load Q (Mvar) | Sync. cond. Q (Mvar) |
|---|---|---|---|---|---|---|
| 295 | L295 | 1.0580 | –4.6000 | 0.0000 | 0.0000 | 0.000 |
| 296 | L296 | 1.0320 | –5.8000 | 154.0000 | 76.3000 | 0.000 |
| 297 | L297 | 1.0280 | –5.6000 | 0.0000 | 0.0000 | 0.000 |
| 298 | L298 | 0.9990 | –5.9000 | 0.0000 | 0.0000 | 0.000 |
| 299 | L299 | 1.0060 | –5.0000 | 178.5000 | 147.0000 | 0.000 |
| 301 | L301 | 1.0000 | –11.9000 | 115.0000 | 43.0000 | 0.000 |
| 303 | L303 | 0.9890 | –7.4000 | 0.0000 | 0.0000 | 0.000 |
| 304 | L304 | 0.9970 | –12.5000 | 170.0000 | 20.8000 | 0.000 |
| 305 | L305 | 0.9810 | –9.0000 | 0.0000 | 0.0000 | 0.000 |
| 306 | L306 | 1.0200 | –9.4000 | 125.0000 | 51.8000 | 0.000 |
| 308 | L308 | 0.9960 | –5.7000 | 0.0000 | 0.0000 | 0.000 |
| 309 | L309 | 0.9970 | –12.6000 | 93.8000 | 18.6000 | 0.000 |
| 311 | L311 | 1.0070 | –7.7000 | 0.0000 | 0.0000 | 0.000 |
| 312 | L312 | 0.9820 | –8.3000 | 33.6000 | 4.1000 | 0.000 |
| 313 | L313 | 1.0030 | –7.5000 | 72.8000 | 24.3000 | 0.000 |
| 314 | L314 | 1.0020 | –10.6000 | 145.0000 | 42.0000 | 0.000 |
| 315 | L315 | 1.0080 | –6.5000 | 0.0000 | 0.0000 | 0.000 |
| 316 | L316 | 1.0090 | –6.6000 | 0.0000 | 0.0000 | 0.000 |
| 327 | L327 | 1.0290 | –8.0000 | 102.0000 | 42.0000 | 0.000 |
| 328 | L328 | 0.9980 | –9.3000 | 227.0000 | 103.8000 | 0.000 |
| 332 | L332 | 1.0140 | –7.0000 | 0.0000 | 0.0000 | 0.000 |
| 333 | L333 | 1.0010 | –11.0000 | 237.0000 | 60.2000 | 0.000 |
| 334 | L334 | 1.0020 | –9.4000 | 49.0000 | 6.2000 | 0.000 |
| 336 | L336 | 0.9820 | –8.5000 | 180.0000 | 26.5000 | 0.000 |
| 337 | L337 | 1.0230 | –8.7000 | 37.8000 | 10.5000 | 0.000 |
| 339 | L339 | 1.0160 | –5.7000 | 0.0000 | 0.0000 | 0.000 |
| 340 | L340 | 1.0310 | –7.7000 | 86.8000 | 35.7000 | 0.000 |
| 343 | L343 | 1.0340 | –7.6000 | 29.0000 | 0.0000 | 0.000 |
| 345 | L345 | 1.0250 | –3.1000 | 76.3000 | 12.9000 | 0.000 |
| 347 | L347 | 1.0180 | –6.4000 | 95.2000 | 35.4000 | 0.000 |
| 349 | L349 | 1.0030 | –8.4000 | 40.5000 | 14.0000 | 0.000 |
| 351 | L351 | 1.0250 | –3.9000 | 139.0000 | 34.6000 | 0.000 |
| 352 | L352 | 1.0290 | –7.7000 | 40.0000 | 30.8000 | 0.000 |
| 353 | L353 | 1.0200 | –7.9000 | 115.0000 | 27.2000 | 0.000 |
| 354 | L354 | 0.9960 | –12.7000 | 124.0000 | 21.6000 | 0.000 |
| 357 | L357 | 1.0130 | –6.3000 | 185.0000 | 114.0000 | 0.000 |
| 359 | L359 | 1.0320 | –5.3000 | 0.0000 | 0.0000 | 0.000 |
| 360 | L360 | 1.0280 | –5.4000 | 39.2000 | 15.1000 | 0.000 |
| 362 | L362 | 0.9990 | –5.3000 | 25.2000 | 2.7000 | 0.000 |
| 365 | L365 | 1.0360 | –7.4000 | 272.0000 | 93.0000 | 0.000 |
| 366 | L366 | 0.9960 | –5.6000 | 85.4000 | 15.7000 | 0.000 |
| 368 | L368 | 1.0090 | –6.6000 | 39.2000 | 13.9000 | 0.000 |
| 371 | L371 | 1.0300 | –2.4000 | 0.0000 | 0.0000 | 0.000 |
| 372 | L372 | 1.0050 | –6.2000 | 0.0000 | 0.0000 | 0.000 |
| 373 | L373 | 1.0130 | –6.6000 | 145.5000 | 70.7000 | 0.000 |
| 375 | L375 | 1.0330 | –4.7000 | 19.6000 | 6.9000 | 0.000 |
| 376 | L376 | 1.0280 | –5.0000 | 19.6000 | 6.9000 | 0.000 |
| 377 | L377 | 1.0070 | –8.0000 | 65.8000 | 23.4000 | 0.000 |
| 378 | L378 | 0.9960 | –4.5000 | 0.0000 | 0.0000 | 0.000 |
| 379 | L379 | 1.0200 | –8.3000 | 44.1000 | 17.5000 | 0.000 |
| 380 | L380 | 1.0040 | –7.9000 | 149.0000 | 80.5000 | 0.000 |
| 381 | L381 | 1.0230 | –6.7000 | 38.5000 | 13.8000 | 0.000 |
| 382 | L382 | 1.0320 | –4.3000 | 0.0000 | 0.0000 | 0.000 |
| 383 | L383 | 1.0050 | –6.5000 | 37.8000 | 4.4000 | 0.000 |
| 385 | L385 | 1.0020 | –8.4000 | 0.0000 | 0.0000 | 0.000 |

**TABLE 1.2 (continued)**
**Table of Load Data Sorted by Node Number**

| Node no. | Name | Load bus voltage | Load bus angle | Load P (MW) | Load Q (Mvar) | Sync. cond. Q (Mvar) |
|---|---|---|---|---|---|---|
| 386 | L386 | 1.0230 | –8.8000 | 0.0000 | 0.0000 | 0.000 |
| 388 | L388 | 1.0060 | –10.6000 | 0.0000 | 0.0000 | 0.000 |
| 389 | L389 | 1.0180 | –9.5000 | 98.0000 | 28.6000 | 0.000 |
| 390 | L390 | 1.0300 | –5.8000 | 228.0000 | 50.0000 | 0.000 |
| 391 | L391 | 1.0350 | –4.1000 | 0.0000 | 0.0000 | 0.000 |
| 401 | L401 | 1.0380 | –5.5000 | 33.6000 | 10.8000 | 0.000 |
| 402 | L402 | 1.0140 | –7.3000 | 42.6000 | 14.7000 | 0.000 |
| 403 | L403 | 1.0080 | –6.3000 | 163.0000 | 52.4000 | 0.000 |
| 404 | L404 | 1.0040 | –8.3000 | 157.0000 | 33.6000 | 0.000 |
| 405 | L405 | 1.0260 | –8.7000 | 150.0000 | 2.1000 | 0.000 |
| 406 | L406 | 1.0170 | –8.6000 | 129.0000 | 41.4000 | 0.000 |
| 409 | L409 | 0.9970 | –5.8000 | 0.0000 | 0.0000 | 0.000 |
| 410 | L410 | 1.0140 | –7.2000 | 38.5000 | 18.4000 | 0.000 |
| 411 | L411 | 1.0140 | –7.3000 | 13.3000 | 2.1000 | 0.000 |
| 412 | L412 | 1.0210 | –9.3000 | 15.4000 | 2.8000 | 0.000 |
| 413 | L413 | 1.0250 | –8.9000 | 32.2000 | 9.8000 | 0.000 |
| 414 | L414 | 1.0150 | –8.5000 | 46.9000 | 15.0000 | 0.000 |
| 415 | L415 | 1.0100 | –9.6000 | 46.9000 | 15.0000 | 0.000 |
| 416 | L416 | 1.0020 | –4.4000 | 0.0000 | 0.0000 | 0.000 |
| 417 | L417 | 1.0120 | –4.4000 | 25.9000 | 7.2000 | 0.000 |
| 418 | L418 | 1.0280 | –4.6000 | 34.3000 | 13.8000 | 0.000 |
| 419 | L419 | 1.0250 | –6.7000 | 10.5000 | 3.9000 | 0.000 |
| 420 | L420 | 1.0300 | –5.0000 | 4.9000 | 1.0000 | 0.000 |
| 421 | L421 | 1.0320 | –4.5000 | 4.9000 | 1.0000 | 0.000 |
| 422 | L422 | 1.0120 | –6.3000 | 44.0000 | 12.8000 | 0.000 |
| 423 | L423 | 1.0240 | –6.1000 | 28.7000 | 9.2000 | 0.000 |
| 424 | L424 | 1.0010 | –10.7000 | 23.8000 | 3.4000 | 0.000 |
| 425 | L425 | 1.0270 | –3.2000 | 0.0000 | 0.0000 | 0.000 |
| 426 | L426 | 1.0260 | –1.2000 | 0.0000 | 0.0000 | 0.000 |
| 427 | L427 | 1.0300 | 2.1000 | 0.0000 | 0.0000 | 0.000 |
| 428 | L428 | 1.0300 | 2.4000 | 0.0000 | 0.0000 | 0.000 |
| 429 | L429 | 0.9940 | –5.5000 | 0.0000 | 0.0000 | 0.000 |
| 446 | L446 | 0.9980 | –5.9000 | 0.0000 | 0.0000 | 0.000 |
| 450 | L450 | 1.0300 | 4.2000 | 0.0000 | 0.0000 | 0.000 |
| 501 | L501 | 0.9820 | –8.8000 | 0.0000 | 0.0000 | 0.000 |
| 518 | L518 | 1.0040 | –6.1000 | 0.0000 | 0.0000 | 0.000 |
| 683 | L683 | 0.9860 | –55.0000 | 101.0000 | 9.1000 | 0.000 |
| 685 | L685 | 1.0000 | –46.1000 | 173.0000 | 16.1000 | 0.000 |
| 687 | L687 | 1.0000 | –53.5000 | 51.8000 | 4.2000 | 0.000 |
| 690 | L690 | 0.9460 | –30.6000 | 0.0000 | 0.0000 | 0.000 |
| 693 | L693 | 0.9540 | –52.4000 | 197.0000 | 18.4000 | 0.000 |
| 695 | L695 | 0.9840 | –7.7000 | 70.4000 | 6.3000 | 0.000 |
| 698 | L698 | 0.9740 | –52.9000 | 0.0000 | 0.0000 | 0.000 |
| 701 | L701 | 0.9960 | –15.8000 | 0.0000 | 0.0000 | 0.000 |
| 702 | L702 | 0.9800 | –8.4000 | 136.5000 | 11.9000 | 0.000 |
| 711 | L711 | 0.9410 | –56.9000 | 168.0000 | 14.7000 | 0.000 |
| 717 | L717 | 0.9960 | –5.1000 | 0.0000 | 0.0000 | 0.000 |
| 926 | L926 | 1.0260 | –5.6000 | 0.0000 | 0.0000 | 0.000 |
| 929 | L929 | 1.0320 | –5.3000 | 0.0000 | 0.0000 | 0.000 |
| 946 | L946 | 1.0240 | –5.7000 | 0.0000 | 0.0000 | 0.000 |

## TABLE 1.2 (continued)
## Table of Generator Reactive Components and Reactive Characteristics

| Node no. | Name | Generator reactive component | Generator reactive Char. - S |
|---|---|---|---|
| 1 | G001 | 0.0000 | –1.0783 |
| 150 | G150 | 0.0000 | 0.0000 |
| 156 | G156 | 0.0000 | 0.6559 |
| 157 | G157 | 0.0000 | 0.0040 |
| 161 | G161 | 0.0000 | 0.0000 |
| 164 | G164 | 0.0000 | –0.0336 |
| 172 | G172 | 0.0000 | 0.0032 |
| 174 | G174 | 0.0000 | –0.0944 |
| 182 | G182 | 0.0000 | 0.0000 |
| 183 | G183 | 0.0000 | –0.8955 |
| 285 | G285 | 0.0000 | –0.1378 |
| 291 | G291 | 0.0000 | 0.2902 |
| 301 | G301 | 0.0000 | 1.4750 |
| 315 | G315 | 0.0000 | 0.0000 |
| 316 | G316 | 0.0000 | 0.0000 |
| 327 | G327 | 0.0000 | 3.7037 |
| 332 | G332 | 0.0000 | 0.0000 |
| 336 | G336 | 0.0000 | 0.0000 |
| 339 | G339 | 0.0000 | 0.4098 |
| 343 | G343 | 0.0000 | 0.0000 |
| 357 | G357 | 0.0000 | 0.5607 |
| 359 | G359 | 0.0000 | 0.0000 |
| 365 | G365 | 0.0000 | –1.3115 |
| 371 | G371 | 0.0000 | 0.2009 |
| 372 | G372 | 0.0000 | 0.0000 |
| 390 | G390 | 0.0000 | 0.3987 |
| 391 | G391 | 0.0000 | 0.4776 |
| 427 | G427 | 0.0000 | 0.0281 |
| 450 | G450 | 0.0000 | –0.1443 |
| 685 | G685 | 0.0000 | 1.2908 |
| 687 | G687 | 0.0000 | 1.2994 |
| 693 | G693 | 0.0000 | 0.0000 |

Reprinted from Energy Utilization of PSE&G for the Middle Atlantic Power Research Committee, Newark, NJ, 1976. With permission.

## TABLE 1.3
## New Off-Nominal Setting(s) for TCUL Transformers (100%)

| Bus no. from | Bus no. to | PBI | Transformer tap |
|---|---|---|---|
| 2 | 295 | 0 | 0.925000 |
| 179 | 180 | 0 | 0.994000 |
| 283 | 282 | 0 | 1.000000 |
| 286 | 288 | 0 | 0.944000 |
| 287 | 288 | 0 | 0.931000 |
| 298 | 299 | 0 | 0.962000 |
| 304 | 305 | 0 | 1.050000 |
| 309 | 336 | 0 | 1.037000 |
| 327 | 332 | 0 | 1.062000 |
| 328 | 332 | 0 | 1.044000 |

**TABLE 1.3 (continued)**
**New Off-Nominal Setting(s) for TCUL Transformers (100%)**

| Bus no. from | Bus no. to | PBI | Transformer tap |
|---|---|---|---|
| 339 | 365 | 0 | 1.000000 |
| 378 | 426 | 0 | 1.006000 |
| 385 | 386 | 0 | 1.000000 |
| 390 | 391 | 0 | 1.031000 |
| 416 | 425 | 0 | 0.969000 |
| 701 | 702 | 0 | 1.050000 |

*Note:* Load flow calculations 100% loading for centralized system.

## Table of Generator Data Sorted by Node Number

| Node no. | Name | Generator voltage | Generator angle | Generator P (MW) | Generator Q (Mvar) |
|---|---|---|---|---|---|
| 1 | G001 | 1.0000 | 0.0000 | 2546.3000 | −183.8000 |
| 150 | G150 | 1.0270 | −19.9000 | 0.0000 | 0.0000 |
| 156 | G156 | 1.0300 | −28.8000 | 147.0000 | 50.7000 |
| 157 | G157 | 1.0250 | −11.4000 | 126.0000 | 50.4000 |
| 161 | G161 | 1.0240 | −14.6000 | 160.0000 | 64.0000 |
| 164 | G164 | 1.0300 | −21.1000 | 330.0000 | 90.9000 |
| 172 | G172 | 1.0300 | −14.0000 | 623.0000 | 35.6000 |
| 174 | G174 | 1.0290 | −19.5000 | 661.0000 | 264.0000 |
| 182 | G182 | 1.0300 | −19.3000 | 216.0000 | −170.0000 |
| 183 | G183 | 1.0310 | −19.4000 | 400.0000 | −200.0000 |
| 285 | G285 | 1.0300 | −22.2000 | 270.0000 | 122.1000 |
| 291 | G291 | 1.0300 | −27.4000 | 58.0000 | 312.7000 |
| 301 | G301 | 1.0000 | −28.6000 | 1.0000 | 99.8000 |
| 315 | G315 | 1.0300 | −14.5000 | 160.0000 | 181.6000 |
| 316 | G316 | 1.0300 | −14.4000 | 320.0000 | 54.7000 |
| 327 | G327 | 1.0300 | −21.6000 | 68.0000 | 27.2000 |
| 332 | G332 | 1.0000 | −20.3000 | 100.0000 | −50.0000 |
| 336 | G336 | 0.9850 | −22.3000 | 20.0000 | 100.0000 |
| 339 | G339 | 1.0270 | −19.7000 | 1143.0000 | 457.2000 |
| 343 | G343 | 1.0280 | −23.0000 | 171.0000 | 68.4000 |
| 357 | G357 | 1.0160 | −20.1000 | 655.0000 | 500.0000 |
| 359 | G359 | 1.0270 | −16.4000 | 200.0000 | 200.0000 |
| 365 | G365 | 1.0290 | −23.1000 | 120.0000 | 200.0000 |
| 371 | G371 | 1.0300 | −16.0000 | 638.0000 | 170.9000 |
| 372 | G372 | 1.0200 | −17.7000 | 140.0000 | 62.5000 |
| 390 | G390 | 1.0300 | −15.1000 | 594.0000 | 128.4000 |
| 391 | G391 | 1.0200 | −14.2000 | 1000.0000 | 116.7000 |
| 427 | G427 | 1.0300 | −7.8000 | 1103.0000 | 328.0000 |
| 450 | G450 | 1.0300 | −3.3000 | 1065.0000 | −77.4000 |
| 685 | G685 | 1.0000 | −63.8000 | 321.0000 | 204.7000 |
| 687 | G687 | 1.0000 | −81.2000 | 160.0000 | 107.3000 |
| 693 | G693 | 1.0000 | −79.7000 | 60.0000 | 271.0000 |

## Table of Load Data Sorted by Node Number

| Node no. | Name | Load bus voltage | Load bus angle | Load P (MW) | Load Q (Mvar) | Sync. cond. Q (Mvar) |
|---|---|---|---|---|---|---|
| 1 | L001 | 1.0000 | 0.0000 | 0.0000 | 0.0000 | 0.000 |
| 2 | L002 | 0.9970 | −10.5000 | 0.0000 | 0.0000 | 0.000 |

**TABLE 1.3 (continued)**
**Table of Load Data Sorted by Node Number**

| Node no. | Name | Load bus voltage | Load bus angle | Load P (MW) | Load Q (Mvar) | Sync. cond. Q (Mvar) |
|---|---|---|---|---|---|---|
| 16 | L016 | 1.0130 | –7.7000 | 0.0000 | 0.0000 | 0.000 |
| 96 | L096 | 1.0250 | –29.1000 | 0.0000 | 0.0000 | 0.000 |
| 125 | L125 | 1.0110 | –30.2000 | 0.0000 | 0.0000 | 0.000 |
| 126 | L126 | 1.0260 | –21.5000 | 0.0000 | 0.0000 | 0.000 |
| 150 | L150 | 1.0270 | –19.9000 | 233.4000 | 5.8000 | 0.000 |
| 151 | L151 | 1.0070 | –30.6000 | 32.0000 | 3.8000 | 0.000 |
| 152 | L152 | 1.0040 | –30.4000 | 20.5000 | 1.7000 | 0.000 |
| 153 | L153 | 1.0090 | –19.8000 | 67.2000 | –11.6000 | 0.000 |
| 155 | L155 | 1.0310 | –19.5000 | 130.7000 | 19.8000 | 0.000 |
| 156 | L156 | 1.0300 | –28.8000 | 68.4000 | 10.9000 | 0.000 |
| 157 | L157 | 1.0250 | –11.4000 | 0.0000 | 0.0000 | 0.000 |
| 158 | L158 | 1.0080 | –22.1000 | 120.2000 | 18.4000 | 0.000 |
| 160 | L160 | 1.0170 | –29.7000 | 3.2000 | 0.6000 | 0.000 |
| 161 | L161 | 1.0240 | –14.6000 | 102.4000 | 5.4000 | 0.000 |
| 162 | L162 | 1.0040 | –23.5000 | 124.0000 | 21.5000 | 0.000 |
| 164 | L164 | 1.0300 | –21.1000 | 20.8000 | –1.7000 | 0.000 |
| 167 | L167 | 1.0210 | –18.9000 | 177.3000 | 21.8000 | 0.000 |
| 168 | L168 | 1.0240 | –16.5000 | 191.5000 | 26.6000 | 0.000 |
| 170 | L170 | 0.9960 | –24.5000 | 204.0000 | 47.4000 | 0.000 |
| 171 | L171 | 1.0110 | –30.0000 | 24.2000 | 16.8000 | 0.000 |
| 172 | L172 | 1.0300 | –14.0000 | 37.2000 | –3.8000 | 0.000 |
| 174 | L174 | 1.0290 | –19.5000 | 390.3999 | 68.9000 | 0.000 |
| 175 | L175 | 1.0030 | –22.9000 | 224.3000 | 50.8000 | 0.000 |
| 177 | L177 | 0.9970 | –30.2000 | 66.0000 | 2.9000 | 0.000 |
| 178 | L178 | 1.0070 | –23.7000 | 52.6000 | 2.7000 | 0.000 |
| 179 | L179 | 0.9970 | –25.5000 | 0.0000 | 0.0000 | 0.000 |
| 180 | L180 | 1.0010 | –23.3000 | 241.8000 | 63.8000 | 0.000 |
| 181 | L181 | 1.0290 | –19.4000 | 30.0000 | 18.0000 | 0.000 |
| 182 | L182 | 1.0300 | –19.3000 | 0.0000 | 0.0000 | 0.000 |
| 183 | L183 | 1.0310 | –19.4000 | 0.0000 | 0.0000 | 0.000 |
| 184 | L184 | 1.0310 | –19.6000 | 119.2000 | 6.8000 | 0.000 |
| 185 | L185 | 1.0300 | –19.8000 | 149.6000 | 46.0000 | 0.000 |
| 186 | L186 | 1.0260 | –20.3000 | 74.6000 | 12.5000 | 0.000 |
| 187 | L187 | 1.0180 | –18.4000 | 92.0000 | 10.6000 | 0.000 |
| 188 | L188 | 1.0170 | –22.9000 | 51.7000 | –5.8000 | 0.000 |
| 189 | L189 | 1.0170 | –23.0000 | 52.4000 | –2.2000 | 0.000 |
| 190 | L190 | 1.0280 | –14.5000 | 61.8000 | 12.9000 | 0.000 |
| 191 | L191 | 1.0080 | –23.6000 | 21.2000 | 4.7000 | 0.000 |
| 192 | L192 | 0.9960 | –30.7000 | 25.9000 | 6.5000 | 0.000 |
| 202 | L202 | 1.0300 | –21.1000 | 0.0000 | 0.0000 | 0.000 |
| 227 | L227 | 1.0110 | –5.4000 | 0.0000 | 0.0000 | 0.000 |
| 231 | L231 | 1.0010 | –20.3000 | 0.0000 | 0.0000 | 0.000 |
| 280 | L280 | 1.0120 | –15.0000 | 53.0000 | 16.9000 | 0.000 |
| 281 | L281 | 1.0090 | –18.8000 | 227.0000 | 37.6000 | 0.000 |
| 282 | L282 | 0.9920 | –25.1000 | 89.0000 | 33.0000 | 0.000 |
| 283 | L283 | 0.9960 | –28.2000 | 213.0000 | 73.5000 | 0.000 |
| 285 | L285 | 1.0300 | –22.2000 | 152.0000 | 60.0000 | 0.000 |
| 286 | L286 | 1.0020 | –20.4000 | 91.0000 | 84.5000 | 0.000 |
| 287 | L287 | 1.0010 | –19.7000 | 91.0000 | 84.5000 | 0.000 |
| 288 | L288 | 1.0330 | –17.0000 | 0.0000 | 0.0000 | 0.000 |
| 289 | L289 | 0.9860 | –21.9000 | 58.0000 | 10.7000 | 0.000 |
| 290 | L290 | 0.9840 | –25.4000 | 167.0000 | 129.0000 | 0.000 |
| 291 | L291 | 1.0300 | –27.4000 | 327.0000 | 10.6000 | 0.000 |
| 295 | L295 | 1.0370 | –14.7000 | 0.0000 | 0.0000 | 0.000 |

**Table 1.3 (continued)**
**Table of Load Data Sorted by Node Number**

| Node no. | Name | Load bus voltage | Load bus angle | Load P (MW) | Load Q (Mvar) | Sync. cond. Q (Mvar) |
|---|---|---|---|---|---|---|
| 296 | L296 | 1.0140 | −19.3000 | 217.0000 | 109.9000 | 0.000 |
| 297 | L297 | 1.0160 | −20.4000 | 0.0000 | 0.0000 | 0.000 |
| 298 | L298 | 1.0020 | −15.2000 | 0.0000 | 0.0000 | 0.000 |
| 299 | L299 | 1.0030 | −14.9000 | 255.0000 | 121.1000 | 0.000 |
| 301 | L301 | 1.0000 | −28.6000 | 168.0000 | 62.3000 | 0.000 |
| 303 | L303 | 0.9790 | −21.8000 | 0.0000 | 0.0000 | 0.000 |
| 304 | L304 | 0.9980 | −29.2000 | 242.0000 | 29.7000 | 0.000 |
| 305 | L305 | 0.9660 | −24.1000 | 0.0000 | 0.0000 | 0.000 |
| 306 | L306 | 0.9940 | −24.6000 | 179.0000 | 74.0000 | 0.000 |
| 308 | L308 | 0.9930 | −19.5000 | 0.0000 | 0.0000 | 0.000 |
| 309 | L309 | 0.9990 | −29.3000 | 134.0000 | 26.3000 | 0.000 |
| 311 | L311 | 1.0060 | −21.7000 | 0.0000 | 0.0000 | 0.000 |
| 312 | L312 | 0.9840 | −22.0000 | 48.0000 | 5.8000 | 0.000 |
| 313 | L313 | 1.0010 | −21.4000 | 104.0000 | 34.7000 | 0.000 |
| 314 | L314 | 0.9970 | −28.6000 | 207.0000 | 60.0000 | 0.000 |
| 315 | L315 | 1.0300 | −14.5000 | 0.0000 | 0.0000 | 0.000 |
| 316 | L316 | 1.0300 | −14.4000 | 0.0000 | 0.0000 | 0.000 |
| 327 | L327 | 1.0300 | −21.6000 | 146.0000 | 60.0000 | 0.000 |
| 328 | L328 | 1.0000 | −23.6000 | 299.0000 | 148.0000 | 0.000 |
| 332 | L332 | 1.0000 | −20.3000 | 0.0000 | 0.0000 | 0.000 |
| 333 | L333 | 0.9950 | −29.0000 | 338.0000 | 86.0000 | 0.000 |
| 334 | L334 | 0.9990 | −24.6000 | 70.0000 | 8.8000 | 0.000 |
| 336 | L336 | 0.9850 | −22.3000 | 257.0000 | 37.9000 | 0.000 |
| 337 | L337 | 1.0070 | −23.3000 | 54.0000 | 15.0000 | 0.000 |
| 339 | L339 | 1.0270 | −19.7000 | 0.0000 | 0.0000 | 0.000 |
| 340 | L340 | 1.0260 | −25.4000 | 124.0000 | 51.0000 | 0.000 |
| 343 | L343 | 1.0280 | −23.0000 | 0.1000 | 0.0000 | 0.000 |
| 345 | L345 | 1.0230 | −16.7000 | 109.0000 | 18.4000 | 0.000 |
| 347 | L347 | 1.0240 | −15.4000 | 136.0000 | 50.6000 | 0.000 |
| 349 | L349 | 0.9940 | −21.8000 | 58.0000 | 20.0000 | 0.000 |
| 351 | L351 | 1.0190 | −17.5000 | 199.0000 | 49.6000 | 0.000 |
| 352 | L352 | 1.0280 | −27.5000 | 57.0000 | 44.0000 | 0.000 |
| 353 | L353 | 1.0130 | −22.6000 | 165.0000 | 39.0000 | 0.000 |
| 354 | L354 | 0.9960 | −29.6000 | 177.0000 | 30.8000 | 0.000 |
| 357 | L357 | 1.0160 | −20.1000 | 265.0000 | 163.4000 | 0.000 |
| 359 | L359 | 1.0270 | −16.4000 | 0.0000 | 0.0000 | 0.000 |
| 360 | L360 | 1.0170 | −20.4000 | 56.0000 | 21.6000 | 0.000 |
| 362 | L362 | 0.9970 | −19.7000 | 36.0000 | 3.9000 | 0.000 |
| 365 | L365 | 1.0290 | −23.1000 | 389.0000 | 133.0000 | 0.000 |
| 366 | L366 | 0.9940 | −19.1000 | 122.0000 | 22.4000 | 0.000 |
| 368 | L368 | 1.0290 | −14.6000 | 56.0000 | 19.8000 | 0.000 |
| 371 | L371 | 1.0300 | −16.0000 | 0.0000 | 0.0000 | 0.000 |
| 372 | L372 | 1.0200 | −17.7000 | 0.0000 | 0.0000 | 0.000 |
| 373 | L373 | 1.0230 | −15.3000 | 208.0000 | 101.4000 | 0.000 |
| 375 | L375 | 1.0230 | −15.3000 | 28.0000 | 9.9000 | 0.000 |
| 376 | L376 | 1.0220 | −15.9000 | 28.0000 | 9.9000 | 0.000 |
| 377 | L377 | 0.9990 | −20.2000 | 94.0000 | 33.4000 | 0.000 |
| 378 | L378 | 1.0000 | −16.9000 | 0.0000 | 0.0000 | 0.000 |
| 379 | L379 | 1.0080 | −23.1000 | 63.0000 | 25.0000 | 0.000 |
| 380 | L380 | 1.0010 | −21.9000 | 213.0000 | 115.0000 | 0.000 |
| 381 | L381 | 1.0240 | −21.4000 | 55.0000 | 19.7000 | 0.000 |
| 382 | L382 | 1.0230 | −16.2000 | 0.0000 | 0.0000 | 0.000 |

**Table 1.3 (continued)**
**Table of Load Data Sorted by Node Number**

| Node no. | Name | Load bus voltage | Load bus angle | Load P (MW) | Load Q (Mvar) | Sync. cond. Q (Mvar) |
|---|---|---|---|---|---|---|
| 383 | L383 | 1.0050 | –17.6000 | 54.0000 | 6.3000 | 0.000 |
| 385 | L385 | 0.9960 | –21.9000 | 0.0000 | 0.0000 | 0.000 |
| 386 | L386 | 0.9990 | –23.7000 | 0.0000 | 0.0000 | 0.000 |
| 388 | L388 | 1.0010 | –28.9000 | 0.0000 | 0.0000 | 0.000 |
| 389 | L389 | 0.9930 | –25.1000 | 140.0000 | 41.0000 | 0.000 |
| 390 | L390 | 1.0300 | –15.1000 | 326.0000 | 71.3000 | 0.000 |
| 391 | L391 | 1.0200 | –14.2000 | 0.0000 | 0.0000 | 0.000 |
| 401 | L401 | 1.0180 | –18.2000 | 48.0000 | 15.5000 | 0.000 |
| 402 | L402 | 1.0030 | –19.8000 | 61.0000 | 21.0000 | 0.000 |
| 403 | L403 | 1.0080 | –19.5000 | 233.0000 | 74.9000 | 0.000 |
| 404 | L404 | 0.9944 | –21.6000 | 224.0000 | 48.0000 | 0.000 |
| 405 | L405 | 1.0050 | –23.0000 | 215.0000 | 3.0000 | 0.000 |
| 406 | L406 | 1.0080 | –23.7000 | 184.0000 | 59.1000 | 0.000 |
| 409 | L409 | 0.9970 | –19.3000 | 0.0000 | 0.0000 | 0.000 |
| 410 | L410 | 1.0010 | –20.3000 | 55.0000 | 26.0000 | 0.000 |
| 411 | L411 | 1.0030 | –20.0000 | 19.0000 | 3.0000 | 0.000 |
| 412 | L412 | 0.9960 | –24.3000 | 22.0000 | 4.0000 | 0.000 |
| 413 | L413 | 1.0020 | –23.5000 | 46.0000 | 14.0000 | 0.000 |
| 414 | L414 | 0.9940 | –23.0000 | 67.0000 | 21.5000 | 0.000 |
| 415 | L415 | 0.9850 | –25.3000 | 67.0000 | 21.5000 | 0.000 |
| 416 | L416 | 0.9980 | –14.1000 | 0.0000 | 0.0000 | 0.000 |
| 417 | L417 | 1.0040 | –14.3000 | 37.0000 | 10.3000 | 0.000 |
| 418 | L418 | 1.0230 | –20.0000 | 49.0000 | 19.8000 | 0.000 |
| 419 | L419 | 1.0100 | –21.7000 | 15.0000 | 5.6000 | 0.000 |
| 420 | L420 | 1.0240 | –15.9000 | 7.0000 | 1.4000 | 0.000 |
| 421 | L421 | 1.0170 | –15.1000 | 7.0000 | 1.4000 | 0.000 |
| 422 | L422 | 1.0030 | –17.8000 | 63.0000 | 18.3000 | 0.000 |
| 423 | L423 | 1.0170 | –17.6000 | 41.0000 | 13.1000 | 0.000 |
| 424 | L424 | 0.9990 | –26.7000 | 34.0000 | 4.8000 | 0.000 |
| 425 | L425 | 1.0110 | –12.0000 | 0.0000 | 0.0000 | 0.000 |
| 426 | L426 | 1.0140 | –11.9000 | 0.0000 | 0.0000 | 0.000 |
| 427 | L427 | 1.0300 | –7.8000 | 0.0000 | 0.0000 | 0.000 |
| 428 | L428 | 1.0280 | –6.7000 | 0.0000 | 0.0000 | 0.000 |
| 429 | L429 | 0.9880 | –18.1000 | 0.0000 | 0.0000 | 0.000 |
| 446 | L446 | 1.0000 | –19.1000 | 0.0000 | 0.0000 | 0.000 |
| 450 | L450 | 1.0300 | –3.3000 | 0.0000 | 0.0000 | 0.000 |
| 501 | L501 | 0.9670 | –23.8000 | 0.0000 | 0.0000 | 0.000 |
| 518 | L518 | 1.0180 | –17.8000 | 0.0000 | 0.0000 | 0.000 |
| 683 | L683 | 0.9770 | –83.0000 | 144.0000 | 13.0000 | 0.000 |
| 685 | L685 | 1.0000 | –63.8000 | 245.0000 | 23.0000 | 0.000 |
| 687 | L687 | 1.0000 | –81.2000 | 73.0000 | 6.0000 | 0.000 |
| 690 | L690 | 0.9360 | –49.1000 | 0.0000 | 0.0000 | 0.000 |
| 693 | L693 | 1.0000 | –79.7000 | 281.0000 | 26.0000 | 0.000 |
| 695 | L695 | 0.9810 | –21.1000 | 102.0000 | 9.0000 | 0.000 |
| 698 | L698 | 1.0000 | –80.3000 | 0.0000 | 0.0000 | 0.000 |
| 701 | L701 | 1.0020 | –31.1000 | 0.0000 | 0.0000 | 0.000 |
| 702 | L702 | 0.9740 | –21.9000 | 195.0000 | 17.0000 | 0.000 |
| 711 | L711 | 0.8960 | –83.3000 | 240.0000 | 21.0000 | 0.000 |
| 717 | L717 | 0.9970 | –18.0000 | 0.0000 | 0.0000 | 0.000 |
| 926 | L926 | 1.0200 | –17.8000 | 0.0000 | 0.0000 | 0.000 |
| 929 | L929 | 1.0270 | –16.4000 | 0.0000 | 0.0000 | 0.000 |
| 946 | L946 | 1.0060 | –16.8000 | 0.0000 | 0.0000 | 0.000 |

**Table 1.3 (continued)**
**Table of Generator Reactive Components and Reactive Characteristics**

| Node no. | Name | Generator reactive component | Generator reactive Char. - S |
|---|---|---|---|
| 1 | G001 | 0.0000 | –0.0722 |
| 150 | G150 | 0.0000 | –0.1172 |
| 156 | G156 | 0.0000 | 0.3449 |
| 157 | G157 | 0.0000 | 0.4000 |
| 161 | G161 | 0.0000 | 0.4000 |
| 164 | G164 | 0.0000 | 0.2755 |
| 172 | G172 | 0.0000 | 0.0571 |
| 174 | G174 | 0.0000 | 0.3994 |
| 182 | G182 | 0.0000 | –0.7870 |
| 183 | G183 | 0.0000 | –0.5000 |
| 285 | G285 | 0.0000 | 0.4522 |
| 291 | G291 | 0.0000 | 5.3914 |
| 301 | G301 | 0.0000 | –0.1172 |
| 315 | G315 | 0.0000 | 1.1350 |
| 316 | G316 | 0.0000 | 0.1709 |
| 327 | G327 | 0.0000 | 0.4000 |
| 332 | G332 | 0.0000 | –0.5000 |
| 336 | G336 | 0.0000 | 5.0000 |
| 339 | G339 | 0.0000 | 0.4000 |
| 343 | G343 | 0.0000 | 0.4000 |
| 357 | G357 | 0.0000 | 0.7634 |
| 359 | G359 | 0.0000 | 1.0000 |
| 365 | G365 | 0.0000 | 1.6667 |
| 371 | G371 | 0.0000 | 0.2679 |
| 372 | G372 | 0.0000 | 0.4464 |
| 390 | G390 | 0.0000 | 0.2162 |
| 391 | G391 | 0.0000 | 0.1167 |
| 427 | G427 | 0.0000 | 0.2974 |
| 450 | G450 | 0.0000 | –0.0727 |
| 685 | G685 | 0.0000 | 0.6377 |
| 687 | G687 | 0.0000 | 0.6706 |
| 693 | G693 | 0.0000 | 4.5167 |

Reprinted from Energy Utilization of PSE&G for the Middle Atlantic Power Research Committee, Newark, NJ, 1976. With permission.

**TABLE 1.4**
**New Off-Nominal Setting(s) for TCUL Transformers (70%)**

| Bus no. from | Bus no. to | PBI | Transformer tap |
|---|---|---|---|
| 2 | 295 | 0 | 0.906000 |
| 179 | 180 | 0 | 0.962000 |
| 283 | 282 | 0 | 0.969000 |
| 286 | 288 | 0 | 0.931000 |
| 287 | 288 | 0 | 0.931000 |
| 298 | 299 | 0 | 0.975000 |
| 304 | 305 | 0 | 1.012000 |
| 309 | 336 | 0 | 1.000000 |
| 327 | 332 | 0 | 1.019000 |
| 328 | 332 | 0 | 1.006000 |
| 339 | 365 | 0 | 0.925000 |

## TABLE 1.4 (continued)
## New Off-Nominal Setting(s) for TCUL Transformers (70%)

| Bus no. from | Bus no. to | PBI | Transformer tap |
|---|---|---|---|
| 378 | 426 | 0 | 0.956000 |
| 385 | 386 | 0 | 0.925000 |
| 390 | 391 | 0 | 1.006000 |
| 416 | 425 | 0 | 0.950000 |
| 701 | 702 | 0 | 0.981000 |

*Note:* Load flow calculations 70% loading for dispersed system.

## Table of Generator Data Sorted by Node Number

| Node no. | Name | Generator voltage | Generator angle | Generator P (MW) | Generator Q (Mvar) |
|---|---|---|---|---|---|
| 1 | G001 | 1.0000 | 0.0000 | 1164.2000 | –642.2000 |
| 151 | G151 | 1.0090 | –11.1000 | 22.4000 | 0.0000 |
| 153 | G153 | 1.0200 | –5.9000 | 12.3000 | 0.0000 |
| 155 | G155 | 1.0340 | –5.6000 | 33.5000 | 0.0000 |
| 156 | G156 | 1.0200 | –11.3000 | 53.4000 | 32.5000 |
| 157 | G157 | 1.0380 | –4.1000 | 0.0000 | 0.6000 |
| 158 | G158 | 1.0310 | –6.7000 | 16.2000 | 0.0000 |
| 161 | G161 | 1.0370 | –5.2000 | 38.4000 | 0.0000 |
| 162 | G162 | 1.0320 | –6.4000 | 2.2000 | 0.0000 |
| 164 | G164 | 1.0300 | –2.8000 | 330.0000 | –57.0000 |
| 167 | G167 | 1.0270 | –3.1000 | 32.4000 | 0.0000 |
| 168 | G168 | 1.0270 | 0.1000 | 52.0000 | 0.0000 |
| 170 | G170 | 1.0300 | –6.6000 | 49.5000 | 0.0000 |
| 172 | G172 | 1.0300 | 2.7000 | 630.7000 | –4.1000 |
| 174 | G174 | 1.0300 | –5.8000 | 320.0000 | –106.4000 |
| 175 | G175 | 1.0310 | –6.8000 | 54.6000 | 0.0000 |
| 177 | G177 | 1.0030 | –10.2000 | 26.1000 | 0.0000 |
| 178 | G178 | 1.0320 | –6.0000 | 10.5000 | 0.0000 |
| 180 | G180 | 1.0340 | –6.7000 | 70.7000 | 0.0000 |
| 181 | G181 | 1.0320 | –5.7000 | 21.0000 | 0.0000 |
| 182 | G182 | 1.0350 | –5.7000 | 0.0000 | 0.0000 |
| 183 | G183 | 1.0350 | –5.6000 | 0.0000 | –300.0000 |
| 184 | G184 | 1.0360 | –5.5000 | 83.5000 | 0.0000 |
| 185 | G185 | 1.0350 | –5.5000 | 105.0000 | 0.0000 |
| 186 | G186 | 1.0320 | –5.2000 | 52.1000 | 0.0000 |
| 187 | G187 | 1.0280 | –3.2000 | 64.4000 | 0.0000 |
| 188 | G188 | 1.0310 | –4.3000 | 36.2000 | 0.0000 |
| 189 | G189 | 1.0320 | –4.6000 | 36.6000 | 0.0000 |
| 190 | G190 | 1.0530 | –4.5000 | 43.2000 | 0.0000 |
| 191 | G191 | 1.0320 | –5.8000 | 14.8000 | 0.0000 |
| 192 | G192 | 1.0040 | –10.4000 | 18.1000 | 0.0000 |
| 280 | G280 | 1.0300 | –5.4000 | 12.8000 | 0.0000 |
| 281 | G281 | 1.0260 | –5.9000 | 31.2000 | 0.0000 |
| 282 | G282 | 1.0290 | –7.0000 | 27.5000 | 0.0000 |
| 285 | G285 | 1.0300 | –5.9000 | 0.0000 | –41.8000 |
| 291 | G291 | 1.0300 | –5.3000 | 588.0000 | 115.2000 |
| 296 | G296 | 1.0400 | –6.3000 | 26.8000 | 0.0000 |
| 299 | G299 | 1.0150 | –5.4000 | 30.8000 | 0.0000 |
| 301 | G301 | 1.0000 | –9.4000 | 173.0000 | 25.6000 |
| 304 | G304 | 1.0010 | –11.6000 | 33.2000 | 0.0000 |
| 306 | G306 | 1.0310 | –6.8000 | 91.1000 | 0.0000 |

**TABLE 1.4 (continued)**
**Table of Generator Data Sorted by Node Number**

| Node no. | Name | Generator voltage | Generator angle | Generator P (MW) | Generator Q (Mvar) |
|---|---|---|---|---|---|
| 309 | G309 | 1.0010 | –11.7000 | 40.0000 | 0.0000 |
| 312 | G312 | 1.0100 | –11.1000 | 15.8000 | 0.0000 |
| 313 | G313 | 1.0050 | –6.3000 | 26.8000 | 0.0000 |
| 314 | G314 | 1.0050 | –7.9000 | 46.4000 | 0.0000 |
| 315 | G315 | 1.0120 | –5.3000 | 0.0000 | 0.0000 |
| 316 | G316 | 1.0120 | –5.3000 | 0.0000 | 0.0000 |
| 327 | G327 | 1.0300 | –6.5000 | 24.0000 | 70.2000 |
| 328 | G328 | 1.0040 | –7.3000 | 3.5000 | 0.0000 |
| 332 | G332 | 1.0220 | –5.5000 | 0.0000 | 0.0000 |
| 334 | G334 | 1.0040 | –7.6000 | 8.9000 | 0.0000 |
| 336 | G336 | 1.0080 | –11.3000 | 0.0000 | 0.0000 |
| 339 | G339 | 1.0240 | –4.3000 | 860.0000 | 400.0000 |
| 340 | G340 | 1.0330 | –5.7000 | 1.3000 | 0.0000 |
| 343 | G343 | 1.0380 | –5.9000 | 61.0000 | 0.0000 |
| 345 | G345 | 1.0260 | –2.2000 | 40.6000 | 0.0000 |
| 347 | G347 | 1.0220 | –4.8000 | 34.8000 | 0.0000 |
| 349 | G349 | 1.0090 | –6.8000 | 1.3000 | 0.0000 |
| 351 | G351 | 1.0290 | –3.3000 | 50.5000 | 0.0000 |
| 352 | G352 | 1.0290 | –5.2000 | 65.0000 | 0.0000 |
| 353 | G353 | 1.0290 | –5.8000 | 52.6000 | 0.0000 |
| 354 | G354 | 0.9980 | –10.9000 | 6.3000 | 0.0000 |
| 357 | G357 | 1.0150 | –5.2000 | 562.8000 | 300.0000 |
| 359 | G359 | 1.0420 | –5.1000 | 0.0000 | 0.0000 |
| 360 | G360 | 1.0320 | –6.3000 | 6.4000 | 0.0000 |
| 362 | G362 | 1.0120 | –7.8000 | 18.7000 | 0.0000 |
| 365 | G365 | 1.0390 | –5.9000 | 112.0000 | –80.0000 |
| 366 | G366 | 1.0110 | –8.5000 | 3.5000 | 0.0000 |
| 371 | G371 | 1.0300 | –1.5000 | 638.0000 | 81.0000 |
| 372 | G372 | 1.0110 | –6.1000 | 0.0000 | 0.0000 |
| 373 | G373 | 1.0160 | –5.2000 | 27.4000 | 0.0000 |
| 375 | G375 | 1.0430 | –4.7000 | 1.2000 | 0.0000 |
| 376 | G376 | 1.0380 | –5.0000 | 1.2000 | 0.0000 |
| 377 | G377 | 1.0120 | –6.2000 | 7.7000 | 0.0000 |
| 380 | G380 | 1.0060 | –6.5000 | 18.8000 | 0.0000 |
| 381 | G381 | 1.0240 | –5.7000 | 16.8000 | 0.0000 |
| 389 | G389 | 1.0290 | –6.9000 | 66.0000 | 0.0000 |
| 390 | G390 | 1.0320 | –4.2000 | 573.0000 | 181.0000 |
| 391 | G391 | 1.0450 | –4.3000 | 344.0000 | 320.0000 |
| 401 | G401 | 1.0470 | –6.0000 | 4.2000 | 0.0000 |
| 402 | G402 | 1.0230 | –6.1000 | 17.1000 | 0.0000 |
| 404 | G404 | 1.0110 | –6.8000 | 26.6000 | 0.0000 |
| 405 | G405 | 1.0370 | –6.3000 | 151.5000 | 0.0000 |
| 406 | G406 | 1.0210 | –6.7000 | 51.2000 | 0.0000 |
| 410 | G410 | 1.0230 | –5.8000 | 38.4000 | 0.0000 |
| 411 | G411 | 1.0230 | –6.0000 | 13.3000 | 0.0000 |
| 412 | G412 | 1.0320 | –6.7000 | 15.4000 | 0.0000 |
| 413 | G413 | 1.0360 | –6.4000 | 32.2000 | 0.0000 |
| 414 | G414 | 1.0250 | –6.3000 | 46.9000 | 0.0000 |
| 415 | G415 | 1.0200 | –7.0000 | 46.9000 | 0.0000 |
| 417 | G417 | 1.0210 | –4.8000 | 25.8000 | 0.0000 |
| 418 | G418 | 1.0310 | –6.0000 | 34.2000 | 0.0000 |
| 419 | G419 | 1.0320 | –6.6000 | 10.5000 | 0.0000 |
| 420 | G420 | 1.0400 | –4.9000 | 4.9000 | 0.0000 |
| 421 | G421 | 1.0420 | –4.5000 | 4.9000 | 0.0000 |
| 422 | G422 | 1.0210 | –5.7000 | 44.0000 | 0.0000 |

## TABLE 1.4 (continued)
## Table of Generator Data Sorted by Node Number

| Node no. | Name | Generator voltage | Generator angle | Generator P (MW) | Generator Q (Mvar) |
|---|---|---|---|---|---|
| 423 | G423 | 1.0340 | –5.5000 | 28.6000 | 0.0000 |
| 424 | G424 | 1.0020 | –8.5000 | 23.8000 | 0.0000 |
| 427 | G427 | 1.0600 | –6.7000 | 0.0000 | –9.1000 |
| 450 | G450 | 1.0470 | –4.8000 | 0.0000 | –157.7000 |
| 683 | G683 | 0.9900 | –23.3000 | 27.2000 | 0.0000 |
| 685 | G685 | 1.0000 | –21.8000 | 177.2000 | 61.4000 |
| 687 | G687 | 1.0000 | –21.8000 | 299.0000 | 75.9000 |
| 693 | G693 | 0.9800 | –23.6000 | 0.0000 | 0.0000 |
| 695 | G695 | 1.0140 | –10.6000 | 19.2000 | 0.0000 |
| 702 | G702 | 1.0120 | –10.3000 | 36.8000 | 0.0000 |
| 711 | G711 | 0.9580 | –26.9000 | 45.2000 | 0.0000 |

## Table of Load Data Sorted by Node Number

| Node no. | Name | Load bus voltage | Load bus angle | Load P (MW) | Load Q (Mvar) | Sync. cond. Q (Mvar) |
|---|---|---|---|---|---|---|
| 1 | L001 | 1.0000 | 0.0000 | 0.0000 | 0.0000 | 0.000 |
| 2 | L002 | 1.0200 | –4.0000 | 0.0000 | 0.0000 | 0.000 |
| 16 | L016 | 1.0330 | –3.9000 | 0.0000 | 0.0000 | 0.000 |
| 96 | L096 | 1.0180 | –11.3000 | 0.0000 | 0.0000 | 0.000 |
| 125 | L125 | 1.0120 | –11.2000 | 0.0000 | 0.0000 | 0.000 |
| 126 | L126 | 1.0310 | –3.5000 | 0.0000 | 0.0000 | 0.000 |
| 150 | L150 | 1.0320 | –5.2000 | 163.0000 | 4.1000 | 0.000 |
| 151 | L151 | 1.0090 | –11.1000 | 22.4000 | 2.7000 | 0.000 |
| 152 | L152 | 1.0060 | –10.9000 | 14.3000 | 1.1000 | 0.000 |
| 153 | L153 | 1.0200 | –5.9000 | 47.0000 | –8.1000 | 0.000 |
| 155 | L155 | 1.0340 | –5.6000 | 91.0000 | 13.8000 | 0.000 |
| 156 | L156 | 1.0200 | –11.3000 | 48.0000 | 7.6000 | 0.000 |
| 157 | L157 | 1.0380 | –4.1000 | 0.0000 | 0.0000 | 0.000 |
| 158 | L158 | 1.0310 | –6.7000 | 84.0000 | 12.9000 | 0.000 |
| 160 | L160 | 1.0130 | –11.1000 | 2.1000 | 0.4000 | 0.000 |
| 161 | L161 | 1.0370 | –5.2000 | 71.0000 | 3.5000 | 0.000 |
| 162 | L162 | 1.0320 | –6.4000 | 87.5000 | 15.0000 | 0.000 |
| 164 | L164 | 1.0300 | –2.8000 | 14.5000 | –1.2000 | 0.000 |
| 167 | L167 | 1.0270 | –3.1000 | 12.4000 | 14.5000 | 0.000 |
| 168 | L168 | 1.0270 | 0.1000 | 134.0000 | 18.6000 | 0.000 |
| 170 | L170 | 1.0300 | –6.6000 | 143.0000 | 33.2000 | 0.000 |
| 171 | L171 | 1.0100 | –11.4000 | 17.0000 | 11.8000 | 0.000 |
| 172 | L172 | 1.0300 | 2.7000 | 26.0000 | –2.7000 | 0.000 |
| 174 | L174 | 1.0300 | –5.8000 | 273.0000 | 48.1000 | 0.000 |
| 175 | L175 | 1.0310 | –6.8000 | 157.0000 | 35.6000 | 0.000 |
| 177 | L177 | 1.0030 | –10.2000 | 46.1000 | 2.0000 | 0.000 |
| 178 | L178 | 1.0320 | –6.0000 | 36.9000 | 1.9000 | 0.000 |
| 179 | L179 | 0.9990 | –7.8000 | 0.0000 | 0.0000 | 0.000 |
| 180 | L180 | 1.0340 | –6.7000 | 169.0000 | 44.5000 | 0.000 |
| 181 | L181 | 1.0320 | –5.7000 | 21.0000 | 12.6000 | 0.000 |
| 182 | L182 | 1.0350 | –5.7000 | 0.0000 | 0.0000 | 0.000 |
| 183 | L183 | 1.0350 | –5.6000 | 0.0000 | 0.0000 | 0.000 |
| 184 | L184 | 1.0360 | –5.5000 | 83.5000 | 4.8000 | 0.000 |
| 185 | L185 | 1.0350 | –5.5000 | 104.0000 | 32.2000 | 0.000 |
| 186 | L186 | 1.0320 | –5.2000 | 52.2000 | 8.4000 | 0.000 |
| 187 | L187 | 1.0280 | –3.2000 | 64.4000 | 7.4000 | 0.000 |
| 188 | L188 | 1.0310 | –4.3000 | 36.2000 | –4.1000 | 0.000 |

**TABLE 1.4 (continued)**
**Table of Load Data Sorted by Node Number**

| Node no. | Name | Load bus voltage | Load bus angle | Load P (MW) | Load Q (Mvar) | Sync. cond. Q (Mvar) |
|---|---|---|---|---|---|---|
| 189 | L189 | 1.0320 | –4.6000 | 36.6000 | –1.5000 | 0.000 |
| 190 | L190 | 1.0530 | –4.5000 | 43.3000 | 9.1000 | 0.000 |
| 191 | L191 | 1.0320 | –5.8000 | 14.8000 | 3.3000 | 0.000 |
| 192 | L192 | 1.0040 | –10.4000 | 18.0000 | 4.6000 | 0.000 |
| 202 | L202 | 1.0300 | –2.9000 | 0.0000 | 0.0000 | 0.000 |
| 227 | L227 | 1.0210 | –2.1000 | 0.0000 | 0.0000 | 0.000 |
| 231 | L231 | 1.0230 | –5.5000 | 0.0000 | 0.0000 | 0.000 |
| 280 | L280 | 1.0300 | –5.4000 | 37.1000 | 11.8000 | 0.000 |
| 281 | L281 | 1.0260 | –5.9000 | 159.0000 | 26.3000 | 0.000 |
| 282 | L282 | 1.0290 | –7.0000 | 62.3000 | 23.1000 | 0.000 |
| 283 | L283 | 1.0030 | –8.0000 | 149.0000 | 51.5000 | 0.000 |
| 285 | L285 | 1.0300 | –5.9000 | 106.0000 | 42.0000 | 0.000 |
| 286 | L286 | 1.0040 | –5.8000 | 63.6000 | 59.0000 | 0.000 |
| 287 | L287 | 1.0040 | –5.4000 | 63.6000 | 59.0000 | 0.000 |
| 288 | L288 | 1.0480 | –5.2000 | 0.0000 | 0.0000 | 0.000 |
| 289 | L289 | 1.0080 | –11.1000 | 40.5000 | 7.4000 | 0.000 |
| 290 | L290 | 1.0200 | –7.1000 | 117.0000 | 90.3000 | 0.000 |
| 291 | L291 | 1.0300 | –5.3000 | 229.0000 | 74.2000 | 0.000 |
| 295 | L295 | 1.0700 | –5.0000 | 0.0000 | 0.0000 | 0.000 |
| 296 | L296 | 1.0400 | –6.3000 | 154.0000 | 76.3000 | 0.000 |
| 297 | L297 | 1.0330 | –6.3000 | 0.0000 | 0.0000 | 0.000 |
| 298 | L298 | 1.0030 | –5.4000 | 0.0000 | 0.0000 | 0.000 |
| 299 | L299 | 1.0150 | –5.4000 | 178.5000 | 147.0000 | 0.000 |
| 301 | L301 | 1.0000 | –9.4000 | 115.0000 | 43.0000 | 0.000 |
| 303 | L303 | 1.0060 | –9.2000 | 0.0000 | 0.0000 | 0.000 |
| 304 | L304 | 1.0010 | –11.6000 | 170.0000 | 20.8000 | 0.000 |
| 305 | L305 | 1.0000 | –10.0000 | 0.0000 | 0.0000 | 0.000 |
| 306 | L306 | 1.0310 | –6.8000 | 125.0000 | 51.8000 | 0.000 |
| 308 | L308 | 1.0110 | –8.4000 | 0.0000 | 0.0000 | 0.000 |
| 309 | L309 | 1.0010 | –11.7000 | 93.8000 | 18.6000 | 0.000 |
| 311 | L311 | 1.0090 | –6.4000 | 0.0000 | 0.0000 | 0.000 |
| 312 | L312 | 1.0100 | –11.1000 | 33.6000 | 4.1000 | 0.000 |
| 313 | L313 | 1.0050 | –6.3000 | 72.8000 | 24.3000 | 0.000 |
| 314 | L314 | 1.0050 | –7.9000 | 145.0000 | 42.0000 | 0.000 |
| 315 | L315 | 1.0120 | –5.3000 | 0.0000 | 0.0000 | 0.000 |
| 316 | L316 | 1.0120 | –5.3000 | 0.0000 | 0.0000 | 0.000 |
| 327 | L327 | 1.0300 | –6.5000 | 102.0000 | 42.0000 | 0.000 |
| 328 | L328 | 1.0040 | –7.3000 | 172.0000 | 103.8000 | 0.000 |
| 332 | L332 | 1.0220 | –5.5000 | 0.0000 | 0.0000 | 0.000 |
| 333 | L333 | 1.0040 | –8.3000 | 237.0000 | 60.2000 | 0.000 |
| 334 | L334 | 1.0040 | –7.6000 | 49.0000 | 6.2000 | 0.000 |
| 336 | L336 | 1.0080 | –11.3000 | 180.0000 | 26.5000 | 0.000 |
| 337 | L337 | 1.0340 | –6.3000 | 37.8000 | 10.5000 | 0.000 |
| 339 | L339 | 1.0240 | –4.3000 | 0.0000 | 0.0000 | 0.000 |
| 340 | L340 | 1.0330 | –5.7000 | 86.8000 | 35.7000 | 0.000 |
| 343 | L343 | 1.0380 | –5.9000 | 29.0000 | 0.0000 | 0.000 |
| 345 | L345 | 1.0260 | –2.2000 | 76.3000 | 12.9000 | 0.000 |
| 347 | L347 | 1.0220 | –4.8000 | 95.2000 | 35.4000 | 0.000 |
| 349 | L349 | 1.0090 | –6.8000 | 40.5000 | 14.0000 | 0.000 |
| 351 | L351 | 1.0290 | –3.3000 | 139.0000 | 34.6000 | 0.000 |
| 352 | L352 | 1.0290 | –5.2000 | 40.0000 | 30.8000 | 0.000 |
| 353 | L353 | 1.0290 | –5.8000 | 115.0000 | 27.2000 | 0.000 |
| 354 | L354 | 0.9980 | –10.9000 | 124.0000 | 21.6000 | 0.000 |
| 357 | L357 | 1.0150 | –5.2000 | 185.0000 | 114.0000 | 0.000 |
| 359 | L359 | 1.0420 | –5.1000 | 0.0000 | 0.0000 | 0.000 |

## TABLE 1.4 (continued)
## Table of Load Data Sorted by Node Number

| Node no. | Name | Load bus voltage | Load bus angle | Load P (MW) | Load Q (Mvar) | Sync. cond. Q (Mvar) |
|---|---|---|---|---|---|---|
| 360 | L360 | 1.0320 | –6.3000 | 39.2000 | 15.1000 | 0.000 |
| 362 | L362 | 1.0120 | –7.8000 | 25.2000 | 2.7000 | 0.000 |
| 365 | L365 | 1.0390 | –5.9000 | 272.0000 | 93.0000 | 0.000 |
| 366 | L366 | 1.0110 | –8.5000 | 85.4000 | 15.7000 | 0.000 |
| 368 | L368 | 1.0130 | –5.3000 | 39.2000 | 13.9000 | 0.000 |
| 371 | L371 | 1.0300 | –1.5000 | 0.0000 | 0.0000 | 0.000 |
| 372 | L372 | 1.0110 | –6.1000 | 0.0000 | 0.0000 | 0.000 |
| 373 | L373 | 1.0160 | –5.2000 | 145.5000 | 70.7000 | 0.000 |
| 375 | L375 | 1.0430 | –4.7000 | 19.6000 | 6.9000 | 0.000 |
| 376 | L376 | 1.0380 | –5.0000 | 19.6000 | 6.9000 | 0.000 |
| 377 | L377 | 1.0120 | –6.2000 | 65.8000 | 23.4000 | 0.000 |
| 378 | L378 | 1.0130 | –8.5000 | 0.0000 | 0.0000 | 0.000 |
| 379 | L379 | 1.0300 | –6.1000 | 44.1000 | 17.5000 | 0.000 |
| 380 | L380 | 1.0060 | –6.5000 | 149.0000 | 80.5000 | 0.000 |
| 381 | L381 | 1.0240 | –5.7000 | 38.5000 | 13.8000 | 0.000 |
| 382 | L382 | 1.0400 | –4.1000 | 0.0000 | 0.0000 | 0.000 |
| 383 | L383 | 1.0080 | –5.6000 | 37.8000 | 4.4000 | 0.000 |
| 385 | L385 | 1.0080 | –6.7000 | 0.0000 | 0.0000 | 0.000 |
| 386 | L386 | 1.0340 | –6.7000 | 0.0000 | 0.0000 | 0.000 |
| 388 | L388 | 1.0090 | –8.0000 | 0.0000 | 0.0000 | 0.000 |
| 389 | L389 | 1.0290 | –6.9000 | 98.0000 | 28.6000 | 0.000 |
| 390 | L390 | 1.0320 | –4.2000 | 228.0000 | 50.0000 | 0.000 |
| 391 | L391 | 1.0450 | –4.3000 | 0.0000 | 0.0000 | 0.000 |
| 401 | L401 | 1.0470 | –6.0000 | 33.6000 | 10.8000 | 0.000 |
| 402 | L402 | 1.0230 | –6.1000 | 42.6000 | 14.7000 | 0.000 |
| 403 | L403 | 1.0110 | –5.3000 | 163.0000 | 52.4000 | 0.000 |
| 404 | L404 | 1.0110 | –6.8000 | 157.0000 | 33.6000 | 0.000 |
| 405 | L405 | 1.0370 | –6.3000 | 150.0000 | 2.1000 | 0.000 |
| 406 | L406 | 1.0210 | –6.7000 | 129.0000 | 41.4000 | 0.000 |
| 409 | L409 | 1.0110 | –8.1000 | 0.0000 | 0.0000 | 0.000 |
| 410 | L410 | 1.0230 | –5.8000 | 38.5000 | 18.4000 | 0.000 |
| 411 | L411 | 1.0230 | –6.0000 | 13.3000 | 2.1000 | 0.000 |
| 412 | L412 | 1.0320 | –6.7000 | 15.4000 | 2.8000 | 0.000 |
| 413 | L413 | 1.0360 | –6.4000 | 32.2000 | 9.8000 | 0.000 |
| 414 | L414 | 1.0250 | –6.3000 | 46.9000 | 15.0000 | 0.000 |
| 415 | L415 | 1.0200 | –7.0000 | 46.9000 | 15.0000 | 0.000 |
| 416 | L416 | 1.0100 | –5.1000 | 0.0000 | 0.0000 | 0.000 |
| 417 | L417 | 1.0210 | –4.8000 | 25.9000 | 7.2000 | 0.000 |
| 418 | L418 | 1.0310 | –6.0000 | 34.3000 | 13.8000 | 0.000 |
| 419 | L419 | 1.0320 | –6.6000 | 10.5000 | 3.9000 | 0.000 |
| 420 | L420 | 1.0400 | –4.9000 | 4.9000 | 1.0000 | 0.000 |
| 421 | L421 | 1.0420 | –4.5000 | 4.9000 | 1.0000 | 0.000 |
| 422 | L422 | 1.0210 | –5.7000 | 44.0000 | 12.8000 | 0.000 |
| 423 | L423 | 1.0340 | –5.5000 | 28.7000 | 9.2000 | 0.000 |
| 424 | L424 | 1.0020 | –8.5000 | 23.8000 | 3.4000 | 0.000 |
| 425 | L425 | 1.0410 | –4.8000 | 0.0000 | 0.0000 | 0.000 |
| 426 | L426 | 1.0600 | –7.1000 | 0.0000 | 0.0000 | 0.000 |
| 427 | L427 | 1.0600 | –6.7000 | 0.0000 | 0.0000 | 0.000 |
| 428 | L428 | 1.0550 | –6.2000 | 0.0000 | 0.0000 | 0.000 |
| 429 | L429 | 1.0230 | –9.6000 | 0.0000 | 0.0000 | 0.000 |
| 446 | L446 | 1.0120 | –7.8000 | 0.0000 | 0.0000 | 0.000 |
| 450 | L450 | 1.0470 | –4.8000 | 0.0000 | 0.0000 | 0.000 |
| 501 | L501 | 1.0020 | –10.0000 | 0.0000 | 0.0000 | 0.000 |
| 518 | L518 | 1.0110 | –6.2000 | 0.0000 | 0.0000 | 0.000 |
| 683 | L683 | 0.9900 | –23.3000 | 101.0000 | 9.1000 | 0.000 |

**TABLE 1.4 (continued)**
**Table of Load Data Sorted by Node Number**

| Node no. | Name | Load bus voltage | Load bus angle | Load P (MW) | Load Q (Mvar) | Sync. cond. Q (Mvar) |
|---|---|---|---|---|---|---|
| 685 | L685 | 1.0000 | –21.8000 | 173.0000 | 16.1000 | 0.000 |
| 687 | L687 | 1.0000 | –21.8000 | 51.8000 | 4.2000 | 0.000 |
| 690 | L690 | 0.9910 | –17.0000 | 0.0000 | 0.0000 | 0.000 |
| 693 | L693 | 0.9800 | –23.6000 | 197.0000 | 18.4000 | 0.000 |
| 695 | L695 | 1.0140 | –10.6000 | 70.4000 | 6.3000 | 0.000 |
| 698 | L698 | 0.9890 | –22.9000 | 0.0000 | 0.0000 | 0.000 |
| 701 | L701 | 0.9990 | –12.4000 | 0.0000 | 0.0000 | 0.000 |
| 702 | L702 | 1.0120 | –10.3000 | 136.5000 | 11.9000 | 0.000 |
| 711 | L711 | 0.9580 | –26.9000 | 168.0000 | 14.7000 | 0.000 |
| 717 | L717 | 1.0120 | –8.5000 | 0.0000 | 0.0000 | 0.000 |
| 926 | L926 | 1.0360 | –4.8000 | 0.0000 | 0.0000 | 0.000 |
| 929 | L929 | 1.0420 | –5.1000 | 0.0000 | 0.0000 | 0.000 |
| 946 | L946 | 1.0350 | –5.0000 | 0.0000 | 0.0000 | 0.000 |

**Table of Generator Reactive Components and Reactive Characteristics**

| Node no. | Name | Generator reactive component | Generator reactive Char. - S |
|---|---|---|---|
| 1 | G001 | 0.0000 | **–0.5516** |
| 151 | G151 | **0.0000** | **0.0000** |
| 153 | **G153** | **0.0000** | **0.0000** |
| 155 | **G155** | **0.0000** | **0.0000** |
| **156** | **G156** | **0.0000** | 0.6086 |
| **157** | **G157** | 0.0000 | –0.1172 |
| **158** | **G158** | 0.0000 | 0.0000 |
| 161 | G161 | 0.0000 | 0.0000 |
| 162 | G162 | 0.0000 | 0.0000 |
| 164 | G164 | 0.0000 | –0.1727 |
| 167 | G167 | 0.0000 | 0.0000 |
| 168 | G168 | 0.0000 | 0.0000 |
| 170 | G170 | 0.0000 | **0.0000** |
| 172 | G172 | 0.0000 | **–0.0065** |
| 174 | G174 | 0.0000 | **–0.3325** |
| 175 | G175 | 0.0000 | **0.0000** |
| 177 | G177 | 0.0000 | **0.0000** |
| 178 | G178 | 0.0000 | 0.0000 |
| 180 | G180 | 0.0000 | 0.0000 |
| 181 | G181 | 0.0000 | 0.0000 |
| 182 | G182 | 0.0000 | –0.1172 |
| 183 | G183 | 0.0000 | –0.1172 |
| 184 | G184 | 0.0000 | 0.0000 |
| 185 | G185 | 0.0000 | 0.0000 |
| 186 | G186 | 0.0000 | 0.0000 |
| 187 | G187 | 0.0000 | 0.0000 |
| 188 | G188 | 0.0000 | 0.0000 |
| 189 | G189 | 0.0000 | 0.0000 |
| 190 | G190 | 0.0000 | 0.0000 |
| 191 | G191 | 0.0000 | 0.0000 |
| 192 | G192 | 0.0000 | 0.0000 |
| 280 | G280 | 0.0000 | 0.0000 |

**TABLE 1.4 (continued)**
**Table of Generator Reactive Components and Reactive Characteristics**

| Node no. | Name | Generator reactive component | Generator reactive Char. - S |
|---|---|---|---|
| 281 | G281 | 0.0000 | 0.0000 |
| 282 | G282 | 0.0000 | 0.0000 |
| 285 | G285 | 0.0000 | –0.1172 |
| 291 | G291 | 0.0000 | 0.1959 |
| 296 | G296 | 0.0000 | 0.0000 |
| 299 | G299 | 0.0000 | 0.0000 |
| 301 | G301 | 0.0000 | 0.1480 |
| 304 | G304 | 0.0000 | 0.0000 |
| 306 | G306 | 0.0000 | 0.0000 |
| 309 | G309 | 0.0000 | 0.0000 |
| 312 | G312 | 0.0000 | 0.0000 |
| 313 | G313 | 0.0000 | 0.0000 |
| 314 | G314 | 0.0000 | 0.0000 |
| 315 | G315 | 0.0000 | –0.1172 |
| 316 | G316 | 0.0000 | –0.1172 |
| 327 | G327 | 0.0000 | 2.9250 |
| 328 | G328 | 0.0000 | 0.0000 |
| 332 | G332 | 0.0000 | –0.1172 |
| 334 | G334 | 0.0000 | 0.0000 |
| 336 | G336 | 0.0000 | –0.1172 |
| 339 | G339 | 0.0000 | 0.4651 |
| 340 | G340 | 0.0000 | 0.0000 |
| 343 | G343 | 0.0000 | 0.0000 |
| 345 | G345 | 0.0000 | 0.0000 |
| 347 | G347 | 0.0000 | 0.0000 |
| 349 | G349 | 0.0000 | 0.0000 |
| 351 | G351 | 0.0000 | 0.0000 |
| 352 | G352 | 0.0000 | 0.0000 |
| 353 | G353 | 0.0000 | 0.0000 |
| 354 | G354 | 0.0000 | 0.0000 |
| 357 | G357 | 0.0000 | 0.5330 |
| 359 | G359 | 0.0000 | –0.1172 |
| 360 | G360 | 0.0000 | 0.0000 |
| 362 | G362 | 0.0000 | 0.0000 |
| 365 | G365 | 0.0000 | –0.1743 |
| 366 | G366 | 0.0000 | 0.0000 |
| 371 | G371 | 0.0000 | 0.1270 |
| 372 | G372 | 0.0000 | –0.1172 |
| 373 | G373 | 0.0000 | 0.0000 |
| 375 | G375 | 0.0000 | 0.0000 |
| 376 | G376 | 0.0000 | 0.0000 |
| 377 | G377 | 0.0000 | 0.0000 |
| 380 | G380 | 0.0000 | 0.0000 |
| 381 | G381 | 0.0000 | 0.0000 |
| 389 | G389 | 0.0000 | 0.0000 |
| 390 | G390 | 0.0000 | 0.3159 |
| 391 | G391 | 0.0000 | 0.9302 |
| 401 | G401 | 0.0000 | 0.0000 |
| 402 | G402 | 0.0000 | 0.0000 |
| 404 | G404 | 0.0000 | 0.0000 |
| 405 | G405 | 0.0000 | 0.0000 |
| 406 | G406 | 0.0000 | 0.0000 |

**TABLE 1.4 (continued)**
**Table of Generator Reactive Components and Reactive Characteristics**

| Node no. | Name | Generator reactive component | Generator reactive Char. - S |
|---|---|---|---|
| 410 | G410 | 0.0000 | 0.0000 |
| 411 | G411 | 0.0000 | 0.0000 |
| 412 | G412 | 0.0000 | 0.0000 |
| 413 | G413 | 0.0000 | 0.0000 |
| 414 | G414 | 0.0000 | 0.0000 |
| 415 | G415 | 0.0000 | 0.0000 |
| 417 | G417 | 0.0000 | 0.0000 |
| 418 | G418 | 0.0000 | 0.0000 |
| 419 | G419 | 0.0000 | 0.0000 |
| 420 | G420 | 0.0000 | 0.0000 |
| 421 | G421 | 0.0000 | 0.0000 |
| 422 | G422 | 0.0000 | 0.0000 |
| 423 | G423 | 0.0000 | 0.0000 |
| 424 | G424 | 0.0000 | 0.0000 |
| 427 | G427 | 0.0000 | –0.1172 |
| 450 | G450 | 0.0000 | –0.1172 |
| 683 | G683 | 0.0000 | 0.0000 |
| 685 | G685 | 0.0000 | 0.3465 |
| 687 | G687 | 0.0000 | 0.2538 |
| 693 | G693 | 0.0000 | –0.1172 |
| 695 | G695 | 0.0000 | 0.0000 |
| 702 | G702 | 0.0000 | 0.0000 |
| 711 | G711 | 0.0000 | 0.0000 |

Reprinted from Energy Utilization of PSE&G for the Middle Atlantic Power Research Committee, Newark, NJ, 1976. With permission.

**TABLE 1.5**
**New Off-Nominal Setting(s) for TCUL Transformers (100%)**

| Bus no. from | Bus no. to | PBI | Transformer tap |
|---|---|---|---|
| 2 | 295 | 0 | 0.906000 |
| 179 | 180 | 0 | 0.981000 |
| 283 | 282 | 0 | 0.994000 |
| 286 | 288 | 0 | 0.944000 |
| 287 | 288 | 0 | 0.931000 |
| 298 | 299 | 0 | 0.956000 |
| 304 | 305 | 0 | 1.037000 |
| 309 | 336 | 0 | 1.025000 |
| 327 | 332 | 0 | 1.062000 |
| 328 | 332 | 0 | 1.037000 |
| 339 | 365 | 0 | 1.000000 |
| 378 | 426 | 0 | 0.956000 |
| 385 | 386 | 0 | 0.994000 |
| 390 | 391 | 0 | 1.031000 |
| 416 | 425 | 0 | 0.950000 |
| 701 | 702 | 0 | 0.994000 |

*Note:* Load flow calculations 100% loading for dispersed system.

**TABLE 1.5 (continued)**
**Table of Generator Data Sorted by Node Number**

| Node no. | Name | Generator voltage | Generator angle | Generator P (MW) | Generator Q (Mvar) |
|---|---|---|---|---|---|
| 1 | G001 | 1.0000 | 0.0000 | 1440.7000 | –573.8999 |
| 151 | G151 | 1.0130 | –5.9000 | 32.0000 | 0.0000 |
| 153 | G153 | 1.0190 | –8.7000 | 17.6000 | 0.0000 |
| 155 | G155 | 1.0520 | –8.2000 | 48.0000 | 0.0000 |
| 156 | G156 | 1.0300 | –4.3000 | 159.0000 | 40.7000 |
| 157 | G157 | 1.0300 | –4.4000 | 45.0000 | –24.7000 |
| 158 | G158 | 1.0240 | –9.2000 | 23.1000 | 0.0000 |
| 161 | G161 | 1.0300 | –5.5000 | 145.6000 | 23.9000 |
| 162 | G162 | 1.0180 | –8.9000 | 3.4000 | 0.0000 |
| 164 | G164 | 1.0300 | –5.6000 | 330.0000 | 16.1000 |
| 167 | G167 | 1.0310 | –6.5000 | 46.4000 | 0.0000 |
| 168 | G168 | 1.0280 | –3.6000 | 74.1000 | 0.0000 |
| 170 | G170 | 1.0120 | –9.3000 | 71.0000 | 0.0000 |
| 172 | G172 | 1.0300 | –1.0000 | 634.0000 | –21.8000 |
| 174 | G174 | 1.0390 | –8.0000 | 661.0000 | –132.0000 |
| 175 | G175 | 1.0200 | –9.3000 | 78.1000 | 0.0000 |
| 177 | G177 | 1.0020 | –8.2000 | 37.3000 | 0.0000 |
| 178 | G178 | 1.0200 | –8.6000 | 15.0000 | 0.0000 |
| 180 | G180 | 1.0180 | –9.1000 | 101.3000 | 0.0000 |
| 181 | G181 | 1.0440 | –8.1000 | 30.0000 | 0.0000 |
| 182 | G182 | 1.0500 | –8.2000 | 0.0000 | 0.0000 |
| 183 | G183 | 1.0530 | –8.2000 | 0.0000 | 0.0000 |
| 184 | G184 | 1.0530 | –8.2000 | 119.2000 | 0.0000 |
| 185 | G185 | 1.0510 | –8.2000 | 149.6000 | 0.0000 |
| 186 | G186 | 1.0440 | –8.1000 | 74.6000 | 0.0000 |
| 187 | G187 | 1.0260 | –5.1000 | 92.0000 | 0.0000 |
| 188 | G188 | 1.0240 | –7.0000 | 51.7000 | 0.0000 |
| 189 | G189 | 1.0250 | –7.3000 | 52.4000 | 0.0000 |
| 190 | G190 | 1.0450 | –5.6000 | 61.8000 | 0.0000 |
| 191 | G191 | 1.0200 | –8.5000 | 21.2000 | 0.0000 |
| 192 | G192 | 1.0030 | –7.5000 | 25.9000 | 0.0000 |
| 280 | G280 | 1.0250 | –6.4000 | 18.3000 | 0.0000 |
| 281 | G281 | 1.0120 | –7.4000 | 44.6000 | 0.0000 |
| 282 | G282 | 1.0080 | –9.7000 | 39.3000 | 0.0000 |
| 285 | G285 | 1.0200 | –7.6000 | 0.0000 | 0.0000 |
| 291 | G291 | 1.0300 | –8.6000 | 620.0000 | 210.7000 |
| 296 | G296 | 1.0340 | –8.4000 | –38.3000 | 0.0000 |
| 299 | G299 | 1.0110 | –6.3000 | 44.0000 | 0.0000 |
| 301 | G301 | 1.0000 | –7.2000 | 493.0000 | 44.9000 |
| 304 | G304 | 1.0010 | –12.0000 | 47.6000 | 0.0000 |
| 306 | G306 | 1.0110 | –9.4000 | 132.2000 | 0.0000 |
| 309 | G309 | 1.0010 | –12.1000 | 97.1000 | 0.0000 |
| 312 | G312 | 0.9950 | –14.2000 | 22.6000 | 0.0000 |
| 313 | G313 | 1.0000 | –8.0000 | 66.3000 | 0.0000 |
| 314 | G314 | 1.0030 | –11.9000 | 0.0000 | 0.0000 |
| 315 | G315 | 1.0300 | –2.4000 | 160.0000 | 187.1000 |
| 316 | G316 | 1.0300 | –2.1000 | 320.0000 | 42.6000 |
| 327 | G327 | 1.0300 | –7.0000 | 204.3000 | –2.7000 |
| 328 | G328 | 1.0030 | –8.8000 | 85.0000 | 0.0000 |
| 332 | G332 | 1.0080 | –6.9000 | 0.0000 | 0.0000 |
| 334 | G334 | 1.0050 | –6.4000 | 12.7000 | 0.0000 |
| 336 | G336 | 0.9930 | –14.4000 | 0.0000 | 0.0000 |
| 339 | G339 | 1.0300 | –5.7000 | 1003.0000 | 310.6001 |
| 340 | G340 | 1.0260 | –8.2000 | 1.8000 | 0.0000 |

**TABLE 1.5 (continued)**
**Table of Generator Data Sorted by Node Number**

| Node no. | Name | Generator voltage | Generator angle | Generator P (MW) | Generator Q (Mvar) |
|---|---|---|---|---|---|
| 343 | G343 | 1.0270 | −7.1000 | 345.0000 | 68.4000 |
| 345 | G345 | 1.0250 | −2.9000 | 58.2000 | 0.0000 |
| 347 | G347 | 1.0250 | −2.8000 | 49.8000 | 0.0000 |
| 349 | G349 | 1.0010 | −8.5000 | 1.8000 | 0.0000 |
| 351 | G351 | 1.0240 | −4.6000 | 72.2000 | 0.0000 |
| 352 | G352 | 1.0280 | −8.7000 | 9.3000 | 0.0000 |
| 353 | G353 | 1.0230 | −7.9000 | 75.3000 | 0.0000 |
| 354 | G354 | 0.9960 | −10.2000 | 9.0000 | 0.0000 |
| 357 | G357 | 1.0120 | −7.1000 | 594.8000 | 500.0000 |
| 359 | G359 | 1.0260 | −6.3000 | 0.0000 | 0.0000 |
| 360 | G360 | 1.0320 | −8.5000 | 9.2000 | 0.0000 |
| 362 | G362 | 1.0060 | −10.0000 | 26.7000 | 0.0000 |
| 365 | G365 | 1.0270 | −7.3000 | 270.2000 | 200.0000 |
| 366 | G366 | 1.0030 | −10.6000 | 5.0000 | 0.0000 |
| 371 | G371 | 1.0300 | −2.1000 | 638.0000 | 101.8000 |
| 372 | G372 | 1.0200 | −4.5000 | 140.0000 | 38.1000 |
| 373 | G373 | 1.0230 | −2.8000 | 39.1000 | 0.0000 |
| 375 | G375 | 1.0230 | −5.7000 | 1.7000 | 0.0000 |
| 376 | G376 | 1.0240 | −6.2000 | 1.7000 | 0.0000 |
| 377 | G377 | 1.0050 | −6.8000 | 13.2000 | 0.0000 |
| 380 | G380 | 1.0020 | −8.2000 | 26.9000 | 0.0000 |
| 381 | G381 | 1.0170 | −7.4000 | 24.0000 | 0.0000 |
| 389 | G389 | 1.0080 | −9.6000 | 94.5000 | 0.0000 |
| 390 | G390 | 1.0300 | −2.6000 | 763.3000 | 115.9000 |
| 391 | G391 | 1.0200 | −5.0000 | 344.0000 | 88.2000 |
| 401 | G401 | 1.0400 | −8.0000 | 6.7000 | 0.0000 |
| 402 | G402 | 1.0090 | −7.7000 | 24.4000 | 0.0000 |
| 404 | G404 | 1.0010 | −8.6000 | 35.1000 | 0.0000 |
| 405 | G405 | 1.0220 | −8.5000 | 215.0000 | 0.0000 |
| 406 | G406 | 1.0110 | −8.2000 | 73.2000 | 0.0000 |
| 410 | G410 | 1.0080 | −7.2000 | 55.0000 | 0.0000 |
| 411 | G411 | 1.0090 | 7.6000 | 19.0000 | 0.0000 |
| 412 | G412 | 1.0130 | −9.2000 | 22.0000 | 0.0000 |
| 413 | G413 | 1.0190 | −8.8000 | 46.0000 | 0.0000 |
| 414 | G414 | 1.0060 | −8.4000 | 67.0000 | 0.0000 |
| 415 | G415 | 0.9990 | −9.7000 | 67.0000 | 0.0000 |
| 417 | G417 | 1.0080 | −5.8000 | 37.0000 | 0.0000 |
| 418 | G418 | 1.0350 | −8.3000 | 49.0000 | 0.0000 |
| 419 | G419 | 1.0260 | −9.0000 | 15.0000 | 0.0000 |
| 420 | G420 | 1.0250 | −6.2000 | 7.0000 | 0.0000 |
| 421 | G421 | 1.0180 | −5.3000 | 7.0000 | 0.0000 |
| 422 | G422 | 1.0080 | −7.1000 | 67.0000 | 0.0000 |
| 423 | G423 | 1.0190 | −6.9000 | 41.0000 | 0.0000 |
| 424 | G424 | 1.0020 | −6.8000 | 34.0000 | 0.0000 |
| 427 | G427 | 1.0570 | −8.4000 | 0.0000 | 0.0000 |
| 450 | G450 | 1.0540 | −6.1000 | 0.0000 | 0.0000 |
| 683 | G683 | 0.9840 | −35.9000 | 38.8000 | 0.0000 |
| 685 | G685 | 1.0000 | −27.9000 | 321.0000 | 72.2000 |
| 687 | G687 | 1.0000 | −34.2000 | 304.8999 | 41.8000 |
| 693 | G693 | 1.0000 | −35.6000 | 55.0000 | 115.6000 |
| 695 | G695 | 1.0010 | −13.6000 | 27.4000 | 0.0000 |
| 702 | G702 | 1.0010 | −13.3000 | 52.6000 | 0.0000 |
| 711 | G711 | 0.9340 | −38.5000 | 64.8000 | 0.0000 |

**TABLE 1.5 (continued)**
**Table of Load Data Sorted by Node Number**

| Node no. | Name | Load bus voltage | Load bus angle | Load P (MW) | Load Q (Mvar) | Sync. cond. Q (Mvar) |
|---|---|---|---|---|---|---|
| 1 | L001 | 1.0000 | 0.0000 | 0.0000 | 0.0000 | 0.000 |
| 2 | L002 | 1.0140 | –5.0000 | 0.0000 | 0.0000 | 0.000 |
| 16 | L016 | 1.0310 | –4.8000 | 0.0000 | 0.0000 | 0.000 |
| 96 | L096 | 1.0270 | –4.6000 | 0.0000 | 0.0000 | 0.000 |
| 125 | L125 | 1.0160 | –5.6000 | 0.0000 | 0.0000 | 0.000 |
| 126 | L126 | 1.0280 | –6.2000 | 0.0000 | 0.0000 | 0.000 |
| 150 | L150 | 1.0450 | –8.1000 | 233.4000 | 5.8000 | 0.000 |
| 151 | L151 | 1.0130 | –5.9000 | 32.0000 | 3.8000 | 0.000 |
| 152 | L152 | 1.0080 | –7.8000 | 20.5000 | 1.7000 | 0.000 |
| 153 | L153 | 1.0190 | –8.7000 | 67.2000 | –11.6000 | 0.000 |
| 155 | L155 | 1.0520 | –8.2000 | 130.7000 | 19.8000 | 0.000 |
| 156 | L156 | 1.0300 | –4.3000 | 68.4000 | 10.9000 | 0.000 |
| 157 | L157 | 1.0300 | –4.4000 | 0.0000 | 0.0000 | 0.000 |
| 158 | L158 | 1.0240 | –9.2000 | 120.2000 | 18.4000 | 0.000 |
| 160 | L160 | 1.0180 | –6.1000 | 3.2000 | 0.6000 | 0.000 |
| 161 | L161 | 1.0300 | –5.5000 | 102.4000 | 5.4000 | 0.000 |
| 162 | L162 | 1.0180 | –8.9000 | 124.0000 | 21.5000 | 0.000 |
| 164 | L164 | 1.0300 | –5.6000 | 20.8000 | –1.7000 | 0.000 |
| 167 | L167 | 1.0310 | –6.5000 | 177.3000 | 21.8000 | 0.000 |
| 168 | L168 | 1.0280 | –3.6000 | 191.5000 | 26.6000 | 0.000 |
| 170 | L170 | 1.0120 | –9.3000 | 204.0000 | 47.4000 | 0.000 |
| 171 | L171 | 1.0140 | –5.5000 | 24.2000 | 16.8000 | 0.000 |
| 172 | L172 | 1.0300 | –1.0000 | 37.2000 | –3.8000 | 0.000 |
| 174 | L174 | 1.0390 | –8.0000 | 390.3999 | 68.9000 | 0.000 |
| 175 | L175 | 1.0200 | –9.3000 | 224.3000 | 50.8000 | 0.000 |
| 177 | L177 | 1.0020 | –8.2000 | 66.0000 | 2.9000 | 0.000 |
| 178 | L178 | 1.0200 | –8.6000 | 52.6000 | 2.7000 | 0.000 |
| 179 | L179 | 0.9990 | –8.8000 | 0.0000 | 0.0000 | 0.000 |
| 180 | L180 | 1.0180 | –9.1000 | 241.8000 | 63.8000 | 0.000 |
| 181 | L181 | 1.0440 | –8.1000 | 30.0000 | 18.0000 | 0.000 |
| 182 | L182 | 1.0500 | –8.2000 | 0.0000 | 0.0000 | 0.000 |
| 183 | L183 | 1.0530 | –8.2000 | 0.0000 | 0.0000 | 0.000 |
| 184 | L184 | 1.0530 | –8.2000 | 119.2000 | 6.8000 | 0.000 |
| 185 | L185 | 1.0510 | –8.2000 | 149.6000 | 46.0000 | 0.000 |
| 186 | L186 | 1.0440 | –8.1000 | 74.6000 | 12.5000 | 0.000 |
| 187 | L187 | 1.0260 | –5.1000 | 92.0000 | 10.6000 | 0.000 |
| 188 | L188 | 1.0240 | –7.0000 | 51.7000 | –5.8000 | 0.000 |
| 189 | L189 | 1.0250 | –7.3000 | 52.4000 | –2.2000 | 0.000 |
| 190 | L190 | 1.0450 | –5.6000 | 61.8000 | 12.9000 | 0.000 |
| 191 | L191 | 1.0200 | –8.5000 | 21.2000 | 4.7000 | 0.000 |
| 192 | L192 | 1.0030 | –7.5000 | 25.9000 | 6.5000 | 0.000 |
| 202 | L202 | 1.0300 | –5.6000 | 0.0000 | 0.0000 | 0.000 |
| 227 | L227 | 1.0170 | –2.4000 | 0.0000 | 0.0000 | 0.000 |
| 231 | L231 | 1.0090 | –6.9000 | 0.0000 | 0.0000 | 0.000 |
| 280 | L280 | 1.0250 | –6.4000 | 53.0000 | 16.9000 | 0.000 |
| 281 | L281 | 1.0120 | –7.4000 | 227.0000 | 37.6000 | 0.000 |
| 282 | L282 | 1.0080 | –9.7000 | 89.0000 | 33.0000 | 0.000 |
| 283 | L283 | 1.0020 | –11.8000 | 213.0000 | 73.5000 | 0.000 |
| 285 | L285 | 1.0200 | –7.6000 | 152.0000 | 60.0000 | 0.000 |
| 286 | L286 | 1.0000 | –7.6000 | 91.0000 | 84.5000 | 0.000 |
| 287 | L287 | 0.9980 | –7.2000 | 91.0000 | 84.5000 | 0.000 |
| 288 | L288 | 1.0320 | –6.5000 | 0.0000 | 0.0000 | 0.000 |
| 289 | L289 | 0.9930 | –14.1000 | 58.0000 | 10.7000 | 0.000 |

**TABLE 1.5 (continued)**
**Table of Load Data Sorted by Node Number**

| Node no. | Name | Load bus voltage | Load bus angle | Load P (MW) | Load Q (Mvar) | Sync. cond. Q (Mvar) |
|---|---|---|---|---|---|---|
| 290 | L290 | 0.9980 | –9.9000 | 167.0000 | 129.0000 | 0.000 |
| 291 | L291 | 1.0300 | –8.6000 | 327.0000 | 10.6000 | 0.000 |
| 295 | L295 | 1.0630 | –6.4000 | 0.0000 | 0.0000 | 0.000 |
| 296 | L296 | 1.0340 | –8.4000 | 217.0000 | 109.9000 | 0.000 |
| 297 | L297 | 1.0310 | –8.6000 | 0.0000 | 0.0000 | 0.000 |
| 298 | L298 | 1.0000 | –4.1000 | 0.0000 | 0.0000 | 0.000 |
| 299 | L299 | 1.0110 | –6.3000 | 255.0000 | 121.1000 | 0.000 |
| 301 | L301 | 1.0000 | –7.2000 | 164.0000 | 62.3000 | 0.000 |
| 303 | L303 | 0.9940 | –10.8000 | 0.0000 | 0.0000 | 0.000 |
| 304 | L304 | 1.0010 | –12.0000 | 242.0000 | 29.7000 | 0.000 |
| 305 | L305 | 0.9850 | –11.3000 | 0.0000 | 0.0000 | 0.000 |
| 306 | L306 | 1.0110 | –9.4000 | 179.0000 | 74.0000 | 0.000 |
| 308 | L308 | 1.0030 | –10.4000 | 0.0000 | 0.0000 | 0.000 |
| 309 | L309 | 1.0010 | –12.1000 | 134.0000 | 26.3000 | 0.000 |
| 311 | L311 | 1.0050 | –8.0000 | 0.0000 | 0.0000 | 0.000 |
| 312 | L312 | 0.9950 | –14.2000 | 48.0000 | 5.8000 | 0.000 |
| 313 | L313 | 1.0000 | –8.0000 | 104.0000 | 34.7000 | 0.000 |
| 314 | L314 | 1.0030 | –11.9000 | 207.0000 | 60.0000 | 0.000 |
| 315 | L315 | 1.0300 | –2.4000 | 0.0000 | 0.0000 | 0.000 |
| 316 | L316 | 1.0300 | –2.1000 | 0.0000 | 0.0000 | 0.000 |
| 327 | L327 | 1.0300 | –7.0000 | 146.0000 | 60.0000 | 0.000 |
| 328 | L328 | 1.0030 | –8.8000 | 246.0000 | 148.0000 | 0.000 |
| 332 | L332 | 1.0080 | –6.9000 | 0.0000 | 0.0000 | 0.000 |
| 333 | L333 | 1.0010 | –12.3000 | 338.0000 | 86.0000 | 0.000 |
| 334 | L334 | 1.0050 | –6.4000 | 70.0000 | 8.8000 | 0.000 |
| 336 | L336 | 0.9930 | –14.4000 | 257.0000 | 37.9000 | 0.000 |
| 337 | L337 | 1.0210 | –8.6000 | 54.0000 | 15.0000 | 0.000 |
| 339 | L339 | 1.0300 | –5.7000 | 0.0000 | 0.0000 | 0.000 |
| 340 | L340 | 1.0260 | –8.2000 | 124.0000 | 51.0000 | 0.000 |
| 343 | L343 | 1.0270 | –7.1000 | 0.1000 | 0.0000 | 0.000 |
| 345 | L345 | 1.0250 | –2.9000 | 109.0000 | 18.4000 | 0.000 |
| 347 | L347 | 1.0250 | –2.8000 | 136.0000 | 50.6000 | 0.000 |
| 349 | L349 | 1.0010 | –8.5000 | 58.0000 | 20.0000 | 0.000 |
| 351 | L351 | 1.0240 | –4.6000 | 199.0000 | 49.6000 | 0.000 |
| 352 | L352 | 1.0280 | –8.7000 | 57.0000 | 44.0000 | 0.000 |
| 353 | L353 | 1.0230 | –7.9000 | 165.0000 | 39.0000 | 0.000 |
| 354 | L354 | 0.9960 | –10.2000 | 177.0000 | 30.8000 | 0.000 |
| 357 | L357 | 1.0120 | –7.1000 | 265.0000 | 163.4000 | 0.000 |
| 359 | L359 | 1.0260 | –6.3000 | 0.0000 | 0.0000 | 0.000 |
| 360 | L360 | 1.0320 | –8.5000 | 56.0000 | 21.6000 | 0.000 |
| 362 | L362 | 1.0060 | –10.0000 | 36.0000 | 3.9000 | 0.000 |
| 365 | L365 | 1.0270 | –7.3000 | 389.0000 | 133.0000 | 0.000 |
| 366 | L366 | 1.0030 | –10.6000 | 122.0000 | 22.4000 | 0.000 |
| 368 | L368 | 1.0290 | –2.4000 | 56.0000 | 19.8000 | 0.000 |
| 371 | L371 | 1.0300 | –2.1000 | 0.0000 | 0.0000 | 0.000 |
| 372 | L372 | 1.0200 | –4.5000 | 0.0000 | 0.0000 | 0.000 |
| 373 | L373 | 1.0230 | –2.8000 | 208.0000 | 101.4000 | 0.000 |
| 375 | L375 | 1.0230 | –5.7000 | 28.0000 | 9.9000 | 0.000 |
| 376 | L376 | 1.0240 | –6.2000 | 28.0000 | 9.9000 | 0.000 |
| 377 | L377 | 1.0050 | –6.8000 | 94.0000 | 33.4000 | 0.000 |
| 378 | L378 | 1.0050 | –10.8000 | 0.0000 | 0.0000 | 0.000 |
| 379 | L379 | 1.0200 | –8.3000 | 63.0000 | 25.0000 | 0.000 |
| 380 | L380 | 1.0020 | –8.2000 | 213.0000 | 115.0000 | 0.000 |
| 381 | L381 | 1.0170 | –7.4000 | 55.0000 | 19.7000 | 0.000 |

**TABLE 1.5 (continued)**
**Table of Load Data Sorted by Node Number**

| Node no. | Name | Load bus voltage | Load bus angle | Load P (MW) | Load Q (Mvar) | Sync. cond. Q (Mvar) |
|---|---|---|---|---|---|---|
| 382 | L382 | 1.0320 | –5.3000 | 0.0000 | 0.0000 | 0.000 |
| 383 | L383 | 1.0090 | –4.5000 | 54.0000 | 6.3000 | 0.000 |
| 385 | L385 | 1.0030 | –8.3000 | 0.0000 | 0.0000 | 0.000 |
| 386 | L386 | 1.0150 | –9.1000 | 0.0000 | 0.0000 | 0.000 |
| 388 | L388 | 1.0060 | –11.9000 | 0.0000 | 0.0000 | 0.000 |
| 389 | L389 | 1.0080 | –9.6000 | 140.0000 | 41.0000 | 0.000 |
| 390 | L390 | 1.0300 | –2.6000 | 326.0000 | 71.3000 | 0.000 |
| 391 | L391 | 1.0200 | –5.0000 | 0.0000 | 0.0000 | 0.000 |
| 401 | L401 | 1.0400 | –8.0000 | 48.0000 | 15.5000 | 0.000 |
| 402 | L402 | 1.0090 | –7.7000 | 61.0000 | 21.0000 | 0.000 |
| 403 | L403 | 1.0120 | –4.9000 | 233.0000 | 74.9000 | 0.000 |
| 404 | L404 | 1.0010 | –8.6000 | 224.0000 | 48.0000 | 0.000 |
| 405 | L405 | 1.0220 | –8.5000 | 215.0000 | 3.0000 | 0.000 |
| 406 | L406 | 1.0110 | –8.2000 | 184.0000 | 59.1000 | 0.000 |
| 409 | L409 | 1.0050 | –9.7000 | 0.0000 | 0.0000 | 0.000 |
| 410 | L410 | 1.0080 | –7.2000 | 55.0000 | 26.0000 | 0.000 |
| 411 | L411 | 1.0090 | –7.6000 | 19.0000 | 3.0000 | 0.000 |
| 412 | L412 | 1.0130 | –9.2000 | 22.0000 | 4.0000 | 0.000 |
| 413 | L413 | 1.0190 | –8.8000 | 46.0000 | 14.0000 | 0.000 |
| 414 | L414 | 1.0060 | –8.4000 | 67.0000 | 21.5000 | 0.000 |
| 415 | L415 | 0.9990 | –9.7000 | 67.0000 | 21.5000 | 0.000 |
| 416 | L416 | 1.0020 | –6.1000 | 0.0000 | 0.0000 | 0.000 |
| 417 | L417 | 1.0080 | –5.8000 | 37.0000 | 10.3000 | 0.000 |
| 418 | L418 | 1.0350 | –8.3000 | 49.0000 | 19.8000 | 0.000 |
| 419 | L419 | 1.0260 | –9.0000 | 15.0000 | 5.6000 | 0.000 |
| 420 | L420 | 1.0250 | –6.2000 | 7.0000 | 1.4000 | 0.000 |
| 421 | L421 | 1.0180 | –5.3000 | 7.0000 | 1.4000 | 0.000 |
| 422 | L422 | 1.0080 | –7.1000 | 63.0000 | 18.3000 | 0.000 |
| 423 | L423 | 1.0190 | –6.9000 | 41.0000 | 13.1000 | 0.000 |
| 424 | L424 | 1.0020 | –6.8000 | 34.0000 | 4.8000 | 0.000 |
| 425 | L425 | 1.0350 | –6.0000 | 0.0000 | 0.0000 | 0.000 |
| 426 | L426 | 1.0540 | –9.0000 | 0.0000 | 0.0000 | 0.000 |
| 427 | L427 | 1.0570 | –8.4000 | 0.0000 | 0.0000 | 0.000 |
| 428 | L428 | 1.0560 | –7.7000 | 0.0000 | 0.0000 | 0.000 |
| 429 | L429 | 1.0130 | –12.2000 | 0.0000 | 0.0000 | 0.000 |
| 446 | L446 | 1.0080 | –9.0000 | 0.0000 | 0.0000 | 0.000 |
| 450 | L450 | 1.0540 | –6.1000 | 0.0000 | 0.0000 | 0.000 |
| 501 | L501 | 0.9860 | –11.3000 | 0.0000 | 0.0000 | 0.000 |
| 518 | L518 | 1.0190 | –4.9000 | 0.0000 | 0.0000 | 0.000 |
| 683 | L683 | 0.9840 | –35.9000 | 144.0000 | 13.0000 | 0.000 |
| 685 | L685 | 1.0000 | –27.9000 | 245.0000 | 23.0000 | 0.000 |
| 687 | L687 | 1.0000 | –34.2000 | 73.0000 | 6.0000 | 0.000 |
| 690 | L690 | 0.9920 | –23.3000 | 0.0000 | 0.0000 | 0.000 |
| 693 | L693 | 1.0000 | –35.6000 | 281.0000 | 26.0000 | 0.000 |
| 695 | L695 | 1.0010 | –13.6000 | 102.0000 | 9.0000 | 0.000 |
| 698 | L698 | 1.0000 | –35.0000 | 0.0000 | 0.0000 | 0.000 |
| 701 | L701 | 1.0030 | –16.5000 | 0.0000 | 0.0000 | 0.000 |
| 702 | L702 | 1.0010 | –13.3000 | 195.0000 | 17.0000 | 0.000 |
| 711 | L711 | 0.9340 | –38.5000 | 240.0000 | 21.0000 | 0.000 |
| 717 | L717 | 1.0040 | –10.7000 | 0.0000 | 0.0000 | 0.000 |
| 926 | L926 | 1.0310 | –6.2000 | 0.0000 | 0.0000 | 0.000 |
| 929 | L929 | 1.0260 | –6.3000 | 0.0000 | 0.0000 | 0.000 |
| 946 | L946 | 1.0260 | –6.6000 | 0.0000 | 0.0000 | 0.000 |

**TABLE 1.5 (continued)**
**Table of Generator Reactive Components and Reactive Characteristics**

| Node no. | Name | Generator reactive component | Generator reactive Char. - S |
|---|---|---|---|
| 1 | G001 | 0.0000 | –0.3983 |
| 151 | G151 | 0.0000 | 0.0000 |
| 153 | G153 | 0.0000 | 0.0000 |
| 155 | G155 | 0.0000 | 0.0000 |
| 156 | G156 | 0.0000 | 0.2560 |
| 157 | G157 | 0.0000 | –0.5489 |
| 158 | G158 | 0.0000 | 0.0000 |
| 161 | G161 | 0.0000 | 0.1641 |
| 162 | G162 | 0.0000 | 0.0000 |
| 164 | G164 | 0.0000 | 0.0488 |
| 167 | G167 | 0.0000 | 0.0000 |
| 168 | G168 | 0.0000 | 0.0000 |
| 170 | G170 | 0.0000 | 0.0000 |
| 172 | G172 | 0.0000 | –0.0344 |
| 174 | G174 | 0.0000 | –0.1997 |
| 175 | G175 | 0.0000 | 0.0000 |
| 177 | G177 | 0.0000 | 0.0000 |
| 178 | G178 | 0.0000 | 0.0000 |
| 180 | G180 | 0.0000 | 0.0000 |
| 181 | G181 | 0.0000 | 0.0000 |
| 182 | G182 | 0.0000 | –0.1172 |
| 183 | G183 | 0.0000 | –0.1172 |
| 184 | G184 | 0.0000 | 0.0000 |
| 185 | G185 | 0.0000 | 0.0000 |
| 186 | G186 | 0.0000 | 0.0000 |
| 187 | G187 | 0.0000 | 0.0000 |
| 188 | G188 | 0.0000 | 0.0000 |
| 189 | G189 | 0.0000 | 0.0000 |
| 190 | G190 | 0.0000 | 0.0000 |
| 191 | G191 | 0.0000 | 0.0000 |
| 192 | G192 | 0.0000 | 0.0000 |
| 280 | G280 | 0.0000 | 0.0000 |
| 281 | G281 | 0.0000 | 0.0000 |
| 282 | G282 | 0.0000 | 0.0000 |
| 285 | G285 | 0.0000 | –0.1172 |
| 291 | G291 | 0.0000 | 0.3398 |
| 296 | G296 | 0.0000 | 0.0000 |
| 299 | G299 | 0.0000 | 0.0000 |
| 301 | G301 | 0.0000 | 0.0911 |
| 304 | G304 | 0.0000 | 0.0000 |
| 306 | G306 | 0.0000 | 0.0000 |
| 309 | G309 | 0.0000 | 0.0000 |
| 312 | G312 | 0.0000 | 0.0000 |
| 313 | G313 | 0.0000 | 0.0000 |
| 314 | G314 | 0.0000 | –0.1172 |
| 315 | G315 | 0.0000 | 1.1694 |
| 316 | G316 | 0.0000 | 0.1331 |
| 327 | G327 | 0.0000 | –0.0132 |
| 328 | G328 | 0.0000 | 0.0000 |
| 332 | G332 | 0.0000 | –0.1172 |
| 334 | G334 | 0.0000 | 0.0000 |
| 336 | G336 | 0.0000 | –0.1172 |

**TABLE 1.5 (continued)**
**Table of Generator Reactive Components and Reactive Characteristics**

| Node no. | Name | Generator reactive component | Generator reactive Char. - S |
|---|---|---|---|
| 339 | G339 | 0.0000 | 0.3097 |
| 340 | G340 | 0.0000 | 0.0000 |
| 343 | G343 | 0.0000 | 0.1983 |
| 345 | G345 | 0.0000 | 0.0000 |
| 347 | G347 | 0.0000 | 0.0000 |
| 349 | G349 | 0.0000 | 0.0000 |
| 351 | G351 | 0.0000 | 0.0000 |
| 352 | G352 | 0.0000 | 0.0000 |
| 353 | G353 | 0.0000 | 0.0000 |
| 354 | G354 | 0.0000 | 0.0000 |
| 357 | G357 | 0.0000 | 0.8406 |
| 359 | G359 | 0.0000 | –0.1172 |
| 360 | G360 | 0.0000 | 0.0000 |
| 362 | G362 | 0.0000 | 0.0000 |
| 365 | G365 | 0.0000 | 0.7402 |
| 366 | G366 | 0.0000 | 0.0000 |
| 371 | G371 | 0.0000 | 0.1596 |
| 372 | G372 | 0.0000 | 0.2721 |
| 373 | G373 | 0.0000 | 0.0000 |
| 375 | G375 | 0.0000 | 0.0000 |
| 376 | G376 | 0.0000 | 0.0000 |
| 377 | G377 | 0.0000 | 0.0000 |
| 380 | G380 | 0.0000 | 0.0000 |
| 381 | G381 | 0.0000 | 0.0000 |
| 389 | G389 | 0.0000 | 0.0000 |
| 390 | G390 | 0.0000 | 0.1518 |
| 391 | G391 | 0.0000 | 0.2564 |
| 401 | G401 | 0.0000 | 0.0000 |
| 402 | G402 | 0.0000 | 0.0000 |
| 404 | G404 | 0.0000 | 0.0000 |
| 405 | G405 | 0.0000 | 0.0000 |
| 406 | G406 | 0.0000 | 0.0000 |
| 410 | G410 | 0.0000 | 0.0000 |
| 411 | G411 | 0.0000 | 0.0000 |
| 412 | G412 | 0.0000 | 0.0000 |
| 413 | G413 | 0.0000 | 0.0000 |
| 414 | G414 | 0.0000 | 0.0000 |
| 415 | G415 | 0.0000 | 0.0000 |
| 417 | G417 | 0.0000 | 0.0000 |
| 418 | G418 | 0.0000 | 0.0000 |
| 419 | G419 | 0.0000 | 0.0000 |
| 420 | G420 | 0.0000 | 0.0000 |
| 421 | G421 | 0.0000 | 0.0000 |
| 422 | G422 | 0.0000 | 0.0000 |
| 423 | G423 | 0.0000 | 0.0000 |
| 424 | G424 | 0.0000 | 0.0000 |
| 427 | G427 | 0.0000 | –0.1172 |
| 450 | G450 | 0.0000 | –0.1172 |
| 683 | G683 | 0.0000 | 0.0000 |
| 685 | G685 | 0.0000 | 0.2249 |
| 687 | G687 | 0.0000 | 0.1371 |
| 693 | G693 | 0.0000 | 2.1018 |

**TABLE 1.5 (continued)**
**Table of Generator Reactive Components and Reactive Characteristics**

| Node no. | Name | Generator reactive component | Generator reactive Char. - S |
|---|---|---|---|
| 695 | G695 | 0.0000 | 0.0000 |
| 702 | G702 | 0.0000 | 0.0000 |
| 711 | G711 | 0.0000 | 0.0000 |

Reprinted from Energy Utilization of PSE&G for the Middle Atlantic Power Research Committee, Newark, NJ, 1976. With permission.

obtained using Equation 1.4 which was developed by the author of this book, Professor Khalil Denno. Computer flow chart for calculating the [B] matrix according to Equation 1.4 is shown in Figure 1.6.

Elements of the transmission loss coefficient matrix for the totally centralized system where fuel cells replaced gas turbines for peak load demand are shown in Tables 1.6 through 1.10. The [B] matrices established are based on system synthesis in the sixth reference frame for minimum transmission losses in the entire power grid system.

## C. SOLUTION FOR ELEMENTS OF THE [K] MATRIX

From data secured through load flow calculations, solution for elements of the [K] matrix were established according to Equation 1.12. Consequently, using respective elements from the [B] and [K] matrices, elements of the [R] matrix established. Diagonal elements of the [R] matrix for the centralized system and the mixed centralized-dispersed system are shown in Table 1.11A and 1.11B.

Elements of the [R] matrix in Table 1.11A were obtained by dividing the diagonal elements of the [B] matrix at 70% loading shown in Table 1.5 by the respective elements of the [K] matrix secured from Equation 1.12.

Elements of the [R] matrix in Table 1.11B is a mixed system of 32 central bus-bars energized by 32 conventional sources and 92 bus bars energized by hydrogen-oxygen fuel cells.

## D. RESULTS

Carrying out the procedure explained earlier for the establishment of the symmetrical resistance diagonal matrices for systems A and B, under all loading conditions, the following information for 70% base loading is listed as typical results for 60, 80, 90 and 100% loads.

Table 1.11A contains the diagonal elements of the [R] matrix for the 32 bus-bar centralized system extracted from the much larger overall [R] matrix.

Table 1.11B contains the diagonal elements of the [R] matrix for the 123 bus-bar dispersed-centralized system extracted from the much larger overall [R] matrix.

The diagonal elements listed in Tables 1.11A and 1.11B represent the elemental resistance path from each bus-bar in the power flow reference frame to the system centroid.

The finite elemental values indicated in Table 1.11A identify the presumed centralized mode of this system.

In Table 1.11B the elemental nonzero values refer to those power bus-bars of centralized location maintained in the new system with respect to total load supplied by them, while the zero elemental values refer to those dispersed bus-bars scattered in the power system at close proximity to the system centroid rendering their resistance path negligible as demonstrated by their zero values.

## TABLE 1.6
## [B] Matrix

60% Loading
Minimum Transmission Loss: = 689.9 MW
$\lambda = 7.6$

| Bus no. | | B | Bus no. | | B | Bus no. | | B |
|---|---|---|---|---|---|---|---|---|
| 1 | 001 | 0.0002309 | 156 | 001 | 0.0004331 | 161 | 001 | -0.0003198 |
| 1 | 156 | 0.0004331 | 156 | 156 | 0.0018760 | 161 | 156 | -0.0001463 |
| 1 | 161 | -0.0003198 | 156 | 161 | -0.0061463 | 161 | 161 | -0.0010145 |
| 1 | 164 | 0.0003564 | 156 | 164 | 0.0011318 | 161 | 164 | -0.0014164 |
| 1 | 172 | 0.0002963 | 156 | 172 | 0.0007068 | 161 | 172 | -0.0006217 |
| 1 | 174 | -0.0000055 | 156 | 174 | -0.0000438 | 161 | 174 | -0.0000355 |
| 1 | 291 | 0.0001961 | 156 | 291 | 0.0006348 | 161 | 291 | -0.0008220 |
| 1 | 315 | -0.0000499 | 156 | 315 | -0.0004182 | 161 | 315 | -0.0002931 |
| 1 | 316 | -0.0000507 | 156 | 316 | -0.0004759 | 161 | 316 | -0.0002561 |
| 1 | 322 | -0.0002494 | 156 | 332 | -0.0035851 | 161 | 332 | -0.0008991 |
| 1 | 336 | -0.0003991 | 156 | 336 | -0.0033456 | 161 | 336 | -0.0023452 |
| 1 | 339 | 0.0001086 | 156 | 339 | 0.0003341 | 161 | 339 | -0.0003970 |
| 1 | 357 | 0.0001235 | 156 | 357 | 0.0004792 | 161 | 357 | -0.0009626 |
| 1 | 371 | 0.0002303 | 156 | 371 | 0.0006287 | 161 | 371 | -0.0006578 |
| 1 | 372 | -0.0001967 | 156 | 372 | -0.0022135 | 161 | 372 | -0.0008339 |
| 1 | 390 | 0.0001674 | 156 | 390 | 0.0005840 | 161 | 390 | -0.0008786 |
| 1 | 683 | -0.0005879 | 156 | 683 | -0.0076562 | 161 | 683 | -0.0022452 |
| 1 | 685 | -0.0000522 | 156 | 685 | -0.0004987 | 161 | 685 | -0.0002587 |
| 1 | 157 | 0.0000532 | 156 | 157 | 0.0003367 | 161 | 157 | 0.0006115 |
| 1 | 182 | -0.0000049 | 156 | 182 | -0.0000378 | 161 | 182 | -0.0000335 |
| 1 | 183 | 0.0000464 | 156 | 183 | 0.0002889 | 161 | 183 | 0.0005728 |
| 1 | 285 | 0.0001832 | 156 | 285 | 0.0008775 | 161 | 285 | -0.0080590 |
| 1 | 301 | 0.0002126 | 156 | 301 | 0.0014665 | 161 | 301 | 0.0018516 |
| 1 | 327 | -0.0000481 | 156 | 327 | -0.0003901 | 161 | 327 | -0.0002971 |
| 1 | 343 | -0.0000049 | 156 | 343 | -0.0000378 | 161 | 343 | -0.0000336 |
| 1 | 359 | -0.0000049 | 156 | 359 | -0.0000378 | 161 | 359 | -0.0000336 |
| 1 | 391 | 0.0000322 | 156 | 391 | 0.0001772 | 161 | 391 | 0.0009183 |
| 1 | 427 | 0.0002322 | 156 | 427 | 0.0004376 | 161 | 427 | -0.0003239 |
| 1 | 450 | 0.0002363 | 156 | 450 | 0.0004512 | 161 | 450 | -0.0003367 |
| 1 | 687 | 0.0001574 | 156 | 687 | 0.0009206 | 161 | 687 | 0.0026762 |
| 1 | 693 | -0.0000634 | 156 | 693 | -0.0005036 | 161 | 693 | -0.0004058 |
| 1 | 711 | -0.0000049 | 156 | 711 | -1.0000374 | 161 | 711 | -0.0000342 |
| 291 | 001 | 0.0001961 | 315 | 001 | -0.0000499 | 316 | 001 | -0.0000507 |
| 291 | 156 | 0.0006348 | 315 | 156 | -0.0004182 | 316 | 156 | -0.0004759 |
| 291 | 161 | -0.0008220 | 315 | 161 | -0.0002931 | 316 | 161 | -0.0002561 |
| 291 | 164 | 0.0004346 | 315 | 164 | -0.0001752 | 316 | 164 | -0.0001852 |
| 291 | 172 | 0.0002990 | 315 | 172 | -0.0000905 | 316 | 172 | -0.0000931 |
| 291 | 174 | -0.0000108 | 315 | 174 | -0.0000262 | 316 | 174 | -0.0000155 |
| 291 | 291 | 0.0002420 | 315 | 291 | -0.0000999 | 316 | 291 | -0.0001059 |
| 291 | 315 | -0.0000999 | 315 | 315 | -0.0001713 | 316 | 315 | -0.0001142 |
| 291 | 316 | -0.0001059 | 315 | 316 | -0.0001142 | 316 | 316 | -0.0000857 |
| 291 | 332 | -0.0005969 | 315 | 332 | -0.0002827 | 316 | 332 | -0.0002406 |
| 291 | 336 | -0.0007993 | 315 | 336 | -0.0013706 | 316 | 336 | -0.0009137 |
| 291 | 339 | 0.0001298 | 315 | 339 | -0.0000504 | 316 | 339 | -0.0000531 |
| 291 | 357 | 0.0001700 | 315 | 357 | -0.0000912 | 316 | 357 | -0.0001001 |
| 291 | 371 | 0.0002573 | 315 | 371 | -0.0000894 | 316 | 371 | -0.0000931 |
| 291 | 372 | -0.0004376 | 315 | 372 | -0.0003011 | 316 | 372 | -0.0002445 |
| 291 | 390 | 0.0002163 | 315 | 390 | -0.0000986 | 316 | 390 | -0.0001058 |
| 291 | 683 | -0.0013683 | 315 | 683 | -0.0007380 | 316 | 683 | -0.0006190 |
| 291 | 685 | -0.0001098 | 315 | 685 | -0.0001122 | 316 | 685 | -0.0000851 |

**TABLE 1.6 (continued)**
**[B] Matrix**

60% Loading
Minimum Transmission Loss: = 689.9 MW
$\lambda = 7.6$

| Bus no. | | B | Bus no. | | B | Bus no. | | B |
|---|---|---|---|---|---|---|---|---|
| 291 | 157 | 0.0000945 | 315 | 157 | -0.0003169 | 316 | 157 | -0.0018301 |
| 291 | 182 | -0.0000095 | 315 | 182 | -0.0000302 | 316 | 182 | -0.0000160 |
| 291 | 183 | 0.0000816 | 315 | 183 | -0.0002316 | 316 | 183 | -0.0007463 |
| 291 | 285 | 0.0002835 | 315 | 285 | -0.0002371 | 316 | 285 | -0.0002849 |
| 291 | 301 | 0.0003926 | 315 | 301 | -0.0150777 | 316 | 301 | 0.0016752 |
| 291 | 327 | -0.0000950 | 315 | 327 | -0.0001963 | 316 | 327 | -0.0001233 |
| 291 | 343 | -0.0000095 | 315 | 343 | -0.0000305 | 316 | 343 | -0.0000161 |
| 291 | 359 | -0.0000095 | 315 | 359 | -0.0000305 | 316 | 359 | -0.0000161 |
| 291 | 391 | 0.0000535 | 315 | 391 | -0.0000711 | 316 | 391 | -0.0001010 |
| 291 | 427 | 0.0001978 | 315 | 427 | -0.0000505 | 316 | 427 | -0.0000513 |
| 291 | 450 | 0.0002033 | 315 | 450 | -0.0000523 | 316 | 450 | -0.0000532 |
| 291 | 687 | 0.0002695 | 315 | 687 | -0.0004874 | 316 | 687 | -0.0008436 |
| 291 | 693 | -0.0001242 | 315 | 693 | -0.0002964 | 316 | 693 | -0.0001769 |
| 291 | 711 | -0.0000095 | 315 | 711 | -0.0000338 | 316 | 711 | -0.0000170 |
| 357 | 001 | 0.0001235 | 371 | 001 | 0.0002303 | 372 | 001 | -0.0001900 |
| 357 | 156 | 0.0004792 | 371 | 156 | 0.0006387 | 372 | 156 | -0.0022135 |
| 357 | 161 | -0.0009626 | 371 | 161 | -0.0006578 | 372 | 161 | -0.0008339 |
| 357 | 164 | 0.0003040 | 371 | 164 | 0.0004638 | 372 | 164 | -0.0007620 |
| 357 | 172 | 0.0001968 | 371 | 172 | 0.0003366 | 372 | 172 | -0.0003678 |
| 357 | 174 | -0.0000097 | 371 | 174 | -0.0000098 | 372 | 174 | -0.0000384 |
| 357 | 291 | 0.0001700 | 371 | 291 | 0.0002573 | 372 | 291 | -0.0004376 |
| 357 | 315 | -0.0000912 | 371 | 315 | -0.0000894 | 372 | 315 | -0.0003011 |
| 357 | 316 | -0.0001001 | 371 | 316 | -0.0000931 | 372 | 316 | -0.0002445 |
| 357 | 332 | -0.0006423 | 371 | 332 | -0.0004939 | 372 | 332 | -0.0007634 |
| 357 | 336 | -0.0007294 | 371 | 336 | -0.0007148 | 372 | 336 | -0.0024085 |
| 357 | 339 | 0.0000901 | 371 | 339 | 0.0001394 | 372 | 339 | -0.0002169 |
| 357 | 357 | 0.0001240 | 371 | 357 | 0.0001747 | 372 | 357 | -0.0004371 |
| 357 | 371 | 0.0001747 | 371 | 371 | 0.0002818 | 372 | 371 | -0.0003741 |
| 357 | 372 | -0.0004371 | 371 | 372 | -0.0003741 | 372 | 372 | -0.0007440 |
| 357 | 390 | 0.0001547 | 371 | 390 | 0.0002268 | 372 | 390 | -0.0004452 |
| 357 | 683 | -0.0014292 | 371 | 683 | -0.0011466 | 372 | 683 | -0.0019380 |
| 357 | 685 | -0.0001043 | 371 | 685 | -0.0000962 | 372 | 685 | -0.0002449 |
| 357 | 157 | 0.0000793 | 371 | 157 | 0.0000686 | 372 | 157 | 0.0013058 |
| 357 | 182 | -0.0000085 | 371 | 182 | -0.0000086 | 372 | 182 | -0.0000376 |
| 357 | 183 | 0.0000683 | 371 | 183 | 0.0000770 | 372 | 183 | 0.0014583 |
| 357 | 285 | 0.0002199 | 371 | 285 | 0.0002799 | 372 | 285 | -0.0014774 |
| 357 | 301 | 0.0003378 | 371 | 301 | 0.0003628 | 372 | 301 | 0.0025749 |
| 357 | 327 | -0.0000859 | 371 | 327 | -0.0000854 | 372 | 327 | -0.0003139 |
| 357 | 343 | -0.0000085 | 371 | 343 | -0.0000086 | 372 | 343 | -0.0000377 |
| 357 | 359 | -0.0000085 | 371 | 359 | -0.0000086 | 372 | 359 | -0.0000377 |
| 357 | 391 | 0.0000431 | 371 | 391 | 0.0000515 | 372 | 391 | -0.0008681 |
| 357 | 427 | 0.0001247 | 371 | 427 | 0.0002322 | 372 | 427 | -0.0001991 |
| 357 | 450 | 0.0001284 | 371 | 450 | 0.0002381 | 372 | 450 | -0.0002066 |
| 357 | 687 | 0.0002209 | 371 | 687 | 0.0002564 | 372 | 687 | -0.1020036 |
| 357 | 693 | -0.0001115 | 371 | 693 | -0.0001121 | 372 | 693 | -0.0004381 |
| 357 | 711 | -0.0000084 | 371 | 711 | -0.0000086 | 372 | 711 | -0.0000390 |
| 157 | 001 | 0.0000532 | 182 | 001 | -0.0000049 | 183 | 001 | 0.0000464 |
| 157 | 156 | 0.0003367 | 182 | 156 | -0.0000378 | 183 | 156 | 0.0002889 |
| 157 | 161 | 0.0006115 | 182 | 161 | -0.0000335 | 183 | 161 | 0.0005728 |
| 157 | 164 | 0.0001666 | 182 | 164 | -0.0000167 | 183 | 164 | 0.0001445 |

**TABLE 1.6 (continued)**
**[B] Matrix**

60% Loading
Minimum Transmission Loss: = 689.9 MW
$\lambda = 7.6$

| Bus no. | | B | Bus no. | | B | Bus no. | | B |
|---|---|---|---|---|---|---|---|---|
| 157 | 172 | 0.0000928 | 182 | 172 | -0.0000088 | 183 | 172 | 0.0000808 |
| 157 | 174 | -0.0000244 | 182 | 174 | -0.0000064 | 183 | 174 | -0.0000188 |
| 157 | 291 | 0.0000945 | 182 | 291 | 0.0000095 | 183 | 291 | 0.0000818 |
| 157 | 315 | -0.0003169 | 182 | 315 | -0.0000302 | 183 | 315 | -0.0002316 |
| 157 | 316 | -0.0018301 | 182 | 316 | -0.0000160 | 183 | 316 | -0.0007463 |
| 157 | 332 | 0.0007218 | 182 | 332 | -0.0000333 | 183 | 332 | 0.0006995 |
| 157 | 336 | -0.0025355 | 182 | 336 | -0.0002415 | 183 | 336 | -0.0018527 |
| 157 | 339 | 0.0000485 | 182 | 339 | -0.0000048 | 183 | 339 | 0.0000421 |
| 157 | 357 | 0.0000793 | 182 | 357 | -0.0000085 | 183 | 357 | 0.0000683 |
| 157 | 371 | 0.0000886 | 182 | 371 | -0.0000086 | 183 | 371 | 0.0000770 |
| 157 | 372 | 0.0013058 | 182 | 372 | -0.0000376 | 183 | 372 | 0.0014583 |
| 157 | 390 | 0.0000905 | 182 | 390 | -0.0000093 | 183 | 390 | 0.0000782 |
| 157 | 683 | 0.0021569 | 182 | 683 | -0.0000 85 | 183 | 683 | 0.0021491 |
| 157 | 685 | -0.0055929 | 182 | 685 | -0.0000155 | 183 | 685 | -0.0011099 |
| 157 | 157 | 0.0000971 | 182 | 157 | -0.0000185 | 183 | 157 | 0.0000806 |
| 157 | 182 | -0.0000185 | 182 | 182 | -0.0000126 | 183 | 182 | -0.0000145 |
| 157 | 183 | 0.0000806 | 182 | 183 | -0.0000145 | 183 | 183 | 0.0000672 |
| 157 | 285 | 0.0001724 | 182 | 285 | -0.0000207 | 183 | 285 | 0.0001472 |
| 157 | 301 | 0.0005096 | 182 | 301 | -0.0001563 | 183 | 301 | 0.0004162 |
| 157 | 327 | -0.0002442 | 182 | 327 | -0.0000402 | 183 | 327 | -0.0001847 |
| 157 | 343 | -0.0000184 | 182 | 343 | -0.0000131 | 183 | 343 | -0.0000144 |
| 157 | 359 | -0.0000184 | 182 | 359 | -0.0000131 | 183 | 359 | -0.0000144 |
| 157 | 391 | 0.0000408 | 182 | 391 | -0.0000057 | 183 | 391 | 0.0000344 |
| 157 | 427 | 0.0000538 | 182 | 427 | -0.0000050 | 183 | 427 | 0.0000469 |
| 157 | 450 | 0.0000556 | 182 | 450 | -0.0000052 | 183 | 450 | 0.0000485 |
| 157 | 687 | 0.0002315 | 182 | 687 | -0.0000357 | 183 | 687 | 0.0001944 |
| 157 | 693 | -0.0002838 | 182 | 693 | -0.0000713 | 183 | 693 | -0.0002182 |
| 157 | 711 | -0.0000175 | 182 | 711 | -0.0000229 | 183 | 711 | -0.0000138 |
| 343 | 001 | -0.0000049 | 359 | 001 | -0.0000049 | 391 | 001 | 0.0000322 |
| 343 | 156 | -0.0000378 | 359 | 156 | -0.0000378 | 391 | 156 | 0.0001772 |
| 343 | 161 | -0.0000336 | 359 | 161 | -0.0000336 | 391 | 161 | 0.0009183 |
| 343 | 164 | -0.0000167 | 359 | 164 | -0.0000167 | 391 | 164 | 0.0000949 |
| 343 | 172 | -0.0000088 | 359 | 172 | -0.0000088 | 391 | 172 | 0.0000550 |
| 343 | 174 | -0.0000065 | 359 | 174 | -0.0000065 | 391 | 174 | -0.0000068 |
| 343 | 291 | -0.0000095 | 359 | 291 | -0.0000095 | 391 | 291 | 0.0000535 |
| 343 | 315 | -0.0000305 | 359 | 315 | -0.0000305 | 391 | 315 | -0.0000711 |
| 343 | 316 | -0.0000161 | 359 | 316 | -0.0000161 | 391 | 316 | -0.0001010 |
| 343 | 332 | -0.0000334 | 359 | 332 | -0.0000334 | 391 | 332 | 0.0033535 |
| 343 | 336 | -0.0002437 | 359 | 336 | -0.0002437 | 391 | 336 | -0.0005686 |
| 343 | 339 | -0.0000048 | 359 | 339 | -0.0000048 | 391 | 339 | 0.0000277 |
| 343 | 357 | -0.0000085 | 359 | 357 | -0.0000085 | 391 | 357 | 0.0000431 |
| 343 | 371 | -0.0000086 | 359 | 371 | -0.0000086 | 391 | 371 | 0.0000515 |
| 343 | 372 | -0.0000377 | 359 | 372 | -0.0000377 | 391 | 372 | -0.0008681 |
| 343 | 390 | -0.0000093 | 359 | 390 | -0.0000093 | 391 | 390 | 0.0000505 |
| 343 | 683 | -0.0000887 | 359 | 683 | -0.0000887 | 391 | 683 | -0.0153528 |
| 343 | 685 | -0.0000150 | 359 | 685 | -0.0000156 | 391 | 685 | -0.0001103 |
| 343 | 157 | -0.0000184 | 359 | 157 | -0.0000184 | 391 | 157 | 0.0000408 |
| 343 | 182 | -0.0000131 | 359 | 182 | -0.0000131 | 391 | 182 | -0.0000057 |
| 343 | 183 | -0.0000144 | 359 | 183 | -0.0000144 | 391 | 183 | 0.0000344 |
| 343 | 285 | -0.0000207 | 359 | 285 | -0.0000207 | 391 | 285 | 0.0000873 |

**TABLE 1.6 (continued)**
**[B] Matrix**

60% Loading
Minimum Transmission Loss: = 689.9 MW
$\lambda = 7.6$

| Bus no. | B | Bus no. | B | Bus no. | B |
|---|---|---|---|---|---|
| 343 | 301-0.0001547 | 359 | 301-0.0001547 | 391 | 301 0.0001928 |
| 343 | 327-0.0000407 | 359 | 327-0.0000407 | 391 | 327-0.0000630 |
| 343 | 343-0.0000136 | 359 | 343-0.0000136 | 391 | 343-0.0000056 |
| 343 | 359-0.0000136 | 359 | 359-0.0000136 | 391 | 359-0.0000056 |
| 343 | 391-0.0000056 | 359 | 391-0.0000056 | 391 | 391 0.0000192 |
| 343 | 427-0.0000050 | 359 | 427-0.0000050 | 391 | 427 0.0000326 |
| 343 | 450-0.0000052 | 359 | 450-0.0000052 | 391 | 450 0.0000337 |
| 343 | 687-0.0000356 | 359 | 687-0.0000356 | 391 | 687 0.0001043 |
| 343 | 693-0.0000725 | 359 | 693-0.0000725 | 391 | 693-0.0000788 |
| 343 | 711-0.0000245 | 359 | 711-0.0000245 | 391 | 711-0.0000055 |
| 164 | 156 0.0011318 | 172 | 156 0.0007068 | 174 | 156-0.0000438 |
| 164 | 161-0.0014164 | 172 | 161-0.0006217 | 174 | 161-0.0000355 |
| 164 | 164 0.0007808 | 172 | 164 0.0005408 | 174 | 164-0.0000190 |
| 164 | 172 0.0005408 | 172 | 172 0.0004136 | 174 | 172-0.0000099 |
| 164 | 174-0.0000190 | 172 | 174-0.0000099 | 174 | 174-0.0000047 |
| 164 | 291 0.0004346 | 172 | 291 0.0002990 | 174 | 291-0.0000108 |
| 164 | 315-0.0001752 | 172 | 315-0.0000905 | 174 | 315-0.0000262 |
| 164 | 316-0.0001852 | 172 | 316-0.0000931 | 174 | 316-0.0000155 |
| 164 | 332-0.0010342 | 172 | 332-0.0004759 | 174 | 332-0.0000348 |
| 164 | 336-0.0014014 | 172 | 336-0.0007238 | 174 | 336-0.0002094 |
| 164 | 339 0.0002334 | 172 | 339 0.0001634 | 174 | 339-0.0000055 |
| 164 | 357 0.0003040 | 172 | 357 0.0001968 | 174 | 357-0.0000097 |
| 164 | 371 0.0004638 | 172 | 371 0.0003366 | 174 | 371-0.0000098 |
| 164 | 372-0.0007620 | 172 | 372-0.0003678 | 174 | 372-0.0000384 |
| 164 | 390 0.0003878 | 172 | 390 0.0002601 | 174 | 390-0.0000106 |
| 164 | 683-0.0023753 | 172 | 683-0.0011134 | 174 | 683-0.0000919 |
| 164 | 685-0.0001919 | 172 | 685-0.0000961 | 174 | 685-0.0000151 |
| 164 | 157 0.0001668 | 172 | 157 0.0000928 | 174 | 157-0.0000244 |
| 164 | 182-0.0000167 | 172 | 182-0.0000088 | 174 | 182-0.0000064 |
| 164 | 183 0.0001445 | 172 | 183 0.0000808 | 174 | 183-0.0000188 |
| 164 | 285 0.0005042 | 172 | 285 0.0003050 | 174 | 285-0.0000243 |
| 164 | 301 0.0006917 | 172 | 301 0.0003759 | 174 | 301-0.0002633 |
| 164 | 327-0.0001668 | 172 | 327-0.0000868 | 174 | 327-0.0000322 |
| 164 | 343-0.0000167 | 172 | 343-0.0000088 | 174 | 343-0.0000065 |
| 164 | 359-0.0000167 | 172 | 359-0.0000088 | 174 | 359-0.0000065 |
| 164 | 391 0.0000949 | 172 | 391 0.0000550 | 174 | 391-0.0000068 |
| 164 | 427 0.0003596 | 172 | 427 0.0002986 | 174 | 427-0.0000056 |
| 164 | 450 0.0003694 | 172 | 450 0.0003053 | 174 | 450-0.0000058 |
| 164 | 687 0.0004767 | 172 | 687 0.0002714 | 174 | 687-0.0000443 |
| 164 | 693-0.0002181 | 172 | 693-0.0001142 | 174 | 693-0.0000520 |
| 164 | 711-0.0000166 | 172 | 711-0.0000088 | 174 | 711-0.0000080 |
| 332 | 001-0.0002494 | 336 | 001-0.0003991 | 339 | 001 0.0001086 |
| 332 | 156-0.0035851 | 336 | 156-0.0033456 | 339 | 156 0.0003341 |
| 332 | 161-0.0008991 | 336 | 161-0.0023452 | 339 | 161-0.0003970 |
| 332 | 164-0.0010342 | 336 | 164-0.0014014 | 339 | 164 0.0002334 |
| 332 | 172-0.0004759 | 336 | 172-0.0007238 | 339 | 172 0.0001634 |
| 332 | 174-0.0000348 | 336 | 174-0.0002094 | 339 | 174-0.0000055 |
| 332 | 291-0.0005969 | 336 | 291-0.0007993 | 339 | 291 0.0001298 |
| 332 | 315-0.0002827 | 336 | 315-0.0013706 | 339 | 315-0.0000504 |
| 332 | 316-0.0002406 | 336 | 316-0.0009137 | 339 | 316-0.0000531 |

**TABLE 1.6 (continued)**
**[B] Matrix**

60% Loading
Minimum Transmission Loss: = 689.9 MW
$\lambda = 7.6$

| Bus no. | B | Bus no. | B | Bus no. | B |
|---|---|---|---|---|---|
| 332 | 332-0.0008073 | 336 | 332-0.0022613 | 339 | 332-0.0002922 |
| 332 | 336-0.0022613 | 336 | 336-0.0109649 | 339 | 336-0.0004031 |
| 332 | 339-0.0002922 | 336 | 339-0.0004031 | 339 | 339 0.0000699 |
| 332 | 357-0.0006423 | 336 | 357-0.0007294 | 339 | 357 0.0000901 |
| 332 | 371-0.0004939 | 336 | 371-0.0007148 | 339 | 371 0.0001394 |
| 332 | 372-0.0007634 | 336 | 372-0.0024085 | 339 | 372-0.0002169 |
| 332 | 390-0.0006219 | 336 | 390-0.0007887 | 339 | 390 0.0001155 |
| 332 | 683-0.0020291 | 336 | 683-0.0059042 | 339 | 683-0.0006731 |
| 332 | 685-0.0002422 | 336 | 685-0.0008975 | 339 | 685-0.0000549 |
| 332 | 157 0.0007218 | 336 | 157-0.0025355 | 339 | 157 0.0000485 |
| 332 | 182-0.0000333 | 336 | 182-0.0002415 | 339 | 182-0.0000048 |
| 332 | 183 0.0006995 | 336 | 183-0.0018527 | 339 | 183 0.0000421 |
| 332 | 285-0.0029623 | 336 | 285-0.0018970 | 339 | 285 0.0001482 |
| 332 | 301 0.0019668 | 336 | 301-0.1206153 | 339 | 301 0.0002005 |
| 332 | 327-0.0002893 | 336 | 327-0.0015704 | 339 | 327-0.0000480 |
| 332 | 343-0.0000334 | 336 | 343-0.0002437 | 339 | 343-0.0000048 |
| 332 | 359-0.0000334 | 336 | 359-0.0002437 | 339 | 359-0.0000048 |
| 332 | 391 0.0033535 | 336 | 391-0.0005686 | 339 | 391 0.0000277 |
| 332 | 427-0.0002526 | 336 | 427-0.0004039 | 339 | 427 0.0001096 |
| 332 | 450-0.0002623 | 336 | 450-0.0004185 | 339 | 450 0.0001125 |
| 332 | 687 0.0040461 | 336 | 687-0.0038988 | 339 | 687 0.0001390 |
| 332 | 693-0.0003981 | 336 | 693-0.0023711 | 339 | 693-0.0000629 |
| 332 | 711-0.0000342 | 336 | 711-0.0002703 | 339 | 711-0.0000048 |
| 390 | 001 0.0001674 | 683 | 001-0.0005879 | 685 | 001-0.0000522 |
| 390 | 156 0.0005840 | 683 | 156-0.0076562 | 685 | 156-0.0004987 |
| 390 | 161-0.0008786 | 683 | 161-0.0022452 | 685 | 161-0.0002587 |
| 390 | 164 0.0003878 | 683 | 164-0.0023753 | 685 | 164-0.0001919 |
| 390 | 172 0.0002601 | 683 | 172-0.0011134 | 685 | 172-0.0000961 |
| 390 | 174-0.0000106 | 683 | 174-0.0000919 | 685 | 174-0.0000151 |
| 390 | 291 0.0002163 | 683 | 291-0.0013683 | 685 | 291-0.0001098 |
| 390 | 315-0.0000986 | 683 | 315-0.0007380 | 685 | 315-0.0001122 |
| 390 | 316-0.0001058 | 683 | 316-0.0006190 | 685 | 316-0.0000851 |
| 390 | 332-0.0006219 | 683 | 332-0.0020291 | 685 | 332-0.0002422 |
| 390 | 336-0.0007887 | 683 | 336-0.0059042 | 685 | 336-0.0008975 |
| 390 | 339 0.0001155 | 683 | 339-0.0006731 | 685 | 339-0.0000549 |
| 390 | 357 0.0001547 | 683 | 357-0.0014292 | 685 | 357-0.0001043 |
| 390 | 371 0.0002268 | 683 | 371-0.0011466 | 685 | 371-0.0000962 |
| 390 | 372-0.0004452 | 683 | 372-0.0019380 | 685 | 372-0.0002449 |
| 390 | 390 0.0001948 | 683 | 390-0.0014123 | 685 | 390-0.0001099 |
| 390 | 683-0.0014123 | 683 | 683-0.0051170 | 685 | 683-0.0006222 |
| 390 | 685-0.0001099 | 683 | 685-0.0006222 | 685 | 685-0.0000846 |
| 390 | 157 0.0000905 | 683 | 157 0.0021569 | 685 | 157-0.0055929 |
| 390 | 182-0.0000093 | 683 | 182-0.0000885 | 685 | 182-0.0000155 |
| 390 | 183 0.0000782 | 683 | 183 0.0021491 | 685 | 183-0.0011099 |
| 390 | 285 0.0002636 | 683 | 285-0.0057349 | 685 | 285-0.0003013 |
| 390 | 301 0.0003795 | 683 | 301 0.0054471 | 685 | 301 0.0014913 |
| 390 | 327-0.0000935 | 683 | 327-0.0007597 | 685 | 327-0.0001205 |
| 390 | 343-0.0000093 | 683 | 343-0.0000887 | 685 | 343-0.0000156 |
| 390 | 359-0.0000093 | 683 | 359-0.0000887 | 685 | 359-0.0000156 |
| 390 | 391 0.0000505 | 683 | 391-0.0153528 | 685 | 391-0.0001103 |

**TABLE 1.6 (continued)**
**[B] Matrix**

60% Loading
Minimum Transmission Loss: = 689.9 MW
$\lambda = 7.6$

| Bus no. | | B | Bus no. | | B | Bus no. | | B |
|---|---|---|---|---|---|---|---|---|
| 390 | 427 | 0.0001689 | 683 | 427 | -0.0005953 | 685 | 427 | -0.0000528 |
| 390 | 450 | 0.0001738 | 683 | 450 | -0.0006180 | 685 | 450 | -0.0000548 |
| 390 | 687 | 0.0002559 | 683 | 687 | 0.0155354 | 685 | 687 | -0.0009651 |
| 390 | 693 | -0.0001219 | 683 | 693 | -0.0010498 | 685 | 693 | -0.0001721 |
| 390 | 711 | -0.0000092 | 683 | 711 | -0.0000911 | 685 | 711 | -0.0000164 |
| 285 | 001 | 0.0001832 | 301 | 001 | 0.0002126 | 327 | 001 | -0.0000481 |
| 285 | 156 | 0.0008775 | 301 | 156 | 0.0014665 | 327 | 156 | -0.0003901 |
| 285 | 161 | -0.0080590 | 301 | 161 | 0.0018516 | 327 | 161 | -0.0002971 |
| 285 | 164 | 0.0005042 | 301 | 164 | 0.0006917 | 327 | 164 | -0.0001668 |
| 285 | 172 | 0.0003050 | 301 | 172 | 0.0003759 | 327 | 172 | -0.0000868 |
| 285 | 174 | -0.0000243 | 301 | 174 | -0.0002633 | 327 | 174 | -0.0000322 |
| 285 | 291 | 0.0002835 | 301 | 291 | 0.0003926 | 327 | 291 | -0.0000950 |
| 285 | 315 | -0.0002371 | 301 | 315 | -0.0150777 | 327 | 315 | -0.0001963 |
| 285 | 316 | -0.0002849 | 301 | 316 | 0.0016752 | 327 | 316 | -0.0001233 |
| 285 | 332 | -0.0029623 | 301 | 332 | 0.0019668 | 327 | 332 | -0.0002893 |
| 285 | 336 | -0.0018970 | 301 | 336 | -0.1206153 | 327 | 336 | -0.0015704 |
| 285 | 339 | 0.0001482 | 301 | 339 | 0.0002005 | 327 | 339 | -0.0000480 |
| 285 | 357 | 0.0002199 | 301 | 357 | 0.0003378 | 327 | 357 | -0.0000859 |
| 285 | 371 | 0.0002799 | 301 | 371 | 0.0003628 | 327 | 371 | -0.0000854 |
| 285 | 372 | -0.0014774 | 301 | 372 | 0.0025749 | 327 | 372 | -0.0003139 |
| 285 | 390 | 0.0002636 | 301 | 390 | 0.0003795 | 327 | 390 | -0.0000935 |
| 285 | 683 | -0.0057349 | 301 | 683 | 0.0054471 | 327 | 683 | -0.0007597 |
| 285 | 685 | -0.0003013 | 301 | 685 | 0.0014913 | 327 | 685 | -0.0001205 |
| 285 | 157 | 0.0001724 | 301 | 157 | 0.0005096 | 327 | 157 | -0.0002442 |
| 285 | 182 | -0.0000207 | 301 | 182 | -0.0001563 | 327 | 182 | -0.0000402 |
| 285 | 183 | 0.0001472 | 301 | 183 | 0.0004162 | 327 | 183 | -0.0001847 |
| 285 | 285 | 0.0004187 | 301 | 285 | 0.0007715 | 327 | 285 | -0.0002182 |
| 285 | 301 | 0.0007715 | 301 | 301 | 0.0030154 | 327 | 301 | -0.0035570 |
| 285 | 327 | -0.0002182 | 301 | 327 | -0.0035570 | 327 | 327 | -0.0002328 |
| 285 | 343 | -0.0000207 | 301 | 343 | -0.0001547 | 327 | 343 | -0.0000407 |
| 285 | 359 | -0.0000207 | 301 | 359 | -0.0001547 | 327 | 359 | -0.0000407 |
| 285 | 391 | 0.0000873 | 301 | 391 | 0.0001928 | 327 | 391 | -0.0000630 |
| 285 | 427 | 0.0001851 | 301 | 427 | 0.0002151 | 327 | 427 | -0.0000486 |
| 285 | 450 | 0.0001911 | 301 | 450 | 0.0002226 | 327 | 450 | -0.0000504 |
| 285 | 687 | 0.0004609 | 301 | 687 | 0.0011365 | 327 | 687 | -0.0004171 |
| 285 | 693 | -0.0002792 | 301 | 693 | -0.0031137 | 327 | 693 | -0.0003630 |
| 285 | 711 | -0.0000203 | 301 | 711 | -0.0001389 | 327 | 711 | -0.0000471 |
| 427 | 001 | 0.0002322 | 450 | 001 | 0.0002363 | 687 | 001 | 0.0001574 |
| 427 | 156 | 0.0004376 | 450 | 156 | 0.0004512 | 687 | 156 | 0.0009206 |
| 427 | 161 | -0.0003239 | 450 | 161 | -0.0003367 | 687 | 161 | 0.0026762 |
| 427 | 164 | 0.0003596 | 450 | 164 | 0.0003694 | 687 | 164 | 0.0004767 |
| 427 | 172 | 0.0002986 | 450 | 172 | 0.0003053 | 687 | 172 | 0.0002714 |
| 427 | 174 | -0.0000056 | 450 | 174 | -0.0000058 | 687 | 174 | -0.0000443 |
| 427 | 291 | 0.0001978 | 450 | 291 | 0.0002033 | 687 | 291 | 0.0002695 |
| 427 | 315 | -0.0000505 | 450 | 315 | -0.0000523 | 687 | 315 | -0.0004874 |
| 427 | 316 | -0.0000513 | 450 | 316 | -0.0000532 | 687 | 316 | -0.0008436 |
| 427 | 332 | -0.0002526 | 450 | 332 | -0.0002623 | 687 | 332 | 0.0040461 |
| 427 | 336 | -0.0004039 | 450 | 336 | -0.0004185 | 687 | 336 | -0.0038988 |
| 427 | 339 | 0.0001096 | 450 | 339 | 0.0001125 | 687 | 339 | 0.0001390 |

## TABLE 1.6 (continued)
## [B] Matrix

60% Loading
Minimum Transmission Loss: = 689.9 MW
$\lambda = 7.6$

| Bus no. | | B | Bus no. | | B | Bus no. | | B |
|---|---|---|---|---|---|---|---|---|
| 427 | 357 | 0.0001247 | 450 | 357 | 0.0001284 | 687 | 357 | 0.0002209 |
| 427 | 371 | 0.0002322 | 450 | 371 | 0.0002381 | 687 | 371 | 0.0002564 |
| 427 | 372 | -0.0001991 | 450 | 372 | -0.0002066 | 687 | 372 | -0.1020036 |
| 427 | 390 | 0.0001689 | 450 | 390 | 0.0001738 | 687 | 390 | 0.0002559 |
| 427 | 683 | -0.0005953 | 450 | 683 | -0.0006180 | 687 | 683 | 0.0155353 |
| 427 | 685 | -0.0000528 | 450 | 685 | -0.0000548 | 687 | 685 | -0.0009651 |
| 427 | 157 | 0.0000538 | 450 | 157 | 0.0000556 | 687 | 157 | 0.0002315 |
| 427 | 182 | -0.0000050 | 450 | 182 | -0.0000052 | 687 | 182 | -0.0000357 |
| 427 | 183 | 0.0000469 | 450 | 183 | 0.0000485 | 687 | 183 | 0.0001944 |
| 427 | 285 | 0.0001851 | 450 | 285 | 0.0001911 | 687 | 285 | 0.0004609 |
| 427 | 301 | 0.0002151 | 450 | 301 | 0.0002226 | 687 | 301 | 0.0011365 |
| 427 | 327 | -0.0000486 | 450 | 327 | -0.0000504 | 687 | 327 | -0.0004171 |
| 427 | 343 | -0.0000050 | 450 | 343 | -0.0000052 | 687 | 343 | -0.0000356 |
| 427 | 359 | -0.0000050 | 450 | 359 | -0.0000052 | 687 | 359 | -0.0000356 |
| 427 | 391 | 0.0000326 | 450 | 391 | 0.0000337 | 687 | 391 | 0.0001043 |
| 427 | 427 | 0.0002336 | 450 | 427 | 0.0002377 | 687 | 427 | 0.0001591 |
| 427 | 450 | 0.0002377 | 450 | 450 | 0.0002419 | 687 | 450 | 0.0001645 |
| 427 | 687 | 0.0001591 | 450 | 687 | 0.0001645 | 687 | 687 | 0.0005770 |
| 427 | 693 | -0.0000641 | 450 | 693 | -0.0000664 | 687 | 693 | -0.0005116 |
| 427 | 711 | -0.0000050 | 450 | 711 | -0.0000051 | 687 | 711 | -0.0000344 |

Reprinted from Energy Utilization of PSE&G for the Middle Atlantic Power Research Committee, Newark, NJ, 1976. With permission.

## TABLE 1.7
## [B] Matrix

70% Loading
Minimum Transmission Loss: = 591.9 MW
$\lambda = 8.0$

| Bus no. | | B | Bus no. | | B | Bus no. | | B |
|---|---|---|---|---|---|---|---|---|
| 1 | 001 | 0.0002047 | 156 | 001 | 0.0003660 | 161 | 001 | -0.0002310 |
| 1 | 156 | 0.0003660 | 156 | 156 | 0.0015749 | 161 | 156 | -0.0036918 |
| 1 | 161 | -0.0002310 | 156 | 161 | -0.0036918 | 161 | 161 | -0.0007452 |
| 1 | 164 | 0.0003160 | 156 | 164 | 0.0009668 | 161 | 164 | -0.0009674 |
| 1 | 172 | 0.0002628 | 156 | 172 | 0.0005998 | 161 | 172 | -0.0004420 |
| 1 | 174 | -0.0000391 | 156 | 174 | -0.0004685 | 161 | 174 | -0.0001504 |
| 1 | 291 | 0.0001606 | 156 | 291 | 0.0005248 | 161 | 291 | -0.0005809 |
| 1 | 315 | -0.0000040 | 156 | 315 | -0.0000305 | 161 | 315 | -0.0000272 |
| 1 | 316 | -0.0000040 | 156 | 316 | -0.0000308 | 161 | 316 | -0.0000267 |
| 1 | 332 | -0.0001668 | 156 | 332 | -0.0020395 | 161 | 332 | -0.0006326 |
| 1 | 336 | -0.0002858 | 156 | 336 | -0.0023614 | 161 | 336 | -0.0016897 |
| 1 | 339 | 0.0000690 | 156 | 339 | 0.0002471 | 161 | 339 | -0.0003253 |

**TABLE 1.7 (continued)**
**[B] Matrix**

70% Loading
Minimum Transmission Loss: = 591.9 MW
$\lambda = 8.0$

| Bus no. | | B | Bus no. | | B | Bus no. | | B |
|---|---|---|---|---|---|---|---|---|
| 1 | 357 | 0.0000771 | 156 | 357 | 0.0003407 | 161 | 357 | -0.0009161 |
| 1 | 371 | 0.0001959 | 156 | 371 | 0.0005358 | 161 | 371 | -0.0004665 |
| 1 | 372 | -0.0001195 | 156 | 372 | -0.0011902 | 161 | 372 | -0.0005463 |
| 1 | 390 | 0.0001166 | 156 | 390 | 0.0004462 | 161 | 390 | -0.0006907 |
| 1 | 683 | -0.0004327 | 156 | 683 | -0.0052055 | 161 | 683 | -0.0016619 |
| 1 | 685 | -0.0000919 | 156 | 685 | -0.0012334 | 161 | 685 | -0.0003266 |
| 1 | 157 | 0.0000451 | 156 | 157 | 0.0002849 | 161 | 157 | 0.0005706 |
| 1 | 182 | 0.0000313 | 156 | 182 | 0.0002170 | 161 | 182 | 0.0002776 |
| 1 | 183 | 0.0000659 | 156 | 183 | 0.0003641 | 161 | 183 | 0.0026897 |
| 1 | 285 | 0.0001778 | 156 | 285 | 0.0008026 | 161 | 285 | -0.0024348 |
| 1 | 301 | 0.0002069 | 156 | 301 | 0.0014054 | 161 | 301 | 0.0019504 |
| 1 | 327 | -0.0000118 | 156 | 327 | -0.0000913 | 161 | 327 | -0.0000790 |
| 1 | 343 | 0.0000314 | 156 | 343 | 0.0002186 | 161 | 343 | 0.0002725 |
| 1 | 359 | 0.0000314 | 156 | 359 | 0.0002186 | 161 | 359 | 0.0002725 |
| 1 | 391 | 0.0000480 | 156 | 391 | 0.0002167 | 161 | 391 | -0.0006571 |
| 1 | 427 | 0.0002059 | 156 | 427 | 0.0003698 | 161 | 427 | -0.0002339 |
| 1 | 450 | 0.0002095 | 156 | 450 | 0.0003814 | 161 | 450 | -0.0002430 |
| 1 | 687 | 0.0001505 | 156 | 687 | 0.0008513 | 161 | 687 | 0.0043183 |
| 1 | 693 | -0.0000183 | 156 | 693 | -0.0001415 | 161 | 693 | -0.0001237 |
| 1 | 711 | 0.0000318 | 156 | 711 | 0.0002386 | 161 | 711 | 0.0002266 |
| 291 | 001 | 0.0001606 | 315 | 001 | -0.0000040 | 316 | 001 | -0.0000040 |
| 291 | 156 | 0.0005248 | 315 | 156 | -0.0000305 | 316 | 156 | -0.0000308 |
| 291 | 161 | -0.0005809 | 315 | 161 | -0.0000272 | 316 | 161 | -0.0000267 |
| 291 | 164 | 0.0003656 | 315 | 164 | -0.0000135 | 316 | 164 | -0.0000136 |
| 291 | 172 | 0.0002477 | 315 | 172 | -0.0000071 | 316 | 172 | -0.0000072 |
| 291 | 174 | -0.0000899 | 315 | 174 | -0.0000065 | 316 | 174 | -0.0000064 |
| 291 | 291 | 0.0001941 | 315 | 291 | -0.0000077 | 316 | 291 | -0.0000077 |
| 291 | 315 | -0.0000077 | 315 | 315 | -0.0000139 | 316 | 315 | -0.0000093 |
| 291 | 316 | -0.0000077 | 315 | 316 | -0.0000093 | 316 | 316 | -0.0000069 |
| 291 | 332 | -0.0003865 | 315 | 332 | -0.0000270 | 316 | 332 | -0.0000264 |
| 291 | 336 | -0.0005706 | 315 | 336 | -0.0001994 | 316 | 336 | -0.0001811 |
| 291 | 339 | 0.0000884 | 315 | 339 | -0.0000039 | 316 | 339 | -0.0000039 |
| 291 | 357 | 0.0001122 | 315 | 357 | -0.0000069 | 316 | 357 | -0.0000069 |
| 291 | 371 | 0.0002100 | 315 | 371 | -0.0000070 | 316 | 371 | -0.0000070 |
| 291 | 372 | -0.0002573 | 315 | 372 | -0.0000305 | 316 | 372 | -0.0000294 |
| 291 | 390 | 0.0001558 | 315 | 390 | -0.0000075 | 316 | 390 | -0.0000076 |
| 291 | 683 | -0.0009973 | 315 | 683 | -0.0000721 | 316 | 683 | -0.0000703 |
| 291 | 685 | -0.0002194 | 315 | 685 | -0.0000130 | 316 | 685 | -0.0000128 |
| 291 | 157 | 0.0000796 | 315 | 157 | -0.0000147 | 316 | 157 | -0.0000154 |
| 291 | 182 | 0.0000578 | 315 | 182 | -0.0000226 | 316 | 182 | -0.0000252 |
| 291 | 183 | 0.0001086 | 315 | 183 | -0.0000114 | 316 | 183 | -0.0000116 |
| 291 | 285 | 0.0002621 | 315 | 285 | -0.0000166 | 316 | 285 | -0.0000168 |
| 291 | 301 | 0.0003782 | 315 | 301 | -0.0001200 | 316 | 301 | -0.0001307 |
| 291 | 327 | -0.0000229 | 315 | 327 | -0.0000264 | 316 | 327 | -0.0000199 |
| 291 | 343 | 0.0000580 | 315 | 343 | -0.0000247 | 316 | 343 | -0.0000277 |
| 291 | 359 | 0.0000580 | 315 | 359 | -0.0000247 | 316 | 359 | -0.0000277 |
| 291 | 391 | 0.0000708 | 315 | 391 | -0.0000045 | 316 | 391 | -0.0000045 |
| 291 | 427 | 0.0001621 | 315 | 427 | -0.0000040 | 316 | 427 | -0.0000040 |
| 291 | 450 | 0.0001667 | 315 | 450 | -0.0000042 | 316 | 450 | -0.0000042 |
| 291 | 687 | 0.0002511 | 315 | 687 | -0.0000284 | 316 | 687 | -0.0000292 |

## TABLE 1.7 (continued)
## [B] Matrix

70% Loading
Minimum Transmission Loss: = 591.9 MW
$\lambda = 8.0$

| Bus no. | | B | Bus no. | | B | Bus no. | | B |
|---|---|---|---|---|---|---|---|---|
| 291 | 693 | -0.0000355 | 315 | 693 | -0.0000468 | 316 | 693 | -0.0000342 |
| 291 | 711 | 0.0000608 | 315 | 711 | -0.0017779 | 316 | 711 | 0.0002535 |
| 357 | 001 | 0.0000771 | 371 | 001 | 0.0001959 | 372 | 001 | -0.0001195 |
| 357 | 156 | 0.0003407 | 371 | 156 | 0.0005358 | 372 | 156 | -0.0011902 |
| 357 | 161 | -0.0009161 | 371 | 161 | -0.0004665 | 372 | 161 | -0.0005463 |
| 357 | 164 | 0.0002063 | 371 | 164 | 0.0004012 | 372 | 164 | -0.0004428 |
| 357 | 172 | 0.0001269 | 371 | 172 | 0.0002885 | 372 | 172 | -0.0002205 |
| 357 | 174 | -0.0001107 | 371 | 174 | -0.0000754 | 372 | 174 | -0.0001172 |
| 357 | 291 | 0.0001122 | 371 | 291 | 0.0002100 | 372 | 291 | -0.0002573 |
| 357 | 315 | -0.0000069 | 371 | 315 | -0.0000070 | 372 | 315 | -0.0000305 |
| 357 | 316 | -0.0000069 | 371 | 316 | -0.0000070 | 372 | 316 | -0.0000294 |
| 357 | 332 | -0.0004832 | 371 | 332 | -0.0003230 | 372 | 332 | -0.0004903 |
| 357 | 336 | -0.0005340 | 371 | 336 | -0.0005105 | 372 | 336 | -0.0016670 |
| 357 | 339 | 0.0000530 | 371 | 339 | 0.0000939 | 372 | 339 | -0.0001355 |
| 357 | 357 | 0.0000738 | 371 | 357 | 0.0001139 | 372 | 357 | -0.0002745 |
| 357 | 371 | 0.0001139 | 371 | 371 | 0.0002359 | 372 | 371 | -0.0002225 |
| 357 | 372 | -0.0002745 | 371 | 372 | -0.0002225 | 372 | 372 | -0.0004595 |
| 357 | 390 | 0.0000960 | 371 | 390 | 0.0001631 | 372 | 390 | -0.0002700 |
| 357 | 683 | -0.0012304 | 371 | 683 | -0.0008356 | 372 | 683 | -0.0012941 |
| 357 | 685 | -0.0002965 | 371 | 685 | -0.0001807 | 372 | 685 | -0.0002472 |
| 357 | 157 | 0.0000630 | 371 | 157 | 0.0000751 | 372 | 157 | 0.0042227 |
| 357 | 182 | 0.0000483 | 371 | 182 | 0.0000535 | 372 | 182 | 0.0004414 |
| 357 | 183 | 0.0000798 | 371 | 183 | 0.0001053 | 372 | 183 | -0.0007599 |
| 357 | 285 | 0.0001740 | 371 | 285 | 0.0002650 | 372 | 285 | -0.0006816 |
| 357 | 301 | 0.0003126 | 371 | 301 | 0.0003513 | 372 | 301 | 0.0035149 |
| 357 | 327 | -0.0000205 | 371 | 327 | -0.0000207 | 372 | 327 | -0.0000866 |
| 357 | 343 | 0.0000487 | 371 | 343 | 0.0000536 | 372 | 343 | 0.0004184 |
| 357 | 359 | 0.0000487 | 371 | 359 | 0.0000536 | 372 | 359 | 0.0004184 |
| 357 | 391 | 0.0000470 | 371 | 391 | 0.0000716 | 372 | 391 | -0.0001840 |
| 357 | 427 | 0.0000779 | 371 | 427 | 0.0001976 | 372 | 427 | -0.0001210 |
| 357 | 450 | 0.0000803 | 371 | 450 | 0.0002026 | 372 | 450 | -0.0001255 |
| 357 | 687 | 0.0001869 | 371 | 687 | 0.0002421 | 372 | 687 | -0.0022032 |
| 357 | 693 | -0.0000318 | 371 | 693 | -0.0000322 | 372 | 693 | -0.0001366 |
| 357 | 711 | 0.0000535 | 371 | 711 | 0.0000554 | 372 | 711 | 0.0002653 |
| 157 | 001 | 0.0000451 | 182 | 001 | 0.0000313 | 183 | 001 | 0.0000659 |
| 157 | 156 | 0.0002849 | 182 | 156 | 0.0002170 | 183 | 156 | 0.0003641 |
| 157 | 161 | 0.0005706 | 182 | 161 | 0.0002776 | 183 | 161 | 0.0026897 |
| 157 | 164 | 0.0001421 | 182 | 164 | 0.0001023 | 183 | 164 | 0.0001960 |
| 157 | 172 | 0.0000789 | 182 | 172 | 0.0000555 | 183 | 172 | 0.0001129 |
| 157 | 174 | 0.0001977 | 182 | 174 | 0.0000747 | 183 | 174 | -0.0008150 |
| 157 | 291 | 0.0000796 | 182 | 291 | 0.0000578 | 183 | 291 | 0.0001086 |
| 157 | 315 | -0.0000147 | 182 | 315 | -0.0000226 | 183 | 315 | -0.0000114 |
| 157 | 316 | -0.0000154 | 182 | 316 | -0.0000252 | 183 | 316 | -0.0000116 |
| 157 | 332 | 0.0007808 | 182 | 332 | 0.0003049 | 183 | 332 | -0.0044376 |
| 157 | 336 | -0.0016169 | 182 | 336 | -0.0081826 | 183 | 336 | -0.0009865 |
| 157 | 339 | 0.0000394 | 182 | 339 | 0.0000290 | 183 | 339 | 0.0000528 |
| 157 | 357 | 0.0000630 | 182 | 357 | 0.0000483 | 183 | 357 | 0.0000798 |
| 157 | 371 | 0.0000751 | 182 | 371 | 0.0000535 | 183 | 371 | 0.0001053 |
| 157 | 372 | 0.0042226 | 182 | 372 | 0.0004414 | 183 | 372 | -0.0007599 |
| 157 | 390 | 0.0000742 | 182 | 390 | 0.0000551 | 183 | 390 | 0.0000979 |

**TABLE 1.7 (continued)**
**[B] Matrix**

70% Loading
Minimum Transmission Loss: = 591.9 MW
$\lambda = 8.0$

| Bus no. | | B | Bus no. | | B | Bus no. | | B |
|---|---|---|---|---|---|---|---|---|
| 157 | 683 | 0.0021618 | 182 | 683 | 0.0008211 | 183 | 683 | -0.0093527 |
| 157 | 685 | 0.0003209 | 182 | 685 | 0.0001402 | 183 | 685 | 0.0098334 |
| 157 | 157 | 0.0000823 | 182 | 157 | 0.0000766 | 183 | 157 | 0.0000852 |
| 157 | 182 | 0.0000766 | 182 | 182 | 0.0000822 | 183 | 182 | 0.0000712 |
| 157 | 183 | 0.0000852 | 182 | 183 | 0.0000712 | 183 | 183 | 0.0000976 |
| 157 | 285 | 0.0001511 | 182 | 285 | 0.0001165 | 183 | 285 | 0.0001901 |
| 157 | 301 | 0.0004732 | 182 | 301 | 0.0004888 | 183 | 301 | 0.0004518 |
| 157 | 327 | -0.0000457 | 182 | 327 | -0.0000756 | 183 | 327 | -0.0000345 |
| 157 | 343 | 0.0000784 | 182 | 343 | 0.0000853 | 183 | 343 | 0.0000723 |
| 157 | 359 | 0.0000784 | 182 | 359 | 0.0000853 | 183 | 359 | 0.0000723 |
| 157 | 391 | 0.0000408 | 182 | 391 | 0.0000315 | 183 | 391 | 0.0000513 |
| 157 | 427 | 0.0000456 | 182 | 427 | 0.0000317 | 183 | 427 | 0.0000667 |
| 157 | 450 | 0.0000472 | 182 | 450 | 0.0000328 | 183 | 450 | 0.0000689 |
| 157 | 687 | 0.0002058 | 182 | 687 | 0.0001746 | 183 | 687 | 0.0002323 |
| 157 | 693 | -0.0000698 | 182 | 693 | -0.0001125 | 183 | 693 | -0.0000531 |
| 157 | 711 | 0.0001071 | 182 | 711 | 0.0001488 | 183 | 711 | 0.0000865 |
| 343 | 001 | 0.0000314 | 359 | 001 | 0.0000314 | 391 | 001 | 0.0000480 |
| 343 | 156 | 0.0002186 | 359 | 156 | 0.0002186 | 391 | 156 | 0.0002167 |
| 343 | 161 | 0.0002725 | 359 | 161 | 0.0002725 | 391 | 161 | -0.0006571 |
| 343 | 164 | 0.0001027 | 359 | 164 | 0.0001027 | 391 | 164 | 0.0001299 |
| 343 | 172 | 0.0000556 | 359 | 172 | 0.0000556 | 391 | 172 | 0.0000794 |
| 343 | 174 | 0.0000726 | 359 | 174 | 0.0000726 | 391 | 174 | -0.0000758 |
| 343 | 291 | 0.0000580 | 359 | 291 | 0.0000580 | 391 | 291 | 0.0000708 |
| 343 | 315 | -0.0000247 | 359 | 315 | -0.0000247 | 391 | 315 | -0.0000045 |
| 343 | 316 | -0.0000277 | 359 | 316 | -0.0000277 | 391 | 316 | -0.0000045 |
| 343 | 332 | 0.0002967 | 359 | 332 | 0.0002967 | 391 | 332 | -0.0003317 |
| 343 | 336 | -0.0140024 | 359 | 336 | -0.0140024 | 391 | 336 | -0.0003520 |
| 343 | 339 | 0.0000291 | 359 | 339 | 0.0000291 | 391 | 339 | 0.0000335 |
| 343 | 357 | 0.0000487 | 359 | 357 | 0.0000487 | 391 | 357 | 0.0000470 |
| 343 | 371 | 0.0000536 | 359 | 371 | 0.0000536 | 391 | 371 | 0.0000716 |
| 343 | 372 | 0.0004184 | 359 | 372 | 0.0004184 | 391 | 372 | -0.0001840 |
| 343 | 390 | 0.0000554 | 359 | 390 | 0.0000554 | 391 | 390 | 0.0000608 |
| 343 | 683 | 0.0007982 | 359 | 683 | 0.0007982 | 391 | 683 | -0.0008428 |
| 343 | 685 | 0.0001370 | 359 | 685 | 0.0001370 | 391 | 685 | -0.0002063 |
| 343 | 157 | 0.0000784 | 359 | 157 | 0.0000784 | 391 | 157 | 0.0000408 |
| 343 | 182 | 0.0000853 | 359 | 182 | 0.0000853 | 391 | 182 | 0.0000315 |
| 343 | 183 | 0.0000723 | 359 | 183 | 0.0000723 | 391 | 183 | 0.0000513 |
| 343 | 285 | 0.0001175 | 359 | 285 | 0.0001175 | 391 | 285 | 0.0001109 |
| 343 | 301 | 0.0005057 | 359 | 301 | 0.0005057 | 391 | 301 | 0.0002032 |
| 343 | 327 | -0.0000832 | 359 | 327 | -0.0000832 | 391 | 327 | -0.0000135 |
| 343 | 343 | 0.0000887 | 359 | 343 | 0.0000887 | 391 | 343 | 0.0000317 |
| 343 | 359 | 0.0000887 | 359 | 359 | 0.0000887 | 391 | 359 | 0.0000317 |
| 343 | 391 | 0.0000317 | 359 | 391 | 0.0000317 | 391 | 391 | 0.0000299 |
| 343 | 427 | 0.0000317 | 359 | 427 | 0.0000317 | 391 | 427 | 0.0000485 |
| 343 | 450 | 0.0000328 | 359 | 450 | 0.0000328 | 391 | 450 | 0.0000501 |
| 343 | 687 | 0.0001774 | 359 | 687 | 0.0001774 | 391 | 687 | 0.0001203 |
| 343 | 693 | -0.0001234 | 359 | 693 | -0.0001234 | 391 | 693 | -0.0000208 |
| 343 | 711 | 0.0001595 | 359 | 711 | 0.0001595 | 391 | 711 | 0.0000350 |
| 164 | 001 | 0.0003160 | 172 | 001 | 0.0002628 | 174 | 001 | -0.0000391 |
| 164 | 156 | 0.0009668 | 172 | 156 | 0.0005998 | 174 | 156 | -0.0004685 |

## TABLE 1.7 (continued)
## [B] Matrix

70% Loading
Minimum Transmission Loss: = 591.9 MW
$\lambda = 8.0$

| Bus no. | B | Bus no. | B | Bus no. | B |
|---|---|---|---|---|---|
| 164 | 161-0.0009674 | 172 | 161-0.0004420 | 174 | 161-0.0001504 |
| 164 | 164 0.0006924 | 172 | 164 0.0004795 | 174 | 164-0.0001527 |
| 164 | 172 0.0004795 | 172 | 172 0.0003667 | 174 | 172-0.0000733 |
| 164 | 174-0.0001527 | 172 | 174-0.0000733 | 174 | 174-0.0000312 |
| 164 | 291 0.0003656 | 172 | 291 0.0002477 | 174 | 291-0.0000899 |
| 164 | 315-0.0000135 | 172 | 315-0.0000071 | 174 | 315-0.0000065 |
| 164 | 316-0.0000136 | 172 | 316-0.0000072 | 174 | 316-0.0000064 |
| 164 | 332-0.0006552 | 172 | 332-0.0003133 | 174 | 332-0.0001310 |
| 164 | 336-0.0009962 | 172 | 336-0.0005171 | 174 | 336-0.0003871 |
| 164 | 339 0.0001654 | 172 | 339 0.0001088 | 174 | 339-0.0000485 |
| 164 | 357 0.0002063 | 172 | 357 0.0001269 | 174 | 357-0.0001107 |
| 164 | 371 0.0004012 | 172 | 371 0.0002885 | 174 | 371-0.0000754 |
| 164 | 372-0.0004428 | 172 | 372-0.0002205 | 174 | 372-0.0001172 |
| 164 | 390 0.0002898 | 172 | 390 0.0001865 | 174 | 390-0.0000992 |
| 164 | 683-0.0016925 | 172 | 683-0.0008117 | 174 | 683-0.0003448 |
| 164 | 685-0.0003696 | 172 | 685-0.0001738 | 174 | 685-0.0000669 |
| 164 | 157 0.0001421 | 172 | 157 0.0000789 | 174 | 157 0.0001977 |
| 164 | 182 0.0001023 | 172 | 182 0.0000555 | 174 | 182 0.0000747 |
| 164 | 183 0.0001960 | 172 | 183 0.0001129 | 174 | 183-0.0008150 |
| 164 | 285 0.0004810 | 172 | 285 0.0002941 | 174 | 285-0.0002808 |
| 164 | 301 0.0006707 | 172 | 301 0.0003654 | 174 | 301 0.0005429 |
| 164 | 327-0.0000402 | 172 | 327-0.0000212 | 174 | 327-0.0000188 |
| 164 | 343 0.0001027 | 172 | 343 0.0000556 | 174 | 343 0.0000726 |
| 164 | 359 0.0001027 | 172 | 359 0.0000556 | 174 | 359 0.0000726 |
| 164 | 391 0.0001299 | 172 | 391 0.0000794 | 174 | 391-0.0000758 |
| 164 | 427 0.0003189 | 172 | 427 0.0002648 | 174 | 427-0.0000396 |
| 164 | 450 0.0003276 | 172 | 450 0.0002707 | 174 | 450-0.0000411 |
| 164 | 687 0.0004522 | 172 | 687 0.0002588 | 174 | 687-0.0067349 |
| 164 | 693-0.0000624 | 172 | 693-0.0000329 | 174 | 693-0.0000296 |
| 164 | 711 0.0001070 | 172 | 711 0.0000568 | 174 | 711 0.0000553 |
| 332 | 001-0.0001668 | 336 | 001-0.0002858 | 339 | 001 0.0000690 |
| 332 | 156-0.0020395 | 336 | 156-0.0023614 | 339 | 156 0.0002471 |
| 332 | 161-0.0006326 | 336 | 161-0.0016897 | 339 | 161-0.0003258 |
| 332 | 164-0.0006552 | 336 | 164-0.0009962 | 339 | 164 0.0001654 |
| 332 | 172-0.0003133 | 336 | 172-0.0005171 | 339 | 172 0.0001088 |
| 332 | 174-0.0001310 | 336 | 174-0.0003871 | 339 | 174-0.0000485 |
| 332 | 291-0.0003865 | 336 | 291-0.0005706 | 339 | 291 0.0000884 |
| 332 | 315-0.0000270 | 336 | 315-0.0001994 | 339 | 315-0.0000039 |
| 332 | 316-0.0000264 | 336 | 316-0.0001811 | 339 | 316-0.0000039 |
| 332 | 332-0.0005496 | 336 | 332-0.0016086 | 339 | 332-0.0002092 |
| 332 | 336-0.0016086 | 336 | 336-0.0078749 | 339 | 336-0.0002929 |
| 332 | 339-0.0002092 | 336 | 339-0.0002929 | 339 | 339 0.0000407 |
| 332 | 357-0.0004832 | 336 | 357-0.0005340 | 339 | 357 0.0000530 |
| 332 | 371-0.0003230 | 336 | 371-0.0005105 | 339 | 371 0.0000939 |
| 332 | 372-0.0004903 | 336 | 372-0.0016670 | 339 | 372-0.0001355 |
| 332 | 390-0.0004284 | 336 | 390-0.0005697 | 339 | 390 0.0000723 |
| 332 | 683-0.0014465 | 336 | 683-0.0042690 | 339 | 683-0.0005386 |
| 332 | 685-0.0002810 | 336 | 685-0.0007903 | 339 | 685-0.0001202 |
| 332 | 157 0.0007808 | 336 | 157-0.0016169 | 339 | 157 0.0000394 |
| 332 | 182 0.0003049 | 336 | 182-0.0081826 | 339 | 182 0.0000290 |

**TABLE 1.7 (continued)**
**[B] Matrix**

70% Loading
Minimum Transmission Loss: = 591.9 MW
$\lambda = 8.0$

| Bus no. | | B | Bus no. | | B | Bus no. | | B |
|---|---|---|---|---|---|---|---|---|
| 332 | 183 | -0.0044376 | 336 | 183 | -0.0009865 | 339 | 183 | 0.0000528 |
| 332 | 285 | -0.0012288 | 336 | 285 | -0.0013038 | 339 | 285 | 0.0001242 |
| 332 | 301 | 0.0022075 | 336 | 301 | -0.0238501 | 339 | 301 | 0.0001890 |
| 332 | 327 | -0.0000779 | 336 | 327 | -0.0005306 | 339 | 327 | -0.0000117 |
| 332 | 343 | 0.0002967 | 336 | 343 | -0.0140024 | 339 | 343 | 0.0000291 |
| 332 | 359 | 0.0002967 | 336 | 359 | -0.0140024 | 339 | 359 | 0.0000291 |
| 332 | 391 | -0.0003317 | 336 | 391 | -0.0003520 | 339 | 391 | 0.0000335 |
| 332 | 427 | -0.0001689 | 336 | 427 | -0.0002892 | 339 | 427 | 0.0000697 |
| 332 | 450 | -0.0001753 | 336 | 450 | -0.0002997 | 339 | 450 | 0.0000717 |
| 332 | 687 | -0.1374043 | 336 | 687 | -0.0025308 | 339 | 687 | 0.0001225 |
| 332 | 693 | -0.0001223 | 336 | 693 | -0.0008548 | 339 | 693 | -0.0000181 |
| 332 | 711 | 0.0002283 | 336 | 711 | 0.0020322 | 339 | 711 | 0.0000308 |
| 390 | 001 | 0.0001166 | 683 | 001 | -0.0004327 | 685 | 001 | -0.0000919 |
| 390 | 156 | 0.0004462 | 683 | 156 | -0.0052055 | 685 | 156 | -0.0012334 |
| 390 | 161 | -0.0006907 | 683 | 161 | -0.0016619 | 685 | 161 | -0.0003266 |
| 390 | 164 | 0.0002898 | 683 | 164 | -0.0016925 | 685 | 164 | -0.0003696 |
| 390 | 172 | 0.0001865 | 683 | 172 | -0.0008117 | 685 | 172 | -0.0001738 |
| 390 | 174 | -0.0000992 | 683 | 174 | -0.0003448 | 685 | 174 | -0.0000669 |
| 390 | 291 | 0.0001558 | 683 | 291 | -0.0009973 | 685 | 291 | -0.0002194 |
| 390 | 315 | -0.0000075 | 683 | 315 | -0.0000721 | 685 | 315 | -0.0000130 |
| 390 | 316 | -0.0000076 | 683 | 316 | -0.0000703 | 685 | 316 | -0.0000128 |
| 390 | 332 | -0.0004284 | 683 | 332 | -0.0014465 | 685 | 332 | -0.0002810 |
| 390 | 336 | -0.0005697 | 683 | 336 | -0.0042690 | 685 | 336 | -0.0007903 |
| 390 | 339 | 0.0000723 | 683 | 339 | -0.0005386 | 685 | 339 | -0.0001202 |
| 390 | 357 | 0.0000960 | 683 | 357 | -0.0012304 | 685 | 357 | -0.0002965 |
| 390 | 371 | 0.0001631 | 683 | 371 | -0.0008356 | 685 | 371 | -0.0001807 |
| 390 | 372 | -0.0002700 | 683 | 372 | -0.0012941 | 685 | 372 | -0.0002472 |
| 390 | 390 | 0.0001291 | 683 | 390 | -0.0011004 | 685 | 390 | -0.0002493 |
| 390 | 683 | -0.0011004 | 683 | 683 | -0.0038081 | 685 | 683 | -0.0007390 |
| 390 | 685 | -0.0002493 | 683 | 685 | -0.0007390 | 685 | 685 | -0.0001443 |
| 390 | 157 | 0.0000742 | 683 | 157 | 0.0021618 | 685 | 157 | 0.0003209 |
| 390 | 182 | 0.0000551 | 683 | 182 | 0.0008211 | 685 | 182 | 0.0001402 |
| 390 | 183 | 0.0000979 | 683 | 183 | -0.0093527 | 685 | 183 | 0.0098334 |
| 390 | 285 | 0.0002253 | 683 | 285 | -0.0031221 | 685 | 285 | -0.0007643 |
| 390 | 301 | 0.0003588 | 683 | 301 | 0.0059653 | 685 | 301 | 0.0010001 |
| 390 | 327 | -0.0000225 | 683 | 327 | -0.0002076 | 685 | 327 | -0.0000377 |
| 390 | 343 | 0.0000554 | 683 | 343 | 0.0007982 | 685 | 343 | 0.0001370 |
| 390 | 359 | 0.0000554 | 683 | 359 | 0.0007982 | 685 | 359 | 0.0001370 |
| 390 | 391 | 0.0000608 | 683 | 391 | -0.0008428 | 685 | 391 | -0.0002063 |
| 390 | 427 | 0.0001178 | 683 | 427 | -0.0004381 | 685 | 427 | -0.0000930 |
| 390 | 450 | 0.0001213 | 683 | 450 | -0.0004547 | 685 | 450 | -0.0000966 |
| 390 | 687 | 0.0002276 | 683 | 687 | -0.0855023 | 685 | 687 | 0.0046918 |
| 390 | 693 | -0.0000348 | 683 | 693 | -0.0003258 | 685 | 693 | -0.0000591 |
| 390 | 711 | 0.0000592 | 683 | 711 | 0.0006093 | 685 | 711 | 0.0001093 |
| 285 | 001 | 0.0001778 | 301 | 001 | 0.0002069 | 327 | 001 | -0.0000118 |
| 285 | 156 | 0.0008026 | 301 | 156 | 0.0014054 | 327 | 156 | -0.0000913 |
| 285 | 161 | -0.0024348 | 301 | 161 | 0.0019504 | 327 | 161 | -0.0000790 |
| 285 | 164 | 0.0004810 | 301 | 164 | 0.0006707 | 327 | 164 | -0.0000402 |
| 285 | 172 | 0.0002941 | 301 | 172 | 0.0003654 | 327 | 172 | -0.0000212 |
| 285 | 174 | -0.0002808 | 301 | 174 | 0.0005429 | 327 | 174 | -0.0000188 |

## TABLE 1.7 (continued)
## [B] Matrix

70% Loading
Minimum Transmission Loss: = 591.9 MW
$\lambda = 8.0$

| Bus no. | | B | Bus no. | | B | Bus no. | | B |
|---|---|---|---|---|---|---|---|---|
| 285 | 291 | 0.0002621 | 301 | 291 | 0.0003782 | 327 | 291 | -0.0000229 |
| 285 | 315 | -0.0000166 | 301 | 315 | -0.0001200 | 327 | 315 | 0.0000264 |
| 285 | 316 | -0.0000168 | 301 | 316 | -0.0001307 | 327 | 316 | -0.0000199 |
| 285 | 332 | -0.0012288 | 301 | 332 | 0.0022075 | 327 | 332 | -0.0000779 |
| 285 | 336 | -0.0013038 | 301 | 336 | -0.0238501 | 327 | 336 | -0.0005306 |
| 285 | 339 | 0.0001242 | 301 | 339 | 0.0001890 | 327 | 339 | -0.0000117 |
| 285 | 357 | 0.0001740 | 301 | 357 | 0.0003126 | 327 | 357 | -0.0000205 |
| 285 | 371 | 0.0002650 | 301 | 371 | 0.0003513 | 327 | 371 | -0.0000207 |
| 285 | 372 | -0.0006816 | 301 | 372 | 0.0035149 | 327 | 372 | -0.0000866 |
| 285 | 390 | 0.0002253 | 301 | 390 | 0.0003588 | 327 | 390 | -0.0000225 |
| 285 | 683 | -0.0031221 | 301 | 683 | 0.0059653 | 327 | 683 | -0.0002076 |
| 285 | 685 | -0.0007643 | 301 | 685 | 0.0010001 | 327 | 685 | -0.0000377 |
| 285 | 157 | 0.0001511 | 301 | 157 | 0.0004732 | 327 | 157 | -0.0000457 |
| 285 | 182 | 0.0001165 | 301 | 182 | 0.0004888 | 327 | 182 | -0.0000756 |
| 285 | 183 | 0.0001901 | 301 | 183 | 0.0004518 | 327 | 183 | -0.0000345 |
| 285 | 285 | 0.0004107 | 301 | 285 | 0.0007527 | 327 | 285 | -0.0000499 |
| 285 | 301 | 0.0007527 | 301 | 301 | 0.0029392 | 327 | 301 | -0.0003905 |
| 285 | 327 | -0.0000499 | 301 | 327 | -0.0003905 | 327 | 327 | -0.0000576 |
| 285 | 343 | 0.0001175 | 301 | 343 | 0.0005057 | 327 | 343 | -0.0000832 |
| 285 | 359 | 0.0001175 | 301 | 359 | 0.0005057 | 327 | 359 | -0.0000832 |
| 285 | 391 | 0.0001109 | 301 | 391 | 0.0002032 | 327 | 391 | -0.0000135 |
| 285 | 427 | 0.0001797 | 301 | 427 | 0.0002093 | 327 | 427 | -0.0000119 |
| 285 | 450 | 0.0001854 | 301 | 450 | 0.0002166 | 327 | 450 | -0.0000124 |
| 285 | 687 | 0.0004455 | 301 | 687 | 0.0011037 | 327 | 687 | -0.0000867 |
| 285 | 693 | -0.0000772 | 301 | 693 | -0.0005870 | 327 | 693 | -0.0000985 |
| 285 | 711 | 0.0001297 | 301 | 711 | 0.0008178 | 327 | 711 | 0.1000663 |
| 427 | 001 | 0.0002059 | 450 | 001 | 0.0002095 | 687 | 001 | 0.0001505 |
| 427 | 156 | 0.0003698 | 450 | 156 | 0.0003814 | 687 | 156 | 0.0008513 |
| 427 | 161 | -0.0002339 | 450 | 161 | -0.0002430 | 687 | 161 | 0.0043182 |
| 427 | 164 | 0.0003189 | 450 | 164 | 0.0003276 | 687 | 164 | 0.0004522 |
| 427 | 172 | 0.0002648 | 450 | 172 | 0.0002707 | 687 | 172 | 0.0002588 |
| 427 | 174 | -0.0000396 | 450 | 174 | -0.0000411 | 687 | 174 | -0.0067349 |
| 427 | 291 | 0.0001621 | 450 | 291 | 0.0001667 | 687 | 291 | 0.0002511 |
| 427 | 315 | -0.0000040 | 450 | 315 | -0.0000042 | 687 | 315 | -0.0000284 |
| 427 | 316 | -0.0000040 | 450 | 316 | -0.0000042 | 687 | 316 | -0.0000292 |
| 427 | 332 | -0.0001689 | 450 | 332 | -0.0001753 | 687 | 332 | -0.1374079 |
| 427 | 336 | -0.0002892 | 450 | 336 | -0.0002997 | 687 | 336 | -0.0025308 |
| 427 | 339 | 0.0000697 | 450 | 339 | 0.0000717 | 687 | 339 | 0.0001225 |
| 427 | 357 | 0.0000779 | 450 | 357 | 0.0000803 | 687 | 357 | 0.0001869 |
| 427 | 371 | 0.0001976 | 450 | 371 | 0.0002026 | 687 | 371 | 0.0002421 |
| 427 | 372 | -0.0001210 | 450 | 372 | -0.0001255 | 687 | 372 | -0.0022032 |
| 427 | 390 | 0.0001178 | 450 | 390 | 0.0001213 | 687 | 390 | 0.0002276 |
| 427 | 683 | -0.0004381 | 450 | 683 | -0.0004547 | 687 | 683 | -0.0855033 |
| 427 | 685 | -0.0000930 | 450 | 685 | -0.0000966 | 687 | 685 | 0.0046918 |
| 427 | 157 | 0.0000456 | 450 | 157 | 0.0000472 | 687 | 157 | 0.0002058 |
| 427 | 182 | 0.0000317 | 450 | 182 | 0.0000328 | 687 | 182 | 0.0001746 |
| 427 | 183 | 0.0000667 | 450 | 183 | 0.0000689 | 687 | 183 | 0.0002323 |
| 427 | 285 | 0.0001797 | 450 | 285 | 0.0001854 | 687 | 285 | 0.0004455 |
| 427 | 301 | 0.0002093 | 450 | 301 | 0.0002166 | 687 | 301 | 0.0011037 |
| 427 | 327 | -0.0000119 | 450 | 327 | -0.0000124 | 687 | 327 | -0.0000867 |

**TABLE 1.7 (continued)**
**[B] Matrix**

70% Loading
Minimum Transmission Loss: = 591.9 MW
$\lambda = 8.0$

| Bus no. | | B | Bus no. | | B | Bus no. | | B |
|---|---|---|---|---|---|---|---|---|
| 427 | 343 | 0.0000317 | 450 | 343 | 0.0000328 | 687 | 343 | 0.0001774 |
| 427 | 359 | 0.0000317 | 450 | 359 | 0.0000328 | 687 | 359 | 0.0001774 |
| 427 | 391 | 0.0000485 | 450 | 391 | 0.0000501 | 687 | 391 | 0.0001203 |
| 427 | 427 | 0.0002071 | 450 | 427 | 0.0002108 | 687 | 427 | 0.0001522 |
| 427 | 450 | 0.0002108 | 450 | 450 | 0.0002145 | 687 | 450 | 0.0001573 |
| 427 | 687 | 0.0001522 | 450 | 687 | 0.0001573 | 687 | 687 | 0.0005540 |
| 427 | 693 | -0.0000186 | 450 | 693 | -0.0000192 | 687 | 693 | -0.0001334 |
| 427 | 711 | 0.0000321 | 450 | 711 | 0.0000333 | 687 | 711 | 0.0002158 |

Reprinted from Energy Utilization of PSE&G for the Middle Atlantic Power Research Committee, Newark, NJ, 1976. With permission.

**TABLE 1.8**
**[B] Matrix**

80% Loading
Minimum Transmission Loss: = 328.4 MW
$\lambda = 8.3$

| Bus no. | | B | Bus no. | | B | Bus no. | | B |
|---|---|---|---|---|---|---|---|---|
| 1 | 001 | 0.0001822 | 156 | 001 | 0.0003117 | 161 | 001 | -0.0001896 |
| 1 | 156 | 0.0003117 | 156 | 156 | 0.0013336 | 161 | 156 | -0.0029533 |
| 1 | 161 | -0.0001896 | 156 | 161 | -0.0029533 | 161 | 161 | -0.0006152 |
| 1 | 164 | 0.0002812 | 156 | 164 | 0.0008311 | 161 | 164 | -0.0007796 |
| 1 | 172 | 0.0002338 | 156 | 172 | 0.0005127 | 161 | 172 | -0.0003609 |
| 1 | 174 | -0.0000822 | 156 | 174 | -0.0076308 | 161 | 174 | -0.0001874 |
| 1 | 291 | 0.0001277 | 156 | 291 | 0.0004305 | 161 | 291 | -0.0004931 |
| 1 | 315 | 0.0000134 | 156 | 315 | 0.0000983 | 161 | 315 | 0.0001019 |
| 1 | 316 | 0.0000134 | 156 | 316 | 0.0000945 | 161 | 316 | 0.0001111 |
| 1 | 332 | -0.0001281 | 156 | 332 | -0.0014889 | 161 | 332 | -0.0005030 |
| 1 | 336 | -0.0002251 | 156 | 336 | -0.0018500 | 161 | 336 | -0.0013414 |
| 1 | 339 | 0.0000275 | 156 | 339 | 0.0001364 | 161 | 339 | -0.0010015 |
| 1 | 357 | 0.0000313 | 156 | 357 | 0.0001763 | 161 | 357 | 0.0009736 |
| 1 | 371 | 0.0001652 | 156 | 371 | 0.0004509 | 161 | 371 | -0.0003849 |
| 1 | 372 | -0.0000833 | 156 | 372 | -0.0007876 | 161 | 372 | -0.0004029 |
| 1 | 390 | 0.0000695 | 156 | 390 | 0.0003109 | 161 | 390 | -0.0008583 |
| 1 | 683 | -0.0003476 | 156 | 683 | -0.0040756 | 161 | 683 | -0.0013543 |
| 1 | 685 | -0.0001392 | 156 | 685 | -0.0048820 | 161 | 685 | -0.0003523 |
| 1 | 157 | 0.0000272 | 156 | 157 | 0.0001805 | 161 | 157 | 0.0002820 |
| 1 | 182 | 0.0000429 | 156 | 182 | 0.0002814 | 161 | 182 | 0.0004604 |
| 1 | 183 | 0.0000674 | 156 | 183 | 0.0003515 | 161 | 183 | -0.0217406 |
| 1 | 285 | 0.0001645 | 156 | 285 | 0.0007132 | 161 | 285 | -0.0016808 |
| 1 | 301 | 0.0001920 | 156 | 301 | 0.0012900 | 161 | 301 | 0.0018885 |
| 1 | 327 | -0.0000008 | 156 | 327 | -0.0000062 | 161 | 327 | -0.0000056 |
| 1 | 343 | 0.0000429 | 156 | 343 | 0.0002846 | 161 | 343 | 0.0004438 |

## TABLE 1.8 (continued)
## [B] Matrix

80% Loading
Minimum Transmission Loss: = 328.4 MW
$\lambda = 8.3$

| Bus no. | | B | Bus no. | | B | Bus no. | | B |
|---|---|---|---|---|---|---|---|---|
| 1 | 359 | 0.0000429 | 156 | 359 | 0.0002846 | 161 | 359 | 0.0004438 |
| 1 | 391 | 0.0000477 | 156 | 391 | 0.0002004 | 161 | 391 | -0.0004126 |
| 1 | 427 | 0.0001832 | 156 | 427 | 0.0003150 | 161 | 427 | -0.0001920 |
| 1 | 450 | 0.0001864 | 156 | 450 | 0.0003249 | 161 | 450 | -0.0001994 |
| 1 | 687 | 0.0001349 | 156 | 687 | 0.0007505 | 161 | 687 | 0.0051722 |
| 1 | 693 | -0.0000014 | 156 | 693 | -0.0000104 | 161 | 693 | -0.0000095 |
| 1 | 711 | 0.0000438 | 156 | 711 | 0.0003267 | 161 | 711 | 0.0003170 |
| 291 | 001 | 0.0001277 | 315 | 001 | 0.0000134 | 316 | 001 | 0.0000134 |
| 291 | 156 | 0.0004305 | 315 | 156 | 0.0000983 | 316 | 156 | 0.0000945 |
| 291 | 161 | -0.0004931 | 315 | 161 | 0.0001019 | 316 | 161 | 0.0001111 |
| 291 | 164 | 0.0003012 | 315 | 164 | 0.0000448 | 316 | 164 | 0.0000441 |
| 291 | 172 | 0.0001999 | 315 | 172 | 0.0000239 | 316 | 172 | 0.0000237 |
| 291 | 174 | -0.0002963 | 315 | 174 | 0.0000239 | 316 | 174 | 0.0000250 |
| 291 | 291 | 0.0001502 | 315 | 291 | 0.0000254 | 316 | 291 | 0.0000248 |
| 291 | 315 | 0.0000254 | 315 | 315 | 0.0000470 | 316 | 315 | 0.0000314 |
| 291 | 316 | 0.0000248 | 315 | 316 | 0.0000314 | 316 | 316 | 0.0000235 |
| 291 | 332 | -0.0002992 | 315 | 332 | 0.0001058 | 316 | 332 | 0.0001209 |
| 291 | 336 | -0.0004506 | 315 | 336 | 0.0014616 | 316 | 336 | 0.0247934 |
| 291 | 339 | 0.0000417 | 315 | 339 | 0.0000124 | 316 | 339 | 0.0000117 |
| 291 | 357 | 0.0000512 | 315 | 357 | 0.0000209 | 316 | 357 | 0.0000192 |
| 291 | 371 | 0.0001669 | 315 | 371 | 0.0000233 | 316 | 371 | 0.0000229 |
| 291 | 372 | -0.0001781 | 315 | 372 | 0.0001329 | 316 | 372 | 0.0001738 |
| 291 | 390 | 0.0000988 | 315 | 390 | 0.0000242 | 316 | 390 | 0.0000232 |
| 291 | 683 | -0.0008146 | 315 | 683 | 0.0002816 | 316 | 683 | 0.0003208 |
| 291 | 685 | -0.0004448 | 315 | 685 | 0.0000477 | 316 | 685 | 0.0000505 |
| 291 | 157 | 0.0000488 | 315 | 157 | 0.0000383 | 316 | 157 | 0.0000320 |
| 291 | 182 | 0.0000764 | 315 | 182 | 0.0000568 | 316 | 182 | 0.0000479 |
| 291 | 183 | 0.0001053 | 315 | 183 | 0.0000350 | 316 | 183 | 0.0000327 |
| 291 | 285 | 0.0002291 | 315 | 285 | 0.0000535 | 316 | 285 | 0.0000513 |
| 291 | 301 | 0.0003466 | 315 | 301 | 0.0002951 | 316 | 301 | 0.0002426 |
| 291 | 327 | -0.0000016 | 315 | 327 | -0.0000059 | 316 | 327 | -0.0000029 |
| 291 | 343 | 0.0000769 | 315 | 343 | 0.0000604 | 316 | 343 | 0.0000505 |
| 291 | 359 | 0.0000769 | 315 | 359 | 0.0000604 | 316 | 359 | 0.0000505 |
| 291 | 391 | 0.0000651 | 315 | 391 | 0.0000145 | 316 | 391 | 0.0000139 |
| 291 | 427 | 0.0001289 | 315 | 427 | 0.0000136 | 316 | 427 | 0.0000135 |
| 291 | 450 | 0.0001326 | 315 | 450 | 0.0000141 | 316 | 450 | 0.0000140 |
| 291 | 687 | 0.0002190 | 315 | 687 | 0.0000860 | 316 | 687 | 0.0000791 |
| 291 | 693 | -0.0000026 | 315 | 693 | -0.0000099 | 316 | 693 | -0.0000049 |
| 291 | 711 | 0.0000835 | 315 | 711 | 0.0002099 | 316 | 711 | 0.0001245 |
| 357 | 001 | 0.0000313 | 371 | 001 | 0.0001652 | 372 | 001 | -0.0000833 |
| 357 | 156 | 0.0001763 | 371 | 156 | 0.0004509 | 372 | 156 | -0.0007876 |
| 357 | 161 | 0.0009736 | 371 | 161 | -0.0003849 | 372 | 161 | -0.0004029 |
| 357 | 164 | 0.0000944 | 371 | 164 | 0.0003454 | 372 | 164 | -0.0003023 |
| 357 | 172 | 0.0000539 | 371 | 172 | 0.0002456 | 372 | 172 | -0.0001527 |
| 357 | 174 | 0.0001011 | 371 | 174 | -0.0001912 | 372 | 174 | -0.0001106 |
| 357 | 291 | 0.0000512 | 371 | 291 | 0.0001669 | 372 | 291 | -0.0001781 |
| 357 | 315 | 0.0000209 | 371 | 315 | 0.0000233 | 372 | 315 | 0.0001329 |
| 357 | 316 | 0.0000192 | 371 | 316 | 0.0000229 | 372 | 316 | 0.0001738 |
| 357 | 332 | -0.0021889 | 371 | 332 | -0.0002473 | 372 | 332 | -0.0003573 |
| 357 | 336 | -0.0004781 | 371 | 336 | -0.0004021 | 372 | 336 | -0.0012743 |

**TABLE 1.8 (continued)**
**[B] Matrix**

80% Loading
Minimum Transmission Loss: = 328.4 MW
$\lambda = 8.3$

| Bus no. | | B | Bus no. | | B | Bus no. | | B |
|---|---|---|---|---|---|---|---|---|
| 357 | 339 | 0.0000197 | 371 | 339 | 0.0000421 | 372 | 339 | -0.0001185 |
| 357 | 357 | 0.0000281 | 371 | 357 | 0.0000500 | 372 | 357 | -0.0002908 |
| 357 | 371 | 0.0000500 | 371 | 371 | 0.0001950 | 372 | 371 | -0.0001539 |
| 357 | 372 | -0.0002908 | 371 | 372 | -0.0001539 | 372 | 372 | -0.0003227 |
| 357 | 390 | 0.0000421 | 371 | 390 | 0.0001023 | 372 | 390 | -0.0002019 |
| 357 | 683 | -0.0070245 | 371 | 683 | -0.0006720 | 372 | 683 | -0.0009584 |
| 357 | 685 | 0.0002291 | 371 | 685 | -0.0003089 | 372 | 685 | -0.0002133 |
| 357 | 157 | 0.0000337 | 371 | 157 | 0.0000458 | 372 | 157 | 0.0009897 |
| 357 | 182 | 0.0000519 | 371 | 182 | 0.0000719 | 372 | 182 | 0.0021277 |
| 357 | 183 | 0.0000526 | 371 | 183 | 0.0001050 | 372 | 183 | -0.0003719 |
| 357 | 285 | 0.0000950 | 371 | 285 | 0.0002392 | 372 | 285 | -0.0004332 |
| 357 | 301 | 0.0002446 | 371 | 301 | 0.0003244 | 372 | 301 | 0.0050392 |
| 357 | 327 | -0.0000014 | 371 | 327 | -0.0000014 | 372 | 327 | -0.0000064 |
| 357 | 343 | 0.0000531 | 371 | 343 | 0.0000723 | 372 | 343 | 0.0015455 |
| 357 | 359 | 0.0000531 | 371 | 359 | 0.0000723 | 372 | 359 | 0.0015455 |
| 357 | 391 | 0.0000263 | 371 | 391 | 0.0000685 | 372 | 391 | -0.0001144 |
| 357 | 427 | 0.0000316 | 371 | 427 | 0.0001666 | 372 | 427 | -0.0000843 |
| 357 | 450 | 0.0000327 | 371 | 450 | 0.0001710 | 372 | 450 | -0.0000874 |
| 357 | 687 | 0.0001180 | 371 | 687 | 0.0002148 | 372 | 687 | -0.0011232 |
| 357 | 693 | -0.0000023 | 371 | 693 | -0.0000024 | 372 | 693 | -0.0000108 |
| 357 | 711 | 0.0000715 | 371 | 711 | 0.0000762 | 372 | 711 | 0.0003829 |
| 157 | 001 | 0.0000272 | 182 | 001 | 0.0000429 | 183 | 001 | 0.0000674 |
| 157 | 156 | 0.0001805 | 182 | 156 | 0.0002814 | 183 | 156 | 0.0003515 |
| 157 | 161 | 0.0002820 | 182 | 161 | 0.0004604 | 183 | 161 | -0.0217409 |
| 157 | 164 | 0.0000877 | 182 | 164 | 0.0001375 | 183 | 164 | 0.0001969 |
| 157 | 172 | 0.0000480 | 182 | 172 | 0.0000754 | 183 | 172 | 0.0001147 |
| 157 | 174 | 0.0000575 | 182 | 174 | 0.0000923 | 183 | 174 | 0.0003068 |
| 157 | 291 | 0.0000488 | 182 | 291 | 0.0000764 | 183 | 291 | 0.0001053 |
| 157 | 315 | 0.0000383 | 182 | 315 | 0.0000568 | 183 | 315 | 0.0000350 |
| 157 | 316 | 0.0000320 | 182 | 316 | 0.0000479 | 183 | 316 | 0.0000327 |
| 157 | 332 | 0.0003533 | 182 | 332 | 0.0005944 | 183 | 332 | -0.0010502 |
| 157 | 336 | -0.0015931 | 182 | 336 | -0.0021710 | 183 | 336 | -0.0007345 |
| 157 | 339 | 0.0000216 | 182 | 339 | 0.0000335 | 183 | 339 | 0.0000382 |
| 157 | 357 | 0.0000337 | 182 | 357 | 0.0000519 | 183 | 357 | 0.0000526 |
| 157 | 371 | 0.0000458 | 182 | 371 | 0.0000719 | 183 | 371 | 0.0001050 |
| 157 | 372 | 0.0009897 | 182 | 372 | 0.0021277 | 183 | 372 | -0.0003719 |
| 157 | 390 | 0.0000439 | 182 | 390 | 0.0000683 | 183 | 390 | 0.0000833 |
| 157 | 683 | 0.0009299 | 182 | 683 | 0.0015614 | 183 | 683 | -0.0029464 |
| 157 | 685 | 0.0001183 | 182 | 685 | 0.0001903 | 183 | 685 | 0.0007908 |
| 157 | 157 | 0.0000491 | 182 | 157 | 0.0000746 | 183 | 157 | 0.0000595 |
| 157 | 182 | 0.0000746 | 182 | 182 | 0.0001133 | 183 | 182 | 0.0000921 |
| 157 | 183 | 0.0000595 | 182 | 183 | 0.0000921 | 183 | 183 | 0.0001007 |
| 157 | 285 | 0.0000978 | 182 | 285 | 0.0001523 | 183 | 285 | 0.0001890 |
| 157 | 301 | 0.0003656 | 182 | 301 | 0.0005536 | 183 | 301 | 0.0004295 |
| 157 | 327 | -0.0000029 | 182 | 327 | -0.0000042 | 183 | 327 | -0.0000023 |
| 157 | 343 | 0.0000775 | 182 | 343 | 0.0001177 | 183 | 343 | 0.0000939 |
| 157 | 359 | 0.0000775 | 182 | 359 | 0.0001177 | 183 | 359 | 0.0000939 |
| 157 | 391 | 0.0000267 | 182 | 371 | 0.0000416 | 183 | 391 | 0.0000525 |
| 157 | 427 | 0.0000276 | 182 | 427 | 0.0000434 | 183 | 427 | 0.0000682 |
| 157 | 450 | 0.0000285 | 182 | 450 | 0.0000449 | 183 | 450 | 0.0000704 |

**TABLE 1.8 (continued)**
**[B] Matrix**

80% Loading
Minimum Transmission Loss: = 328.4 MW
$\lambda = 8.3$

| Bus no. | | B | Bus no. | | B | Bus no. | | B |
|---|---|---|---|---|---|---|---|---|
| 157 | 687 | 0.0001401 | 182 | 687 | 0.0002161 | 183 | 687 | 0.0002222 |
| 157 | 693 | -0.0000049 | 182 | 693 | -0.0000071 | 183 | 693 | -0.0000038 |
| 157 | 711 | 0.0001393 | 182 | 711 | 0.0002052 | 183 | 711 | 0.0001183 |
| 343 | 001 | 0.0000429 | 359 | 001 | 0.0000429 | 391 | 001 | 0.0000477 |
| 343 | 156 | 0.0002846 | 359 | 156 | 0.0002846 | 391 | 156 | 0.0002004 |
| 343 | 161 | 0.0004438 | 359 | 161 | 0.0004438 | 391 | 161 | -0.0004126 |
| 343 | 164 | 0.0001382 | 359 | 164 | 0.0001382 | 391 | 164 | 0.0001260 |
| 343 | 172 | 0.0000756 | 359 | 172 | 0.0000756 | 391 | 172 | 0.0000781 |
| 343 | 174 | 0.0000906 | 359 | 174 | 0.0000906 | 391 | 174 | -0.0007207 |
| 343 | 291 | 0.0000769 | 359 | 291 | 0.0000769 | 391 | 291 | 0.0000651 |
| 343 | 315 | 0.0000604 | 359 | 315 | 0.0000604 | 391 | 315 | 0.0000145 |
| 343 | 316 | 0.0000505 | 359 | 316 | 0.0000505 | 391 | 316 | 0.0000139 |
| 343 | 332 | 0.0005556 | 359 | 332 | 0.0005556 | 391 | 332 | -0.0002133 |
| 343 | 336 | -0.0025238 | 359 | 336 | -0.0025238 | 391 | 336 | -0.0002708 |
| 343 | 339 | 0.0000341 | 359 | 339 | 0.0000341 | 391 | 339 | 0.0000204 |
| 343 | 357 | 0.0000531 | 359 | 357 | 0.0000531 | 391 | 357 | 0.0000263 |
| 343 | 371 | 0.0000723 | 359 | 371 | 0.0000723 | 391 | 371 | 0.0000685 |
| 343 | 372 | 0.0015455 | 359 | 372 | 0.0015455 | 391 | 372 | -0.0001144 |
| 343 | 390 | 0.0000692 | 359 | 390 | 0.0000692 | 391 | 390 | 0.0000466 |
| 343 | 683 | 0.0014624 | 359 | 683 | 0.0014624 | 391 | 683 | -0.0005834 |
| 343 | 685 | 0.0001862 | 359 | 685 | 0.0001862 | 391 | 685 | -0.0006085 |
| 343 | 157 | 0.0000775 | 359 | 157 | 0.0000775 | 391 | 157 | 0.0000267 |
| 343 | 182 | 0.0001177 | 359 | 182 | 0.0001177 | 391 | 182 | 0.0000416 |
| 343 | 183 | 0.0000939 | 359 | 183 | 0.0000939 | 391 | 183 | 0.0000525 |
| 343 | 285 | 0.0001542 | 359 | 285 | 0.0001542 | 391 | 285 | 0.0001071 |
| 343 | 301 | 0.0005770 | 359 | 301 | 0.0005770 | 391 | 301 | 0.0001907 |
| 343 | 327 | -0.0000046 | 359 | 327 | -0.0000046 | 391 | 327 | -0.0000009 |
| 343 | 343 | 0.0001224 | 359 | 343 | 0.0001224 | 391 | 343 | 0.0000421 |
| 343 | 359 | 0.0001224 | 359 | 359 | 0.0001224 | 391 | 359 | 0.0000421 |
| 343 | 391 | 0.0000421 | 359 | 391 | 0.0000421 | 391 | 391 | 0.0000301 |
| 343 | 427 | 0.0000434 | 359 | 427 | 0.0000434 | 391 | 427 | 0.0000481 |
| 343 | 450 | 0.0000449 | 359 | 450 | 0.0000449 | 391 | 450 | 0.0000497 |
| 343 | 687 | 0.0002209 | 359 | 687 | 0.0002209 | 391 | 687 | 0.0001118 |
| 343 | 693 | -0.0000077 | 359 | 693 | -0.0000077 | 391 | 693 | -0.0000015 |
| 343 | 711 | 0.0002200 | 359 | 711 | 0.0002200 | 391 | 711 | 0.0000481 |
| 164 | 001 | 0.0002812 | 172 | 001 | 0.0002338 | 174 | 001 | -0.0000822 |
| 164 | 156 | 0.0008311 | 172 | 156 | 0.0005127 | 174 | 156 | -0.0076308 |
| 164 | 161 | -0.0007796 | 172 | 161 | -0.0003609 | 174 | 161 | -0.0001874 |
| 164 | 164 | 0.0006161 | 172 | 164 | 0.0004267 | 174 | 164 | -0.0004076 |
| 164 | 172 | 0.0004267 | 172 | 172 | 0.0003263 | 174 | 172 | -0.0001646 |
| 164 | 174 | -0.0004076 | 172 | 174 | -0.0001646 | 174 | 174 | -0.0000612 |
| 164 | 291 | 0.0003012 | 172 | 291 | 0.0001999 | 174 | 291 | -0.0002963 |
| 164 | 315 | 0.0000448 | 172 | 315 | 0.0000239 | 174 | 315 | 0.0000239 |
| 164 | 316 | 0.0000441 | 172 | 316 | 0.0000237 | 174 | 316 | 0.0000250 |
| 164 | 332 | -0.0004925 | 172 | 332 | -0.0002391 | 174 | 332 | -0.0001464 |
| 164 | 336 | -0.0007820 | 172 | 336 | -0.0004069 | 174 | 336 | -0.0003440 |
| 164 | 339 | 0.0000786 | 172 | 339 | 0.0000464 | 174 | 339 | 0.0001744 |
| 164 | 357 | 0.0000944 | 172 | 357 | 0.0000539 | 174 | 357 | 0.0001011 |
| 164 | 371 | 0.0003454 | 172 | 371 | 0.0002456 | 174 | 371 | -0.0001912 |
| 164 | 372 | -0.0003023 | 172 | 372 | -0.0001527 | 174 | 372 | -0.0001106 |

**TABLE 1.8 (continued)**
**[B] Matrix**

80% Loading
Minimum Transmission Loss: = 328.4 MW
$\lambda = 8.3$

| Bus no. | | B | Bus no. | | B | Bus no. | | B |
|---|---|---|---|---|---|---|---|---|
| 164 | 390 | 0.0001894 | 172 | 390 | 0.0001153 | 174 | 390 | 0.0032284 |
| 164 | 683 | -0.0013390 | 172 | 683 | -0.0006490 | 174 | 683 | -0.0003948 |
| 164 | 685 | -0.0006462 | 172 | 685 | -0.0002741 | 174 | 685 | -0.0001129 |
| 164 | 157 | 0.0000877 | 172 | 157 | 0.0000480 | 174 | 157 | 0.0000575 |
| 164 | 182 | 0.0001375 | 172 | 182 | 0.0000754 | 174 | 182 | 0.0000923 |
| 164 | 183 | 0.0001969 | 172 | 183 | 0.0001147 | 174 | 183 | 0.0003068 |
| 164 | 285 | 0.0004414 | 172 | 285 | 0.0002712 | 174 | 285 | -0.0077352 |
| 164 | 301 | 0.0006213 | 172 | 301 | 0.0003388 | 174 | 301 | 0.0003949 |
| 164 | 327 | -0.0000027 | 172 | 327 | -0.0000015 | 174 | 327 | -0.0000014 |
| 164 | 343 | 0.0001382 | 172 | 343 | 0.0000756 | 174 | 343 | 0.0000906 |
| 164 | 359 | 0.0001382 | 172 | 359 | 0.0000756 | 174 | 359 | 0.0000906 |
| 164 | 391 | 0.0001260 | 172 | 391 | 0.0000781 | 174 | 391 | -0.0007207 |
| 164 | 427 | 0.0002838 | 172 | 427 | 0.0002356 | 174 | 427 | -0.0000833 |
| 164 | 450 | 0.0002915 | 172 | 450 | 0.0002409 | 174 | 450 | -0.0000867 |
| 164 | 687 | 0.0004051 | 172 | 687 | 0.0002320 | 174 | 687 | 0.0004590 |
| 164 | 693 | -0.0000046 | 172 | 693 | -0.0000024 | 174 | 693 | -0.0000023 |
| 164 | 711 | 0.0001471 | 172 | 711 | 0.0000782 | 174 | 711 | 0.0000756 |
| 332 | 001 | -0.0001281 | 336 | 001 | -0.0002251 | 339 | 001 | 0.0000275 |
| 332 | 156 | -0.0014889 | 336 | 156 | -0.0018500 | 339 | 156 | 0.0001364 |
| 332 | 161 | -0.0005030 | 336 | 161 | -0.0013414 | 339 | 161 | -0.0010015 |
| 332 | 164 | -0.0004925 | 336 | 164 | -0.0007820 | 339 | 164 | 0.0000786 |
| 332 | 172 | -0.0002391 | 336 | 172 | -0.0004069 | 339 | 172 | 0.0000464 |
| 332 | 174 | -0.0001464 | 336 | 174 | -0.0003440 | 339 | 174 | 0.0001744 |
| 332 | 291 | -0.0002992 | 336 | 291 | -0.0004506 | 339 | 291 | 0.0000417 |
| 332 | 315 | 0.0001058 | 336 | 315 | 0.0014616 | 339 | 315 | 0.0000124 |
| 332 | 316 | 0.0001209 | 336 | 316 | 0.0247934 | 339 | 316 | 0.0000117 |
| 332 | 332 | -0.0004255 | 336 | 332 | -0.0012646 | 339 | 332 | -0.0002787 |
| 332 | 336 | -0.0012646 | 336 | 336 | -0.0062124 | 339 | 336 | -0.0002501 |
| 332 | 339 | -0.0002787 | 336 | 339 | -0.0002501 | 339 | 339 | 0.0000146 |
| 332 | 357 | -0.0021889 | 336 | 357 | -0.0004781 | 339 | 357 | 0.0000197 |
| 332 | 371 | -0.0002473 | 336 | 371 | -0.0004021 | 339 | 371 | 0.0000421 |
| 332 | 372 | -0.0003573 | 336 | 372 | -0.0012743 | 339 | 372 | -0.0001185 |
| 332 | 390 | -0.0003983 | 336 | 390 | -0.0004632 | 339 | 390 | 0.0000322 |
| 332 | 683 | -0.0011437 | 336 | 683 | -0.0033823 | 339 | 683 | -0.0007722 |
| 332 | 685 | -0.0002783 | 336 | 685 | -0.0006741 | 339 | 685 | 0.0005529 |
| 332 | 157 | 0.0003533 | 336 | 157 | -0.0015931 | 339 | 157 | 0.0000216 |
| 332 | 182 | 0.0005944 | 336 | 182 | -0.0021710 | 339 | 182 | 0.0000335 |
| 332 | 183 | -0.0010502 | 336 | 183 | -0.0007345 | 339 | 183 | 0.0000382 |
| 332 | 285 | -0.0008287 | 336 | 285 | -0.0010106 | 339 | 285 | 0.0000732 |
| 332 | 301 | 0.0022785 | 336 | 301 | -0.0144129 | 339 | 301 | 0.0001554 |
| 332 | 327 | -0.0000056 | 336 | 327 | -0.0000443 | 339 | 327 | -0.0000008 |
| 332 | 343 | 0.0005556 | 336 | 343 | -0.0025238 | 339 | 343 | 0.0000341 |
| 332 | 359 | 0.0005556 | 336 | 359 | -0.0025238 | 339 | 359 | 0.0000341 |
| 332 | 391 | -0.0002133 | 336 | 391 | -0.0002708 | 339 | 391 | 0.0000204 |
| 332 | 427 | -0.0001297 | 336 | 427 | -0.0002278 | 339 | 427 | 0.0000278 |
| 332 | 450 | -0.0001346 | 336 | 450 | -0.0002360 | 339 | 450 | 0.0000287 |
| 332 | 687 | -0.0059121 | 336 | 687 | -0.0019301 | 339 | 687 | 0.0000834 |
| 332 | 693 | -0.0000095 | 336 | 693 | -0.0000746 | 339 | 693 | -0.0000013 |
| 332 | 711 | 0.0003222 | 336 | 711 | 0.0031439 | 339 | 711 | 0.0000416 |
| 390 | 001 | 0.0000695 | 683 | 001 | -0.0003476 | 685 | 001 | -0.0001392 |

**TABLE 1.8 (continued)**
**[B] Matrix**

80% Loading
Minimum Transmission Loss: = 328.4 MW
$\lambda = 8.3$

| Bus no. | | B | Bus no. | | B | Bus no. | | B |
|---|---|---|---|---|---|---|---|---|
| 390 | 156 | 0.0003109 | 683 | 156 | -0.0040756 | 685 | 156 | -0.0048820 |
| 390 | 161 | -0.0008583 | 683 | 161 | -0.0013543 | 685 | 161 | -0.0003523 |
| 390 | 164 | 0.0001894 | 683 | 164 | -0.0013390 | 685 | 164 | -0.0006462 |
| 390 | 172 | 0.0001153 | 683 | 172 | -0.0006490 | 685 | 172 | -0.0002741 |
| 390 | 174 | 0.0032284 | 683 | 174 | -0.0003948 | 685 | 174 | -0.0001129 |
| 390 | 291 | 0.0000988 | 683 | 291 | -0.0008146 | 685 | 291 | -0.0004448 |
| 390 | 315 | 0.0000242 | 683 | 315 | 0.0002816 | 685 | 315 | 0.0000477 |
| 390 | 316 | 0.0000232 | 683 | 316 | 0.0003208 | 685 | 316 | 0.0000505 |
| 390 | 332 | -0.0003983 | 683 | 332 | -0.0011437 | 685 | 332 | -0.0002783 |
| 390 | 336 | -0.0004632 | 683 | 336 | -0.0033823 | 685 | 336 | -0.0006741 |
| 390 | 339 | 0.0000322 | 683 | 339 | -0.0007722 | 685 | 339 | 0.0005529 |
| 390 | 357 | 0.0000421 | 683 | 357 | -0.0070244 | 685 | 357 | 0.0002291 |
| 390 | 371 | 0.0001023 | 683 | 371 | -0.0006720 | 685 | 371 | -0.0003089 |
| 390 | 372 | -0.0002019 | 683 | 372 | -0.0009584 | 685 | 372 | -0.0002133 |
| 390 | 390 | 0.0000727 | 683 | 390 | -0.0010925 | 685 | 390 | -0.0024699 |
| 390 | 683 | -0.0010925 | 683 | 683 | -0.0030748 | 685 | 683 | -0.0007503 |
| 390 | 685 | -0.0024699 | 683 | 685 | -0.0007503 | 685 | 685 | -0.0002094 |
| 390 | 157 | 0.0000439 | 683 | 157 | 0.0009299 | 685 | 157 | 0.0001183 |
| 390 | 182 | 0.0000683 | 683 | 182 | 0.0015614 | 685 | 182 | 0.0001903 |
| 390 | 183 | 0.0000833 | 683 | 183 | -0.0029464 | 685 | 183 | 0.0007908 |
| 390 | 285 | 0.0001664 | 683 | 285 | -0.0022699 | 685 | 285 | -0.0031241 |
| 390 | 301 | 0.0003142 | 683 | 301 | 0.0060114 | 685 | 301 | 0.0008077 |
| 390 | 327 | -0.0000015 | 683 | 327 | -0.0000150 | 685 | 327 | -0.0000027 |
| 390 | 343 | 0.0000692 | 683 | 343 | 0.0014624 | 685 | 343 | 0.0001862 |
| 390 | 359 | 0.0000692 | 683 | 359 | 0.0014624 | 685 | 359 | 0.0001862 |
| 390 | 391 | 0.0000466 | 683 | 391 | -0.0005834 | 685 | 391 | -0.0006085 |
| 390 | 427 | 0.0000703 | 683 | 427 | -0.0003519 | 685 | 427 | -0.0001410 |
| 390 | 450 | 0.0000725 | 683 | 450 | -0.0003651 | 685 | 450 | -0.0001467 |
| 390 | 687 | 0.0001790 | 683 | 687 | -0.0177441 | 685 | 687 | 0.0010565 |
| 390 | 693 | -0.0000026 | 683 | 693 | -0.0000252 | 685 | 693 | -0.0000046 |
| 390 | 711 | 0.0000807 | 683 | 711 | 0.0008585 | 685 | 711 | 0.0001506 |
| 285 | 001 | 0.0001645 | 301 | 001 | 0.0001920 | 327 | 001 | -0.0000008 |
| 285 | 156 | 0.0007132 | 301 | 156 | 0.0012900 | 327 | 156 | -0.0000062 |
| 285 | 161 | -0.0016808 | 301 | 161 | 0.0018885 | 327 | 161 | -0.0000056 |
| 285 | 164 | 0.0004414 | 301 | 164 | 0.0006213 | 327 | 164 | -0.0000027 |
| 285 | 172 | 0.0002712 | 301 | 172 | 0.0003388 | 327 | 172 | -0.0000015 |
| 285 | 174 | -0.0077352 | 301 | 174 | 0.0003949 | 327 | 174 | -0.0000014 |
| 285 | 291 | 0.0002291 | 301 | 291 | 0.0003466 | 327 | 291 | -0.0000016 |
| 285 | 315 | 0.0000535 | 301 | 315 | 0.0002951 | 327 | 315 | -0.0000059 |
| 285 | 316 | 0.0000513 | 301 | 316 | 0.0002426 | 327 | 316 | -0.0000029 |
| 285 | 332 | -0.0008287 | 301 | 332 | 0.0022785 | 327 | 332 | -0.0000056 |
| 285 | 336 | -0.0010106 | 301 | 336 | -0.0144129 | 327 | 336 | -0.0000443 |
| 285 | 339 | 0.0000732 | 301 | 339 | 0.0001554 | 327 | 339 | -0.0000008 |
| 285 | 357 | 0.0000950 | 301 | 357 | 0.0002446 | 327 | 357 | -0.0000014 |
| 285 | 371 | 0.0002392 | 301 | 371 | 0.0003244 | 327 | 371 | -0.0000014 |
| 285 | 372 | -0.0004332 | 301 | 372 | 0.0050392 | 327 | 372 | -0.0000064 |
| 285 | 390 | 0.0001664 | 301 | 390 | 0.0003142 | 327 | 390 | -0.0000015 |
| 285 | 683 | -0.0022699 | 301 | 683 | 0.0060114 | 327 | 683 | -0.0000150 |
| 285 | 685 | -0.0031241 | 301 | 685 | 0.0008077 | 357 | 685 | -0.0000027 |
| 285 | 157 | 0.0000978 | 301 | 157 | 0.0003656 | 327 | 157 | -0.0000029 |

**TABLE 1.8 (continued)**
**[B] Matrix**

80% Loading
Minimum Transmission Loss: = 328.4 MW
$\lambda = 8.3$

| Bus no. | | B | Bus no. | | B | Bus no. | | B |
|---|---|---|---|---|---|---|---|---|
| 285 | 182 | 0.0001523 | 301 | 182 | 0.0005536 | 327 | 182 | -0.0000042 |
| 285 | 183 | 0.0001890 | 301 | 183 | 0.0004295 | 327 | 183 | -0.0000023 |
| 285 | 285 | 0.0003816 | 301 | 285 | 0.0006990 | 327 | 285 | -0.0000034 |
| 285 | 301 | 0.0006990 | 301 | 301 | 0.0027297 | 327 | 301 | -0.0000229 |
| 285 | 327 | -0.0000034 | 301 | 327 | -0.0000229 | 327 | 327 | -0.0000041 |
| 285 | 343 | 0.0001542 | 301 | 343 | 0.0005770 | 327 | 343 | -0.0000046 |
| 285 | 359 | 0.0001542 | 301 | 359 | 0.0005770 | 327 | 359 | -0.0000046 |
| 285 | 391 | 0.0001071 | 301 | 391 | 0.0001907 | 357 | 391 | -0.0000009 |
| 285 | 427 | 0.0001662 | 301 | 427 | 0.0001942 | 327 | 427 | -0.0000008 |
| 285 | 450 | 0.0001714 | 301 | 450 | 0.0002010 | 327 | 450 | -0.0000008 |
| 285 | 687 | 0.0004042 | 301 | 687 | 0.0010160 | 327 | 687 | -0.0000057 |
| 285 | 693 | -0.0000056 | 301 | 693 | -0.0000384 | 327 | 693 | -0.0000071 |
| 285 | 711 | 0.0001778 | 301 | 711 | 0.0010866 | 327 | 711 | -0.0000443 |
| 427 | 001 | 0.0001832 | 450 | 001 | 0.0001864 | 687 | 001 | 0.0001349 |
| 427 | 156 | 0.0003150 | 450 | 156 | 0.0003249 | 687 | 156 | 0.0007505 |
| 427 | 161 | -0.0001920 | 450 | 161 | -0.0001994 | 687 | 161 | 0.0051722 |
| 427 | 164 | 0.0002838 | 450 | 164 | 0.0002915 | 687 | 164 | 0.0004051 |
| 427 | 172 | 0.0002356 | 450 | 172 | 0.0002409 | 687 | 172 | 0.0002320 |
| 427 | 174 | -0.0000833 | 450 | 174 | -0.0000867 | 687 | 174 | 0.0004590 |
| 427 | 291 | 0.0001289 | 450 | 291 | 0.0001326 | 687 | 291 | 0.0002190 |
| 427 | 315 | 0.0000136 | 450 | 315 | 0.0000141 | 687 | 315 | 0.0000860 |
| 427 | 316 | 0.0000135 | 450 | 316 | 0.0000140 | 687 | 316 | 0.0000791 |
| 427 | 332 | -0.0001297 | 450 | 332 | -0.0001346 | 687 | 332 | -0.0059121 |
| 427 | 336 | -0.0002278 | 450 | 336 | -0.0002360 | 687 | 336 | -0.0019301 |
| 427 | 339 | 0.0000278 | 450 | 339 | 0.0000287 | 687 | 339 | 0.0000834 |
| 427 | 357 | 0.0000316 | 450 | 357 | 0.0000327 | 687 | 357 | 0.0001180 |
| 427 | 371 | 0.0001666 | 450 | 371 | 0.0001710 | 687 | 371 | 0.0002148 |
| 427 | 372 | -0.0000843 | 450 | 372 | -0.0000874 | 687 | 372 | -0.0011232 |
| 427 | 390 | 0.0000703 | 450 | 390 | 0.0000725 | 687 | 390 | 0.0001790 |
| 427 | 683 | -0.0003519 | 450 | 683 | -0.0003651 | 687 | 683 | -0.0177442 |
| 427 | 685 | -0.0001410 | 450 | 685 | -0.0001467 | 687 | 685 | 0.0010565 |
| 427 | 157 | 0.0000276 | 450 | 157 | 0.0000285 | 687 | 157 | 0.0001401 |
| 427 | 182 | 0.0000434 | 450 | 182 | 0.0000449 | 687 | 182 | 0.0002161 |
| 427 | 183 | 0.0000682 | 450 | 183 | 0.0000704 | 687 | 183 | 0.0002222 |
| 427 | 285 | 0.0001662 | 450 | 285 | 0.0001714 | 687 | 285 | 0.0004042 |
| 427 | 301 | 0.0001942 | 450 | 301 | 0.0002010 | 687 | 301 | 0.0010160 |
| 427 | 327 | -0.0000008 | 450 | 327 | -0.0000008 | 687 | 327 | -0.0000057 |
| 427 | 343 | 0.0000434 | 450 | 343 | 0.0000449 | 687 | 343 | 0.0002209 |
| 427 | 359 | 0.0000434 | 450 | 359 | 0.0000449 | 687 | 359 | 0.0002209 |
| 427 | 391 | 0.0000481 | 450 | 391 | 0.0000497 | 687 | 391 | 0.0001118 |
| 427 | 427 | 0.0001843 | 450 | 427 | 0.0001876 | 687 | 427 | 0.0001364 |
| 427 | 450 | 0.0001876 | 450 | 450 | 0.0001909 | 687 | 450 | 0.0001410 |
| 427 | 687 | 0.0001364 | 450 | 687 | 0.0001410 | 687 | 687 | 0.0004970 |
| 427 | 693 | -0.0000014 | 450 | 693 | -0.0000014 | 687 | 693 | -0.0000095 |
| 427 | 711 | 0.0000443 | 450 | 711 | 0.0000458 | 687 | 711 | 0.0002932 |

Reprinted from Energy Utilization of PSE&G for the Middle Atlantic Power Research Committee, Newark, NJ, 1976. With permission.

## TABLE 1.9
## [B] Matrix

90% Loading
Minimum Transmission Loss: = 2298.1 MW
$\lambda = 8.1$

| Bus no. | | B | Bus no. | | B | Bus no. | | B |
|---|---|---|---|---|---|---|---|---|
| 1 | 001 | 0.0001603 | 156 | 001 | 0.0002614 | 161 | 001 | -0.0001953 |
| 1 | 156 | 0.0002614 | 156 | 156 | 0.0011118 | 161 | 156 | -0.0041035 |
| 1 | 161 | -0.0001953 | 156 | 161 | -0.0041035 | 161 | 161 | -0.0006265 |
| 1 | 164 | 0.0002475 | 156 | 164 | 0.0007040 | 161 | 164 | -0.0008341 |
| 1 | 172 | 0.0002058 | 156 | 172 | 0.0004316 | 161 | 172 | -0.0003759 |
| 1 | 174 | -0.0001664 | 156 | 174 | 0.0010128 | 161 | 174 | -0.0002261 |
| 1 | 291 | 0.0000885 | 156 | 291 | 0.0003279 | 161 | 291 | -0.0006647 |
| 1 | 315 | 0.0000030 | 156 | 315 | 0.0000229 | 161 | 315 | 0.0000217 |
| 1 | 316 | 0.0000030 | 156 | 316 | 0.0000227 | 161 | 316 | 0.0000220 |
| 1 | 332 | -0.0001315 | 156 | 332 | -0.0017522 | 161 | 332 | -0.0005123 |
| 1 | 336 | -0.0002132 | 156 | 336 | -0.0017734 | 161 | 336 | -0.0012819 |
| 1 | 339 | -0.0000388 | 156 | 339 | -0.0031430 | 161 | 339 | -0.0001015 |
| 1 | 357 | -0.0000333 | 156 | 357 | -0.0004554 | 161 | 357 | -0.0001276 |
| 1 | 371 | 0.0001317 | 156 | 371 | 0.0003680 | 161 | 371 | -0.0004257 |
| 1 | 372 | -0.0000852 | 156 | 372 | -0.0008554 | 161 | 372 | -0.0004104 |
| 1 | 390 | 0.0000099 | 156 | 390 | 0.0000674 | 161 | 390 | 0.0000892 |
| 1 | 683 | -0.0003253 | 156 | 683 | -0.0041074 | 161 | 683 | -0.0013088 |
| 1 | 685 | -0.0002228 | 156 | 685 | 0.0032797 | 161 | 685 | -0.0004102 |
| 1 | 157 | -0.0000099 | 156 | 157 | -0.0000804 | 161 | 157 | -0.0000619 |
| 1 | 182 | 0.0000300 | 156 | 182 | 0.0002011 | 161 | 182 | 0.0002765 |
| 1 | 183 | 0.0000496 | 156 | 183 | 0.0002680 | 161 | 183 | 0.0013620 |
| 1 | 285 | 0.0001405 | 156 | 285 | 0.0006009 | 161 | 285 | -0.0023011 |
| 1 | 301 | 0.0001649 | 156 | 301 | 0.0011031 | 161 | 301 | 0.0015290 |
| 1 | 327 | -0.0000169 | 156 | 327 | -0.0001340 | 161 | 327 | -0.0001102 |
| 1 | 343 | 0.0000300 | 156 | 343 | 0.0002031 | 161 | 343 | 0.0002705 |
| 1 | 359 | 0.0000300 | 156 | 359 | 0.0002031 | 161 | 359 | 0.0002705 |
| 1 | 391 | 0.0000294 | 156 | 391 | 0.0001395 | 161 | 391 | -0.0019350 |
| 1 | 427 | 0.0001613 | 156 | 427 | 0.0002642 | 161 | 427 | -0.0001978 |
| 1 | 450 | 0.0001641 | 156 | 450 | 0.0002726 | 161 | 450 | -0.0002056 |
| 1 | 687 | 0.0001062 | 156 | 687 | 0.0005986 | 161 | 687 | 0.0020517 |
| 1 | 693 | -0.0000129 | 156 | 693 | -0.0000992 | 161 | 693 | -0.0000872 |
| 1 | 711 | 0.0000305 | 156 | 711 | 0.0002282 | 161 | 711 | 0.0002182 |
| 291 | 001 | 0.0000885 | 315 | 001 | 0.0000030 | 316 | 001 | 0.0000030 |
| 291 | 156 | 0.0003279 | 315 | 156 | 0.0000229 | 316 | 156 | 0.0000227 |
| 291 | 161 | -0.0006647 | 315 | 161 | 0.0000217 | 316 | 161 | 0.0000220 |
| 291 | 164 | 0.0002230 | 315 | 164 | 0.0000103 | 316 | 164 | 0.0000102 |
| 291 | 172 | 0.0001423 | 315 | 172 | 0.0000055 | 316 | 172 | 0.0000054 |
| 291 | 174 | 0.0006050 | 315 | 174 | 0.0000052 | 316 | 174 | 0.0000052 |
| 291 | 291 | 0.0000993 | 315 | 291 | 0.0000058 | 316 | 291 | 0.0000058 |
| 291 | 315 | 0.0000058 | 315 | 315 | 0.0000107 | 316 | 315 | 0.0000072 |
| 291 | 316 | 0.0000058 | 315 | 316 | 0.0000072 | 316 | 316 | 0.0000054 |
| 291 | 332 | -0.0003578 | 315 | 332 | 0.0000218 | 316 | 332 | 0.0000224 |
| 291 | 336 | -0.0004362 | 315 | 336 | 0.0001927 | 316 | 336 | 0.0002218 |
| 291 | 339 | -0.0001948 | 315 | 339 | 0.0000030 | 316 | 339 | 0.0000031 |
| 291 | 357 | -0.0000919 | 315 | 357 | 0.0000053 | 316 | 357 | 0.0000055 |
| 291 | 371 | 0.0001169 | 315 | 371 | 0.0000053 | 316 | 371 | 0.0000053 |
| 291 | 372 | -0.0001966 | 315 | 372 | 0.0000254 | 316 | 372 | 0.0000266 |
| 291 | 390 | 0.0000177 | 315 | 390 | 0.0000053 | 316 | 390 | 0.0000050 |
| 291 | 683 | -0.0008590 | 315 | 683 | 0.0000583 | 316 | 683 | 0.0000600 |

**TABLE 1.9 (continued)**
**[B] Matrix**

90% Loading
Minimum Transmission Loss: = 2298.1 MW
$\lambda = 8.1$

| Bus no. | | B | Bus no. | | B | Bus no. | | B |
|---|---|---|---|---|---|---|---|---|
| 291 | 685 | 0.0136738 | 315 | 685 | 0.0000103 | 316 | 685 | 0.0000104 |
| 291 | 157 | -0.0000199 | 315 | 157 | 0.0000128 | 316 | 157 | 0.0000157 |
| 291 | 182 | 0.0000529 | 315 | 182 | 0.0000147 | 316 | 182 | 0.0000137 |
| 291 | 183 | 0.0000748 | 315 | 183 | 0.0000083 | 316 | 183 | 0.0000081 |
| 291 | 285 | 0.0001770 | 315 | 285 | 0.0000125 | 316 | 285 | 0.0000123 |
| 291 | 301 | 0.0002906 | 315 | 301 | 0.0000794 | 316 | 301 | 0.0000744 |
| 291 | 327 | -0.0000335 | 315 | 327 | 0.0000401 | 316 | 327 | 0.0000608 |
| 291 | 343 | 0.0000533 | 315 | 343 | 0.0000158 | 316 | 343 | 0.0000147 |
| 291 | 359 | 0.0000533 | 315 | 359 | 0.0000158 | 316 | 359 | 0.0000147 |
| 291 | 391 | 0.0000402 | 315 | 391 | 0.0000034 | 316 | 391 | 0.0000033 |
| 291 | 427 | 0.0000893 | 315 | 427 | 0.0000031 | 316 | 427 | 0.0000031 |
| 291 | 450 | 0.0000921 | 315 | 450 | 0.0000032 | 316 | 450 | 0.0000032 |
| 291 | 687 | 0.0001653 | 315 | 687 | 0.0000207 | 316 | 687 | 0.0000202 |
| 291 | 693 | -0.0000250 | 315 | 693 | 0.0001551 | 316 | 693 | -0.0002114 |
| 291 | 711 | 0.0000581 | 315 | 711 | 0.0000886 | 316 | 711 | 0.0000626 |
| 357 | 001 | -0.0000333 | 371 | 001 | 0.0001317 | 372 | 001 | -0.0000852 |
| 357 | 156 | -0.0004554 | 371 | 156 | 0.0003680 | 372 | 156 | -0.0008554 |
| 357 | 161 | -0.0001276 | 371 | 161 | -0.0004257 | 372 | 161 | -0.0004104 |
| 357 | 164 | -0.0001316 | 371 | 164 | 0.0002857 | 372 | 164 | -0.0003130 |
| 357 | 172 | -0.0000626 | 371 | 172 | 0.0001990 | 372 | 172 | -0.0001568 |
| 357 | 174 | -0.0000426 | 371 | 174 | -0.0009515 | 372 | 174 | -0.0001224 |
| 357 | 291 | -0.0000919 | 371 | 91 | 0.0001169 | 372 | 291 | -0.0001966 |
| 357 | 315 | 0.0000053 | 371 | 315 | 0.0000053 | 372 | 315 | 0.0000254 |
| 357 | 316 | 0.0000055 | 371 | 316 | 0.0000053 | 372 | 316 | 0.0000266 |
| 357 | 332 | -0.0001076 | 371 | 332 | -0.0002653 | 372 | 332 | -0.0003639 |
| 357 | 336 | -0.0002979 | 371 | 336 | -0.0003833 | 372 | 336 | -0.0012306 |
| 357 | 339 | -0.0000201 | 371 | 339 | -0.0000943 | 372 | 339 | -0.0000623 |
| 357 | 357 | -0.0000267 | 371 | 357 | -0.0000675 | 372 | 357 | -0.0000900 |
| 357 | 371 | -0.0000675 | 371 | 371 | 0.0001506 | 372 | 371 | -0.0001612 |
| 357 | 372 | -0.0000900 | 371 | 372 | -0.0001612 | 372 | 372 | -0.0003287 |
| 357 | 390 | 0.0000243 | 371 | 390 | 0.0000168 | 372 | 390 | 0.0001681 |
| 357 | 683 | -0.0002765 | 371 | 683 | -0.0006489 | 372 | 683 | -0.0009446 |
| 357 | 685 | -0.0000788 | 371 | 685 | -0.0007326 | 372 | 685 | -0.0002326 |
| 357 | 157 | -0.0000146 | 371 | 157 | -0.0000177 | 372 | 157 | -0.0000618 |
| 357 | 182 | 0.0000766 | 371 | 182 | 0.0000504 | 372 | 182 | 0.0005680 |
| 357 | 183 | -0.0039342 | 371 | 183 | 0.0000771 | 372 | 183 | -0.0005106 |
| 357 | 285 | -0.0002513 | 371 | 285 | 0.0001983 | 372 | 285 | -0.0004682 |
| 357 | 301 | 0.0004253 | 371 | 301 | 0.0002769 | 372 | 301 | 0.0032033 |
| 357 | 327 | -0.0000263 | 371 | 327 | -0.0000300 | 372 | 327 | -0.0001152 |
| 357 | 343 | 0.0000740 | 371 | 343 | 0.0000506 | 372 | 343 | 0.0005170 |
| 357 | 359 | 0.0000740 | 371 | 359 | 0.0000506 | 372 | 359 | 0.0005170 |
| 357 | 391 | -0.0000974 | 371 | 391 | 0.0000434 | 372 | 391 | -0.0001438 |
| 357 | 427 | -0.0000337 | 371 | 427 | 0.0001329 | 372 | 427 | -0.0000862 |
| 357 | 450 | -0.0000350 | 371 | 450 | 0.0001365 | 372 | 450 | -0.0000894 |
| 357 | 687 | 0.0014465 | 371 | 687 | 0.0001678 | 372 | 687 | -0.0016289 |
| 357 | 693 | -0.0000211 | 371 | 693 | -0.0000226 | 372 | 693 | -0.0000959 |
| 357 | 711 | 0.0000538 | 371 | 711 | 0.0000531 | 372 | 711 | 0.0002589 |
| 157 | 001 | -0.0000099 | 182 | 001 | 0.0000300 | 183 | 001 | 0.0000496 |
| 157 | 156 | -0.0000804 | 182 | 156 | 0.0002011 | 183 | 156 | 0.0002680 |
| 157 | 161 | -0.0000619 | 182 | 161 | 0.0002765 | 183 | 161 | 0.0013620 |

**TABLE 1.9 (continued)**
**[B] Matrix**

90% Loading
Minimum Transmission Loss: = 2298.1 MW
$\lambda = 8.1$

| Bus no. | | B | Bus no. | | B | Bus no. | | B |
|---|---|---|---|---|---|---|---|---|
| 157 | 164 | -0.0000343 | 182 | 164 | 0.0000972 | 183 | 164 | 0.0001482 |
| 157 | 172 | -0.0000179 | 182 | 172 | 0.0000530 | 183 | 172 | 0.0000851 |
| 157 | 174 | -0.0000160 | 182 | 174 | 0.0000559 | 183 | 174 | 0.0001182 |
| 157 | 291 | -0.0000199 | 182 | 291 | 0.0000529 | 183 | 291 | 0.0000748 |
| 157 | 315 | 0.0000128 | 182 | 315 | 0.0000147 | 183 | 315 | 0.0000083 |
| 157 | 316 | 0.0000157 | 182 | 316 | 0.0000137 | 183 | 316 | 0.0000081 |
| 157 | 332 | -0.0000593 | 182 | 332 | 0.0003188 | 183 | 332 | -0.0064264 |
| 157 | 336 | -0.0003158 | 182 | 336 | -0.0030152 | 183 | 336 | -0.0007355 |
| 157 | 339 | -0.0000089 | 182 | 339 | 0.0000358 | 183 | 339 | 0.0001097 |
| 157 | 357 | -0.0000146 | 182 | 357 | 0.0000766 | 183 | 357 | -0.0039340 |
| 157 | 371 | -0.0000177 | 182 | 371 | 0.0000504 | 183 | 371 | 0.0000771 |
| 157 | 372 | -0.0000618 | 182 | 372 | 0.0005680 | 183 | 372 | -0.0005106 |
| 157 | 390 | -0.0000382 | 182 | 390 | 0.0000274 | 183 | 390 | 0.0000219 |
| 157 | 683 | -0.0001566 | 182 | 683 | 0.0008826 | 183 | 683 | -0.0072214 |
| 157 | 685 | -0.0000314 | 182 | 685 | 0.0001147 | 183 | 685 | 0.0002675 |
| 157 | 157 | -0.0000174 | 182 | 157 | -0.0000960 | 183 | 157 | -0.0000322 |
| 157 | 182 | -0.0000960 | 182 | 182 | 0.0000789 | 183 | 182 | 0.0000648 |
| 157 | 183 | -0.0000322 | 182 | 183 | 0.0000648 | 183 | 183 | 0.0000733 |
| 157 | 285 | -0.0000438 | 182 | 285 | 0.0001093 | 183 | 285 | 0.0001452 |
| 157 | 301 | -0.0005103 | 182 | 301 | 0.0004299 | 183 | 301 | 0.0003551 |
| 157 | 327 | -0.0000368 | 182 | 327 | -0.0001229 | 183 | 327 | -0.0000518 |
| 157 | 343 | -0.0001116 | 182 | 343 | 0.0000819 | 183 | 343 | 0.0000660 |
| 157 | 359 | -0.0001116 | 182 | 359 | 0.0000819 | 183 | 359 | 0.0000660 |
| 157 | 391 | -0.0000121 | 182 | 391 | 0.0000283 | 183 | 391 | 0.0000354 |
| 157 | 427 | -0.0000100 | 182 | 427 | 0.0000303 | 183 | 427 | 0.0000502 |
| 157 | 450 | -0.0000104 | 182 | 450 | 0.0000314 | 183 | 450 | 0.0000519 |
| 157 | 687 | -0.0000830 | 182 | 687 | 0.0001555 | 183 | 687 | 0.0001683 |
| 157 | 693 | -0.0000363 | 182 | 693 | -0.0000751 | 183 | 693 | -0.0000372 |
| 157 | 711 | 0.0001385 | 182 | 711 | 0.0001429 | 183 | 711 | 0.0000825 |
| 343 | 001 | 0.0000300 | 359 | 001 | 0.0000300 | 391 | 001 | 0.0000294 |
| 343 | 156 | 0.0002031 | 359 | 156 | 0.0002031 | 391 | 156 | 0.0001395 |
| 343 | 161 | 0.0002705 | 359 | 161 | 0.0002705 | 391 | 161 | -0.0019350 |
| 343 | 164 | 0.0000976 | 359 | 164 | 0.0000976 | 391 | 164 | 0.0000832 |
| 343 | 172 | 0.0000531 | 359 | 172 | 0.0000531 | 391 | 172 | 0.0000495 |
| 343 | 174 | 0.0000556 | 359 | 174 | 0.0000556 | 391 | 174 | 0.0000875 |
| 343 | 291 | 0.0000533 | 359 | 291 | 0.0000533 | 391 | 291 | 0.0000402 |
| 343 | 315 | 0.0000158 | 359 | 315 | 0.0000158 | 391 | 315 | 0.0000034 |
| 343 | 316 | 0.0000147 | 359 | 316 | 0.0000147 | 391 | 316 | 0.0000033 |
| 343 | 332 | 0.0003075 | 359 | 332 | 0.0003075 | 391 | 332 | -0.0003648 |
| 343 | 336 | -0.0037933 | 359 | 336 | -0.0037933 | 391 | 336 | -0.0002708 |
| 343 | 339 | 0.0000353 | 359 | 339 | 0.0000353 | 391 | 339 | 0.0001670 |
| 343 | 357 | 0.0000740 | 359 | 357 | 0.0000740 | 391 | 357 | -0.0000974 |
| 343 | 371 | 0.0000506 | 359 | 371 | 0.0000506 | 391 | 371 | 0.0000434 |
| 343 | 372 | 0.0005170 | 359 | 372 | 0.0005170 | 391 | 372 | -0.0001438 |
| 343 | 390 | 0.0000285 | 359 | 390 | 0.0000285 | 391 | 390 | 0.0000095 |
| 343 | 683 | 0.0008479 | 359 | 683 | 0.0008479 | 391 | 683 | -0.0008141 |
| 343 | 685 | 0.0001136 | 359 | 685 | 0.0001136 | 391 | 685 | 0.0002248 |
| 343 | 157 | -0.0001116 | 359 | 157 | -0.0001116 | 391 | 157 | -0.0000121 |
| 343 | 182 | 0.0000819 | 359 | 182 | 0.0000819 | 391 | 182 | 0.0000283 |
| 343 | 183 | 0.0000660 | 359 | 183 | 0.0000660 | 391 | 183 | 0.0000354 |

**TABLE 1.9 (continued)**
**[B] Matrix**

90% Loading
Minimum Transmission Loss: = 2298.1 MW
$\lambda = 8.1$

| Bus no. | | B | Bus no. | | B | Bus no. | | B |
|---|---|---|---|---|---|---|---|---|
| 343 | 285 | 0.0001104 | 359 | 285 | 0.0001104 | 391 | 285 | 0.0000755 |
| 343 | 301 | 0.0004463 | 359 | 301 | 0.0004463 | 391 | 301 | 0.0001550 |
| 343 | 327 | -0.0001373 | 359 | 327 | -0.0001373 | 391 | 327 | -0.0000200 |
| 343 | 343 | 0.0000852 | 359 | 343 | 0.0000852 | 391 | 343 | 0.0000286 |
| 343 | 359 | 0.0000852 | 359 | 359 | 0.0000852 | 391 | 359 | 0.0000286 |
| 343 | 391 | 0.0000286 | 359 | 391 | 0.0000286 | 391 | 391 | 0.0000179 |
| 343 | 427 | 0.0000304 | 359 | 427 | 0.0000304 | 391 | 427 | 0.0000297 |
| 343 | 450 | 0.0000314 | 359 | 450 | 0.0000314 | 391 | 450 | 0.0000307 |
| 343 | 687 | 0.0001587 | 359 | 687 | 0.0001587 | 391 | 687 | 0.0000800 |
| 343 | 693 | -0.0000820 | 359 | 693 | -0.0000820 | 391 | 693 | -0.0000147 |
| 343 | 711 | 0.0001532 | 359 | 711 | 0.0001532 | 391 | 711 | 0.0000334 |
| 164 | 001 | 0.0002475 | 172 | 001 | 0.0002058 | 174 | 001 | 0.0001664 |
| 164 | 156 | 0.0007040 | 172 | 156 | 0.0004316 | 174 | 156 | 0.0010128 |
| 164 | 161 | -0.0008341 | 172 | 161 | -0.0003759 | 174 | 161 | -0.0002261 |
| 164 | 164 | 0.0005422 | 172 | 164 | 0.0003755 | 174 | 164 | -0.0020996 |
| 164 | 172 | 0.0003755 | 172 | 172 | 0.0002872 | 174 | 172 | -0.0003938 |
| 164 | 174 | -0.0020996 | 172 | 174 | -0.0003938 | 174 | 174 | -0.0001074 |
| 164 | 291 | 0.0002230 | 172 | 291 | 0.0001423 | 174 | 291 | 0.0006050 |
| 164 | 315 | 0.0000103 | 172 | 315 | 0.0000055 | 174 | 315 | 0.0000052 |
| 164 | 316 | 0.0000102 | 172 | 316 | 0.0000054 | 174 | 316 | 0.0000052 |
| 164 | 332 | -0.0005173 | 172 | 332 | -0.0002471 | 174 | 332 | -0.0001697 |
| 164 | 336 | -0.0007422 | 172 | 336 | -0.0003856 | 174 | 336 | -0.0003388 |
| 164 | 339 | -0.0001862 | 172 | 339 | -0.0000771 | 174 | 339 | -0.0000397 |
| 164 | 357 | -0.0001316 | 172 | 357 | -0.0000626 | 174 | 357 | -0.0000426 |
| 164 | 371 | 0.0002857 | 172 | 371 | 0.0001990 | 174 | 371 | -0.0009515 |
| 164 | 372 | -0.0003130 | 172 | 372 | -0.0001568 | 174 | 372 | -0.0001224 |
| 164 | 390 | 0.0000324 | 172 | 390 | 0.0000176 | 174 | 390 | 0.0000184 |
| 164 | 683 | -0.0012643 | 172 | 683 | -0.0006090 | 174 | 683 | -0.0004269 |
| 164 | 685 | -0.0014879 | 172 | 685 | -0.0004773 | 174 | 685 | -0.0001800 |
| 164 | 157 | -0.0000343 | 172 | 157 | -0.0000179 | 174 | 157 | -0.0000160 |
| 164 | 182 | 0.0000972 | 172 | 182 | 0.0000530 | 174 | 182 | 0.0000559 |
| 164 | 183 | 0.0001482 | 172 | 183 | 0.0000851 | 174 | 183 | 0.0001182 |
| 164 | 285 | 0.0003794 | 172 | 285 | 0.0002322 | 174 | 285 | 0.0005355 |
| 164 | 301 | 0.0005341 | 172 | 301 | 0.0002911 | 174 | 301 | 0.0003082 |
| 164 | 327 | -0.0000581 | 172 | 327 | -0.0000305 | 174 | 327 | -0.0000278 |
| 164 | 343 | 0.0000976 | 172 | 343 | 0.0000531 | 174 | 343 | 0.0000556 |
| 164 | 359 | 0.0000976 | 172 | 359 | 0.0000531 | 174 | 359 | 0.0000556 |
| 164 | 391 | 0.0000832 | 172 | 391 | 0.0000495 | 174 | 391 | 0.0000875 |
| 164 | 427 | 0.0002497 | 172 | 427 | 0.0002073 | 174 | 427 | -0.0001690 |
| 164 | 450 | 0.0002565 | 172 | 450 | 0.0002120 | 174 | 450 | -0.0001770 |
| 164 | 687 | 0.0003228 | 172 | 687 | 0.0001834 | 174 | 687 | 0.0002390 |
| 164 | 693 | -0.0000437 | 172 | 693 | -0.0000231 | 174 | 693 | -0.0000215 |
| 164 | 711 | 0.0001026 | 172 | 711 | 0.0000545 | 174 | 711 | 0.0000520 |
| 332 | 001 | -0.0001315 | 336 | 001 | -0.0002132 | 339 | 001 | -0.0000388 |
| 332 | 156 | -0.0017522 | 336 | 156 | -0.0017734 | 339 | 156 | -0.0031431 |
| 332 | 161 | -0.0005123 | 336 | 161 | -0.0012819 | 339 | 161 | -0.0001015 |
| 332 | 164 | -0.0005173 | 336 | 164 | -0.0007422 | 339 | 164 | -0.0001862 |
| 332 | 172 | -0.0002471 | 336 | 172 | -0.0003856 | 339 | 172 | -0.0000771 |
| 332 | 174 | -0.0001697 | 336 | 174 | -0.0003388 | 339 | 174 | -0.0000397 |
| 332 | 291 | -0.0003578 | 336 | 291 | -0.0004362 | 339 | 291 | -0.0001948 |

## TABLE 1.9 (continued)
## [B] Matrix

90% Loading
Minimum Transmission Loss: = 2298.1 MW
$\lambda = 8.1$

| Bus no. | | B | Bus no. | | B | Bus no. | | B |
|---|---|---|---|---|---|---|---|---|
| 332 | 315 | 0.0000218 | 336 | 315 | 0.0001927 | 339 | 315 | 0.0000030 |
| 332 | 316 | 0.0000224 | 336 | 316 | 0.0002218 | 339 | 316 | 0.0000031 |
| 332 | 332 | -0.0004333 | 336 | 332 | -0.0012127 | 339 | 332 | -0.0000807 |
| 332 | 336 | -0.0012127 | 336 | 336 | -0.0058794 | 339 | 336 | -0.0001859 |
| 332 | 339 | -0.0000807 | 336 | 339 | -0.0001859 | 339 | 339 | -0.0000169 |
| 332 | 357 | -0.0001076 | 336 | 357 | -0.0002979 | 339 | 357 | -0.0000201 |
| 332 | 371 | -0.0002653 | 336 | 371 | -0.0003833 | 339 | 371 | -0.0000943 |
| 332 | 372 | -0.0003639 | 336 | 372 | -0.0012306 | 339 | 372 | -0.0000623 |
| 332 | 390 | 0.0001011 | 336 | 390 | -0.0013263 | 339 | 390 | 0.0000116 |
| 332 | 683 | -0.0011142 | 336 | 683 | -0.0031926 | 339 | 683 | -0.0002050 |
| 332 | 685 | -0.0003146 | 336 | 685 | -0.0006609 | 339 | 685 | -0.0000705 |
| 332 | 157 | -0.0000593 | 336 | 157 | -0.0003158 | 339 | 157 | -0.0000089 |
| 332 | 182 | 0.0003188 | 336 | 182 | -0.0030152 | 339 | 182 | 0.0000358 |
| 332 | 183 | -0.0064263 | 336 | 183 | -0.0007355 | 339 | 183 | 0.0001097 |
| 332 | 285 | -0.0009660 | 336 | 285 | -0.0009671 | 339 | 285 | -0.0020352 |
| 332 | 301 | 0.0017698 | 336 | 301 | -0.0157741 | 339 | 301 | 0.0001977 |
| 332 | 327 | -0.0001072 | 336 | 327 | -0.0006461 | 339 | 327 | -0.0000157 |
| 332 | 343 | 0.0003075 | 336 | 343 | -0.0037933 | 339 | 343 | 0.0000353 |
| 332 | 359 | 0.0003075 | 336 | 359 | -0.0037933 | 339 | 359 | 0.0000353 |
| 332 | 391 | -0.0003648 | 336 | 391 | -0.0002708 | 339 | 391 | 0.0001670 |
| 332 | 427 | -0.0001332 | 336 | 427 | -0.0002158 | 339 | 427 | -0.0000393 |
| 332 | 450 | -0.0001382 | 336 | 450 | -0.0002236 | 339 | 450 | -0.0000409 |
| 332 | 687 | 0.0076069 | 336 | 687 | -0.0019243 | 339 | 687 | 0.0001988 |
| 332 | 693 | -0.0000862 | 336 | 693 | -0.0006057 | 339 | 693 | -0.0000123 |
| 332 | 711 | 0.0002206 | 336 | 711 | 0.0020361 | 339 | 711 | 0.0000303 |
| 390 | 001 | 0.0000099 | 683 | 001 | -0.0003253 | 685 | 001 | -0.0002228 |
| 390 | 156 | 0.0000674 | 683 | 156 | -0.0041074 | 685 | 156 | 0.0032797 |
| 390 | 161 | 0.0000892 | 683 | 161 | -0.0013088 | 685 | 161 | -0.0004102 |
| 390 | 164 | 0.0000324 | 683 | 164 | -0.0012643 | 685 | 164 | -0.0014879 |
| 390 | 172 | 0.0000176 | 683 | 172 | -0.0006090 | 685 | 172 | -0.0004773 |
| 390 | 174 | 0.0000184 | 683 | 174 | -0.0004269 | 685 | 174 | -0.0001800 |
| 390 | 291 | 0.0000177 | 683 | 291 | -0.0008590 | 685 | 291 | 0.0136739 |
| 390 | 315 | 0.0000053 | 683 | 315 | 0.0000583 | 685 | 315 | 0.0000103 |
| 390 | 316 | 0.0000050 | 683 | 316 | 0.0000600 | 685 | 316 | 0.0000104 |
| 390 | 332 | 0.0001011 | 683 | 332 | -0.0011142 | 685 | 332 | -0.0003146 |
| 390 | 336 | -0.0013264 | 683 | 336 | -0.0031926 | 685 | 336 | -0.0006609 |
| 390 | 339 | 0.0000116 | 683 | 339 | -0.0002050 | 685 | 336 | -0.0000705 |
| 390 | 357 | 0.0000243 | 683 | 357 | -0.0002765 | 685 | 357 | -0.0000788 |
| 390 | 371 | 0.0000168 | 683 | 371 | -0.0006489 | 685 | 371 | -0.0007326 |
| 390 | 372 | 0.0001681 | 683 | 372 | -0.0009446 | 685 | 372 | -0.0002326 |
| 390 | 390 | 0.0000095 | 683 | 390 | 0.0002785 | 685 | 390 | 0.0000376 |
| 390 | 683 | 0.0002785 | 683 | 683 | -0.0028687 | 685 | 683 | -0.0007945 |
| 390 | 685 | 0.0000376 | 683 | 685 | -0.0007945 | 685 | 685 | -0.0003092 |
| 390 | 157 | -0.0000382 | 683 | 157 | -0.0001566 | 685 | 157 | -0.0000314 |
| 390 | 182 | 0.0000274 | 683 | 182 | 0.0008826 | 685 | 182 | 0.0001147 |
| 390 | 183 | 0.0000219 | 683 | 183 | -0.0072214 | 685 | 183 | 0.0002675 |
| 390 | 285 | 0.0000366 | 683 | 285 | -0.0022610 | 685 | 285 | 0.0017031 |
| 390 | 301 | 0.0001490 | 683 | 301 | 0.0049050 | 685 | 301 | 0.0006320 |
| 390 | 327 | -0.0000465 | 683 | 327 | -0.0002841 | 685 | 327 | -0.0000548 |
| 390 | 343 | 0.0000285 | 683 | 343 | 0.0008479 | 685 | 343 | 0.0001136 |

**TABLE 1.9 (continued)**
**[B] Matrix**

90% Loading
Minimum Transmission Loss: = 2298.1 MW
$\lambda = 8.1$

| Bus no. | | B | Bus no. | | B | Bus no. | | B |
|---|---|---|---|---|---|---|---|---|
| 390 | 359 | 0.0000285 | 683 | 359 | 0.0008479 | 685 | 359 | 0.0001136 |
| 390 | 391 | 0.0000095 | 683 | 391 | -0.0008141 | 685 | 391 | 0.0002248 |
| 390 | 427 | 0.0000101 | 683 | 427 | -0.0003293 | 685 | 427 | -0.0002259 |
| 390 | 450 | 0.0000104 | 683 | 450 | -0.0003418 | 685 | 450 | -0.0002358 |
| 390 | 687 | 0.0000528 | 683 | 687 | 0.0579783 | 685 | 687 | 0.0005268 |
| 390 | 693 | -0.0000276 | 683 | 693 | -0.0002293 | 685 | 693 | -0.0000425 |
| 390 | 711 | 0.0000515 | 683 | 711 | 0.0005899 | 685 | 711 | 0.0001035 |
| 285 | 001 | 0.0001405 | 301 | 001 | 0.0001649 | 327 | 001 | -0.0000169 |
| 285 | 156 | 0.0006009 | 301 | 156 | 0.0011031 | 327 | 156 | -0.0001340 |
| 285 | 161 | -0.0023011 | 301 | 161 | 0.0015290 | 327 | 161 | -0.0001102 |
| 285 | 164 | 0.0003794 | 301 | 164 | 0.0005341 | 327 | 164 | -0.0000581 |
| 285 | 172 | 0.0002322 | 301 | 172 | 0.0002911 | 327 | 172 | -0.0000305 |
| 285 | 174 | 0.0005355 | 301 | 174 | 0.0003082 | 327 | 174 | -0.0000278 |
| 285 | 291 | 0.0001770 | 301 | 291 | 0.0002906 | 327 | 291 | -0.0000335 |
| 285 | 315 | 0.0000125 | 301 | 315 | 0.0000794 | 327 | 315 | 0.0000401 |
| 285 | 316 | 0.0000123 | 301 | 316 | 0.0000744 | 327 | 316 | 0.0000608 |
| 285 | 332 | -0.0009660 | 301 | 332 | 0.0017698 | 327 | 332 | -0.0001072 |
| 285 | 336 | -0.0009671 | 301 | 336 | -0.0157741 | 327 | 336 | -0.0006461 |
| 285 | 339 | -0.0020351 | 301 | 339 | 0.0001977 | 327 | 339 | -0.0000157 |
| 285 | 357 | -0.0002513 | 301 | 357 | 0.0004253 | 327 | 357 | -0.0000263 |
| 285 | 371 | 0.0001983 | 301 | 371 | 0.0002769 | 327 | 371 | -0.0000300 |
| 285 | 372 | -0.0004682 | 301 | 372 | 0.0032033 | 327 | 372 | -0.0001152 |
| 285 | 390 | 0.0000366 | 301 | 390 | 0.0001490 | 327 | 390 | -0.0000465 |
| 285 | 683 | -0.0022610 | 301 | 683 | 0.0049050 | 327 | 683 | -0.0002841 |
| 285 | 685 | 0.0017031 | 301 | 685 | 0.0006320 | 327 | 685 | -0.0000548 |
| 285 | 157 | -0.0000438 | 301 | 157 | -0.0005103 | 327 | 157 | -0.0000368 |
| 285 | 182 | 0.0001093 | 301 | 182 | 0.0004299 | 327 | 182 | -0.0001229 |
| 285 | 183 | 0.0001452 | 301 | 183 | 0.0003551 | 327 | 183 | -0.0000518 |
| 285 | 285 | 0.0003248 | 301 | 285 | 0.0005994 | 327 | 285 | -0.0000730 |
| 285 | 301 | 0.0005994 | 301 | 301 | 0.0023432 | 327 | 301 | -0.0006588 |
| 285 | 327 | -0.0000730 | 301 | 327 | -0.0006588 | 327 | 327 | -0.0000825 |
| 285 | 343 | 0.0001104 | 301 | 343 | 0.0004463 | 327 | 343 | -0.0001373 |
| 285 | 359 | 0.0001104 | 301 | 359 | 0.0004463 | 327 | 359 | -0.0001373 |
| 285 | 391 | 0.0000755 | 301 | 391 | 0.0001550 | 327 | 391 | -0.0000200 |
| 285 | 427 | 0.0001420 | 301 | 427 | 0.0001668 | 327 | 427 | -0.0000172 |
| 285 | 450 | 0.0001465 | 301 | 450 | 0.0001726 | 327 | 450 | -0.0000178 |
| 285 | 687 | 0.0003245 | 301 | 687 | 0.0008511 | 327 | 687 | -0.0001318 |
| 285 | 693 | -0.0000540 | 301 | 693 | -0.0004046 | 327 | 693 | -0.0000897 |
| 285 | 711 | 0.0001242 | 301 | 711 | 0.0007730 | 327 | 711 | 0.0004653 |
| 427 | 001 | 0.0001613 | 450 | 001 | 0.0001641 | 687 | 001 | 0.0001062 |
| 427 | 156 | 0.0002642 | 450 | 156 | 0.0002726 | 687 | 156 | 0.0005986 |
| 427 | 161 | -0.0001978 | 450 | 161 | -0.0002056 | 687 | 161 | 0.0020517 |
| 427 | 164 | 0.0002497 | 450 | 164 | 0.0002565 | 687 | 164 | 0.0003228 |
| 427 | 172 | 0.0002073 | 450 | 172 | 0.0002120 | 687 | 172 | 0.0001834 |
| 427 | 174 | -0.0001690 | 450 | 174 | -0.0001770 | 687 | 174 | 0.0002390 |
| 427 | 291 | 0.0000893 | 450 | 291 | 0.0000921 | 687 | 291 | 0.0001653 |
| 427 | 315 | 0.0000031 | 450 | 315 | 0.0000032 | 687 | 315 | 0.0000207 |
| 427 | 316 | 0.0000031 | 450 | 316 | 0.0000032 | 687 | 316 | 0.0000202 |
| 427 | 332 | -0.0001332 | 450 | 332 | -0.0001382 | 687 | 332 | 0.0076068 |
| 427 | 336 | -0.0002158 | 450 | 336 | -0.0002236 | 687 | 336 | -0.0019243 |

## TABLE 1.9 (continued)
## [B] Matrix

90% Loading
Minimum Transmission Loss: = 2298.1 MW
$\lambda = 8.1$

| Bus no. | | B | Bus no. | | B | Bus no. | | B |
|---|---|---|---|---|---|---|---|---|
| 427 | 339 | -0.0000393 | 450 | 339 | -0.0000409 | 687 | 339 | 0.0001988 |
| 427 | 357 | -0.0000337 | 450 | 357 | -0.0000350 | 687 | 357 | 0.0014465 |
| 427 | 371 | 0.0001329 | 450 | 371 | 0.0001365 | 687 | 371 | 0.0001678 |
| 427 | 372 | -0.0000862 | 450 | 372 | -0.0000894 | 687 | 372 | -0.0016289 |
| 427 | 390 | 0.0000101 | 450 | 390 | 0.0000104 | 687 | 390 | 0.0000528 |
| 427 | 683 | -0.0003293 | 450 | 683 | -0.0003418 | 687 | 683 | 0.0579769 |
| 427 | 685 | -0.0002259 | 450 | 685 | -0.0002358 | 687 | 685 | 0.0005268 |
| 427 | 157 | -0.0000100 | 450 | 157 | -0.0000104 | 687 | 157 | -0.0000830 |
| 427 | 182 | 0.0000303 | 450 | 182 | 0.0000314 | 687 | 182 | 0.0001555 |
| 427 | 183 | 0.0000502 | 450 | 183 | 0.0000519 | 687 | 183 | 0.0001683 |
| 427 | 285 | 0.0001420 | 450 | 285 | 0.0001465 | 687 | 285 | 0.0003245 |
| 427 | 301 | 0.0001668 | 450 | 301 | 0.0001726 | 687 | 301 | 0.0008511 |
| 427 | 327 | -0.0000172 | 450 | 327 | -0.0000178 | 687 | 327 | -0.0001318 |
| 427 | 343 | 0.0000304 | 450 | 343 | 0.0000314 | 687 | 343 | 0.0001587 |
| 427 | 359 | 0.0000304 | 450 | 359 | 0.0000314 | 687 | 359 | 0.0001587 |
| 427 | 391 | 0.0000297 | 450 | 391 | 0.0000307 | 687 | 391 | 0.0000800 |
| 427 | 427 | 0.0001622 | 450 | 427 | 0.0001651 | 687 | 427 | 0.0001074 |
| 427 | 450 | 0.0001651 | 450 | 450 | 0.0001680 | 687 | 450 | 0.0001111 |
| 427 | 687 | 0.0001074 | 450 | 687 | 0.0001111 | 687 | 687 | 0.0003890 |
| 427 | 693 | -0.0000130 | 450 | 693 | -0.0000135 | 687 | 693 | -0.0000936 |
| 427 | 711 | 0.0000308 | 450 | 711 | 0.0000319 | 687 | 711 | 0.0002051 |

Reprinted from Energy Utilization of PSE&G for the Middle Atlantic Power Research Committee, Newark, NJ, 1976. With permission.

## TABLE 1.10
## [B] Matrix

100% Loading
Minimum Transmission Loss: = 450.1 MW
$\lambda = 7.5$

| Bus no. | | B | Bus no. | | B | Bus no. | | B |
|---|---|---|---|---|---|---|---|---|
| 1 | 001 | 0.0001374 | 156 | 001 | 0.0002088 | 161 | 001 | -0.0002550 |
| 1 | 156 | 0.0002088 | 156 | 156 | 0.0008806 | 161 | 156 | 0.0304658 |
| 1 | 161 | -0.0002550 | 156 | 161 | 0.0304658 | 161 | 161 | -0.0007850 |
| 1 | 164 | 0.0002121 | 156 | 164 | 0.0005701 | 161 | 164 | -0.0012627 |
| 1 | 172 | 0.0001763 | 156 | 172 | 0.0003465 | 161 | 172 | -0.0005106 |
| 1 | 174 | -0.0003994 | 156 | 174 | 0.0005156 | 161 | 174 | -0.0003031 |
| 1 | 291 | 0.0000318 | 156 | 291 | 0.0001632 | 161 | 291 | 0.0005202 |
| 1 | 315 | -0.0000365 | 156 | 315 | -0.0003271 | 161 | 315 | -0.0002157 |
| 1 | 316 | -0.0000372 | 156 | 316 | -0.0004100 | 161 | 316 | -0.0001896 |
| 1 | 332 | -0.0001804 | 156 | 332 | -0.0055280 | 161 | 332 | -0.0006638 |
| 1 | 336 | -0.0002489 | 156 | 336 | -0.0021713 | 161 | 336 | -0.0015038 |
| 1 | 339 | -0.0002299 | 156 | 339 | 0.0002984 | 161 | 339 | -0.0001752 |

**TABLE 1.10 (continued)**
**[B] Matrix**

100% Loading
Minimum Transmission Loss: = 450.1 MW
$\lambda = 7.5$

| Bus no. | B | Bus no. | B | Bus no. | B |
|---|---|---|---|---|---|
| 1 | 357-0.0001620 | 156 | 357 0.0006965 | 161 | 357-0.0002633 |
| 1 | 371 0.0000891 | 156 | 371 0.0002726 | 161 | 371-0.0008135 |
| 1 | 372-0.0001264 | 156 | 372-0.0017802 | 161 | 372-0.0005690 |
| 1 | 390-0.0000927 | 156 | 390 0.0016159 | 161 | 390-0.0002388 |
| 1 | 683-0.0003648 | 156 | 683-0.0064480 | 161 | 683-0.0015154 |
| 1 | 685-0.0004026 | 156 | 685 0.0012254 | 161 | 685-0.0005443 |
| 1 | 157-0.0000798 | 156 | 157-0.0017677 | 161 | 157-0.0003123 |
| 1 | 182-0.0000090 | 156 | 182-0.0000721 | 161 | 182-0.0000593 |
| 1 | 183 0.0000089 | 156 | 183 0.0000616 | 161 | 183 0.0000694 |
| 1 | 285 0.0001037 | 156 | 285 0.0004551 | 161 | 285 0.0055115 |
| 1 | 301 0.0001234 | 156 | 301 0.0008302 | 161 | 301 0.0010167 |
| 1 | 327-0.0000636 | 156 | 327-0.0005953 | 161 | 327-0.0003621 |
| 1 | 343-0.0000090 | 156 | 343-0.0000718 | 161 | 343-0.0000595 |
| 1 | 359-0.0000090 | 156 | 359-0.0000718 | 161 | 359-0.0000595 |
| 1 | 391-0.0000157 | 156 | 391-0.0002017 | 161 | 391-0.0000736 |
| 1 | 427 0.0001382 | 156 | 427 0.0002110 | 161 | 427-0.0002585 |
| 1 | 450 0.0001406 | 156 | 450 0.0002177 | 161 | 450-0.0002690 |
| 1 | 687 0.0000602 | 156 | 687 0.0003652 | 161 | 687 0.0005985 |
| 1 | 693-0.0000543 | 156 | 693-0.0004509 | 161 | 693-0.0003442 |
| 1 | 711-0.0000090 | 156 | 711-0.0000684 | 161 | 711-0.0000622 |
| 291 | 001 0.0000318 | 315 | 001-0.0000365 | 316 | 001-0.0000372 |
| 291 | 156 0.0001632 | 315 | 156-0.0003271 | 316 | 156-0.0004100 |
| 291 | 161 0.0005202 | 315 | 161-0.0002157 | 316 | 161-0.0001896 |
| 291 | 164 0.0000942 | 315 | 164-0.0001294 | 316 | 164-0.0001388 |
| 291 | 172 0.0000544 | 315 | 172-0.0000664 | 316 | 172-0.0000688 |
| 291 | 174 0.0000664 | 315 | 174-0.0000582 | 316 | 174-0.0000560 |
| 291 | 291 0.0000326 | 315 | 291-0.0000974 | 316 | 291-0.0001656 |
| 291 | 315-0.0000974 | 315 | 315-0.0001250 | 316 | 315-0.0000833 |
| 291 | 316-0.0001656 | 315 | 316-0.0000833 | 316 | 316-0.0000625 |
| 291 | 332 0.0009267 | 315 | 332-0.0002054 | 316 | 332-0.0001742 |
| 291 | 336-0.0006277 | 315 | 336-0.0009214 | 316 | 336-0.0005985 |
| 291 | 339 0.0000384 | 315 | 339-0.0000336 | 316 | 339-0.0000324 |
| 291 | 357 0.0000769 | 315 | 357-0.0000569 | 316 | 357-0.0000533 |
| 291 | 371 0.0000462 | 315 | 371-0.0000683 | 316 | 371-0.0000750 |
| 291 | 372-0.0015441 | 315 | 372-0.0002128 | 316 | 372-0.0001695 |
| 291 | 390 0.0001099 | 315 | 390-0.0000600 | 316 | 390-0.0000541 |
| 291 | 683 0.0165531 | 315 | 683-0.0005206 | 316 | 683-0.0004270 |
| 291 | 685 0.0001439 | 315 | 685-0.0001132 | 316 | 685-0.0001070 |
| 291 | 157 0.0007640 | 315 | 157-0.0001016 | 316 | 157-0.0000848 |
| 291 | 182-0.0000191 | 315 | 182-0.0000467 | 316 | 182-0.0000267 |
| 291 | 183 0.0000146 | 315 | 183 0.0001667 | 316 | 183 0.0000455 |
| 291 | 285 0.0000855 | 315 | 285-0.0001820 | 316 | 285-0.0002360 |
| 291 | 301 0.0001923 | 315 | 301 0.0070000 | 316 | 301 0.0007778 |
| 291 | 327-0.0001869 | 315 | 327-0.0001939 | 316 | 327-0.0001340 |
| 291 | 343-0.0000190 | 315 | 343-0.0000476 | 316 | 343-0.0000270 |
| 291 | 359-0.0000190 | 315 | 359-0.0000476 | 316 | 359-0.0000270 |
| 291 | 391-0.0001197 | 315 | 391-0.0000289 | 316 | 391-0.0000226 |
| 291 | 427 0.0000322 | 315 | 427-0.0000370 | 316 | 427-0.0000377 |
| 291 | 450 0.0000333 | 315 | 450-0.0000383 | 316 | 450-0.0000391 |
| 291 | 687 0.0000794 | 315 | 687-0.0005909 | 316 | 687 0.0016250 |

**TABLE 1.10 (continued)**
**[B] Matrix**

100% Loading
Minimum Transmission Loss: = 450.1 MW
$\lambda = 7.5$

| Bus no. | B | Bus no. | B | Bus no. | B |
|---|---|---|---|---|---|
| 291 | 693-0.0001238 | 315 | 693-0.0002400 | 316 | 693-0.0001464 |
| 291 | 711-0.0000174 | 315 | 711-0.0000604 | 316 | 711-0.0000307 |
| 357 | 001-0.0001620 | 371 | 001 0.0000891 | 372 | 001-0.0001264 |
| 357 | 156 0.0006965 | 371 | 156 0.0002726 | 372 | 156-0.0017802 |
| 357 | 161-0.0002633 | 371 | 161-0.0008135 | 372 | 161-0.0005690 |
| 357 | 164-0.0031180 | 371 | 164 0.0002091 | 372 | 164-0.0004954 |
| 357 | 172-0.0003997 | 371 | 172 0.0001392 | 372 | 172-0.0002372 |
| 357 | 174-0.0001306 | 371 | 174 0.0003636 | 372 | 174-0.0001804 |
| 357 | 291 0.0000769 | 371 | 291 0.0000462 | 372 | 291-0.0015441 |
| 357 | 315-0.0000569 | 371 | 315-0.0000683 | 372 | 315-0.0002128 |
| 357 | 316-0.0000533 | 371 | 316-0.0000750 | 372 | 316-0.0001695 |
| 357 | 332-0.0002105 | 371 | 332-0.0004636 | 372 | 332-0.0005100 |
| 357 | 336-0.0003929 | 371 | 336-0.0004608 | 372 | 336-0.0015101 |
| 357 | 339-0.0000755 | 371 | 339 0.0002108 | 372 | 339-0.0001043 |
| 357 | 357-0.0001025 | 371 | 357 0.0016248 | 372 | 357-0.0001679 |
| 357 | 371 0.0016248 | 371 | 371 0.0000957 | 372 | 371-0.0002749 |
| 357 | 372-0.0001679 | 371 | 372-0.0002749 | 372 | 372-0.0004762 |
| 357 | 390-0.0000841 | 371 | 390-0.0004155 | 372 | 390-0.0001653 |
| 357 | 683-0.0004608 | 371 | 683-0.0008421 | 372 | 683-0.0012219 |
| 357 | 685-0.0002186 | 371 | 685 0.0014559 | 372 | 685-0.0003395 |
| 357 | 157-0.0000970 | 371 | 157-0.0001936 | 372 | 157-0.0002456 |
| 357 | 182-0.0000149 | 371 | 182-0.0000161 | 372 | 182-0.0000640 |
| 357 | 183 0.0000160 | 371 | 183 0.0000149 | 372 | 183 0.0000909 |
| 357 | 285 0.0003192 | 371 | 285 0.0001385 | 372 | 285-0.0010802 |
| 357 | 301 0.0002283 | 371 | 301 0.0002047 | 372 | 301 0.0014286 |
| 357 | 327-0.0000971 | 371 | 327-0.0001209 | 372 | 327-0.0003479 |
| 357 | 343-0.0000149 | 371 | 343-0.0000161 | 372 | 343-0.0000645 |
| 357 | 359-0.0000149 | 371 | 359-0.0000161 | 372 | 359-0.0000645 |
| 357 | 391-0.0000214 | 371 | 391-0.0000332 | 372 | 391-0.0000629 |
| 357 | 427-0.0001646 | 371 | 427 0.0000900 | 372 | 427-0.0001279 |
| 357 | 450-0.0001726 | 371 | 450 0.0000926 | 372 | 450-0.0001328 |
| 357 | 687 0.0001211 | 371 | 687 0.0000951 | 372 | 687 0.0012207 |
| 357 | 693-0.0000880 | 371 | 693-0.0000986 | 372 | 693-0.0003593 |
| 357 | 711-0.0000152 | 371 | 711-0.0000157 | 372 | 711-0.0000706 |
| 157 | 001-0.0000798 | 182 | 001-0.0000090 | 183 | 001 0.0000089 |
| 157 | 156-0.0017677 | 182 | 156-0.0000721 | 183 | 156 0.0000616 |
| 157 | 161-0.0003123 | 182 | 161-0.0000593 | 183 | 161 0.0000694 |
| 157 | 164-0.0003356 | 182 | 164-0.0000310 | 183 | 164 0.0000292 |
| 157 | 172-0.0001529 | 182 | 172-0.0000162 | 183 | 172 0.0000157 |
| 157 | 174-0.0001069 | 182 | 174-0.0000149 | 183 | 174 0.0000155 |
| 157 | 291 0.0007640 | 182 | 291-0.0000191 | 183 | 291 0.0000146 |
| 157 | 315-0.0001016 | 182 | 315-0.0000467 | 183 | 315 0.0001667 |
| 157 | 316-0.0000848 | 182 | 316-0.0000267 | 183 | 316 0.0000455 |
| 157 | 332-0.0002731 | 182 | 332-0.0000582 | 183 | 332 0.0000723 |
| 157 | 336-0.0007147 | 182 | 336-0.0003584 | 183 | 336 0.0018637 |
| 157 | 339-0.0000618 | 182 | 339-0.0000086 | 183 | 339 0.0000090 |
| 157 | 357-0.0000970 | 182 | 357-0.0000149 | 183 | 357 0.0000160 |
| 157 | 371-0.0001936 | 182 | 371-0.0000161 | 183 | 371 0.0000149 |
| 157 | 372-0.0002456 | 182 | 372-0.0000640 | 183 | 372 0.0000909 |
| 157 | 390-0.0000924 | 182 | 390-0.0000162 | 183 | 390 0.0000182 |

**TABLE 1.10 (continued)**
**[B] Matrix**

100% Loading
Minimum Transmission Loss: = 450.1 MW
$\lambda = 7.5$

| Bus no. | | B | Bus no. | | B | Bus no. | | B |
|---|---|---|---|---|---|---|---|---|
| 157 | 683 | -0.0006407 | 182 | 683 | -0.0001522 | 183 | 683 | 0.0002021 |
| 157 | 685 | -0.0001977 | 182 | 685 | -0.0000294 | 183 | 685 | 0.0000312 |
| 157 | 157 | -0.0001302 | 182 | 157 | -0.0000292 | 183 | 157 | 0.0000374 |
| 157 | 182 | -0.0000292 | 182 | 182 | -0.0000232 | 183 | 182 | -0.0000543 |
| 157 | 183 | 0.0000374 | 182 | 183 | -0.0000543 | 183 | 183 | 0.0000125 |
| 157 | 285 | -0.0012503 | 182 | 285 | -0.0000395 | 183 | 285 | 0.0000332 |
| 157 | 301 | 0.0005646 | 182 | 301 | -0.0004070 | 183 | 301 | 0.0001458 |
| 157 | 327 | -0.0001683 | 182 | 327 | -0.0000689 | 183 | 327 | 0.0001776 |
| 157 | 343 | -0.0000294 | 182 | 343 | -0.0000241 | 183 | 343 | -0.0000500 |
| 157 | 359 | -0.0000294 | 182 | 359 | -0.0000241 | 183 | 359 | -0.0000500 |
| 157 | 391 | -0.0000321 | 182 | 391 | -0.0000089 | 183 | 391 | 0.0000132 |
| 157 | 427 | -0.0000808 | 182 | 427 | -0.0000091 | 183 | 427 | 0.0000090 |
| 157 | 450 | -0.0000840 | 182 | 450 | -0.0000095 | 183 | 450 | 0.0000093 |
| 157 | 687 | 0.0003826 | 182 | 687 | -0.0000776 | 183 | 687 | 0.0000459 |
| 157 | 693 | -0.0001668 | 182 | 693 | -0.0001042 | 183 | 693 | -0.0015033 |
| 157 | 711 | -0.0000314 | 182 | 711 | -0.0000420 | 183 | 711 | -0.0000265 |
| 343 | 001 | -0.0000090 | 359 | 001 | -0.0000090 | 391 | 001 | -0.0000157 |
| 343 | 156 | -0.0000718 | 359 | 156 | -0.0000718 | 391 | 156 | -0.0002017 |
| 343 | 161 | -0.0000595 | 359 | 161 | -0.0000595 | 391 | 161 | -0.0000736 |
| 343 | 164 | -0.0000309 | 359 | 164 | -0.0000309 | 391 | 164 | -0.0000605 |
| 343 | 172 | -0.0000162 | 359 | 172 | -0.0000162 | 391 | 172 | -0.0000293 |
| 343 | 174 | -0.0000149 | 359 | 174 | -0.0000149 | 391 | 174 | -0.0000228 |
| 343 | 291 | -0.0000190 | 359 | 291 | -0.0000190 | 391 | 291 | -0.0001197 |
| 343 | 315 | -0.0000476 | 359 | 315 | -0.0000476 | 391 | 315 | -0.0000289 |
| 343 | 316 | -0.0000270 | 359 | 316 | -0.0000270 | 391 | 316 | -0.0000226 |
| 343 | 332 | -0.0000585 | 359 | 332 | -0.0000585 | 391 | 332 | -0.0000665 |
| 343 | 336 | -0.0003661 | 359 | 336 | -0.0003661 | 391 | 336 | -0.0002058 |
| 343 | 339 | -0.0000086 | 359 | 339 | -0.0000086 | 391 | 339 | -0.0000132 |
| 343 | 357 | -0.0000149 | 359 | 357 | -0.0000149 | 391 | 357 | -0.0000214 |
| 343 | 371 | -0.0000161 | 359 | 371 | -0.0000161 | 391 | 371 | -0.0000332 |
| 343 | 372 | -0.0000645 | 359 | 372 | -0.0000645 | 391 | 372 | -0.0000629 |
| 343 | 390 | -0.0000162 | 359 | 390 | -0.0000162 | 391 | 390 | -0.0000213 |
| 343 | 683 | -0.0001532 | 359 | 683 | -0.0001532 | 391 | 683 | -0.0001605 |
| 343 | 685 | -0.0000295 | 359 | 685 | -0.0000295 | 391 | 685 | -0.0000431 |
| 343 | 157 | -0.0000294 | 359 | 157 | -0.0000294 | 391 | 157 | -0.0000321 |
| 343 | 182 | -0.0000241 | 359 | 182 | -0.0000241 | 391 | 182 | -0.0000089 |
| 343 | 183 | -0.0000500 | 359 | 183 | -0.0000500 | 391 | 183 | 0.0000132 |
| 343 | 285 | -0.0000393 | 359 | 285 | -0.0000383 | 391 | 285 | -0.0001198 |
| 343 | 301 | -0.0003889 | 359 | 301 | -0.0003889 | 391 | 301 | 0.0002108 |
| 343 | 327 | -0.0000700 | 359 | 327 | -0.0000700 | 391 | 327 | -0.0000470 |
| 343 | 343 | -0.0000250 | 359 | 343 | -0.0000250 | 391 | 343 | -0.0000089 |
| 343 | 359 | -0.0000250 | 359 | 359 | -0.0000250 | 391 | 359 | -0.0000089 |
| 343 | 391 | -0.0000089 | 359 | 391 | -0.0000089 | 391 | 391 | -0.0000083 |
| 343 | 427 | -0.0000091 | 359 | 427 | -0.0000091 | 391 | 427 | -0.0000159 |
| 343 | 450 | -0.0000094 | 359 | 450 | -0.0000094 | 391 | 450 | -0.0000165 |
| 343 | 687 | -0.0000762 | 359 | 687 | -0.0000762 | 391 | 687 | 0.0002073 |
| 343 | 693 | -0.0001072 | 359 | 693 | -0.0001072 | 391 | 693 | -0.0000494 |
| 343 | 711 | -0.0000450 | 359 | 711 | -0.0000450 | 391 | 711 | -0.0000099 |
| 164 | 001 | 0.0002121 | 172 | 001 | 0.0001763 | 174 | 001 | -0.0003994 |
| 164 | 156 | 0.0005701 | 172 | 156 | 0.0003465 | 174 | 156 | 0.0005156 |

**TABLE 1.10 (continued)**
**[B] Matrix**

100% Loading
Minimum Transmission Loss: = 450.1 MW
$\lambda = 7.5$

| Bus no. | B | Bus no. | B | Bus no. | B |
|---|---|---|---|---|---|
| 164 | 161-0.0012627 | 172 | 161-0.0005106 | 174 | 161-0.0003031 |
| 164 | 164 0.0004646 | 172 | 164 0.0003218 | 174 | 164 0.0012858 |
| 164 | 172 0.0003218 | 172 | 172 0.0002461 | 174 | 172-0.0022449 |
| 164 | 174 0.0012858 | 172 | 174-0.0022449 | 174 | 174-0.0001812 |
| 164 | 291 0.0000942 | 172 | 291 0.0000544 | 174 | 291 0.0000664 |
| 164 | 315-0.0001294 | 172 | 315-0.0000664 | 174 | 315-0.0000582 |
| 164 | 316-0.0001388 | 172 | 316-0.0000688 | 174 | 316-0.0000560 |
| 164 | 332-0.0007863 | 172 | 332-0.0003491 | 174 | 332-0.0002347 |
| 164 | 336-0.0008756 | 172 | 336-0.0004517 | 174 | 336-0.0003997 |
| 164 | 339 0.0007470 | 172 | 339-0.0012789 | 174 | 339-0.0001046 |
| 164 | 357-0.0031180 | 172 | 357-0.0003997 | 174 | 357-0.0001306 |
| 164 | 371 0.0002091 | 172 | 371 0.0001392 | 174 | 371 0.0003636 |
| 164 | 372-0.0004954 | 172 | 372-0.0002372 | 174 | 372-0.0001804 |
| 164 | 390-0.0005481 | 172 | 390-0.0001936 | 174 | 390-0.0000999 |
| 164 | 683-0.0014864 | 172 | 683-0.0006926 | 174 | 683-0.0005025 |
| 164 | 685 0.0329089 | 172 | 685-0.0011028 | 174 | 685-0.0002854 |
| 164 | 157-0.0003356 | 172 | 157-0.0001529 | 174 | 157-0.0001069 |
| 164 | 182-0.0000310 | 172 | 182-0.0000162 | 174 | 182-0.0000149 |
| 164 | 183 0.0000292 | 172 | 183 0.0000157 | 174 | 183 0.0000155 |
| 164 | 285 0.0002881 | 172 | 285 0.0001732 | 174 | 285 0.0002461 |
| 164 | 301 0.0004020 | 172 | 301 0.0002183 | 174 | 301 0.0002196 |
| 164 | 327-0.0002279 | 172 | 327-0.0001161 | 174 | 327-0.0000999 |
| 164 | 343-0.0000309 | 172 | 343-0.0000162 | 174 | 343-0.0000149 |
| 164 | 359-0.0000309 | 172 | 359-0.0000162 | 174 | 359-0.0000149 |
| 164 | 391-0.0000605 | 172 | 391-0.0000293 | 174 | 391-0.0000228 |
| 164 | 427 0.0002140 | 172 | 427 0.0001777 | 174 | 427-0.0004083 |
| 164 | 450 0.0002198 | 172 | 450 0.0001817 | 174 | 450-0.0004365 |
| 164 | 687 0.0001893 | 172 | 687 0.0001052 | 174 | 687 0.0001128 |
| 164 | 693-0.0001886 | 172 | 693-0.0000982 | 174 | 693-0.0000888 |
| 164 | 711-0.0000304 | 172 | 711-0.0000161 | 174 | 711-0.0000151 |
| 332 | 001-0.0001804 | 336 | 001-0.0002489 | 339 | 001-0.0002299 |
| 332 | 156-0.0055280 | 336 | 156-0.0021713 | 339 | 156 0.0002984 |
| 332 | 161-0.0006638 | 336 | 161-0.0015038 | 339 | 161-0.0001752 |
| 332 | 164-0.0007863 | 336 | 164-0.0008756 | 339 | 164 0.0007470 |
| 332 | 172-0.0003491 | 336 | 172-0.0004517 | 339 | 172-0.0012790 |
| 332 | 174-0.0002347 | 336 | 174-0.0003997 | 339 | 174-0.0001046 |
| 332 | 291 0.0009267 | 336 | 291-0.0006277 | 339 | 291 0.0000384 |
| 332 | 315-0.0002054 | 336 | 315-0.0009214 | 339 | 315-0.0000336 |
| 332 | 316-0.0001742 | 336 | 316-0.0005985 | 339 | 316-0.0000324 |
| 332 | 332-0.0005750 | 336 | 332-0.0014408 | 339 | 332-0.0001357 |
| 332 | 336-0.0014408 | 336 | 336-0.0068333 | 339 | 336-0.0002311 |
| 332 | 339-0.0001357 | 336 | 339-0.0002311 | 339 | 339-0.0000604 |
| 332 | 357-0.0002105 | 336 | 357-0.0003929 | 339 | 357-0.0000755 |
| 332 | 371-0.0004636 | 336 | 371-0.0004608 | 339 | 371 0.0002108 |
| 332 | 372-0.0005100 | 336 | 372-0.0015101 | 339 | 372-0.0001043 |
| 332 | 390-0.0001979 | 336 | 390-0.0004165 | 339 | 390-0.0000577 |
| 332 | 683-0.0013384 | 336 | 683-0.0036745 | 339 | 683-0.0002905 |
| 332 | 685-0.0004307 | 336 | 685-0.0007799 | 339 | 685-0.0001649 |
| 332 | 157-0.0002731 | 336 | 157-0.0007147 | 339 | 157-0.0000618 |
| 332 | 182-0.0000582 | 336 | 182-0.0003584 | 339 | 182-0.0000086 |

**TABLE 1.10 (continued)**
**[B] Matrix**

100% Loading
Minimum Transmission Loss: = 450.1 MW
$\lambda = 7.5$

| Bus no. | | B | Bus no. | | B | Bus no. | | B |
|---|---|---|---|---|---|---|---|---|
| 332 | 183 | 0.0000723 | 336 | 183 | 0.0018637 | 339 | 183 | 0.0000090 |
| 332 | 285 | -0.0047368 | 336 | 285 | -0.0012037 | 339 | 285 | 0.0001424 |
| 332 | 301 | 0.0010805 | 336 | 301 | -0.2869953 | 339 | 301 | 0.0001270 |
| 332 | 327 | -0.0003416 | 336 | 327 | -0.0014174 | 339 | 327 | -0.0000578 |
| 332 | 343 | -0.0000585 | 336 | 343 | -0.0003661 | 339 | 343 | -0.0000086 |
| 332 | 359 | -0.0000585 | 336 | 359 | -0.0003661 | 339 | 359 | -0.0000886 |
| 332 | 391 | -0.0000665 | 336 | 391 | -0.0002058 | 339 | 391 | -0.0000132 |
| 332 | 427 | -0.0001827 | 336 | 427 | -0.0002519 | 339 | 427 | -0.0002350 |
| 332 | 450 | -0.0001899 | 336 | 450 | -0.0002610 | 339 | 450 | -0.0002512 |
| 332 | 687 | 0.0006954 | 336 | 687 | -0.0033681 | 339 | 687 | 0.0000652 |
| 332 | 693 | -0.0003342 | 336 | 693 | -0.0018091 | 339 | 693 | -0.0000513 |
| 332 | 711 | -0.0000620 | 336 | 711 | -0.0004802 | 339 | 711 | -0.0000087 |
| 390 | 001 | -0.0000927 | 683 | 001 | -0.0003648 | 685 | 001 | -0.0004026 |
| 390 | 156 | 0.0016159 | 683 | 156 | -0.0064480 | 685 | 156 | 0.0012254 |
| 390 | 161 | -0.0002388 | 683 | 161 | -0.0015154 | 685 | 161 | -0.0005443 |
| 390 | 164 | -0.0005481 | 683 | 164 | -0.0014864 | 685 | 164 | 0.0329089 |
| 390 | 172 | -0.0001936 | 683 | 172 | -0.0006926 | 685 | 172 | -0.0011028 |
| 390 | 174 | -0.0000999 | 683 | 174 | -0.0005025 | 685 | 174 | -0.0002854 |
| 390 | 291 | 0.0001099 | 683 | 291 | 0.0165531 | 685 | 291 | 0.0001439 |
| 390 | 315 | -0.0000600 | 683 | 315 | -0.0005206 | 685 | 315 | -0.0001132 |
| 390 | 316 | -0.0000541 | 683 | 316 | -0.0004270 | 685 | 316 | -0.0001070 |
| 390 | 332 | -0.0001979 | 683 | 332 | -0.0013384 | 685 | 332 | -0.0004307 |
| 390 | 336 | -0.0004165 | 683 | 336 | -0.0036745 | 685 | 336 | -0.0007799 |
| 390 | 339 | -0.0000577 | 683 | 339 | -0.0002905 | 685 | 339 | -0.0001649 |
| 390 | 357 | -0.0000841 | 683 | 357 | -0.0004608 | 685 | 357 | -0.0002186 |
| 390 | 371 | -0.0004155 | 683 | 371 | -0.0008421 | 685 | 371 | 0.0014559 |
| 390 | 372 | -0.0001653 | 683 | 372 | -0.0012219 | 685 | 372 | -0.0003395 |
| 390 | 390 | -0.0000739 | 683 | 390 | -0.0004450 | 685 | 390 | -0.0001756 |
| 390 | 683 | -0.0004450 | 683 | 683 | -0.0031667 | 685 | 683 | -0.0009361 |
| 390 | 685 | -0.0001756 | 683 | 685 | -0.0009361 | 685 | 685 | -0.0004694 |
| 390 | 157 | -0.0000924 | 683 | 157 | -0.0006407 | 685 | 157 | -0.0001977 |
| 390 | 182 | -0.0000162 | 683 | 182 | -0.0001522 | 685 | 182 | -0.0000294 |
| 390 | 183 | 0.0000182 | 683 | 183 | 0.0002021 | 685 | 183 | 0.0000312 |
| 390 | 285 | 0.0006303 | 683 | 285 | -0.0041767 | 685 | 285 | 0.0005711 |
| 390 | 301 | 0.0002641 | 683 | 301 | 0.0030930 | 685 | 301 | 0.0004443 |
| 390 | 327 | -0.0001014 | 683 | 327 | -0.0008581 | 685 | 327 | -0.0001935 |
| 390 | 343 | -0.0000162 | 683 | 343 | -0.0001532 | 685 | 343 | -0.0000295 |
| 390 | 359 | -0.0000162 | 683 | 359 | -0.0001532 | 685 | 359 | -0.0000295 |
| 390 | 391 | -0.0000213 | 683 | 391 | -0.0001605 | 685 | 391 | -0.0000431 |
| 390 | 427 | -0.0000940 | 683 | 427 | -0.0003694 | 685 | 427 | -0.0004095 |
| 390 | 450 | -0.0000980 | 683 | 450 | -0.0003836 | 685 | 450 | -0.0004309 |
| 390 | 687 | 0.0001483 | 683 | 687 | 0.0022506 | 685 | 687 | 0.0002330 |
| 390 | 693 | -0.0000945 | 683 | 693 | -0.0008638 | 685 | 693 | -0.0001742 |
| 390 | 711 | -0.0000168 | 683 | 711 | -0.0001650 | 685 | 711 | -0.0000300 |
| 285 | 001 | 0.0001037 | 301 | 001 | 0.0001234 | 327 | 001 | -0.0000636 |
| 285 | 156 | 0.0004551 | 301 | 156 | 0.0008302 | 327 | 156 | -0.0005953 |
| 285 | 161 | 0.0055115 | 301 | 161 | 0.0010167 | 327 | 161 | -0.0003621 |
| 285 | 164 | 0.0002881 | 301 | 164 | 0.0004020 | 327 | 164 | -0.0002279 |
| 285 | 172 | 0.0001732 | 301 | 172 | 0.0002183 | 327 | 172 | -0.0001161 |
| 285 | 174 | 0.0002461 | 301 | 174 | 0.0002196 | 327 | 174 | -0.0000999 |

**TABLE 1.10 (continued)**
**[B] Matrix**

100% Loading
Minimum Transmission Loss: = 450.1 MW
$\lambda = 7.5$

| Bus no. | | B | Bus no. | | B | Bus no. | | B |
|---|---|---|---|---|---|---|---|---|
| 285 | 291 | 0.0000855 | 301 | 291 | 0.0001923 | 327 | 291 | -0.0001869 |
| 285 | 315 | -0.0001820 | 301 | 315 | 0.0070000 | 327 | 315 | -0.0001939 |
| 285 | 316 | -0.0002360 | 301 | 316 | 0.0007778 | 327 | 316 | -0.0001340 |
| 285 | 332 | -0.0047369 | 301 | 332 | 0.0010805 | 327 | 332 | -0.0003416 |
| 285 | 336 | -0.0012037 | 301 | 336 | -0.2869953 | 327 | 336 | -0.0014174 |
| 285 | 339 | 0.0001424 | 301 | 339 | 0.0001270 | 327 | 339 | -0.0000578 |
| 285 | 357 | 0.0003192 | 301 | 357 | 0.0002283 | 327 | 357 | -0.0000971 |
| 285 | 371 | 0.0001385 | 301 | 371 | 0.0002047 | 327 | 371 | -0.0001209 |
| 285 | 372 | -0.0010802 | 301 | 372 | 0.0014286 | 327 | 372 | -0.0003479 |
| 285 | 390 | 0.0006303 | 301 | 390 | 0.0002641 | 327 | 390 | -0.0001014 |
| 285 | 683 | -0.0041767 | 301 | 683 | 0.0030930 | 327 | 683 | -0.0008581 |
| 285 | 685 | 0.0005711 | 301 | 685 | 0.0004443 | 327 | 685 | -0.0001935 |
| 285 | 157 | -0.0012503 | 301 | 157 | 0.0005646 | 327 | 157 | -0.0001683 |
| 285 | 182 | -0.0000395 | 301 | 182 | -0.0004070 | 327 | 182 | -0.0000689 |
| 285 | 183 | 0.0000332 | 301 | 183 | 0.0001458 | 327 | 183 | 0.0001776 |
| 285 | 285 | 0.0002359 | 301 | 285 | 0.0004459 | 327 | 285 | -0.0003334 |
| 285 | 301 | 0.0004459 | 301 | 301 | 0.0017500 | 327 | 301 | 0.0042129 |
| 285 | 327 | -0.0003334 | 301 | 327 | 0.0042129 | 327 | 327 | -0.0003041 |
| 285 | 343 | -0.0000393 | 301 | 343 | -0.0003889 | 327 | 343 | -0.0000700 |
| 285 | 359 | -0.0000393 | 301 | 359 | -0.0003889 | 327 | 359 | -0.0000700 |
| 285 | 391 | -0.0001198 | 301 | 391 | 0.0002108 | 327 | 391 | -0.0000470 |
| 285 | 427 | 0.0001048 | 301 | 427 | 0.0001249 | 327 | 427 | -0.0000644 |
| 285 | 450 | 0.0001082 | 301 | 450 | 0.0001292 | 327 | 450 | -0.0000667 |
| 285 | 687 | 0.0001942 | 301 | 687 | 0.0005815 | 327 | 687 | -0.0015072 |
| 285 | 693 | -0.0002483 | 301 | 693 | -0.0042026 | 327 | 693 | -0.0003617 |
| 285 | 711 | -0.0000373 | 301 | 711 | -0.0002605 | 327 | 711 | -0.0000853 |
| 427 | 001 | 0.0001382 | 450 | 001 | 0.0001406 | 687 | 001 | 0.0000602 |
| 427 | 156 | 0.0002110 | 450 | 156 | 0.0002177 | 687 | 156 | 0.0003652 |
| 427 | 161 | -0.0002585 | 450 | 161 | -0.0002690 | 687 | 161 | 0.0005985 |
| 427 | 164 | 0.0002140 | 450 | 164 | 0.0002198 | 687 | 164 | 0.0001893 |
| 427 | 172 | 0.0001777 | 450 | 172 | 0.0001817 | 687 | 172 | 0.0001052 |
| 427 | 174 | -0.0004083 | 450 | 174 | -0.0004365 | 687 | 174 | 0.0001128 |
| 427 | 291 | 0.0000322 | 450 | 291 | 0.0000333 | 687 | 291 | 0.0000794 |
| 427 | 315 | -0.0000370 | 450 | 315 | -0.0000383 | 687 | 315 | -0.0005909 |
| 427 | 316 | -0.0000377 | 450 | 316 | -0.0000391 | 687 | 316 | 0.0016250 |
| 427 | 332 | -0.0001827 | 450 | 332 | -0.0001899 | 687 | 332 | 0.0006954 |
| 427 | 336 | -0.0002519 | 450 | 336 | -0.0002610 | 687 | 336 | -0.0033681 |
| 427 | 339 | -0.0002350 | 450 | 339 | -0.0002512 | 687 | 339 | 0.0000652 |
| 427 | 357 | -0.0001646 | 450 | 357 | -0.0001726 | 687 | 357 | 0.0001211 |
| 427 | 371 | 0.0000900 | 450 | 371 | 0.0000926 | 687 | 371 | 0.0000951 |
| 427 | 372 | -0.0001279 | 450 | 372 | -0.0001328 | 687 | 372 | 0.0012207 |
| 427 | 390 | -0.0000940 | 450 | 390 | -0.0000980 | 687 | 390 | 0.0001483 |
| 427 | 683 | -0.0003694 | 450 | 683 | -0.0003836 | 687 | 683 | 0.0022506 |
| 427 | 685 | -0.0004095 | 450 | 685 | -0.0004309 | 687 | 685 | 0.0002330 |
| 427 | 157 | -0.0000808 | 450 | 157 | -0.0000840 | 687 | 157 | 0.0003826 |
| 427 | 182 | -0.0000091 | 450 | 182 | -0.0000095 | 687 | 182 | -0.0000776 |
| 427 | 183 | 0.0000090 | 450 | 183 | 0.0000093 | 687 | 183 | 0.0000459 |
| 427 | 285 | 0.0001048 | 450 | 285 | 0.0001082 | 687 | 285 | 0.0001942 |
| 427 | 301 | 0.0001249 | 450 | 301 | 0.0001292 | 687 | 301 | 0.0005815 |
| 427 | 327 | -0.0000644 | 450 | 327 | -0.0000667 | 687 | 327 | -0.0015072 |

**TABLE 1.10 (continued)**
**[B] Matrix**

100% Loading
Minimum Transmission Loss: = 450.1 MW
$\lambda = 7.5$

| Bus no. | B | Bus no. | B | Bus no. | B |
|---|---|---|---|---|---|
| 427 | 343-0.0000091 | 450 | 343-0.0000094 | 687 | 343-0.0000762 |
| 427 | 359-0.0000091 | 450 | 359-0.0000094 | 687 | 359-0.0000762 |
| 427 | 391-0.0000159 | 450 | 391-0.0000165 | 687 | 391 0.0002073 |
| 427 | 427 0.0001390 | 450 | 427 0.0001415 | 687 | 427 0.0000609 |
| 427 | 450 0.0001415 | 450 | 450 0.0001440 | 687 | 450 0.0000630 |
| 427 | 687 0.0000609 | 450 | 687 0.0000630 | 687 | 687 0.0002167 |
| 427 | 693-0.0000550 | 450 | 693-0.0000570 | 687 | 693-0.0005553 |
| 427 | 711-0.0000091 | 450 | 711-0.0000094 | 687 | 711-0.0000638 |

Reprinted from Energy Utilization of PSE&G for the Middle Atlantic Power Research Committee, Newark, NJ, 1976. With permission.

## E. CONCLUSIONS DRAWN FROM EXAMPLE 1

Economic evaluation, stability, reliability, and the overall energy system security can be given direct and prompt analysis once the load flow calculations and optimum transmission loss coefficients information obtained for several energy system alternatives are established on different grounds.

From this example we may draw the following conclusions:

1. An overall [R] matrix for an optimum energy system reflecting network design in the energy flow reference frame can be established for all loadings, based on data compiled from load flow calculations and optimum [B] matrices.
2. A diagonal [R] matrix can be extracted from the overall matrix, to indicate on a smaller scale (especially in a power system with large numbers of bus-bars), the direct resistive elemental path from each energy equivalent bus-bar to the system centroid.
3. Inspection of the order of magnitudes of the diagonal matrices under all percentages of total received loads for each optimum system can serve as a basic criterion for identifying that arbitrary interconnecting network and its eventual design in the actual reference frame.
   a. Therefore, an inspection of Table 1.11A, which lists the elements of diagonal matrices for an optimum centralized energy system, under all percentages of loading, reveals that all of those elements are nonzero and of sizable values. This implies the feasibility of the optimal form of this centralized system, and consequently its design in the first reference frame.
   b. Also, inspection of Table 1.11B indicates that all the newly established dispersed energy bus-bars have a zero resistance path with respect to the system reference point, which those nonzero values of the diagonal matrices refer to the originally existing centralized bus-bars. Hence this represents again the exact identification and feasibility of the presumed arbitrary interconnecting network for a dispersed-centralized energy system and its design and physical realization in the first reference frame.

## TABLE 1.11A
## Self-Symmetric Resistance Matrix for Centralized System

| Bus no. | 70% Loading |
|---|---|
| 1 | 73.9802 |
| 2 | 1.3380 |
| 3 | –396.5701 |
| 4 | 62.0394 |
| 5 | 8.5583 |
| 6 | –22.0731 |
| 7 | 149.2670 |
| 8 | –14.2234 |
| 9 | –7.1399 |
| 10 | –303.6730 |
| 11 | –3961.8000 |
| 12 | 11.7583 |
| 13 | 64.4223 |
| 14 | 299.5341 |
| 15 | –255.2030 |
| 16 | 18.3579 |
| 17 | 613880.8 |
| 18 | –69.4038 |
| 19 | 80.3259 |
| 20 | 38.4454 |
| 21 | 98.2755 |
| 22 | 429.6367 |
| 23 | 3078.50 |
| 24 | –38.7570 |
| 25 | 41.4405 |
| 26 | 29.4890 |
| 27 | 0.7789 |
| 28 | 29.4290 |
| 29 | 3.7398 |
| 30 | 267.4327 |
| 31 | –95.4486 |
| 32 | 736.7194 |

*Note*: Values listed are $10^6$ times their true per unit values.

From Denno, K., Power system identification in the power reference frame, *J. Appl. Sci. Eng.*, 2, 141—153, 1977. With permission.

## TABLE 1.11B
## Self-Symmetric Resistance Matrix for Dispersed-Centralized System

| Bus no. | 70 % Loading | Bus no. | 70% Loading |
|---|---|---|---|
| 1 | 58.1807 | 57 | 37.8970 |
| 2 | 0.0000 | 58 | 0.0000 |
| 3 | 0.0000 | 59 | 49.1009 |
| 4 | 0.0000 | 60 | 384.8020 |

**TABLE 1.11B (continued)**
**Self-Symmetric Resistance Matrix for Dispersed-Centralized System**

| Bus no. | 70 % Loading | Bus no. | 70% Loading |
|---|---|---|---|
| 5 | 0.0000 | 61 | 0.0000 |
| 6 | 0.0000 | 62 | 0.0000 |
| 7 | 333.7475 | 63 | 0.0000 |
| 8 | -24.7995 | 64 | 0.0000 |
| 9 | 0.0000 | 65 | 3.8601 |
| 10 | 0.0000 | 66 | 0.0000 |
| 11 | 0.0000 | 67 | 5.1711 |
| 12 | 61.8234 | 68 | 0.0000 |
| 13 | 0.0000 | 69 | 0.0000 |
| 14 | 0.0000 | 70 | 0.0000 |
| 15 | 0.0000 | 71 | 0.0000 |
| 16 | 0.0000 | 72 | 0.0000 |
| 17 | 14.9525 | 73 | –0.5968 |
| 18 | 0.6518 | 74 | –83.9000 |
| 19 | 0.0000 | 75 | 0.0000 |
| 20 | 0.0000 | 76 | 0.0000 |
| 21 | 0.0000 | 77 | 0.0000 |
| 22 | 0.0000 | 78 | 0.0000 |
| 23 | 0.0000 | 79 | 0.0044 |
| 24 | 0.0000 | 80 | –339.6110 |
| 25 | 0.0000 | 81 | 0.0000 |
| 26 | 0.0000 | 82 | 0.0000 |
| 27 | 0.0000 | 83 | 0.0000 |
| 28 | 0.0000 | 84 | 0.0000 |
| 29 | 0.0000 | 85 | 0.0000 |
| 30 | 0.0000 | 86 | 0.0000 |
| 31 | 0.0000 | 87 | 0.0000 |
| 32 | 0.0000 | 88 | 0.0000 |
| 33 | 0.0000 | 89 | 5.4057 |
| 34 | 0.0000 | 90 | –0.3814 |
| 35 | 0.0000 | 91 | 0.0000 |
| 36 | 0.0000 | 92 | 0.0000 |
| 37 | 0.0000 | 93 | 0.0000 |
| 38 | –8.3863 | 94 | 0.0000 |
| 39 | 0.0000 | 95 | 0.0000 |
| 40 | 0.0000 | 96 | 0.0000 |
| 41 | 0.0000 | 97 | 0.0000 |
| 42 | 0.0000 | 98 | 0.0000 |
| 43 | 0.0000 | 99 | 0.0000 |
| 44 | 1.3834 | 100 | 0.0000 |
| 45 | 0.0000 | 101 | 0.0000 |
| 46 | 0.0000 | 102 | 0.0000 |
| 47 | 0.0000 | 103 | 0.0000 |
| 48 | 0.1237 | 104 | 0.0000 |
| 49 | 0.0000 | 105 | 0.0000 |
| 50 | 0.0000 | 106 | 0.0000 |
| 51 | 0.0000 | 107 | 0.0000 |
| 52 | 0.0000 | 108 | 0.0000 |
| 53 | 0.0000 | 109 | 0.0000 |
| 54 | 0.0000 | 110 | 0.0000 |
| 55 | 0.0000 | 111 | 0.0000 |
| 56 | 75.4960 | 112 | 0.0000 |

**TABLE 1.11B (continued)**
**Self-Symmetric Resistance Matrix for Dispersed-Centralized System**

| Bus no. | 70 % Loading | Bus no. | 70% Loading |
|---|---|---|---|
| 113 | 0.0000 | 119 | 0.0000 |
| 114 | 0.0000 | 120 | –11.6660 |
| 115 | 0.0000 | 121 | 0.0000 |
| 116 | 0.0000 | 122 | 0.0000 |
| 117 | 0.0000 | 123 | 7.0156 |
| 118 | 0.0000 | | |

*Note*: Values listed are $10^6$ times their true per unit values.

From Denno, K., Power system identification in the power reference frame, *J. Appl. Sci. Eng.*, 2, 141—153, 1977. With permission.

c. The above procedure of network identification and its physical realization for the two optimum systems A and B, in fact serves as an example in comparing several energy system alternatives having different numbers of bus-bars, to be established under different constraints, as mentioned in the introductory part of this paper.

4. Identification of an energy system in the sixth reference frame (known as the power flow frame) can lead to system representation in each of the other preceding five frames, by applying the corresponding transformation matrices given by Kron. In the case of actual optimum energy system design, its identification in the first reference frame (individual currents and actual interconnection) represents the direct operational form.
5. Analyzing any energy system in the power flow reference frame can be very economical with respect to computer time and memory, since in this frame there will be a smaller total number of bus bars and a smaller number of interconnecting branches.

## VII. OPTIMAL SOLUTION FOR THE TRANSMISSION LOSS COEFFICIENTS[1-15] MATRIX IN A MULTIAREA ENERGY POOL SYSTEM*

Optimization of economic dispatch for a multiarea energy pool is the most sensitive problem facing the power utilities, which requires rigorous and fast evaluation leading to reliable, comprehensive, and universal solutions.

One method of optimization established in earlier investigation is known as the Pool $\lambda$ method which is based on a set of penalty factors representing ratios between the on line running cost of any area in the energy pool with respect to the reference running cost. However, this method requires the immediate availability of a generalized [B] matrix at the central computer, where the control will perform periodic dispatch calculations for the entire energy pool for the purpose of solving all penalty vectors of the individual area members.

Also, in this method of optimization for the economic power dispatch, the central dispatch center undertakes the total task for complete assessment of information relevant to the composite incremental cost curve for each member in the power pool, losses within that area, tie power flow out of the area, and allocation of generation in accord to the relative cost with respect to the on-line reference value.

*  Reprinted with permission from Denno, K., Power system identification in the power reference frame, *J. Appl. Sci. Eng.*, 2, 141—153, 1977.

Basic data of information that must be fed in the central computer dispatch center is the transmission loss coefficients matrix for each single area and tie energy flow out of each area.

A principle reason for error recurrence in the economic dispatch results could be attributed to the fact that the conventional forms of the [B] matrix, whether the simple quadratic or the linear-quadratic, are derived with respect to one-base loading conditions, and presumed to remain invariant under all other loading levels.

Recently, an optimal form for the [B] matrix was developed for one area only, but without consideration to the elements of area tie flows. This section considered rigorous solution for the [B] matrix with direct presence of tie flows, and with the fact that it is an implicit function of all the power generating sources within the energy pool area.

Current literature indicates that representations for the tie flow could be considered either as independent energy sources with respect to total transmission losses, in terms of averaging the results of a number of load flows, or by assuming that each area can be expressed by a simple resistance to ground. The last assumption implies that the total transmission loss per area is proportional to the total tie flow power squared and is used in the procedure for the optimal solution of the [B] matrix.

## VIII. OBJECTIVES OF MULTIAREA ENERGY SYSTEM*

Given several alternatives of optimum energy systems guided by two states of coordination and constraints according to Equations 1.29 and 1.30, each area system is characterized by the following features:

1. Location of the generating sources
2. Output of each source within its range or capacity
3. Fuel cost and rate of consumption
4. Characteristics of voltage magnitudes and phase angles

The coordination equation is expressed below:

$$\frac{\partial F_i}{\partial P_i} + \lambda \frac{\partial P_L}{\partial P_i} + \lambda \frac{\partial P_T}{\partial P_i} = \lambda \tag{1.29}$$

While the constraint equation is

$$\psi\left(P_1, P_2 — P_n\right) = P_i - P_L - P_T - P_r = 0 \tag{1.30}$$

$$P_L = \sum_i \sum_j P_i B_{ij} P_j \tag{1.31}$$

and

$$P_T = k\sqrt{P_L} \tag{1.32}$$

* © IEEE, 1978. Reprinted with permission from Denno, K., Power system identification in the power flow reference frame in the presence of tie flows, Control of Power Systems Conference and Exposition, Oklahoma City, No. 78 CH-1282-3, REG5, IEEE, 1978, 90—95.

k is a constant

$$\frac{1}{P_r} = k \tag{1.33}$$

where $\lambda$ = cost of received power in dollars per megawatt hour; $P_L$ = total transmission loss in a single area in megawatts; $P_T$ = net tie flow across an area in megawatts; $P_r$ = given received load of an area in megawatts; $P_i$ = capacity of plant i within an area in megawatts; and $F_i$ = fuel cost of plant i in dollars per hour.

Dependence among generating sources within a single area is expressed as:

$$P_j = g(P_i) \tag{1.34}$$

$$B_{ij} = G(P_i) \tag{1.35}$$

$$P_T = f(P_i, B_{ij} P_j) = k\sqrt{P_L} \tag{1.36}$$

The problem centers on obtaining a general optimal solution in closed form for the [B] matrix for a single energy area in terms of source outputs within their range, their economic cost, and with consideration of the net tie flow across an area.

## IX. SOLUTION OF THE [B] MATRIX[1-15] *

Rewrite Equation 1.29.

$$\frac{\partial F_i}{\partial P_i} + \frac{\partial P_L}{\partial P_i} + \frac{\partial P_T}{\partial P_i} = \lambda \tag{1.37}$$

Then from:

$$\frac{\partial F_i}{\partial P_i} = F_{ii} P_i + f_i \tag{1.38}$$

where $F_{ii}$ = slope of incremental fuel cost curve and $f_i$ = incremental cost of plant i at zero output.

$$\frac{\partial P_L}{\partial P_i} = B_{ij} P_j + P_i \frac{\partial B_{ij}}{\partial P_i} P_j + P_i B_{ij} \frac{\partial P_j}{\partial P_i} \tag{1.39}$$

$$\frac{\partial P_T}{\partial P_i} = \frac{k}{2} \frac{B_{ij} P_j + P_i \frac{\partial B_{ij}}{\partial P_i} P_j + P_i B_{ij} \frac{\partial P_j}{\partial P_i}}{\sqrt{\sum_i \sum_j P_i B_{ij} P_j}} \tag{1.40}$$

* © Elsevier Scientific Publishing, 1977. Reprinted with permission from Denno, K., Power system identification in the power reference frame, *J. Appl. Sci. Eng.*, 2, 141—153, 1977.

Upon substitution in Equation 1.37, two compatible differential equations are obtained as below:

$$\frac{\partial F_i}{\partial P_i} + \lambda\left[B_{ij}P_j + P_i\frac{\partial B_{ij}}{\partial P_i}P_j + P_iB_{ij}\frac{\partial P_j}{\partial P_i}\right]\left[1 + \frac{\frac{k}{2}}{\sqrt{\sum_i\sum_j P_iB_{ij}P_j}}\right] = \lambda \tag{1.41}$$

$$\frac{\partial F_j}{\partial P_j} + \lambda\left[\frac{\partial P_i}{\partial P_j}B_{ij}P_j + P_i\frac{\partial B_{ij}}{\partial P_j}P_j + P_iB_{ij}\right]\left[1 + \frac{\frac{k}{2}}{\sum_i\sum_j P_iB_{ij}P_j}\right] = \lambda \tag{1.42}$$

Equation 1.37 may be expressed in terms of the following:

$$G\left(P_i, P_j, B_{ij}, \frac{\partial B_{ij}}{\partial P_i}, \frac{\partial B_{ij}}{\partial P_j}\right) = 0 \tag{1.43}$$

and

$$F\left(P_i, P_j, B_{ij}, \frac{\partial B_{ij}}{\partial P_i}, \frac{\partial B_{ij}}{\partial P_j}\right) = 0 \tag{1.44}$$

$$F - G = \phi = 0 \tag{1.45}$$

Using the method of characteristics, through which Equation 1.45 has been converted to a canonical system of subdifferential equations, the following equation is obtained.

$$F_{jj}P^2 - F_{ii}Q^2 = C^2 \tag{1.46}$$

where

$$P = \frac{\partial B_{ij}}{\partial P_i}, Q = \frac{\partial B_{ij}}{\partial P_j} \tag{1.47}$$

P and Q are obtained by solving simultaneously Equations 1.41 and 1.42.

The value of C is defined from the following boundary conditions:

$$P_i = \frac{\lambda - f_i}{F_{ii}} \tag{1.48}$$

and

$$P_j = \frac{\lambda - f_j}{F_{jj}} \tag{1.49}$$

from above in Equation 1.46, C = 0.

From Equation 1.46, the following solution is obtained.

$$B'_{ij} = B_{ij}\left[1 + \frac{\frac{k}{2}}{\sqrt{P_L}}\right] = \frac{H_2 F_{ii}\left(\lambda - F_{ii}P_i - f_i\right)}{H_1 P_i F_{jj}\lambda + H_2 P_j F_{ii}} \tag{1.50}$$

where

$$H_1 = \frac{F_{ii}}{F_{jj}} - \frac{\lambda - F_{ii}P_i - f_i}{\lambda - F_{jj}P_j - f_j} \tag{1.51}$$

and

$$H_2 = \frac{\lambda - F_{jj}P_{ji} - f_i}{\lambda - F_{ii}P_i - f_i} - \frac{F_{jj}}{F_{ii}} \tag{1.52}$$

$$k = \frac{1}{P_r} \tag{1.53}$$

where $P_r$ = received load in megawatts.

The solution established by Equation 1.50 for $B_{ij}$ represents elements of the transmission loss coefficients matrix with the direct effect of the net tie flows across a single area in a multiarea grid system.

$B_{ij}$ in Equation 1.50 reflects on the elements of the [B] matrix without consideration of tie flows.

The corrective factor for the effect of tie flows is expressed in terms of the constant k, which is a measure of the reciprocal of the received load in megawatts, with respect to the square root of the total transmission losses within a single area.

## X. CASE STUDY $2^{1\text{-}15}$ *

A specific eight energy sources in a single area having the following data, has been selected to calculate the $B_{ij}$ matrix.

This system is described below:

1.

| Plant | $F_{ii}$ | $f_i$ |
|---|---|---|
| 1 | 0.0082 | 1.28 |
| 2 | 0.0044 | 0.795 |
| 3 | 0.0019 | 1.809 |
| 4 | 0.00429 | 0.657 |
| 5 | 0.00222 | 0.889 |
| 6 | 0.0120 | 0.300 |
| 7 | 0.0208 | 0.635 |
| 8 | 0.0127 | 0.572 |

**TABLE 1.12**

| Loading (%) | Corrective factor due to tie flow |
|---|---|
| 100 | $1 + 3.33 \times 10^{-4}$ |
| 67 | $1 + 7.15 \times 10^{-4}$ |
| 41 | $1 + 14.1 \times 10^{-4}$ |

2. **Total peak of generation = 2000 MW**

| $P_1$ | $P_2$ | $P_3$ | $P_4$ | $P_5$ | $P_6$ | $P_7$ | $P_8$ |
|---|---|---|---|---|---|---|---|
| 260 | 210 | 270 | 420 | 310 | 240 | 110 | 180 |
| | | | **Total generation = 1340 MW** | | | | |
| 145 | 210 | 75 | 285 | 310 | 150 | 75 | 85 |
| | | | **Total generation = 820 MW** | | | | |
| 45 | 210 | −100 | 160 | 310 | 80 | 45 | 60 |

Elements of $B_{ij}$ the transmission loss coefficients matrix have been calculated by Equation 1.50 through a simple computer program. Values of $\lambda$ selected in the calculation, were those values corresponding to cases where the total transmission loss for a single area are minimum (without tie flow).

Three matrices for $B_{ij}$, at 100, 67, and 41% total generation, are calculated and listed in Table 1.12.

The correct factor for each degree of loading and its minimum transmission loss has been calculated and listed in Table 1.13.

From the preceding we may draw the following conclusions.

1. The [B] matrix derived in this example for a single area within a multiarea grid power system with direct consideration of net tie flow, represents a true and actual reflection for the interaction among the area power generating sources, especially it took into account the fact that each element of this matrix is an implicit function of load changes, follows the correct rules of system optimization, and represents the actual optimal form.
2. The solution obtained, besides its role in optimizing the economic power dispatch, enables the factual design of an optimum power system selected from a given group of system alternatives to be established on different grounds with respect to distribution of generating sources, characteristics of bus-bars, patterns of loads, specified total generation, specified plant capacity, and minimum total transmission losses.
3. The most significant new aspect in the solution of the [B] matrix $B_{ij}$ is the corrective role of the tie flow, which in fact depends upon the order of magnitude of the total generation and the total transmission losses, both expressed in megawatts. Values for corrective factors showed a pattern of increase at lower degree of loading and less transmission loss as indicated in Table 1.14.

## XI. SUMMARY[1-15]

This chapter presents a procedural method for selecting and designing an acceptable optimum energy system configuration from a group of system alternatives to be established in a single area or multiarea mode.

## Table 1.13[1–15]
## $B_{ij}$

Maximum Load = 2000 MW
D–om = $10^{-m}$

**Total Peak Generation, $\lambda$ = 2.9 $P_{L-min}$ = 0.56 MW**

| | | | | | | | |
|---|---|---|---|---|---|---|---|
| 0.1000D 01 | –0.1815D–02 | –0.4448D–02 | –0.1493D–02 | –0.8433D–03 | –0.2468D–03 | –0.2994D–04 | 0.5906D–04 |
| –0.1815D–02 | 0.1000D 01 | 0.5825D–03 | 0.4147D–03 | 0.8186D–03 | –0.6306D–03 | –0.3816D–04 | 0.6693D–04 |
| –0.4448D–02 | 0.5825D–03 | 0.1000D 01 | 0.2576D–03 | 0.4657D–03 | –0.6280D–03 | –0.2986D–04 | 0.5116D–04 |
| –0.1493D–02 | 0.4147D–03 | 0.2576D–03 | 0.1000D 01 | 0.3380D–03 | –0.3607D–03 | –0.1914D–04 | 0.3313D–04 |
| –0.8433D 03 | 0.1886D–03 | 0.4657D–03 | –0.3380D–03 | –0.1000D 01 | –0.3725D–03 | –0.2574D–04 | 0.4587D–04 |
| –0.2468D–03 | –0.6306D 03 | –0.6280D–03 | –0.3607D–03 | –0.3725D–03 | 0.1000D 01 | –0.3185D–04 | 0.6799D–04 |
| –0.2994D–04 | –0.3816D–04 | –0.2986D–04 | –0.1914D–04 | –0.2574D–04 | –0.3185D–04 | 0.1000D 01 | –0.6622D–04 |
| 0.5906D–04 | 0.6693D–04 | 0.5116D–04 | 0.3313D 04 | 0.4587D–04 | 0.6799D–04 | –0.6622D–04 | 0.1000D 01 |

**67% Total Generation, $\lambda$ = 2.0 $P_{L-min}$ = 0.28 MW**

| | | | | | | | |
|---|---|---|---|---|---|---|---|
| 0.1000D 01 | 0.7326D–02 | 0.1767D–03 | 0.8373D–03 | –0.1572D–02 | –0.2825D–03 | –0.5534D–03 | 0.2129D–02 |
| 0.7326D–02 | 0.1000D 01 | 0.1088D–03 | 0.1812D–03 | 0.3125D–03 | –0.3192D–03 | –0.6173D–03 | 0.5524D–03 |
| 0.1767D–02 | 0.1088D–03 | 0.1000D 01 | 0.7693D–04 | 0.7611D–04 | 0.2134D–03 | 0.4304D–03 | 0.2541D–03 |
| 0.8373D–03 | 0.1812D–03 | 0.7693D–04 | 0.1000D 01 | 0.1539D–03 | –0.3118D–03 | –0.5964D–03 | 0.3281D–03 |
| –0.1572D 02 | 0.3125D–03 | 0.7611D–04 | 0.1593D–03 | –0.1000D 01 | –0.1821D–03 | –0.3540D–03 | 0.4585D–03 |
| –0.2825D–03 | 0.3192D 03 | 0.2134D–03 | –0.3118D–03 | –0.1821D–03 | 0.1000D 01 | –0.3291D–03 | –0.1192D–02 |
| –0.5534D–03 | –0.6173D–03 | 0.4304D–03 | –0.5964D–03 | –0.3540D–03 | –0.3291D–03 | 0.1000D 01 | –0.2266D–02 |
| 0.2129D–02 | 0.5524D–03 | 0.2541D–03 | 0.3281D–03 | 0.4385D–03 | –0.1192D–02 | –0.2266D–02 | 0.1000D 01 |

**41% Total Generation, $\lambda$ = 1.6 $P_{L-min}$ = 0.19 MW**

| | | | | | | | |
|---|---|---|---|---|---|---|---|
| 0.1000D 01 | –0.1340D–03 | –0.1908D–02 | –0.2023D–03 | –0.1436D–03 | –0.4166D–03 | 0.9868D–03 | –0.5922D–03 |
| –0.1340D–03 | 0.1000D 01 | –0.6120D–04 | –0.1188D–02 | 0.9462D–04 | –0.1144D–01 | 0.9107D–04 | 0.2191D–02 |
| –0.1908D–02 | –0.6120D–04 | 0.1000D 01 | –0.7094D–04 | –0.3019D–04 | –0.1387D–03 | –0.1074D–03 | –0.1769D–03 |
| –0.2023D–03 | –0.1188D–02 | –0.7094D–04 | 0.1000D 01 | 0.7598D–04 | 0.7989D–03 | 0.1098D–03 | 0.7482D–03 |
| –0.1436D–03 | 0.9462D–04 | –0.3019D–04 | 0.7598D–04 | 0.1000D 01 | 0.1414D–03 | 0.4936D–04 | 0.1646D–03 |
| –0.4166D–03 | –0.1144D–01 | –0.1387D–03 | 0.7989D–03 | 0.1414D–03 | 0.1000D 01 | 0.2162D–03 | 0.1310D–02 |
| 0.9868D–03 | 0.9107D–04 | –0.1074D–03 | 0.1098D–03 | 0.4936D–03 | 0.2162D–03 | 0.1000D 01 | 0.2792D 03 |
| –0.5922D–03 | 0.2191D–02 | –0.1769D–03 | 0.7482D–03 | 0.1646D–03 | 0.1310D–02 | 0.2792D–03 | 0.1000D 01 |

The procedural method developed is based on compiling data obtained from load flow calculations with that of the optimum transmission loss coefficients matrix [B] for each system, in order to come up with an optimum design of any power system network in the sixth reference frame.

Identification of the optimum energy network is in terms of the symmetrical resistance matrix as indicated Equation 1.54:

$$[R] = [K][B]^{-1} \tag{1.54}$$

where [R] is the symmetric resistance matrix; [B] is the optimum transmission loss coefficient matrix; and[K] is the matrix function of load flow calculation parameters.

By inspection of the [R] matrices for a group of optimum energy system alternatives, established under various percentages of total load received, the most economically optimum system can be identified, followed by a series of matrix transformation to have its form in the actual or first reference frame.

Load flow calculations using Newton-Raphson or Gauss-Seidel methods for energy system optimization have been applied on a 23,000 MW capacity of a centralized and a mixed centralized-dispersed energy systems (containing conventional and renewable energy sources) under all loadings to calculate the [K] and the optimum [B] matrices, respectively. Then by Equation 1.21 above, elements of the [R] matrices reflecting energy system representation in the power flow frame have been established for all systems and subsystems from which the most economically optimum power network is selected relying on the elements of the diagonal [R] matrices since they represent the direct path from each equivalent energy source to the system centroid.

It can be stated that analyzing any arbitrary energy system in the energy flow reference frame according to the method presented in this chapter can be very economical with respect to consumption of computer time and memory since in this frame there are a substantially smaller number of total energy bus-bars and branches than that in the actual energy network.

Optimization of economic dispatch for a multiarea energy pool is the most sensitive and critical problem facing the power utilities and requires rigorous and fast evaluation leading to a comprehensive and universal solution.

One method of optimization established in earlier investigation is known as the Pool $\lambda$ method. It is based on a set of penalty factors resembling ratios between the on-line running cost of any area in the power pool with respect to the reference running cost. However, this method requires the immediate availability of a generalized [B] matrix (transmission loss coefficients) at the central computer where the control will perform periodic dispatch calculations for the entire energy pool for the purpose of solving all of the penalty vectors of the individual area members.

Basic data of information that must be fed in the central computer dispatch center is the transmission loss coefficient matrix for each single area of the energy pool and tie flow energy out of each area (since they serve as important elements in the system of constraint equations).

Available basis for the data of the transmission loss coefficient matrix is on the assumption of either constant ratio of bus-bar load current to the total system current or in a form of linear function ratio. In the first case, a simple quadratic form and, in the second, a linear quadratic form of the [B] matrix will result.

A principle and important reason for error recurrence in the economic dispatch results could be attributed to the fact that the conventional form of the [B] matrix, whether the simple quadratic or the linear-quadratic, are derived with respect to one-base loading conditions, and presumed to remain invariant at all other loadings.

**Table 1.14**
**Design for the Self-Symmetric Resistance Matrix for the "Centralized-Dispersed" Case**

| | | Loading | | | | |
|---|---|---|---|---|---|---|
| **No.** | **Bus no.** | **60%** | **70%** | **80%** | **90%** | **100%** |
| 1 | 1 | 232.7405 | 58.1807 | 50.0874 | 12.6649 | 28.296 |
| 2 | 150 | 0 | 0 | 0 | 0 | 0 |
| 3 | 151 | 0 | 0 | 0 | 0 | 0 |
| 4 | 152 | 0 | 0 | 0 | 0 | 0 |
| 5 | 153 | 0 | 0 | 0 | 0 | 0 |
| 6 | 155 | 0 | 0 | 0 | 0 | 0 |
| 7 | 156 | 199.7291 | 333.7475 | 71.6012 | 119.2799 | 60.5789 |
| 8 | 157 | 27.2476 | –24.7995 | 21.6802 | 78.7583 | 33.69004 |
| 9 | 158 | 0 | 0 | 0 | 0 | 0 |
| 10 | 161 | 0 | 0 | –222.6271 | 0 | 0 |
| 11 | 162 | 0 | 0 | 0 | 0 | 0 |
| 12 | 164 | 70.3657 | 61.8234 | 120.1663 | 83.7759 | 88.057 |
| 13 | 167 | 0 | 0 | 0 | 0 | 0 |
| 14 | 168 | 0 | 0 | 0 | 0 | 0 |
| 15 | 170 | 0 | 0 | 0 | 0 | 0 |
| 16 | 172 | 9.2792 | 14.9525 | 13.78256 | 3.5535 | 3.576 |
| 18 | 174 | 24.7215 | 0.6518 | –0.154 | –0.7353 | –0.6737 |
| 19 | 175 | 0 | 0 | 0 | 0 | 0 |
| 20 | 177 | 0 | 0 | 0 | 0 | 0 |
| 21 | 178 | 0 | 0 | 0 | 0 | 0 |
| 22 | 180 | 0 | 0 | 0 | 0 | 0 |
| 23 | 181 | 0 | 0 | 0 | 0 | 0 |
| 24 | 184 | 0 | 0 | 0 | 0 | 0 |
| 25 | 185 | 0 | 0 | 0 | 0 | 0 |
| 26 | 186 | 0 | 0 | 0 | 0 | 0 |
| 27 | 187 | 0 | 0 | 0 | 0 | 0 |
| 28 | 188 | 0 | 0 | 0 | 0 | 0 |
| 29 | 189 | 0 | 0 | 0 | 0 | 0 |
| 30 | 190 | 0 | 0 | 0 | 0 | 0 |
| 31 | 191 | 0 | 0 | 0 | 0 | 0 |
| 32 | 192 | 0 | 0 | 0 | 0 | 0 |
| 33 | 193 | 0 | 0 | 0 | 0 | 0 |
| 34 | 280 | 0 | 0 | 0 | 0 | 0 |
| 35 | 281 | 0 | 0 | 0 | 0 | 0 |
| 36 | 282 | 0 | 0 | 0 | 0 | 0 |
| 37 | 283 | 0 | 0 | 0 | 0 | 0 |
| 38 | 285 | 11.1651 | –8.3863 | 4.4923 | 11.4764 | 17.8185 |
| 39 | 286 | 0 | 0 | 0 | 0 | 0 |
| 40 | 287 | 0 | 0 | 0 | 0 | 0 |
| 41 | 288 | 0 | 0 | 0 | 0 | 0 |
| 42 | 289 | 0 | 0 | 0 | 0 | 0 |
| 43 | 290 | 0 | 0 | 0 | 0 | 0 |
| 44 | 291 | 14.3162 | 1.3834 | 0.6222 | –0.6429 | –1.36074 |
| 45 | 296 | 0 | 0 | 0 | 0 | 0 |
| 46 | 298 | 0 | 0 | 0 | 0 | 0 |
| 47 | 299 | 0 | 0 | 0 | 0 | 0 |
| 48 | 301 | 0 | –0.1237 | 0.4195 | 1.3208 | 1.927 |
| 49 | 304 | 0 | 0 | 0 | 0 | 0 |
| 50 | 305 | 0 | 0 | 0 | 0 | 0 |
| 51 | 306 | 0 | 0 | 0 | 0 | 0 |
| 52 | 309 | 0 | 0 | 0 | 0 | 0 |
| 53 | 312 | 0 | 0 | 0 | 0 | 0 |

**Table 1.14 (continued)**
**Design for the Self-Symmetric Resistance Matrix for the "Centralized-Dispersed" Case**

| | | Loading | | | | |
|---|---|---|---|---|---|---|
| **No.** | **Bus no.** | **60%** | **70%** | **80%** | **90%** | **100%** |
| 54 | 313 | 0 | 0 | 0 | 0 | 95.9768 |
| 55 | 314 | 0 | 0 | 0 | 0 | 0 |
| 56 | 315 | –69.41225 | –75.496 | –51.9564 | 0 | 0 |
| 57 | 316 | –34.8433 | –37.897 | –2.6081 | 0 | 0 |
| 58 | 327 | 0 | 0 | 0 | 0 | 0 |
| 59 | 328 | 5.7243 | 49.1009 | 0 | 0 | 0 |
| 60 | 332 | –406.2994 | –384.802 | –326.518 | –274.4125 | –223.6036 |
| 61 | 333 | 0 | 0 | 0 | 0 | 0 |
| 62 | 334 | 49.7521 | 0 | 0 | 0 | 0 |
| 63 | 336 | 0 | 0 | 0 | 0 | 0 |
| 64 | 337 | 0 | 0 | 0 | 0 | 0 |
| 65 | 339 | 22.2 | 3.8601 | –0.6725 | –27.3766 | –4.7944 |
| 66 | 340 | 0 | 0 | 0 | 0 | 0 |
| 67 | 343 | 5.9322 | –5.1711 | 1.4737 | 11.184 | 2.1394 |
| 68 | 345 | 0 | 0 | 0 | 0 | 0 |
| 69 | 349 | 0 | 0 | 0 | 0 | 519.8188 |
| 70 | 351 | 0 | 0 | 0 | 0 | 0 |
| 71 | 353 | 0 | 0 | 0 | 0 | 0 |
| 72 | 354 | 0 | 0 | 0 | 0 | 0 |
| 73 | 357 | 2.4494 | –0.5968 | –7.2435 | –9.1713 | –18.4476 |
| 74 | 360 | 0 | –83.9 | 67.8684 | 14.1348 | 253.1313 |
| 75 | 362 | 0 | 0 | 0 | 0 | 0 |
| 76 | 365 | 0 | 0 | 0 | 0 | 0 |
| 77 | 366 | 11.1651 | –8.3863 | 4.4923 | 11.4764 | 17.8185 |
| 78 | 368 | 0 | 0 | 0 | 0 | 0 |
| 79 | 371 | 25.7709 | 0.0044 | 0.7 | 0.5817 | 0.5987 |
| 80 | 372 | –364.7648 | –339.611 | –277.2269 | –219.60304 | 0 |
| 81 | 0 | 0 | 0 | 0 | 0 | 0 |
| 82 | 0 | 0 | 0 | 0 | 0 | 0 |
| 83 | 376 | 0 | 0 | 0 | 0 | 0 |
| 84 | 379 | 0 | 0 | 0 | 0 | 0 |
| 85 | 380 | 0 | 0 | 0 | 0 | 0 |
| 86 | 381 | 0 | 0 | 0 | 0 | 0 |
| 87 | 383 | 0 | 0 | 0 | 0 | 0 |
| 88 | 389 | 0 | 0 | 0 | 0 | 0 |
| 89 | 390 | 11.4417 | 5.4057 | –0.6336 | –4.528 | –4.5613 |
| 90 | 391 | 0 | 0 | 0 | 0 | 0 |
| 91 | 401 | 0 | 0 | 0 | 0 | 0 |
| 92 | 402 | 0 | 0 | 0 | 0 | 0 |
| 93 | 403 | 0 | 0 | 0 | 0 | 0 |
| 94 | 404 | 0 | 0 | 0 | 0 | 0 |
| 95 | 405 | 0 | 0 | 0 | 0 | 0 |
| 96 | 410 | 0 | 0 | 0 | 0 | 0 |
| 97 | 406 | 0 | 0 | 0 | 0 | 0 |
| 98 | 411 | 0 | 0 | 0 | 0 | 0 |
| 99 | 412 | 0 | 0 | 0 | 0 | 0 |
| 100 | 413 | 0 | 0 | 0 | 0 | 0 |
| 101 | 414 | 0 | 0 | 0 | 0 | 0 |
| 102 | 415 | 0 | 0 | 0 | 0 | 0 |
| 103 | 417 | 0 | 0 | 0 | 0 | 0 |
| 104 | 418 | 0 | 0 | 0 | 0 | 0 |
| 105 | 419 | 0 | 0 | 0 | 0 | 0 |

**Table 1.14 (continued)**
**Design for the Self-Symmetric Resistance Matrix for the "Centralized-Dispersed" Case**

| | | Loading | | | | |
|---|---|---|---|---|---|---|
| **No.** | **Bus no.** | **60%** | **70%** | **80%** | **90%** | **100%** |
| 106 | 420 | 0 | 0 | 0 | 0 | 0 |
| 107 | 422 | 0 | 0 | 0 | 0 | 0 |
| 109 | 424 | 0 | 0 | 0 | 0 | 0 |
| 110 | 432 | 18.4988 | 0 | 0 | 0 | 0 |
| 111 | 433 | 0 | 0 | 0 | 0 | 0 |
| 112 | 434 | 0 | 0 | 0 | 0 | 0 |
| 113 | 436 | 0 | 0 | 0 | 0 | 0 |
| 114 | 437 | 0 | 0 | 0 | 0 | 0 |
| 115 | 683 | –566.4243 | 0 | 0 | 0 | 0 |
| 116 | 685 | 0 | 0 | 0 | 0 | 0 |
| 117 | 423 | 0 | 0 | 0 | 0 | 0 |
| 118 | 687 | 0 | 0 | 0 | 0 | 0 |
| 119 | 690 | 0 | 0 | 0 | 0 | 0 |
| 120 | 693 | 27.8 | –11.666 | 10.0973 | 0 | 0 |
| 121 | 695 | 0 | 0 | 0 | 0 | 0 |
| 122 | 702 | 0 | 0 | 0 | 0 | 0 |
| 123 | 711 | 0 | –7.0156 | 6.143 | 22.2623 | 41.009 |

*Note*: All values listed are $10^6$ times greater than their true per unit value

From Denno, K., Power system identification in the power reference frame, *J. Appl. Sci. Eng.*, 2, 141—153, 1977. With permission.

## XII. PROBLEMS

1.1 For

$$P_L = \sum_i^n \sum_j^n P_i B_{ij} P_j$$

$$\frac{dF_i}{dP_i} = F_{ii} P_i + F_i$$

Obtain solution of $B_{ij}$ shown in Equation 1.4 by solving the differential Equation of 1.1.

1.2 Using information of load flow calculations at 70% loading for centralized energy system from Table 1.2 establish solution for the [K] matrix.

1.3 Using elements of the [K] matrix obtained in Problem 2 and data of the [B] matrix for a centralized energy system at 70% loading given in Table 1.7, establish solution for the system synthesis in the sixth reference frame, namely, the [R] matrix.

1.4 Repeat Problem 2, but for 100% loading.

1.5 Repeat Problem 3, but for 100% loading.

1.6 Repeat Problem 2, but for 70% dispersed energy system.

1.7 Repeat Problem 3, but for 70% dispersed energy system.

1.8 Through proper computer program, convert solution of the [R] matrix established in Problem 3 into a new matrix in the principle coordinate system. Such a matrix contains only diagonal elements and can be secured from any nonsingular matrix by securing solution of λs from the following determinant equation:

$$\begin{bmatrix} a_{11}- & a_{12} & a_{13} & a_{1n} \\ a_{21} & a_{22} & \cdots & a_{2n} \\ \cdots & \cdots & \cdots & \cdots \\ \cdots & \cdots & \cdots & \cdots \\ \cdots & \cdots & \cdots & \cdots \\ a_{n1} & & & a_{nn}- \end{bmatrix} = 0$$

Solution of all λs will be the diagonal elements of the principle matrix.

1.9 Repeat Problem 8 for the [R] matrix established in Problem 5.

1.10 Repeat Problem 8 for the [R] matrix established in Problem 7.

1.11 From systematic sequence of equations in Section IX, derive the solution of the transmission loss coefficient matrix [B] for a multiarea energy pool with tie power flow expressed in Equation 1.50.

1.12 Equation 1.50 was derived on the basis that:

$$P_T = \frac{\sqrt{P_L}}{P_r}$$

where $P_r$ is constant.
Establish another solution for $B_{ij}$ for

$$P_T = \text{root - mean - square value of } \sqrt{\frac{P_L}{P_r}}$$

1.13 Repeat Problem 12 for $B_{ij}$ for $P_T$ = geometrical mean of:

$$\sqrt{\frac{P_L}{P_r}}$$

for example,

$$P_T = \sqrt{\frac{P_L}{P_r}}$$

1.14 Table 1.13 shows elements of $B_{ij}$ at 100% loading for the eight power plants with tie power flows. Using data in Table 1.12 for corrective factor establish transmission loss coefficient matrix without tie power flow.

1.15 Repeat Problem 14, but for 67% loading.

1.16 Repeat Problem 14, but for 41% loading.

1.17 Corrective factor for tie power flow from Equation 1.50 is expressed by:

$$C.F. = \left(1 + \frac{\frac{k}{2}}{\sqrt{P_{L-min}}}\right)$$

Refer to Table 1.6 which shows the [B] matrix for centralized system in which fuel cells supply peak power demand at 60% loading to establish [B] with tie power flow.

1.18 Repeat Problem 17, but for 70% loading.

1.19 Repeat Problem 17, but for 80% loading.

1.20 Repeat Problem 17, but for 100% loading.

1.21 Table 1.14 shows the diagonal elements of the regular symmetric [R] matrix for a centralized-dispersed system, where fuel cells generating an assembled system supplies power demand at newly planned generators as well as at locations of new load bus-bars. Treat the case of 100% loading. Using load flow calculations data for such system, establish the [B′] matrix without tie power flow.

1.22 Repeat Problem 21, but with tie power flow existing, i.e., establish the [B′] or $B_{ij}$ matrix.

1.23 Through appropriate computer program, convert the [R] matrix in Problem 21 into the principle coordinate system, i.e., a new matrix with only forced diagonal elements.

1.24 Also, through appropriate computer program, convert the [R] matrix of Problem 22 into the principle coordinate system.

## REFERENCES


1. **Boshier, J. R.,** Economic operation for electric power systems, *IEE Electronics and Power*, May 1974, 418—420.
2. **Denno, K. I.,** Power System Synthesis from Solution of Optimum Transmission Loss Coefficients, paper C73462-9 presented at the IEEE, PES Summer Meeting in Vancouver, Canada, July 1973.
3. **Denno, K.,** Power system identification in the power flow reference frame, *J. Appl. Sci. Eng.*, 2, 141—153, 1977.
4. **Denno, K.,** Optimal Solution for the Transmission Loss Coefficients Matrix in a Multi-Area Pool System, Proc. Control of Power Systems, IEEE, No. 77CH1168-4 REG. 5, 1977, 124—127.
5. **Denno, K.,** Steady State and Dynamic Investigations for Determining Optimum Electrochemical — Electro-mechanical Interconnected Power Systems, report published by NJIT for a research grant sponsored by the Middle Atlantic Power Research Committee, 1975.
6. **Davis, T. W. and Palmer, R. W.,** *Computer-Aided Analysis of Electrical Networks*, Charles E. Merrill Publishing Co., Ohio, 1973.
7. **Fink, L. H.,** An Economic Dispatch Technique for PJM, Rep. E-195, Philadelphia Electric Company, August 1970.
8. **Happ, H. J. and Nour, N. E.,** Multi-area network modeling for power pools, *IEEE Trans Power Appar. Syst.*, March—April, 1976.
9. **Kirchmayer, L. K.,** *Economic Operation of Power Systems*, John Wiley & Sons, New York, 1958.
10. **Kron, G.,** Tensorial analysis of integrated transmission systems, *AIEE Trans. Power Syst. and Appar.*, 70, 1239, 1951.
11. **Mickel, M. H. and Sze, T. W.,** *Optimization in Systems Engineering*, Intex Educational Publishers, San Francisco, 1972.
12. **Mollo, C. R. and Denno, K.,** The Feasibility of Fuel Cells in Modern Power Systems, M.S. thesis presented in partial fulfillment of the requirements of Master of Science degree in Electrical Engineering, New Jersey Institute of Technology, Newark, NJ, 1973.
13. **Stagg, G. W. and El-Abiad, A. H.,** *Computer Methods in Power System Analysis*, McGraw-Hill Book Company, New York, 1968.
14. **Stagg, G. W. and El-Abiad, A. H.,** *Computer Methods in Power System Analysis*, McGraw-Hill, New York 1968.

Chapter 2

# ECONOMIC FEASIBILITY OF FUEL CELLS AND STORAGE BATTERIES WITHIN CONVENTIONAL ENERGY SYSTEMS*

## I. INTRODUCTION[1-13]

In the forefront of various modes of renewable energy sources are the fuel cell and storage battery. Both are electrochemical energy devices that deliver direct current output power. Therefore, the fuel cell or the storage battery has to be linked to a power inverter to generate an alternating power, followed by a filtering system to secure a pure sinusoidal wave form, and finally, stepping the output alternating current voltage through a transformer system.

Fuel cells fall into two major categories, namely, the low temperature mode which is the hydrogen-oxygen cell and the high temperature cell which is the carbon monoxide-oxygen cell. The oxidizing agent in both fuel cell modes is oxygen or preheated air.

Basic electrochemical equations for the hydrogen-oxygen cell are shown below.

At the anode:

$$2H_2 \rightarrow 4H^+ + 4\bar{e} \tag{2.1}$$

At the cathode:

$$4H^+ + 4e + O_2 \rightarrow 2H_2O \tag{2.2}$$

The overall electrochemical equation becomes

$$2H_2 + O_2 \rightarrow 2H_2O \tag{2.3}$$

Separating the anode from the cathode is an ion exchange membrane for the movement of hydrogen ions.

For the high temperature fuel cell where carbon monoxide acts as the fuel and oxygen or preheated air as the oxidizer, the basic electrochemical equations are expressed below.

At the anode:

$$CO + CO_3^{--} \rightarrow 2CO_2 + 2e \tag{2.4}$$

At the cathode:

$$CO_2 + \frac{1}{2}O_2 + 2e \rightarrow CO_3^{--} \tag{2.5}$$

And hence, the overall electrochemical equation becomes

$$CO + \frac{1}{2}O_2 \rightarrow CO_2 \tag{2.6}$$

Regarding the storage battery, the basic reactants are not unique as in the case of fuel cells.

Operational batteries include the conventional lead-acid battery, nickel-cadmium, zinc-nickel oxide, and alkali-metal batteries.

Among the alkali-metal batteries, the lithium-sulfur (Li-S) battery is considered as a reliable power source for bulk power output, although the sodium-sulfur (Na-S) and (Li-S) of the alkali-metal group have been in the process of progressive development.

## II. FUEL COST CURVES

### A. FUEL CELL

Fuel cost for a fuel cell unit is projected at \$90/MBtu associated with an escalation factor to account for inflation, and with heat energy dissipated by the cell to remain constant at 8500 Btu/kWh. Therefore, the incremental fuel cost of the fuel cell becomes

$$\frac{dF}{dP} = \left(8.5 \times 10^{-3} \text{ million Btu/kWh}\right)\left(\$0.90/\text{million Btu}\right) = 7.65 \text{ mills/kWh} \quad (2.7)$$

### B. STORAGE BATTERY

The principle criterion for calculating the fuel cost curve for the storage battery is expressed by

1. Incremental fuel cost = the system off-peak incremental fuel cost per storage battery efficiency
2. Nominal efficiency = 80% (usually)

Applications of the storage battery are intended to supply peak loading demand, and in this respect, they may take part with the gas turbines or even replace them in meeting peak loads. However, batteries recharging for cost effectiveness, could be conducted at off-peak loading.

From the normal load duration curve, the total megawatt hours (MWh) that storage batteries would supply could be determined exactly. The load duration curve is a correlation for the percentage of load demand with respect to total annual hours.

Therefore, the total energy that the battery system will supply is the value determined from the load duration curve divided by the battery efficiency which is of the order of 80%.

The next step in the process of establishing the incremental fuel cost of the battery system is the identification of an equal area under the load duration curve which is equal to the total energy the battery supplies; this is in effect the same amount needed to recharge the battery system.

Frequently, and in most cases as data in the literature indicates, if the total energy for recharging is below the minimum total energy demand anywhere within the load duration curve, the incremental fuel cost for the battery system will be considered equal to the minimum value available within the entire generating sources.

## III. INTEGRATION OF ELECTROCHEMICAL GENERATORS[1-13] (A CASE STUDY OF UTILITY SYSTEM)*

Engineering economics of electrochemical generators, notably fuel cells and storage batteries, will be examined and demonstrated through an integration process where these two renewable energy sources will be used to supply base and peak power loadings.

The particular power system in which fuel cells and/or storage batteries will be integrated is a large grid power system supplied by the PSE&G of New Jersey for a total load growth of about

* © 1973, Reprinted with permission from M.Sc. theses authored by C. R. Mollo and W. L. Yang, under supervision of K. Denno. Title of each thesis "The Feasibility of Fuel Cells in a Modern Power System".

5000 MW and for a total peak load of about 13,000 MW. The 5000 MW growth is to be spanned over a period of 5 years.

A total of seven alternative systems for the allocation of power sources include conventional sources such as (1) fossil-steam operated alternators, (2) pumped-hydro plants, (3) gas turbines, and (4) nuclear operated alternators in connection with fuel cells and storage batteries for base as well as peak load demands.

Those seven options of integrated power system alternatives include totally centralized power plants as well as combinations of centralized-dispersed systems.

Dispersed subsystems will be formed for the new planned sites of additional generators. New centers of load demands will be met by fuel cells and or storage batteries located at these new load centers.

The new dispersed subsystem, through its integration with an existing central system of conventional energy sources, will form a new combination of centralized-dispersed interconnected energy systems.

Taking the above into consideration, the alternative systems were reasonably chosen and were defined as follows.

**Alternative A: The Conventional System** — It consists of nuclear and pumped-hydro units for the base loading with steam-fossil and gas-turbine generators for the off-peak and peak conditions, respectively. This plan was chosen as the reference plan that will be compared with each alternative plan.

**Alternative B: The Centralized Nuclear, Pumped-Hydro and Fuel Cell System** — In this system, all of the steam-fossil and gas-turbine generators were replaced by the fuel cell units. Therefore, the new plan consists of nuclear, pumped-hydro operated generators and fuel-cell assembled units.

**Alternative C: The Peak Loading Fuel Cell System** — In this system, all of the gas-turbine generators planned for the peak loading conditions were replaced by the fuel-cell assembled units. The new plan now consists of nuclear, pumped-hydro, and steam-fossil generators, and fuel-cell assembled units.

**Alternative D: The Off-Peak Loading Fuel Cell System** — In this system, all of the steam-fossil generators planned for off-peak loading condition were replaced by the fuel-cell assembled units. The reasoning for this alternative is that the steam-fossil unit has very high operation and maintenance cost and high incremental fuel cost with respect to fuel cells. In this case, the new alternative system consists of nuclear, pumped-hydro, and gas-turbine generators, and fuel-cell assembled units.

**Alternative E: The Centralized-Dispersed Fuel Cell System** — In this system, the fuel cell units were installed at those buses where there is an increase in load from its initial level. The purpose of this alternative is to study the impact of minimum transmission losses and environmental impacts.

**Alternative F: The Peak Loading Assembled Battery System** — In this system, all of the gas-turbine generators planned for the peak loading conditions were replaced by the assembled storage battery system. The advantage of using storage batteries is that such units can be charged up during off-peak loading with lower incremental fuel cost and will supply the peaking energy demand which otherwise will require higher incremental fuel cost. By doing so, the fuel cost of the entire system could be minimized. This new plan consists of nuclear, pumped-hydro, and steam-fossil generators, and the storage battery assembled system.

**Alternative G: The Fuel Cell and Battery System I** — In this system alternative, all of the steam-fossil generators planned for the off-peak condition are replaced by the fuel-cell assembled units, and all of the gas-turbine generators planned for the peak loading condition were replaced by the storage battery system. The new plan here consists of nuclear, pumped-hydro generators, fuel cell units, and storage battery systems.

**Alternative H: The Fuel Cell and Battery System II** — In this system alternative, all of the

gas-turbine generators planned for the peak loading condition are replaced by both the fuel-cell assembled units and storage batteries in a 50:50 ratio basis. The new plan consists of nuclear, pumped-hydro, steam-fossil generators, fuel-cell assembled units, and the storage battery system.

After all alternative plans have been defined, the calculation of cost effectiveness for each plan can begin. However, it should be noted that all computation to be carried out is done on the annual savings basis with respect to the conventional reference centralized plan. A positive value represents a savings compared to the conventional plan, while negative value means economic losses compared to the conventional reference plan.

There are three major economic areas that should be considered for this study. They are the capital cost, the operation and maintenance cost, and the fuel cost. The capital cost includes the initial investment of expanding the generating facility and transmission network. The operation and maintenance cost includes the fixed and variable operation and maintenance costs. Fuel cost includes the cost of various types of fuel used in the various generating units. After the annual savings were calculated for all the three costs, the total annual savings for each alternative plan, with respect to the conventional reference plan, will be computed simply by adding all three costs together. In this chapter, the plan using fuel cell generators as well as storage batteries in an integral mode with conventional energy system will be evaluated on a short-term as well as a long-term scope.

## IV. ECONOMIC EVALUATION OF ALTERNATIVE ENERGY SYSTEMS[1-13]*

The objective of economic evaluation for alternative energy systems should be accomplished by comparison of the total cost which includes the initial capital cost, fuel cost, and operation and maintenance cost on an annual savings basis. The theoretical concept for economic evaluation is shown in Sections IV.A and IV.B.

### A. ANNUAL CAPITAL COST EVALUATION

The annual capital cost includes the expansion investment for the generating units and transmission network. The cost data was given by the PSE&G of New Jersey in Table 2.1. The basic formula for this computation is described below.

The annual capital cost for each energy source or bus-bar can be calculated from:

$$CC_p = \left[(GC + TC)KP_p\right] / (CR)_i^n \tag{2.8}$$

where $CC_p$ = the annual capital cost for bus P in dollars; GC = the generation expansion capital cost for bus P in dollars per kilowatt; TC = the transmission capital cost for bus P in dollars per kilowatt; $P_p$ = the total generation for bus P in megawatts; $K = 10^3$, a conversion factor from megawatts to kilowatts; and (CR) = the capital recovery factor for n life year of the unit and i the percent interest.

Total annual capital cost for plan Y can be computed by adding all annual capital costs for each energy bus as follows:

$$TCCy = \sum_P CC_p \tag{2.9}$$

* © 1973, Reprinted with permission from M.Sc. theses authored by C. R. Mollo and W. L. Yang, under supervision of K. Denno. Title of each thesis "The Feasibility of Fuel Cells in a Modern Power System".

**TABLE 2.1**
**Operation & Maintenance Cost for Various Modes of Generating Units**

| Unit type | Average life (years) | Fixed O&M ($/kW/year) | Variable O&M (mills/kWh) | Annual maintenance (weeks) |
|---|---|---|---|---|
| Steam-fossil | 45 | 2.0 | 0.3 | 4 |
| Gas turbine | 30 | Negligible | 2.0 | 2 |
| Nuclear | 35 | 1.0 | 0.1 | 4 |
| Pumped-hydro | 50 | Negligible | Negligible | 4 |
| Fuel cell | 20 | Negligible | 1.5 | 1 |
| Storage battery | 20 | Negligible | 1.0 | 1 |

*Note:* Based on the above table, calculation of the annual O&M cost for each alternative plan is to be performed in the following process: AOMCp = FAOMCp + VAOMCp where $AOMC_n$ = the annual O&M cost for bus P in dollars; $FAOMC_n$ = the fixed annual O&M cost for bus P in dollars; and $VAOMC_n$ = the variable annual O&M cost for bus P in dollars.

From Energy Utilization of PSE&G for the Middle Atlantic Power Research Committee, Newark, NJ, 1976. With permission.

where TCCy = the total annual capital cost for plan Y in dollars; P = the bus-bar number; and $CC_p$ = the annual capital cost for bus P in dollars.

## B. ANNUAL OPERATION AND MAINTENANCE COST EVALUATION

There are fixed and variable operation and maintenance (O&M) costs. Both data were given in Table 2.1.

Calculation of the annual O&M cost for each alternative plan is to be performed in the following process:

$$AOMC_p = FAOMC_p + VAOMC_p \tag{2.9A}$$

where $AOMC_n$ = the annual O&M cost for bus P in dollars; $FAOMC_n$ = the fixed annual O&M cost for bus P in dollars; and $VAOMC_n$ = the variable annual O&M cost for bus P in dollars.

By simply adding all annual O&M cost for each energy bus, the total annual cost for plan Y can be obtained as follows:

$$TAOMC_p = \sum_P AOMC_p \tag{2.10}$$

where $TAOMC_p$ = the total annual O&M cost for plan Y in dollars and $AOMC_p$ = the annual O&M cost for bus P in dollars.

## C. ANNUAL FUEL COST EVALUATION[1-13]

The process of computing the annual fuel cost is a complex and lengthy one. First, the calculation of fuel input cost for a particular plant is obtained by solving the coordination equation below.

$$\frac{dF_i}{dP_i} + \lambda \frac{\partial P_L}{\partial P_i} = \lambda \tag{2.11}$$

where

$$F_t = \sum_{i=1}^{n} F_i$$

$P_L$ = the total transmission losses in megawatts; $F_i$ = the input cost to unit i in dollars per hour; $P_i$ = the output of unit n in megawatts; $F_t$ = total cost of all plants; $\partial F_i/\partial P_i$ = the incremental production cost in dollars per megawatt hour for plant i; $\partial P_L = \partial P_i$ = the incremental transmission losses in megawatts per megawatts; and $\lambda$ = cost of received power in dollars per megawatt hour.

The incremental transmission losses for plant i can be expressed as follows:

$$\frac{\partial P_L}{\partial P_i} = \sum_{i,j}^{n,m} 2B_{ij}P_j \tag{2.12}$$

where $B_{ij}$ = the loss formula coefficient and $P_i$ = the output of unit i in megawatts.

To calculate the total system losses, the following equation can be used

$$P_L = \sum_{i}^{n} \sum_{j}^{m} P_i B_{ij} P_j$$

The incremental production cost for a given plant can be represented by:

$$\frac{\partial F_i}{\partial P_i} = F_{ii}P_i + f_i \tag{2.13}$$

where $F_{ii}$ = the slope of incremental production cost curve and $f_i$ = the intercept of incremental production cost curve.

Substituting Equations 2.11 and 2.12 into 2.10 gives

$$F_{ii}P_i + f_i + \lambda \sum_{i}^{n} B_{ij}F_j = \lambda \tag{2.14}$$

In a metropolitan (condensed) system like the one used in this study, the effect of the transmission network is neglected in the scheduling of generation, so the optimum loading can be expressed in the following way by assuming $B_{ij}$ to be zero.

$$\lambda = F_{ii}P_i + f_i \tag{2.15}$$

therefore,

$$\frac{\partial F_t}{\partial P_i} = \lambda \tag{2.16}$$

It should be noted, Equation 2.15 is true only in a metropolitan or condensed system where losses are assumed to be negligible ($P_L = 0$).

The meaning of Equation 2.15 is very important for the following reasons. When Equation 2.15 is satisfied, the total input cost ($F_t$) to a system is at its minimum. However, total output power ($P_i$) is at its optimum limit. In other words, the minimum input (dollars per hour) for a given load is obtained when all generating units are operated at the same incremental cost ($\lambda$) found in Equation 2.15. Any change in $\lambda$ will cause the same change in total generation as

indicated in the equation. Therefore, if $\lambda$ is known for any generating capacity, one can be sure the most economic scheduling of generation is obtained. The fuel cost computed from this $\lambda$ will be the most economic fuel cost.

The procedures of calculating fuel cost after the computation of $\lambda$ are as follows. Since $\lambda$ for each loading of generating units is known, an incremental cost curve ($\lambda$ vs. power output) can be plotted for every generating unit. By integrating such a curve, the fuel cost curve (input fuel cost vs. total power received) can be obtained. The fuel cost curve provides only the information of fuel cost (dollars per hour) at various loadings. To calculate the total annual fuel cost, the load duration curve (percent power vs. percent time) must be introduced. From this curve, the amount of hours for a specific power loading can be secured. Therefore, by using a load duration curve, the fuel cost curve can be replotted in a fuel cost (dollars per hour) vs. total hours (hours) basis. Take the area under such a curve; this area represents the total annual fuel cost.

## V. INCREMENTAL FUEL COST CURVES

In the following, incremental fuel cost curves for a conventional centralized power system having a total of 32 bus-bars powered by fossil-steam, pumped-hydroelectrics, nuclear as well as gas turbine are shown.

## VI. OPTIMUM RATE OF FUEL COST[1-13]

The most economical or optimum scheduling of power allocation from individual energy sources for each system alternative could be determined by using the economic power coordination in Equation 2.11. $P_L$ is negligible in this case study which involves a grid system of a metropolitan consuming region for both centralized and, of course, dispersed systems.

## VII. EVALUATION OF OPTIMUM ECONOMICS*

### A. TOTAL ANNUAL ECONOMIC CHANGE

From the optimum fuel cost curves determined earlier, it is possible to find the annual optimum fuel cost savings or losses for each system with respect to the alternative system A. Furthermore, from the installation cost data supplied by PSE&G, New Jersey, it is possible to determine the annual equivalent initial cost savings or losses for each system, again using the alternative system A. The combination of these two economic values will determine the most economic system, i.e., the optimum as well as the relative additional cost of each alternative. Finally, from the O&M cost data supplied by PSE&G, it is possible to integrate the effect of the speculated O&M cost of the different system alternatives into the final economic picture of each system alternative.

### B. ANNUAL FUEL COST DIFFERENTIAL

The first step in determining the annual fuel cost differential is to find the difference between the fuel cost (dollars per hour) of each system with respect to alternative A. The resulting differential plots of $\delta$ (dollars per hour) vs. power received are shown in Figures 2.34 through 2.40. Once these curves are established, they are interacted with the load duration curve shown in Figure 2.41, to obtain plots of $\delta$ (dollars per hour) vs. total annual hours. The annual economic edge which could be either savings or losses are then found simply by finding the area under these curves [$\delta$ (dollars per hour) $\times$ hours = $\delta$ dollars]. This load duration curve was approximated by two straight lines, as indicated on the curve. The equations of these lines were

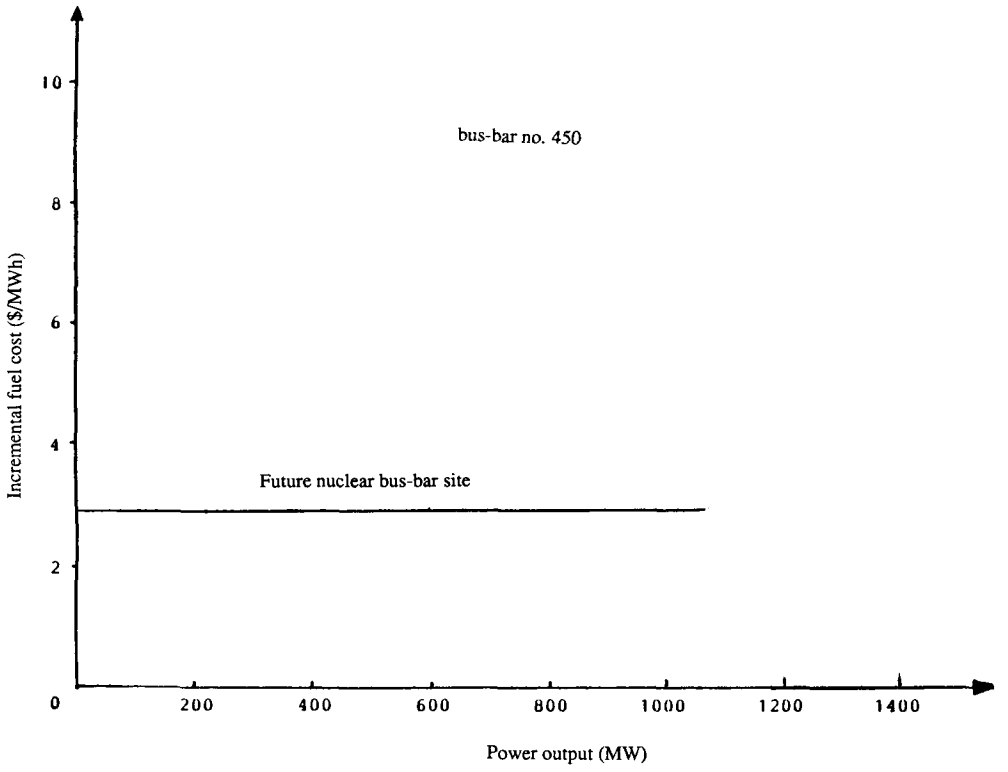


FIGURE 2.1 Incremental fuel cost curve (bus-bar no. 450). (From Mollo, C. and Yang, W., The Feasibility of Fuel Cells in Modern Power Systems, M.Sc. thesis, supervised by K. Denno, New Jersey Institute of Technology, 1973; and sponsored by PSE&G, Newark, NJ. With permission.)

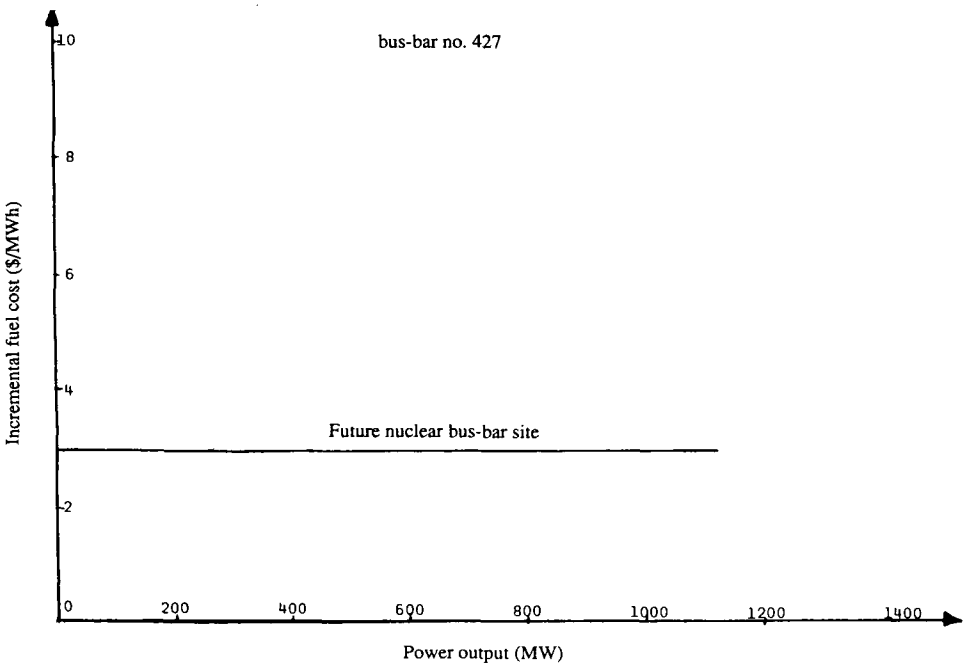


FIGURE 2.2 Incremental fuel cost curve (bus-bar no. 427). (From Mollo, C. and Yang, W., The Feasibility of Fuel Cells in Modern Power Systems, M.Sc. thesis, supervised by K. Denno, New Jersey Institute of Technology, 1973; and sponsored by PSE&G, Newark, NJ. With permission.)

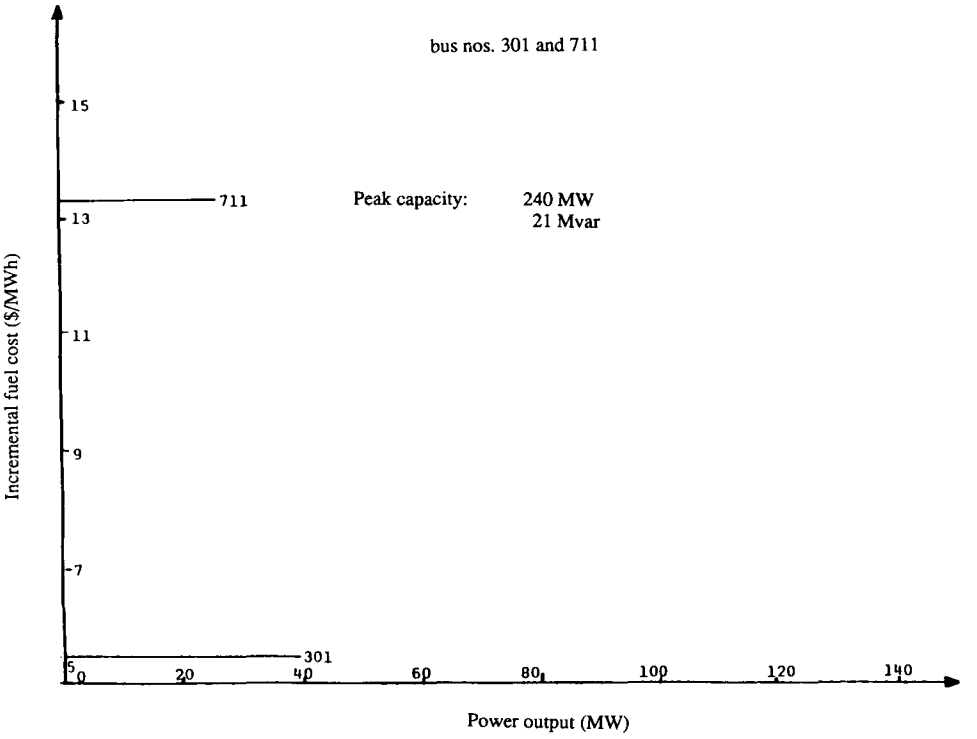


FIGURE 2.3 Incremental fuel cost curve (bus-bar nos. 301 and 711). (From Mollo, C. and Yang, W., The Feasibility of Fuel Cells in Modern Power Systems, M.Sc. thesis, supervised by K. Denno, New Jersey Institute of Technology, 1973; and sponsored by PSE&G, Newark, NJ. With permission.)

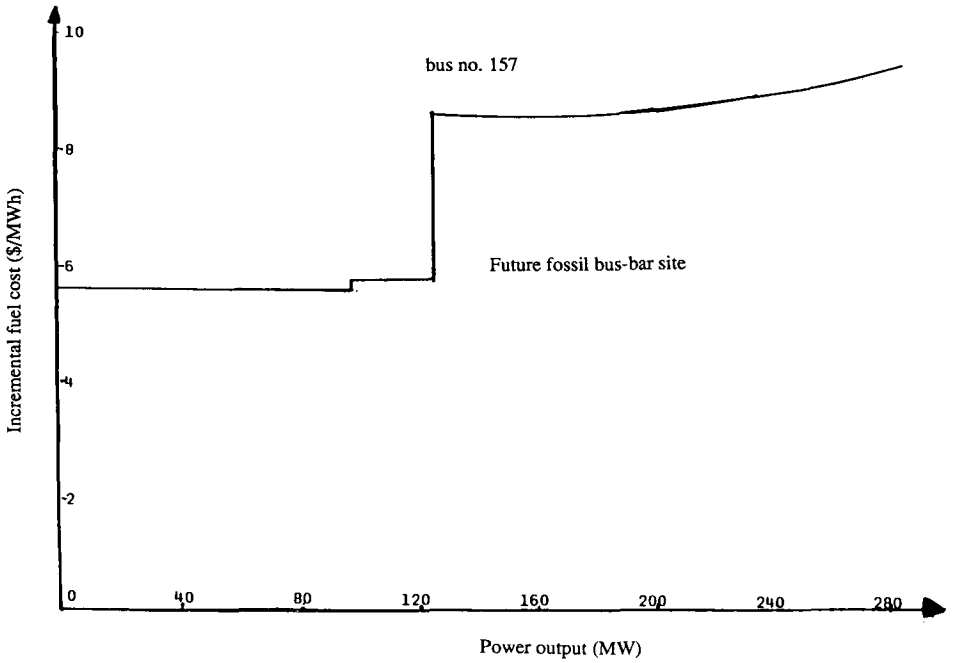


FIGURE 2.4 Incremental fuel cost curve (bus-bar no. 157). (From Mollo, C. and Yang, W., The Feasibility of Fuel Cells in Modern Power Systems, M.Sc. thesis, supervised by K. Denno, New Jersey Institute of Technology, 1973; and sponsored by PSE&G, Newark, NJ. With permission.)

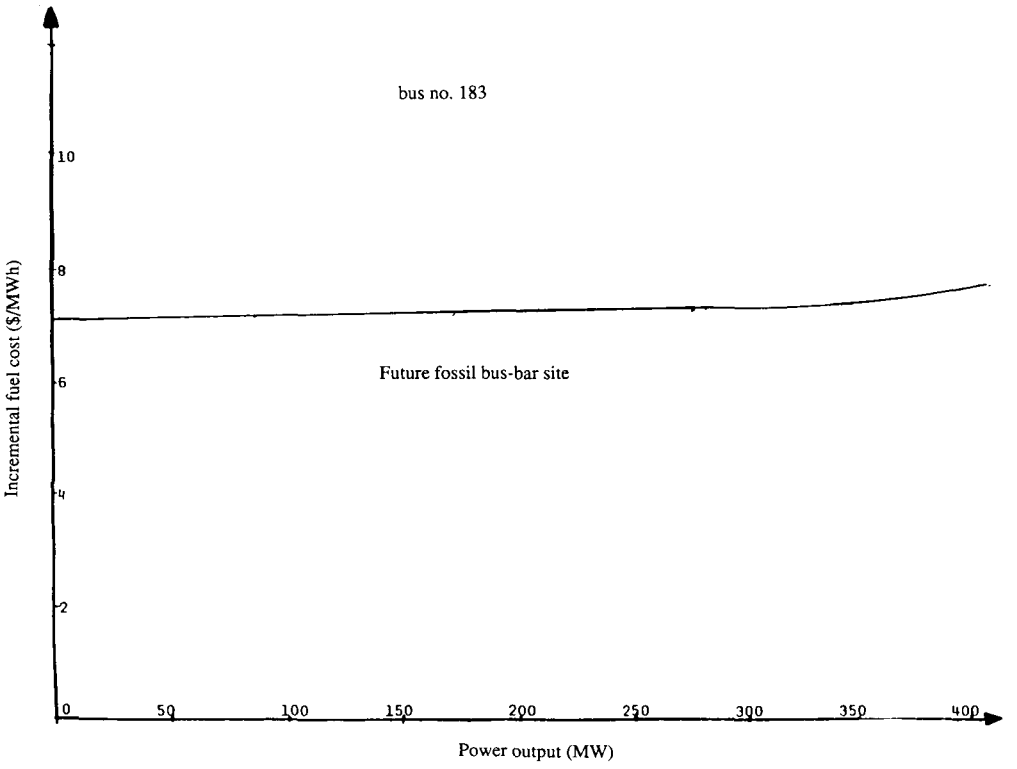


FIGURE 2.5 Incremental fuel cost curve (bus no. 183). (From Mollo, C. and Yang, W., The Feasibility of Fuel Cells in Modern Power Systems, M.Sc. thesis, supervised by K. Denno, New Jersey Institute of Technology, 1973; and sponsored by PSE&G, Newark, NJ. With permission.)

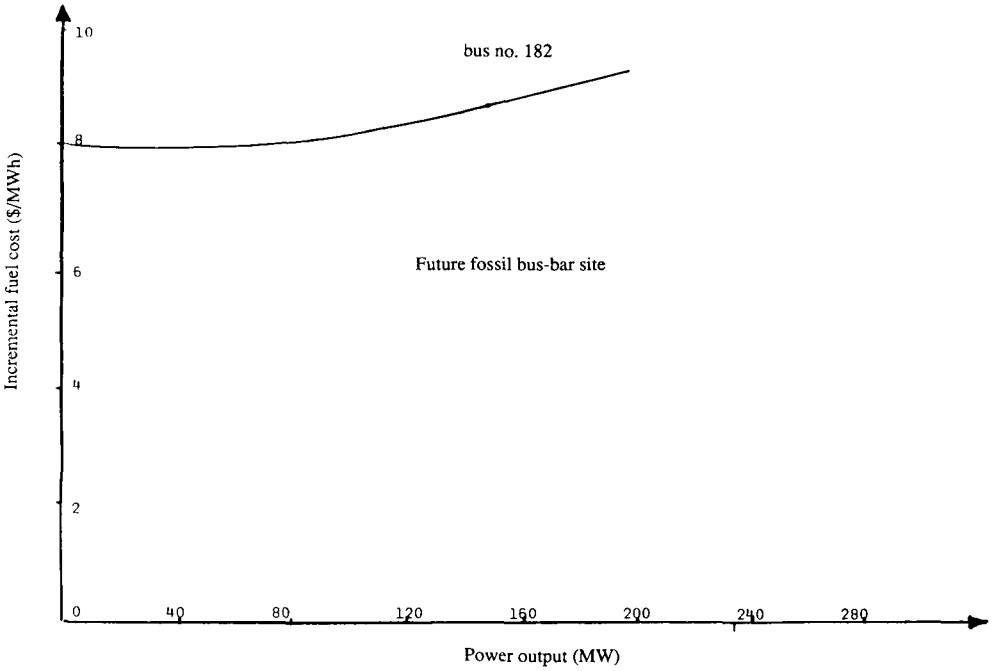


FIGURE 2.6 Incremental fuel cost curve (bus no. 182). (From Mollo, C. and Yang, W., The Feasibility of Fuel Cells in Modern Power Systems, M.Sc. thesis, supervised by K. Denno, New Jersey Institute of Technology, 1973; and sponsored by PSE&G, Newark, NJ. With permission.)

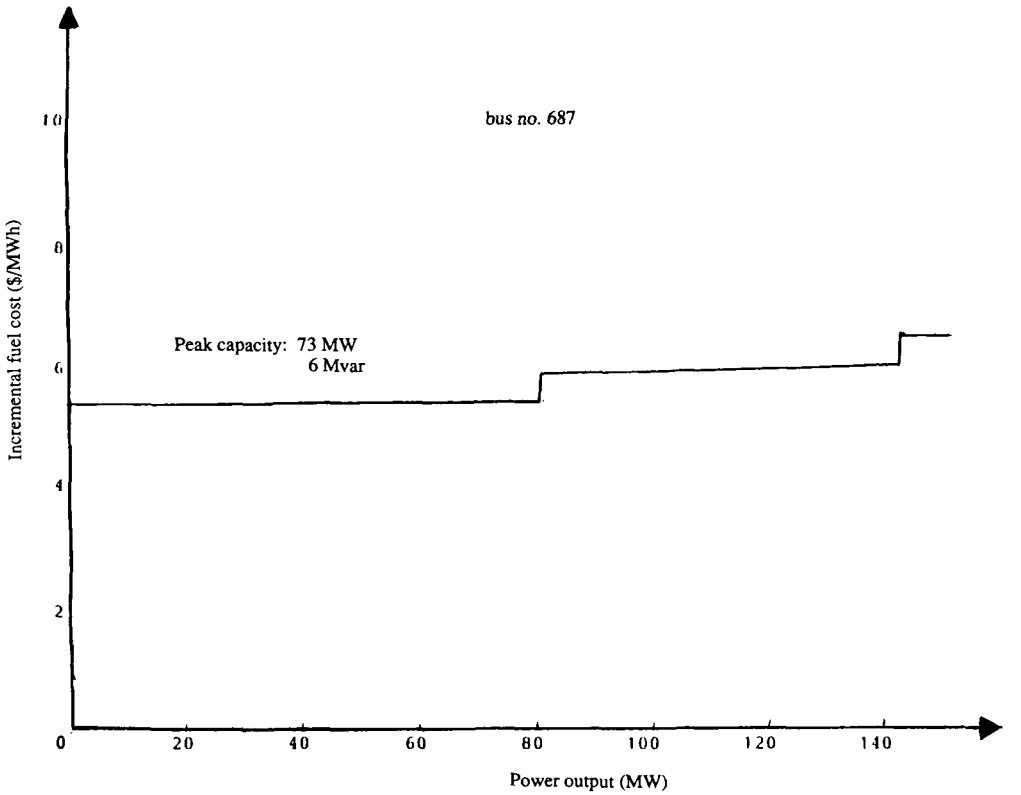


FIGURE 2.7 Incremental fuel cost curve (bus no. 687). (From Mollo, C. and Yang, W., The Feasibility of Fuel Cells in Modern Power Systems, M.Sc. thesis, supervised by K. Denno, New Jersey Institute of Technology, 1973; and sponsored by PSE&G, Newark, NJ. With permission.)

then fed into the computer with a program that converted power into a percent of the total load power, enabling us to obtain a dispatch of power vs. total annual hours. From this dispatch it is possible to convert the $\delta$ (dollars per hour) vs. power received curve to a $\delta$ (dollars per hour) vs. total annual hours curve simply by replacing the power received by total annual hours as indicated in the dispatch. The computer program and flow chart for this dispatch is shown in Figure 2.42, while the $\delta$ (dollars per hour) vs. total annual hours curves are shown in Figures 2.43 to 2.49. As mentioned previously, the area under these curves represents the annual fuel cost savings or losses as indicated.

Therefore through computer programming involving the incremental fuel cost curves shown in Figures 2.1 to 2.26 and the flow diagram of Figure 2.42, the economic scheduling of generation for all bus-bars have been secured.

Next, the interaction of results for the economic scheduling of generation for every bus-bar for power system plans A through H, expressed in megawatts vs. total received load, with the incremental fuel cost curves in dollars per megawatt hour, a new set of optimal economic pictures have been established as shown in Figures 2.27 through 2.33.

## VIII. CAPITAL COST CALCULATIONS

The capital cost of each alternative system ought to be based on the generation expansion planned for that alternative. The individual power generation allocation together with the mode of generation have been established earlier. The initial cost is secured by multiplying the

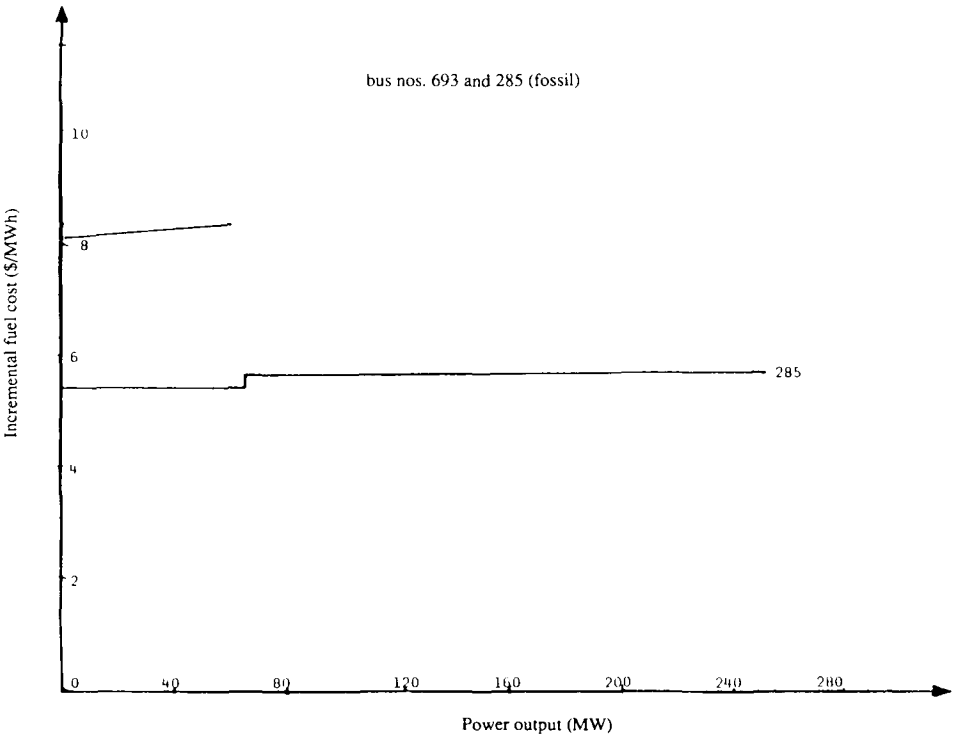


FIGURE 2.8 Incremental fuel cost curve (bus nos 693 and 285, fossil). (From Mollo, C. and Yang, W., The Feasibility of Fuel Cells in Modern Power Systems, M.Sc. thesis, supervised by K. Denno, New Jersey Institute of Technology, 1973; and sponsored by PSE&G, Newark, NJ. With permission.)

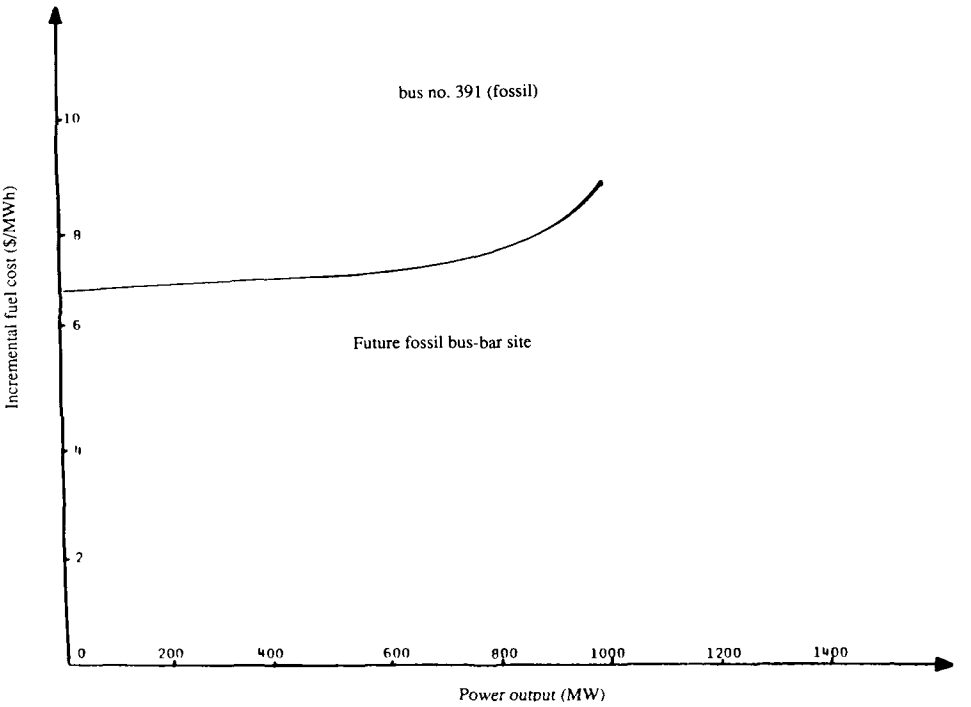


FIGURE 2.9 Incremental fuel cost curve (bus no. 391, fossil). (From Mollo, C. and Yang, W., The Feasibility of Fuel Cells in Modern Power Systems, M.Sc. thesis, supervised by K. Denno, New Jersey Institute of Technology, 1973; and sponsored by PSE&G, Newark, NJ. With permission.)

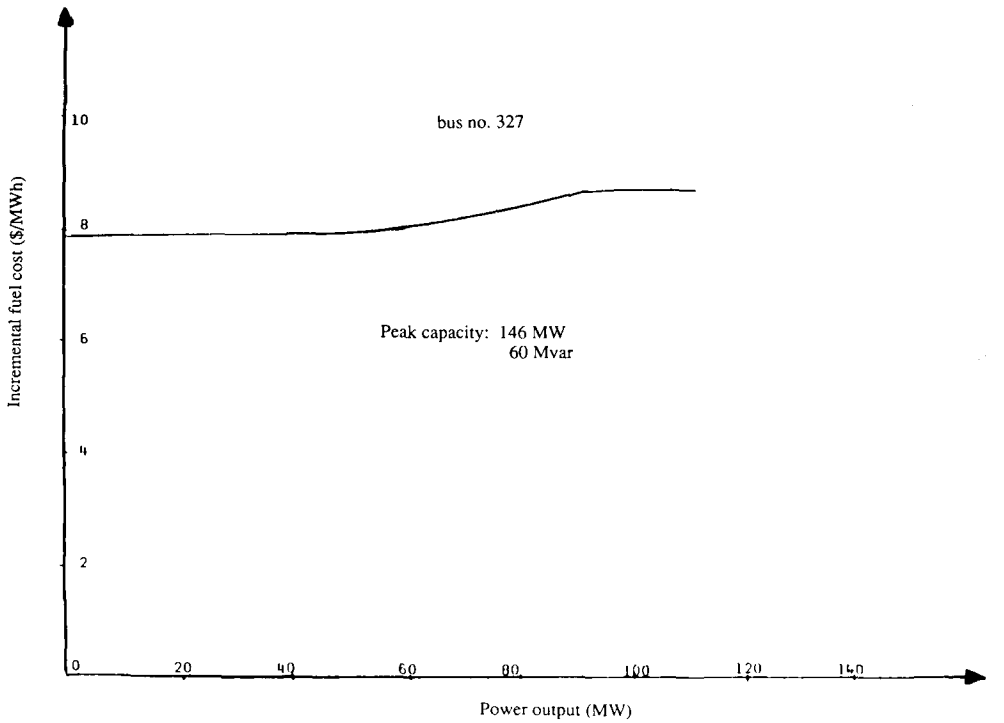


FIGURE 2.10 Incremental fuel cost curve (bus no. 327). (From Mollo, C. and Yang, W., The Feasibility of Fuel Cells in Modern Power Systems, M.Sc. thesis, supervised by K. Denno, New Jersey Institute of Technology, 1973; and sponsored by PSE&G, Newark, NJ. With permission.)

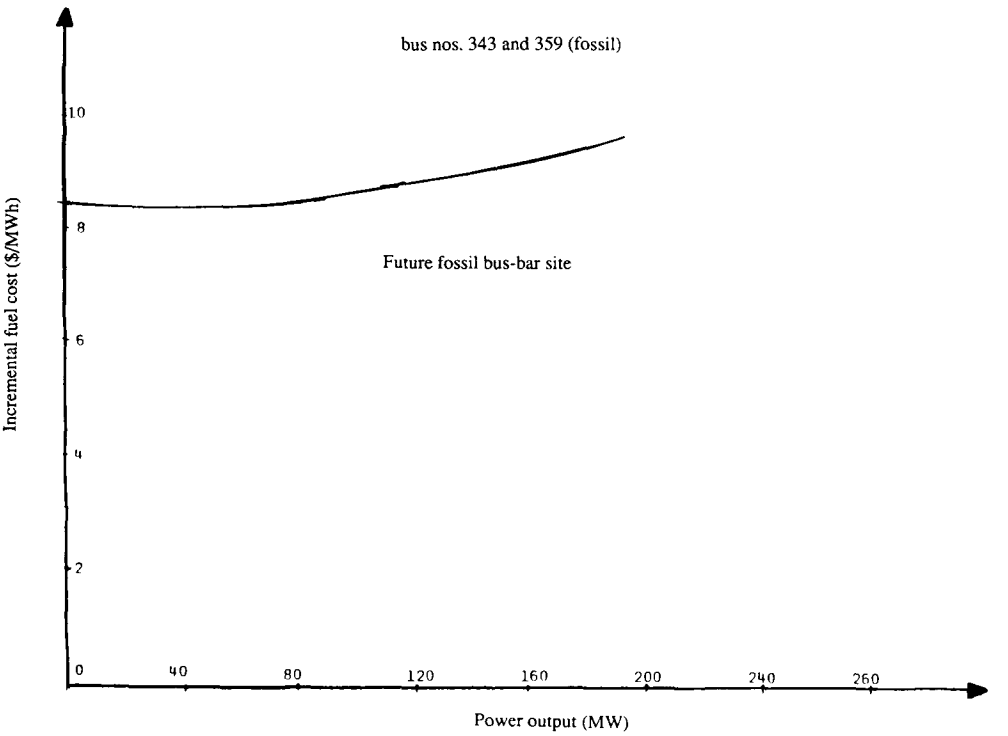


FIGURE 2.11 Incremental fuel cost curve (bus nos. 343 and 359, fossil). (From Mollo, C. and Yang, W., The Feasibility of Fuel Cells in Modern Power Systems, M.Sc. thesis, supervised by K. Denno, New Jersey Institute of Technology, 1973; and sponsored by PSE&G, Newark, NJ. With permission.)

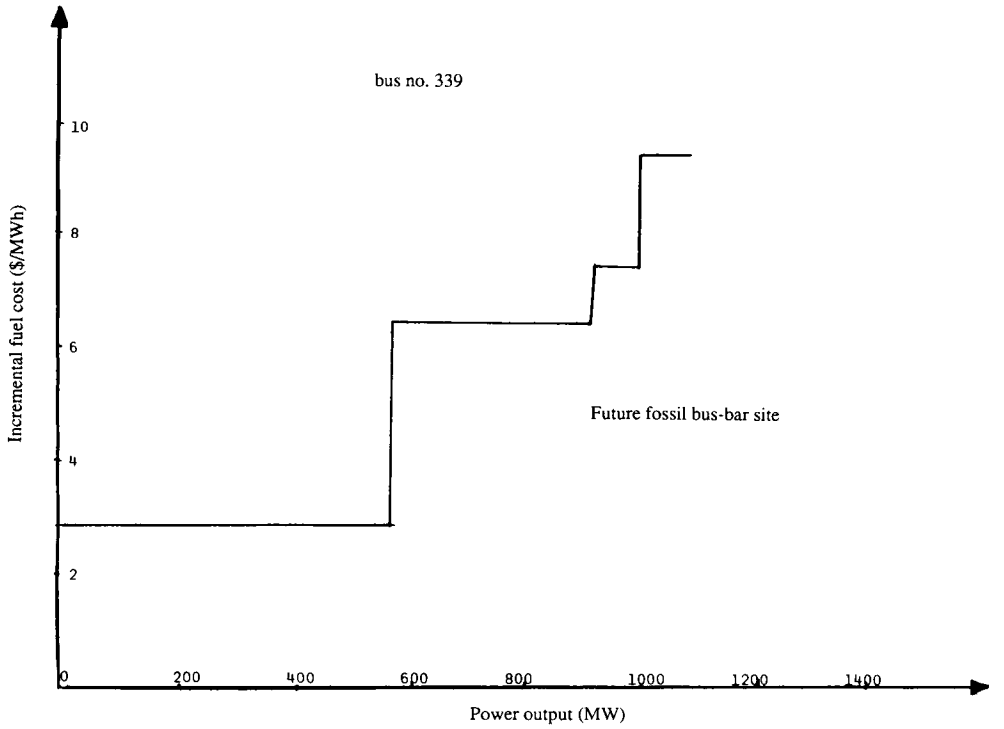


FIGURE 2.12 Incremental fuel cost curve (bus no. 339). (From Mollo, C. and Yang, W., The Feasibility of Fuel Cells in Modem Power Systems, M.Sc. thesis, supervised by K. Denno, New Jersey Institute of Technology, 1973; and sponsored by PSE&G, Newark, NJ. With permission.)

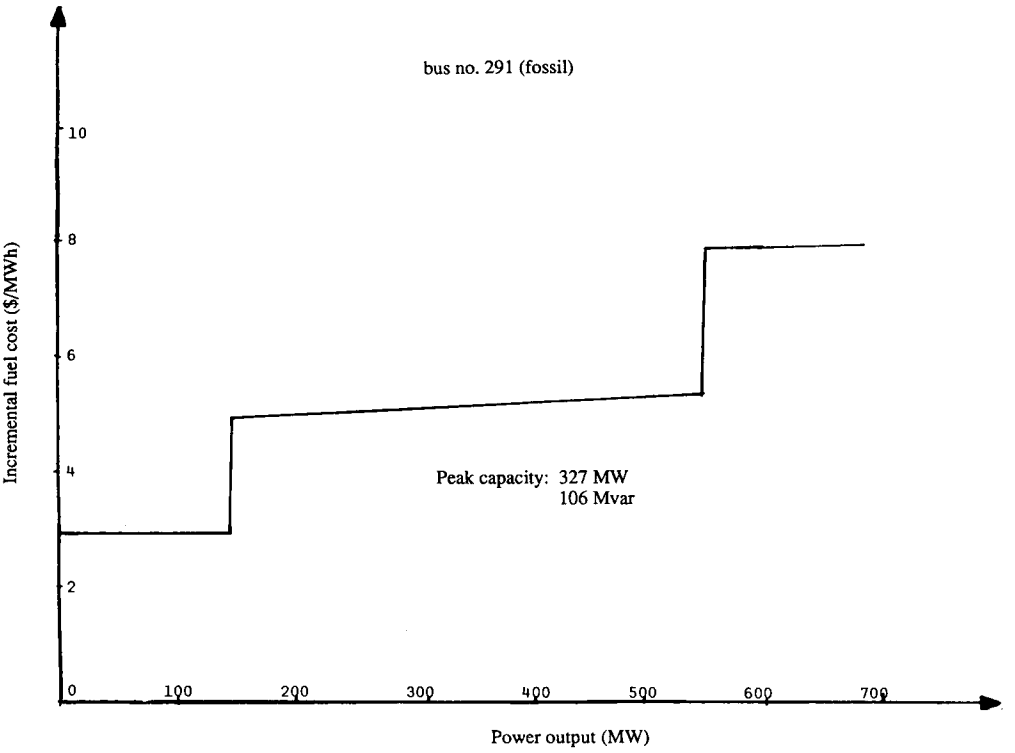


FIGURE 2.13 Incremental fuel cost curve (bus no. 291, fossil). (From Mollo, C. and Yang, W., The Feasibility of Fuel Cells in Modem Power Systems, M.Sc. thesis, supervised by K. Denno, New Jersey Institute of Technology, 1973; and sponsored by PSE&G, Newark, NJ. With permission.)

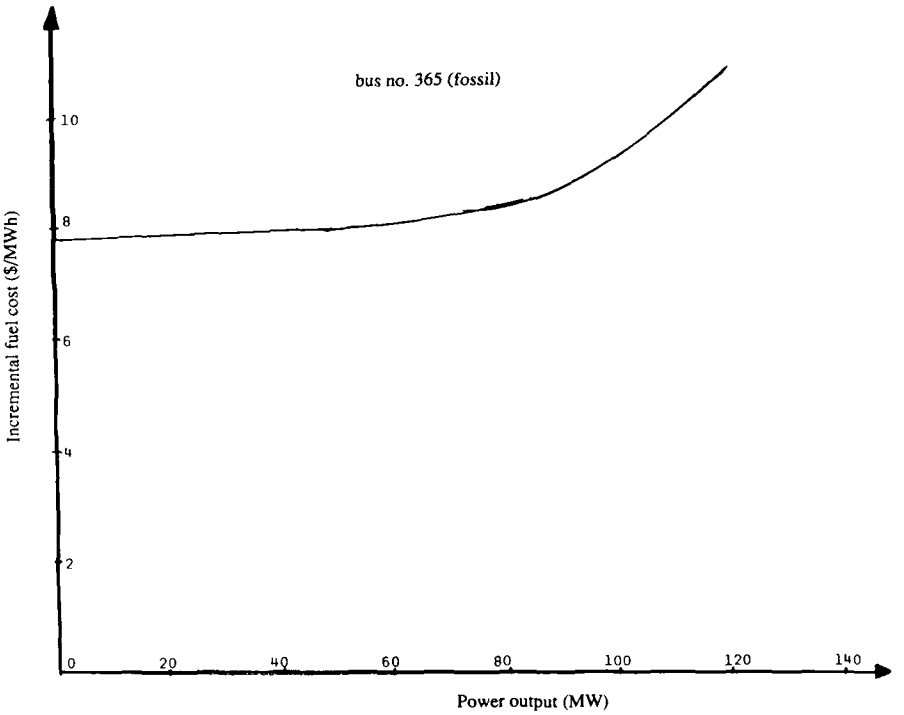


FIGURE 2.14 Incremental fuel cost curve (bus no. 365, fossil). (From Mollo, C. and Yang, W., The Feasibility of Fuel Cells in Modern Power Systems, M.Sc. thesis, supervised by K. Denno, New Jersey Institute of Technology, 1973; and sponsored by PSE&G, Newark, NJ. With permission.)

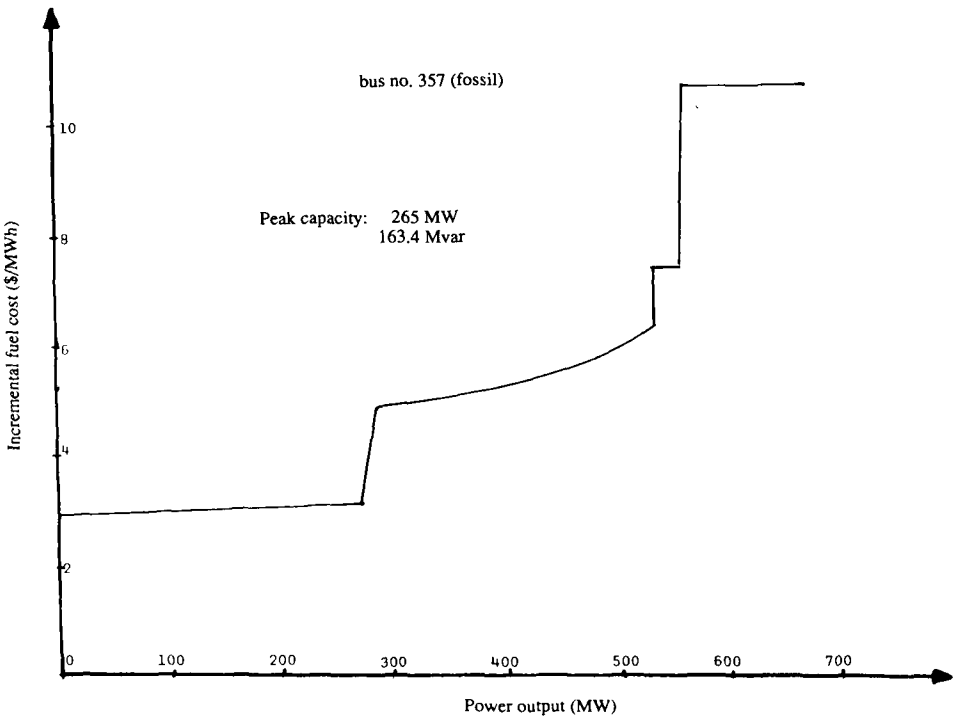


FIGURE 2.15 Incremental fuel cost curve (bus no. 357, fossil). (From Mollo, C. and Yang, W., The Feasibility of Fuel Cells in Modern Power Systems, M.Sc. thesis, supervised by K. Denno, New Jersey Institute of Technology, 1973; and sponsored by PSE&G, Newark, NJ. With permission.)

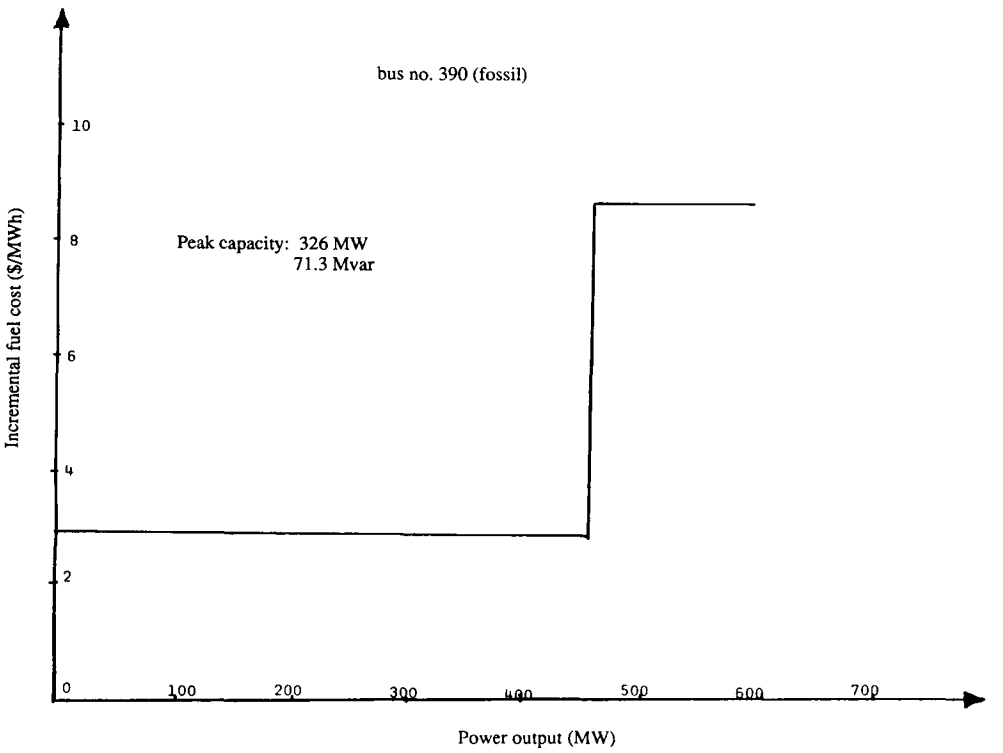


FIGURE 2.16 Incremental fuel cost curve (bus no. 390, fossil). (From Mollo, C. and Yang, W., The Feasibility of Fuel Cells in Modern Power Systems, M.Sc. thesis, supervised by K. Denno, New Jersey Institute of Technology, 1973; and sponsored by PSE&G, Newark, NJ. With permission.)

optimum generating allocation in megawatts by the initial capital cost of that particular mode of generation in dollars per megawatt. The total initial cost of a given system is then found by summing the cost of every new generator planned for that system alternative.

Typical values of initial capital cost for conventional power sources are shown below.

| Generation | Initial cost ($/kW) |
|---|---|
| Nuclear | 315 |
| Gas-turbine | 110 |
| Steam-fossil | 180—200 |

For alternative power system A, Table 2.2 shows planned incremental generation expansion over four phases. Each mode of generation has installation cost in dollars per kilowatt as well as annual capital cost in millions of dollars. The installation cost is associated with a certain escalation factor to account for a nominal inflation, while the annual capital cost is calculated on the basis of the generator life span and a nominal interest.

$$\text{Annual capital cost} = (\text{capactiy})(\text{cost})(\text{CR})_i^n \tag{2.17}$$

where $[\text{CR}_i^n]$ is a capital recovery factor with n as the life span in years and i as the interest.

The life span of each mode of generation is as shown below:

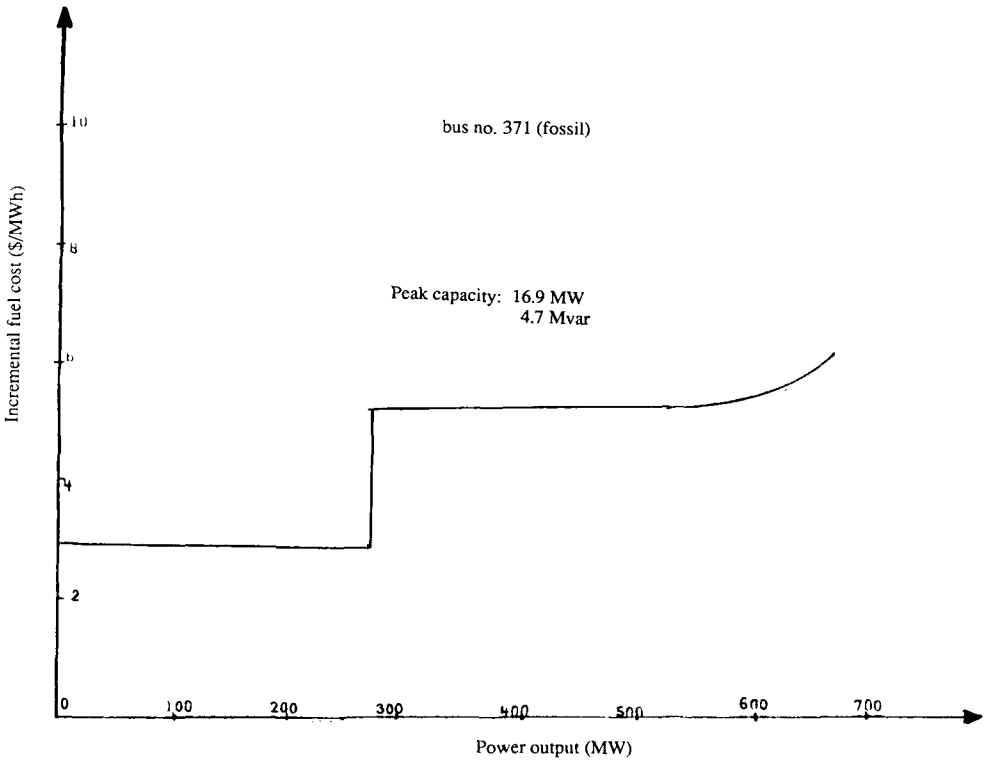


FIGURE 2.17 Incremental fuel cost curve (bus-bar no. 371, fossil). (From Mollo, C. and Yang, W., The Feasibility of Fuel Cells in Modern Power Systems, M.Sc. thesis, supervised by K. Denno, New Jersey Institute of Technology, 1973; and sponsored by PSE&G, Newark, NJ. With permission.)

- Nuclear: 35 years
- Steam-fossil: 45 years
- Gas turbine: 30 years

For example, for alternative power system A, the total annual cost due to installation is shown in Table 2.3.

Similar calculations have been carried out for the other system alternatives and are shown in Table 2.4.

The annual differential cost for system alternatives is shown in Table 2.5.

## IX. OPERATION AND MAINTENANCE ANNUAL COST

These are fixed and variable costs, based on data supplied by the PSE&G of New Jersey. Table 2.6 shows ratings of calculating annual costs.

Total operation and maintenance on an annual basis for each system alternative is shown in Table 2.7.

Based on the data of Table 2.7, the differential element for 0&M annual cost for the system alternative with respect to alternative system A is shown in Table 2.8.

The final step for comprehensive annual cost for each system alternative has been obtained by adding the annual costs for fuel, installation, capital, as well as O&M, then comparing the total with reference alterative A as shown in Table 2.9.

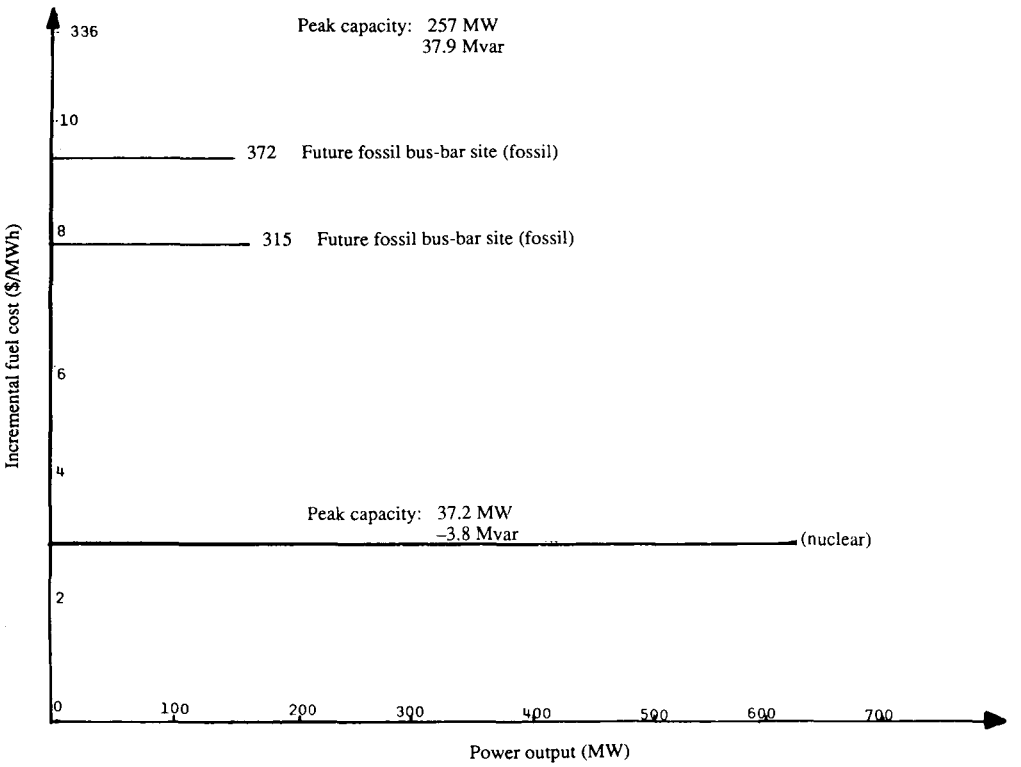


FIGURE 2.18 Incremental fuel cost curve (bus-bar nos. 315 and 372, fossil). (From Mollo, C. and Yang, W., The Feasibility of Fuel Cells in Modern Power Systems, M.Sc. thesis, supervised by K. Denno, New Jersey Institute of Technology, 1973; and sponsored by PSE&G, Newark, NJ. With permission.)

## X. GENERAL CONCLUSIONS

### A. THE STEADY STATE CONCLUSIONS

The economic optimization study was based on eight major power systems and is known as plans A, B, C, D, E, F, G and H.

The economic optimization study conducted was based on minimum dollars input annually for each system. The cost of power production and cost of power delivery to the load were both integral parts of this study.

Throughout the economic calculations that were carried out on those systems for various load percentages, the network interconnections were assumed to be arbitrary in nature and the transmission losses were assumed to be zero.

The nominal capacities of the power bus-bars were maintained; however, optimum scheduling of generation for all the eight major power systems was performed under the constraint of minimum dollars input annually.

Network identification or design was sought in terms of the total establishment of the symmetric [R] matrix in the power flow or the sixth reference frame.

Calculation of the symmetric [R] matrices was obtained with the aid of the optimum [B] matrices, also calculated, and information from the load flow data conducted at the ITT Computer Center in Paramus, New Jersey.

Therefore, by combining the results of the economic optimization for an arbitrary unknown network and those of the specific network design, we are able to make the following conclusions for a steady state system. The optimum systems are listed below in the order of the most

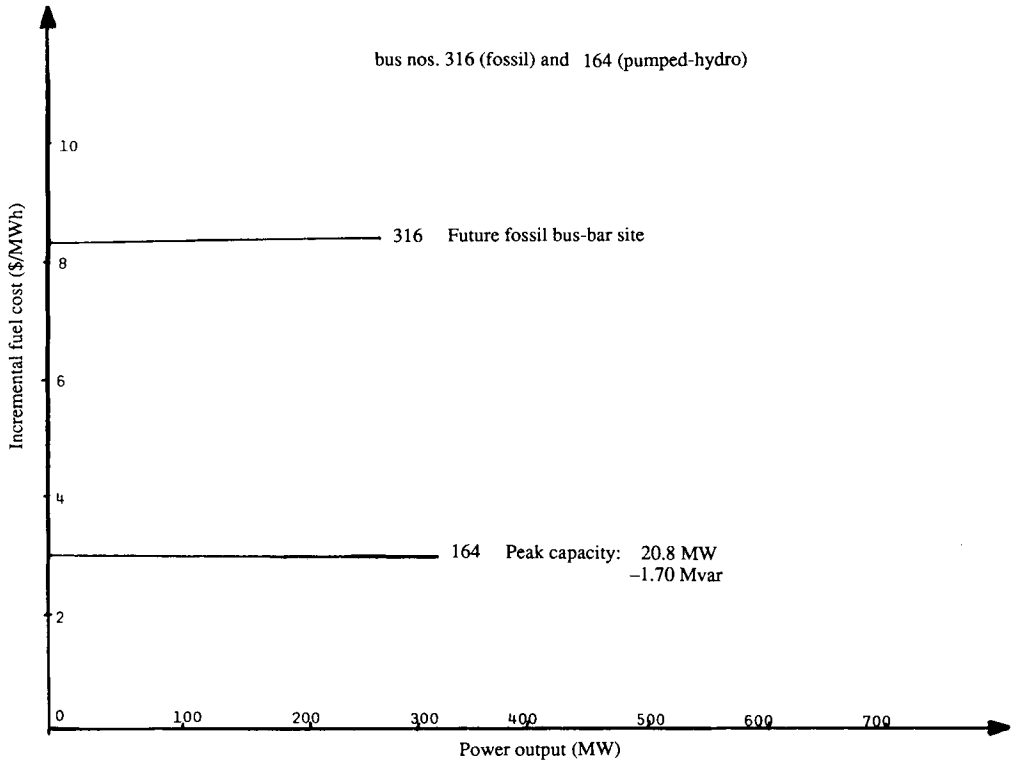


FIGURE 2.19 Incremental fuel cost curve (bus-bar nos. 316, fossil and 164, pumped-hydro). (From Mollo, C. and Yang, W., The Feasibility of Fuel Cells in Modern Power Systems, M.Sc. thesis, supervised by K. Denno, New Jersey Institute of Technology, 1973; and sponsored by PSE&G, Newark, NJ. With permission.)

economically optimum and feasible alternatives for this set of connected systems. The conventional reference alternative power system with a diagonal [R] matrix in the sixth reference frame is known as Plan A and is taken as the base of comparison (see Table 2.10).

**1. Plan E — Combination of Centralized-Dispersed Power System**

A combination of a centralized-dispersed power system known as plan E, in which fuel cell generators are located at each new power bus-bar demanding additional power. An overall load of more than 22,000 MW is assumed to be supplied by this interconnected system involving a large number of fuel cell generators linked to a centralized conventional power system of 8000 MW.

The information gathered from the economic optimizaton (based on minimum annual cost plus the least amount of losses), with the network identification in the sixth reference frame in terms of the [R] matrices (diagonal [R] matrices shown in tables) taken as bases of inspection, were combined. The results clearly indicate that plan E is the most economically and practically feasible system. This system includes about 20 central power generation bus-bars interconnected by a conventional network and more than 140 isolated or dispersed bus-bars. The central bus-bars are either totally conventional or conventionally topped to a fuel cell coupled to a solid state inverter. However, the isolated or dispersed bus-bars are fuel cell generators coupled to solid state inverters. The [R] matrix of alternative plan E is shown in Chapter 1, Table A because of its relevance there.

Such a combination of centralized-dispersed system, besides its economic and design feasi-

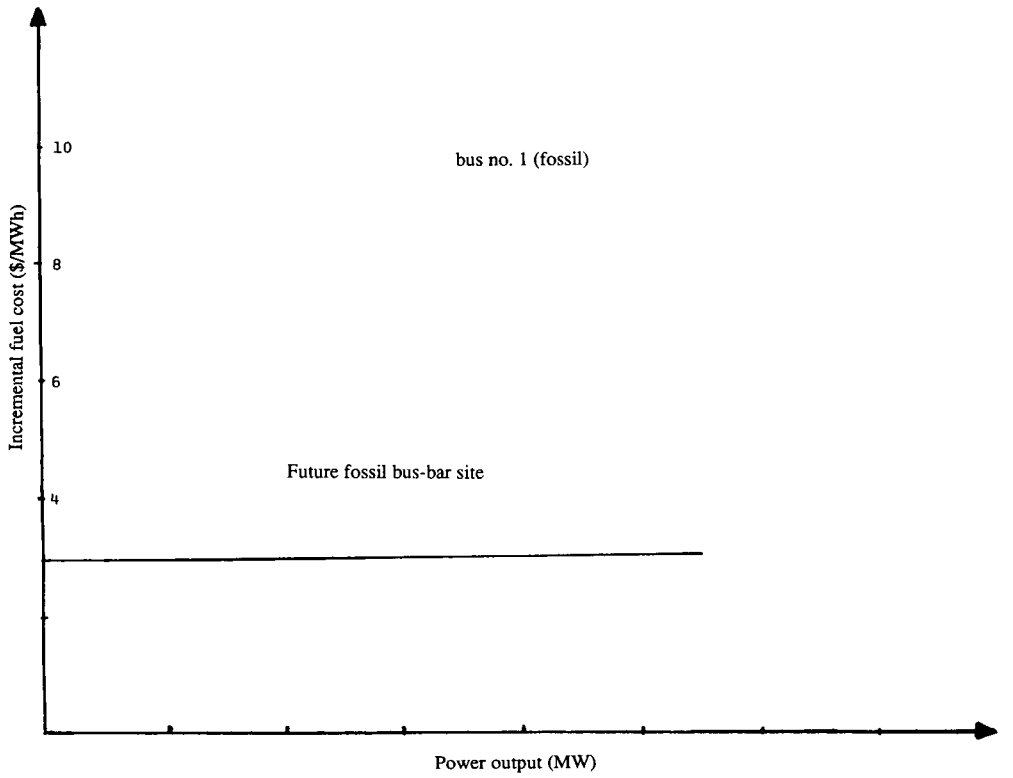


FIGURE 2.20 Incremental fuel cost curve (bus no. 1, fossil). (From Mollo, C. and Yang, W., The Feasibility of Fuel Cells in Modern Power Systems, M.Sc. thesis, supervised by K. Denno, New Jersey Institute of Technology, 1973; and sponsored by PSE&G, Newark, NJ. With permission.)

bility, has the added attractive feature of impacting minimially on the environment because it has a large number of dedicated or dispersed electrochemical generators located at its load centers. These isolated generator load stations can be established, operated, and controlled locally by including the utilization of an existing natural gas supply system to feed the reformer system of the fuel cell. (This is, of course, feasible for a fuel cell generator of the order of 1 MW on several hundred kilowatt capacities.)

Hence, this study concludes that a combination centralized-dispersed power system is the most feasible alternative for an electrochemical-electromechanical interconnected power system.

**2. Plan B — Fuel Cells for Peak and Base Power Demand**

Compiling the results of economic optimization with network identification (described earlier: see Table 2.11 for the diagonal [R] matrix) for plan B, i.e., fuel cell generators supply peak loads in place of gas turbines and base loads in place of fossil-steam generators, it can be stated that this alternative can become economically and feasibly acceptable if the fuel cell generators are confined to supplying peak loads only. This modified alternative, known as system C (see Table 2.12 for the diagonal [R] matrix), is a system with central power generators of fuel cells interconnected through their appropriate inverters to the other intermechanical bus-bars.

Therefore, this study recommends a central power system of fuel cell generators (supplying peak loads) interconnected to other conventional electromechanical bus-bars as a second alternative for a practical optimum system.

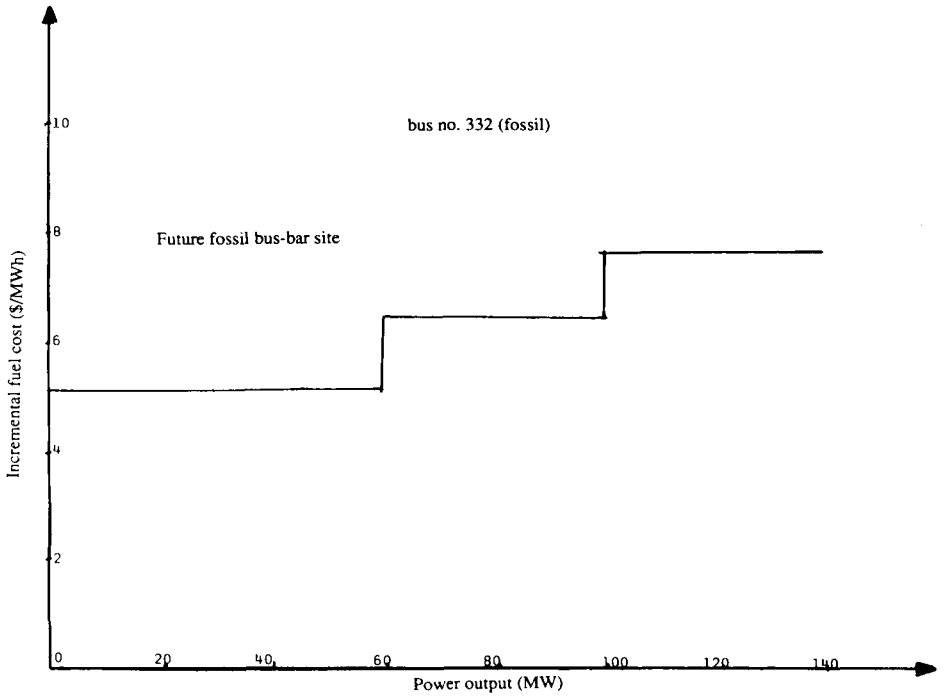


FIGURE 2.21 Incremental fuel cost curve (bus no. 332, fossil). (From Mollo, C. and Yang, W., The Feasibility of Fuel Cells in Modern Power Systems, M.Sc. thesis, supervised by K. Denno, New Jersey Institute of Technology, 1973; and sponsored by PSE&G, Newark, NJ. With permission.)

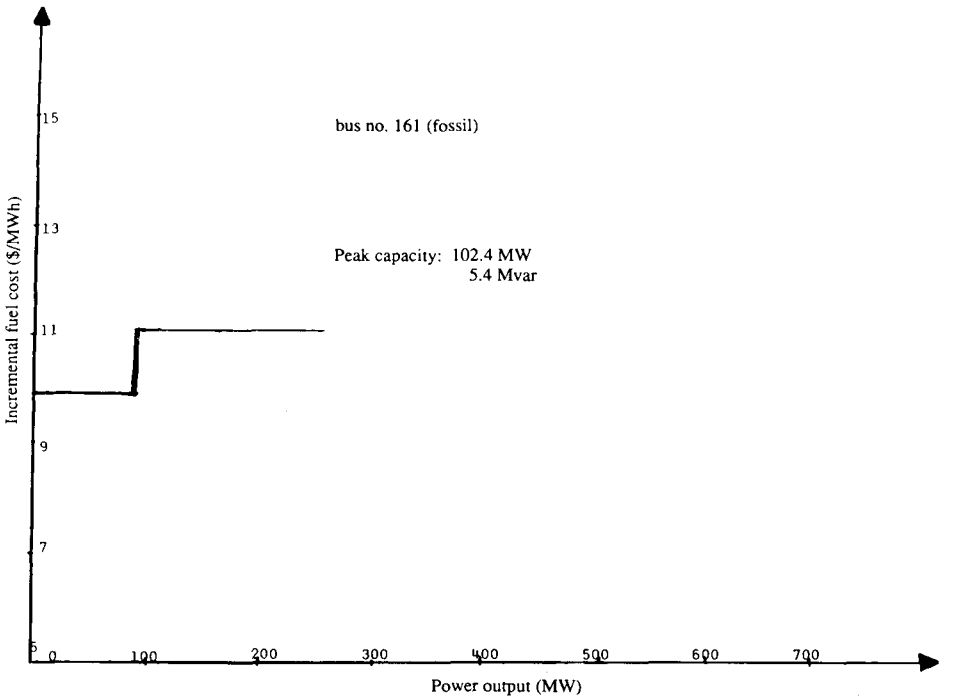


FIGURE 2.22 Incremental fuel cost curve (bus no. 161, fossil). (From Mollo, C. and Yang, W., The Feasibility of Fuel Cells in Modern Power Systems, M.Sc. thesis, supervised by K. Denno, New Jersey Institute of Technology, 1973; and sponsored by PSE&G, Newark, NJ. With permission.)

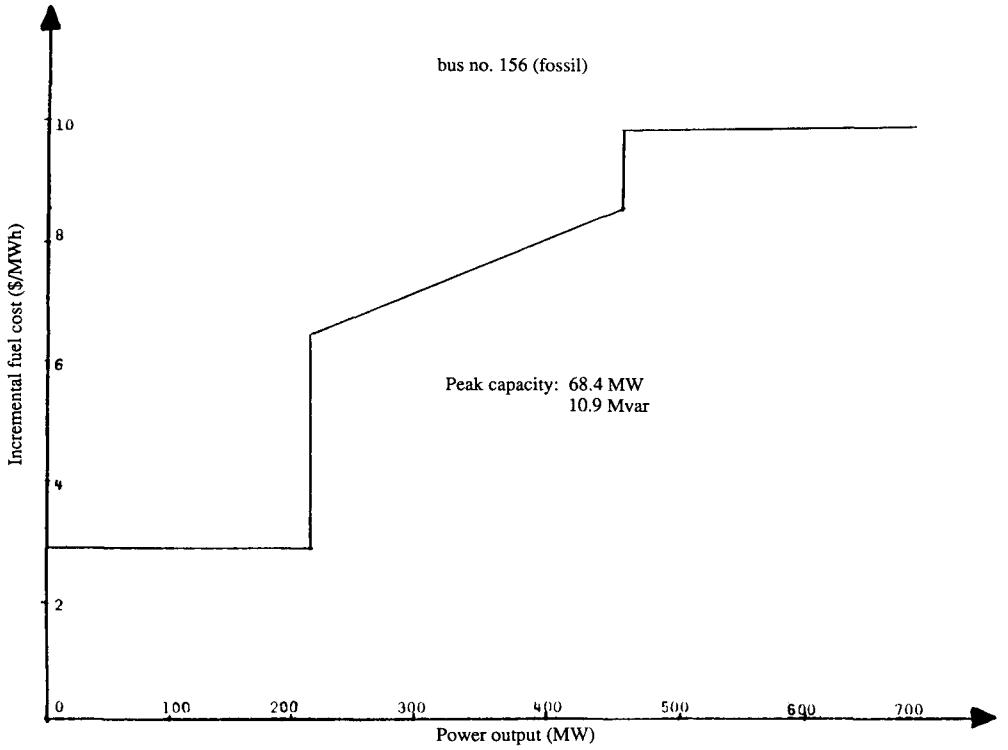


FIGURE 2.23 Incremental fuel cost curve (bus no. 156, fossil). (From Mollo, C. and Yang, W., The Feasibility of Fuel Cells in Modern Power Systems, M.Sc. thesis, supervised by K. Denno, New Jersey Institute of Technology, 1973; and sponsored by PSE&G, Newark, NJ. With permission.)

### 3. Plan D — Fuel Cells for Base Power Demand

This study proceeds to recommend as another alternative, a central interconnected power system known as plan D, which consists of fuel cell generators supplying base load demand in place of fossil-steam generators. The structure of this electrochemical-electromechanical system is the same as the conventional reference system known as alternative A except that each fossil-steam generator must be replaced by a fuel cell coupled to an appropriate inverter.

The centralized nature of this interconnected system is represented by the diagonal matrix of the symmetric resistances in the sixth reference frame and shown in Table 2.13. Economic feasibility could be accepted as a fourth alternative plan.

### 4. Plan F — Storage Batteries and Fuel Cells for Peak Power Demand

This study concludes its analysis by stating that a central interconnected system, where storage batteries supply peak demands instead of gas-turbine generators, known as plan F, is not feasible economically. Also, the same conclusion applies to a central system where storage batteries and fuel cell generators supply an equal share of peak demand known as plan H. Network identifications for plans F and H are shown in Tables 2.14 and 2.15, respectively.

### 5. Plan G — Storage Batteries for Peak Power Demand

Information gathered from the results of economic optimization and network design in terms of the [R] matrix, indicates that a power system in which storage batteries supply peak loads, can only be economically and practically feasible if its role is confined to load demand between base level and peak limit.

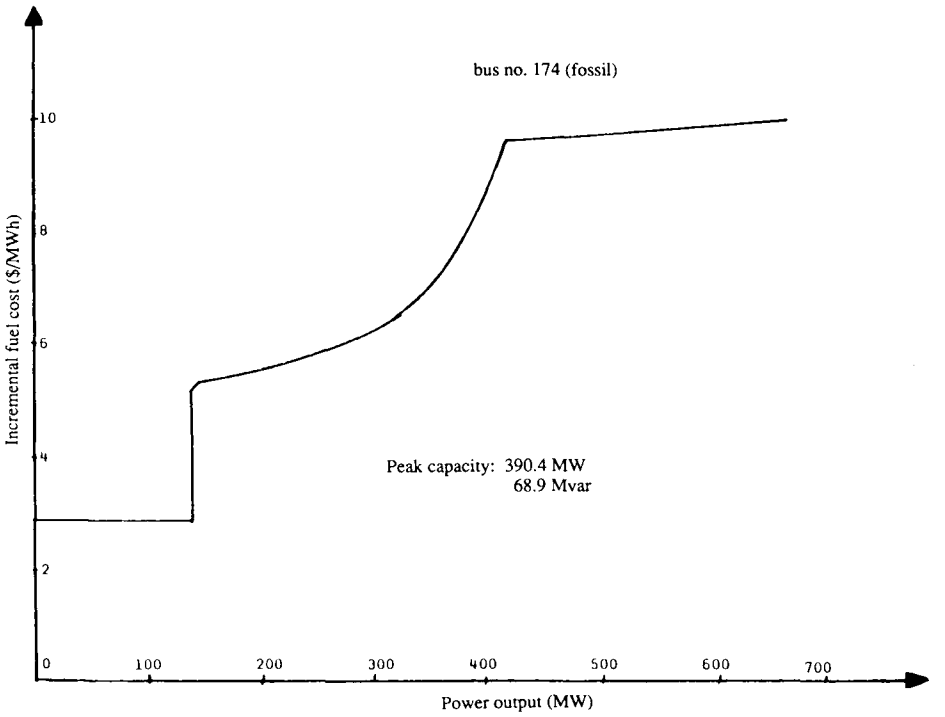


FIGURE 2.24 Incremental fuel cost curve (bus no. 174, fossil). (From Mollo, C. and Yang, W., The Feasibility of Fuel Cells in Modern Power Systems, M.Sc. thesis, supervised by K. Denno, New Jersey Institute of Technology, 1973; and sponsored by PSE&G, Newark, NJ. With permission.)

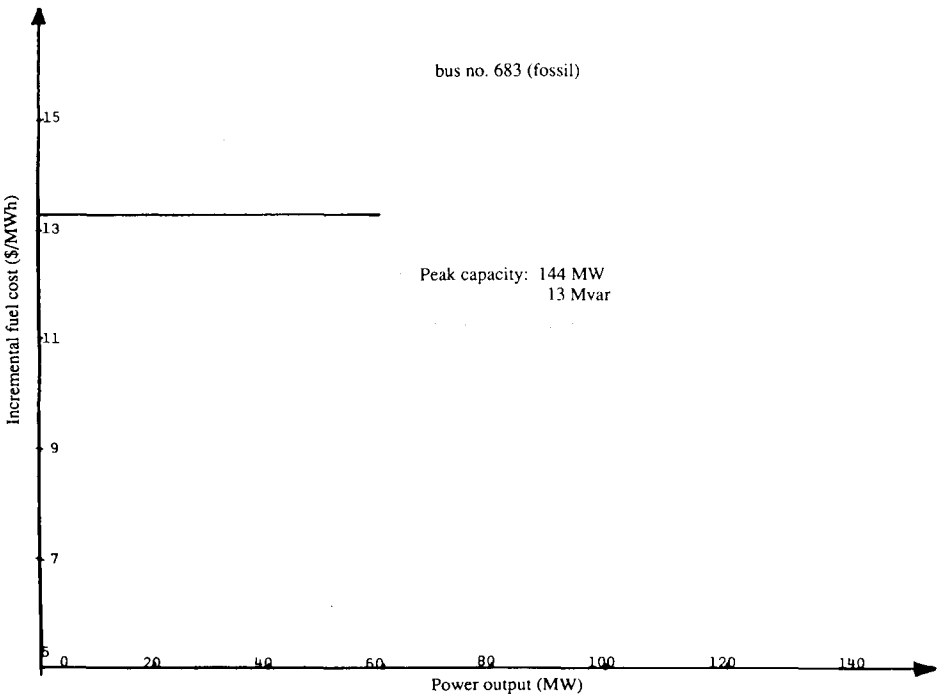


FIGURE 2.25 Incremental fuel cost curve (bus no. 683, fossil). (From Mollo, C. and Yang, W., The Feasibility of Fuel Cells in Modern Power Systems, M.Sc. thesis, supervised by K. Denno, New Jersey Institute of Technology, 1973; and sponsored by PSE&G, Newark, NJ. With permission.)

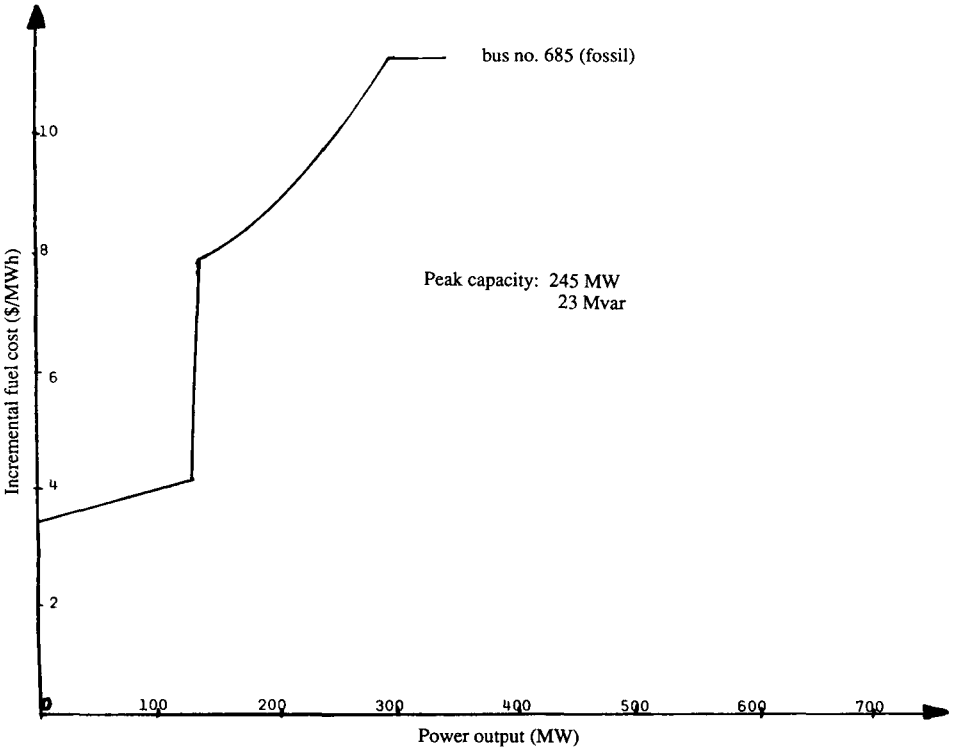


FIGURE 2.26 Incremental fuel cost curve (bus no. 685, fossil). (From Mollo, C. and Yang, W., The Feasibility of Fuel Cells in Modern Power Systems, M.Sc. thesis, supervised by K. Denno, New Jersey Institute of Technology, 1973; and sponsored by PSE&G, Newark, NJ. With permission.)

Such an interconnected system is known as plan G, with its diagonal [R] matrix and is shown in Table 2.16. Therefore, such an interconnected system could be recommended as a third alternative. Gas turbine bus-bars in the new bulk load of over 22,000 MW could be assumed as either storage battery bus-bars or fuel cells, both coupled to the appropriate inverters.

Conclusions described in the preceeding paragraphs clearly identify the best optimum power sytem, plan E, which is a combination of a relatively small number of centralized interconnected bus-bars and a much larger number of dispersed isolated or dedicated electrochemical bus-bars.

## XI. SUMMARY

The purpose of this case study has been to identify the optimum aspects of an electrochemical-electromechanical interconnected power system.

Economic optimization and optimum network identifiation were the two major considerations of this case study. Optimum [B] matrices were established in Chapter 1 in order to determine optimum economic criteria for the design of any power system. The data which were studied were initial cost, maximum power generating capacity, lifetime, and fuel costs.

Optimum [R] matrices were calculated using more than 35 power systems to determine optimum network identification. The information was obtained from load flow calculations and the [B] matrices.

Two systems were identified as best fulfilling the optimum conditions. They were a centralized system in which fuel cell generating units supplied peak demand and a dispersed-centralized system in which fuel cell generating units were scattered on isolated locations to

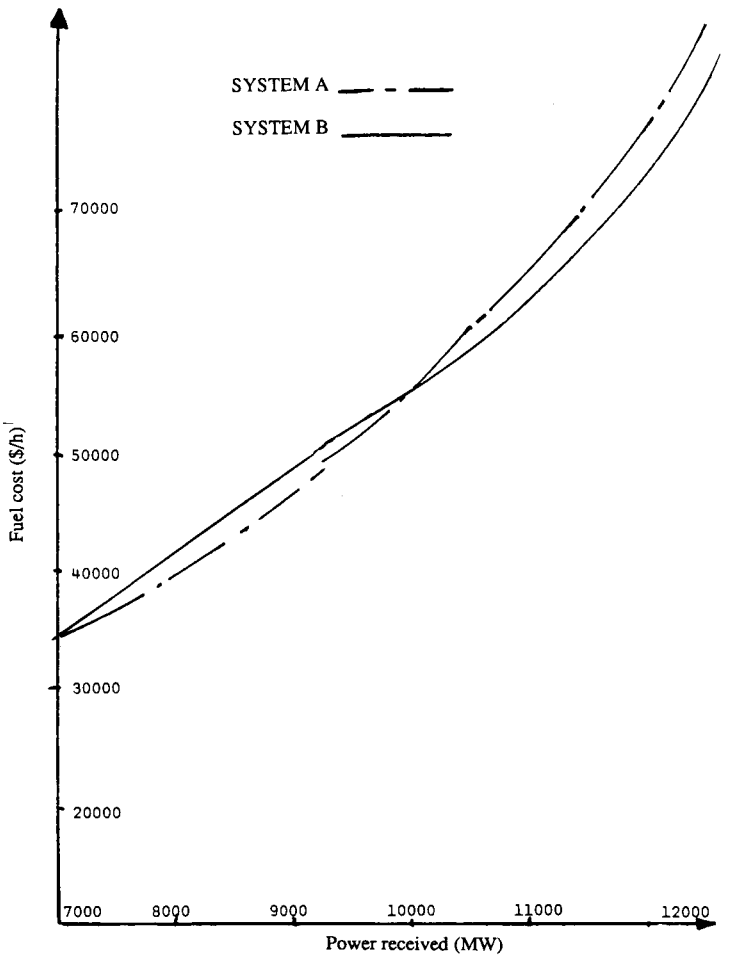


FIGURE 2.27 Fuel cost curve (systems A and B). (From Mollo, C. and Yang, W., The Feasibility of Fuel Cells in Modern Power Systems, M.Sc. thesis, supervised by K. Denno, New Jersey Institute of Technology, 1973; and sponsored by PSE&G, Newark, NJ. With permission.)

supply their own load. Less optimum than the two systems already mentioned were two other systems: the first was a centralized system where fuel cell generating units supplied base loads and the second system consisted of storage batteries which supplied peak loads only.

I would like to indicate that economic data used in the case study presented in this chapter may not be in line with current levels of economic cost of all aspects required to have the energy system operational. These aspects cover fuel costs, capital and installation costs, as well as maintenance and operation costs.

The main objective for the economic study presented in this chapter, and any relevant material in Chapter 1, is to provide an analytical methodology and procedural approach for determining the economic outlook of any energy system seeking to integrate fuel cells and storage batteries, in a dispersed or central pattern, which would have a meaningful contribution as a viable, renewable energy source that is economically acceptable and practically applicable.

Therefore, given economic costs that are presently valid, a new economic outlook may emerge when used in all aspects of analysis that have been carried out in this chapter and the case study undertaken.

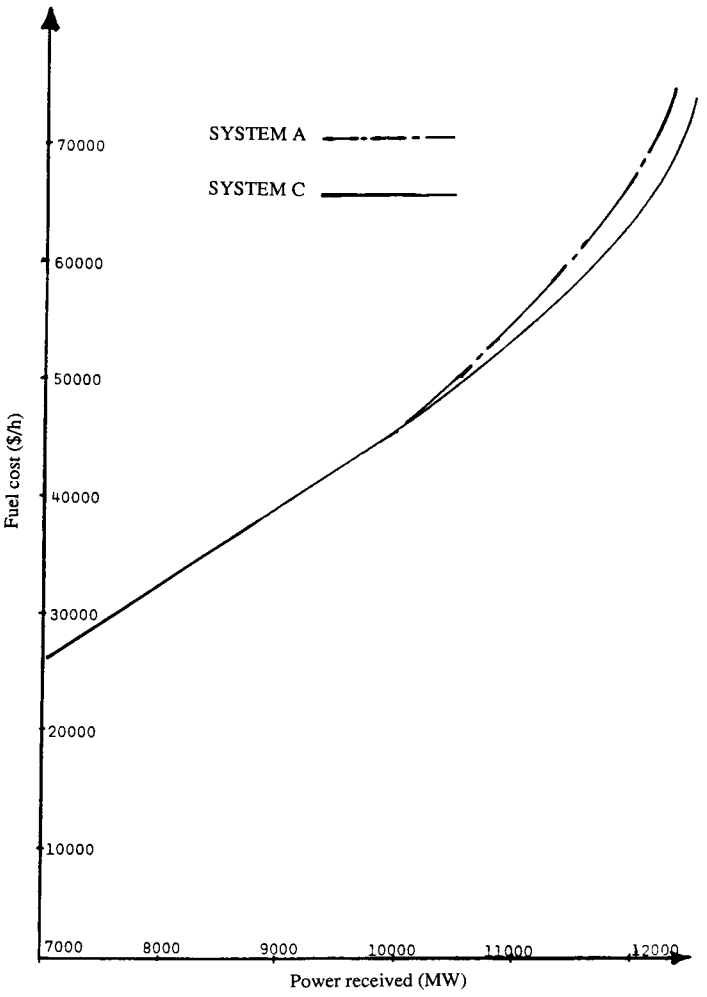


FIGURE 2.28 Fuel cost curve (systems A and B). (From Mollo, C. and Yang, W., The Feasibility of Fuel Cells in Modern Power Systems, M.Sc. thesis, supervised by K. Denno, New Jersey Institute of Technology, 1973; and sponsored by PSE&G, Newark, NJ. With permission.)

## XII. PROBLEMS

In the following problems, where relevant, consider $P_L = 0$ in solving the coordination equation.

2.1 Through resorting to reference material, describe the mathematical expressions for the electromotive force (emf) of fuel cells under the condition of any pressure (P) and temperature (T). What is the linkage between P and T for the fuel cell emf to remain invariant at the standard level?

2.2 Repeat Problem 2.1 for the standard efficiency of the fuel cell.

2.3 Refer to Table 2.2 and sketch graphs for the incremental fuel cost curve ($/MWh vs. MW) for the following power bus-bars taking into account inflationary factor of Δ percent. The bus-bar numbers are: F339, F372, PH164, and N172.

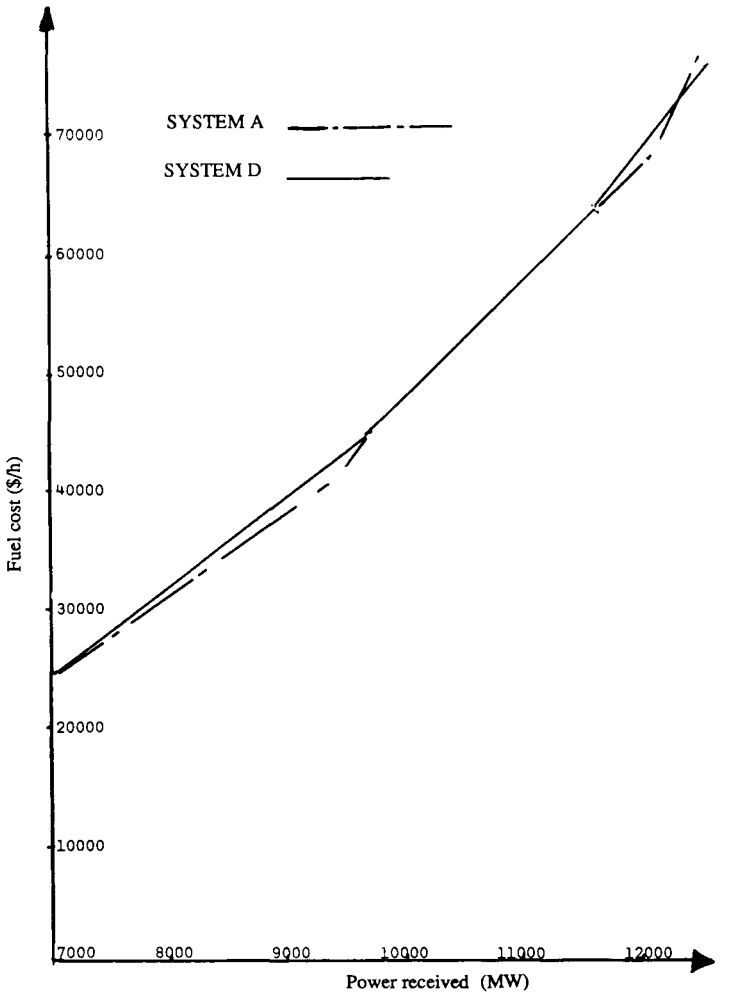


FIGURE 2.29 Fuel cost curve (systems A and B). (From Mollo, C. and Yang, W., The Feasibility of Fuel Cells in Modern Power Systems, M.Sc. thesis, supervised by K. Denno, New Jersey Institute of Technology, 1973; and sponsored by PSE&G, Newark, NJ. With permission.)

2.4 Repeat Problem 3 for the following bus-bars: GT343, FGT391, N427, and F285.

2.5 Refer to Figure 2.2, establish a new curve for the fuel cost in dollars per hour for the alternative system B under the condition that the incremental fuel cost for nuclear and pumped-hydro generators is tripled the values listed in Tables 2.2 and 2.3. Consider inflation escalation to be at the rate of 7.5% instead of the 5% used in arriving at Figure 2.2.

2.6 Repeat Problem 2.5 regarding alternative system C, where fuel-cell assembled units replaced the gas-turbine generator to provide peak load demand.

2.7 Repeat Problem 2.5 regarding alternative system E, where fuel cell assembled units are installed to supply any increase in load demand. This includes new generating units as well as the creation of new load centers, at which fuel cell assemblies would be installed.

2.8 Repeat Problem 2.5 regarding alternative system F where storage battery units are installed replacing gas-turbine generators for peak loading. Let incremental fuel cost for

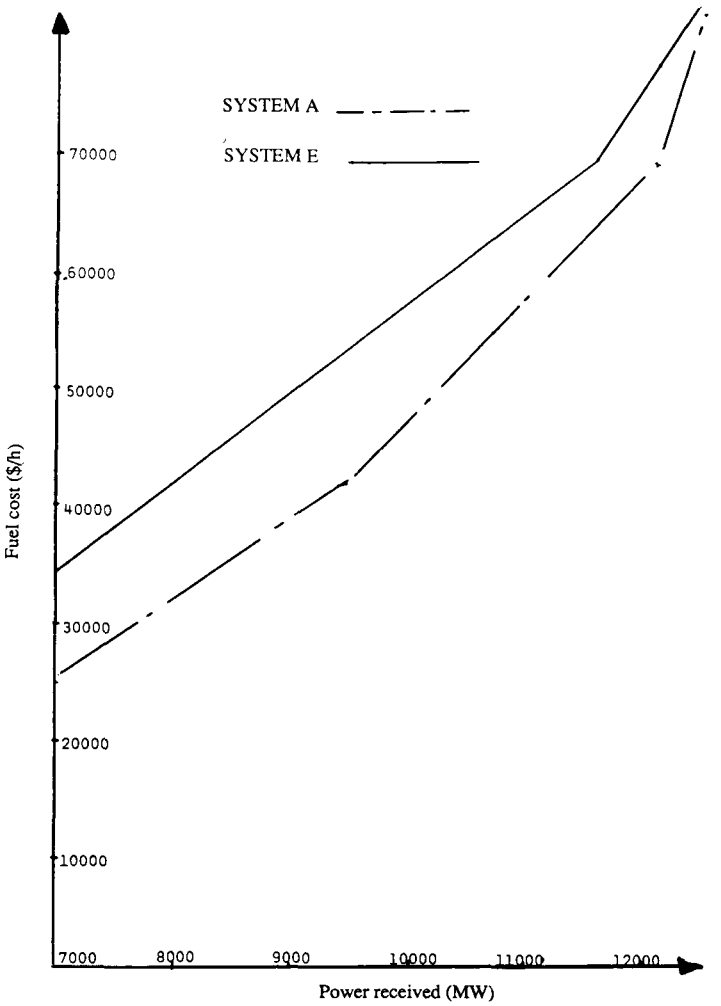


FIGURE 2.30 Fuel cost curve (systems A and B). (From Mollo, C. and Yang, W., The Feasibility of Fuel Cells in Modern Power Systems, M.Sc. thesis, supervised by K. Denno, New Jersey Institute of Technology, 1973; and sponsored by PSE&G, Newark, NJ. With permission.)

the storage batteries equal to twice the rate for alternative reference A during off-peak incremental fuel cost be divided by 0.8. Consider the rate of fuel cost at off-peak loading equals 4 mills/kWh.

2.9 Repeat Problem 2.5 regarding alternative system H where peak load demand usually supplied by gas turbines is replaced by fuel cells and storage batteries on a 50% basis. Consider incremental fuel cost for fuel cells equal to 1.3 mills/kW and for storage batteries equal to 5 mills/kWh.

2.10 Repeat Problem 2.5 regarding system alternative G where all fossil-steam generators for off-peak loading are replaced by fuel cells units, and all gas-turbine generators are replaced by storage-battery units. Let incremental fuel cost for fuel cells = 1.5 mills/kW and incremental fuel cost for storage batteries = 5 mills/kWh.

2.11 Refer to results secured in Problem 2.5 and through association with the load duration

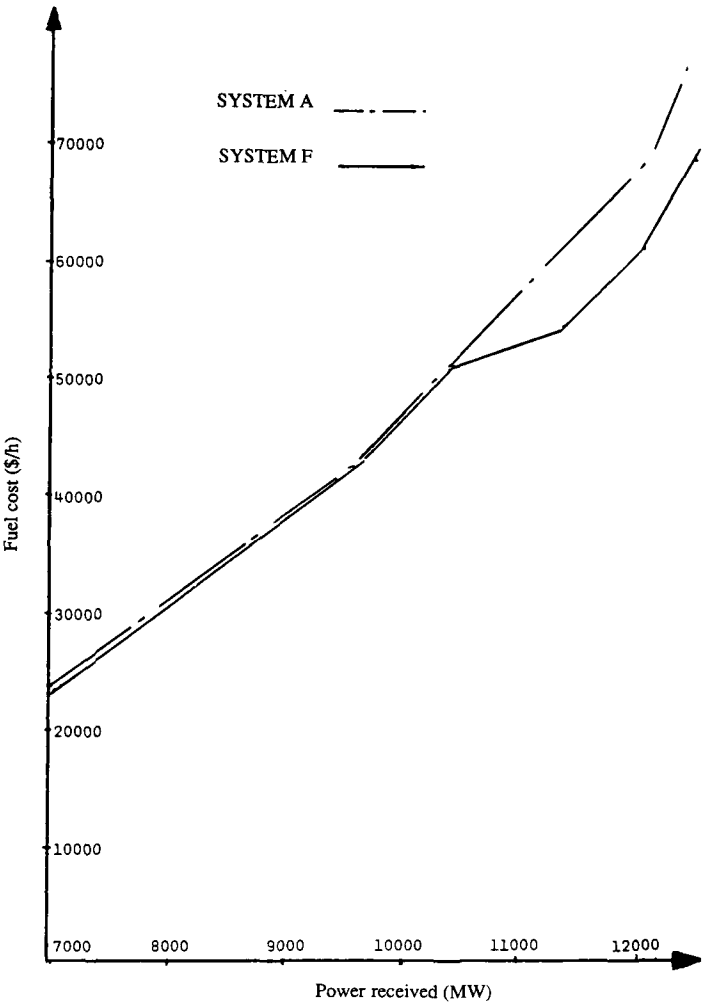


FIGURE 2.31 Fuel cost curve (systems A and B). (From Mollo, C. and Yang, W., The Feasibility of Fuel Cells in Modern Power Systems, M.Sc. thesis, supervised by K. Denno, New Jersey Institute of Technology, 1973; and sponsored by PSE&G, Newark, NJ. With permission.)

curve, establish a graphical pattern for the differential fuel cost in dollars per hour vs. total annual hours, i.e., similar to Figure 2.18.

2.12 For the results of Problem 2.6 and with the aid of the load duration curve, establish a graphical structure for the differential fuel cost (with respect to reference system A) in dollars per hour vs. total annual hours.

2.13 Similar to the statement of Problem 2.11 establish the differential fuel cost curve vs. total annual hours for the system described in Problem 2.7.

2.14 Repeat Problem 2.13 for the system described in Problem 2.8.

2.15 Repeat Problem 2.13 for the system described in problem 2.9.

2.16 Repeat Problem 2.13 for the system described in problem 2.10.

2.17 A ten power plant system with transmission loss $P_L$ is described below.

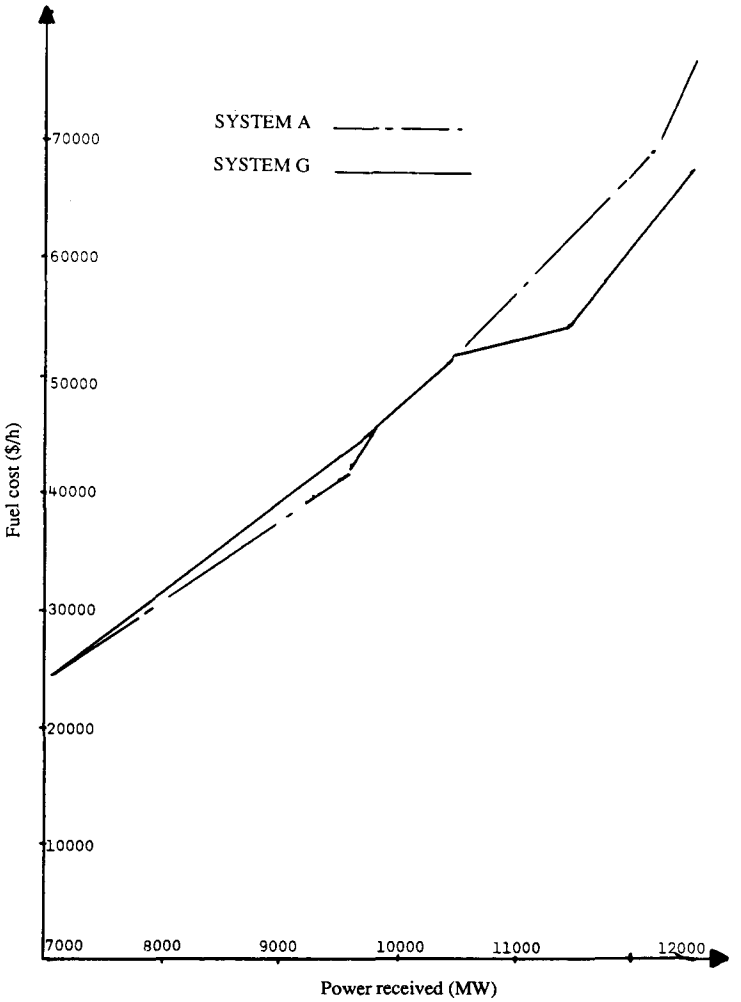


FIGURE 2.32 Fuel cost curve (systems A and B). (From Mollo, C. and Yang, W., The Feasibility of Fuel Cells in Modern Power Systems, M.Sc. thesis, supervised by K. Denno, New Jersey Institute of Technology, 1973; sponsored by PSE&G, Newark, NJ. With permission.)

| Plant | $F_{ii}$ | $L_i$ |
|---|---|---|
| 1 | 0.006 | 1.24 |
| 2 | 0.005 | 1.00 |
| 3 | 0.002 | 0.82 |
| 4 | 0.004 | 0.72 |
| 5 | 0.003 | 0.64 |
| 6 | 0.007 | 0.78 |
| 7 | 0.0064 | 0.64 |
| 8 | 0.0088 | 0.54 |
| 9 | 0.009 | 0.36 |
| 10 | 0.0010 | 0.92 |

*Note:* Total peak generation = 3150 MW.

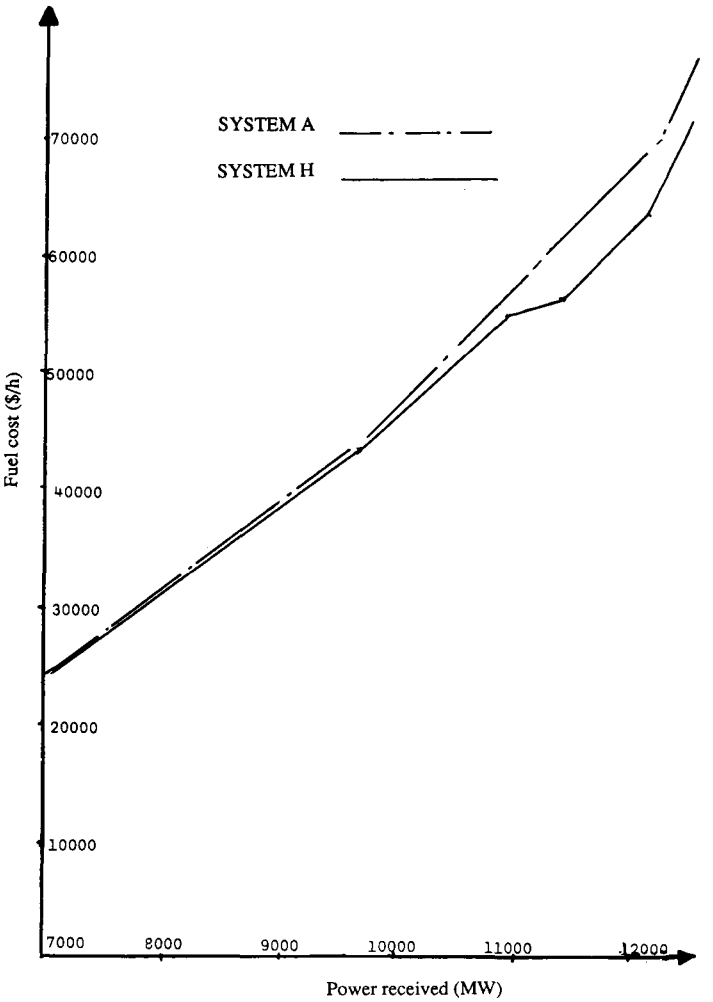


FIGURE 2.33 Fuel cost curve (systems A and B). (From Mollo, C. and Yang, W., The Feasibility of Fuel Cells in Modern Power Systems, M.Sc. thesis, supervised by K. Denno, New Jersey Institute of Technology, 1973; and sponsored by PSE&G, Newark, NJ. With permission.)

**Peak Generator Capacities in MW**

| P1 | P2 | P3 | P4 | P5 | P6 | P7 | P8 | P9 | P10 |
|---|---|---|---|---|---|---|---|---|---|
| 250 | 250 | 200 | 400 | 250 | 350 | 650 | 200 | 300 | 300 |

Establish the [B] matrix according to Equation 1.4 and minimum $P_L$ at peak total generation of 3150 MW.

2.18 From data and results secured in Problem 2.17, establish an economic scheduling of generation for the ten generators using the coordination equation.

2.19 In problem 2.17 replace generators P1, P3, and P10 with fuel-cell assembled units. Using the following information for the incremental fuel cost pattern of fuel cells, establish the [B] matrix using Equation 2.14 and also find $P_L$ minimum for peak generation. Incremental fuel cost for fuel cell = 1.2 mills/kWh.

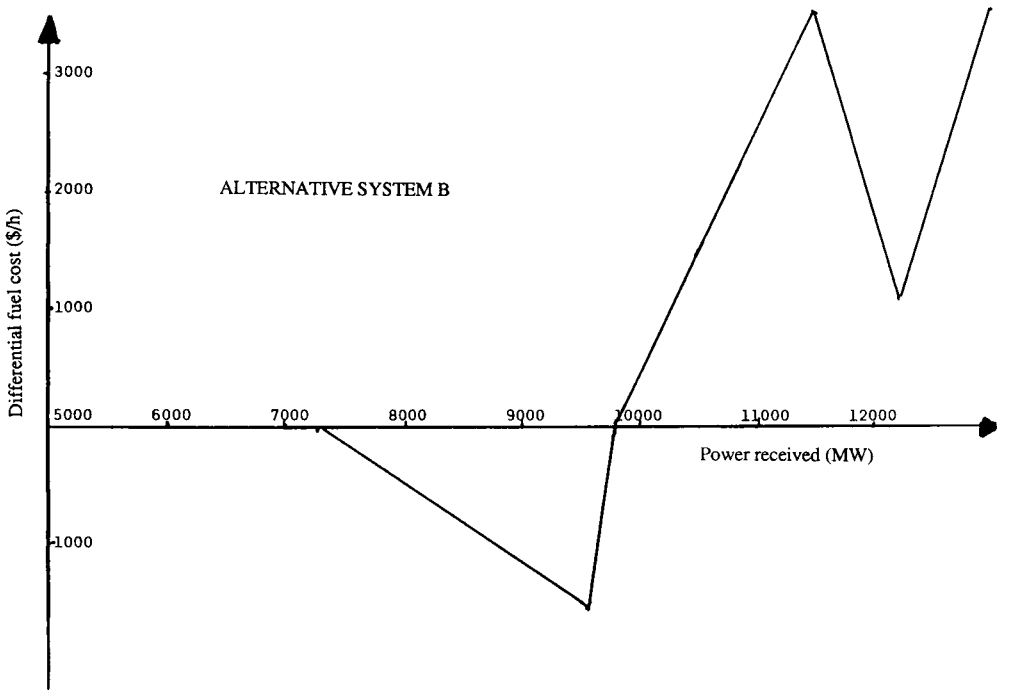


FIGURE 2.34 Differential fuel cost curve (alternative system B). (From Mollo, C. and Yang, W., The Feasibility of Fuel Cells in Modern Power Systems, M.Sc. thesis, supervised by K. Denno, New Jersey Institute of Technology, 1973; and sponsored by PSE&G, Newark, NJ. With permission.)

2.20 From data and results secured in Problem 2.19, establish an economic scheduling of generation for the ten generating units using the coordination equation.

2.21 From relevant results secured in Problems 2.19 and 2.20, establish the differential fuel cost in dollars per hour vs. power received.

2.22 Using relevant results from Problems 2.19, 2.20, and 2.21, establish, with the aid of the usual load duration curve, graphical pattern for the differential fuel cost in dollars per hour vs. total annual hours.

2.23 For alternative power system B given the symmetric [R] matrix in Table 2.14 and the corresponding [B] matrix for this system presented in Chapter 1, establish the [K] matrix. Check for the singularity character of the [K] matrix.

2.24 Repeat Problem 2.23 for alternative power system E. Check for the singularity character of the [K] matrix.

2.25 Repeat Problem 2.23 for alternative power system C. Check for the singularity character of the [K] matrix. Comment on the nature of the [K] matrix.

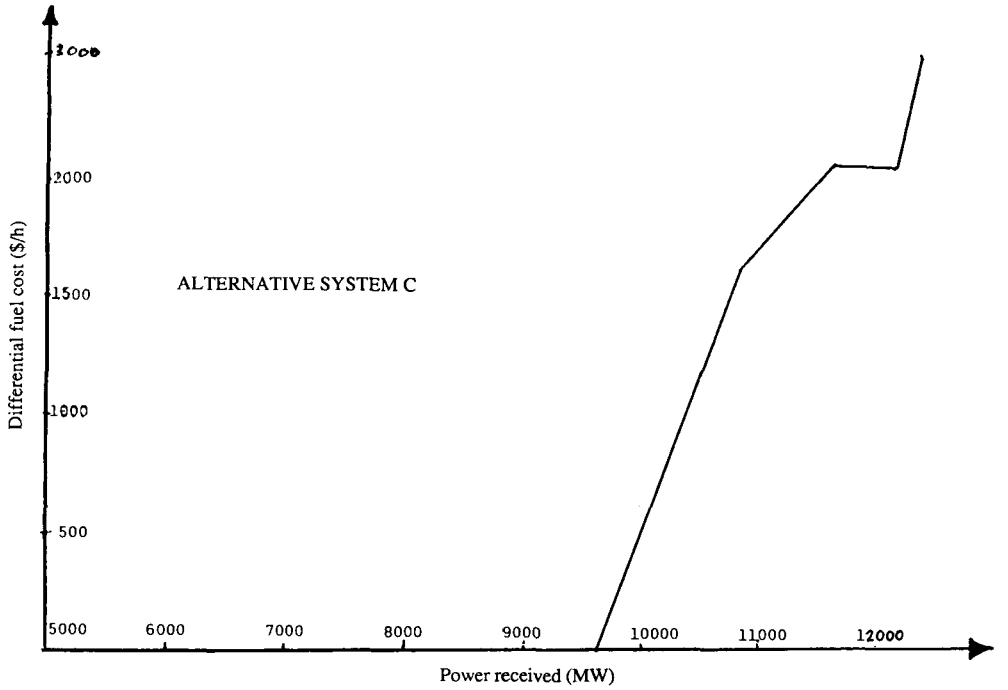


FIGURE 2.35 Differential fuel cost curve (alternative system C). (From Mollo, C. and Yang, W., The Feasibility of Fuel Cells in Modern Power Systems, M.Sc. thesis, supervised by K. Denno, New Jersey Institute of Technology, 1973; and sponsored by PSE&G, Newark, NJ. With permission.)

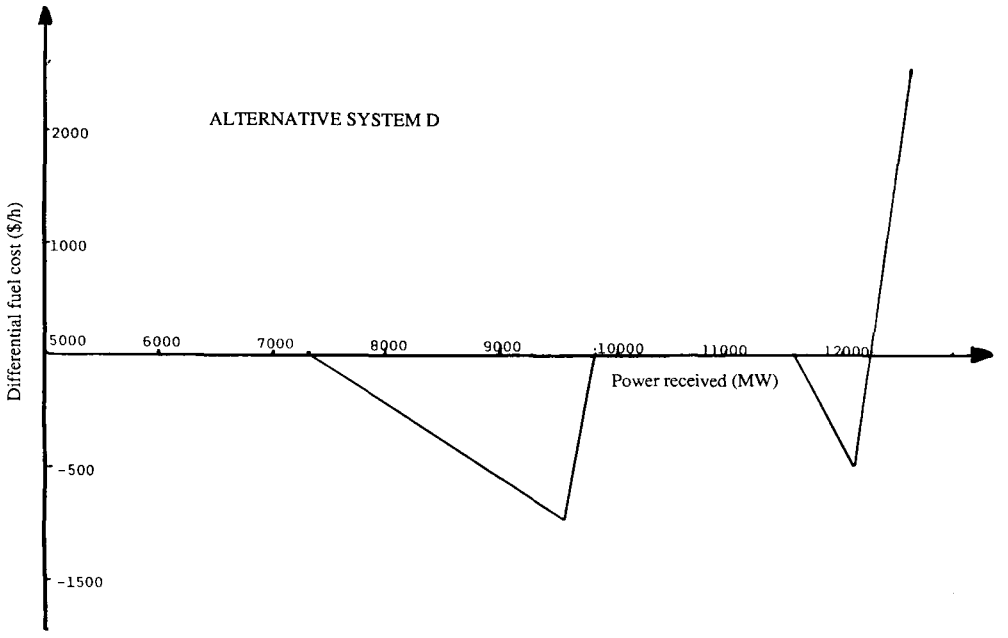


FIGURE 2.36 Differential fuel cost curve (alternative system D). (From Mollo, C. and Yang, W., The Feasibility of Fuel Cells in Modern Power Systems, M.Sc. thesis, supervised by K. Denno, New Jersey Institute of Technology, 1973; and sponsored by PSE&G, Newark, NJ. With permission.)

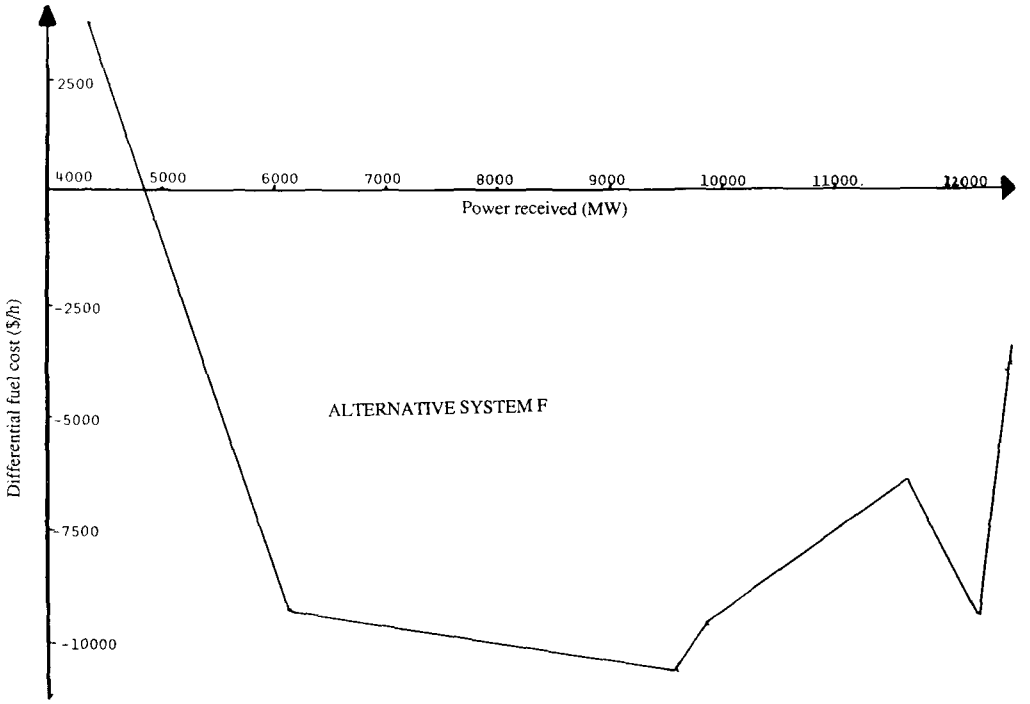


FIGURE 2.37 Differential fuel cost curve (alternative system F). (From Mollo, C. and Yang, W., The Feasibility of Fuel Cells in Modern Power Systems, M.Sc. thesis, supervised by K. Denno, New Jersey Institute of Technology, 1973; and sponsored by PSE&G, Newark, NJ. With permission.)

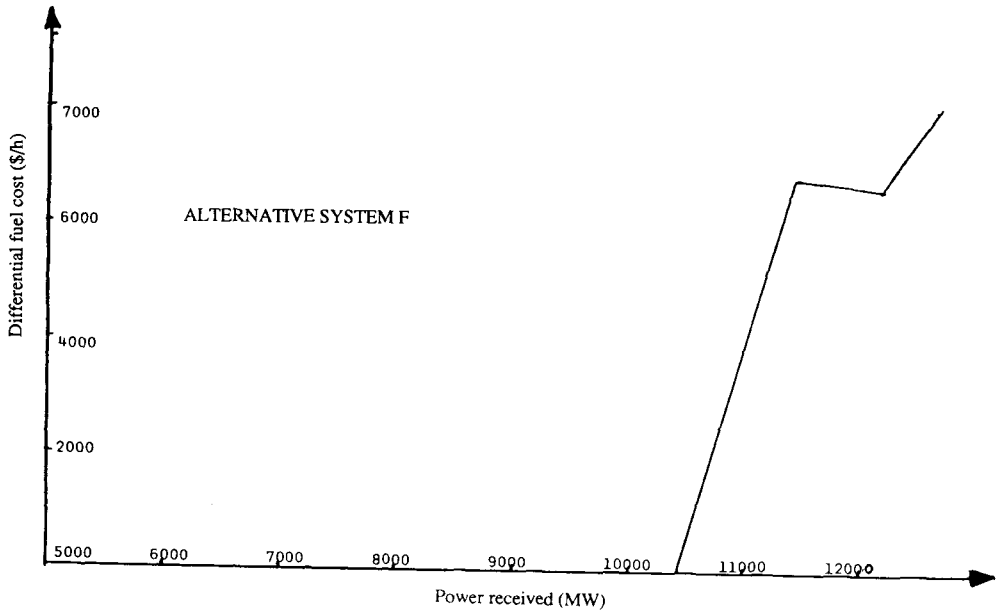


FIGURE 2.38 Differential fuel cost curve (alternative system F). (From Mollo, C. and Yang, W., The Feasibility of Fuel Cells in Modern Power Systems, M.Sc. thesis, supervised by K. Denno, New Jersey Institute of Technology, 1973; and sponsored by PSE&G, Newark, NJ. With permission.)

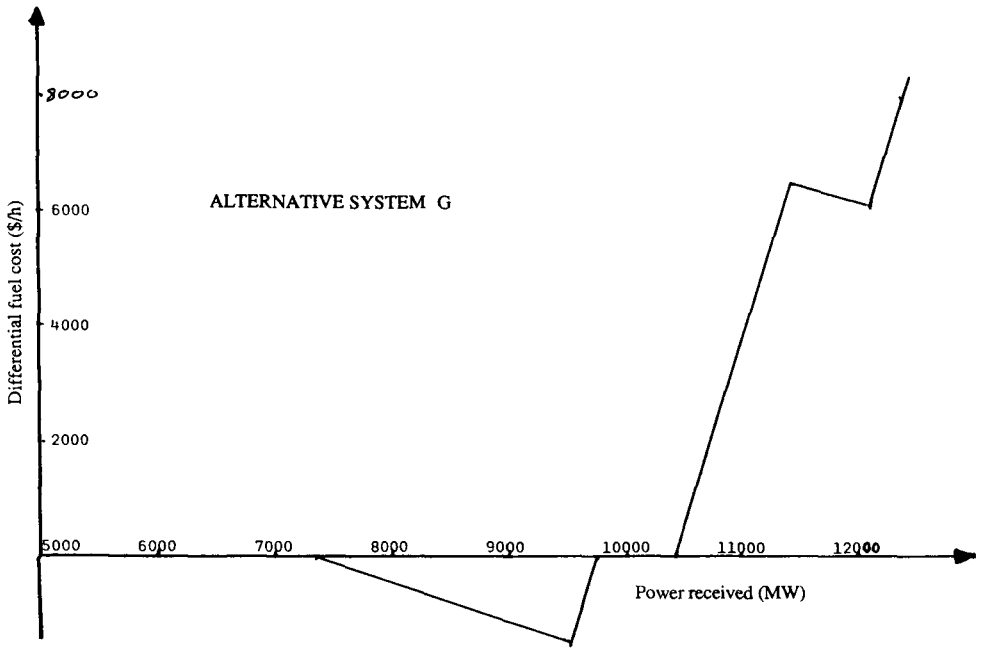


FIGURE 2.39 Differential fuel cost curve (alternative system G). (From Mollo, C. and Yang, W., The Feasibility of Fuel Cells in Modern Power Systems, M.Sc. thesis, supervised by K. Denno, New Jersey Institute of Technology, 1973; and sponsored by PSE&G, Newark, NJ. With permission.)

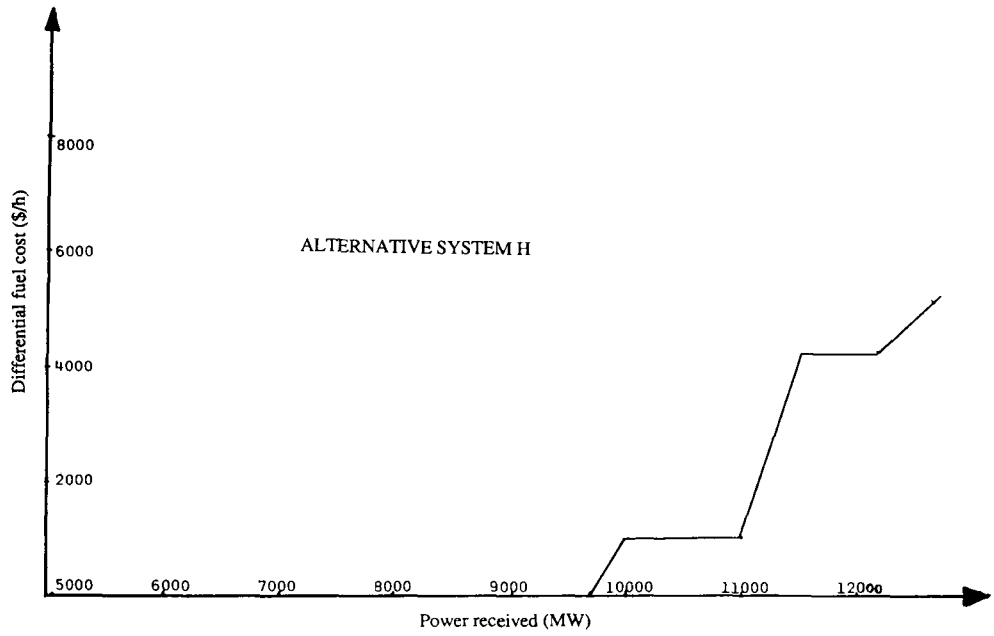


FIGURE 2.40 Differential fuel cost curve (alternative system H). (From Mollo, C. and Yang, W., The Feasibility of Fuel Cells in Modern Power Systems, M.Sc. thesis, supervised by K. Denno, New Jersey Institute of Technology, 1973; and sponsored by PSE&G, Newark, NJ. With permission.)

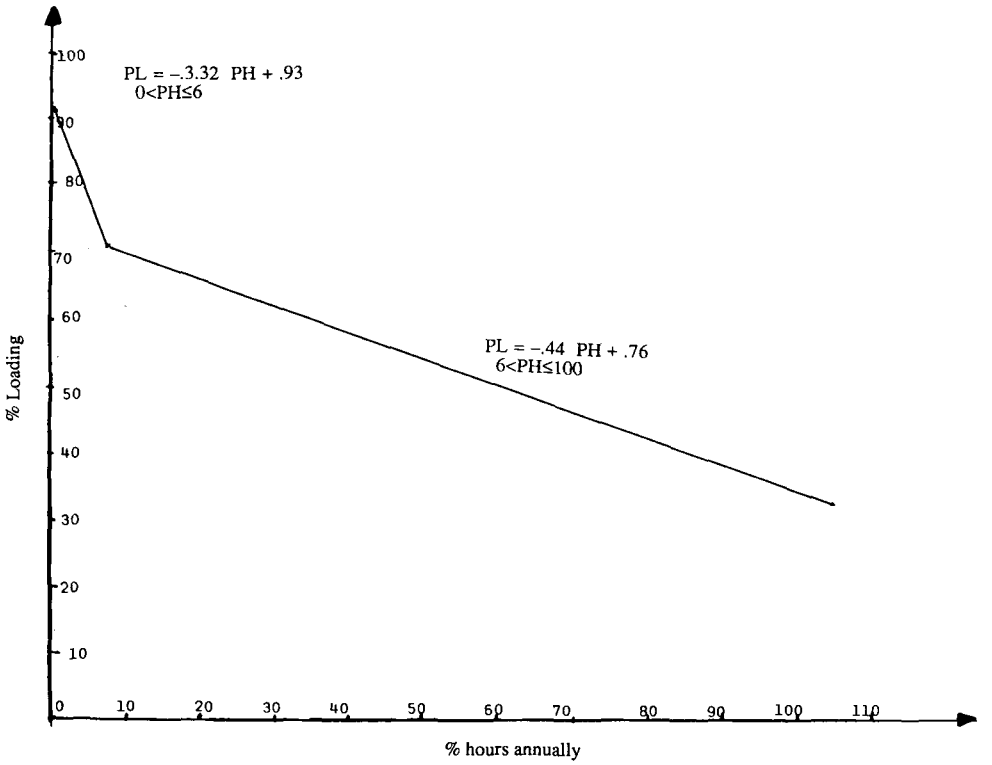


FIGURE 2.41 Load duration curve. (From Mollo, C. and Yang, W., The Feasibility of Fuel Cells in Modern Power Systems, M.Sc. thesis, supervised by K. Denno, New Jersey Institute of Technology, 1973; and sponsored by PSE&G, Newark, NJ. With permission.)

```
   Program: Power - Time Dispatch
   DO 1  I = 5000,13300,25
   P = I
   IF(P - 9700.) 2,2,3
2  PL = P/13291.
   PH = (PL - .76)*8760./(-.44)
   GO TO 1
3  PL = P/13291.
   PH = (PL - .93)* 8760./(-3.33)
1  Print P,PH
   STOP
   END
```

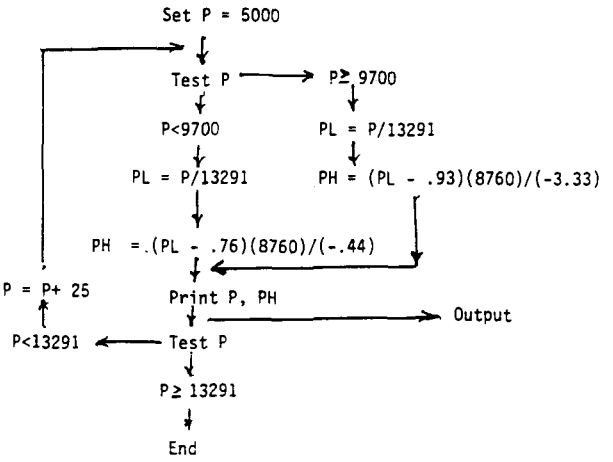


FIGURE 2.42 Power time dispatch. (From Mollo, C. and Yang, W., The Feasibility of Fuel Cells in Modern Power Systems, M.Sc. thesis, supervised by K. Denno, New Jersey Institute of Technology, 1973; and sponsored by PSE&G, Newark, NJ. With permission.)

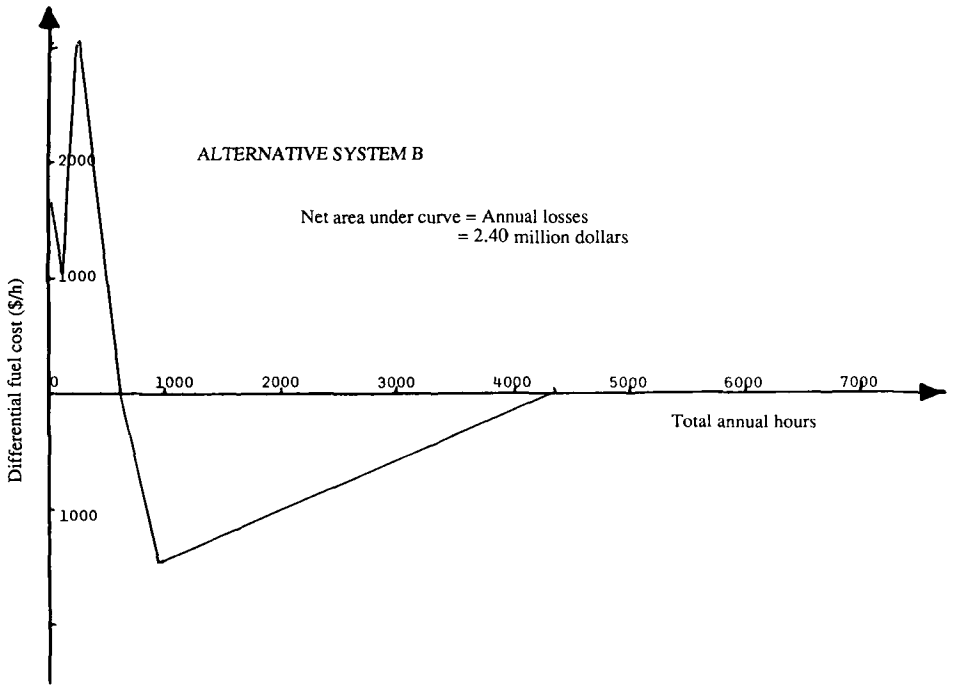


FIGURE 2.43 Relative annual cost (alternative system B). (From Mollo, C. and Yang, W., The Feasibility of Fuel Cells in Modern Power Systems, M.Sc. thesis, supervised by K. Denno, New Jersey Institute of Technology, 1973; and sponsored by PSE&G, Newark, NJ. With permission.)

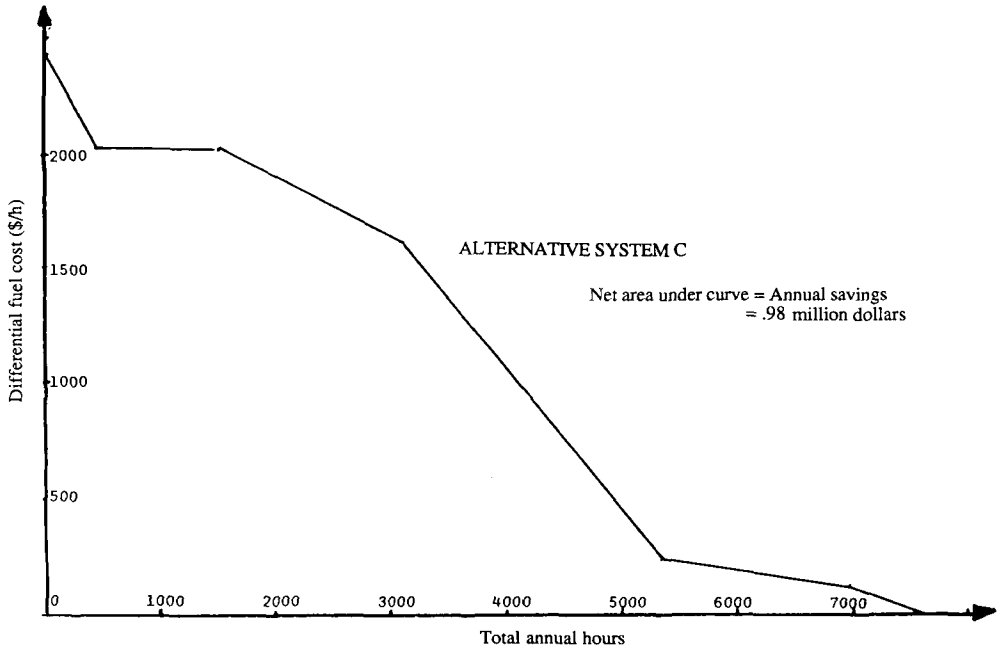


FIGURE 2.44 Relative annual cost (alternative system C). (From Mollo, C. and Yang, W., The Feasibility of Fuel Cells in Modern Power Systems, M.Sc. thesis, supervised by K. Denno, New Jersey Institute of Technology, 1973; and sponsored by PSE&G, Newark, NJ. With permission.)

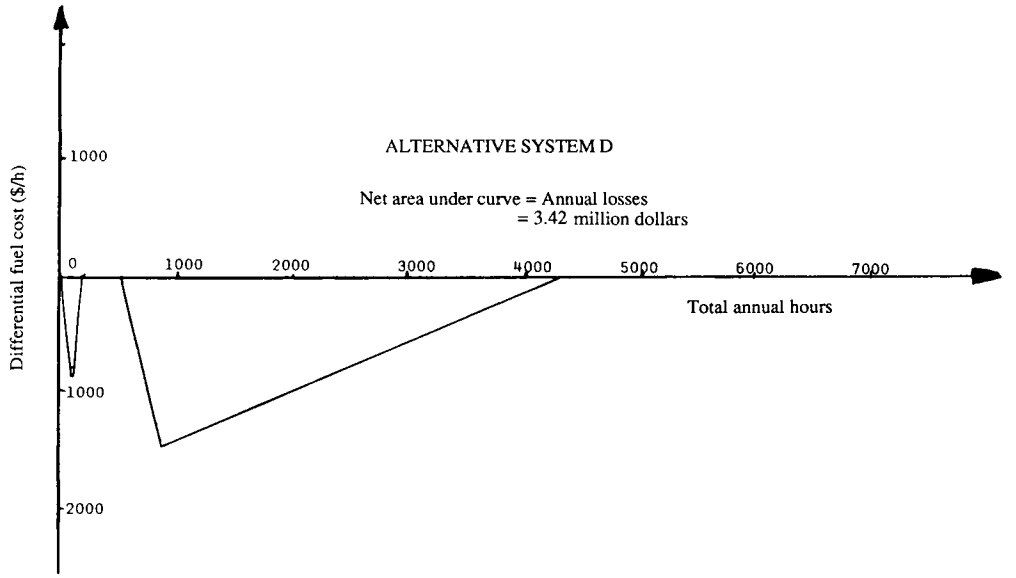


FIGURE 2.45 Relative annual cost (alternative system D). (From Mollo, C. and Yang, W., The Feasibility of Fuel Cells in Modern Power Systems, M.Sc. thesis, supervised by K. Denno, New Jersey Institute of Technology, 1973; and sponsored by PSE&G, Newark, NJ. With permission.)

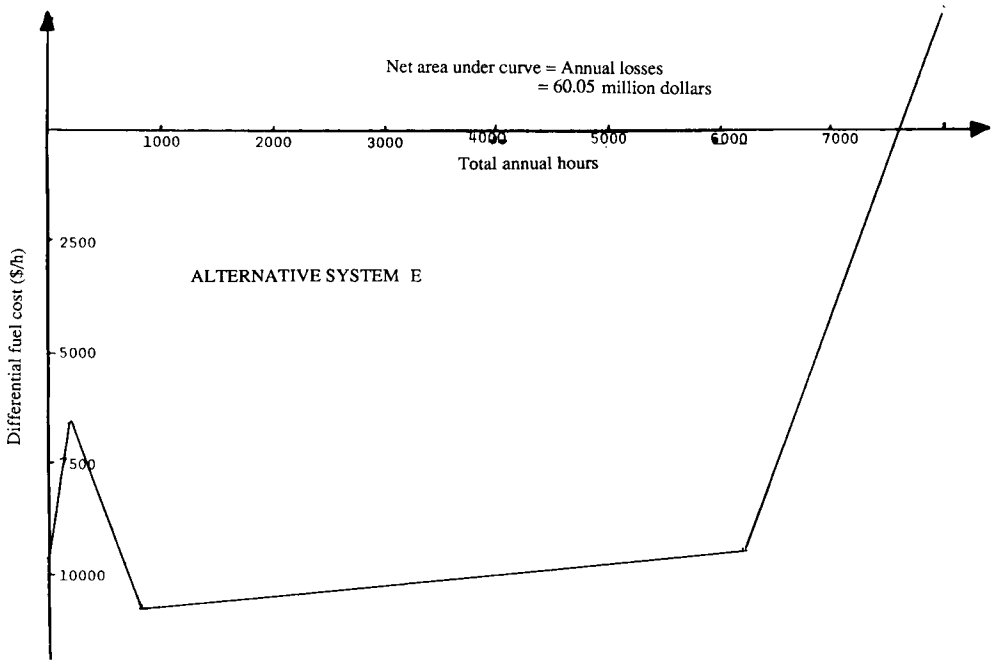


FIGURE 2.46 Relative annual cost (alternative system E). (From Mollo, C. and Yang, W., The Feasibility of Fuel Cells in Modern Power Systems, M.Sc. thesis, supervised by K. Denno, New Jersey Institute of Technology, 1973; and sponsored by PSE&G, Newark, NJ. With permission.)

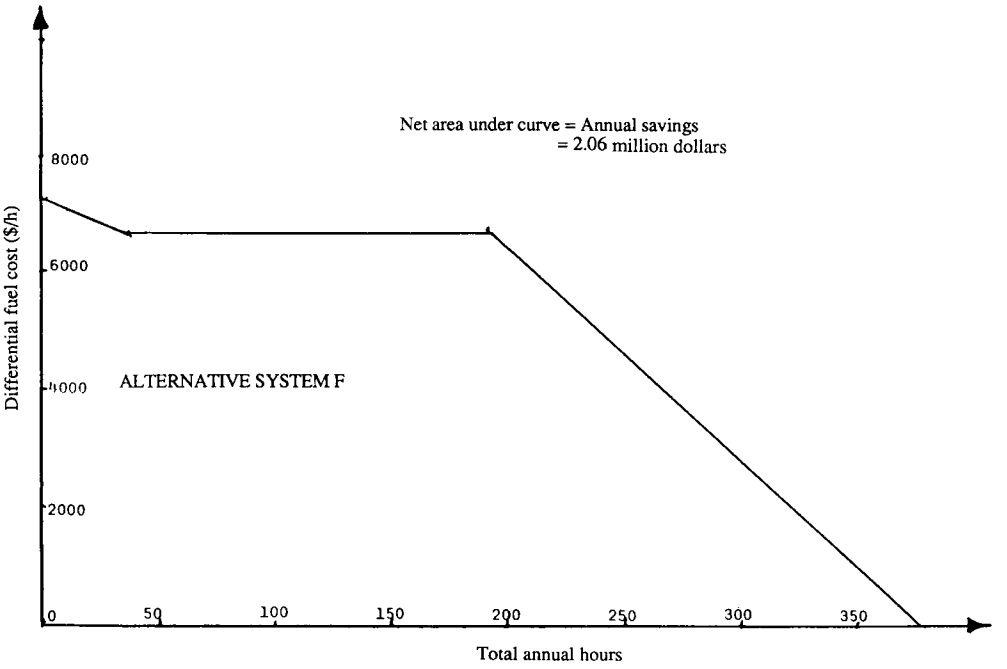


FIGURE 2.47 Relative annual cost (alternative system F). (From Mollo, C. and Yang, W., The Feasibility of Fuel Cells in Modern Power Systems, M.Sc. thesis, supervised by K. Denno, New Jersey Institute of Technology, 1973; and sponsored by PSE&G, Newark, NJ. With permission.)

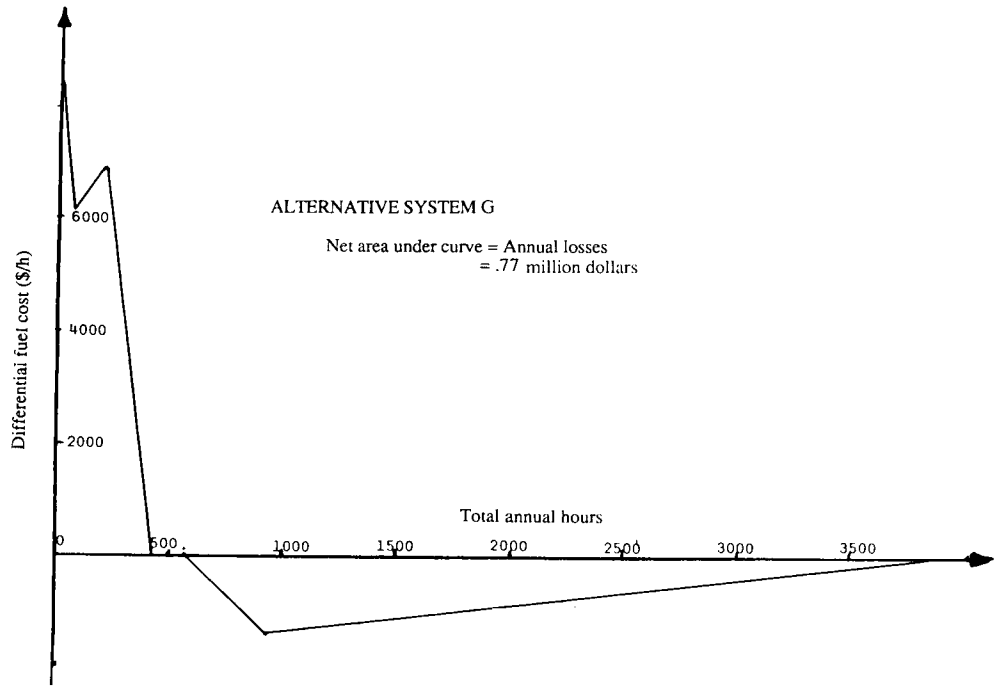


FIGURE 2.48 Relative annual cost (alternative system G). (From Mollo, C. and Yang, W., The Feasibility of Fuel Cells in Modern Power Systems, M.Sc. thesis, supervised by K. Denno, New Jersey Institute of Technology, 1973; and sponsored by PSE&G, Newark, NJ. With permission.)

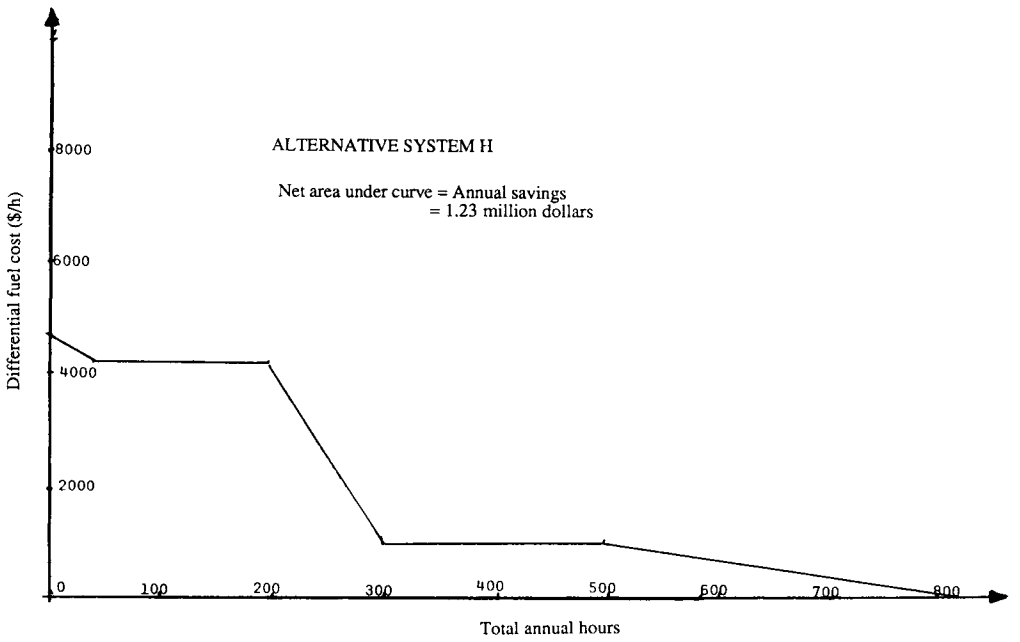


FIGURE 2.49 Relative annual cost (alternative system H). (From Mollo, C. and Yang, W., The Feasibility of Fuel Cells in Modern Power Systems, M.Sc. thesis, supervised by K. Denno, New Jersey Institute of Technology, 1973; and sponsored by PSE&G, Newark, NJ. With permission.)

**TABLE 2.2**
**Future Generation Expansion**

| Generation | MW | $/MW | Annual cost (million $) |
|---|---|---|---|
| $\Delta G_1$: | | | |
| Nuclear | 538 | 330.75 | 10.76 |
| Gas turbine | 828 | 115.50 | 6.25 |
| Steam-fossil | 40 | 119.50 | 0.27 |
| Total | | | 17.26 |
| $\Delta G_2$: | | | |
| Nuclear | 1077 | 347.29 | 22.84 |
| Gas turbine | 280 | 121.28 | 1.58 |
| Steam-fossil | 270 | 192.45 | 3.01 |
| Steam-fossil | 60 | 209.48 | 0.71 |
| Steam-fossil | 226 | 220.50 | 3.55 |
| Total | | | 31.69 |
| $\Delta G_3$: | | | |
| Nuclear | 558 | 364.65 | 12.43 |
| Steam-fossil | 800 | 219.95 | 9.90 |
| Total | | | 22.33 |
| $\Delta G_4$: | | | |
| Steam-fossil | 400 | 218.79 | 5.60 |
| Total | | | 5.60 |

*Note*: Where $\Delta G_i$ = change in power generation of plant i.

From Mollo, C. R. and Yang, W. L., The Feasibility of Fuel Cells in a Modern Power System, M.Sc. thesis, supervised by K. Denno, New Jersey Institute of Technology, 1973. With permission.

## TABLE 2.3
## Annual Installation Cost

| Type of generation | Total capacity (MW) | Total annual cost (million $) |
|---|---|---|
| Nuclear | 2168 | 46.03 |
| Steam-fossil | 1856 | 23.04 |
| Gas Turbine | 1028 | 7.81 |
| Total | | 76.88 |

From Mollo, C. R. and Yang, W. L., The Feasibility of Fuel Cells in a Modern Power System, M.Sc. thesis, supervised by K. Denno, New Jersey Institute of Technology, 1973. With permission.

## TABLE 2.4
## Annual Capital Cost for System Alternatives

| Generation mode | Capacity (MW) | Cost ($/MW) | Annual cost (million $) |
|---|---|---|---|
| Alternative B | | | |
| Nuclear | 2168 | | 46.03 |
| Fuel cells | 2884 | 175 | 40.50 |
| Total | | | 86.53 |
| Alternative C | | | |
| Nuclear | 2168 | | 46.03 |
| Steam-fossil | 1856 | | 23.04 |
| Fuel cells | 1028 | 175 | 14.43 |
| Total | | | 83.50 |
| Alternative D | | | |
| Nuclear | 2168 | | 46.03 |
| Gas turbine | 1028 | | 7.81 |
| Fuel cells | 1856 | 175 | 26.06 |
| Total | | | 79.90 |
| Alternative E | | | |
| Fuel Cells | 5052 | 175 | 70.94 |
| Alternative F | | | |
| Nuclear | 2168 | | 46.03 |
| Fossil-steam | 1856 | | 23.04 |
| Storage battery | 1028 | 200 | 16.50 |
| Total | | | 85.57 |
| Alternative G | | | |
| Nuclear | 2168 | | 46.03 |
| Fossil-steam | 1856 | 175 | 26.06 |
| Storage battery | 1028 | 200 | 16.50 |
| Total | | | 88.59 |
| Alternative H | | | |
| Nuclear | 2168 | | 46.03 |
| Steam-fossil | 1856 | | 23.04 |
| Fuel cells | 514 | 175 | 7.22 |
| Storage battery | 514 | 200 | 8.25 |
| Total | | | 84.54 |

*Note*: Life span for storage batteries = 20 years.

From Mollo, C. R. and Yang, W. L., The Feasibility of Fuel Cells in a Modern Power System, M.Sc. thesis, supervised by K. Denno, New Jersey Institute of Technology, 1973. With permission.

## TABLE 2.5
## Annual Capital Differential Cost For System Alternatives

| Alternative | Annual cost cost W.R.T.A.[a] (million $) | Relative differential loss in (million $) | Annual gain or loss (million $) |
|---|---|---|---|
| A | 76.88 | | |
| B | 86.53 | –9.65 | 9.65 loss |
| C | 83.50 | –6.62 | 6.62 loss |
| D | 79.90 | –3.02 | 3.02 loss |
| E | 70.94 | 5.94 | 5.94 gain |
| F | 85.57 | –8.69 | 8.69 loss |
| G | 88.59 | –11.71 | 11.71 loss |
| H | 84.54 | –7.66 | 7.66 loss |

[a] W.R.T.A. = with respect to plan A.

From Mollo, C. R. and Yang, W. L., The Feasibility of Fuel Cells in a Modern Power System, M.Sc. thesis, supervised by K. Denno, New Jersey Institute of Technology, 1973. With permission.

## TABLE 2.6
## O&M Cost

| Generation mode | Fixed O&M ($/kW/year) | Variable O&M (mills/kWh) | Annual maintenance (weeks) |
|---|---|---|---|
| Nuclear | 1.0 | 0.1 | 4 |
| Steam-fossil | 2.0 | 0.3 | 4 |
| Gas turbine | — | 2.0 | 2 |
| Fuel cell | — | 1.5 | 1 |
| Storage battery | — | 1.0 | 1 |

From Mollo, C. R. and Yang, W. L., The Feasibility of Fuel Cells in a Modern Power System, M.Sc. thesis, supervised by K. Denno, New Jersey Institute of Technology, 1973. With permission.

## TABLE 2.7
## Total O&M Cost

| Alternative | Generation mode | Annual fixed O&M cost (million $) | Annual variable O&M cost (million $) | Total annual O&M cost (million $) |
|---|---|---|---|---|
| A | Nuclear | 2.168 | 0.145 | 2.315 |
| | Gas turbine | | 0.691 | 0.691 |
| | Steam-fossil | 3.712 | 0.374 | 4.088 |
| | Total | | | 7.090 |
| B | Nuclear | 2.168 | 0.145 | 2.315 |
| | Fuel cells | — | 0.726 | 0.726 |
| | Total | | | 3.039 |
| C | Nuclear | 2.168 | 0.145 | 2.315 |
| | Steam-fossil | 3.712 | 0.374 | 4.086 |
| | Fuel cells | — | 0.259 | 0.259 |
| | Total | | | 6.658 |

## TABLE 2.7 (continued)
## Total O&M Cost

| Alternative | Generation mode | Annual fixed O&M cost (*million* $) | Annual variable O&M cost (*million* $) | Total annual O&M cost (*million* $) |
|---|---|---|---|---|
| D | Nuclear | 2.168 | 0.145 | 2.315 |
| | Gas turbine | — | 0.691 | 0.691 |
| | Fuel cells | — | 0.468 | 0.468 |
| | Total | | | 3.472 |
| E | Fuel cells | — | 1.270 | 1.270 |
| | Total | | | 2.170 |
| F | Nuclear | 2.168 | 0.145 | 2.315 |
| | Steam-fossil | 3.712 | 0.374 | 4.086 |
| | Storage batteries | — | 0.173 | 0.172 |
| | Total | | | 6.572 |
| G | Nuclear | 2.168 | 0.145 | 2.312 |
| | Fuel cells | — | 0.468 | 0.463 |
| | Storage batteries | — | 0.173 | 0.172 |
| | Total | | | 2.957 |
| H | Nuclear | 2.168 | 0.145 | 2.315 |
| | Fossil-steam | 3.172 | 0.374 | 4.086 |
| | Fuel cells | — | 0.129 | 0.129 |
| | Storage batteries | — | 0.086 | 0.086 |
| | Total | | | 6.61 |

From Mollo, C. R. and Yang, W. L., The Feasibility of Fuel Cells in a Modern Power System, M.Sc. thesis, supervised by K. Denno, New Jersey Institute of Technology, 1973. With permission.

## TABLE 2.8
## Differential O&M Cost

| Alternative | Total annual cost O&M (*million* $) | Annual gain or loss (*million* $) |
|---|---|---|
| A | 7.09 | Reference |
| B | 3.04 | 4.05 |
| C | 6.66 | 0.43 |
| D | 3.47 | 3.62 |
| E | 1.27 | 5.82 |
| F | 6.57 | 0.52 |
| G | 2.95 | 4.14 |
| H | 6.61 | 0.48 |

From Mollo, C. R. and Yang, W. L., The Feasibility of Fuel Cells in a Modern Power System, M.Sc. thesis, supervised by K. Denno, New Jersey Institute of Technology, 1973; and sponsored by PSE&G, Newark, NJ. With permission.

## TABLE 2.9
## Economic Picture of Alternative Power System Plans with Respect to Conventional Plan A

| Alternative | Annual initial or capital cost (million $) | Annual fuel cost (million $) | Annual O&M (million $) | Total savings or loss (million $) | % |
|---|---|---|---|---|---|
| A | Reference[a] | | | | |
| B | –9.65 | –2.4 | 4.05 | –8.0 | 2.49 |
| C | –6.62 | 0.98 | 0.43 | –5.21 | 1.62 |
| D | –3.02 | –3.42 | 3.62 | –2.82 | 0.87 |
| E | 5.94 | –60.05 | 5.82 | –48.2 | 15.00 |
| F | –8.69 | 2.06 | 0.52 | –6.11 | 1.90 |
| G | –11.71 | 0.77 | 4.14 | –8.34 | 2.59 |
| H | –7.66 | 1.23 | 0.48 | –5.95 | 1.85 |

[a] Refer to conventional plan A.

From Mollo, C. R. and Yang, W. L., The Feasibility of Fuel Cells in a Modern Power System, M.Sc. thesis, supervised by K. Denno, New Jersey Institute of Technology, 1973; and sponsored by PSE&G, Newark, NJ. With permission.

## TABLE 2.10
## Design for the Self-Symmetric Resistance Matrix for Plan A

| | | Loading | | | | |
|---|---|---|---|---|---|---|
| No. | Bus no. | 60% | 70% | 80% | 90% | 100% |
| 1 | 1—1 | 30 | 74 | 25.5461 | 5.2948 | 18.3021 |
| 2 | 156—156 | 1,190 | 1,347.051 | 462.195 | 356.3037 | 289.6976 |
| 3 | 161—161 | 480 | –377.3679 | –290.2955 | –397.7508 | –393.0586 |
| 4 | 164—164 | 20 | 62.475 | 36.134 | 7.8631 | 17.2112 |
| 5 | 172—172 | 10 | 8.6184 | 22.8502 | 9.3277 | 9.5093 |
| 6 | 174—174 | 10 | –17.5725 | –15.0119 | –29.3407 | –40.3621 |
| 7 | 291—291 | 230 | 153.3516 | 29.2962 | 23.4773 | 10.1149 |
| 8 | 315—315 | –60 | 0 | 46.6069 | –457.2831 | –30.5149 |
| 9 | 316—316 | –30 | 0 | 23.3498 | –22.9096 | –2.0222 |
| 10 | 332—332 | –390 | –285.1644 | –195.613 | –294.2089 | –290.0895 |
| 11 | 336—336 | –4,940 | –3,804.2 | –2,770.0476 | –3,390.7502 | –3,075.95 |
| 12 | 339—339 | 20 | 12.7752 | 6.1862 | –0.2235 | –17.0691 |
| 13 | 357—357 | 90 | 69.7488 | 15.7405 | –18.7635 | –22.4475 |
| 14 | 371—371 | 170 | 30.0423 | 10.8441 | 7.9081 | 6.3914 |
| 15 | 372—372 | –350 | –235.2496 | –139.5694 | –246.0342 | –237.7283 |
| 16 | 390—390 | 30 | 19.2112 | 12.0852 | –2.5044 | –6.0936 |
| 17 | 683—683 | –4,980 | –1,821.8 | –1402.7555 | –1,607.4692 | –1,474.3 |
| 18 | 685—685 | –20 | –62.5 | 0 | 0 | 0 |
| 19 | 157—157 | –50 | –68.1525 | –13.2275 | –101.7685 | –55.3677 |
| 20 | 182—182 | –150 | –130.9763 | –64.1915 | –147.621 | –36.429 |
| 21 | 183—183 | 90 | 108.7597 | 123.8365 | 2.9759 | .2585 |
| 22 | 285—285 | 440 | 441.6566 | 3.464 | 147.9623 | 25.0036 |
| 23 | 301—301 | 3,160 | 3,157.4417 | 2,861.5463 | 2,066.9847 | 1,788.6734 |
| 24 | 327 | –80 | –18.9725 | 30.1299 | 0 | 0 |
| 25 | 343 | –300 | –102.0663 | –113.733 | –284.1548 | –133.39 |
| 26 | 359 | –150 | –102.4630 | –54.8963 | –136.8692 | 151.2471 |
| 27 | 391 | –200 | –194.3907 | –173.2672 | –228.5479 | –13.5362 |
| 28 | 427 | 50 | 0.7843 | 3.7 | 9.363 | 13.3358 |
| 29 | 450 | 0 | 3.7661 | 2.1609 | 0.8923 | 1.8834 |
| 30 | 687 | 320 | 27.7690 | 0 | 0 | 0 |
| 31 | 693 | –460 | –60.6083 | 50.1456 | –178.3677 | 0 |
| 32 | 711 | –4,170 | –11,018.544 | –8,494.1238 | –9,695.5671 | –8,995.9204 |

*Note:* All values listed are $10^6$ times greater than their true per unit value.

From Mollo, C. R. and Yang, W. L., The Feasibility of Fuel Cells in a Modern Power System, M.Sc. thesis, supervised by K. Denno, New Jersey Institute of Technology, 1973; and sponsored by PSE&G, Newark, NJ. With permission.

## TABLE 2.11
## Design for the Self-Symmetric Resistance Matrix for Plan B

| No. | Bus no. | Loading 60% | 70% | 80% | 90% | 100% |
|---|---|---|---|---|---|---|
| 1 | 1 | 32.521 | 78.2342 | 24.7193 | 5.5959 | 18.8668 |
| 2 | 156 | 1190.2486 | 1412.1301 | 445.6685 | 382.197 | 302.8404 |
| 3 | 161 | –476.03 | –239.2782 | –372.3141 | –275.315 | –332.6847 |
| 4 | 164 | 21.782339 | 65.6069 | 34.9645 | 8.3102 | 17.74218 |
| 5 | 172 | 14.2156 | 9.0504 | 22.1106 | 9.8581 | 9.80276 |
| 6 | 174 | 7.5734 | 14.831 | –25.0701 | –18.1871 | –33.9532 |
| 7 | 291 | 234.3997 | 182.7257 | 24.936 | 34.9818 | 15.37 |
| 8 | 315 | –60.1107 | 102.3375 | –12.371 | 41.4284 | –5.7946 |
| 9 | 316 | –30.1148 | 51.3716 | –6.1981 | 20.7554 | –0.384 |
| 10 | 332 | –390.9161 | –152.0667 | –272.4651 | –180.6832 | –234.1436 |
| 11 | 336 | –4939.433 | –2670.8843 | –3417.874 | –2447.3073 | –2629.9373 |
| 12 | 339 | 22.7219 | 20.0887 | 1.4519 | 0 | –12.9272 |
| 13 | 357 | 94.80 | 108.0416 | 4.575 | –2.88625 | –16.87124 |
| 14 | 371 | 170.3366 | 33.6968 | 9.8782 | 9.5838 | 7.3293 |
| 15 | 372 | –352.3437 | –91.7633 | –222.4387 | –123.821 | –178.2961 |
| 16 | 390 | 29.9415 | 25.3479 | 8.0748 | 4.112 | –3.8847 |
| 17 | 683 | –4981.66 | –1397.9582 | –1648.9843 | –1244.3694 | –1300.5437 |
| 18 | 685 | –22.7541 | –12.8352 | 0 | 0 | 0 |
| 19 | 157 | –46.47 | –45.7567 | –25.13 | –54.0723 | –44.42 |
| 20 | 182 | –149.2743 | –15.6385 | –116.2613 | –69.2173 | –27.3675 |
| 21 | 183 | 13.8331 | 13.3038 | 36.26 | 5.5885 | 0.3436 |
| 22 | 285 | 19.9315 | 197.0936 | 0.4387 | 53.6561 | 4.1352 |
| 23 | 301 | 3158.604 | 3725.0753 | 2550.008 | 2523.727 | 2081.929 |
| 24 | 327 | –79.232 | 123.5541 | –53.1275 | 0 | 0 |
| 25 | 343 | 26.9076 | 133.0382 | 72.52 | 146.49 | 26.0277 |
| 26 | 359 | 13.8331 | 133.5553 | 35.0041 | 70.5603 | 29.512 |
| 27 | 391 | 5.5114 | 52.9058 | 13.9463 | 28.1121 | 0.625 |
| 28 | 427 | 52.3777 | 0.8237 | 3.58 | 9.8954 | 13.7472 |
| 29 | 450 | 0.6587 | 3.9549 | 2.0909 | 0.9431 | 1.9415 |
| 30 | 687 | 17.223 | 154.2539 | 0 | 0 | 0 |
| 31 | 693 | 93.3157 | 382.8292 | 103.689 | 208.0343 | 0 |
| 32 | 711 | –4170.3 | –8514.449 | –9945.92 | –7550.3364 | –7956.7357 |

*Note:* All values listed are $10^6$ times greater than their true per unit value.

From Mollo, C. R. and Yang, W. L., The Feasibility of Fuel Cells in a Modern Power System, M.Sc. thesis, supervised by K. Denno, New Jersey Institute of Technology, 1973; and sponsored by PSE&G, Newark, NJ. With permission.

## TABLE 2.12
## Design for the Self-Symmetric Resistance Matrix for Plan C

| No. | Bus no. | Loading 60% | 70% | 80% | 90% | 100% |
|---|---|---|---|---|---|---|
| 1 | 1 | 33.5884 | 73.9802 | 25.2272 | 5.2527 | 18.1516 |
| 2 | 156 | 1,222.6544 | 1.338 | 455.8237 | 352.6841 | 286.191 |
| 3 | 161 | –377.8778 | –396.5701 | –321.9187 | –414.867 | –409.1584 |
| 4 | 164 | 22.4971 | 62.0394 | 35.6823 | 7.8 | 17.4696 |
| 5 | 172 | 14.6821 | 8.5583 | 22.5651 | 9.2535 | 9.4311 |
| 6 | 174 | 41.0448 | –22.0731 | –18.89 | –30.9 | –42.0713 |
| 7 | 291 | 258.3174 | 149.267 | 27.615 | 21.868 | 8.7141 |
| 8 | 315 | 16.2214 | –14.2234 | 23.8673 | –57.9111 | –37.1062 |
| 9 | 316 | 8.1268 | –7.1399 | 11.9574 | –29.0131 | –2.459 |
| 10 | 332 | –294.097 | –303.673 | –225.2441 | –310.08 | –305.0083 |

**TABLE 2.12 (continued)**
**Design for the Self-Symmetric Resistance Matrix for Plan C**

| | | Loading | | | | |
|---|---|---|---|---|---|---|
| **No.** | **Bus no.** | **60%** | **70%** | **80%** | **90%** | **100%** |
| 11 | 336 | –4,122.7117 | –3,961.8 | –3,019.8118 | –3,531.76 | –3,194.8883 |
| 12 | 339 | 27.4905 | 11.7583 | 4.361 | 0.2821 | –18.1738 |
| 13 | 357 | 1,141.679 | 64.4223 | 11.4361 | –20.9824 | –23.9352 |
| 14 | 371 | 182.1171 | 29.5341 | 10.4717 | 7.6738 | 6.1412 |
| 15 | 372 | –247.3774 | –255.203 | –171.5213 | –263.1198 | –253.576 |
| 16 | 390 | 33.9317 | 18.3579 | 10.5389 | –3.4292 | –6.6827 |
| 17 | 683 | –4,319.5262 | –1,880.8 | –1,497.688 | –1,658.23 | –1,520.6362 |
| 18 | 685 | 5.1085 | –69.40338 | 0 | 0 | 0 |
| 19 | 186 | 0.4275 | 80.3259 | 9.3525 | 0 | –26.9275 |
| 20 | 182 | 67.0469 | 38.4454 | 60.217 | 0 | –2.8988 |
| 21 | 183 | 142.3706 | 98.2755 | 106.8499 | 2.28 | 1.571 |
| 22 | 285 | 501.02523 | 429.6367 | 3.3059 | 142.8485 | 24.0768 |
| 23 | 301 | 3,556.917 | 3,078.5 | 2,741.4401 | 2,003.126 | 1,730.144 |
| 24 | 327 | 25.9888 | –38.757 | –1.7188 | 0 | 0 |
| 25 | 343 | 139.7455 | 41.4405 | 129.8163 | –9.58817 | –11.91033 |
| 26 | 359 | 71.8428 | 29.4290 | 62.6594 | –4.6183 | –13.5047 |
| 27 | 427 | 54.0964 | 0.7789 | 3.6538 | 9.28863 | 13.2261 |
| 28 | 391 | 49.438 | 29.429 | 30.7263 | –0.9426 | –0.47629 |
| 29 | 450 | 0.68 | 3.7398 | 2.13389 | 0.8852 | 1.8679 |
| 30 | 687 | 371.4351 | 267.4327 | 0 | 0 | 0 |
| 31 | 693 | –35.5412 | –95.4486 | –5.9217 | –208.07844 | 0 |
| 32 | 711 | 383.7076 | 736.7194 | 1,153.9238 | –85.7268 | –235.9871 |

*Note:* All values listed are $10^6$ times greater than their true per unit value.

From Mollo, C. R. and Yang, W. L., The Feasibility of Fuel Cells in a Modern Power System, M.Sc. thesis, supervised by K. Denno, New Jersey Institute of Technology, 1973; and sponsored by PSE&G, Newark, NJ. With permission.

**TABLE 2.13**
**Design for the Self-Symmetric Resistance Matrix for Plan D**

| | | Loading | | | | |
|---|---|---|---|---|---|---|
| **No.** | **Bus no.** | **60%** | **70%** | **80%** | **90%** | **100%** |
| 1 | 1 | 32.395 | 72.9015 | 25.2274 | 5.5959 | 18.9999 |
| 2 | 156 | 1186.4127 | 1319.239 | 455.8237 | 382.197 | 305.958 |
| 3 | 161 | –487.6442 | –436.4545 | –321.9186 | –275.315 | –318.5241 |
| 4 | 164 | 21.6977 | 61.1349 | 35.6832 | 8.3102 | 17.86675 |
| 5 | 172 | 14.1604 | 8.4335 | 22.5651 | 9.8581 | 9.8715 |
| 6 | 174 | 3.6869 | –31.4249 | –18.8901 | –18.1871 | –32.45 |
| 7 | 291 | 231.5694 | 140.7829 | 27.615 | 34.9818 | 16.6024 |
| 8 | 315 | –69.1384 | –43.7942 | 23.8673 | 41.4284 | 0 |
| 9 | 316 | –34.6376 | –21.9838 | 11.9574 | 20.7554 | 0 |
| 10 | 332 | –402.373 | –342.1157 | –225.2441 | –180.6832 | –221.0209 |
| 11 | 336 | –5036.08 | –4289.13 | –3019.8118 | –2447.3073 | –2525.3163 |
| 12 | 339 | 22.158 | 9.6458 | 4.3612 | –0.0429 | –11.9556 |
| 13 | 357 | 92.5087 | 53.3633 | 11.4361 | –2.8862 | –15.5633 |
| 14 | 371 | 168.943 | 28.479 | 10.4717 | 9.5838 | 7.5493 |
| 15 | 372 | –364.765 | –296.648 | –171.5213 | –123.8211 | –164.3559 |
| 16 | 390 | 29.0692 | 16.586 | 10.5389 | 4.112 | –3.36656 |
| 17 | 683 | –5060.02 | –2031.516 | –1497.688 | –1244.3694 | –1259.7856 |
| 18 | 685 | –26.048 | –83.748 | 0 | 0 | 0 |
| 19 | 157 | –60.3282 | –65.7457 | –2.339 | –3.7376 | –13.2059 |
| 20 | 182 | –156.7083 | –141.7757 | –84.2679 | –69.2172 | –25.2419 |

## TABLE 2.13 (continued)
## Design for the Self-Symmetric Resistance Matrix for Plan D

| | | Loading | | | | |
|---|---|---|---|---|---|---|
| **No.** | **Bus no.** | **60%** | **70%** | **80%** | **90%** | **100%** |
| 21 | 183 | 82.0695 | 76.5092 | 106.84998 | 7.9555 | 0.7274 |
| 22 | 285 | 10.0917 | 26.9764 | 0.7853 | 53.6561 | 5.2512 |
| 23 | 301 | 68.119 | 182.091 | 614.4605 | 691.9926 | 343.28 |
| 24 | 327 | –91.6952 | –79.9286 | –1.7188 | 0 | 0 |
| 25 | 343 | –314.5057 | –142.4249 | –156.4171 | –119.5351 | –88.43159 |
| 26 | 359 | –161.6867 | –142.9785 | –75.499 | –57.5765 | –100.27 |
| 27 | 391 | 17.7358 | 14.006 | 25.3488 | 24.1442 | 0.3529 |
| 28 | 427 | 52.1743 | 0.7675 | 3.6538 | 9.8994 | 13.8437 |
| 29 | 450 | 0.6561 | 3.6853 | 2.1339 | 0.9431 | 1.9551 |
| 30 | 687 | 8.7204 | 21.1129 | 0 | 0 | 0 |
| 31 | 693 | 47.2474 | 52.3983 | 185.6098 | 208.0354 | 0 |
| 32 | 693 | 47.2474 | 52.3983 | 185.6098 | 208.0354 | 0 |
| 33 | 711 | –4234.53 | –1209.0012 | –9053.8635 | –7550.3364 | –7712.9788 |

*Note:* All values are $10^6$ times greater than their true per unit value.

From Mollo, C. R. and Yang, W. L., The Feasibility of Fuel Cells in a Modern Power System, M.Sc. thesis, supervised by K. Denno, New Jersey Institute of Technology, 1973; and sponsored by PSE&G, Newark, NJ. With permission.

## TABLE 2.14
## Design for the Self-Symmetric Resistance Matrix for Plan F

| | | Loading | | | | |
|---|---|---|---|---|---|---|
| **No** | **Bus no.** | **60%** | **70%** | **80%** | **90%** | **100%** |
| 1 | 1 | 32.1374 | 75.9834 | 25.2274 | 5.2948 | 18.4488 |
| 2 | 156 | 1178.592 | 1372.9084 | 455.8237 | 356.3037 | 293.1135 |
| 3 | 161 | –511.335 | –322.5014 | –321.9186 | –397.7508 | –377.3772 |
| 4 | 164 | 21.5252 | 63.7193 | 35.6832 | 7.8631 | 17.3491 |
| 5 | 172 | 14.0479 | 87.9009 | 22.5651 | 9.3277 | 9.5855 |
| 6 | 174 | –2.9725 | –4.7275 | –18.8901 | –29.3407 | –38.6976 |
| 7 | 291 | 225.7965 | 165.02161 | 27.615 | 23.4773 | 11.4807 |
| 8 | 315 | –87.5581 | 40.6592 | 23.8673 | –45.7283 | –24.095 |
| 9 | 316 | –43.8657 | 20.4102 | 11.9574 | –22.9096 | –1.5917 |
| 10 | 332 | –425.7375 | –232.3814 | –225.2441 | –294.2089 | –275.5583 |
| 11 | 336 | –5233.16 | –3353.913 | –3019.8118 | –3398.7502 | –2960.1051 |
| 12 | 339 | 21.0068 | 15.6815 | 4.3612 | –0.2235 | –15.9932 |
| 13 | 357 | 87.8345 | 84.9632 | 11.4361 | –18.7365 | –20.9992 |
| 14 | 371 | 166.0997 | 31.4943 | 10.4717 | 7.90811 | 6.635 |
| 15 | 372 | –390.0951 | –178.2379 | –171.5213 | –246.0342 | –222.2917 |
| 16 | 390 | 28.5062 | 21.6494 | 10.5389 | –2.5044 | –5.5191 |
| 17 | 683 | –5219.81 | –1653.397 | –1497.688 | –1607.4692 | –1429.1694 |
| 18 | 685 | –32.7602 | –42.7609 | 0 | 0 | 0 |
| 19 | 157 | 48831.894 | 46158.94 | 7205.5985 | 15047.185 | 6073.7431 |
| 20 | 182 | 618.1367 | 575.386 | 500.2645 | 426.0709 | 90.26627 |
| 21 | 183 | 69.059 | 138.7011 | 106.8499 | 2.9759 | 0.3571 |
| 22 | 285 | 418.7447 | 476.0024 | 3.3059 | 147.9623 | 25.9065 |
| 23 | 301 | 3015.35 | 3382.98 | 2741.4401 | 2066.9857 | 1845.6969 |
| 24 | 327 | –117.08 | 37.656 | –1.7188 | 0 | 0 |
| 25 | 343 | 1288.38 | 620.2114 | 1078.4748 | 913.1864 | 370.867 |
| 26 | 359 | 662.3519 | 622.63 | 520.5553 | 439.8552 | 420.5151 |
| 27 | 391 | 0 | 0 | 0 | 0 | 0 |
| 28 | 427 | 51.7595 | 0.8 | 3.6538 | 9.363 | 13.4426 |
| 29 | 450 | 0.6509 | 3.8411 | 2.1339 | 0.8923 | 1.8984 |

**TABLE 2.14 (continued)**
**Design for the Self-Symmetric Resistance Matrix for Plan F**

| | | Loading | | | | |
|---|---|---|---|---|---|---|
| **No** | **Bus no.** | **60%** | **70%** | **80%** | **90%** | **100%** |
| 30 | 687 | 295.48 | 307 | 0 | 0 | 0 |
| 31 | 693 | –608.52 | 38.9 | –5.921 | –178.3677 | 0 |
| 32 | 711 | 31824.7 | 99197.8 | 86246.013 | 73451.578 | 66106.438 |

*Note:* All values listed are $10^6$ times greater than their true per unit value.

From Mollo, C. R. and Yang, W. L., The Feasibility of Fuel Cells in a Modern Power System, M.Sc. thesis, supervised by K. Denno, New Jersey Institute of Technology, 1973; and sponsored by PSE&G, Newark, NJ. With permission.

**TABLE 2.15**
**Design for the Self-Symmetric Resistance Matrix for Plan H**

| | | Loading | | | | |
|---|---|---|---|---|---|---|
| **No.** | **Bus no.** | **60%** | **70%** | **80%** | **90%** | **100%** |
| 1 | 1 | 32.137 | 72.901 | 23.979 | 5.694 | 20.05 |
| 2 | 156 | 1178.592 | 1319.203 | 430.88 | 319.693 | 0 |
| 3 | 161 | –510.501 | –435.622 | –444.839 | –234.403 | –204.506 |
| 4 | 164 | 21.225 | 61.134 | 33.918 | 8.467 | 18.863 |
| 5 | 172 | 26.52 | 15.921 | 40.493 | 18.939 | 19.675 |
| 6 | 174 | –4.561 | –31.424 | –34.068 | –14.527 | –20.423 |
| 7 | 291 | 227.637 | 142.282 | 21.397 | 39.275 | 26.908 |
| 8 | 315 | –87.558 | –43.794 | –65.150 | 17.02 | 46.3825 |
| 9 | 316 | –43.865 | –21.983 | –32.639 | 35.080 | 3.0738 |
| 10 | 332 | –424.87 | –341.257 | –340.375 | –142.688 | –115.299 |
| 11 | 336 | –5233.157 | –4289.131 | –3997.512 | –2135.11 | –1688.3588 |
| 12 | 339 | 21.006 | 9.645 | –2.779 | 0.016 | –4.182 |
| 13 | 357 | 87.834 | 53.363 | –5.425 | 2.331 | –5.097 |
| 14 | 371 | 167.651 | 28.802 | 9.155 | 10.267 | 9.452 |
| 15 | 372 | –390.095 | –296.647 | –296.585 | –83.723 | –52.828 |
| 16 | 390 | 28.506 | 16.585 | 4.487 | 6.282 | 0.779 |
| 17 | 683 | –5219.809 | –2003.151 | –1869.293 | 125.229 | –933.724 |
| 18 | 685 | –32.76 | –83.748 | 0 | 0 | 0 |
| 19 | 157 | 97.05 | 51.651 | –7.119 | 22.511 | 4.828 |
| 20 | 182 | 465.765 | 346.0912 | 255.153 | 249.486 | 46.697 |
| 21 | 183 | 69.059 | 67.509 | 40.356 | 9.589 | 1.44 |
| 22 | 285 | 421.367 | 407.390 | 2.709 | 197.722 | 36.044 |
| 23 | 301 | 15.347 | 2914.55 | 0.002 | 2673.600 | 2471.625 |
| 24 | 327 | –117.079 | –79.9 | –127.635 | 0 | 0 |
| 25 | 343 | 1288.377 | 595.055 | 1025.128 | 982.151 | 403.231 |
| 26 | 359 | 662.351 | 597.368 | 494.806 | 473.073 | 457.212 |
| 27 | 391 | 21.337 | 0 | 5.874 | 38.973 | 2.063 |
| 28 | 427 | 51.76 | 0.767 | 3.473 | 10.07 | 14.615 |
| 29 | 450 | 0.65 | 3.685 | 2.028 | 0.959 | 2.064 |
| 30 | 687 | 295.48 | 246.128 | 0 | 0 | 0 |
| 31 | 693 | –606.122 | –166.765 | –223.532 | 104.875 | 0 |
| 32 | 711 | –374 | 323.717 | –96.44 | 1711.622 | 1768.172 |

*Note*: The [R] matrix for a centralized-dispersed system has been presented in Chapter 1. All values are $10^6$ times greater than their true per unit value.

From Mollo, C. R. and Yang, W. L., The Feasibility of Fuel Cells in a Modern Power System, M.Sc. thesis, supervised by K. Denno, New Jersey Institute of Technology, 1973; and sponsored by PSE&G, Newark, NJ. With permission.

## TABLE 2.16
## Design for the Self-Symmetric Resistance Matrix for Plan G

| No. | Bus no. | Loading 60% | 70% | 80% | 90% | 100% |
|---|---|---|---|---|---|---|
| 1 | 1 | 31.8731 | 72.3412 | 24.71936 | 5.2948 | 18.4488 |
| 2 | 156 | 1170.56 | 1309.439 | 445.6685 | 356.3037 | 293.3113 |
| 3 | 161 | −535.648 | −457.1732 | −372.3141 | −397.7508 | −377.3772 |
| 4 | 164 | 21.3482 | 60.665 | 34.9645 | 7.8631 | 17.3491 |
| 5 | 172 | 139.3235 | 836.875 | 22.1106 | 9.3277 | 9.5855 |
| 6 | 174 | −12.8715 | −36.2843 | −25.0701 | −29.3407 | −38.6976 |
| 7 | 291 | 219 | 136.3768 | 24.936 | 23.4773 | 11.4807 |
| 8 | 315 | −106.4709 | −59.1444 | −12.3716 | −45.7283 | −24.0954 |
| 9 | 316 | −53.34 | −29.689 | −6.1981 | −22.9096 | −1.5967 |
| 10 | 332 | −449.7249 | −362.0854 | −272.4651 | −294.0899 | −275.5583 |
| 11 | 336 | −5435.51 | −4459.176 | −3417.8744 | −3398.7502 | −3960.1051 |
| 12 | 339 | 19.8254 | 8.5487 | 1.4519 | −0.2235 | −15.9932 |
| 13 | 357 | 83.0376 | 47.612 | 4.575 | −18.7635 | −20.992 |
| 14 | 371 | 163.181 | 27.93024 | 9.8782 | 7.9081 | 6.635 |
| 15 | 372 | −416.101 | −318.1754 | −222.438 | −246.0342 | −222.2917 |
| 16 | 390 | 27.5177 | 15.6649 | 8.0748 | −2.5044 | −5.5196 |
| 17 | 683 | −5383.86 | −2066.745 | −1648.9843 | −1607.4692 | −1429.1694 |
| 18 | 685 | −39.6568 | −91.2024 | 0 | 0 | 0 |
| 19 | 157 | 356.0904 | 230.4142 | 24.31865 | 0.745 | −16.0986 |
| 20 | 182 | 613.0521 | 540.7805 | 490.1892 | 426.07099 | 90.2662 |
| 21 | 183 | −21.441 | 6.1943 | 36.2606 | 0.3654 | 0.05137 |
| 22 | 285 | −30.8945 | 9.1768 | 3.508798 | 0.61812 | 0.4387 |
| 23 | 301 | 2916.68 | 2829.398 | 2550.0075 | 2066.9857 | 1845.6969 |
| 24 | 327 | −143.160 | −101.3159 | −53.1275 | 0 | 0 |
| 25 | 343 | 1277.77 | 590.4824 | 1056.7547 | 913.1864 | 370.867 |
| 26 | 359 | 656.9037 | 592.7773 | 510.0714 | 439.8552 | 420.5151 |
| 27 | 391 | 702.1129 | 512.6921 | 363.4106 | 173.7908 | 3.5262 |
| 28 | 427 | 51.3337 | 0.761 | 3.5802 | 9.3630 | 13.4426 |
| 29 | 450 | 0.6455 | 3.657 | 2.0909 | 0.89236 | 1.8984 |
| 30 | 687 | −26.696 | 7.1821 | 0 | 0 | 0 |
| 31 | 693 | −144.6421 | 17.2848 | 103.689 | 13.6042 | 0 |
| 32 | 711 | 31562.518 | 94437.84 | 84507.167 | 73451.578 | 66106.438 |

*Note:* All values are $10^6$ times greater than their true per unit value.

From Mollo, C. R. and Yang, W. L., The Feasibility of Fuel Cells in a Modern Power System, M.Sc. thesis, supervised by K. Denno, New Jersey Institute of Technology, 1973; and sponsored by PSE&G, Newark, NJ. With permission.

# REFERENCES


1. **Denno, K.,** Steady State and Dynamic Investigation for Determining Optimum Electrochemical-Electromechanical Interconnected Power Systems, report sponsored by a Middle Atlantic Power Research Committee research grant, New Jersey Institute of Technology, Newark, NJ, March 1976.
2. **Denno, K.,** Power System Synthesis from Solution of Optimum Transmission Loss Coefficients, Paper no. C-73-4C2-9 presented at the IEEE Power Engineering Society Meeting in Vancouver, Canada, July 1973.
3. **Denno, K.,** Steady State and Dynamic Modeling of an Integrated Power System, Proc. Can. Commun. and Power Conf., IEEE no. 74CH0894-6 REG. 7, Montreal, November 1974.
4. **Denno, K.,** Optimal Solution for the Transmission Loss Coefficients Matrix in a Multi-Area Pool System, Proc. of Control of Power Syst., IEEE no. 77CH1168-4 REG. 5, 1977, 124.
5. **Denno, K.,** Power system identification in the power flow reference frame, *J. of Appl. Sci. and Eng.* A, 2, 141, 1977.

6. **Denno, K.,** *Power System Design and Applications for Alternative Energy Sources*, Prentice-Hall, Englewood Cliffs, NJ, 1988.
7. **Kirchmayer, L. K.,** *Economic Operation of Power Systems*, John Wiley & Sons, NY, 1958.
8. **Mollo, C. R.,** The Feasibility of Fuel Cells in Modern Power System, M.Sc. thesis, Newark College of Engineering, 1973.
9. **Mollo, C., Yang, W. and Denno, K.,** Economic Optimization for an Integrated Power System, Midwest Power Symp. Proc., University of Missouri, Rolla, October 1974.
10. **Stagg, G. W., and El-Abiad, A. H.,** *Computer Methods in Power System Analysis*, McGraw-Hill, New York, 1968.
11. **Wood, A. J. and Wollenberg, B. F.,** *Power Generation, Operation and Control*, John Wiley & Sons, New York, 1984.
12. **Walsh, E. M.,** *Energy Conversion*, The Ronald Press Co., New York, 1967.
13. **Yang, W. K. L.,** The Feasibility of Fuel Cells in a Modern Power System, M.Sc. thesis, Newark College of Engineering, NJ, 1973.

Chapter 3

# THE ECONOMICS OF THE REDOX FLOW CELL ENERGY CONVERSION SYSTEM (RFEC)*

## I. EQUIVALENT CIRCUIT MODEL OF THE REDOX FLOW CELL ENERGY SYSTEM[33,34]

The redox flow cell as energy generator and storage device operates on the principle of oxidation-reduction in which the redox couple $Fe^{+3}/Fe^{+2}$; $Ti^{+3}/Ti^{+4}$ remain soluble in their electrolyte in either the oxidized or reduced state.

Previous research work carried out by this author[6,7] identified basic gyromagnetic characteristics, as well as a quantum parametric characterization for the ferromagnetic fluid flow in the catholyte continuum of the redox flow cell, which were needed as reliable information to design the proper mechanism for neutralizing the internal circulating currents and hence, extending their redox flow cell performance at all levels of loading and output voltage. Those previous results indicated clearly that at ferro-resonance, the catholyte gyromagnetic resistance, as well as the magnetic susceptibility became very large at which point the induced internal circulating currents almost disappeared. At ferro-resonance the loading specific magnetomotive force was established as well as peak values for the gyromagnetic energy, resistance, and magnetic susceptibility.

Further work[6-8] had been carried out centering on the state of magnetization and relaxation of the neutral particles for water based ferromagnetic fluid under pulsed application of an external magnetic field. The above-mentioned work identified theoretically and experimentally the pattern of alignment of particles which chain with a strong tendency, especially when influenced by a stationary magnetic field. Magnetization and subsequent relaxaton were attributed to particle alignment as well as moment rotation which are the two principal factors for the state of magnetization. Experimentally verified time constants have been confirmed to be of the order of 1 ms, depending on particle diameter, surfactant thickness, and concentration of particles.

Also magnetization of water based ferro-fluid was proved to be a direct function of particle diameter, thickness of surfactant, hydrodynamic mobility, fluid viscosity, and particle concentration.

This section presents another chapter of research efforts to enhance the operational performance aspects of the redox flow cell working fluid, namely to unfolding the basic parametric structure for its equivalent circuit in space and time domains.

Derivation of central criteria for the redox flow cell working fluid will proceed along the established proven facts; that magnetization and relaxation are generated by internal action on the fluid ionic state and external magnetization on the ferro-fluid neutral chain of particles.

Derivation of the basic parametric principles of the redox flow cell working ferro-fluid sets soundly the direct mechanism for total elimination of the induced circulating current at any load and voltage level, while the mathematical model defines the required spectrum for the steady state and transient performance as well as the stability limitations. The importance of the redox flow cell could be realized as a reliable electric generator and also as a device for bulk energy storage where it occupies a physical size of no more than 3% of a comparable hydroelectric plant of the same megawatt (MW) capacity.

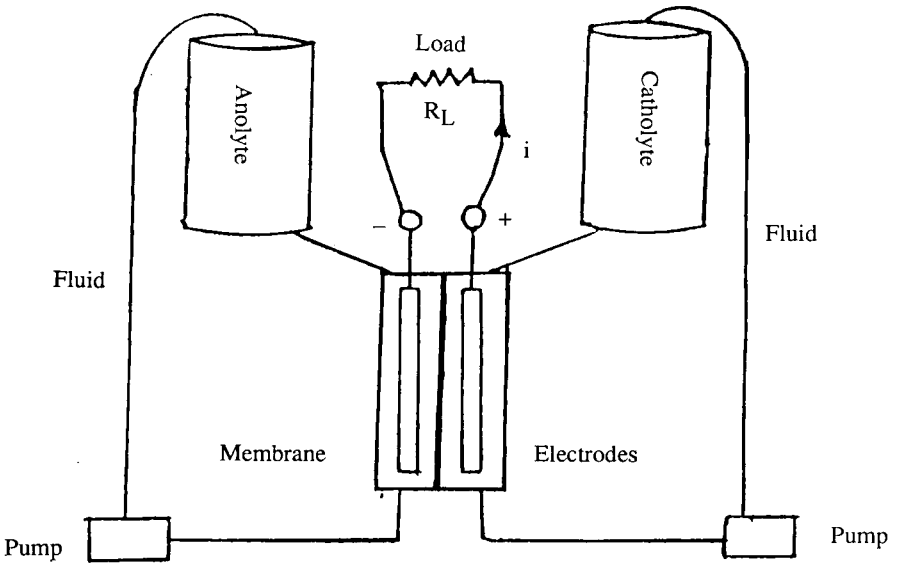


FIGURE 3.1 Two tank redox flow cell. (From Thaler, L., Electrically Rechargeable Redox Flow Cells, NASA-TM-X-71540, Lewis Research Center, Cleveland, OH, 1974. With permission.)

## II. THE REDOX FLOW CELL[33,34]

Refer to Figure 3.1 for a two tank model of the rechargeable redox flow cell for bulk energy storage. This device operates on the basis of an oxidation-reduction reaction where the ions of the redox couple remain soluble in their electrolyte in either oxidized or reduced states. The redox couple could be a titanium solution for the anolyte and ferro-fluid for the catholyte. On discharge the ferric-fluid $Fe^{+3}$ ions will be reduced to a ferrous solution ($Fe^{+2}$) and the $Ti^{+3}$ ions will be oxidized to $Ti^{+4}$ ions. The selective membrane could be a hydrogen ion ($H^+$) type or a chlorine ($C1^-$) type. The redox cell is electrically rechargeable by reversing the direction of flow of electric current. The working fluid in the catholyte chamber is always a water based ferromagnetic fluid during the processes of discharge and recharge, and ferro-particles are indeed in ionic as well as neutral states. Hence the catholyte working fluid during discharge and recharge will experience magnetization and relaxation with respect to the local stationary magnetic field produced by the discharge and recharge electric currents. It had been established in recent research efforts[33] that internally induced circulating current within the redox cell adversely affected the compatible output performance of this energy producing device. Also, it was shown by this author that one of the causing elements of the induced internal circulating currents inside the redox cell was due to the process of magnetic alignment and relaxation within the catholyte working fluid.

Previous published results[2,6,7] centered on the aspect of local and internal ionic-magnetic alignment of the ferro-fluid magnetic dipoles as a result of a nonzero value for the gyromagnetic factor of the ions, which is a ratio of magnetic moment to the angular momentum of the ferro-dipole.

Those results identified clearly the presence of a magneto-fluid interaction represented by the nonlinear pattern of gyromagnetic absorbed energy with respect to the local stationary magnetic field and the existence of Bloch wall energy distribution along the continuum of the moving ferro-fluid.

Other published results by this author[6-8] presented a magnetization pattern of a ferric solution under the influence of a sustained magnetic field which indicated that symmetrical magnetiza-

tion couples with relaxation around impulsive behavior at resonance. Also magnetic susceptibility presented an almost zero attitude with impulsive presence of ferro-resonance. The analysis in the above-mentioned published results were centered on the theory that magnetic dipolar ions interact with the sustained stationary magnetic field according to Debye-Langevin criterion, where the dipoles are assumed loose and freely rotating.

However, the author's approach of the above-mentioned analysis overlooked the effect of the external magnetization and relaxation influence on the ferro-fluid neutral particles and their clusters. Research work carried out by Bogardus et al.[3] identified clearly the magnetization and relaxation of ferro-fluids under a pulsed-applied stationary magnetic field. Their work pinpointed the fact that particle rotation as well as moment orientation contributed effectively to the process of magnetization and relaxation of ferro-fluids. However, serious differences emerged from that work with respect to a large gap between the theoretical and experimental values for the rotational time constant and the moment time constant of the particles that was rectified by the presentation of a specific relation between the particle hydrodynamic diameter and the surfactant thickness and particle chaining number as a parameter.

In the redox flow cell throughout the discharge and recharge processes, two modes of magnetization and relaxation are taking place:

1. Internal with respect to ferro-magnetic fluid ions such as $Fe^{+3}$ or $Fe^{+2}$.
2. External with respect to ferro-fluid particles and their chaining which includes particle rotation and moment orientation.

Theoretical and experimental work carried out by the author identified clearly various aspects of ferro-fluid magnetization of dipolar ions under a sustained-applied stationary magnetic field. This author now will present a simple review of the basic principles of paramagnetism and ferromagnetism and its application to the magnetization of dipolar ions and also a review of basic relationships for the phenomenon of particle rotation and moment orientation of water based ferro-fluid under an external magnetic field.

## III. REVIEW OF MAGNETIZATION OF WATER BASED FERRO-FLUID*

The following analysis was carried out and published by Bogardus et al.[3] Relevant parameters to the process of magnetization and relaxation of magnetites are

$\tau_n$ = Neél relaxation time constant, for particle moment/rotation.
$\tau_r$ = Particle rotation time constant.

Both $\tau_r$ and $\tau_n$ apply for a single particle and for a linear chain of particles.

### A. MOMENT ROTATION

Debye derivation for the dependence of noninteracting particle dipole moments under an external magnetic field led to a well known partial differential equation with variable coefficients. The form of the differential equation is referred to Reference 2 in which the following variable parameters have been represented:

1. Magnetic moment per unit volume.
2. Rotational mobility.

3. Normalized space variable.
4. External magnetic field applied.
5. Variable solid angle.
6. Concentration of dipoles per unit volume.
7. $M_s$ = saturation magnetization level.
8. $\gamma$ = rotational mobility.
9. V = volume of magnetite particles.

Magnetization is given by:

$$M(h,t) = MsVn \int_{-1}^{1} f \cos\theta \, d\Omega \tag{3.1}$$

From 3.1 in another form

$$\frac{dM}{dt} + \frac{2MTk}{\gamma} = \frac{nM_s^2V^2H}{\gamma} \int_{-1}^{1} \left(1 - x^2\right) f\left(x^2\right) dx \tag{3.2}$$

where M = magnetic moment/unit volume; k, T = Boltzman constant and absolute temperature, respectively; $\gamma$ = rotational mobility; x = normalized space variable along the principal axis of the ferro-fluid continuum; H = external magnetic field vector in a-t/m; and n = magnetite concentration/unit volume.

Equation 3.2 is based on a magnetizing pulse duration of normalized unit time.

## B. ROTATION OF CHAINS OF PARTICLES

Chains are assumed rigid and may be approximated by a prolated spheroid with an aspect ratio of B.

B = semiminor axis
A = semimajor axis

Brenner[2,3] has assumed *Sticking B.C.*, i.e., the fluid at the surface of the particle moves with the particle.

Hu of Zwanzig et al.[2] gave numerical results for *Slip B.C.*

But in view of the large size of the magnetite particles relative to the water molecules, the *Stick B.C.* are adopted.

There are two contributions for single domain magnetite particles:

1. Crystalline anisotropy

$$E = K_1V\left(B_1^2B_2^2 + B_2^2B_3^2 + B_3^2B_1^2\right) \tag{3.3}$$

B's are the direction cosines of the magnetic moment relative to the crystal axes.

2. Demagnetization effects for a single particle giving rise to an energy barrier

$$= \pi VM_S^2 (1\text{-}3n_a)/2$$

The eccentricity to be used is for the particle magnetite itself. For spherical magnetite $n_a = n_b = {}^1/_3$, and hence there is no demagnetization.

Now the question is, what configuration could give the observed relaxation? From there,

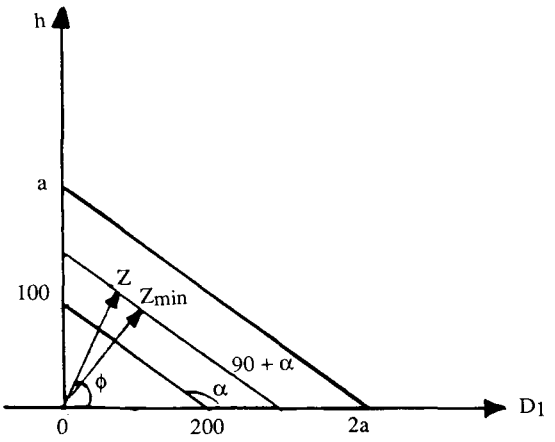


FIGURE 3.2 Locus of surfactant thickness with respect to magnetite diameter. (From Denno, K., Equivalent circuit parametric model requirements of the redox flow cell for bulk energy storage, *Alternative Energy Sources*, Vol. III, 1983, 417—432. With permission.)

Bogardus et al.[3] presented contour of relationships among particle diameters, surfactant thickness, and chain number of particles that would give $\tau_r$ the order of 1 ms.

## IV. MATHEMATICAL LOCI FOR $\tau_r$ AND $\tau_n$*

### A. LOCUS FOR $\tau_r$

According to Bogardus et al., slopes of $\tau_r$ contours are $-1/2$ including effects of viscosity with the magnetite particles as prolate spheroids.

In reference to Figure 3.2 where h = surfactant thickness and $D_1$ = particle diameter:

$$\begin{aligned} z &= |z|e^{j(\phi \pm \theta)} \\ h &= |z| \sin(\phi \pm \theta) \\ D_1 &= Z\cos(\phi \pm \theta) \end{aligned} \tag{3.4}$$

and

$$Z_{min} = Z_o e^{\pm j\alpha} \tag{3.5}$$

But

$$Z = D_1 + j\left(a - \frac{D_1}{2}\right) \tag{3.6}$$

where a = surfactant layer thickness for $D_1 = 0$ and $D_1$ = particle diameter.

* © 1978. Reprinted with permission from Bogardus, E. H., Krueger, D. A., and Thompson, D. A., Dynamic magnetization in ferrofluids, *J. Appl. Phys.*, 49, 3422—3429, 1978.

$$|z| = 5D_1^2 - aD_1 + a^2$$

$$\alpha = |z| \text{ min in the } hv_s D_1 \text{ plane.} \tag{3.7}$$

Then for local viscosity:

$$\tau_r = \gamma_1 (2kT)^{-1} \tag{3.8}$$

where

$$\gamma_1 = 2n_1 V_h \left(a^2 + b^2\right)\left(n_a A^2 + n_b B^2\right)^{-1} \tag{3.9}$$

where l = number of neutral particles in a chain and A,B = semimajor and semiminor axes of prolate spheroid.

$$\tau_r = 2n_1 \left(D_1 + 2h\right)^3 \left(A^2 + B^2\right) / \left(n_a A^2 + n_b B^2\right) \tag{3.10}$$

where $D_1$ and h are constrained by straight lines with a slope of $-1/2$.

**B. LOCUS OF $\tau_n$***

$$\tau_n = \frac{-1}{2}\left(1K_1 V\right) + \frac{1}{2} 1\pi V M_s^2 (1 - 3na) + 1V^2 M_s^2 D_2^3 k' \tag{3.11}$$

$$D_2 = D_1 + 2h \tag{3.12}$$

$$V = \frac{\pi}{6} D_1^2 \tag{3.13}$$

where $k_1$ is anisotropy constant.

Now referring to Figure 3.2 and considering l = 2 and A/B = 2 and 4, respectively, and approximating each nonlinear curve by a meanwise straight line:

$$l = 2, \; A / B = 1.0 \tag{3.14}$$

$$h = -0.6D_1 + 120 \tag{3.15}$$

and

$$l = 2, \; A / B = 1.0$$

$$h = 0.7D_1 + 140 \tag{3.16}$$

which gives an increase of –0.1 in slope as the spheroid aspect ratio increases from 1.0 to 1.10.

$$l = 4, \; A / B = 1.0$$

$$h = 1.075D_1 + 140 \tag{3.17}$$

* © 1978. Reprinted with permission from Bogardus, E. H., Krueger, D. A., and Thompson, D. A., Dynamic magnetization in ferrofluids, *J. Appl. Phys.*, 49, 3422—3429, 1978.

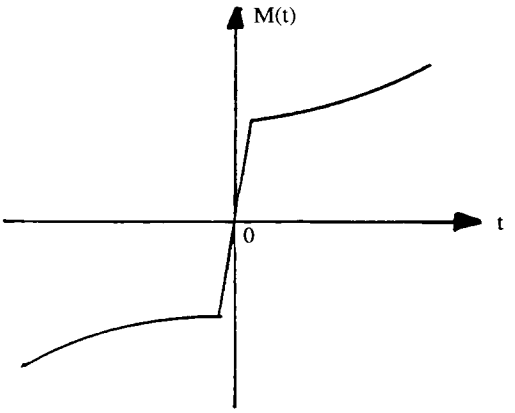


FIGURE 3.3 Time response for the state of magetization. (From Denno, K., Equivalent circuit parametric model requirements of the redox flow cell for bulk energy storage, *Alternative Energy Sources*, Vol. III, 1983, 417—432. With permission.)

and

$$l = 4,\ A / B = 1.10$$

$$h = 1.25D_1 + 160 \tag{3.18}$$

which gives an increase of –0.15 in slope as the spheroid aspect ratio increases from 1.0 to 1.10.

Another observation is that the slope of the mean straight line representation for $h\ v_s\ D_1$ for the same aspect ratio but with an increase of chain particles from 2 to 4 is of the order of –0.50.

Also with the approximation involved in the case of the aspect ratio, it can be concluded that the increase in slope is on the average of about –0.125 from the case of A/B = 1.0 to that of 1.10.

## V. SOLUTION OF THE DISTRIBUTION FUNCTION f(x)*

From the Equations 3.1 and 3.2 of magnetization given in References 2 and 3 and illustrated in Figures 3.3 and 3.4, we can write,

$$\int_{-1}^{1} \left(1 - x^2\right) f(x)dx = 0 \tag{3.19}$$

Therefore,

$$\left(1 - x^2\right) f(x) = 0$$

$$x = \pm 1$$

* © 1983. Reprinted with permission from Denno, K., Equivalent circuit parametric model requirements of the redox flow cell for bulk energy storage, *Alternative Energy Sources*, Vol. III, 1983, 417—432; © 1978. Reprinted with permission from Bogardus, E. H., Krueger, D. A., and Thompson, D. A., Dynamic magnetization in ferrofluids, *J. Appl. Phys.*, 49, 3422—3429, 1978.

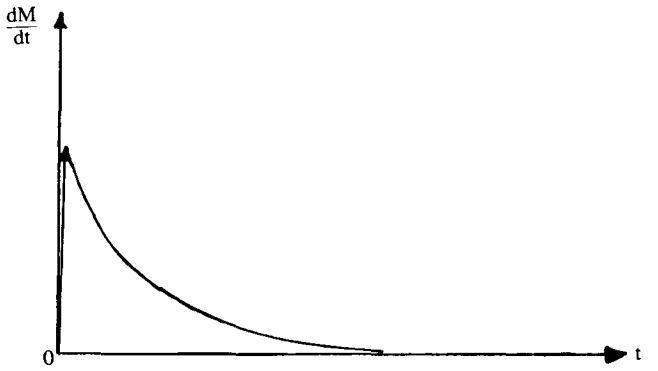


FIGURE 3.4 Time response for the rate of magetization. (From Denno, K., Equivalent circuit parametric model requirements of the redox flow cell for bulk energy storage, *Alternative Energy Sources*, Vol. III, 1983, 417—432. With permission.)

From Equation 3.19 we obtain

$$\frac{f'(x)}{f'''(x)} = \frac{3}{4}\left[\frac{3}{20} - \frac{x_3}{6} + \frac{x_5}{60}\right] \tag{3.20}$$

and

$$(6x+4)f''(x) + 2f'(x) = \left(1-x^2\right)f'''(x)f''(x) = \frac{11}{10} - x^2 - \frac{x^3}{9} + \frac{x^5}{90} / (4+6x) \tag{3.21}$$

Let

$$y(x) = f''(x)$$

$$y'(x) = f'''(x) \tag{3.22}$$

A solution for $y(x) = f''(x)$ is obtained with approximation on the basis that x is small

$$f''(x) = \int_{-1}^{1}\left[\frac{40x}{11} + \frac{30x^2}{11} + \frac{400x^3}{363} + \frac{2900x^4}{1178} \cdots\right]dx \tag{3.23}$$

To obtain reliable solution for $f'(x)$, a plot has been established first and shown in Figure 3.5 which shows a curved and slowly ascending slope for $0 < x < 1$ and the graph accelerates steeply as x increases to the terminal limit of $\pm 1$. Therefore, from Figure 3.5 three distinct subfunctions are obtained.

$$f_1''(x) = 194x^3 \quad \text{for} \quad 0 < x < \frac{1}{2} \tag{3.24}$$

$$f_2''(x) = 244 + 552x \quad \text{for} \quad \frac{1}{2} < x < \frac{3}{4} \tag{3.25}$$

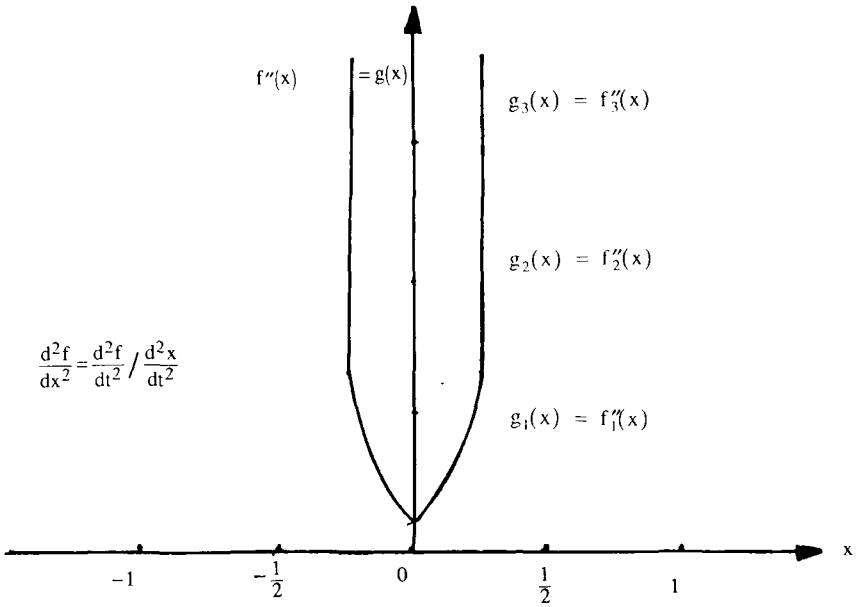


FIGURE 3.5 Second differential for magnetites distribution fraction. (From Denno, K., Equivalent circuit parametric model requirements of the redox flow cell for bulk energy storage, *Alternative Energy Sources*, Vol. III, 1983, 417—432. With permission.)

and

$$f_3''(x) = 19222 + 2585x \qquad \text{for } \frac{3}{4} < x < 1 \tag{3.26}$$

$$f_1''(x) = 9.7x^5 \qquad \text{for } 0 < x < \frac{1}{2} \tag{3.27}$$

$$f_2''(x) = 9611x^2 + \frac{12928}{3}x^3 \qquad \text{for } \frac{1}{2} < x < \frac{3}{4} \tag{3.28}$$

and

$$f_3''(x) = 122x^2 + 92x^3 \qquad \text{for } \frac{3}{4} < x < 1 \tag{3.29}$$

And hence the approximate solution for f″(x) and f(x) in the spatial duration of $-1 < x < 1$ are given by Equation 3.30 and Figure 3.5.

$$f''(x) = \left(9.7x^5\right) + \left(-9611x^2 + \frac{12928}{3}x^3\right) + \left(-122x^2 + 92x^3\right) \tag{3.30}$$

The plot of f(x) is shown in Figure 3.6.

## VI. DISCUSSION

The subject matter presented in the last six sections is the phenomenon of magnetization and

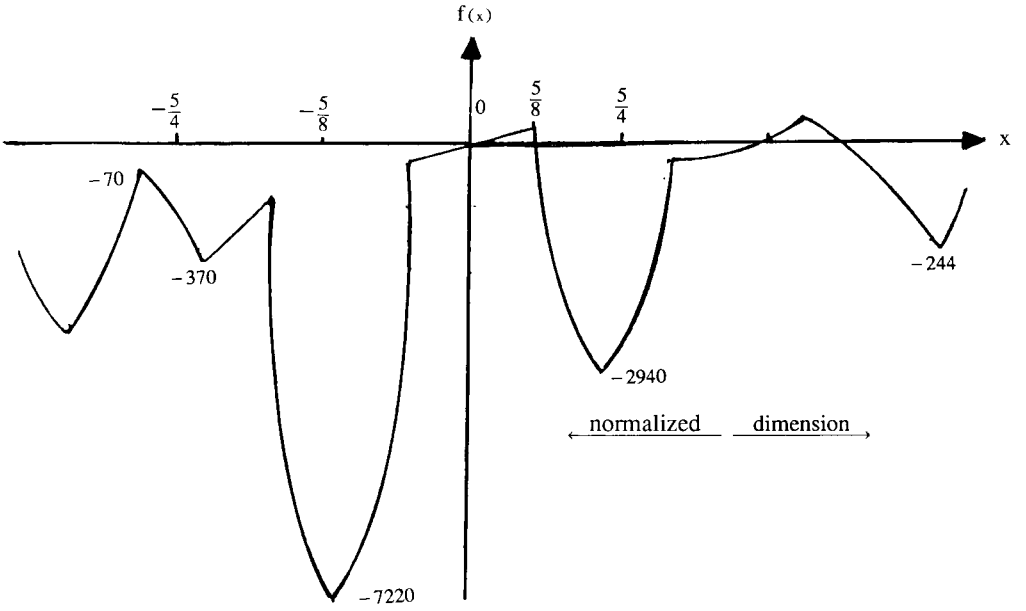


FIGURE 3.6. Magnetites distribution function. (From Denno, K., Equivalent circuit parametric model requirements of the redox flow cell for bulk energy storage, *Alternative Energy Sources*, Vol. III, 1983, 417—432. With permission.)

subsequent relaxation of water-based ferromagnetic fluids at ambient temperature such as ferric and ferrous solutions in the catholyte of the redox flow cell. The continuum in the catholyte channel is either Fe $C1_3$ and Fe $C1_2$ in the neutral state and then in an ionic state during the processes of discharge and recharge. In order to establish a true and total representation of the redox cell equivalent circuit, full and reliable information about every reaction occurring in this energy device has to be revealed and studied carefully. It had been found experimentally that various aspects of the redox cell performance especially the weight-cost factor and the number of interconnected modules, as well as efficiency, respond in an adverse pattern as the cell terminal voltage increases. From previously published work[33,34] I established that internally induced circulating currents within the cell catholyte channel is one of several causes which contribute to the catholyte internal currents.

Hence various aspects of magneto-fluid interactions ought to be looked upon to determine their contribution to the state of induction of circulating currents within the catholyte channel.

Since the catholyte fluid could be a mixture of neutral ferromagnetic particles, clustered particles, as well as ferric or ferrous ions, two states of magnetization and relaxation will most likely take place inside the ferro-fluid continuum.

The two processes are

1. Magnetic alignment of ferro-fluid ionic dipoles whose outer shell of electrons are unfilled and have nonzero gyromagnetic factor. Those ions of course could be singles or clusters. As a result of the load current during discharge and its own magnetic field, an energy will be expended to align the ferro-fluid dipoles along the field direction. Comprehensive analysis of this phenomenon including the pattern of behavior of the expended gyromagnetic power and resistance, the state of magnetization and magnetic susceptibility, and the occurrence of ferro-resonance has been investigated in depth by this author in a previously published work.[8]
2. Magnetization and relaxation for the single ferro-fluid particles and the cluster of particles under the influence of the discharge and recharge electric current generated a magnetic

field. Work published by Bogardus et al.[3] indicated that particle rotation has a dominant role and that moments orientation, to a lesser extent, are the magneto-fluid interaction tools of magnetization and subsequent relaxation, and that in effect advances through a fast component followed by a slow component. Also their work pointed out that a rotational time constant of the order of 1 ms is attributed to a specific relationship between the surfactant layer thickness and the particle diameter with an implicit function dependence on local viscosity.

## VII. REDOX FLOW CELLS, CONVENTIONAL FUEL CELLS, AND STORAGE BATTERIES AS OPTIMAL POWER SOURCES FOR BUILDINGS*

Application of new modes of direct energy conversion systems in supplying total power demands by residential, commercial, and industrial buildings point to clearly feasible compatibility. Direct energy subsystems for buildings could include conventional storage batteries, conventional hydrogen fuel cells, and the redox flow cells for energy supply and storage. Any individual or interconnected direct energy system could be realized in either dispersed form, central form, or their combination and could be placed in a hybrid connected pattern with the present traditional electromechanical system. Furthermore, in order to supply the required AC power for load from the buildings, a solid state power inverter of a suitable mode of commutation followed with a proper harmonics filter must be linked at the terminals of the direct energy generation and storing system.

The following few sections present analytical work for testing the optimal compatibility for a reliance on fuel cells, conventional storage batteries, and the redox flow cells in separate or interconnected forms for meeting the total power demand (23,000) by a large number (totaling 125) of dispersed isolated systems of load centers. Each load center is considered a direct simulation of one building complex or a cluster of complexes and is characterized with varying megawatt loading, terminal voltage levels, as well as phase angles. The analytical work involved in carrying out load flow calculations at different distinct loading levels, as well as the optimal forms of the linking loss coefficient matrices, helped to establish the optimal design matrices of the entire system in the power flow reference frame. The main conclusions secured from the design matrix are that the dispersed system of load centers is the most optimum pattern to be supplied from hydrogen fuel cells throughout base loading, conventional storage batteries at peak loading, while the redox flow cells supply power at base as well as peaking loading. Also during the off-peak load period, the redox flow cells with the conventional batteries will be recharged for energy storage.

Also, based on the internal and external performance constraints for the fuel cells interconnected to the storage batteries, and then coupled to their appropriate power inverter which is the auxiliary impulse commutation type, another conclusion established was the optimal level of the output DC voltage, which may reach up to 2 kV, while in the case of the redox flow cells it should be around 200 V, requiring the utilization of two distinct diverse levels of voltage stepping up transformation ratios, in case the need arises.

In summary, electric power supply to a large building complex, cluster of buildings, or a system of clusters could be accomplished by a dispersed system of on-site substations of fuel cells, redox flow cells, and storage batteries coupled to the appropriate type of power inverter.

Consequently, the following problem will be addressed. Given the physical structure of dispersed load centers simulating large clusters of commercial, industrial, and residential building complexes, required is presentation of a comprehensive feasibility study for the actual

determination of optimum and compatible energy supply systems containing conventional sources, hydrogen fuel cells, redox flow cells, and storage batteries coupled to the appropriate power inverters.

## VIII. THE PROPOSED ENERGY SYSTEM SPECTRUM[1-4]*

A group of alternative plans of interconnected power systems are listed below, each plan reflects a power network containing more than 120 buses and 250 branches.

**Plan A** — Totally conventional central power system, consisting of fossil fueled, nuclear, gas-turbine, and pumped-hydro, generators in order to meet the present and substantial future load expansion.

**Plan B** — A central system in which the future expansion will be met only with nuclear and fuel cell generating buses. Therefore, this system is comprised of fossil conventional, gas-turbine, pumped-hydro, nuclear, and fuel cell generating buses. An alternative to conventional hydrogen fuel cells, the redox flow cells as supply and storage energy sources will be considered in this power system plan.

**Plan C** — A central system where conventional storage batteries will supply peak loading by substituting for gas turbines and hydrogen fuel cells and for base loading by substituting for fossil-steam generators. Also an alternative in this plan involves the utilization of redox flow cells for supplying base as well as peak loads.

**Plan D** — This is a hybrid system involving the combination of a central conventional energy system interconnected to large dispersed load centers. The dispersed load centers simulating building complexes will be supplied by on site individual hydrogen fuel cells or redox flow cells coupled to power inverters of appropriate commutation.

## IX. LOAD FLOW CALCULATIONS AND OPTIMUM SCHEDULING OF GENERATION*

Load flow calculations using the Newton-Raphson method based on nonlinear equations for expressing the specified real and reactive powers in terms of bus voltages have been carried out by a computer program on the IBM 360 computer, for base, peak, and off peak, loadings.

Load flow calculations were carried out for centralized interconnected power systems as well as dispersed systems, and included in addition to usual results, bus voltage magnitude, phase angle, real and reactive powers, and total net transmission losses.

Load flow calculations were followed by obtaining optimum scheduling of generation for each of Plan A through D of the proposed power system spectrum. The optimum scheduling of generation used the usual criterion of coordination between incremental fuel cost and the cost of received power. However, the new element in the scheduling process was the presence of fuel cells as well as storage batteries and redox flow cells among conventional fossil generators, nuclear, gas-turbine and pumped hydro-generating buses. For the fuel cells, the incremental fuel cost is assumed constant up to its maximum range and with specified thermal conversion efficiency. (Incremental fuel cost is assumed to be $1.80 per MBtu, and with thermal conversion efficiency of 8500 Btu/kWh).

As for the storage battery, the cost of charging is assumed to be equal to the incremental fuel cost of fossil generators during the off-peak period and multiplied by a factor of 1.25 to account for the battery efficiency.

However, the incremental cost of the redox flow cells including initial, as well as maintenance and operation costs, is not compatible with that of hydrogen fuel cells and batteries.

* © 1980. Reprinted with permission from Denno, K., Redox flow cells, conventional fuel cells, and storage batteries as optimal power sources for buildings, *IASTED J. Energy Syst.*, 2(2), 109—113, 1980.

**TABLE 3.1**
**Redox Flow Cell-Power Inverter**
**Efficiency-Normalized Weight-Cost Factor With**
**Respect to an Output Voltage of 375 V**

| V | Efficiency | Weight-cost | K |
|---|---|---|---|
| 400 | 1 | .06 | 0.60 |
| 350 | .98 | .105 | 1.03 |
| 300 | .98 | .11 | 1.078 |
| 250 | .97 | .12 | 1.164 |
| 200 | .96 | .14 | 1.344 |
| 150 | .92 | .18 | 1.656 |
| 100 | .86 | .26 | 2.236 |
| 50 | .64 | .50 | 3.20 |
| 25 | 0 | 1 | 0 |

*Note:* Where K is the combined factor for efficiency and weight-cost.

Present information in the literature indicates that a normalized weight-cost factor as well as the efficiency of the redox cell coupled to a solid state auxiliary impulse commutated inverter are implicit functions of the redox cell DC output voltage as shown in Table 3.1.

## X. ECONOMIC EVALUATION OF ENERGY SYSTEMS*

### A. FUEL CONSUMPTION COST

1. The optimum scheduling of generation for each plan of power systems proposed in the spectrum from A through D established (assuming total copper loss in the interconnecting network to be zero) based on information from load flow calculations.
2. Step 1 is followed by calculating and plotting the difference in fuel input in dollars per hour vs. total generation for each power system plan from A through D.
3. Step 2 is followed by establishing the savings or loss in dollars per hour vs. total received power for each power system in the spectrum with respect to plan A as a reference system. Plan A is that of a totally conventional system for present and future load expansion.
4. Step 3 is followed by establishing for each power system plan, using the data from a load duration curve, the fuel input savings or loss in dollars per hour vs. total hours across the year. The total net area under each curve indicates the total annual dollars of savings or loss incurred in each alternative plan in the centralized and central-dispersed systems with respect to plan A. These are shown in Figures 3.7, 3.8, and 3.9.

### B. INSTALLATION AND MAINTENANCE COST

Table 3.2 gives the fixed generation and transmission costs for each type of generation together with cost escalation factor, excluding the redox cell which is included in Table 3.1.

Table 3.3 gives information concerning fixed and variable operation and maintenance costs for various types of generation and their life times. For each type of generation there is the installation cost in dollars per kilowatt and annual cost. The installation cost for each type of generation varies for each year to account for a 5% escalation cost. The annual cost is calculated

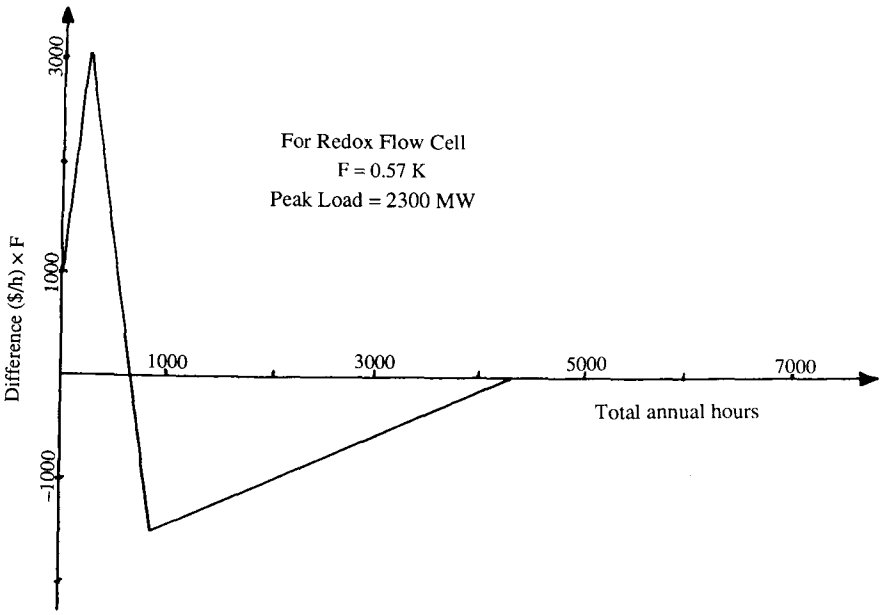


FIGURE 3.7 Annual saving curve. (From Denno, K., Redox flow cells, conventional fuel cells, and storage batteries as optimal power sources for buildings, *IASTED J. Energy Syst.*, 2(2), 109—113, 1980. With permission.)

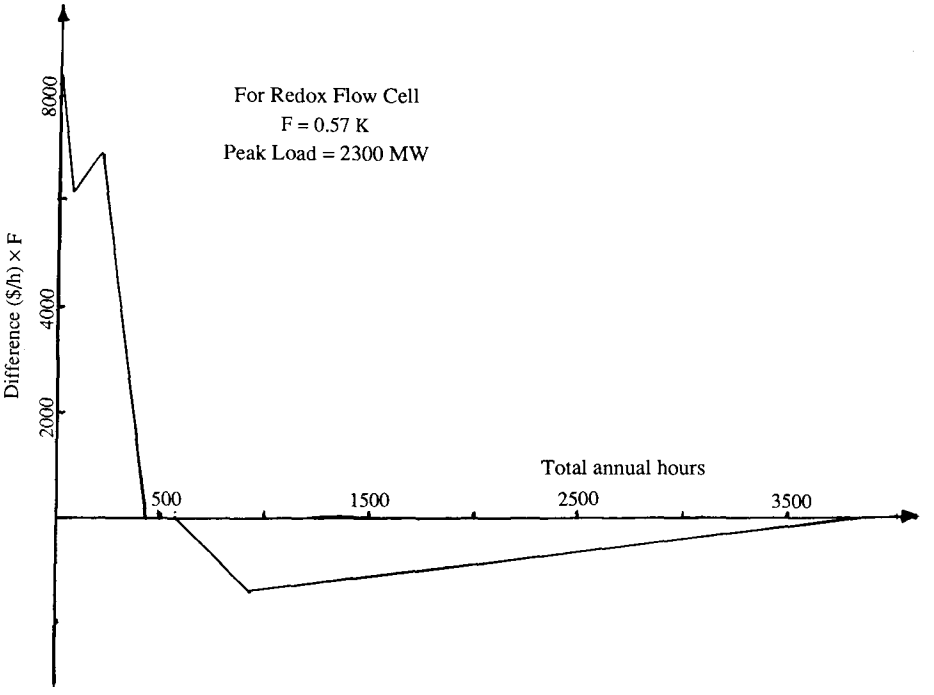


FIGURE 3.8 Annual saving curve. (From Denno, K., Redox flow cells, conventional fuel cells, and storage batteries as optimal power sources for buildings, *IASTED J. Energy Syst.*, 2(2), 109—113, 1980. With permission.)

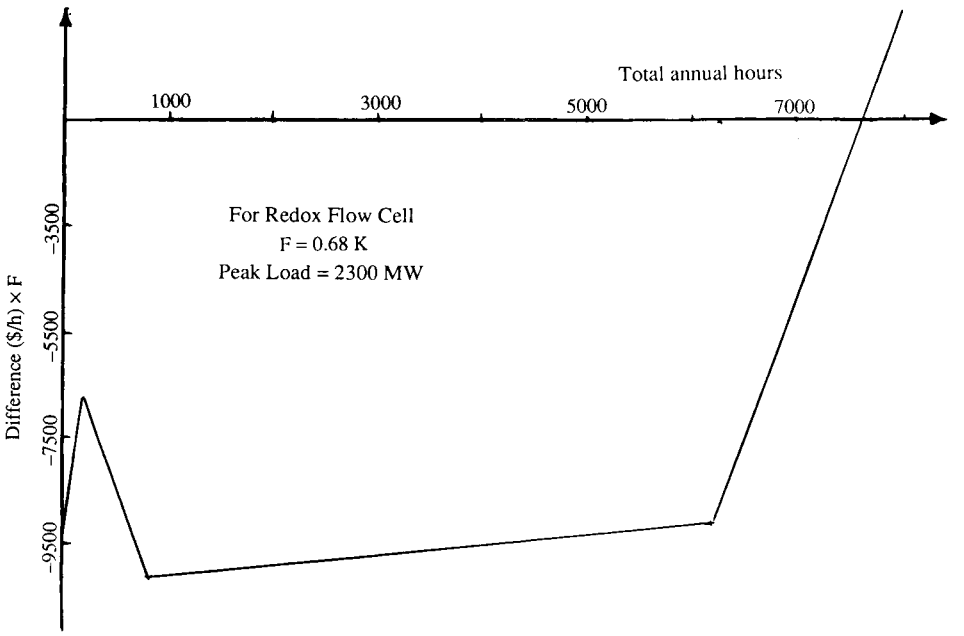


FIGURE 3.9 Annual saving curve. (From Denno, K., Redox flow cells, conventional fuel cells, and storage batteries as optimal power sources for buildings, *IASTED J. Energy Syst.*, 2(2), 109—113, 1980. With permission.)

**TABLE 3.2**
**Tentative Initial Cost in Dollars**

| | **Cost ($ × 1.5)** |
|---|---|
| Type of generation | 1/kW |
| Steam-fossil | 180—200 |
| Gas turbine | 100 |
| Nuclear | 250—330 |
| Fuel-cells (1/2 MW) | 300 |
| (2 MW) | 250 |
| (5—500) MW | 175 |
| Storage batteries | |
| (1/2 MW) | 300 |
| (2 MW) | 250 |
| (5—500) MW | 200 |

by multiplying the megawatt capacity of a particular generator and the installation cost by a capital recovery factor.

Total annual cost, which is a combination of initial cost plus that due to operation and maintenance, has been calculated for each plan, from which the total cost of plan A is subtracted, giving the annual savings or loss for each plan. Such calculations were carried out for Plans B to D, and shown in Figures 3.7, 3.8, and 3.9.

**TABLE 3.3**
**Operation and Maintenance (O&M) Costs**

| Generation | Life (years) | Fixed 0&M ($/kW/year) | Variable 0&M (mills/kWh) |
|---|---|---|---|
| Nuclear | 35 | 1.0 | 0.1 |
| Steam-fossil | 45 | 2.0 | 0.3 |
| Gas turbine | 30 | — | 2.0 |
| Fuel-cells | 20 | — | 1.5 |
| Batteries | 20 | — | 1.0 |
| Redox cells | 40 (total modification factor K is stated in Table 3.1) | | |

*Note:* Annual cost = (capacity) (cost) $(CR)_n$, where $(CR)_n$ is a capital recovery factor accounting for the lifetime years (n) and percent interest (i). This factor converts total initial cost into an equivalent annual cost spread over the generator life time.

## XI. ENERGY SYSTEM DESIGN*

Calculations for the optimum transmission loss coefficient matrices [B] were carried out for each energy system alternative in addition to load flow data obtained earlier. Design of any energy systems that were in the sixth or power flow reference frame can be expressed in terms of elements of the symmetric resistance matrix as written as follows:

$$[R] = [K][B]^{-1}$$

where [R] is the symmetric resistance matrix, [B] is the optimum transmission loss coefficients matrix, and [K] is a matrix function of load flow parameters.

Computer calculations on the IBM 360 computer have been carried out to secure the [R] matrix for system alternatives B, C, and D as expressed in Tables 3.4, 3.5, and 3.6.

## XII. MODELING OF THE REDOX FLOW CELL, FUEL CELL, STORAGE BATTERY, AND HARMONICALLY COMMUTATED INVERTER**

In the quest to adequately meet the accelerating demand for electric energy which is coupled to the problems associated with increasing cost and decreasing availability of conventional fuels, new modes of power generating and storing systems are being proposed. These systems include, among others, the electrically rechargeable redox flow cell, the fuel cell, and a new mode of the conventional storage battery, all coupled to a solid state inverter to deliver an output AC power at the conventional power frequency.

Problems encountered in bringing the redox power system to the operational levels include major reduction in the circulating internal currents, optimizing the generated electric power output density and perfecting the selectivity of the ionic exchange membrane.

Conventional fuel cells operate on the principle of an electrochemical reaction between $H_2$ and $O_2$ to produce DC power and fluidic byproducts. Fuel cells and storage batteries are expected

* © 1980. Reprinted with permission from Denno, K., Redox flow cells, conventional fuel cells, and storage batteries as optimal power sources for buildings, *IASTED J. Energy Syst.*, 2(2), 109—113, 1980.

** © 1976, IEEE. Reprinted with permission from Denno, K., Modeling of Redox Flow Cell, Fuel Cell, Storage Battery and Harmonically Commutated Inverter, Proc. Can. Commun. Power Conf., 1976, 403—406.

## TABLE 3.4
## Design for the Self-Symmetric Resistance Matrix for Plan B

Fuel Cells or Redox Flow Cells and Conventional Generators

| No. of bus-bar | Loading 60% | 80% | 100% | K[a] |
|---|---|---|---|---|
| 1 | 32.521 | 24.7193 | 18.8668 | 1 |
| 2 | 1190.2486 | 445.6685 | 302.8404 | 0.10 |
| 3 | –476.03 | –372.3141 | –332.6847 | 0.10 |
| 4 | 21.782339 | 34.9645 | 17.74218 | 0.10 |
| 5 | 14.2156 | 22.1106 | 9.80276 | 0.10 |
| 6 | 7.5734 | –25.0701 | 33.9532 | 0.10 |
| 7 | 234.3997 | 24.936 | 15.37 | 0.10 |
| 8 | –60.1107 | –12.371 | –0.7946 | 0.10 |
| 9 | –30.1148 | –6.1981 | –0.384 | 0.10 |
| 10 | –390.9161 | –272.4651 | –234.1436 | 0.10 |
| 11 | 4939.433 | –3417.874 | –2629.9373 | 0.10 |
| 12 | 22.7219 | 1.4519 | 12.9272 | 0.10 |
| 13 | 94.80 | 4.575 | –16.87124 | 0.10 |
| 14 | 170.3366 | 9.8782 | 7.73293 | 0.10 |
| 15 | –352.3437 | –222.4387 | –178.2961 | 0.10 |
| 16 | 29.9415 | 8.0748 | –3.8847 | 0.10 |
| 17 | 4981.66 | 1648.9843 | 1300.5437 | 0.10 |
| 18 | –22.7541 | 0 | 0 | 0.10 |
| 19 | –46.47 | –25.13 | –44.42 | 0.10 |
| 20 | –149.2743 | –116.2613 | 0.3675 | 0.10 |
| 21 | 13.8331 | 36.26 | 0.3436 | 0.10 |
| 22 | 19.9315 | 0.4387 | 0.1352 | 0.10 |
| 23 | 3158.604 | 2550.008 | 2081.929 | 0.10 |
| 24 | –79.232 | –53.1275 | 0 | 0.10 |
| 25 | 26.9076 | 72.52 | 26.0277 | 0.10 |
| 26 | 13.8331 | 5.0041 | 29.512 | 0.10 |
| 27 | 5.5114 | 13.9463 | 0.625 | 0.10 |
| 28 | 52.3777 | 3.58 | 13.7472 | 1 |
| 29 | 0.6587 | 2.0909 | 1.9415 | 1 |
| 30 | 17.223 | 0 | 0 | 0.1 |
| 31 | 93.3157 | 103.689 | 0 | 0.1 |
| 32 | –4170.3 | 9945.92 | –7956.7357 | 0.1 |

*Note:* All values listed are $10^6$ times greater than their true per unit value.

[a] K is the cost multiplying factor.

From Denno, K., Modeling of Redox Flow Cell, Fuel Cell, Storage Battery and Harmonically Commutated Inverter, Proc. Can. Commun. Power Conf., IEEE, 1976, 403—406. With permission.

to meet base loading, peaking, and storage power due to an occasional random increase in energy demand.

The following few sections address the feasibility of integrating the redox flow cell, the conventional fuel cell, and the storage battery within the present traditional power system. For the redox flow cell, theoretical as well as experimental work has been done to identify the causes of its internal circulating current, the cell internal gyromagnetic resistance, and the phenomenon of gyromagnetic resonance, all leading to the establishment of a circuit parameter model and a dynamic model of the redox cell.

**TABLE 3.5**
**Design for the Self-Symmetric Resistance Matrix for Plan C**

Fuel Cell and Storage Batteries, or Redox Flow Cells and Conventional Generators

| No. of bus-bars | Loading 60% | 80% | 100% | K[a] |
|---|---|---|---|---|
| 1 | 31.8731 | 24.71936 | 18.4488 | 1 |
| 2 | 1170.56 | 445.6685 | 293.3113 | 0.1 |
| 3 | 535.648 | –372.3141 | –377.3772 | 0.1 |
| 4 | 21.3482 | 34.9645 | 17.3491 | 0.1 |
| 5 | 139.3235 | 22.1106 | 9.5655 | 0.1 |
| 6 | –12.8715 | –25.0701 | –38.6976 | 0.1 |
| 7 | 219 | 24.936 | 11.4897 | 0.1 |
| 8 | –106.4709 | –6.1981 | –1.5967 | 0.1 |
| 9 | –30.115 | –6.200 | –0.3842 | 0.1 |
| 10 | –449.7249 | –272.4651 | –275.5583 | 0.1 |
| 11 | –5435.51 | –3417.8744 | 3960.1051 | 0.1 |
| 12 | 19.8254 | 1.4519 | –15.9932 | 0.1 |
| 13 | 83.0376 | 4.575 | 20.992 | 0.1 |
| 14 | 163.181 | 9.8782 | 6.635 | 0.1 |
| 15 | 416.101 | –222.438 | –222.2917 | 0.1 |
| 16 | 27.5177 | 8.0748 | –5.5196 | 0.1 |
| 17 | –5383.86 | –1648.9843 | –1429.1694 | 0.1 |
| 18 | –39.6568 | 0 | 0 | 0.1 |
| 19 | 356.0904 | 24.31865 | –16.0986 | 0.1 |
| 20 | 613.0521 | 490.1892 | 90.2662 | 0.1 |
| 21 | –21.441 | 36.2606 | .4387 | 0.1 |
| 22 | –30.8945 | 3.508798 | 1845.6969 | 0.1 |
| 23 | 2916.68 | 1056.7547 | 0 | 0.1 |
| 24 | –143.160 | –53.1275 | 0 | 0.1 |
| 25 | 1277.77 | 1056.7547 | 370.867 | |
| 26 | 656.9037 | 592.0714 | 420.5151 | 0.1 |
| 27 | 702.1129 | 363.4106 | 3.5262 | |
| 28 | 51.3337 | 3.5802 | 13.4426 | 1 |
| 29 | 0.6455 | 2.0909 | 1.8984 | 1 |
| 30 | 26.696 | 0 | 0 | 0.1 |
| 31 | –144.6421 | 103.689 | 0 | 0.1 |
| 32 | 31562.518 | 84507.167 | 66106.438 | 0.1 |

*Note*: All values listed are $10^6$ times greater than their true per unit value.

[a] K is the cost multiplying factor.

From Denno, K., Modeling of Redox Flow Cell, Fuel Cell, Storage Battery and Harmonically Commutated Inverter, Proc. Can. Commun. Power Conf., IEEE, 1976, 403—406. With permission.

Lumped parametric representation for the fuel cell has been established on the basis of a complete electrochemical reaction and the existence of the reactivity and invariance characteristics. A dynamic model has been developed for the fuel cell with the aid of irreversibility as a reality for the electrochemical generator.

Modeling for the storage battery is developed on the principles of the charged carrier transport theory in a conducting medium followed by the transform of stored electrochemical energy. This analytical work is culminated with the development of a dynamic model for a harmonically commutated inverter, for delivery of an AC output.

## TABLE 3.6
## Design for the Self-Symmetric Resistance Matrix for the Centralized-Dispersed Case

Fuel Cells, Storage Batteries, or Redox Flow Cells and Conventional Generators

| No. of bus-bars | Loading | | | K[a] |
|---|---|---|---|---|
| | 60% | 80% | 100% | |
| 1 | 232.7405 | 50.0874 | 28.296 | 0.1 |
| 2 | 0 | 0 | 0 | 0.1 |
| 3 | 0 | 0 | 0 | 0.1 |
| 4 | 0 | 0 | 0 | 0.1 |
| 5 | 0 | 0 | 0 | 0.1 |
| 6 | 0 | 0 | 0 | 0.1 |
| 7 | 199.7291 | 71.6012 | 60.5789 | 0.1 |
| 8 | 27.2476 | 21.6802 | 33.69004 | 0.1 |
| 9 | 0 | 0 | 0 | 0.1 |
| 10 | 0 | –222.6271 | 0 | 0.1 |
| 11 | 0 | 0 | 0 | 0.1 |
| 12 | 70.3657 | 120.1663 | 88.057 | 0.075 |
| 13 | 0 | 0 | 0 | 0.1 |
| 14 | 0 | 0 | 0 | 0.1 |
| 15 | 0 | 0 | 0 | 0.1 |
| 16 | 0 | 0 | 0 | 0.1 |
| 17 | 9.2792 | 13.78256 | 3.576 | 0.075 |
| 18 | 24.7215 | 0.154 | –0.6737 | 0.075 |
| 19 | 0 | 0 | 0 | 0.10 |
| 20 | 0 | 0 | 0 | 0.10 |
| 21 | 0 | 0 | 0 | 0.10 |
| 22 | 0 | 0 | 0 | 0.10 |
| 23 | 0 | 0 | 0 | 0.10 |
| 24 | 0 | 0 | 0 | 0.10 |
| 25 | 0 | 0 | 0 | 0.10 |
| 26 | 0 | 0 | 0 | 0.10 |
| 27 | 0 | 0 | 0 | 0.10 |
| 28 | 0 | 0 | 0 | 0.10 |
| 29 | 0 | 0 | 0 | 0.10 |
| 30 | 0 | 0 | 0 | 0.10 |
| 31 | 0 | 0 | 0 | 0.10 |
| 32 | 0 | 0 | 0 | 0.10 |
| 33 | 0 | 0 | 0 | 0.10 |
| 34 | 0 | 0 | 0 | 0.10 |
| 35 | 0 | 0 | 0 | 0.10 |
| 36 | 0 | 0 | 0 | 0.10 |
| 37 | 0 | 0 | 0 | 0.10 |
| 38 | 11.1651 | 4.4923 | 17.8185 | 0.10 |
| 39 | 0 | 0 | 0 | 0.10 |
| 40 | 0 | 0 | 0 | 0.10 |
| 41 | 0 | 0 | 0 | 0.10 |
| 42 | 0 | 0 | 0 | 0.10 |
| 43 | 0 | 0 | 0 | 0.10 |
| 44 | 14.3162 | 0.6222 | –1.36074 | 0.075 |
| 45 | | | | |
| 46 | 0 | 0 | 0 | 0.10 |
| 47 | 0 | 0 | 0 | 0.10 |
| 48 | 0 | 0.4195 | 1.927 | 1 |
| 49 | 0 | 0 | 0 | 1 |

**TABLE 3.6 (continued)**
**Design for the Self-Symmetric Resistance Matrix for the Centralized-Dispersed Case**

Fuel Cells, Storage Batteries, or Redox Flow Cells and Conventional Generators

| No. of bus-bars | Loading | | | K[a] |
|---|---|---|---|---|
| | 60% | 80% | 100% | |
| 50 | 0 | 0 | 0 | 1 |
| 51 | 0 | 0 | 0 | 0.10 |
| 52 | 0 | 0 | 0 | 1 |
| 53 | 0 | 0 | 0 | 1 |
| 54 | 0 | 0 | 95.9768 | |
| 55 | 0 | 0 | 0 | 0.10 |
| 56 | –69.41225 | –51.9564 | 0 | 1 |
| 57 | –34.8433 | –2.6081 | 0 | 1 |
| 58 | 0 | 0 | 0 | 0.075 |
| 59 | 5.7243 | 0 | 0 | 0.075 |
| 60 | –406.2994 | –326.518 | –223.6036 | 0.10 |
| 61 | 0 | 0 | 0 | 0.10 |
| 62 | 49.7521 | 0 | 0 | 0.10 |
| 63 | 0 | 0 | 0 | 1 |
| 64 | 0 | 0 | 0 | 0.10 |
| 65 | 22.2 | –0.6725 | –4.7944 | 1 |
| 66 | 0 | 0 | 0 | 0.10 |
| 67 | 5.9322 | 1.4737 | 2.1394 | 1 |
| 68 | 0 | 0 | 0 | 0.10 |
| 69 | 0 | 0 | 519.8188 | 0.10 |
| 70 | 0 | 0 | 0 | 0.10 |
| 71 | 0 | 0 | 0 | 0.10 |
| 72 | 0 | 0 | 0 | 0.10 |
| 73 | 2.4494 | –7.2435 | –18.4476 | 0.075 |
| 74 | 0 | 67.8684 | 253.1313 | 0.10 |
| 75 | 0 | 0 | 0 | 0.10 |
| 76 | 0 | 0 | 0 | 0.075 |
| 77 | 0 | 0 | 0 | 0.10 |
| 78 | 0 | 0 | 0 | 1 |
| 79 | 25.7709 | 0.7 | 0.5987 | 1 |
| 80 | –364.7648 | –277.2269 | 0 | 1 |
| 81 | 0 | 0 | 0 | 0.10 |
| 82 | 0 | 0 | 0 | 0.10 |
| 83 | 0 | 0 | 0 | 0.10 |
| 84 | 0 | 0 | 0 | 0.10 |
| 85 | 0 | 0 | 0 | 0.10 |
| 86 | 0 | 0 | 0 | 0.10 |
| 87 | 0 | 0 | 0 | 0.10 |
| 88 | 0 | 0 | 0 | 0.10 |
| 89 | 11.4417 | –0.6336 | –4.5613 | 0.075 |
| 90 | 0.9876 | 0.3233 | 0.0347 | 1.0 |
| 91 | 0 | 0 | 0 | 0.1 |
| 92 | 0 | 0 | 0 | 0.1 |
| 93 | 0 | 0 | 0 | 0.1 |
| 94 | 0 | 0 | 0 | 0.1 |
| 95 | 0 | 0 | 0 | 0.1 |
| 96 | 0 | 0 | 0 | 0.1 |
| 97 | 0 | 0 | 0 | 0.1 |
| 98 | 0 | 0 | 0 | 0.1 |

**TABLE 3.6 (continued)**
**Design for the Self-Symmetric Resistance Matrix for the Centralized-Dispersed Case**

Fuel Cells, Storage Batteries, or Redox Flow Cells and Conventional Generators

| No. of bus-bars | Loading | | | K[a] |
|---|---|---|---|---|
| | 60% | 80% | 100% | |
| 99 | 0 | 0 | 0 | 0.1 |
| 100 | 0 | 0 | 0 | 0.1 |
| 102 | 0 | 0 | 0 | 0.1 |
| 103 | 0 | 0 | 0 | 0.1 |
| 104 | 0 | 0 | 0 | 0.1 |
| 105 | 0 | 0 | 0 | 0.1 |
| 106 | 0 | 0 | 0 | 0.1 |
| 107 | 0 | 0 | 0 | 0.1 |
| 108 | 0 | 0 | 0 | 0.1 |
| 109 | 0 | 0 | 0 | 0.1 |
| 110 | 18.4988 | 0 | 0 | 0.1 |
| 111 | 0 | 0 | 0 | 0.1 |
| 112 | 0 | 0 | 0 | 0.1 |
| 113 | 0 | 0 | 0 | 0.1 |
| 114 | 0 | 0 | 0 | 1.0 |
| 115 | –566.4243 | 0 | 0 | 1.0 |
| 116 | 0 | 0 | 0 | 1.0 |
| 117 | 0 | 0 | 0 | 1.0 |
| 118 | 0 | 0 | 0 | 1.0 |
| 119 | 0 | 0 | 0 | 1.0 |
| 120 | 27.8 | 10.0973 | 0 | 1.0 |
| 121 | 0 | 0 | 0 | 1.0 |
| 122 | 0 | 0 | 0 | 1.0 |
| 123 | 0 | 6.143 | 41.009 | 1.0 |

*Note*: All values listed are $10^6$ times greater than their true per unit value.

[a] K is the cost multiplying factor.

From Denno, K., Modeling of Redox Flow Cell, Fuel Cell, Storage Battery and Harmonically Commutated Inverter, Proc. Can. Commun. Power Conf., IEEE, 1976, 403—406. With permission.

Due to the operational linkage which practically exists among the redox cell, the hydrogen cell, and the storage battery, the following characterizations will be discussed.

**The redox flow cell** — The main task is to identify a lumped circuit model containing characteristics of the gyromagnetic phenomenon such as the shunt resistance, the internal circulating current, and resonance.

**The conventional fuel cell** — Its physical realization is to establish a dynamic model in the frequency domain based on the principles of electrochemical transform of fuel input to a DC power output.

**The conventional storage battery** — Its physical realization is to develop a dynamic model in the frequency domain taking into account the electrical transform of energy.

**The harmonically commutated inverter** — Development of a dynamic model in the frequency domain for the harmonically commutated inverter will identify the basis as its physical realization.

# XIII. GYROMAGNETIC CHARACTERISTICS IN THE REDOX FLOW CELL*

## A. THEORETICAL CONSIDERATION

In the catholyte of a redox flow cell, the working fluid could be a ferric ionic solution containing individual and/or clusters of ion and chlorine in a random pattern. Presence of the ferric dipolar medium in a fluid state resembles a continuum of freely rotating magnetic dipoles restrained by their total angular momentum quantum number which limits the degrees of freedom through which each dipole may align itself with the direction of magnetization.

According to the classical theory of paramagnetism, the magnetic moment (M) per unit volume can be calculated with the same approach in accordance with the Debye-Langevin theory, where

$$M = N\mu L\left[\frac{\mu H}{kt}\right] \tag{3.31}$$

where

$$L\left(\frac{\mu H}{kT}\right)$$

is the Langevin function, N = dipole concentration, $\mu$ = magnetic dipole moment, H = external magnetic field, k = Boltzman constant, T = absolute temperature in degrees kelvin, and if $\mu H << kT$, Equation 3.31 becomes

$$M \simeq \frac{N\mu^2 H}{3kT} \tag{3.32A}$$

However, the quantum theory of paramagnetism limits the degrees of freedom for a dipolar alignment with respect to an external field, depending on the value of its angular momentum quantum number (J).

Calculations have been carried out using Hund's rules and Pauli's principles which identified the ferric flow in the redox cell that is possessing magnetic tendencies.

The external magnetic field in the operation of the redox flow cell is due to the current to be delivered by the unit itself to the load.

Therefore, the static energy density (E) taken from the cell power output can be expressed as

$$E = \overline{H}.\overline{M} \tag{3.32B}$$

$$E = \frac{N\mu^2 H^2}{3kT} \tag{3.33}$$

The field H is due to a current passing in a solenoid,

$$H = \frac{ni}{l} \tag{3.34}$$

* © 1963. Reprinted with permission from Dekker, A. J., *Solid State Physics*, Prentice-Hall, Englewood Cliffs, NJ, 1963.

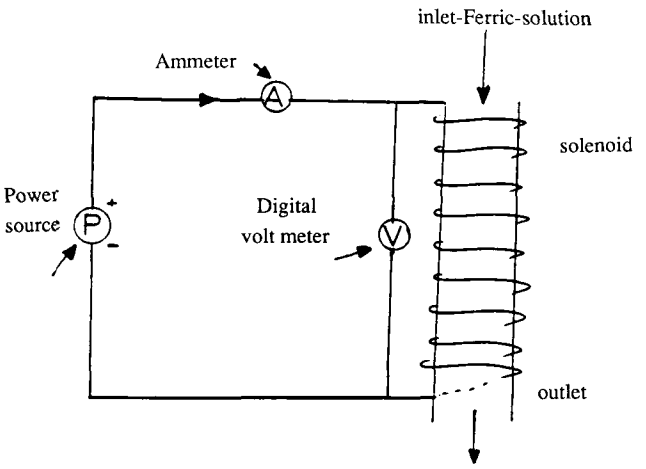


FIGURE 3.10 Experiment to identify gyromagnetic power.

where n = number of turns in the solenoid, l = axial length of the solenoid, and i = solenoid current. Then,

$$E = \frac{N\mu^2 n^2 i^2}{3kTl^2} \tag{3.35}$$

However, the ferric flow in the redox cell usually is pumped at an adjustable velocity (v), and hence, those dipoles will interact with the local magnetic field while they are in motion. In other words, the redox flow dipoles will find themselves in a different state of local motion during the process of magnetization.

Let dM/dt = the local volume displacement per second for the ferric dipoles and $W_{gm}$ = the gyromagnetic power delivered from the source of the external magnetic field.

$$\frac{dM}{dt} = W_{gm} / E \tag{3.36}$$

## XIV. EXPERIMENTAL IDENTIFICATION OF THE GYROMAGNETIC PHENOMENON IN FERRIC FLOW*

The ferric solution is adjusted mechanically to flow at a certain pumping velocity, simulating those ranges compatible to that in the catholyte channel of the redox battery. The catholyte channel flow is surrounded by a solenoid of 100 turns closely wound around the cylindrical channel.

The experimental set-up is shown in Figure 3.10.

At each velocity of the ferric solution, readings were taken for the net voltage drop across the solenoid, total current supplied, and a precise value for the solenoid resistance. From those data the gyromagnetic power supplied from the source $W_{gm}$ is obtained from the equation:

$$W_{gm} = P - V_L^2 / R_L \tag{3.37}$$

* © 1983. Reprinted with permission from Denno, K., Equivalent circuit parametric model requirements of the redox flow cell for bulk energy storage, *Alternative Energy Sources*, Vol. III, 1983, 417—432.

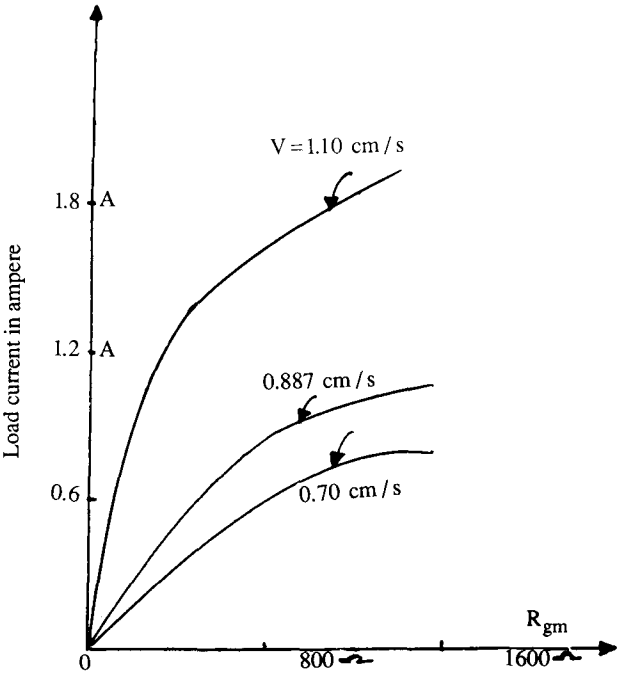


FIGURE 3.11 Gyromagnetic resistance and current.

where P = total power input, $V_L$ = voltage across the solenoid, and $R_L$ = DC resistance of the solenoid.

The gyromagnetic current ($i_{gm}$) is obtained from the relationship:

$$W_{gm} = i_{gm}^2 R_{Fe} \tag{3.38}$$

where $R_{Fe}$= the gyromagnetic resistance of the ferric flow.

In Figure 3.11 three curves are shown illustrating the pattern of change between the source current and the gyromagnetic resistance at three different flow velocities of the ferric solution.

Figure 3.12 shows the behavior of the gyromagnetic power ($W_{gm)}$ and current ($i_{gm}$) with respect to the total load current, where the real feature of resonance is clearly shown.

Then using the concept of charged carriers in a continuum together with the coupling effects of the gyromagnetic current and resistance, a lumped circuit model for the redox flow cell is shown in Figure 3.13.

From the preceding, we may proceed to outline the following remarks:

1. Identification for the causes of internal circulating currents in the catholyte of the redox flow cell is the first step in developing efficient direct energy systems meeting actual variational load conditions.
2. Dynamic modeling of the redox cell has direct dependence on the phenomenon of paramagnetic resonance, especially the gyromagnetic power, circulating current, and shunt resistance (see Figure 3.13).

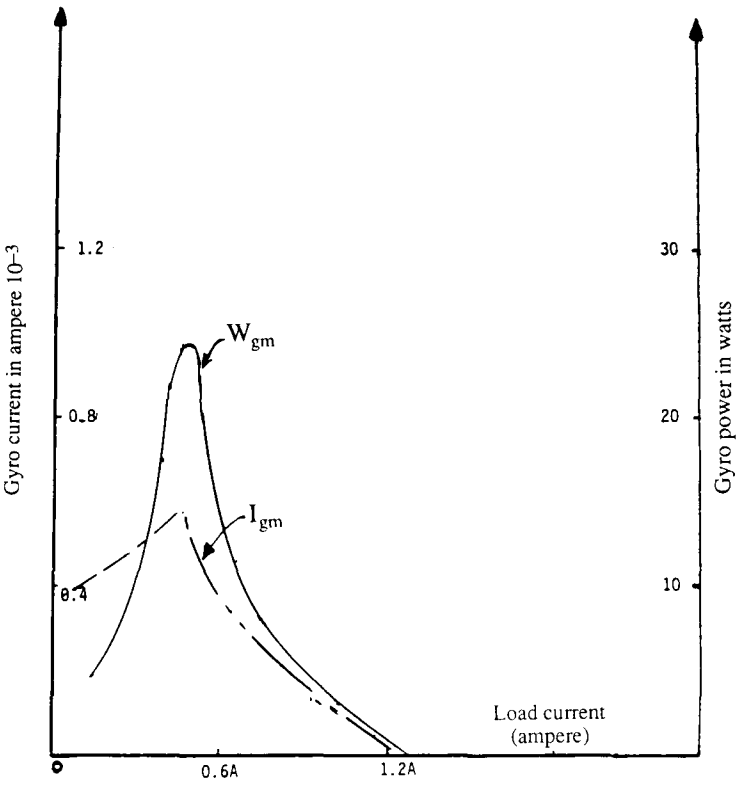


FIGURE 3.12 Gyromagnetic power and current against load current.

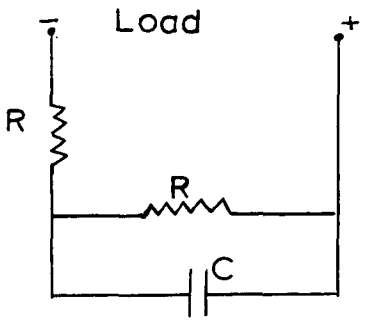


FIGURE 3.13 Parametric model redox flow cell.

## XV. COMPATIBILITY BETWEEN THE STORAGE BATTERY, FUEL CELL, PHOTOVOLTAIC, AND THE REDOX FLOW CELL*

Present efforts on the road of research and development with respect to direct energy devices such as conventional storage batteries, conventional fuel cells, photovoltaics, etc., point to a

* © 1978, IEEE. Reprinted with permission from Denno, K., Compatibility of Direct Energy Storage Devices with AC Processing Power System Components, IEEE Region V Annual Conf., Tulsa, OK, 1978, 6—10.

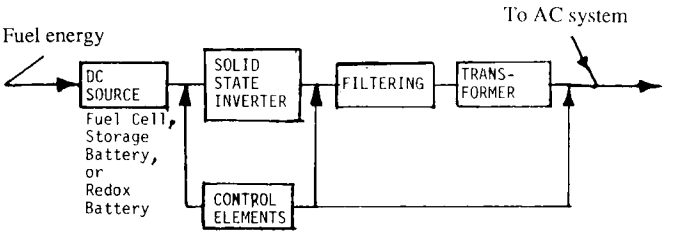


FIGURE 3.14 Renewable energy for AC output. (From Denno, K., Compatibility of Direct Energy Storage Devices with AC Processing Power System Components, IEEE Region V Annual Conf., Tulsa, OK, 1978, 6—10. With permission.)

serious problem centered on the compatibility of those devices and their operational link with supplementing AC power processing components.

Parameters of compatibility include efficiency, weight-cost factor, and peak power handling capability. Important components for the delivery of pure AC power output include solid state power inverters of an appropriate mode of commutation, an associated control system, and a filter system as well as a stepping up transformer, as shown in Figure 3.14.

It has been established by current research efforts that the bridge type inverter of auxiliary impulse commutation offers an optimum range of operation around a mean input DC voltage of 2 kV, while the weight-cost normalized factor for a modulated connection of redox storage batteries varies inversely with the level of the output DC voltage of the module and it is low at 2 kV. It is also reported that while the efficiency of conventional hydrogen fuel cell increases with the level of its output DC voltage; the reverse trend exists in the case of the redox flow battery.

As with respect to performance merit of the power inverter, present data point to the fact that it is indeed the main limiting element for the entire direct AC power output system. By proper scaling, other components in the subsystem can be designed to achieve the desired efficiency and other performance characteristics.

The number of interconnected modules of a direct energy device proved to be decisive with respect to a normalized level of the weight-cost factor. The increase in number of the interconnected modules in the case of conventional storage batteries and fuel cells toward an enlarged DC voltage resulted in an improved normalized weight-cost factor and efficiency, while in the case of redox flow storage battery, an output voltage beyond 200 V required the forced trade-off of low weight-cost factor with respect to efficiency. At the same time it has been reported that a redox battery with 400 V terminal voltage offers a maximum efficiency on one hand, but results in a poor level of normalized weight-cost factor.

From the preceding presentation it must be pointed out that an interconnected power system linking varous kinds of direct energy devices in any series-parallel mode of combination through working AC power output components involves incompatible device characteristics of poor efficiency, high cost, and weight. This problem will certainly lead to amplified diverse performance output if the direct AC output system is coupled in a hybrid system of connection with the conventional or the traditional electromechanical power system.

In this chapter, the problem of compatibility among renewable energy sources is demonstrated by considering the following case.

Given a direct energy system for delivering pure AC power output as indicated in Figure 3.14, it is required to develop an analytical approach through which the criteria of compatibility could identify desired and working performance characteristics for the direct energy device, the solid state power inverter, the filter system, the transformer, and any associative controlling function.

# XVI. BASIS FOR MODELING*

## A. STORAGE BATTERY & FUEL CELL

Irreversibility is expressed by

$$E = \frac{|\Delta G| - |W_e|}{nF} nF \tag{3.39}$$

where $W_e$ = reversible electric power output, F = electrochemical equivalent, F = 96,493 coulombs, n = total reactants concentration, and G = Gibbs free energy, defined as the maximum amount of energy available at constant pressure and temperature.

Also,

$$\Delta G = \sum_{i=1}^{l=j} \mu_i dni \tag{3.40}$$

where $\mu_i$ = electrochemical potential of ith reactant and $n_i$ = concentration of ith reactant.

## B. REDOX FLOW BATTERY

Based on present research data which indicate that this device efficiency, with respect to its terminal DC voltage, follows a curve very similar to the familiar B-H curve of ferromagnets, and that the normalized weight-cost factor, with respect to the battery terminal DC voltages, is hyperbolic, the following two analytical relations have been developed:

$$\eta = \frac{36\sqrt{E}}{E + 320} \tag{3.41}$$

and

$$N = \frac{25}{E}$$

where E = the redox battery output DC voltage, $\eta$ = the redox battery efficiency, and N = normalized weight-cost factor.

From Equation 3.38, it is possible to find out the limitation on the redox flow cell voltage for maximum efficiency which had been determined as E/320 V leading to an ideal level for efficiency of 100%.

# XVII. TOOLS FOR COMPATIBILITY*

Using performance characteristics for the storage battery, hydrogen fuel cell, and the redox flow battery outlined above, dynamic models in the complex frequency domain are developed for each device.

Also from previous work, dynamic models in the complex frequency domain were developed for the following modes of solid state power inverters:

1. Direct line commutated mode
2. Parallel capacitor commutated mode

$$G = k\sqrt{S}\left\{\left(S + \frac{r_g}{R}\right) + \frac{V_c(S)}{V_c(0)}\left[S\left(1 - \frac{r_g}{R}\right) - r_g S^2\right]\right\}$$

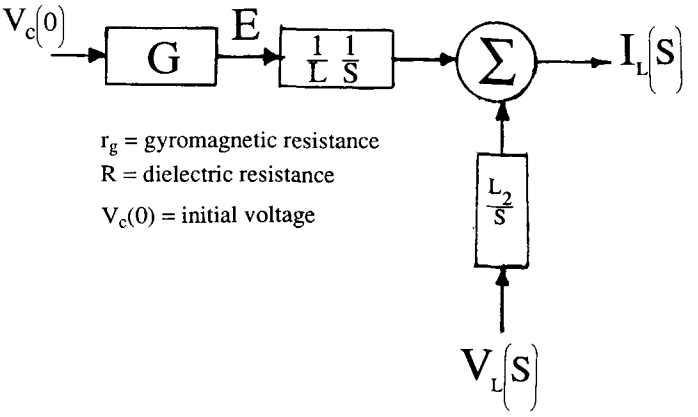


FIGURE 3.15 Model for redox battery coupled to direct line inverter. (From Denno, K., Compatibility of Direct Energy Storage Devices with AC Processing Power System Components, IEEE Region V Annual Conf., Tulsa, OK, 1978, 6—10. With permission.)

3. Series capacitor commutated mode
4. Transformer commutated mode
5. Auxiliary impulse commutated mode

Then from the data assembled for the direct energy devices and power inverters, unified models have been established for the redox storage battery coupled separately to each mode of power inverter; these are shown in Figures 3.15 to 3.18.

From the preceding sections, we can proceed to list these remarks:

1. In order to establish compatible unified power systems for pure AC output from non-mechanical energy devices linked through solid state power inverters and transformers, consistent change in performance pattern must be secured before proceeding to interconnect those energy devices in cascade. To ensure the existence of compatibility, dynamic models for direct energy bus-bars containing every internal component could reveal a total pattern for the steady state as well as the time domain including economic merit factors.
2. Steady state response from the unified model could determine the best acceptable mode of power inverters for optimum AC power output.
3. Mathematical representation describing steady state behavior for the redox flow battery has been established in terms of efficiency and normalized weight-cost factor, both with respect to the battery terminal DC voltage.

## XVIII. SUMMARY

This chapter presents the following conclusions which set more solidly the central basis for establishing a true equivalent circuit for the redox flow cell.

A mathematical locus for a particle rotation time constant has been expressed in a plane correlating the surfactant thickness with particle diameter. The locus is in terms of minimum

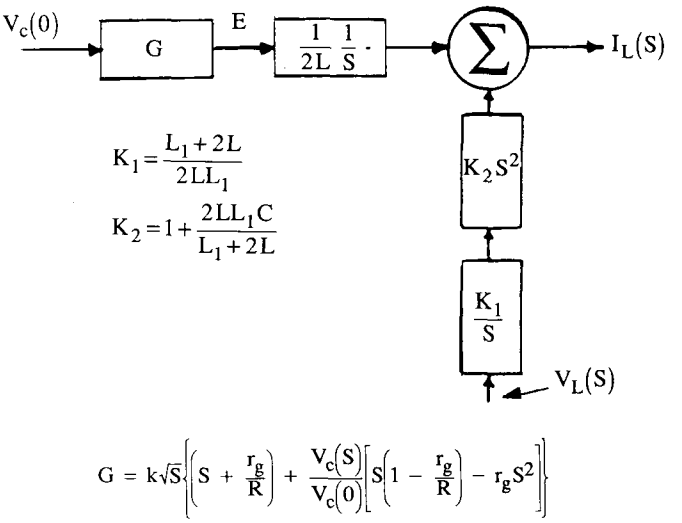


FIGURE 3.16 Model for redox battery coupled to parallel capacitor inverter. (From Denno, K., Compatibility of Direct Energy Storage Devices with AC Processing Power System Components, IEEE Region V Annual Conf., Tulsa, OK, 1978, 6—10. With permission.)

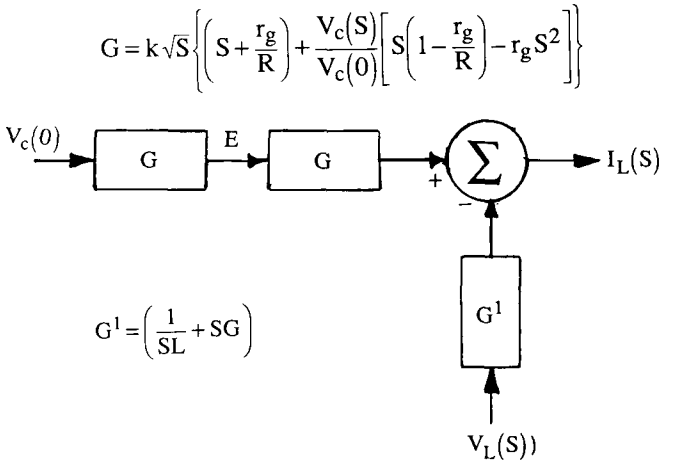


FIGURE 3.17 Model for redox battery coupled to transformer inverter. (From Denno, K., Compatibility of Direct Energy Storage Devices with AC Processing Power System Components, IEEE Region V Annual Conf., Tulsa, OK, 1978, 6—10. With permission.)

value of the radial vector as well as the surfactant thickness and the straight line contours of h $V_s D_1$.

A straight line representation with respect to the Neél time constant, which is a measure of moment rotation with a defined charge in slope, has been derived for h $V_s D_1$ with respect to particle chaining and the aspect ratio of the prolate spheroid.

A closed form of mathematical solution for the state of magnetization M(t) has been obtained in terms of particles distribution function f(x), mobility, and the initial value M which is $M_o$ subject to the application of a sustained DC magnetic field.

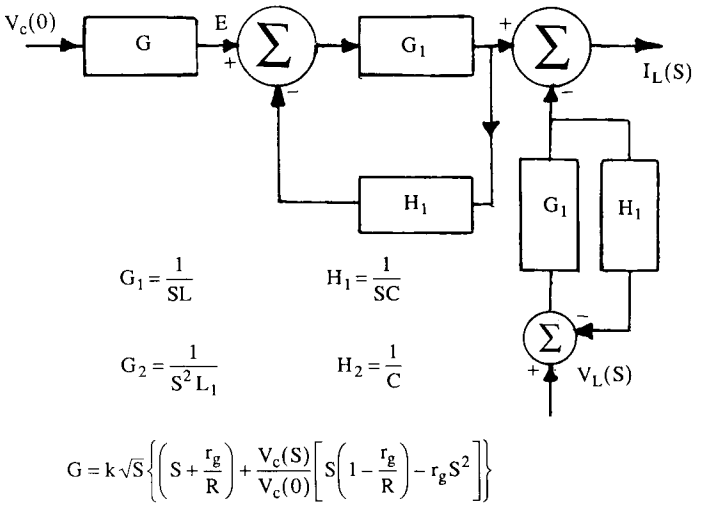


FIGURE 3.18 Model for redox battery coupled to series inverter. (From Denno, K., Compatibility of Direct Energy Storage Devices with AC Processing Power System Components, IEEE Region V Annual Conf., Tulsa, OK, 1978, 6—10. With permission.)

The time rate of change of M(t) is derived in the form of an impulse followed with a decaying step function, again in terms of the particles distribution function, mobility, and the initial level of magnetization $M_o$.

A solution was obtained for the space second derivative of the distribution function f(x) in the space domain in the form of a bell curve, which could serve a direct measure for particles acceleration as well as the second time derivative of f(x). A plot of f″(x) is shown in Figure 3.5.

An approximate solution for the distribution function f(x) is established in three distinct regions confined in the main spatial region for x, i.e., $-1 < x < 1$.

The three regions are

$$f_1(x) \quad \text{for} \quad -\frac{1}{2} < x < \frac{1}{2}$$

$$f_2(x) \quad \text{for} \quad \pm\frac{1}{2} < x < \pm\frac{3}{4}$$

$$f_3(x) \quad \text{for} \quad \pm\frac{3}{4} < x < \pm 1$$

Information secured in this chapter with respect to the pattern of magnetization and its space and time variations of ferro-fluids in the catholyte of the redox flow cell, together with the solution of the particles distribution function and its spatial derivative, will provide concrete and reliable data for establishing a true and representative equivalent circuit for the redox flow cell.

Economic evaluation of fuel costs for centralized power systems B and C indicates encouraging results for significant annual savings with respect to conventional Plan A as overall load demand increases.

The total annual capital cost covering the sum of initial, operation and maintenance costs for each of the alternative plans investigated indicates a slight rise over base Plan A.

The fuel cost for a dispersed power system in which fuel cells supply a major part of the overall load would result in a substantial increase as total load increases; however, that is offset to some degree by a decrease in total initial maintenance and operation cost.

The dispersed power system is based on assigned load centers, with zero total losses, but independent of the type and mode of the interconnecting network linking the various generating buses. Therefore, the economic forecast indicated above ought to be taken on qualified viewpoint.

The inclusion of redox flow cells, coupled to an auxiliary impulse inverter in a central or dispersed energy system, results in a substantial increase in cost if the redox cell DC voltage exceeds 100 V. Therefore a trade-off mechanism has to be devised where the redox cell coupled to its inverter will perform in compatibility with other direct energy sources.

In a dispersed energy system, redox flow cells coupled to an auxiliary impulse power inverter and operating for an output DC voltage around 2 kV, provides a very economical and efficient energy system but requires an improvement in the redox cell performance for a 2 kV output voltage.

The design for an optimum energy system in the power flow or the sixth reference frame sets the central storage for the design in the first or the actual frame by carrying out a set of matrix transformations. Designs of two central systems and a dispersed-central system are set in Tables 3.4, 3.5, and 3.6.

Problems encountered in bringing the redox power system to the operational levels include major reduction in the circulating internal currents, optimizing the generated electric power output density, and perfecting the selectivity of the ionic exchange membrane.

The development of a dynamic model for the redox flow cell characterized the causes and effects of the circulating currents on the steady state and time varying performance, especially the power density and stability of the terminal voltage. The model also demonstrates the phenomenon of gyroparamagnetization of the $Fe^{+3}/Fe^{+2}$ ionic dipoles as a result of their interaction with the magnetization effects of the load current supplied externally.

Theoretical calculations based on classical as well as quantum theories established basic characteristics for the internal shunt resistance of the redox flow cell as a result of induced gyromagnetic internal currents, followed with a unique representation in the dynamic model.

This work also presents dynamic modeling for the harmonically commutated inverter, including the two modes of commutation namely, the n-phase externally and internally commutated types.

A unified model has been established for the redox flow cell interconnected to the harmonically commutated inverter, as a composite unified electrochemical AC bus-bar for supplying and storing bulk electric power.

The total model developed established basic criterion for stabilizing the AC terminal voltage of the power inverter and identified several avenues for neutralizing the circulating currents in the redox flow cell and optimizing its power density and efficiency. The total model in general is extremely useful in providing reliable information about steady state and transient behavior of this interfaced energy system when linked with the conventional power grid system.

## XIX. PROBLEMS

3.1 Consider a centralized power system of 32 bus-bars containing nuclear, fossil-steam, and pumped-hydro generators supplying base loading demands while redox flow cell generating bus-bars will supply only peak demand instead of gas-turbine generators. This is known as alternative system C in Chapters 1 and 2.

3.2 Assuming the incremental fuel cost for the redox flow cell to be equal to twice that for the conventional fuel cell generating system which is \$7.36/kWh and using Equation 1.4, establish all elements of the [B] matrix for minimum transmission loss, with its optimum Lagrange multiplier $\lambda$. Let $P_r$ = 10,000 MW.

3.3 In Chapter 2, the symmetric resistance matrix [R] for alternative system C is listed. With

the assumption that the [R] matrix is valid and with the [B] matrix secured in Problem 3.4, obtain all elements of the [K] matrix in the power flow reference frame.

3.4 From results secured in Problem 3.7 for the [K] matrix of an alternative power system where the redox flow cells supply peak loading instead of gas turbines, proceed to calculate unit values for voltage magnitudes and phase angles of the 32 bus-bars. You may use Equation 1.12 in Chapter 1.

3.5 Assuming that alternative system C analyzed in Problems 3.1, 3.3, and 3.4 is subdivided into a multiarea interconnected energy system, calculate all elements of the [B] matrix using Equation 1.50 in chapter 1 for a total power received ($P_r$) = 9000 MW, under the constraint of minimum $P_L$. Identify the optimum Lagrange multiplier $\lambda$.

3.6 Using the generalized economic coordination equation for a multiarea power pool (Equation 1.37 in Chapter 1), calculate the net tie power flow across an area in megawatts. Assume any feasible condition to secure $P_T$.

3.7 From the solution of the [B] matrix in Problem 3.9, and using the [R] matrix for alternative system C given in Chapter 2, calculate all elements of the [K] matrix in the power flow reference frame for the multiarea interconnected power system.

3.8 From solution of the [B] matrix in Problem 3.6 for alternative system C where the redox flow cells are used to supply peak loads instead of gas turbines, establish a set for economic scheduling of generation for all generating plants for $P_r$ = 10,000 MW.

3.9 Repeat Problem 3.8, but for the data secured in Problem 3.5 for the multiarea interconnected system. Let $P_r$ = 9000 MW.

3.10 Repeat Problem 3.8 but for $P_r$ = 7000 MW. This requires first the calculation of elements of the [B] matrix and then the economic allocation of generation for all plants.

3.11 Repeat Problem 3.9, but for $P_r$ = 7000 MW. Again this first requires calculation for elements of the [B] matrix.

3.12 Using the economic scheduling of generation for all plants in Problem 3.8 for $P_r$ = 10,000 MW and the pattern of the load duration curve, establish a set of results for the economic cost in dollars per hour vs. total annual hours for each plant.

3.13 Repeat Problem 3.12, but for the results and data of Problem 3.9.

3.14 From economic costs secured from Problem 3.12 and 3.3, establish the differential cost in dollars per hour of the one area system for alternative system C with respect to an interconnected multiarea of the same system.

3.15 Using Equation 1.4 in chapter 1, calculate through an appropriate computer program for alternative system E in which the redox flow cells will meet loading demands for all new planned generating central bus-bars plus the on-site supply generators of any new load centers for a total $P_r$ = 10,000 MW where $P_r$ = 5000 MW. Identification of bus-bars and their fuel cost data is shown in Chapter 1. Assume incremental fuel cost for the redox flow cell generating bus-bars to be equal to \$15.3/kWh.

3.16 From results secured in Problem 3.15 and for the same system, establish the economic power allocation for each bus-bar for $P_r$ = 13,000 MW. This represents 100% loading.

3.17 Using results for the [B] matrix of alternative system E secured in Problem 3.16 and in reference to the [R] matrix shown in Chapter 2 for this system, calculate elements of the [K] matrix.

3.18 Using Equation 1.12 in chapter 1, calculate voltage magnitudes with their phase angles with respect to the slack bus for system E.

3.19 Compare data secured in Problem 3.18 with those given in Chapter 1 obtained through load flow calculations for system E.

3.20 Develop a parametric model for the redox flow cell valid over a load drawn current ranging between 0.6 A to 0.8 A with a catholyte fluid flow at 0.75 cm/s. Note: Use curves shown in Figures 3.11 and 3.12 with approximate manipulation.

3.21 Repeat Problem 3.20 for $0.6 \leq i_L \leq 1.2$ A and $0.7 \leq v \leq 1.10$ cm/s.

3.22 Figure 3.15 represents a mathematical model in the (s) domain for the redox flow cell coupled to an auxiliary impulse commutated inverter. Determine the correlation between $H_1(s)$ and $G_1(s)$ such that $I_L(s) = 0$ and $V_c(0) = V/S$. Assume zero initial conditions for all cases $V_c(0)$ is the initial stored voltage across the capacitor.

3.23 Again with respect to Figure 3.18, if

$$\frac{G_1}{1 + G_1 H_1} = -1$$

$$V_c(0) = 1$$

and

$$\frac{r_g}{R} = \frac{1}{10s}$$

obtain an expression for $I_L(s)$ in the steady state.

3.24 Direct compatibility between Figure 3.15 for the redox flow cell coupled to a direct line inverter and Figure 3.16 for the redox flow cell coupled to a parallel capacitor commutated inverter requires $I_L(s)$ output for the two systems to be identical. Under steady state conditions, establish the correlation between $V_c(0)$ for each system, then show the necessary constraint for pure sinusoidal outputs.

3.25 Direct compatibility between two systems representing a redox battery connected to a series capacitor commutated inverter in one system and to a transformer commutated inverter in the second system requires $I_L(s)$ to be identical in both systems. Find the correlation between $V_c(0)$ in each system in the steady state under the following conditions:

$$r_g \ll R$$

$$L \to \infty$$

3.26 Find the overall transform function for a system comprised of the redox flow cell coupled to a transformer commutated inverter. Identify constraints under which

$$I_L(s) = \mathcal{L}\ I_m \sin\ wt$$

where $\mathcal{L}$ means the Laplace transform.

3.27 The conventional hydrogen-oxygen fuel cell with irreversibility as a basic character of its performance, is known to work according to the following energy linkage equations:

$$NFE = G - NFE \tag{a}$$

$$dV = TdQ - dG \tag{b}$$

where dV = total differential energy change, dQ = entropy differential, n = concentration function of any reactant, N = functional representation for the electro-chemical reaction, F = Faraday's constant = 96,493 coulombs, E = fuel cell developed emf, and dG = change

in Gibbs free energy. Carrying out a process of time variation on equation (a) and neglecting any volume change, obtain a dynamic model for the fuel cell in the complex frequency domain. The dynamic model sought is in the form of a feedback control system with V(s) as the input function and E(s) as the output response.

3.28 The figure at the left represents a parametric circuit model for the storage battery, where $R_L$ is the loading resistance, C is the storage element in the form of capacitance, and S is the Laplace variable or the complex frequency. Develop a mathematical model for the storage battery in the (s) domain, that is in the form of a feedback control system with $E_o/S$ as the input variable and E(s) is the output response. $E_o$ as the initial voltage stored in the battery capacitance c.

3.29 Using the redox flow cell parametric model shown in Figure 3.13, derive a mathematical model for the redox cell in the (s) domain. You may use the energy linkage equation stated in Problem 3.27.

3.30 From the principle of direct compability between the storage battery and the redox flow cell derived in Problems 3.28 and 3.29, and considering that incremental fuel cost for the redox cell is (m) times that for the storage battery, establish for minimum fuel cost for the interconnected storage battery and redox cell system criterion of parametric linkage with respect to (s). Next reform the resulting criterion for validity in the steady state.

3.31 Repeat Problem 3.30 for a new criterion for the interconnection between the conventional fuel cell and a redox flow cell.

3.32 Let the principle of direct compatibility among conventional hydrogen fuel cell, the redox flow cell and a storage battery exist. The incremental fuel cost for the redox flow cell is (m) times that of the conventional cell and is (m) times that for the storage battery. For minimum total fuel cost for the three cells with respect to (s) as an independent variable, establish a linking criterion valid to ensure the state of compatibility in the steady state.

3.33 Consider an energy system comprised of the interconnection of conventional fuel cells, redox flow cells and storage batteries. If the incremental fuel cost for the redox flow cell is ($m_1$) times that of the conventional fuel cell and for the storage battery is ($m_2$) times that of the fuel cell, establish for minimum fuel cost the optimum number of units to be connected from each energy source indicated.

3.34 An interconnected energy system involves parallel coupling at a bus-bar of a redox battery terminated to a direct line inverter, and a conventional alternator powered by a fossil-steam prime mover. Derive a mathematical model for the conventional AC generator in the (s) domain. Under compatible AC voltage for the two power sources, establish steady state criterion for sinusoidal AC output assume the AC alternator is a cylindrical rotor.

3.35 For the interconnected system of Problem 3.34, obtain a solution in the time domain for AC electric current output due to a sudden disconnection of the conventional AC generator.

3.36 Repeat Problem 3.34 where the renewable energy generator is that of a redox flow cell coupled to a transformer commutated inverter.

3.37 Repeat for the statement of Problem 3.34 with respect to Problem 3.36.

## REFERENCES

1. **Ateya, B. G. and Austin, L. G.**, The Kinetics of $Fe^{2+}$/Fe $C1_2$/Hc (ag) on Pyrolytic Graphite Electrodes, *J. Electrochem. Sci. Tech.*, September 1973.
2. **Bogardus, E. H., Scraton, R., and Thompson, D. A.**, Pulse magnetization measurements in ferrofluids, *IEEE Trans. Magnetics*, Mag-11, No.5, 1364, 1975.

3. **Bogardus, E. H., Krueger, D. A., and Thompson, D. A.,** Dynamic magnetization in ferrofluids, *J. Appl. Phys.*, 49, 3422, 1978.
4. **Cobine, J. D.,** *Gaseous Conductors*, Dover Publications, New York, 1958.
5. **Dekker, A. J.,** *Solid State Physics*, Prentice-Hall, Inc., Englewood Cliffs, NJ, 1963.
6. **Denno, K.,** Modeling of Redox Flow Cell, Fuel Cell, Storage Battery and Harmonically Commutated Inverter, Proc. Can. Commun. Power Conf.,1976, 403.
7. **Denno, K.,** Problems in the Redox Flow Cell Power System for Bulk Energy Storage, Proc. Inst. Environ. Sci., Seattle, WA, May 1979, 322.
8. **Denno, K.,** Magnetic transport properties of dipolar conducting liquids at ambient temperature, *J. Electrostatics*, 7, 345, 1979.
9. **Smity, A. C., Janak, J. F., and Adler, R. B.,** *Electronic Conduction in Solids*, McGraw-Hill, New York, 1967.
10. **Rabinowitch, E. and Stockmayer, W. H.,** Associate of Ferric Ions with Chloride, Bromide and Hydroxyl Ions, Contribution No. 482 from the Research Laboratory of Physical Chemistry, and Publication No. 9, Solar Energy Conversion Research Project, MIT, Cambridge, MA, 1942.
11. **Boshier, J. F.,** Economic operation for electric power systems, *IEE Electronics and Power*, 20(10), May 1974.
12. **Denno, K.,** Steady State and Dynamic Investigations for Determining Optimum Electrochemical-Electromechanical Interconnected Power Systems, published report for a research grant sponsored by the Middle Atlantic Power Research Committee, Newark, NJ, January 1975.
13. **Denno, K.,** Power System Synthesis from Solution of Optimum Transmission Loss Coefficients, Paper C. 73-462-9, IEEE Conf., Vancouver, July 1973.
14. **Denno, K.,** Power system identification in the power flow reference frame, *J. Appl. Sci. Eng.*, 2, 141, 1977.
15. **Kirchmayer, L. K.,** *Economic Operation of Power Systems*, John Wiley & Sons, Inc., New York, 1958.
16. **Kron, G.,** Tensorial analysis of integrated transmission systems, *AIEE Trans. Power Syst. Apparatus*, 70, 1239, 1950.
17. **Stagg, G. W. and El-Abiad, A. H.,** *Computer Methods in Power System Analysis*, McGraw-Hill, New York, 1968.
18. **Walsh, E. M.,** *Energy Conversion*, Ronald Press Co., New York, 1967.
19. **Mukhopadhyay, B. K. and Malik, O. P.,** Specific Optimal Control of a Non-Linear Closed-Loop Power System, conference paper presented at IEEE Power Eng. Soc., Vancouver, Summer 1973.
20. **Reikert, L.,** The conversion of energy in chemical reactions, *Energ. Convers., Int. J.*, 15, 81, 1976.
21. **Smith, A. C., Janak, J. F., and Adler, R. B.,** *Electronic Conduction in Solids*, McGraw-Hill, New York, 1967.
22. **Woodson, H. H. and Melcher, J. R.,** *Electromechanical Dynamics*, Vol. I, II, and III, John Wiley & Sons, Inc., New York, 1968.
23. **Cains, and Liebhafsky,** *Fuel Cells and Fuel Batteries*, McGraw-Hill, New York, 1970.
24. **Christensen, G. S. and El-Hawary, M. E.,** Functional Optimization of Hydro-Thermal Systems with Trapezoidal Reservoirs and Variable Efficiency, conference paper presented at IEEE Power Eng. Soc., 1973.
25. **Denno, K.,** Modeling of Redox Flow Cell, Fuel Cell, Storage Battery and Harmonically Commutated Inverter, Proc. Can. Commun. Power Conf., October 1976.
26. **Denno, K.,** Modeling of Basic Types of Solid State Power Inverters, Proc. Midwest Power Symp., October 1976.
27. **Dekker, A. J.,** *Solid State Physics*, Prentice-Hall, Englewood Cliffs, NJ, 1963.
28. **Crouch, D. A.,** Batteries and the Economics of Load Leveling in Large Power Systems, IEEE Power Eng. Soc., New York, Winter 1973.
29. **Mantell, C.,** *Batteries and Energy Systems*, McGraw-Hill, New York, 1970.
30. **Humphrey, A. J.,** Inverter Commutation Circuits, Applications, *IEEE Trans. Industr Gen. Applications*, Vol. 4, 1968.
31. **Thaler, L.,** Electrically Rechargeable Redox Flow Cells, NASA-TM-X-71540, Lewis Research Center, Cleveland, OH, 1974.
32. **Warshay, M. and Wright, L. O.,** Cost and Size Estimates for an Electrochemical Bulk Energy Storage Concept, NASA-TM-X-3192, Lewis Research Center, Cleveland, Ohio 1975.
33. **Denno, K.,** *Power System Design and Applications for Alternative Energy Sources*, Prentice-Hall, Englewood Cliffs, NJ, 1989.
34. **Denno, K.,** Equivalent circuit parametric model requirements of the redox flow cell for bulk energy storage, *Alternative Energy Sources*, Vol. III, 1983, 417.
35. **Denno, K.,** Redox flow cells, conventional fuel cells, and storage batteries as the optimal power sources for buildings, *IASTED J. of Energy Systems*, 2(2), 109—113, 1980.
36. **Denno, K.,** Compatibility of Direct Energy Storage Devices with AC Processing Power System Components, IEEE, Region V Annual Conf. Record, Tulsa, OK, 1978, 6—10.

Chapter 4

# THE ECONOMICS OF BIOELECTROCHEMICAL ENERGY CONVERSION SYSTEMS (BEEC)

## I. SIMULATING CRITERION FOR BIOCHEMICAL CONVERSION OF REFUSE TO SYNTHETIC FUEL AND ELECTRIC POWER*

This section presents, through the mechanism of simulation, synthetic fuel production and the process of bioelectrochemical energy conversion.

Generation of electric energy from refuse through the process of bioconversion is performed by the bioelectrochemical fuel cell. The bio-organic matter is prepared from refuse and then injected as fuel to the anode, with preheated air as an oxidizer to the cathode, where both are coupled through an organic electrolyte such as potassium hydroxide.

Resorting to the criterion that useful electric energy output from the bioelectrochemical fuel cell is the transformed product secured from the interaction of the local reactants with the material environment coupled with the criteria of total continuity of the cell fluids, reliable results have been developed through a systematic simulation describing the biochemical local kinetics and dynamics, thermal effects, electric field generated by electrochemical energy transformation, as well as local entropy and enthalpy within the cell continuum. The same principle of local reactants to material environment interaction and the continuity equation have been used successfully in the development of system models simulating the kinetic as well as the dynamic characteristics for the pure biochemical process of synthetic fuel extraction from organic refuse. The process of biochemical conversion takes place with a prepared refuse that will be digested with anaerobic bacteria, producing multigrades of unsaturated as well as saturated hydrocarbon of the order of $C_mH_{2m+2}$ (n is the grade of the hydrocarbon).

From the preceding analysis, mathematical simulation in the form of coupled partial differential equations associated with variable coefficients in the time domain, followed by a total dynamic model in the state variables domain, have been established for the overall bioelectrochemical energy extraction from synthetic fuel, as well as for the biochemical conversion of organic wastes to synthetic fuel.

From the above-mentioned, simulating mathematical as well as dynamic models have been developed and useful information has been obtained, defining several operational criteria for optimum performance of bioconversion of organic refuse to synthetic fuel and then eventually to useful electric energy in terms of equivalent bioelectrochemical potentials of reactants, order of hydrocarbons, and their concentrations, as well as local conditions of entropy and enthalpy. Stability aspects concluded from the dynamic models identified a reliable spectrum of fluctuation for the electric terminal voltage and/or electric field intensity in terms of cell operational parameters.

## II. BIOCHEMICAL CONVERSION

This involves transformation of prepared refuse to synthetic hydrocarbon fuel $C_mH_{2m+2}$, where m is the fuel order. Previous work[3,4] carried out by this author established unique mathematical models for this process based on the principles of refuse interaction with oxidizing environmental forces.

The models developed previously in the complex frequency domain are distinctly identified with respect to the number of frequency poles in the transformed energy function and the order of that function.

Simulating procedure for the process of energy conversion to be presented here is centered on the principles of mass conservation and biochemical reaction kinetics, as well as the continuity equation of fluids.

$$\frac{\partial n_i}{\partial t} = + \bar{\nabla} \cdot n_i \bar{v}_i = \sum_{i-1}^{n} Y_i \tag{4.1}$$

where $n_i$ = lumped concentration of the ith reaction process, $v_i$ = mean velocity of the ith reaction process, and $\Sigma Y_i$ = total sum of rate of concentration on sources and sinks.

Equation 4.1 could also be written as

$$\frac{\partial n_i}{\partial t} + n_i\left(\bar{\nabla}\bar{v}_i + \left(\bar{v}_i\bar{\nabla}\right)n_i\right) = \sum_i Y_i \tag{4.2}$$

From the equation of energy conservation and equation of continuity,

$$\frac{\partial U}{\partial t} = \frac{\partial H}{\partial t} - T_o\frac{\partial Q}{\partial t} + n_i\frac{\partial W_e}{\partial t}\left[W_c^o + RT_o \ln\frac{M}{m}\right]\left[\sum_i Y_i - \bar{\nabla} \cdot n_i\bar{v}_i\right] \tag{4.3}$$

where U = maximum energy per mole extracted from refuse; H,Q = enthalpy and entropy, respectively; $w^i$ = maximum energy change per mole due to variation in chemical composition of ith reactant of the prepared refuse; and $w^o$ = maximum energy developed per mole from prepared refuse.

Equation 4.3 can be written in another form with the order of the hydrocarbon m varying,

$$\frac{\partial U}{\partial t} = \frac{\partial H}{\partial t} - T_o\frac{\partial Q}{\partial t} + \sum_i \frac{n_i}{m} RT_o\frac{\partial m}{\partial t} + W_c^i\frac{\partial n_i}{\partial t} \tag{4.4}$$

Then from Equation 4.2

$$\frac{\partial U}{\partial t} = \frac{\partial H}{\partial t} - T_o\frac{\partial Q}{\partial t} + \sum_i -RT_o\frac{n_i}{m}\frac{\partial m}{\partial t} + W_i\left[\sum_i Y_i - n_i\frac{\partial v_i}{\partial x} - v_i\frac{\partial n_i}{\partial x}\right] \tag{4.5}$$

Also the transform of Equation 4.2 in the (s) domain is secured as follows:

$$v_i(s) = \frac{3S}{Y_i}\sum_{k=1}^{P}\frac{A_l(s_k)}{B_l'(s_k)}n_i(s - s_k) \tag{4.6}$$

where

$$v_i(s) = \frac{A_l(s_k)}{B_l(s_k)} \tag{4.7}$$

Then since,

$$n_i(s) = \frac{Y_i}{2s^2} - \frac{1}{2}\sum_{k=1}^{P} \frac{M(s_k)}{N'(s_k)} V_i(s - s_k) \tag{4.8}$$

Hence from Equations 4.6 and 4.8,

$$\frac{n_i(s)}{V_i(s)} = \frac{\frac{3s}{Y_i}\sum_{k=1}^{P} \frac{A_1(s_k)}{B_1'(s_k)} n_i(s - s_k)}{\frac{Y_i}{2s^2} - \frac{1}{2}\sum_{k=1}^{P} \frac{M(s_k)}{N'(s_k)} V_i(s - s_k)} \tag{4.9}$$

For conditions of peak energy transfer; from Equation 4.4 under a state of time variation, peak energy extraction through the mth order hydrocarbon is expressed by the following condition:

$$T_o \frac{\partial Q_i}{\partial t} - \frac{\partial H_i}{\partial t} = W_i \frac{\partial n_i}{\partial t} - \frac{n_i}{m} RT_o \frac{\partial m}{\partial t} \tag{4.10}$$

and similarly with respect to space displacements across the reactants continuum, the condition is:

$$T_o \frac{\partial Q_i}{\partial x} - \frac{\partial H_i}{\partial x} = W_i \frac{\partial n_i}{\partial t} - \frac{RT_o}{M} \frac{n_i}{m} \frac{\partial m}{\partial x} \tag{4.11}$$

For stable reactants continuum $v_i = \partial v_i/\partial x = 0$, the constraint equation in the time domain becomes

$$W_i^o + RT_o \ln \frac{M}{m} = \frac{1}{Y_i}\left[\left(T_o \frac{\partial Q_i}{\partial t} - \frac{\partial H_i}{\partial t}\right) + \frac{n_i}{m} RT_o \frac{\partial m}{\partial t}\right] \tag{4.12}$$

while the constraint equation in the space domain becomes

$$\frac{\partial m}{\partial x} = \frac{Mm}{RT_o n_i} kx + \frac{Mm}{RT_o n_i} \frac{\partial n_i}{\partial x}\left[\frac{k_t}{Y_i} - \frac{RT_o n_i}{Y_i m} \frac{\partial m}{\partial t}\right] \tag{4.13}$$

where

$$k_t = T_o \frac{\partial Q_i}{\partial t} - \frac{\partial H_i}{\partial t}, \qquad k_x = T_o \frac{\partial Q_i}{\partial x} - \frac{\partial H_i}{\partial x} \tag{4.14}$$

and the zero gradient of the developed hydrocarbon becomes

$$\frac{\partial m}{\partial t} = \frac{1}{RT_o} \frac{m}{RT_o}\left[k_t - kx / \frac{\partial n_i}{\partial x}\right] \tag{4.15}$$

# III. MODELING OF BIOELECTROCHEMICAL CONVERSION OF REFUSE TO ENERGY*

This section proceeds to show, through the mechanism of modeling, the operational prospects for the production of synthetic fuel from prepared refuse and then the controlling process of bioelectrochemical energy conversion. The principles of interaction between local reactants and material environments have been applied successfully in the development of system models simulating the kinetic as well as the dynamic characteristics for the two combined processes of synthetic fuel extraction from organic refuse coupled with the generation of electric energy through the biochemical fuel cell.

The process of biochemical fuel conversion is secured from the organic prepared refuse through digestion with anaerobic bacteria, generating multigrades of unsaturated as well as saturated hydrocarbon of the order of $C_mH_{2m+2}$ (m is the hydrocarbon order). Then the following operation of electric power output is accomplished by electrochemical conversion where synthetic hydrocarbon is injected as fuel to the cell anode, preheated air as an oxidizer to the cathode, where both will interact through an organic electrolyte such as potassium hydroxide.

Modeling methodology for the processes of fuel extraction and electric power generation is a very effective tool for synthesizing the kinetics as well as the dynamics of various energy functions for every reactant involved up to final outputs. Mathematical synthesis of energy functions through modeling will define clear physical realization in practice for the total process.

For the practical and feasible economic development of the bioelectrochemical fuel cell as a reliable energy conversion mechanism, methodology of mathematical modeling of generalized energy functions are developed for the ultimate purpose of total physical realization of extracting electric energy from refuse.

The modeling methodology is based on generalized functional realizations of various biochemical as well as electrochemical reactions in the complex frequency domain, for the condition of simple order and multiple order of energy functions, as well as other kinetic and dynamic parameters.

The energy functions and reaction parameters are

1. Concentration of organic fuel.
2. Order of biochemical and electrochemical equivalence of potential reactions.
3. Energy content function of the extracted synthetic fuel entropy, enthalpy, and temperature.
4. Status of the cell terminal electric potential.

# IV. STAGES OF ENERGY CONVERSION*

## A. CONVERSION OF PREPARED REFUSE TO SYNTHETIC FUEL

### 1. First Order and Finite Number of Poles in the Transform of Energy Functions

For equations 4.16 and 4.17, let

$U$ = maximum energy content per mole extracted from synthetic fuel through interaction of prepared refuse with environmental continuum.

$W_c^i$ = maximum energy change per mole due to variation i of chemical composition of ith reactant of prepared refuse.

$W_c^o$ = maximum energy change per mole developed from prepared refuse.

* © 1979. Reprinted with permission from Denno, K., Modeling of bio-electro-chemical conversion of refuse to energy, Proc. 2nd Int. Conf. Math. Modeling, University of Missouri, Rolla, 1979, 1031—1040.

m = chemical order of synthetic fuel ($C_mH_{2+2M}$).
T = absolute temperature.
N = functional order of bioelectrochemical equivalence of potentials.
$n_i$ = concentration function of ith reactant.
H,Q = enthalpy and entropy functions, respectively.

The equation linking the production of synthetic fuel to prepared energy content obtained in previous work[18-20] is

$$\frac{\partial U}{\partial t} = \frac{\partial H}{\partial t} - T_o \frac{\partial Q}{\partial t} + n_i \frac{\partial W_c}{\partial t}\left( W_c^o + RT_o \ln \frac{M}{m} \right) \frac{\partial n_i}{\partial t} \tag{4.16}$$

Then from Equation 4.16, the transformed relationship in the complex frequency domain is

$$\frac{U(S)}{n(S)} = \frac{S}{n(S)} H(S) - T_o Q(S) + SRT_o \ln \frac{M}{m} + \sum_{k=1}^{P} \frac{C_1(S_{k1}) C_2(S - S_{k1})}{D_1'(S_{k1}) D_2(S - S_{k1})} (2S - S_k) \tag{4.17}$$

where $S_k$ are poles of

$$W_c^o(S) = \frac{C_2(S)}{D_1(S)}$$

and

$$n(S) = \frac{C_1(S)}{D_2(S)}$$

**2. Multiple Order and Finite Number of Poles in the Transform of Energy Functions**

Let each energy function in the time domain be single valued almost everywhere for t >/0 and proceed according to the following rule:

$$\mathcal{L}\left[ f_1(t) \cdot f_2(t) \right] = \sum_{k=1}^{P} \sum_{j=1}^{m_k} \frac{(-1)^{m_k - j_k} kj}{(m_k - j)!} \frac{d^{m_k - j}}{dS^{m_k}} F_2(s) \tag{4.18}$$

where

$$K_{kj} = \frac{1}{(j-1)!} \left[ \frac{d^{j-1}}{dS^{j-1}} (S - S_k)^{m_k} \cdot F(s)_1 \right], \tag{4.19}$$

P = number of poles in $F_1(s)$, and $m_k$ = order of pole $S_k$.

Then from Equations 4.16, 4.18, and 4.19, a mathematical model in the transform domain relating energy content in the output synthetic fuel with respect to the concentration function of the ith reactant is expressed below:

$$U(S) - H(S) + T_o Q(S) = \frac{1}{S} \sum_{k_1=1}^{P_1} \sum_{j_1=1}^{m_{k1}} \frac{(-1)^{m_{k1} K} K_{kj1}}{(m_{k1} - j_1)!} \frac{d^{m_{k1} - j_1}}{dS^{m_{k1} - jl}} \rightsquigarrow (S) \downarrow \tag{4.20}$$

$$S = S - S_k$$

where

$$K_{kj1} = \frac{1}{(J_1 - 1)!} \frac{d^{j_1 - 1}}{dS^{j_1 - 1}} (S - S_{k1})^{m_{k1}} S W_c^i(S) \Big\downarrow_{S = S_{k1}} \tag{4.21}$$

and

$$(S) = \sum_{k_2=1}^{P_2} \sum_{j_2=i}^{m_{k2}} \frac{(-1)^{m_{k2} - j2} K_{kj2}}{(m_{k2} - j2)!} \left[ \frac{d^{m_{k2} - j2}}{dS^{m_{k2} - j2}} \right] n(S) \Big\downarrow_{S = S - S_{k2}} \tag{4.22}$$

$$K_{kj2} = \frac{1}{(J2 - 1)!} \left[ \frac{d^{j2-1}}{dS^{j2-1}} (S - S_{k2})^{m_{k2}} S\, n\,(S) \right] \Big\downarrow_{S = S_{k1}} \tag{4.23}$$

$P_1$ = number of poles in $\frac{\partial W_c^i}{\partial t}$ with order $m_{k1}$, and $P_2$ = number of poles in $\frac{\partial n}{\partial t}$ with order $m_{k2}$.

Then from Equation 4.20,

$$\int \cdots \int_{m_{k1} - j1} S[U(S) - H(S) + T_o Q(S)] ds = \sum_{k_1=1}^{P_1} \sum_{j_1=1}^{m_{k1}} \frac{(-1)^{m_{k1} - j1}}{(m_{k1} - j1)!} \left[ K_{kj1}\, \omega - \int_1 \cdots \int_{m_{k1} - j1} \omega dK_{kj1} \right] \tag{4.24}$$

and from Equation 4.22,

$$\int_1 \cdots \int_{m_{k2} - j_2} \omega(S) dS = \sum_{k2=1}^{P_2} \sum_{j2=1}^{m_{k2}} \frac{(-1)^{m_{k2} - j2}}{(m_{k2} - j2)} \left[ n K_{jk2} - \int_1 \cdots \int_{m_{k2} - j1} n dK_{kj2} \right] \tag{4.25}$$

From Equations 4.24 and 4.25, an implicit transformation model for the concentration function in terms of thermal energy functions, including the output fuel energy content as well as reaction parameters, can be obtained.

## B. BIOELECTROCHEMICAL CONVERSION OF SYNTHETIC FUEL*

### 1. First Order and Finite Number of Poles in the Transform of Energy Functions

The bioelectrochemical reactions are as follows.

At the anode:

* © 1979. Reprinted with permission from Denno, K., Modeling of bio-electro-chemical conversion of refuse to energy, Proc. 2nd Int. Conf. Math. Modeling, University of Missouri, Rolla, 1979, 1031—1040.

$$\frac{1}{2}CH_2O_{\downarrow} + 2OH\frac{1}{2}CO_2 + \frac{3}{2}H_2O + 2e \text{ biofuel}$$

At the cathode:

$$\frac{1}{2}O_2 + H_2O \rightarrow 2OH - 2e \tag{4.26}$$

The overall reaction is

$$\frac{1}{2}CH_2O + \frac{1}{2}O_2 \rightarrow \frac{1}{2}CO_2 + \frac{1}{2}H_2O$$

The linking partial differential equation for the total reactions in the time domain is

$$\frac{\partial U}{\partial t} = T\frac{\partial Q}{\partial t} - F\left[(n+N)\frac{\partial E}{\partial t} + E\frac{\partial n}{\partial t} + \frac{\partial N}{\partial t}\right] \tag{4.27}$$

where F = Faraday's constant and E = biocell electric terminal potential function.

$$n = \sum_{i=1}^{n'} n_i \tag{4.28}$$

where $n_i$ = concentration of ith reactant, $n_i$ = concentration function of the biosynthetic fuel, $n_2$ = concentration of oxygen or preheated air, and $n'$ = number of reactants.

From Equation 4.27, the transformed model in the (S) domain is expressed as

$$\frac{E(S)}{U(S)} = G - \frac{U_o/S}{U(S)}G + \frac{E_o/S}{U(S)}G' - \frac{1/FS}{U(S)}G'' \tag{4.29}$$

where $U_o$, $E_o$ = initial values for the biofuel energy content and the fuel cell terminal potential, respectively, and G,G',G'' = transform closed loop feedback functions in the (s) domain.

$$E(S) = \frac{E_o}{S} - \sum_{i=1}^{m'} \Delta\frac{E_o}{S}\, e^{-n\Delta ts} \tag{4.30}$$

where e(t) is assumed to be a stepping down constant function with each decrement of $\Delta E_o$ in $\Delta t$.

**2. Multiple Order and Finite Number of Poles in the Transform of Energy Functions and Reaction Parameters**

If Le'(t) is a rational function of $p_3$ number of poles and order $m_{k3}$, and also the e(t) is a rational function of $p_4$ number of poles and order $m_{k4}$, then from Equation 4.27,

$$\sum_{k3,k4=1}^{P3,p4} \sum_{j3,j4=1}^{m_{k3},m_{k4}} \frac{(-1)^{m_{k3}-j_3}K_{k3,4^{-j_{3,4}}}}{\left(m_{k3},m_{k4}-j_{3,4}\right)} \frac{d^{m_{k3}-j_3}}{dS^{m_{k3}-j_3}} \left[n(S)+N(s)\right]_{S=S-S_{k1}} \tag{4.31}$$

Equation 4.31 is valid for $m_{k3}\text{-}j_3 < m_{k4}\text{-}j_4$ where

$$K_{k3,j3} = \frac{1}{(j3-1)!}\left[\frac{d^{j3-1}}{dS^{j3-1}} S - S_{k3}\, m_{k3} \cdot SE(S)\right]_{S=S_{k3}} \tag{4.32}$$

$$K_{k4,j4} = \frac{1}{(j4-1)!}\left[\frac{d^{j4-1}}{dS^{j4-1}} S - S_{k4}\, m_{k4} \cdot E(S)\right]_{S=S_{k4}} \tag{4.33}$$

Equation 4.31 is an implicit transformation model in the complex frequency domain for the combined reaction functions of n(S) and N(S). Also a solution or a mathematical model function for [N(S) + n(S)] could be written as

$$\int\cdots\int\left[SU(S) - \mathcal{L}TQ'^{ds} = \sum_{k3,k4=1}^{P3,p4} \sum_{j3,j4=1}^{m_{k3},m_{k4}} (-1)\frac{m_{k3,4}-j_{3,4}}{(m_{k3},m_{k4}-j_{3,4})}\right.$$

$$\left.\begin{matrix} K_{k3,j3} \\ k4,j4 \end{matrix}(n+N) - \int\cdots\int_{m_{k3}-j_3} (n+N)dK_{\begin{matrix} k3,j3 \\ k4,j4 \end{matrix}}\right] \tag{4.34}$$

Indeed Equation 4.34 is almost explicit in identifying the (n + N) function in terms of thermal energy functions of the output synthetic fuel energy content.

## V. CRITERION FOR OVERALL CONVERSION OF PREPARED REFUSE TO ELECTRIC POWER*

The common link between the two processes of synthetic fuel extraction from refuse and that of securing electric power is the amount of energy fuel content. Therefore, substituting in Equation 4.31 the term of fuel energy content from Equation 4.20, the following integro-differential equation in the complex frequency domain is the generalized criterion for the overall bioelectrochemical energy conversion setting the required constraint among various reactants such as concentration, equivalent order of electrochemical potentials, variations in chemical compositions on one side, and thermal energy functions on the other side. The generalized relationship is

$$\left[SH - ST_oQ + \sum_{k_1=1}^{P_1} \sum_{j_1=1}^{m_{k1}} \frac{(-1)^{m_{k1}-j_1} K_{kj1}}{(m_{k1}-j_1)!}\left(\frac{d^{m_{k1}-j1}}{dS^{m_{k1}-j1}}\right)\right] - \mathcal{L}TQ' =$$

$$\sum_{k3,k4=1}^{P3,p4} \sum_{j3,j3=1}^{m_{k3},m_{k4}} \frac{(-1)^{m_{k3,4}-j_{3,4}} K_{k-j_{3,4}}}{(m_{k3},m_{k4}-j_{3,4})3,4}\left(\frac{d^{m_{k3}-j_3}}{dS^{m_{k3}-j_3}}\right)(n+N) \tag{4.35}$$

* © 1979. Reprinted with permission from Denno, K., Modeling of bio-electro-chemical conversion of refuse to energy, Proc. 2nd Int. Conf. Math. Modeling, University of Missouri, Rolla, 1979, 1031—1040.

Equation 4.35 is valid for the case of a finite number of poles and of arbitrary multiplicity in the thermal energy functions, as well as for all reaction parameters.

Returning to the case of simple poles of arbitrary order, the generalized constraint could be set up by substituting the transform of the hydrocarbon fuel energy from Equation 4.17 into Equation 4.29, resulting in a transform of the relatively simple relationship between the biocell terminal electric potential and the reactant concentration function.

In order for bioelectrochemical energy conversion from organic refuse to become practically realizable for the generation of bulk electric power, more reliable information for the kinetic and dynamic characteristics for all stages of reactions has to be established.

Mathematical modeling for the processes of conversion from prepared organic refuse to pure synthetic fuel, followed by the electrochemical performance of the biocell for the generation of electric power, revealed extremely reliable constraints and feasibility conditions on various thermal energy functions with respect to reactants properties.

The methodology for securing useful mathematical models is based physically on the principle of pure interaction between various local bioelectrochemical reactants and material environments, while mathematically it is centered on the existence of the number of poles and their order in the transforms of thermal energy functions, as well as the reactant properties.

Mathematical models in the form of simple transforms as well as transformable integro-differential equations will be secured for the following:

1. Conversion of prepared organic refuse to synthetic fuel for the existence of a simple pole and multiple poles of any arbitrary order in the transform of thermal energy functions, as well as in parametric functions such as reactant concentration, temperature, and electrochemical order of potential reactions.
2. Conversion through the bioelectrochemical cell of the synthetic hydrocarbon fuel to bulk electric power output for the case of a simple pole, as well as multiple poles of any arbitrary order in the transform of thermal energy functions, and all parametric functions characterizing the kinetic as well as dynamic properties of reactants.
3. From 1 and 2, a unified mathematical model in the form of a transformable integro-differential equation in the complex frequency domain will then be established linking the generation of bulk electric energy output to the thermal, kinetic, and dynamic properties of the organic prepared refuse and various internal energy functions.
4. Reduction in poles multiplicity leads to a simpler mathematical model for every process of conversion and faster physical realization for an equivalent circuit model and stable steady state operation.

## VI. MODELING OF ALTERNATIVE PLANS FOR FUEL PRODUCTION AND STORAGE*

Alternative renewable energy systems for generation, storage, and transport which can be implemented without limit include conventional fuel cells, redox flow cells, solar cells, bioelectrochemical cells, and ocean thermal energy systems.

This paper undertakes direct utilization of direct energy systems for the storage of electric power in chemical form, which includes the recharging of the redox flow cell, conversion of prepared refuse to multigrades of hydrocarbon, and the production of hydrogen and ammonia through ocean thermal energy conversion (OTEC) plantship.

A working model has been established for the recharging of the redox flow cell for the

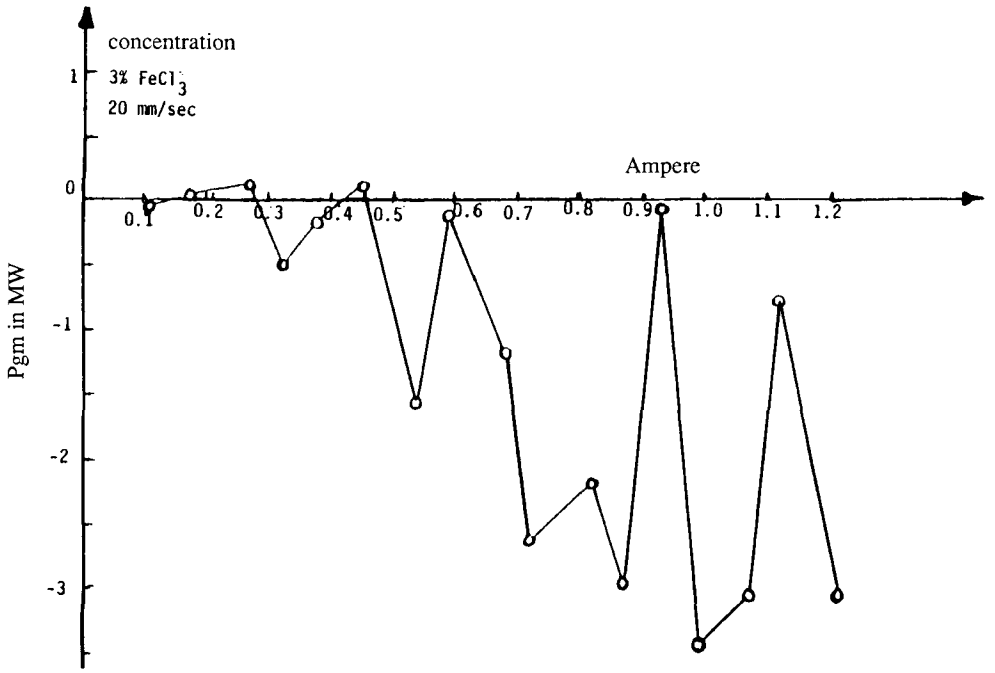


FIGURE 4.1 Tow tank redox flow cell. (From Thaler, L., Electrically Rechargeable Redox Flow Cells, NASA-TM-X-71540, Lewis Research Center, Cleveland, OH, 1974. With permission.)

conversion of ferrous catholyte fluid into ferric–solution in terms of local pressure and temperatures concentration of reactants and products.

For production of synthetic fuel from prepared refuse, specific solutions for molar energy content have been obtained under a variety of local conditions such as enthalpy, entropy, concentration, and standard energy release due to an environmental exerting interaction.

## VII. RECHARGE ELECTROCHEMICAL EQUATIONS

The process of electrochemical oxidation of ferrous solution to ferric–liquid of a ferromagnetic fluid implies the storage of electrical energy input in a stable chemical form 9 (see Figure 4.1).

The equations of the reaction are

$$Ti^{=4} + e \rightarrow Ti^{+3} \qquad \text{at the anolyte}$$

and

$$FE^{+2} \rightarrow e + Fe^{+3} \qquad \text{at the catholyte}$$

In terms of reactants activities:

$$P^{a'}_{Fe^{+2}} \rightarrow P^{b'}_{e} + P_{Fe^{+3}}$$

$$P^{a'}_{Ti^{+4}} + P^{b'}_{e} \rightarrow P^{c'}_{Ti} + 3$$

where a, b, and c, as well as a′, b′, and c′, are concentrations of reactants and products, respectively.

The associative electrothermal equation is

$$\Delta E_{Fe} = \frac{RT_{Ti}}{n_{Fe}} \ln \frac{P_{Fe^{+2}}}{P_e - P_{Fe^{+3}}} \tag{4.36}$$

Similarly, for the anolyte channel of Ti solution,

$$\Delta E_{Ti} = \frac{RT_{Ti}}{n_{Ti}} \ln \frac{P_{Ti^{+4}} R_e}{P_{Ti^{+3}}} \tag{4.37}$$

where $\Delta E_{Fe}$ = voltage differential at the catholyte channel, and $\Delta E\tau_i$ = voltage differential at the anolyte channel.

$FeCl_2 + Cl^- = FeCl_3 + e$, $TiCl_4 + e = TiCl_3 + Cl^-$, and the total equation of the reaction is

$$FeCl_2 + TiCl_4 \rightarrow FeCl_3 + TiCl_3$$

$$P_{Fe}^a + 2 \rightarrow P_e^b + P_{Fe}^c + 3$$

$$P_{Ti^{+4}}^{a'} + P_e^b \rightarrow P_{Ti^{+4}}^{c'}$$

Hence, from the above electrochemical equations, we can proceed to state the following:

$$\Delta E_{net} = \frac{RT}{n} \ln \frac{P_{FeCl_2} P_{TiCl_3}}{P_{FeCl_2} P_{TiCl_4}} \tag{4.38}$$

Electric DC power input $P_{DC}$

$$P_{DC} = JA \frac{RT}{\Gamma n} \ln \frac{P_{FeCl_3} P_{TiCl_3}}{P_{FeCl_2} P_{TiCl_4}} \tag{4.39}$$

Now with the introduction of the following thermoelectrochemical equations:

$$PV = RT \tag{4.40}$$

$$\Delta G = G - G_o = RT \ln \frac{P}{P_o} \tag{4.41}$$

$$G = V_i + PV - TS \tag{4.42}$$

where R = universal fluid constant, G = Gibbs free energy or maximum electrical energy released per kilogram-mole, $G_o$ = Gibbs energy at standard pressure and temperature (SPT), $V_i$ = internal energy, P,T,S = pressure, temperature, and entropy, respectively, V = volume of catholyte or anolyte channel, and $P_o$ = 1 atm.

Using the above relationships, Equation 4.41 can be rewritten as:

$$G = RT \ln P \tag{4.43}$$

Electrochemical, as well as thermodynamic, interactions throughout the recharge process could be totally orderly with the absence of any entropy or more likely the combination of orderly and disorderly with the presence of entropy and release of both electrical and thermal energies.

The first is the general case of combined orderly and disorderly energy release and with

$$\partial G + V\partial P - S\partial T \tag{4.44}$$

A general criterion linking the electrical and thermodynamic characteristics of the recharging process of the redox flow cell, where the input electrochemical couples are $FeC1_2$ and $TiC1_4$ excited with a locally present electric DC input power ($P_{DC}$), while the output is $FeC1_3$ and $TiC1_3$, has been derived and expressed by the following mathematical model:

$$\ln\left[P_{FeCl_3}P_{TiCl_3}\right]^{R-S} = \ln\left[P_{FeCl_2}P_{TiCl_4}\right]^{(R-S)} + \frac{n\Gamma P_{pc}}{JAV^2T_m} \tag{4.45}$$

The second case is for the orderly energy release confined to the involvement of electrical form of energy only, where S = 0, criterion Equation 4.45 becomes,

$$\ln\left[P_{FeCl_3}P_{TiCl_3}\right]^{R} = \ln\left[P_{FeCl_2}P_{TiCl_4}\right]^{R} + \frac{n\Gamma P_{pc}}{JAV^2T_m} \tag{4.46}$$

The third case is in between the preceding two cases, that is, the modified adiabatic expansion case, i.e.,

$$\frac{T_o}{T_i} = \left(\frac{P_o}{P_i}\right)^{k\left(\frac{\gamma-1}{\gamma}\right)} \tag{4.47}$$

where $k = v_L/V_{o.c.}$, and $v_L$, $V_{o.c.}$ = load terminal voltage and open-circuit voltage, respectively. If

$$P_{FeCl_3} = P_{TiCl_3} = P_o \tag{4.48}$$

$\therefore$

$$P_{FeCl_2} = P_{TiCl_4} = P_i \tag{4.49}$$

The criterion obtained in Equation 4.45 becomes:

$$\frac{\alpha(R-S)}{k(\alpha-1)}\ln\frac{T_o}{T_i} = \frac{n\Gamma}{JAV^2T_m}P_{DC} \tag{4.50}$$

where $T_o$ = working temperature of produced ferric-fluid, $T_i$ = working temperature of the input ferrous fluid, $P_{DC}$ = direct current input recharging power, and $\alpha = C_p/C_v$.

To enhance effectiveness of the recharging process of the redox flow cell for energy storage, a set of experiments has been conducted on samples of ferricchloride solutions of different concentrations and with a flow velocity of 20 mm/s. Plots for the patterns of gyromagnetic resistance and power absorbed are shown in Figures 4.2 through 4.4.

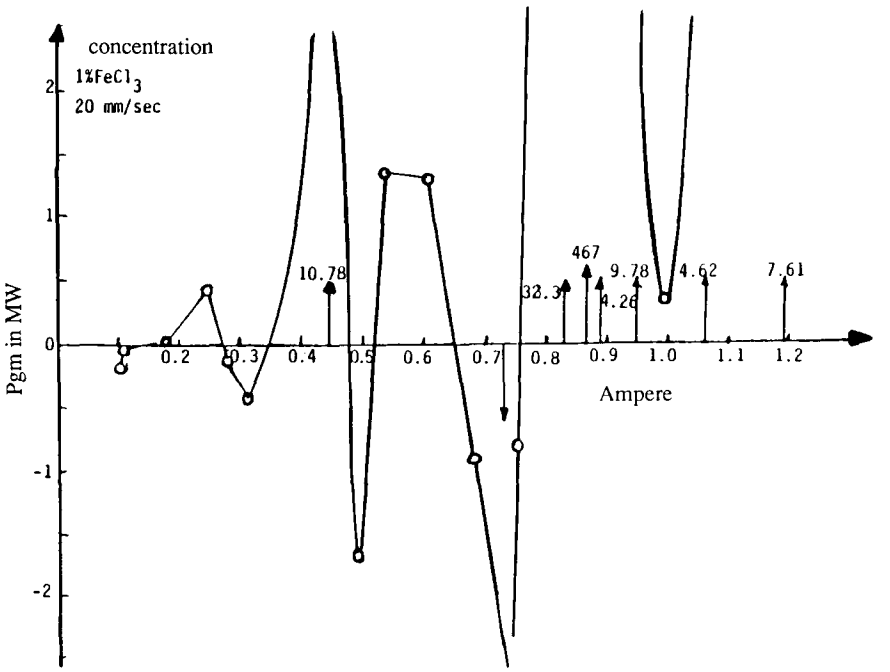


FIGURE 4.2 Magnetization power of ferro-fluids.

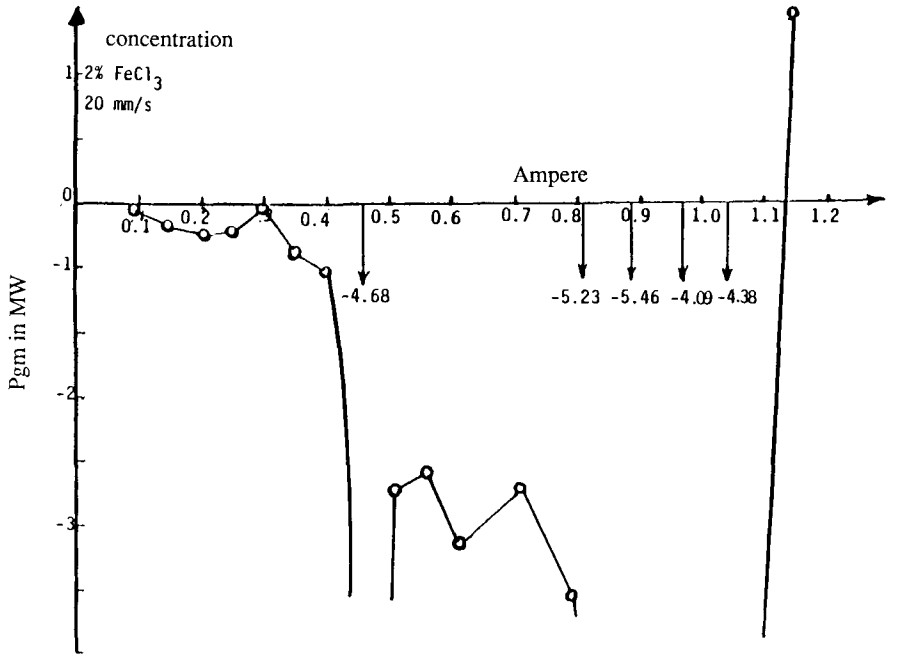


FIGURE 4.3 Magnetization power of ferro-fluids.

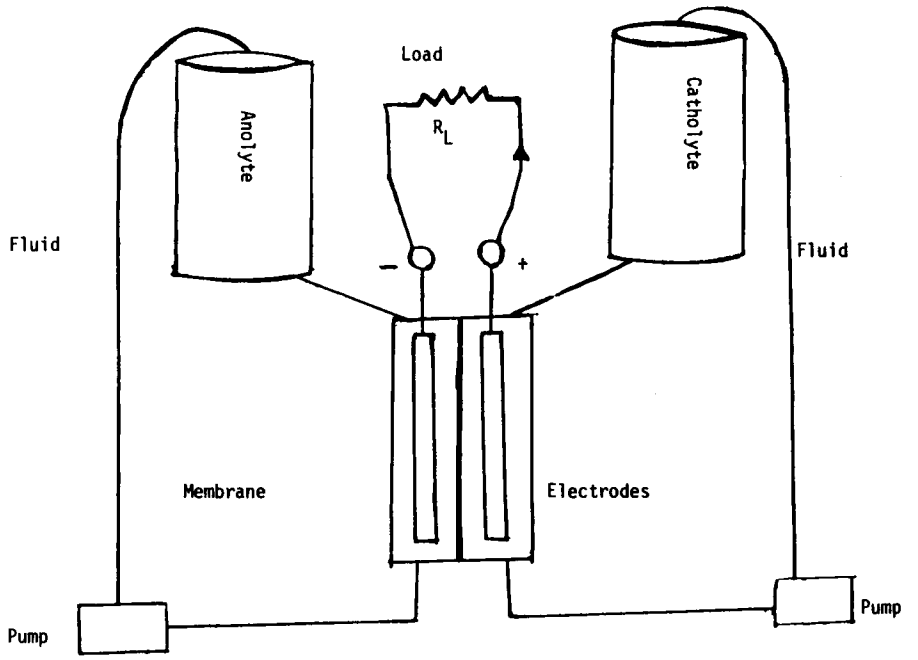


FIGURE 4.4 Magnetization power of ferro-fluids.

## VIII. SYNTHETIC FUEL FROM PREPARED REFUSE*

Interaction of prepared organic refuse with oxidizing environmental elements will result in the production of hydrocarbon fuel of the order $C_mH_{2m+2}$.

Let $W_c^o$ = maximum energy developed per mole in functional form, m = order of the hydrocarbon fuel = 1,2,3 --- N, U = maximum energy content per mole extracted from synthetic fuel in functional form, T = absolute temperature, H,Q = enthalpy and entropy functions for reactants and products, $n_i$ = concentration function of ith reactant, and $w_c$ = maximum energy change per mole due to variation in chemical composition of ith reactant of refuse.

The differential equation linking electrical, thermal, and chemical interactions is expressed as follows:

$$\frac{\partial U}{\partial t} = \frac{\partial H}{\partial t} - T_o \frac{\partial Q}{\partial t} + n_i \frac{\partial W_c}{\partial t}\left(W_c^o + RT_o \ln \frac{M}{m}\right)\frac{\partial n_i}{\partial t} \tag{4.51}$$

Solutions of Equation 4.51 under different and distinct functional forms for H(t), Q(t), Wc(t), and n(t) are listed as follows:

**Case A** — Orderly and disorderly reaction where ni(t), H(t), Q(t), and Wc(t) are each a constant and sustained function.

The solution of U(t) representing the energy content of $C_mH_{2\,m+2}$ is expressed as follows:

$$U(t) = H\delta(t) + \left(nRT_o \ln_m^M + 2n^2 W_c^{i^2}\right)U - 1(t) - T_o Qnt \tag{4.52}$$

* © 1982. Reprinted with permission from Denno, K., Modelling of Alternative Plans for Fuel Production and Storage, *Symp. Proc. Energy Modelling II, Planning for Energy Disruptions*, sponsored by Institute of Gas Technology, Chicago, IL, 1982, 664—680.

where R = universal gas constant, $T_o$ = reference temperature of reaction, M = constant of reaction, and d(t) = Delta-dirac function.

Time of reaction must not exceed $t_\infty$.

$$t_\infty = \left( nRT_o \ln \frac{M}{m} + 2n^2 W_i^o \right) \Big/ T_o Qn \tag{4.53}$$

**Case B** — Orderly and disorderly reaction where n(t) = nt, $W^i = W_c t$ sustained linear increase for each function at all times, H(t) = Ht, and Q(t) = Qt,

The solution of U(t) for $C_m H_{2m+2}$ is:

$$U(t) = HU_{-1}(t) + \frac{1}{6}\left(n^2 W_c^2 - T_o Qn\right)t^3 + RnT_o \ln \frac{M}{m} U_{-1(t)} \tag{4.54}$$

The time of reaction must not exceed $t_\infty$.

$$t_\infty = \frac{6\left[H + nRT_o \ln \frac{M}{m}\right]^{\frac{1}{3}}}{n^2 W_c^2 - T_o Qn} \tag{4.55}$$

**Case C** — Orderly and disorderly reaction where n(t) = nt and $W^i = W_c t$ which are sustained linear increase and $H(t) = HU_{-1}(t)$ and $Q(t) = QU_{-1}(t)$.are sustained constant values.

The solution of U(t) is

$$U(t) = HU_{-1}(t) - T_o Qn \frac{t^2}{2} + RnT_o \ln \frac{M}{m} U_{-1}(t) + \frac{W_c^2 n^2}{6} t^3 \tag{4.56}$$

To ensure orderly stability, reaction time must not exceed $t_\infty$ where

$$t_\infty = \frac{6\left[H + nRT_o \ln \frac{M}{m}^{\frac{1}{3}}\right]}{W_c^2 n^2}$$

**Case D** — Orderly reaction only, i.e., Q = 0, and $n(t) = nU_{-1}(t)$, $H(t) = HU_{-1}(t)$, and $W_c = WcU_{-1}(t)$ are all sustained functions.

The solution of U(t) is as follows:

$$U(t) = \left[H + nRT_o \ln \tfrac{M}{m}\right] U_{-1}(t) + 2n^2 W_c t \tag{4.57}$$

Time of reaction must not exceed $t_\infty$, where

$$t_\infty = \left[H + nRT_o \ln \tfrac{M}{m}\right] \Big/ 2n^2 W_c$$

**Case E** — Orderly and disorderly reaction where $n(t) = ne^{-at}$, $W^i = W_c e$, $H(t) = He^{at}$, and $Q(t) = Qe^{-at}$.

The solution of U(t) is

$$U(t) = \left(\left[H + nT_oR \ln \frac{M}{m}\right] + \left[\delta(t) - \delta(o)e^{-at} - atU_{-1}(t) + a^2t^2\right] + \left[anW_c - nQT_o - 2an^2W_c^2\right] + te^{-at} + 2n^2W_ce^{-at}\right) \quad (4.58)$$

For an orderly reaction where Q = 0,

$$U(t) = \left(\left[H + nT_oR \ln \frac{M}{m}\right] + \left[\delta(t) - atU_{-1}(t) + a^2t^2\right] + \left[anW_c - 2an^2W_c^2\right] + te^{-at} + 2n^2W_ce^{-at}\right) \quad (4.59)$$

To ensure stability of orderly, reaction time must not exceed $t_\infty$.

$$t_\infty = \frac{a \pm \sqrt{a^2 + 4a^2k^2}}{2a^2} \quad (4.60)$$

where

$$k^2 = \frac{2an^2W_c^2 - anW_c}{H + nRT_o \ln \frac{M}{m}} \quad (4.61)$$

## IX. PRODUCTION OF $H_2$ AND $NH_3$*

Hydrogen, ($H_2$) is produced through the endothermic decomposition of ocean water using thermal energy input from OTEC plant. Then $NH_3$ is produced by combining $H_2$ and $N_2$, which is realized from the process of air liquification.

From previous work[10] carried out by this author, the molar concentration of $H_2$ obtained from the endothermic and the conventional electrolysis of water is

$$M_c = \frac{\eta OH \eta 1H^{E_oE_2}}{H_{2h}} + \frac{\eta_4}{\eta_3 H_{2h}(Q_1 + Q_2)} \quad (4.62)$$

where $H_{2h}$ = molar enthalpy change for combined endothermic and conventional electrolysis; $\eta OH = E_1/E_o$ for $H_2$; $\eta 1H = E_2/E_1$ for $H_2$; $\eta_3 = Q_4/Q_1 + Q_2$; $\eta_4 = H_{2h} P_{22}/Q_4$; $E_o$ = total energy input into OTEC plant; $E_1$ = energy output from OTEC plant; $E_2$ = energy content from endothermic process; and $Q_1$, $Q_2$ = heat rejection of OTEC and endothermic electrolysis, respectively.

$$Q_3 = Q_1 + Q_2 \quad (4.63)$$

$Q_4$ = energy content of conventional electrolysis output.

$$P_{22} = \frac{\eta_4}{\eta_3 H_{2h}(Q_1 + Q_2)} \quad (4.64)$$

* © 1982. Reprinted with permission from Denno, K., Modelling of Alternative Plans for Fuel Production and Storage, *Symp. Proc. Energy Modelling II, Planning for Energy Disruptions*, sponsored by Institute of Gas Technology, Chicago, IL, 1982, 664—680.

And then for released $NH_3$ molar concentration

$$M_{NH_3} = \eta_{OH}\eta_{kH}\eta_{1H}E_oE_2 + \frac{\eta_4}{\eta_3(Q_1 + Q_2)} \tag{4.65}$$

For safeguards against the impacts of energy supply disruptions, alternative domains of storage during availability and low demand periods are presented in this section as follows.

AC electric power after rectification could be stored in chemical form through recharging of the redox flow cell. The recharging process will exert the cycle of oxidation on the ferrous solution in the catholyte to the ferric phase while the anolyte fluid will reduce the $TiC1_4$ into $TiC1_3$ solution.

Analytical as well as experimental criteria for the recharging reactions of the oxidation-recharging process through the application of available electric energy have been derived and demonstrated. Also, a special state for disorderly and orderly reaction have been considered in connection with modified adiabatic expansion.

Production of synthetic fuel hydrocarbon $C_mH_{2m+2}$ is realized by extracting prepared organic refuse through interaction with external environmental forces. The solutions in the time domain have been established for the molecular energy content of extracted synthetic fuel with respect to several kinds of thermally exciting functions. Duration of feasible reactions are presented for every case.

Thermal and electric energies could be used effectively in conjunction with OTEC heat energy to reproduce $H_2$ through the endothermic and the conventional electrolysis of water, as well as the production of ammonia with nitrogen obtained from liquified air.

## X. OPTIMUM SCHEDULING OF GENERATION FOR CENTRAL BIOCHEMICAL POWER PLANTS*

Let $F_{i1}$ = cost of conversion of prepared refuse into synthetic fuel, namely $C_mH_{2m+2,}$ where m = the hydrocarbon order, $F_{i2}$ = cost of partial or total oxidation of the hydrocarbon fuel by oxygen or preheated natural gas such as to $C\,H_2O$ in dollars per hour ($/h). $F_i$ = cost effective of potential fuel for the bioelectrochemical cell.

$$F_i = F_{i1} + F_{i2} \quad (\text{in dollars per hour}) \tag{4.66}$$

Also let each plant be characterized by the following:

a = location of the generating sources
b = output of each generating source within its range or capacity
c = fuel cost and the rate of consumption
d = characterization of voltage magnitude and its phase angle

The coordination equation for optimum scheduling of generation is expressed by

$$\frac{\partial F_i}{\partial P_i} + \lambda\frac{\partial P_L}{\partial P_i} = \lambda \tag{4.67}$$

* © 1982. Reprinted with permission from Denno, K., Modelling of Alternative Plans for Fuel Production and Storage, *Symp. Proc. Energy Modelling II, Planning for Energy Disruptions*, sponsored by Institute of Gas Technology, Chicago, IL, 1982, 664—680.

Constraint equations associated with Equation 4.67 are

$$(P_1, P_2 \cdots P_a) = \sum_i^n P_1 - P_L - P_r = 0 \tag{4.68}$$

where

$$P_L = \sum_i \sum_j P_i B_{ij} P_j, \tag{4.69}$$

$P_L$ = total transmission loss for a centralized system in megawatts and $\lambda$ = cost of received power in dollars per megawatt hour.

Similar to Chapter 1,

$$P_j = \phi_1(P_i) \tag{4.70}$$

$$B_{ij} = \phi_2(P_i) \tag{4.71}$$

where $B_{ij}$ is any element of the transmission loss coefficient matrix shown in Equation 4.71.

Also,

$$\frac{\partial F_i}{\partial P_i} = F_{ii} P_i + f_i \tag{4.72}$$

where $F_{ii}$ = slope of the incremental fuel cost curve for the bioelectrochemical central plant, and $f_i$ = incremental cost of plant i at no-load.

The solution of Equation 4.67 subject to all constraints expressed in Equations 4.68 to 4.72 will lead to an expression for $B_{ij}$, as indicated in Reference 16 and written as follows:

$$B_{ij} = \left[-F_{ii}F_{jj}P_iP_j + \left(\lambda F_{ii} - F_{ii}f_j\right)P_i + \left(\lambda F_{jj} - F_{jj}f_i\right)P_j + \left(\lambda f_i + f_j - f_i f_j - ^2\lambda\right)\right]$$

$$\left[2\lambda F_{ii}P_i^2 + 2\lambda F_{jj}P_j^2 + \left(2\lambda f_i - 2_\lambda^2\right)P_i + \left(2\lambda f_j - 2_\lambda^2\right)P_j\right] \tag{4.73}$$

## XI. OPTIMUM SCHEDULING OF POWER GENERATION IN A DISPERSED BIOCHEMICAL PLANT*

The topographical layout of a set of dispersed bioelectrochemical energy systems is visualized as having a number of dispersed plants, coupled among themselves by an electromagnetic power coupling coefficient $M_{ij}$ and every plant being subjected to an optimal power levelling balance. $P_L\Delta$ megawatts, where

$$P_m = \sum_i^N \sum_j^N P_i M_{ij} B_j \tag{4.74}$$

* © 1982. Reprinted with permission from Denno, K., Modelling of Alternative Plans for Fuel Production and Storage, *Symp. Proc. Energy Modelling II, Planning for Energy Disruptions*, sponsored by Institute of Gas Technology, Chicago, IL, 1982, 664—680.

$$\Delta P_L = k\sqrt{P_m} \tag{4.75}$$

In Equation 4.74, $P_M$ could be realized physically as total power accumulation due to electromagnetic linkage for balanced power allocation among all bioelectrochemical plants. Mathematically, $P_M$ is very compatible to $P_L$, the total transmission losses due to a set of interconnected central power plants.

Regarding $\Delta P_L$, identified as the optimal power levelling balance to ensure compatible power allocation, it could be positive or negative, i.e., that particular plant may in effect receive or deliver power in order to accomplish an optimum dispersed system.

The new coordination equation for the dispersed bioelectrochemical set of power plants is:

$$\frac{\partial F_i}{\partial P_i} + \lambda \frac{\partial P_l}{\partial P_i} + \lambda \frac{\partial P_m}{\partial P_i} = \lambda \tag{4.76}$$

where $\lambda$ = cost of power delivery in dollars per megawatt hour.

Also, as indicated earlier,

$$F_i = F_{i1} + F_{i2} \tag{4.77}$$

which is the total fuel cost at plant i in dollars per hour and

$$\frac{\partial F_i}{\partial P_i} = F_{ii} P_i + F_i \tag{4.78}$$

Also, it is useful for the sake of completeness to restate the constraint equations associated with the coordination Equation 4.76.

$$P_j = \psi_1(P_i) \tag{4.79}$$

$$M_{ij} = \psi_2(P_i) \tag{4.80}$$

$$\Delta P_L = \psi_3(P_i, M_{ij}, P_j) = kP_M \tag{4.81}$$

$$P_m = \psi_4(P_i, M_{ij}, P_j) \tag{4.82}$$

and

$$\psi(P_1, P_2 \ldots P_n) = \sum_i P_i - P_m - \Delta P_L - P_r = 0 \tag{4.83}$$

The solution of the coordination equation under its stated constraints, will lead to a solution for $M_{ij}$ in terms of optimal power scheduling delivery for all bioelectrochemical plants, their fuel cost data, as well as $P_M$ and $\Delta P_L$.

Using the principle of duality, the solution of $M_{ij}$ is exactly the same as that for $B_{ij}$ for a set of interconnected multiarea power pool systems.

Referring to the solution of $B_{ij}$ shown in Chapter 1, Equation 1.50, we can proceed to write the solution for $M_{ij}$:

$$M_{ij} = B_{ij}\left[1 + k/2/\sqrt{\Delta P_{\Delta}}\right] = \frac{H_2 F_{ii}\left(\lambda - F_{ii}P_i - F_i\right)}{H_1 P_i F_{jj} + H_2 P_j F_{ii}\lambda} \tag{4.84}$$

where $M_{ij}$ = power system linkage coefficient, where

$$H_1 = \frac{F_{ii}\lambda}{F_{jj}\lambda} - \frac{F_{ii}P_j - F_i}{F_{jj}P_j - F_j} \tag{4.85}$$

$$H_2 = \frac{\lambda - F_{jj}P_j - L_i}{\lambda - F_{ii}P_i - L_j} \tag{4.86}$$

and where $P_r$ = power received in MW and $\Delta P_L$ = optimal power levelling balance at any on-site bioelectrochemical plant.

## XII. FUNCTIONAL DEPENDENCE OF [B] MATRIX

To establish criterion for calculating the [B] matrix of a certain area energy system, in the case of fuel cost incremental curve changes for a new renewable energy source such as the bioelectrochemical system, a functional review of $B_{ij}$ shown in Chapter 1, Equation 1.4 is

$$\frac{\partial F_i}{\partial P_i} = F_{ii}P_i + F_i \tag{4.87}$$

where $F_{ii}$ = slope of incremental fuel cost curve and $f_i$ = incremental cost of plant (i) at no-load.

Returning to Chapter 1, Equation 1.4 the functional form of [B], first in terms of $F_{ii}$ and then in terms of $f_i$ is indicated as follows. Let $F_{ii} = x$ and all other parameters be constants, since they are different or independent of $F_{ii}$. Then

$$B_{ij} = \frac{ax + bx + c}{a'x + b'} = \frac{(a+b)x + c}{a'x + b'} = \frac{Ax + c}{a'x + b'} \tag{4.88}$$

where

$$A = (a + b) \tag{4.89}$$

and

$$A = -F_{jj}P_iP_j + \left(\lambda P_i - f_j P_i\right) \tag{4.90}$$

$$C = P_j\left[\lambda F_{jj} - F_{jj}f_i\right] + \lambda F_i + F_j - F_iF_j \tag{4.91}$$

$$a' = 2\lambda P_i^2 \tag{4.92}$$

$$b' = 2\lambda F_{jj}P_j^2 + P_i\left(2f_i - 2\lambda^2\right) + P_j\left(2\lambda F_j - 2\lambda^2\right) \tag{4.93}$$

If $B_{ij}$ in Chapter 1, Equation 1.4 remains invariant, the set of Chapter 1, Tables 1.6 through 1.10 could be used in processes of economic evaluation and system identification.

Energy system identification or, in other words, its design could be established and inspected by either structuring a new symmetric [R] matrix or for an immediate design. The set of Tables 1.11A in Chapter 1, as well as those tables in Chapter 2, namely, Tables 2.13 through 2.19, will be referred to throughout the presentation, analysis, and evaluation of energy systems in this book.

Therefore, for $B_{ij}$ to remain invariant under a change in fuel cost, we can write

$$F_{ii-new} = kF_{ii-old} \tag{4.94}$$

$$\gamma = 1$$

From Equation 4.94, three criteria can be concluded.

$$\gamma B_{ij} = \frac{AKX + c}{a'kx + b'} \tag{4.95}$$

where

$$KX = kF_{ii} \tag{4.96}$$

and k is a multiplying factor for the slope of the incremental fuel cost curve and could be any value including zero.

From Equations 4.88 and 4.95,

$$\gamma B_{ij}/B_{ij} = \gamma = \frac{AKX + C}{a'kx + b'}\frac{a'x + b'}{AX + C} \tag{4.97}$$

$$\approx \left[K + \frac{C}{AX} - \frac{KC}{AX} - \frac{C^2}{A^2X^2} + \ldots\right]\left[\frac{1}{k} + \frac{b'}{a'Kx} - \frac{b'}{a'k^2x} - \frac{b'^2}{a'^2k^2x^2} + \ldots\right], \tag{4.98}$$

we can state the following:

I.

$$\frac{C}{AX} - \frac{KC}{AX} - \frac{C^2}{A^2X^2} + \ldots = 0$$

Therefore,

$$K \cong \left(1 - \frac{C}{A}\right) \tag{4.99}$$

II.

$$\frac{b'}{a'Kx} - \frac{b'}{a'k^2x} - \frac{b'^2}{(a'kx)^2} + \ldots = 0 \tag{4.100}$$

From Equation 4.106

$$K \cong \left(1 + \frac{b'}{a'x}\right) \tag{4.101}$$

III.

$$\left[K+\frac{C}{AX}-\frac{KC}{AX}-\frac{C^2}{A^2X^2}+\ldots\right]\left[\frac{1}{K}+\frac{b'}{a'Kx}-\frac{b'}{a'k^2x}-\frac{b'2}{(a'kx)^2}+\ldots\right]=1 \tag{4.102}$$

The value of k that can be extracted from Equation 4.102 is much more complicated than those expressed by Equations 4.99 and 4.101. However, the third criterion in Equation 4.102 offers another option for the ultimate goal of economic evaluation for energy systems in the power flow reference frame.

Now the second expected change in fuel cost is the incremental cost in dollars per megawatt hour under no load, i.e., $f_i$ for plant (i).

Let $f_i = x$, and

$$B_{ij}=\frac{A_1+C_1X}{D_1+E_1X} \tag{4.103}$$

where

$$A_1=-F_{ii}F_{jj}P_iP_j+\left(\lambda F_{ii}-F_{ii}F_j\right)P_i+\lambda F_{jj}P_j+F_j-\lambda^2 \tag{4.104}$$

$$C_1=-F_{jj}P_j+\lambda-F_j \tag{4.105}$$

$$D_1=2\lambda F_{ii}P_i+2\lambda F_{jj}P_j-2\lambda^2P_i-2\lambda^2P_j-2\lambda F_jP_j \tag{4.106}$$

$$E_1=2\lambda P_i$$

For a change in $F_i$ to k $F_j$,

$$\gamma' B_{ij}=\frac{A_1+k'C_1X}{D_1+k'E_1X} \tag{4.107}$$

$\therefore$

$$\gamma' B_{ij}\Big/B_{ij}=\left(\frac{A_1+k'C_1X}{D_1+k'E_1X}\right)\left(\frac{D_1+E_1X}{A_1+C_1X}\right) \tag{4.108}$$

Repeating a procedure similar to the case where $F_{ii}$ was the variable, the following criteria were obtained in the case of having $B_{ij}$ remain invariant:

I′.

$$K\cong 1-\frac{A_1}{C_1X} \tag{4.109}$$

II′.

$$K\cong 1+\frac{D_1}{E_1X} \tag{4.110}$$

III. This third criterion which could be deduced from Equation 4.108 will be similar to that of Equation 4.102. This is left as a problem for the student.

The third case is where the entire incremental fuel cost curve pertaining to the no-load cost and the slope will be changing, i.e., $F_{ii}$ and $f_i$ are variables at the same time.

$$\frac{\partial F_i}{\partial P_i} = K_1 F_{ii} + k_2 f_i \tag{4.111}$$

From Chapter 1, Equation 1.4 let

$$F_{ii\text{-}old} = X \text{ and } f_{i\text{-}old} = Y$$

$$F_{ii\text{-}new} = K_1 X \text{ and } f_{i\text{-}new} = K_2 Y$$

Therefore,

$$B_{ij} = \frac{A_2 X + C_2 Y + D_2}{A_2 X + C_2 Y + D_2} \tag{4.112}$$

where

$$A_2 = -F_{jj} P_i P_j + (\lambda - f_i) P_i \tag{4.113}$$

$$C_2 = -F_{jj} P_j \tag{4.114}$$

$$D_2 = F_{jj} P_j \tag{4.115}$$

$$A_2' = 2\lambda P_i^2 \tag{4.116}$$

$$C_2 = 2\lambda P_i \tag{4.117}$$

and

$$D_2' = 2\lambda F_{jj} P_j^2 - 2\lambda^2 P_j + P_j(2\lambda f_j - 2\lambda^2) \tag{4.118}$$

Now we can write,

$$\gamma B_{jj} = \frac{A_2 k_1 X + C_2 k_2 Y + D_2}{A_2' k_1 X + C_2' k_2 Y + D_2'} \tag{4.119}$$

From Equations 4.112 and 4.119, for $B_{ij}$ to remain invariant, $\gamma = 1$. Therefore,

$$\gamma = \frac{B_{ij}}{B_{ij}'}$$

$$= \frac{A_2 k_1 X + C_2 k_2 Y + D_2}{A_2' k_1 X + C_2' k_2 Y + D_2'} \bullet \frac{A_2' X + C_2' Y + D_2'}{A_2 X + C_2 Y + D_2} \tag{4.120}$$

From Equation 4.120 above, since both $F_{ii}$ and $f_i$ are changing by a factor of $K_1$ and $K_2$, respectively, only one criterion has been secured from the condition that,

$$\gamma = 1$$

The criterion is

$$\left[K_1 + \frac{C_2K_2 - C_2K_1Y}{A_2X} + \frac{D_2 - K_1D_2}{A_2X}\right]\left[\frac{1}{K_1} + \frac{C_2\left(1-\frac{K_2}{K_1}\right)}{A_2' K_1X} + \frac{D_2 - K_1\frac{D_2}{K_1}}{A_2' K_1X}\right] = 1 \quad (4.121)$$

The preceding criteria regarding conditions for keeping any [B] matrix in the power flow reference frame invariant are based on having the following changes in the incremental fuel cost curve:

1. Change in the curve slope, i.e., $F_{ii}$
2. Change in the curve vertical intercept defining the incremental cost at the no-load, i.e., $f_i$
3. Changes in both the slope and the vertical intercept of the incremental fuel cost, i.e., $F_{ii}$ and $f_i$ as shown in the following:

$$\frac{\partial F_i}{\partial P_i} = F_{ii}P_i + f_i \quad (4.122)$$

or

$$\frac{\partial F_i}{\partial P_j} = F_{jj}P_j + f_j \quad (4.123)$$

## XIII. FUNCTIONAL DEPENDENCE OF THE PARAMETER K

Relevant to system optimization and economic scheduling of power delivery from a set of bioelectrochemical energy sources, we will proceed now to look into the functional dependence on the cost multiplying factor under the following economic constraints as examples. Variable $F_{ii}$ where

$$K \cong 1 - \frac{C}{AX} \quad (4.124)$$

$$\cong 1 - \frac{P_jF_{jj}(\lambda - f_i) + \lambda f_i + f_j - F_iF_j - \lambda^2}{\lambda P_i(1 - f_j)F_{ii}} \quad (4.125)$$

As shown in Equation 4.125 that k = function of $P_i$, $P_j$, $f_i$, and $F_j$, as specified parameters and $F_{ii}$ as the variable parameter, where $P_i$ and $P_j$ each represent scheduled power capacity for the ith and jth source, respectively, and $\lambda$ is the cost of power delivery in dollars per megawatt hour or the Lagrange multiplier.

To economize k with respect to $\lambda$, differentiate Equation 4.125 with respect to $\lambda$, and then equate to zero to obtain the condition required.

$$\frac{\partial k}{\partial \lambda} = \frac{\left[P_i F_{ii}\left(1-f_j\right)\right]\left[P_j F_{jj} + f_i - 2\lambda\right] - \left[P_j F_{jj}\left(\lambda - f_i\right) + \lambda f_i + f_j - f_i F_j - \lambda^2\right]\left[P_i F_{ii}\left(1-f_j\right)\right]}{\left[\lambda P_i\left(1-f_j\right)F_{ii}{}^2\right]} = 0 \tag{4.126}$$

The condition k = 0 will eventually imply the following in dollars per megawatt hour:

$$\lambda = \sqrt{f_i f_j + f_i P_j F_{jj} - f_j} \tag{4.127}$$

The value of λ expressed by Equation 4.127 will ensure invariance of an established [B] as well as [R] matrices and an optimum level of cost fluctuation represented by the factor k.

Similar criteria on λ that could be secured for other cases analyzed in this section will be left as exercises for the student.

## XIV. CASE STUDY

Given a centrally distributed energy system (32 bus-bars) where all base loadings are met by fossil-steam generating plants and pumped-hydroelectrics and nuclear fission plants, while peak loadings are supplied by bioelectrochemical plants.

Consider the overall average loading to be at 60% of a total 10,000 MW.

Incremental fuel cost for the bioelectrochemical power plants have a multiplying factor k, based on a charge involving the vertical intercept of the incremental fuel cost curve with respect to that of conventional storage batteries.

Calculate the new resistance symmetric matrix of the new system where the bioelectrochemical units supply peak load instead of storage batteries.

Also determine the expression for optimum k.

**Solution** — From Equation 4.109, the corresponding multiplying factor k is given by

$$\begin{aligned} K &= 1 - \frac{A_1}{C_1 f_1} \\ &= 1 - \frac{-F_{ii}F_{jj}P_iP_j + P_iF_{ii}\left(\lambda - f_j\right) + \lambda F_{jj}P_j + f_j - \lambda^2}{f_i\left(\lambda - f_j - P_jF_{jj}\right)} \end{aligned} \tag{4.128}$$

In Equation 4.128 above, $f_i$ is the incremental cost in dollars per megawatt hour for the storage battery power plant, while the incremental cost for the bioelectrochemical plant = k $f_i$ or k $f_j$.

Therefore, the [B] matrix for this system at 60% loading remains invariant which is indicated in Table 1.6 in Chapter 1.

Consequently, the [R] matrix for the new central system involving bioelectrochemical generators supplying peak loading is that shown in Table 2.15 Chapter 2 under the column of 60% loading.

Next, the optimum value of k could be obtained by the following step:

$$\begin{aligned} \frac{\partial k}{\partial f_i} &= 0 \\ &= \frac{\left[F_{ii}F_{jj}P_iP_j - P_iF_{ii}\left(\lambda - f_j\right) - \lambda F_{jj}P_j + f_j - \lambda^2\right]\left[\lambda - f_j - P_jF_{jj}\right]}{\left[f_i\left(\lambda - f_j - P_jF_{jj}\right)\right]^2} = 0 \end{aligned} \tag{4.129}$$

Now, from Equation 4.129, the following condition for optimum k develops which is centered on specifying criterion for representing the cost of power delivery in dollars per megawatt hour.

$$F_{ii}F_{jj}P_iP_j - \lambda P_iF_{ii} + f_jP_iF_{ii} - \lambda P_jF_{jj} + \lambda^2 = \lambda - P_jF_{jj}$$

Therefore,

$$\lambda^2 - \lambda\left(1 + P_iF_{ii} + P_jF_{jj}\right) + \left[F_{ii}F_{jj}P_iP_j + f_jP_iF_{ii} + P_jF_{jj}\right] = 0 \tag{4.130}$$

And hence,

$$\lambda = \frac{1}{2}\left[1 + P_iF_{ii} + P_jF_{jj} \pm \sqrt{1 + P_i^2F_{ii}^2 + P_j^2F_{jj}^2F_{ii}F_{jj}P_iP_j - P_jF_{jj} + P_iF_{ii} + 4f_jP_iF_{ii}}\right] \tag{4.131}$$

The above expression for $\lambda$ could be incorporated in a computer program for the calculation of optimum scheduling of generation for all power sources in this system.

## XV. SUMMARY

This chapter presents simulation criteria for unfolding useful information on the kinetic and dynamic performance properties of the bioelectrochemical cell. Research work by this author[2-18] identified operational constraints for maximum energy extraction from prepared refuse by the output hydrocarbon with variable order, in terms of space as well as time domains. Calculations also secured a closed form solution for the electric field intensity within the biocell continuum in terms of all parameters, indicating the direct measure of electric energy output.

Alternative methods of generation, storage, and transport of electric energy are compatible in effectively meeting any emergency situation that may arise from any disruptive action. Modeling criteria have been developed for the energy storage in chemical form for a redox flow energy system, a bioelectrochemical system, as well as for a hydrogen and ammonia production system.

Examination of the redox flow system is demonstrated by characterization of the ferromagnetic fluid used in either the discharge or recharge cycle. Patterns showing the modes of change for the gyromagnetic resistance with respect to the local magnetic field are obtained, indicating regimes of transfer from magnetization into relaxation and vice versa.

On the production of synthetic hydrocarbon fuel, several criteria have been presented regarding expressions for the molecular energy content with respect to probable functional varieties of concentrations, enthalpy, and entropy as well as base energy release.

Also, models of hydrogen generation through endothermic as well as conventional electrolysis of ocean water are expressed using thermal energy extracted by OTEC plantship.

Fuel generation, storage, and transport could be secured in a system of interconnection comprised of the biochemical cells and redox flow cells centered around the OTEC plant, with promising expectations economically and with respect to reliability.

This chapter also carried out theoretical analysis for the ultimate goal of securing mathematical models, in the complex frequency domain, of the main processes of energy conversion of organic prepared refuse to synthetic hydrocarbon fuel, followed by the stage of generating electric power at the terminal of the bioelectrochemical fuel cell.

Mathematical models, for the energy conversion processes in the form of transformable integro-differential equations, are secured through the central physical principle of interactions between local reactants and interfacing material environments. The mathematical reasoning is based on the existence of rational thermal energy functions as well as kinetic and dynamic parameters having simple and multiple poles of arbitrary order.

Also, a unified model with a direct link between the generated electric power output and the organic prepared refuse, with both kinetic and dynamic characteristics, is established.

To consider the problem of energy system design in the power flow reference frame in terms of the symmetric resistance matrix [R], a procedure of invariancy of the already established [B] matrices in Chapter 1, as well as the [R] matrices set up in Chapters 1 and 2, was obtained.

Under the procedure developed, the [B] and the [R] matrices developed in Chapters 1 and 2 could be used directly if a special change in the incremental fuel cost curve through a multiplying factor is valid.

The special multiplying cost factor (k) could be related to a change in the vertical intercept, that is the cost in dollars per megawatt hour under all loadings, the slope of the incremental fuel cost curve, and when both the vertical intercept as well as the slope of the incremental fuel cost curve are under a change.

The new cost multiplying factor (k) is a function of the cost of power delivery ($\lambda$), power scheduling for any plant in the system, and parameters of the incremental fuel cost curve.

## XVI. PROBLEMS

4.1 Equation 4.9 represents the transform function for the concentration with respect to the mean velocity of reactants within the bioelectrochemical cell. Express the solution for the given transform function in the steady state under a sinusoidal time variation, i.e., $\partial/\partial t = jw$.

4.2 Repeat Problem 4.1 with respect to Equation 4.17 as the first order transform function.

4.3 Refer to Equations 4.16, 4.18, 4.19, 4.24 and 4.25, then proceed to finalize a transform function of multiple order and finite number of poles in the complex frequency domain.

4.4 Convert the transform function of Problem 4.3 to the time domain and in the steady state.

4.5 Using Equation 4.108, proceed to simplify and obtain one or more expressions for the fuel cost multiplying factor k, based on the criterion for invariant [B] matrix.

4.6 Equation 4.73 represents the optimal [B] matrix for a certain area power pool in terms of source's power capacities and their fuel cost data. For bioelectrochemical sources, the incremental fuel cost curve has only the vertical intercept of that curve, i.e., $f_i$, and hence $F_{ii} = 0$. Therefore, using Equation 4.109, obtain a new expression for the [B] matrix, where k is the fuel cost multiplying factor for the bioelectrochemical sources for the invariant [B] matrix.

4.7 Repeat Problem 4.6, but use Equation 4.110 for the multiplying factor, k.

4.8 Repeat Problem 4.6 by using the new expression for k that was obtained in Problem 4.5.

4.9 Using the new [B] matrix obtained in Problem 4.6 and the conventional power coordination equation, and taking into account the fact that $P_j = f(P_i)$, obtain an expression for the incremental fuel cost curve for plant i.

4.10 Repeat Problem 4.9 with respect to the [B] matrix obtained in Problem 4.7.

4.11 Repeat Problem 4.9 with respect to the new [B] matrix obtained in Problem 4.8.

4.12 Using the new [B] matrix established in Problem 4.6 and the incremental fuel cost curves shown in Chapter 2, calculate using an appropriate computer format elements of the invariant [B] matrix for a centralized power system in which peak loading is supplied by a set of bioelectrochemical bus-bars, at 60% loading. Assume fuel cost for the bioelectrochemical cell is k times the incremental fuel cost of a storage battery. Compare the result with that shown in Chapter 1. Also, let the incremental fuel cost for the storage battery $\lambda = 7.65$ ¢/MWh.

4.13 From the results obtained in Problem 4.12 together with information from the multiplying factor (k), which is a function of power source capacities and fuel cost, calculate the total yearly cost in dollars for supplying the peak load by the bioelectrochemical bus-bars. Use the load duration curves shown in Chapter 2.

4.14 From the solution of the new [B] matrix obtained in Problem 4.6 and using the symmetric [R] matrix for this system given in Chapter 2, solve for the corresponding [K] matrix. Inspect elements of the [K] matrix for those bus-bars operating as bioelectrochemical sources.

4.15 Using the value of $\lambda$ expressed in Equation 4.127 and for optimal value of K, modify the [B] matrix in Equation 4.73. Then using the general conventional coordination equation, obtain a solution for $\partial F_i/\partial P_i$, where $F_i$ is the cost of plant (i) in dollars per hour.

4.16 Using the results of Problem 4.15 and data on the incremental fuel cost curves shown in Chapter 2, solve for the optimum scheduling of generation of all plants in a 32 bus-bar centralized energy system where peak loading is supplied by bioelectrochemical bus-bars.

4.17 Equations 4.54 and 4.56 represent the energy content of the hydrocarbon extracted from prepared refuse under the two cases of (1) orderly and (2) disorderly reaction. Solve for the order of the hydrocarbon (m) when V(t) of Section VIII Case B at a time, t, equals to V(t) of Section VIII Case C at $t = t_\infty$.

4.18 Equation 4.57 describes the energy content for $C_mH_{2m+2}$. At time of reaction $t \rightarrow t_\infty$, solve for V(t) under the minimum m and highest possible value of m. Consider functional status as given in Section VIII Case D.

4.19 Equation 4.58 describes the energy content for $C_mH_{2m+2}$ under orderly and disorderly restraints indicated under Section VIII Case E. Solve for an optimum V(t) where m is an expressed function of the following form:

$$m = \sqrt{n(t)\,Q(t)}$$

Optimization is centered on the process of differentiation for V(t) with respect to m as an implicit function for both n(t) and Q(t).

4.20 Equation 4.59 describes the energy content of orderly release of the hydrocarbon $C_mH_{2m+2}$. Obtain a generalized criterion for optimal U(t) under concurrent variations of n, m, H and t.

4.21 Equation 4.65 presents an expression for the molar concentration of $NH_3$ through endothermic decomposition and conventional electrolysis of water from OTEC output. Carry out an optimization process on $M_{NH_3}$ with respect to $M_{OH}$, $1_{1H}$, and $H_{2L}$ to ensure stable release of $NH_3$. Stability here is tied to the maximum possible steady-state level for $M_{NH_3}$.

4.22 Figure 4.4 represents the behavior of expended power for magnetites realignment known as gyromagnetic power vs. electric current. Calculate the total energy expended for the redox sytem characterized over a period of time of 1 h.

4.23 Repeat Problem 4.22, as if the exciting currents along the horizontal line of Figure 4.4 are the RMS values of an AC sinusoidal current.

4.24 Consider a dispersed power system where various power plants supply electric energy by bioelectrochemical interconnected units. In Equation 4.84, $M_{ij}$ is represented in terms of a $B_{ij}$ matrix for centrally interconnected generators, as well as the functions $H_1$ and $H_2$ and $\Delta P_L$. Modify Equation 4.84 for an invariant $B_{ij}$ by using the constraint expressed by Equation 4.109. Obtain the simplest possible form for $M_{ij}$.

4.25 Repeat Problem 4.24 by using the constraint expressed by Equation 4.110. Obtain the simplest possible form for the new $M_{ij}$.

4.26 Modify Equation 4.84 for $M_{ij}$ when the incremental fuel cost curve is a constant horizontal line. Also establish a new form for $P_p$ in a quadratic form, as well as in quadratic plus linear terms of $B_{ij}$.

4.27 Repeat Problem 4.24 for when the incremental fuel cost curve is a straight line passing

into the origin within the capacity of bioelectrochemical generating units. Obtain a new form for $M_{ij}$ through the constraint expressed by Equation 4.99.

4.28 Repeat Problem 4.27 by using the constraint expressed by Equation 4.100. Obtain the most simplified form for $M_{ij}$.

4.29 Consider an interconnected energy supply system involving m center areas sparsely linked through a transmission network. Each center contains m bioelectrochemical generating sources also linked through a transmission network. Let the incremental fuel cost curve for the bioelectrochemical sources as in $f_i$ be in dollars per Kilowatt hour and of course constant. Establish a solution for the generalized [B] matrix for the dispersed-centralized system such that power scheduling of generation for every plant in the entire system is optimum.

4.30 If the incremental fuel cost curve in Problem 4.29 is multiplied by an adjustment factor of K, obtain one or two solutions for K such that the [B] matrix of the system described in Problem 4.29 will remain invariant. Explain the effect of K on the process of optimum scheduling of generation on each center area.

4.31 Equation 4.52 presents the energy content for the hydrocarbon $C_mH_{2m+2}$ extracted from prepared refuse. Using the economic coordination equation and the facts that $P_i$ and $P_L$ are implicit functions of n, H, Q, and $W_c$, obtain a solution for the cost of received power in dollars per megawatt hour, i.e., $\lambda$. This system refers to the case of an orderly and disorderly electrochemical reaction. Identify criteria under which $\lambda$ may attain a minimum value.

4.32 Repeat Problem 4.31 with respect to Equation 4.54 which is another case of an orderly-disorderly electrochemical reaction.

4.33 Repeat Problem 4.31 with respect to Equation 4.57 for the case of an orderly electrochemical reaction.

4.34 Repeat Problem 4.31 with respect to Equation 4.58 which is another case of a disorderly electrochemical reaction.

4.35 Repeat Problem 4.31 with respect to Equation 4.59 which is for an orderly electrochemical reaction.

4.36 From solutions of $\lambda$ secured in Problems 4.31 through 4.35, identify the most possible optimum system in which $\lambda$ may attain the least minimum level in terms of n(t), H(t), Q(t), and $W_L(t)$.

## REFERENCES


1. **Angel, E. and Bellman, R.,** *Dynamic Programming and Partial Differential Equations*, Bellman, R., Ed., Academic Press, New York, 1972.
2. **Denno, K.,** Modeling of bio-electro-chemical conversion of refuse to energy, Proc. Second Int. Conf. Math. Modeling, University of Missouri, Rolla, 1979, 1030.
3. **Denno, K.,** Bio-electrochemical conversion of refuse to energy, Proc. 25th Annu. Tech. Meet. Inst. Environ. Sci., Institute of Environmental Sciences, Seattle WA, 1979, 316.
4. **Denno, K.,** Redox flow cells, conventional fuel cells and storage batteries as the optimal power sources to buildings, *IASTED J. Energ. Syst.*, 2(2), 109, 1980.
5. **Denno., K.,** Simulating criterion for bio-chemical conversion of refuse to synthetic fuel and electric power, Proc. Condens. Pap., Third Miami Int. Conf. Alternative Energ. Sources, University of Miami, Coral Gables, FL, 1980, 594.
6. **Denno, K. and Sohn, K.,** Spatial distribution of quantum parameters in the continuum of ferromagnetic liquid insulation, *Proc. 15th Electr./Electron. Insulation Conf.*, IEEE, Chicago, IL, 1981.
7. **Denno, K.,** Hybrid system of OTEC plantship coupled to MHD and hydrogen fuel cell generating plants, *Proc. Fourth Int. Conf. Alternative Energy Sources*, Ann Arbor Science, MI, 1981.

8. **Denno, K.,** Ocean thermal energy conversion, storage and transport through water-based ferro-magnetic fluid, *Proc. Fourth Miami Int. Conf. Alternative Energy Sources*, Ann Arbor Science, MI, 1981.
9. **Colichman, E. L.,** Preliminary biochemical fuel cell investigations, *IEEE Proc.*, 51, 812—819, 1963.
10. **Denno, K.,** Mathematical modeling of storage battery and fuel-cell, *Proc. Int. Telephone Energy Conf.*, IEEE, Washington, D.C., 1978, 237.
11. **Denno, K.,** Modeling of redox flow cell, fuel cell, storage battery and harmonically commutated inverter, *Proc. Can. Commun. Power Conf.*, IEEE, Montreal, Canada, 1976, 403.
12. **Dunlap, W. C.,** *An Introduction to Semiconductors*, John Wiley & Sons, New York, 1957.
13. **Denno, K.,** Power System Synthesis From Solution of Transmission Loss Coefficients, Paper c/73.4C2-9, presented at the IEEE Power Eng. Soc. Meet., Vancouver, Canada, July 1973.
14. **Denno, K.,** Power system identification in the power flow reference frame, *J. Appl. Sci. Eng.*, A. 2, 141, 1977.
15. **Denno, K.,** Simulating criterion for bio-chemical conversion of refuse to synthetic fuel and electric power, *Alternative Energy Sources III*, Vol. 7, 1980, 241.
16. **Sohn, K. and Denno, K.,** *Modelling of Alternative Plans for Fuel Production and Storage*, Energy Modelling IV (planning for energy disruptions) of the Institute of Gas Technology, Ann Arbor Science, MI, 1982, 663 .

Chapter 5

# ECONOMICS OF MAGNETOHYDRODYNAMIC POWER GENERATION (MHD)

**(Utilization of Nonfossil Fuel as Working Fluid)**

In this chapter, major review and presentation of energy systems for the generation of bulk power output ranging from conventional electromechanical systems using fossil fuel, to the dependence on nuclear fission, and then to nuclear fusion as well as other sources of renewable fuels, will be reviewed and their economic expectations structured mathematically.

The economic/analytical review will be centered on a relativistic approach balancing the evolution of global need for energy consumption from all kinds of sources, with respect to public concern, economic availability, and environmental preservation.

The inclusion of MHD power generation in this book is centered on using nonfossil fuel such as the exhaust plasma of nuclear fusion reactors as a working fluid which could be recycled for multiple use on one hand, and a preheated synthetic fuel $C_mH_{2m+2}$ that could be extracted from prepared refuse as another source of a renewable energy system.

## I. THE GLOBAL NUCLEAR ENERGY EQUATION[12,13]

This section presents an open and frank perspective global model which is centered around the utilization of nuclear energy in the U.S. and abroad. The physical model based on the pattern of the special theory of relativity, will identify various milestones of nuclear energy utilization including fission and fusion processes, with respect to the alternative energy sources as well.

The physical global model will stress the relativistic future situation that bulk amounts of energy could be extracted in a timely manner from nuclear modes besides the fossil fuel resources. However, since fossil fuel is in a time dwindling state, reliance on nuclear energy to meet the huge demand by industry and other load centers requires the bold acceptance of nuclear power as the answer for increasing future energy needs coupled with increased safeguards.

The physical model points out the necessary safeguards or general concern for the safety of populated zones and the protection of the environment as prerequisite milestones in the location of nulcear power plants.

The model presents a balanced criterion for the acceptability of nuclear fission and nuclear fusion in the U.S. and abroad with respect to the total concern for the probability of radiation which is higher in fission nuclear reaction than in nuclear fusion, the safety of populations in close proximity to nuclear centers, and the total environmental safeguards of our world.

The established relativistic balanced energy model, identifies with an open mind the clear platform with individual planks along with a sound nuclear energy policy, coupled to public education regarding nuclear power and the minimization of its perils, while taking the maximum benefits from the huge energy release out of nuclear reaction which could be pursued at the global level.

The relativistic model of nuclear energy balance presented in this book will evolve around the time axis along which the nondimensional energy index increases from zero level to unity. The nondimensional energy index is the ratio of nuclear energy dependency with respect to its fossil energy counterpart.

Therefore, as the time element proceeds, global energy needs will approach asymptotic total reliance on nuclear power, while dependency on fossil fuel will diminish also asymptotically.

Hence, after a relatively long time span which could be determined, total dependency on nuclear energy (fission and fusion) will become an established fact.

A similar argument applies to the intensity of public concern, evolving around safety and conservation of the environment, where such intensity will diminish as the time element forces the global acceptance of nuclear energy.

Interaction between the fuel sufficiency tensor and its public concern counterpart has to have a special mathematical linkage to realize their physical formulation. It will be shown later in the chapter that such a link will take a special mode to preserve the required balance between the concept of increased dependency on nuclear energy and keeping tight control on public safety and preservation of our environment.

## II. BALANCED ENERGY SUFFICIENCY[12]

Energy demand will center on the continuous development of all aspects of life in any society, locally or on a global level. Fuel supply will be met by fossil and nonfossil resources. Also, the nonfossil kind of fuel draws its sources from nuclear fission, nuclear fusion, and other modes of alternative energy sources. Alternative energy sources could be hydrogen energy systems, ocean thermal energy conversion systems (OTEC), wind energy systems, solar energy systems, bioelectrochemical systems, and others. However, realistically, the bulk amount of energy demand could only be derived from fossil fuel and nuclear power (fission and fusion).

Adequate sufficiency for life aspects could be looked upon as an evolving physical phenomenon properly formulated in four-dimensional space time coordinate systems, with translational movement, along any space axis to reflect on the time element. This concept is modeled on the same principles of the four-dimensional system for the special relativity theory.

The four-dimensional model of balanced energy demand, with respect to public concern, could be visualized as a transformed four-dimensional vector, reflecting on time as central axis for evolution.

$$X_i' = a_{ij} X_j \qquad i, j = 1, 2, 3, 4 \tag{5.1}$$

or

$$\begin{bmatrix} X_1' \\ X_2' \\ X_3' \\ X_4' \end{bmatrix} = \begin{bmatrix} \alpha & 0 & 0 & i\alpha\tau \\ 0 & 1 & 0 & 0 \\ 0 & 0 & 1 & 0 \\ -i\alpha\tau & 0 & 0 & \end{bmatrix} \begin{bmatrix} X_1 \\ X_2 \\ X_3 \\ X_4 \end{bmatrix} \tag{5.2}$$

where $X_1$ = health and social services ... fuel sufficiency vector, $X_2$ = educational development ... fuel sufficiency vector, $X_3$ = industry and commerce ... fuel sufficiency vector, $X_4$ = agriculture and other services ... fuel sufficiency vector, $a_{ij}$ = Lorentz transformation matrix, $X_j$ = is the preceeding energy sufficiency vector, $X_i'$ = is the superceding sufficiency vector, and $\tau = V/C$.

$$\alpha = \left[1 - \frac{V^2}{C^2}\right]^{-\frac{1}{2}} \tag{5.3}$$

V = perturbational nuclear energy demand index, C = total fossil energy demand index, and i is an imaginary symbol reflecting on the time axis as the fourth coordinate axis.

## III. BALANCED PUBLIC CONCERN[12]

Increasing fuel demand in effect means an ultimate increase in nuclear power which has to be balanced carefully with total public concern for population safety against nuclear accident and assurance of environmental safeguards.

As expressed in the case of a fuel sufficiency vector, a similar, balanced, four-dimensional vector equation representing safety and public environmental concerns is expressed as follows:

$$Y_i' = b_{ij} Y_j \qquad i, j = 1, 2, 3, 4 \tag{5.4}$$

where $b_{ij}$ = Lorentz transformation matrix, $Y_j$ = preceding concern vector, and $Y_i$ = superceding concern vector.

$$\begin{bmatrix} Y_1' \\ Y_2' \\ Y_3' \\ Y_4' \end{bmatrix} = \begin{bmatrix} \alpha' & 0 & 0 & i\alpha'\tau' \\ 0 & 1 & 0 & 0 \\ 0 & 0 & 1 & 0 \\ -i & \alpha'\tau' & 0 & \alpha' \end{bmatrix} \begin{bmatrix} Y_1 \\ Y_2 \\ Y_3 \\ Y_4 \end{bmatrix} \tag{5.5}$$

where $Y_1$ = population safety index, $Y_2$ = wildlife safety index, $Y_3$ = ground environmental index, $Y_4$ = air and sea environmental index, V = perturbational nuclear public concern index, and C = maximum level of safety and environmental concern index.

$$\tau' = \frac{V'}{C'} \tag{5.6}$$

$$\alpha' = \left[1 - \frac{V^2}{C^2}\right]^{-\frac{1}{2}} \tag{5.7}$$

## IV. LINKAGE BETWEEN SUFFICIENCY AND CONCERN[12]

Adequate sufficiency in energy, which in effect calls for accelerating dependency on nuclear power has to be balanced with equal emphasis on safeguarding population centers and preserving the environment in all aspects.

For a safer world, maintaining energy sufficiency and taking parallel action for the safety of population centers from nuclear accident, as well as preserving the entire environment, imply that

$$[X] = 1/[Y] \tag{5.8}$$

or

$$X_{ik}\, Y_{kl} = 1 \qquad i, k, l = 1, 2, 3, 4 \tag{5.9}$$

The implication of Equation 5.9 is that an increase in the establishment of nuclear power plants must be associated with equal safeguards regarding population safety and careful planning to preserve our environments.

Faced with the realistic and relativistic global picture that fossil fuels are in a continuous state of dwindling which requires accelerating dependence on nuclear power for bulk power production, the following model based on the theory of relativity is characterized by the following:

1. Sufficiency in fuel (fossil and nuclear) to meet all the demands of local or global society is represented as a four dimensional relativistic vector associated with translational motion in the coordinate system to reflect on time elements as a true resemblance of world continuous development, growth, and evolution.
2. The concerns of society are represented also in terms of a four-dimensional vector associated with translational motion in the coordinate system reflecting the time element for recognizing the changing world.
3. The linkage between asserting fuel sufficiency and adequate public concern is represented in a new tensorial product property as expressed in Equation 5.9, where the product of sufficiency and concern tensors is equal to the scalar value of unity.
4. Every expansion in nuclear power establishment will be countered by equal but reverse intensive action of public concern against nuclear accidents and the careful preservation of public safety and the environment. As long as the balance equation is strictly and carefully observed, the movement for establishment of nuclear energy centers could proceed without conflict with public concern.

## V. MHD POWER GENERATION[1-3,12,17,18]*

Conventional power generating systems depend on fossil fuel as their primary energy source. However, fossil fuel reserves, although still vast from a global viewpoint, are becoming increasingly limited in supply. This impending shortage is already acute in some areas where the demands for energy exceed the supply of energy. Consequently, it is imperative that serious consideration be given toward establishment of certain controlling guidelines for optimum usage of energy.

Constraints on resources of fossil fuels include, in addition to limited reserves, increased regulation and control of environmental degradation processes and the increase in energy demand from new and additional sectors such as in transportation and other industrial consuming areas.

The present energy conversion efficiency for fossil fuel is about 34%. Such inefficiency increases pollution and contributes to fuel supply problems.

Therefore, there is a great need to seek new, primary, energy resources while at the same time establishing other power generating schemes that result in an eventual increase of primary to secondary efficiency. The ultimate effect will be to prolong the life of the present fossil fuel reserves and also reduce the pollutants released to the environment.

Magnetohydrodynamic power generating cycles augmenting a cycle for conventional steam systems will result in an increase in conversion efficiency to the order of 50 to 60%. This is because MHD cycles operate at a higher temperature, resulting in increased thermal efficiency. The fossil fuel suitable for an open cycle MHD power plant could be natural gas, petroleum, coal, or charcoal. The fuel would be burned in preheated and/or oxygen-enriched compressed air to produce temperatures in the range from 4000 to 5000°F.

It has been predicted that with fossil fuels MHD would bring about a savings in fuel of about one third. In addition, MHD affords the opportunity of reducing thermal pollution and related undesirables.

* © 1970. Reprinted with permission from Hals, F. A., Environmental pollution control through MHD power generation, report issued by AVCO-Everett Research Lab, 1970.

Integration of an open cycle MHD central station supplementing either steam or gas turbines and using gas, oil, coal, or coal-derived fuel, either as a base load or for peaking and emergency cases, could have a clear and positive impact on improving the environment and on economy in the use of fossil fuel. There appears to be a trend toward development of an open cycle, coal-fired MHD plant topping a conventional steam or gas turbine resulting in an efficiency boost and a reduction in thermal pollution. An increase in thermal efficiency from 40 to 50% reduces the heat rejection per unit power output by one third, and an increase from 40 to 60% reduces heat rejection by 55%.

Since conventional fossil fuel plants and those with MHD topping cycles will discharge roughly equivalent fractions of heat up the stack, the reductions in cooling water requirements are correspondingly large. Such reduction in heat rejection may result in further boosting the overall power generating capacity that can be served by one source of cooling water, hence permitting additional flexibility compared with conventional fossil fuel stations. Considering the problem of air pollution, it may be stated frankly that an MHD topped unit could offer an improvement in reducing the ejection of nitrogen oxide (NOx) into the atmosphere by maximizing its content in the effluent. In this way, recovery of fixed nitrogen and nitric acid becomes economically attractive. Also, the possibility exists to minimize the NOx content in the effluent so that it is acceptable for direct emission to the atmosphere.

As with respect to SOx, since $SO_3$ readily dissolves in water, with the help of NOx, $SO_2$ can be converted to $SO_3$ which can produce sulphuric acid. However, the contribution of MHD to an improvement in air pollution is still controversial.

Concerning closed cycle MHD, it is still in the early stages for consideration as a reliable means of bulk power generation, principally because of problems in obtaining sufficient nonequilibrium electrical conductivity in the gas.

Theoretical and experimental research and development are progressing, but not fast enough. More rigorous studies are needed in order to prove the feasibility of open cycle MHD on a commercial level.

Problems to be solved relate to optimum channel dimensions, protection of channel walls from the hot conducting plasma, and fuel preparation (such as hydrogen production, natural gas, oil, coal, and coal-derived fuel). Other problems concern thermal efficiency of the channel, air preheater, and electrode distribution and orientation.

## VI. FEASIBILITY OF MHD POWER[15-20]

MHD power generation is a power producing system whereby a high temperature, weakly or moderately ionized working fluid, replaces the armature of conventional electromechanical generators.

Figure 5.1 shows an illustration of an MHD electric generator and a conventional turbo electric power generator.

The MHD generator has the following distinct advantages over conventional electric power generation methods.

1. It can handle extremely high temperatures.
2. It can handle very high power levels.
3. It has no moving parts or close tolerances.
4. It can start and reach full power very rapidly.

As a result, no other energy conversion process holds such great promise for bulk generation of electricity at high efficiency and at low cost. However, the resulting environmental aspects of MHD are probably of even greater significance. The MHD energy conversion process promises a dramatic reduction in pollution of air and water (Figure 5.2).

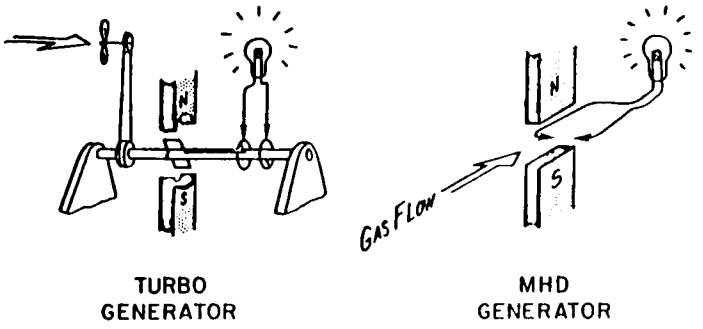


FIGURE 5.1 Comparison of turbogenerator and magnetohydrodynamic (MHD) generator. (From Hals, F. A., Environmental pollution control through MHD power generation, report issued by AVCO-Everett Research Lab, 1970. With permission.)

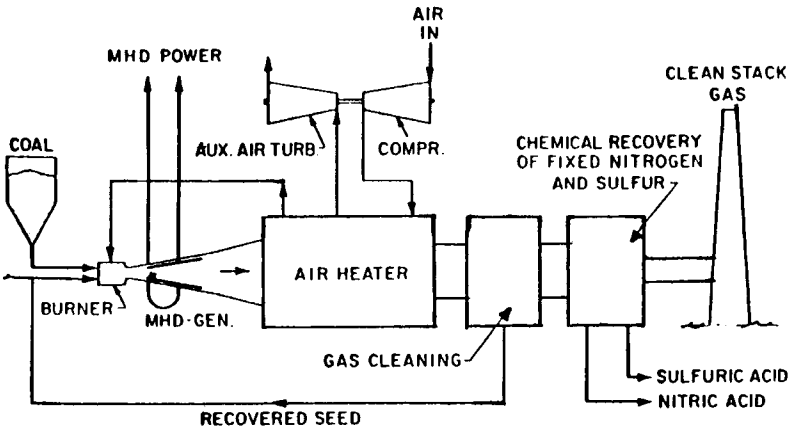


FIGURE 5.2 MHD power cycle. (From Hals, F. A., Environmental pollution control through MHD power generation, report issued by AVCO-Everett Research Lab, 1970. With permission.)

## VII. THEORY OF MHD PHENOMENON[9-11]

Consider a control volume of fluid in the presence of an electromagnetic field. The fluid is assumed to have the normal properties of fluids. The mathematical equations describing the fluid flow are not independent from the electromagnetic field equations. The two sets of equations are coupled.

### A. FLOW FIELD EQUATIONS

#### 1. Continuity Equation

The continuity equation is

$$\frac{\partial p}{\partial t} + \bar{\nabla} \cdot (\rho \bar{V}) = 0 \tag{5.10}$$

where (-) indicates vector quantity and p = fluid mass density.

Equation 5.10 can be rewritten as

$$\frac{\partial p}{\partial t} + \rho \, \bar{\nabla} \cdot \bar{V} + \bar{V} \cdot \bar{\nabla} \rho = 0 \tag{5.11}$$

Then,

$$\left( \frac{\partial p}{\partial t} + \bar{V} \cdot \nabla \rho \right)$$

can be replaced with the convective derivative term Dp/Dt and Equation 5.11 becomes

$$\frac{Dp}{Dt} + \rho \, \bar{\nabla} \cdot \bar{V} = 0 \tag{5.12}$$

The continuity equation is unaffected by the electromagnetic effects since forces never appear in it.

The definition for an incompressible fluid is that the convective derivative is equal to zero. Therefore, Equation 5.12 becomes

$$\bar{\nabla} \cdot \bar{V} = 0 \tag{5.13}$$

**2. Momentum Equation**

The contribution to momentum flux comes from surface forces due to pressures acting on the control volume surface and body forces such as magnetic, electric, and gravitational forces.

Surface forces are represented by the pressure tensor:

$$\bar{\bar{P}} = -\bar{\bar{P}}\bar{\bar{I}} + \tau_{ij} \tag{5.14}$$

where P = hydrostatic pressure, I = unit tensor, and $\tau_{ij}$ = viscosity tensor. The electromagnetic forces are given by the Lorentz equation:

$$\bar{F}_{em} = \bar{j} \times \bar{B} + P_e \, \bar{E} \tag{5.15}$$

where E = electric field intensity and $P_e$ = excess electric charge density. The surface and body forces can be combined in a momentum equation:

$$\frac{D}{Dt} \int_v (pV) dv = \int_S \bar{F}_s \cdot \bar{n} \, ds + \int_V F_b \, dv \tag{5.16}$$

where $\bar{F}_s$ = surface force vector and $\bar{F}_b$ = body force vector.

Then, for an arbitrary volume of incompressible and inviscid fluid, with no applied electric field and neglecting gravitational force, the momentum equation becomes

$$P \left( \bar{V} \cdot \bar{\nabla} \right) \bar{V} = -\bar{\nabla} P + \bar{j} \times \bar{B} \tag{5.17}$$

where $\bar{B}$ = magnetic flux density vector.

**3. Energy Equation**

Conservation of energy in magnetohydrodynamic flow is represented by the following:

a. The rate of increase of the fluid energy is the sum of the rate of increase of kinetic energy and the rate of increase of internal energy.
b. The rate of energy input comes from the sum of

- The rate at which electromagnetic energy enters.
- The rate at which energy due to heat conduction and diffusion enters.
- The rate of energy input resulting from surface forces.

Then for incompressible, inviscid and steady flow the energy equation is given by

$$P\left(\bar{\nabla}\cdot\bar{\nabla}\right)\left[\frac{1}{2}V^2+\frac{P}{\rho}+C_V T\right]=\bar{E}\cdot\bar{j} \tag{5.18}$$

where E = total electric field intensity in volt per meter, $C_v$ = specific heat at constant volume, T = temperature in K, and j = current density in amperes per meter squared.

## B. ELECTROMAGNETIC FIELD EQUATIONS

### 1. The Charge Continuity Equation

$$\bar{\nabla}\cdot\bar{j}+\frac{\partial Pe}{\partial t}=0 \tag{5.19}$$

### 2. Ampere's Law

$$\bar{\nabla}\times\bar{B}=\bar{j}_t \tag{5.20}$$

where $\bar{j}_t$ = total current density vector.

$$\bar{\nabla}\cdot\bar{B}=0 \tag{5.21}$$

### 3. Faraday's Equation

$$\bar{\nabla}\times\bar{E}=-\frac{\partial\bar{B}}{\partial t} \tag{5.22}$$

The remaining Maxwell equation which relates the divergence of the electric field to the net charge density can be replaced by the condition that electron and ion densities are equal in magnetohydrodynamic flows.

### 4. Ohm's Law

$$\bar{j}_c=\left(\bar{E}_a+\bar{V}\times\bar{B}\right) \tag{5.23}$$

where $\bar{j}_c$ = conduction current density vector neglecting the Hall effect and ion slip, $\sigma$ = electrical conductivity, and $\bar{E}_a$ = applied electric field intensity vector.

### 5. The Energy Equation

$$W_{em}=\bar{E}_a\cdot\bar{j}_t-j_c^2 \tag{5.24}$$

where $W_{em}$ is the rate at which electromagnetic energy enters the flow field.

If $E_a = 0$:

$$W_{em} = \frac{j_c^2}{\sigma} \tag{5.25}$$

For MHD flow having the properties of being incompressible, inviscid, and steady and with no applied electric field the magnetohydrodynamic equations are

$$\begin{aligned} \bar{\nabla} \cdot \bar{V} &= 0 \\ P\left(\bar{V} \cdot \bar{\nabla}\right) \bar{V} &= -\bar{\nabla} P + \sigma \left(\bar{V} \times \bar{B}\right) \times \bar{B} \\ \bar{\nabla} \cdot \bar{B} &= 0 \\ \bar{\nabla} \times \bar{B} &= {}_o \mu^j \\ \left(\bar{V} \cdot \bar{\nabla}\right)\left[\frac{1}{2} V^2 + \frac{P}{\rho} + C\,T\right] &= -j_c^2 / \sigma \end{aligned} \tag{5.26}$$

if the Hall effect and ion slip are neglected.

## VIII. THE MHD GENERATOR PROBLEM[1-3, 15-24]

This is divided mainly into two parts. Part one undertakes the solution of all magnetofluid components of MHD generators where the fluid is a real synthetic gas usually considered to be viscous, incompressible, thermally conducting, and of scalar function electrical conductivity. The magnetic field is nonuniform due to two line conductors (see Figure 5.3). The solution of the magnetofluid components will be based on three dimensions. Part two will undertake development of an optimization theory and then establishment of criteria for optimum channel efficiency and fluid velocity. The physical features are

1. The gas mass density, P = P (P T).
2. The gas enthalpy, H = H (P T).
3. The gas electron mobility, $\mu = \mu$ (P T).
4. The gas electrical conductivity, $\sigma = \sigma$ (P T), where P T are the gas pressure and temperature of the real gas.
5. The heat loss per unit volume, G = G (P T U).
6. The wall-friction force per unit volume, F = F (P T U).
7. The applied magnetic field would be produced by a set of line conductors carrying DC or AC embedded under the lower channel plant and also over the upper channel plant, or by a set of magnetic dipoles, or even by a single line conductor below and above the channel plates.
8. The electrical loading function can be taken as only one parameter by applying certain restrictions.
9. Variations of MHD components could be taken in three dimensions along the direction of flow (X direction), transverse to the flow between the two electrodes (direction), and across the channel width (direction). The optimization could be applied on the following types of MHD generators:

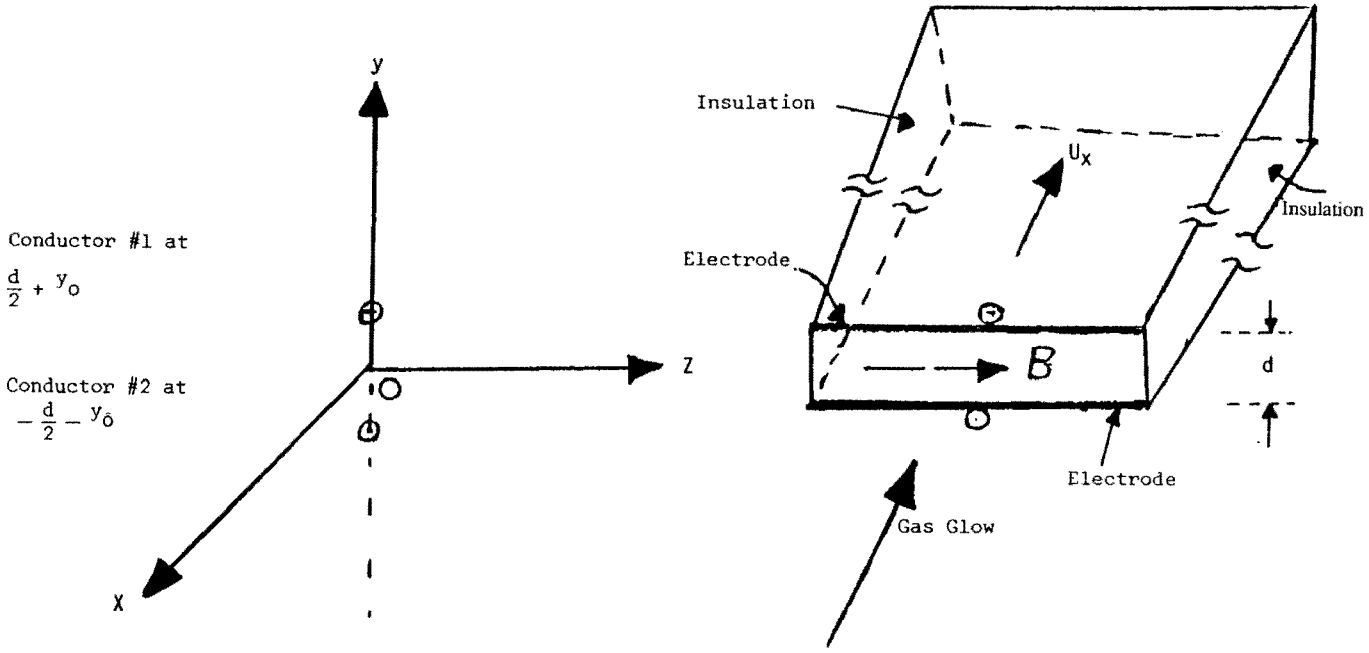


FIGURE 5.3 Generator channel.

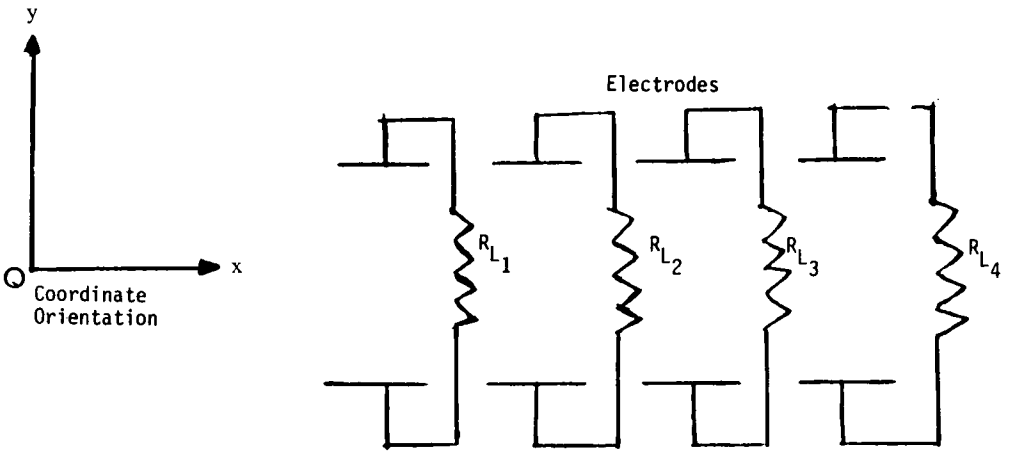


FIGURE 5.4 Multiple load for segmented generator.

a. The segmented electrode Faraday generator with multiple loading (See Figure 5.4).
b. Multiple load cross-connected generator (See Figure 5.5).
c. Single load cross-connected generator (See Figure 5.6).

10. Properties of thermal and electrical characterizations for the real gas could be modified to represent that of synthetic fuel extracted from refuse, namely $C_mH_{2+2m}$ by eliminating nitrogen from the equations as real gas mentioned above.

## IX. MAGNETOFLUID AND OPTIMIZATION PARAMETERS

$B_x$, $B_y$ = transverse magnetic field components
$E_x$, $E_y$ and $E_z$ = axial and transverse induced electric field components
$U_x$, $U_y$ and $U_z$ = axial and transverse fluid velocities
T = fluid temperature
P = fluid pressure
$T_s$ = fluid stagnation temperature
$P_s$ = fluid stagnation pressure
$K_n$ = channel dimensions
$\Gamma$= electrical loading function
F = wall friction force per unit volume
G = heat loss per unit volume

The electrical loading function $\Gamma$ could be any one of the following loading functions:

1. The isentropic efficiency where

$$n = \frac{\bar{J} \cdot \bar{E}}{\bar{V}\left(\bar{J} \times \bar{B}\right)} \tag{5.27}$$

$\eta$ is the ratio of power output per unit volume to total work exerted by the fluid against the electromagnetic decelerating force.

2. $$\lambda = J_x / \beta J_y \tag{5.28}$$

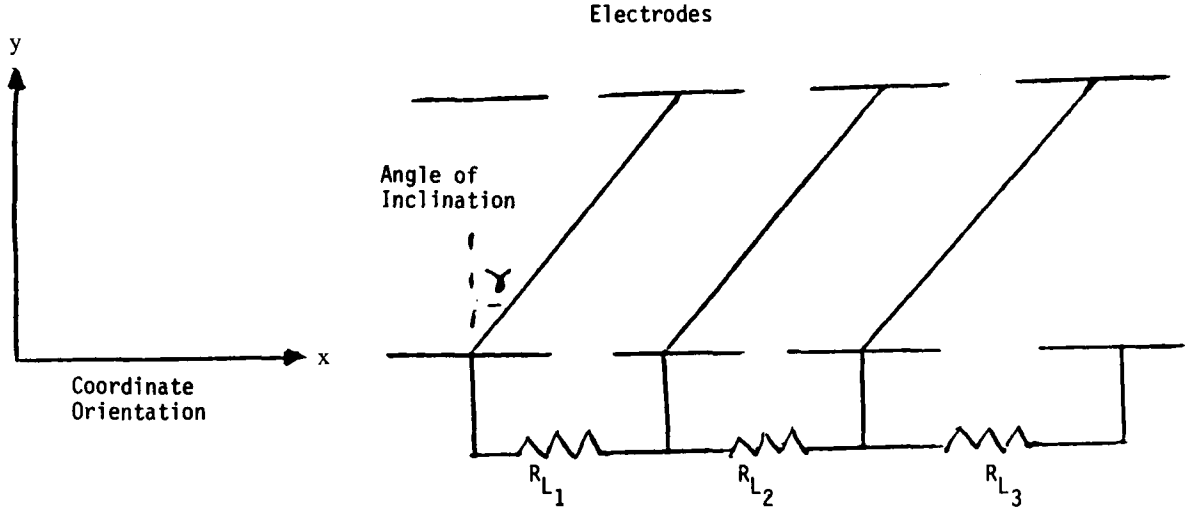


FIGURE 5.5 Multiple load cross-connected generator.

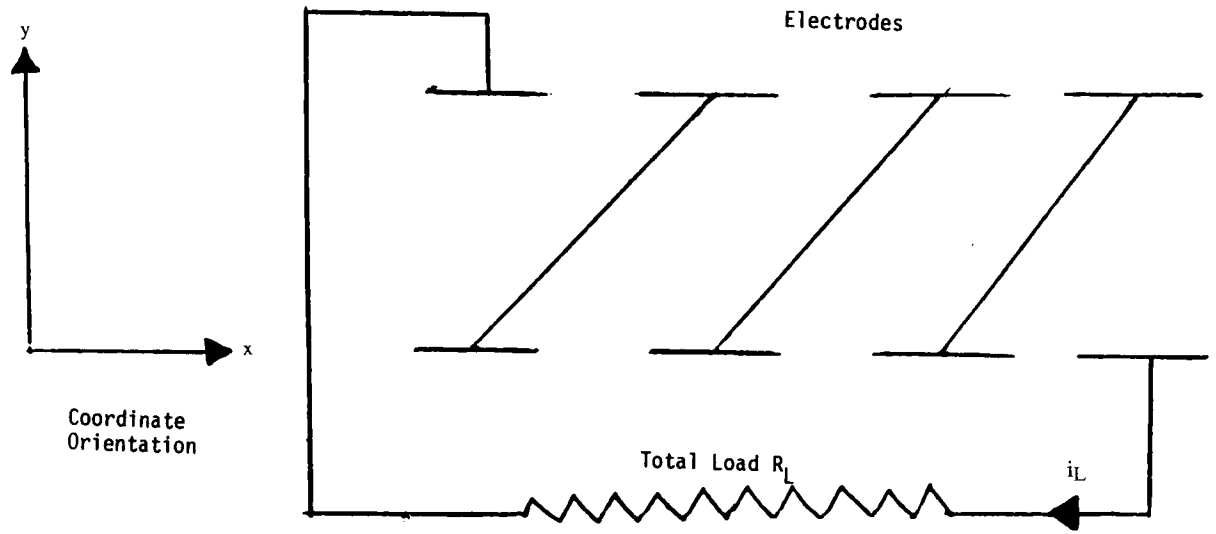


FIGURE 5.6 Single load cross-connected generator.

as the ratio of axial to transverse current densities and $\beta$ is the Hall parameter.

3. $$\theta = -E_y / E_x \tag{5.29}$$

as the ratio of transverse to axial electric fields.

4. $$M = E_x / E_{xo} \tag{5.30}$$

as a load parameter relating the electric field along the channel to the open circuited field.

5. $$i_L = A \frac{\bar{J}\,\bar{E}}{E_x} \tag{5.31}$$

as the total current crossing an equipotential plan in the generator. A = duct cross-section.

## X. THE PROBLEM OBJECTIVES

### A. TO OBTAIN SOLUTIONS FOR THE FOLLOWING MAGNETOFLUID COMPONENTS:

1. $B_{xt}$, $B_y$ and $B_t$ — total axial and transverse magnetic fields, (applied and induced).
2. $E_y$ and $E_x$ — induced electric fields.
3. $U_x$, $U_y$ and U — total gas velocity components.
4. $\bar{\nabla}P$, P — pressure gradient and total pressure components.
5. $\bar{\nabla}P_m$, $P_m$ — magnetic pressure gradient and magnetic pressure components.
6. Induced current densities $J_x$ and $J_y$.
7. To obtain solutions for:

   - output power density $(\bar{j}.\bar{E})$.
   - body force density $(\bar{J} \times \bar{B})$.
   - friction force per unit volume, F, which is a function of the velocity flow.
   - convective heat loss per unit volume, G, which is a function of the flow velocity.

### B. TO DEVELOP A SUITABLE OPTIMIZATION THEORY FOR THESE PROBLEMS:

1. To seek optimum MHD channel length and cross-sectional area by minimizing the integral of the ratio of total flow discharge to total power output density, that is

$$\text{To minimize} \rightarrow \left[\frac{\text{Total flow discharge}}{\text{Total power output density}}\right] \tag{5.32}$$

2. To establish the optimum gas velocity and efficiency between inlet and exit of the channel.
3. To establish the value of the cross-connected angle for optimum efficiency.

## XI. FUSION REACTION EXHAUST PLASMA[4-12, 15, 17, 23, 24]

This section presents a characterization of the fusion reactor (The Tokamak) exhaust plasma and its feasible application as a nonfossil fuel for MHD generators.

The nuclear fusion reaction is based on the perfect union of the two heavy isotopes of hydrogen, namely deuterium and tritium, producing a lighter atom, with the loss in mass

converted to energy. The fusion process is characterized by chemical–free pollution, cheap and inexhaustible fuel, negligible radioactive waste product ($10^{-6}$ with respect to the fission process), and predictably high efficiency.

Reliable operational criterion for nuclear fusion is the attainment of a reaction zone temperature of the order of $10^8$ °C, $10^{15}$ ions per cubic centimeter. and confinement time of 0.5 to 1 s.

This section presents a detailed review of fusion research which started in 1953 and culminated with the recent breakthrough accomplished by Princeton Laboratory production of a fusion temperature of $60 \times 10^6$ °C and a confinement time of 0.1 s in the design of the Tokamak Fusion Test Reactor.[1,2,23]

Also, work in this section includes modification in the magnetic field coils system near the reactor divertor for the goal of providing additional ohmic heating, positive cumulative pattern on confining the separatrix surface off the torodial field coils, and better streamlining for the entire divertor magnetic field pattern.

Further proceedings to consider the direct as well as indirect aspects of energy extraction from the nuclear fusion reactor system. Energy calculations are carried out for the direct modes associated with the main reaction plasma zone, as well as for the exhaust plasma where separation of charge carriers into groups according to their energy content is secured to impinge upon a series of appropriately biased collecting electrodes. Another direct mode of energy extraction considered is through the main plasma expansion work against a magnetic piston.

As for the indirect modes of energy conversion, work has been carried out for utilizing the thermal fusion energy released in producing hydrogen fuel through the endothermic electrolysis of water (for eventual use in fuel cells) and for steam production for conventional electric power plant operations. Another mode of indirect energy conversion considered was that of utilizing the exhaust chamber, and its plasma content, of the fusion reactor divertor as a channel for the AC magnetohydrodynamic electric power generation, including the induction as well as the synchronous modes.

The operational prospects of the nuclear fusion reactor is seen as very feasible within 10 to 15 years which, with the ample availability of its fuel isotopes (deterium is derived from the hydrogen in sea water and tritium could be extracted from lithium), will produce a vast portion of our nation's need of clean energy, free from any combustion products.

The main objective is to review realities of various modes of energy extraction from the Tokamak fusion reactor.

Direct modes include:

1. Energy extraction from the exhaust divertor plasma.
2. Energy extraction from the main plasma reaction zone.

Indirect modes include:

1. Expansion as a magnetic piston for the fusion main plasma as well as the exhaust.
2. Hydrogen fuel generation by endothermic and conventional electrolysis of water by thermal energy content of both the main plasma and exhaust.
3. MHD power generation using the divertor channel with its exhaust plasma.
4. MHD blanket and plasma blanket confining the main plasma zone.

## XII. DIRECT ENERGY[4-12,15,17,23,24]

This involves the processes of magnetic deflections for the electrons and all other ion impurities followed by charge collection through a multielectrode biased system.

Figure 5.7 represents a half cross-section of the Tokamak fusion reactor with the addition of

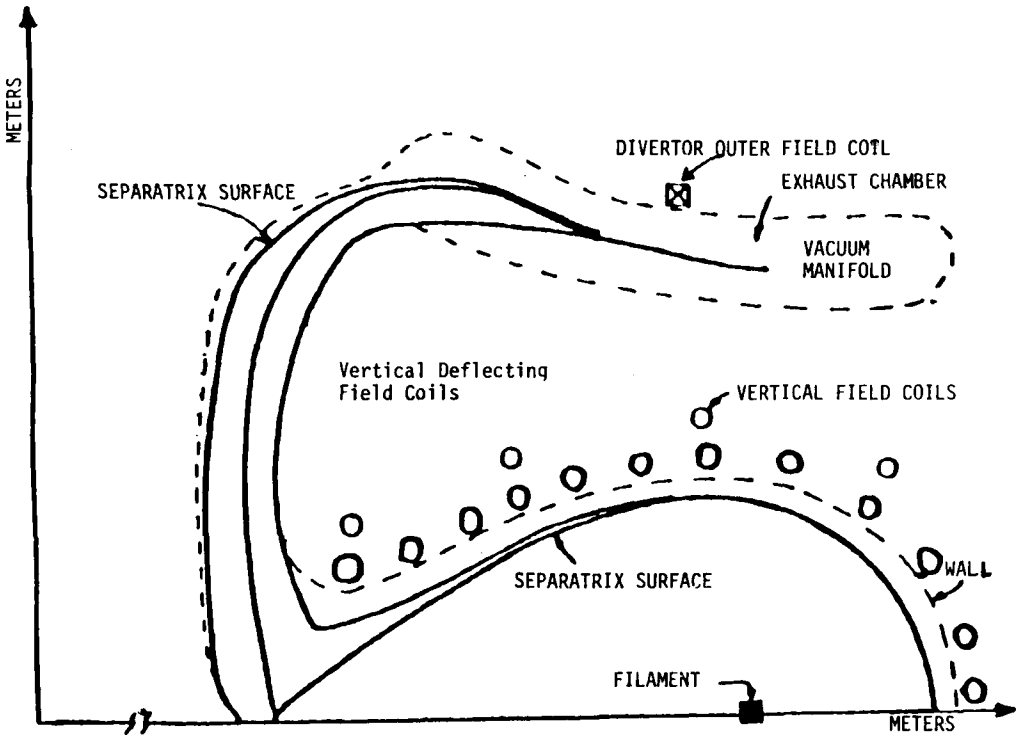


FIGURE 5.7 A half cross-section of the Tokamak Fusion Reactor. (From Tenney, F. H., A 2000 MW Fusion Reactor, An Overview, Proc. 5th Symp. on Engineering Problems of Fusion Research, IEEE, 1973, 65—68. With permission.)

another set of vertical field coils, whose function it is to impose the required mechanism for electrons deflection.

Also this additional set of coils may contribute to streamlining the separatrix field surface. A system of charge collections for the main zone could be set similar to that of the divertor channel. Calculations have been carried out for a radial spectrum of magnetic deflections, the number of cyclindrical electrode collecting shells, the spatial arrangement of deflecting coils, as well as a functional form for the terminal voltage.

## XIII. ENERGY EXTRACTION[4-12, 15, 17, 23, 24]

### A. THROUGH MAGNETIC PISTON ACTION

This mode of energy conversion is realized by letting either the main reaction plasma or the weakened exhaust plasma do work in a compressions pattern against a beam of dense magnetic flux density. A feasible application could demonstrate the divertor exhaust plasma exerting compression work against a circumferential magnetic field produced by a set of coils stationed at the terminal section of the exhaust chamber. Solutions have been obtained for the levels of magnetic compressions established by the moving exhaust plasma against the circumferential magnetic field, as well as rotational properties for the induced magnetic inductions at various radii of electron motion.

### B. HYDROGEN FUEL GENERATION

Endothermic as well as conventional electrolysis of water for the generation of $H_2$ and $O_2$ could be accomplished by utilizing the vast thermal energy content of the main reaction fusion plasma and the divertor exhaust plasma. Provided an effective procedure of separation for $H_2$

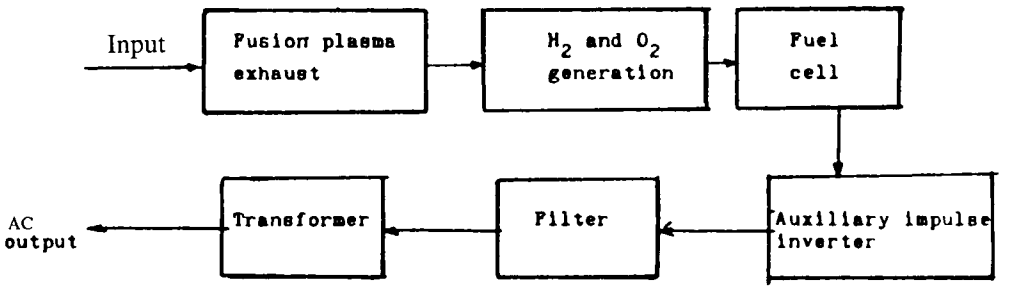


FIGURE 5.8 System diagram of electric power generation coupled to hydrogen release operation.

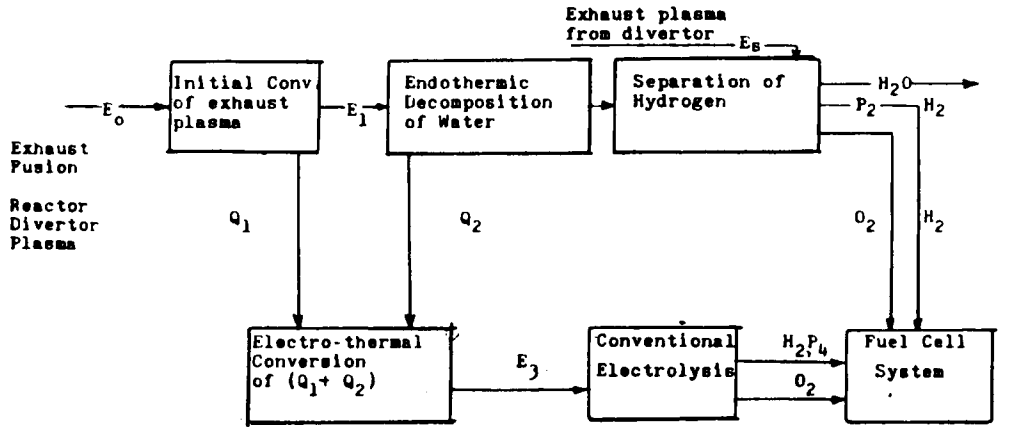


FIGURE 5.9 System diagram for the generation of $H_2$-$O_2$ endothermic and conventional electrolysis.

and $O_2$ could be devised, the hydrogen output would be fed as fuel in the process of electric power generation through a system of fuel cells. Eventually AC output could be secured through an appropriate inverter coupled to a compatible harmonic filter and required step up transformer. See Figure 5.8.

Calculations have been carried out to develop a systematic process for the generation of $H_2$ and $O_2$ by endothermic and conventional electrolysis of water using the thermal energy content of the fusion reactor exhaust plasma as shown in Figure 5.9, from which a dynamic model in the complex frequency domain could be developed. From the dynamic model stability aspects, steady state and time responses can be obtained for the net concentration of hydrogen energy content with respect to energy input of fusion plasma.

The fact is that with lower values for water enthalpy, an increase in the incremental level of $H_2$ release, with respect to initial fusion plasma energy content, will result. Eventually, $H_2$ secured from water through electrolysis could be fed as excellent potential fuel in the process of electric power generation.

## XIV. MHD POWER FROM THE DIVERTOR[4-12,15,17,23,24]

This system could be secured through direct utilization of the divertor channel with its plasma content near the scraper off region, then by placing a set of primary linear superconductors on both sides of the channel, biased with time varying field for plasma excitation, and followed by another set of secondary coils set for receiving an amplified induced voltage output. Also,

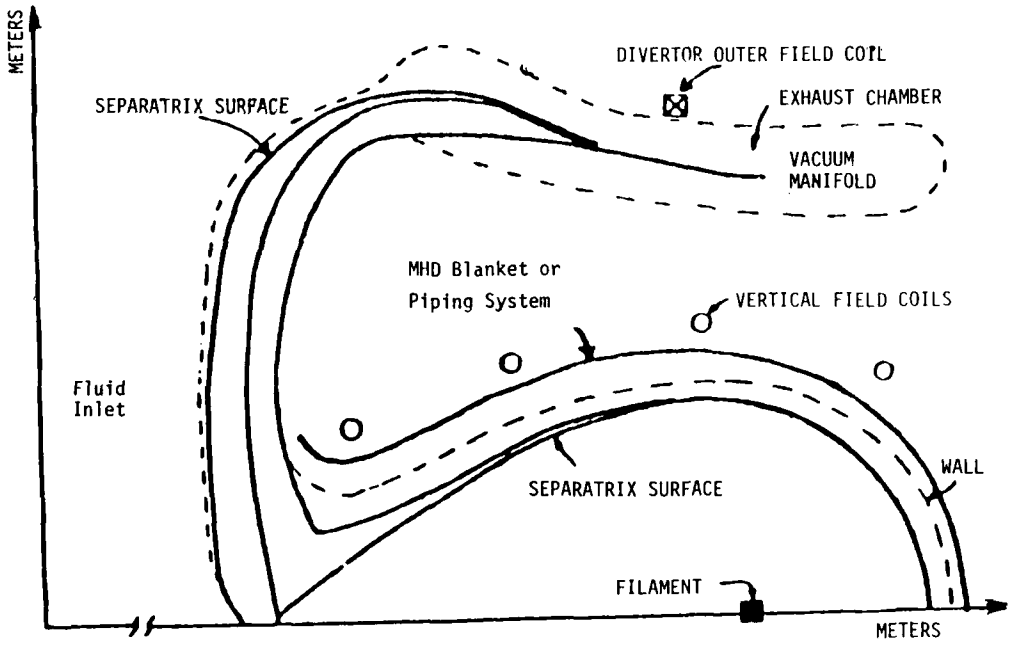


FIGURE 5.10 MHD blanket within fusion reactor. (From Tenney, F. H., A 2000 MW Fusion Reactor, An Overview, Proc. 5th Symp. on Engineering Problems of Fusion Research, IEEE, 1973, 65—68. With permission.)

insertion of the primary coils field will add to an improvement in streamlining of the poloidal divertor field.

Calculations have been carried out for all magneto-fluid perturbations in the divertor channel as well as MHD power generation performance parameters.

## A. MHD INDUCTION GENERATOR

By modifying the exhaust chamber into a cylindrical channel and exciting the plasma with a time varying current sheet, AC electric power output could be secured through a conventional winding enclosing the current sheet with a highly permeable cylindrical iron shell. Calculations[5-7] have been carried out for the functional distribution of the amplified magnetic field, current density, and the MHD generator performance parameters.

## B. ACCELERATOR INDUCTION MHD GENERATOR[14]

The divertor plasma would be accelerated through the inward half of the exhaust chamber by an external electric field, while the outer half could be used as a channel for an MHD induction generator.

Calculations[5] have been carried out for the pattern of accelerator parameters with respect to the operating range of magnetic amplification ratios, the design concept for the AC MHD generator, the optimum range for the outward exhaust channel, and output waveform purity.

## C. MHD BLANKET

A coaxial segmented channel could be designed and inserted within the fluid blanket surrounding the main reaction plasma zone (shown in Figure 5.10). The MHD fluid at ambient temperature could be fed through the channel inlet at a velocity close to or around sonic level in a circumferential direction. The injected fluid blanket will absorb heat energy through conduction for a level which could be set in accordance with the limit of the maximum degree of ionization suitable for MHD operation, namely that the magnetic Reynolds number of the

MHD plasma must not exceed 10%. A set of vertical field coils could be placed beneath the internal and external walls of the MHD shell for exciting the MHD working fluid and, at the same time, streamlining the separatrix surface. Electric power output could be delivered to an external set of load resistors connected to the system of electrode segments of the MHD channel.

Another useful and more practical utilization of the main fusion reaction zone thermal energy is as a heating source for a plasma blanket, which may take the configuration of a coaxial shell around the main plasma zone, or could be a system of multiaxial piping system carrying MHD fluid. In both cases of the coaxial shell and piping system, the heating plasma will be delivered at the exit to a separate MHD power generating plant as a suitable working fluid. The level of plasma temperature acquired by the injected cold fluid is determined by the criterion established earlier, that is, the magnetic Reynolds number should not exceed 10%, i.e.,

$$R_m = \mu_o \left[\sigma_o y_o V_o\right]$$

where $\mu_o$, $\sigma_o$ = plasma permeability and electrical conductivity, respectively, $y_o$,$V_o$ = plasma reference distance and initial velocity, respectively. Figure 5.10 shows simply the feasible location of MHD or the plasma blanket or the piping heating system.

## XV. MHD SYNCHRONOUS GENERATOR[9]

The exhaust plasma of the fusion reactor, usually at low level in pressure and velocity, will be accelerated through the action of any model of the linear induction accelerators. Structural components of the synchronous MHD generator are comprised of a coaxial, perfectly conducting, cylinder, with the inner cylinder having a set of lateral tangential blades whose function is to impart the rotor with the desired mechanical velocity for synchronous operation from the impinging plasma.

Electric AC power would be developed through induction in a sinusoidally distributed three phase conventional winding close to the inner cylinder.

Magnetic fluid interaction solutions, as well as electromechanical outcome power expressions, have been secured for actual concept design.

The following relationships are expressed due to their significance

$$W_m = \frac{V_x + V_o}{\gamma} \tag{5.33}$$

where $w_m$ = mechanical angular velocity imparted to the inner cylindrical shell rotor, $v_o$ = the final value of accelerated velocity for the exhaust plasma, $v_x$ = plasma velocity perturbation due to MHD interaction, and r = radius of the inner cylindrical rotor. The induced magnetic induction at the walls of the cylindrical rotor,

$$B_{ind} = \sum_{n=1}^{\infty} \frac{9A}{n^2 \pi^2} \sin\frac{n\pi}{3} \sin\frac{n\pi x}{a} - \sum_{n=0}^{\infty} \frac{6A}{n\pi} \sin\frac{n\pi x}{a} \tag{5.34}$$

The axial velocity perturbation $v_x$ is controlled by the magnetic Reynolds number ($R_m$) and the magnetic interaction parameters (I), i.e.,

$$X = \gamma \cos\theta$$

$$V_x = F\left(L, r, R_m, J, \theta\right) \tag{5.35}$$

L = width of the coaxial plasma medium and r, θ = radial depth and angular displacement within the plasma annulus.

The mean, time varying emf, induced in the three phase, sinusoidally distributed, conventional winding, is written below:

$$\text{Eph} = \frac{4.44\ \text{fkw}\ N_{ph}}{c}\left[\frac{2/D}{p}\left(\sum_{n=1}^{\infty}\frac{9A}{n^2\pi^2}\ \sin\frac{n\pi}{3}\ \sin\frac{n\pi x}{a} - \sum_{n=1}^{\infty}\frac{6A}{n\pi}\ \sin\frac{n\pi x}{a}\right)\right] \tag{5.36}$$

where $k_w$ = pitch distribution winding factor, c = number of stator circuits per phase, A = peak value of B field induced, l, D = axial length and diameter of the plasma annulus, and a = circumferential separation of line conductors producing the external magnetic field.

Sections XII through XVI spanned several feasible systems for energy extraction from the fusion reactor, namely the Tokamak Princeton Test Reactor. Alternatives are confined into two main mechanisms which are direct and indirect systems.

The direct mechanisms are

1. Separation and collection of plasma electrons through a set of DC biased electrodes where high voltage terminal output could be collected. This system could be applied to either the main fusion plasma or the exhaust divertor plasma.
2. Letting either the main fusion plasma or the divertor exhaust do work as a magnetic piston against the beam of magnetic flux.

The indirect mechanisms are

1. Hydrogen generation, through endothermic as well as conventional electrolysis of water, which, after successful separation, could be used as fuel in the electrochemical reaction of the fuel cell.
2. MHD electric power generation could be extracted from the divertor exhaust plasma as the working fluid, after its temperature is reduced to a level suitable for MHD operation, and the exhaust chamber, through geometrical modification, could be used as an accelerator MHD generator.
3. The main fusion plasma zone could be the potential heating source for an MHD blanket through a coaxial shell or a multiaxial piping system enclosing the main reaction zone.

## XVI. MHD CENTRALIZED POWER SYSTEM

MHD operational plants, using fusion reactors exhaust plasma as their working fluid or thermally ionized synthetic fuel extracted from refuse, can feasibly be seen as an ideal alternative to replace nuclear fission plants in the centralized mode for power generation and its eventual delivery.

The centralized system of power generation known as plan A in Chapters 1 and 2 in which power sources are identified as nuclear and pumped-hydro, provide base power loads, while fossil-steam generators provide for off-peak loads, and gas turbines provide for peak loading.

Central topography for MHD power plants can be identified as replacing all nuclear plants identified in Chapters 1 and 2 in terms of their [B] matrices, [R] matrices, as well as their incremental fuel cost curves given in Chapter 2.

Information for the [B] matrices (known as the power linkage matrices), as well as of their corresponding symmetric [R] matrices, can provide an effective and reliable base for the design of any other power system even if there are significant changes in fuel cost of new power sources.

Therefore, replacing nuclear power plants in the system plan A described in Chapters 1 and

2 will render a definite change in the incremental fuel cost curves for the new MHD generating plants.

To use the [B] and the [R] matrices, whose data is given in Chapters 1 and 2, we may proceed to keep those matrices as invariants so that they could be continued to be used as reliable tools for design basis of a new power system in the power flow reference frame.

Invariancy of the [B] matrix in a system containing MHD power plants with pumped-hydro generators supplying base loads, while fossil-steam generators supplying off-peak loads and gas-turbine plants supplying peak loads, the following cases of fuel cost are restated from Chapter 4.

A new incremental fuel cost curve with the same vertical intercept, i.e., $F'_{ii} = k\, F_{ii}$, $f_i$ remains constant. Restating conditions for the multiplying factor k:

$$k_{1\text{-MHD}} \cong 1 - \frac{C}{A} \tag{5.37}$$

$$k_{2-\text{MHD}} \cong 1 + \frac{b'}{a'x} \tag{5.38}$$

$k_{3\text{-MHD}}$ which can be extracted from Chapter 4, Equation 4.102.

A new incremental fuel cost curve in which the slope is the same but with a new vertical intercept, i.e., $F_{ii}$ remains constant.

$$f'_i = k\, f_i \tag{5.39}$$

Restating conditions for the new multiplying factor from Chapter 4 such that the [B] matrix remains invariant.

$$k'_{1-\text{MHD}} = 1 - \frac{A_1}{C_1 X} \tag{5.40}$$

$$k'_2 - \text{MHD} = 1 + \frac{D_1}{E_1 X} \tag{5.41}$$

$k'_{3\text{-MHD}}$ is one that is similar in principle to that of Chapter 4, Equation 4.102.

A new incremental fuel cost curve in which both $F_i$ and $F_{ii}$ will have a new, unified, multiplying factor k. $k_{MHD}$ is similar to one that can be extracted from Chapter 4, Equation 4.121.

In Equations 5.48 through 5.52, all parmeters $C_1$ A, a , b have been described in Chapter 4.

## XVII. MHD DISPERSED POWER SYSTEM

MHD power generating plants using nonfossil plasma as their working fluids, or thermally ionized synthetic fuel extracted from prepared refuse, can be utilized to provide electric power in closely or remotely dispersed system.

Power system plan E, described in Chapters 1 and 2, in which new generators and new load centers, with respect to the limit of original loads, are supplied by fuel cell power plants, now will be supplied by MHD power generating plants with new incremental fuel cost curves.

In Chapter 2, the [B] matrix for a dispersed system linked through optimal power coefficients was presented and is given below because of its importance:

$$B'_{ij} = B_{ij}\left(1 + \frac{P_T}{2\,P_L}\right) \tag{5.42}$$

or

$$B'_{ij} = \frac{H_z F_{ii}(\lambda - F_{ii}P_i - f_i)}{H_i P_i F_{jj}\ \lambda + H_2 P_j F_{ii}\lambda} \tag{5.42a}$$

where

$$H_1 = \frac{F_{ii}}{F_{jj}} - \frac{(\lambda - F_{ii}P_i - f_i)}{\lambda \cdot F_{jj}P_j - f_j} \tag{5.43}$$

$$H_2 = \frac{F_{jj}P_j - f_j}{F_{ii}P_i - f_i} - \frac{F_{jj}}{F_{ii}} \tag{5.44}$$

Consider the case where the incremental fuel cost curve for the MHD power plants is constant, i.e., $F_{ii}, - F_{jj} = 0$ and only $F_i$ and $F_j$ are constants.

The $B_{ij}$ matrix is looked upon as the central basis of system identification for a power system that is a combination of central topology and dispersed and, with its corresponding [R], the symmetric resistance matrix, provides a system design in the sixth or what is known as the power flow reference frame.

To look at system optimal performance, in terms of the role of the [B′] matrix, we can carry out differentiation of [B′] with respect to ($L_i$), then set the expression of $\partial B_{ij}/\partial L_i$ as equal to zero.

From the process of

$$\frac{\partial B_{ij}}{\partial f_i} = 0$$

as expected, the secured condition came to be that of $\lambda = f_i$.

In Chapters 1 and 2, the [B] matrix was given for a centralized-dispersed system containing about 128 bus-bars, where dispersed power plants were supplied by fuel cell generators.

Invariancy of the [B′] matrix can be used as the central base through its corresponding [R] matrix to reflect on system design in the power flow reference frame.

Securing a system design in the sixth or power flow reference frame can lead to eventual identification in the first, or the actual, frame through a set of matrix transformations from the sixth, the fifth, the fourth, the third, the second and then finally, to the first, which is the actual frame in which the linking network is identified in terms of impedances, power sources in terms of real and reactive powers, as well as voltage magnitudes and phase angles of power and load bus-bars.

Now, to use an established [B] matrix and its associated [R] matrix for a power system containing new power sources with a new incremental fuel cost curve, as in this new case, where MHD plants replace fuel cell generators to supply new load centers and new planned generators as described in plan E in Chapters 1 and 2, a new multiplying factor for the MHD incremental fuel cost curve be expressed so that the [B] matrix for the centralized-dispersed system remains invariant.

The incremental fuel cost curve for the MHD plants will have zero slope, but a new vertical intercept, $L_i$, such that, $f_i = k\, f_i$. The new but invariant [B] matrix becomes

$$B'_{2-ij} = \frac{(\lambda - kf_i)^2 (f_j - kf_i)}{(kf_i - f_j)(\lambda - f_j) P_i + (f_j - kf_i)(\lambda - kf_i) P_j \lambda} \tag{5.45}$$

while the originally established $[B'_{1\text{-}ij}]$ has the form,

$$B'_{1\text{-}ij} = \frac{(\lambda - f_i)^2 (f_j - f_i)}{(f_i - f_j)(\lambda - f_j)P_i + (f_j - f_i)(\lambda - f_i)P_j\lambda} \tag{5.46}$$

For the [B'] matrix to remain invariant; $B_{2\text{-}ij} = B'_{i\text{-}ij.}$

Therefore from Equations 5.56 and 5.57 the value expression for the multiplying cost correction factor (k) is

$$k_{MHD} = \frac{\beta \pm \sqrt{\beta^2 - 4\alpha\gamma}}{2\alpha} \tag{5.47}$$

where

$$\alpha = f_i^3 - P_j f_i^2 \lambda \left(B'_{1\text{-}ij}\right) \tag{5.48}$$

$$\beta = \left[\lambda f_i + f_j f_i^2 + \lambda P_i (\lambda - f_i) f_i \left(B'_{1-ij}\right) - \lambda P_j f_i f_j \left(B'_{1-ij}\right)\right] \tag{5.49}$$

$$\gamma = \left[\lambda f_j - \lambda P_i (\lambda - f_j) f_j B'_{1-ij} - \lambda^2 j f_j \left(B'_{1-ij}\right) + \lambda^2 f_i P_j \left(B'_{1-ij}\right)\right] \tag{5.50}$$

## XVIII. CASE STUDY

This case refers to Case Study or Example 2, presented in Chapter 2 with eight plants located in a dispersed mode and with the power linking various dispersed plants.

Optimum scheduling of generation for the eight plants was calculated at a peak generation limit as well as at 67% and 41% generation limits.

The [B'] matrix was also calculated as shown in Table 1.13 in Chapter 1 with minimum transmission losses taken as criterion for the optimal value for the cost of received power in dollars per megawatt hour which is λ. The corresponding values of λ are 2.9, 2.0, 1.6, and 1 MWh for minimum transmission losses.

The present case is calling for replacing all plants by MHD power generating plants such that the original [B] will remain invariant as the principle base for designing the new MHD interconnected grid system. The case calls for calculating the MHD power multiplying factor such that the [B] matrix remains invariant.

To find $k_{MHD}$ for every plant in the eight plants system, we will proceed according to a sample demonstration to show how to calculate every element involved for k for any plant.

Elements for $k_{MHD}$ are indicated in Equations 5.40, 5.41, and Chapter 4, Equation 4.102.

As a procedural example, we will show the initial step of calculating for plant number 1:

$$\alpha = f_i^3 - \lambda P_j f_i^2 \qquad B_{1\text{-}ij}$$

where $B'_{1-ij}$ is the original [B'] matrix already calculated and shown in Chapter 1, Table 1.13.

Using incremental fuel cost data describing the eight plants system, shown in Chapter 1, Tables 1.12 and 1.13 for the original [B'] matrices, the following sample of calculations is provided.

To calculate $\alpha_1$ for plant #1 as MHD power plant at peak loading:

$$\alpha_1 = (1.28)^3 - 2.9 \times 1.28^2[-210 \times 0.815 \times 10^{-2} - 270 \times 0.44 \times 10^{-2} - 420 \times 0.149 \times 10^{-2}$$
$$-310 \times 0.8433 \times 10^{-3} - 240 \times 0.2408 \times 10^{-3} - 1100.299 \times 10^{-4} + 180 \times 0.59 \times 10^{-4}]$$

Therefore, $\alpha_1 = 20.328993$.

Similarly, calculations can be carried out for finding values of $\beta_1$ and $\gamma_1$, where $k_1$ for plant #1 will be obtained.

Proceeding now for the fuel cost multiplying factor for MHD plant #2:

$$\alpha_2 = (0.795)^3 - 2.9 \times (0.795)^2[-260 \times 0.815 \times 10^{-2} + 270 \times 0.582 \times 10^{-3} + 420$$
$$\times 0.414 \times 10^{-3} + 31 \times 0.818 \times 10^{-3} - 240 \times 0.63 \times 10^{-3} - 110 \times 0.3816 \times 10^{-4} + 180$$
$$\times 0.009 \times 10^{-4}]$$
$$\alpha_2 = 2.1802154.$$

For MHD plant #3:

$$\alpha_3 = (1.809)^2 - 2.9 \times (1.809)^2[-260 \times 0.444 \times 10^{-2} + 210 \times 0.5825 \times 10^{-3} + 420$$
$$\times 0.25 \times 10^{-3} - 310 \times 0.465 \times 10^{-3} - 240 \times 0.625 \times 10^{-3} - 110 \times 0.298 \times 10^{-4} + 180$$
$$\times 0.5116 \times 10^{-4}]$$
$$\alpha_3 = 19.446237$$

For MHD plant #4:

$$\alpha_4 = (0.657)^3 - 2.9 \times (0.657)^2[-260 \times 0.149 \times 10^{-2} + 210 \times 0.414 \times 10^{-3} + 270$$
$$\times 0.2576 \times 10^{-3} + 310 \times 0.338 \times 10^{-3} + 240 \times 0.3607 \times 10^{-3} - 110 \times 0.191 \times 10^{-4}$$
$$+ 180 \times 0.331 \times 10^{-4}]$$
$$\alpha_4 = 0.5450141$$

Other remaining values for $\alpha$, as well as all values of $\beta$ and $\gamma$ for all MHD plants could be calculated, where the multiplying factor (k) for every MHD plant would be secured.

It is important to recognize the fact that the economic multiplying factor (k) is rigidly associated with the economic optimal scheduling of power generation for every source in the system, which would assure total controlled economy.

## XIX. SUMMARY

This chapter presented an open and frank perspective global model centered around the utilization of nuclear energy in the U.S. and abroad. The physical model identified various milestones of nuclear energy utilization, including fission and fusion processes, with respect to the availability of fossil fuel energy sources and the feasibility of alternative energy sources as well.

The physical global model stresses the realistic future situation that the bulk amount of energy could be extracted from nuclear modes as well as fossil fuel resources. However, since the later is in a dwindling state, reliance on nuclear energy to meet the huge demand by industry and other load centers, requires the bold acceptance of the fact that nuclear fusion power is the answer for meeting the increasing future energy needs.

The physical model also points out the safeguards, for the safety of populated zones and the protection of the environment, as prerequisite milestones in the location of nuclear power plants.

The model presents a balanced equation for the acceptability of nuclear fission and fusion in the U.S. and abroad with respect to the probability of radiation, which is much higher in fission reaction than in fusion, the safety of population in close proximity to nuclear centers, and the environmental safeguards of our world.

This chapter as a whole touched on a comprehensive review of various feasible modes of securing electric power output from the Tokamak Reactor. A direct mechanism includes the procedure of charge separation and collection through a system of biased electrodes, for either the main fusion plasma and/or the exhaust divertor plasma.

Indirect mechanisms include magnetic piston action by either or both the main plasma and the divertor plasma, hydrogen production by endothermic and conventional electrolysis of water through thermal energy content of the main plasma and the divertor, MHD power generation using the divertor and the exhaust chamber with their plasma content, and the system of MHD or plasma blanket enclosing the main fusion reaction zone.

In addition to the preceding presentation, this chapter emphasized the main aspects of economic utilization of MHD power using renewable fuel such as the exhaust plasma from the fusion nuclear reactors or thermally ionized synthetic fuel extracted from prepared refuse. The presentation included determination of the economic cost of fuel for the MHD power plants based on the criteria of invariant power linkage matrices already established.

Consideration of the optimal fuel cost multiplying factor has been linked to centralized systems, where MHD plants have been integrated with fossil-steam, gas-turbine, and nuclear power plants.

Also, utilization of MHD plants fueled by renewable resources have been considered to operate and supply energy in a dispersed pattern and in connection with other centralized sources. Economic utilization of such MHD plants has been evaluated and the feasibility of optimal cost was established based on the invariancy of the [B] matrix, better now identified as the power linkage matrix.

The incremental fuel cost multiplying factor has been determined for optimal scheduling of generation for the centralized-dispersed integrated system.

## XX. PROBLEMS

5.1 Matrix Equation 5.2 represents a four-dimensional model for a balanced energy demand with respect to public concern. Transform this matrix equation into the principle coordinate system, where all diagonal elements exist in the new matrix. Comment on the implications the new matrix would have on the distribution of energy at the global, as well as the national level.

5.2 Repeat the state of Problem 5.1 with respect to Equation 5.5.

5.3 Establish a point-by-point comparison between the conventional turbo generator and the MHD generator shown in Figure 5.1.

5.4 Given a parallel plate MHD channel of 0.2 m height, 4 m length with a front cross-section in the x-y plant. The applied B magnetic field and the flow velocity field are expressed as follows:

$$B = \left(a_x 0.8Y + a_y 1.5x + a_z 0.1x^2\right) \quad \text{tesal}$$

$$\bar{v} = \left(a_y 150x + a_x 50Y + a_z 200\right) \quad \text{m / s}$$

Calculate the induced electric field and b the potential difference built across a channel width of 0.1 m. If the MHD channel loading factor = 0.7, calculate the actual terminal

voltage across the channel width (loading factor = actual terminal voltage divided by the induced voltage).

5.5 Supplemental to the data in Problem 5.4, give the moving fluid electrical conductivity $\sigma = \alpha e^{-}(a/xt)$, calculate the induced electric density and then the net electric charge density, where t is time in seconds and a is a constant.

5.6 Using the data of Problems 5.4 and 5.5 above, and if there is no applied electric field, calculate the energy density developed in the MHD channel.

5.7 The set of Equations 5.29 through 5.37 represents characterization for the thermal and electrical properties of a real mixture of hydrocarbon fuel. Modify this set of equations as if the real gas is a synthetic fuel $C_mH_{2m+2}$ extracted from prepared refuse.

5.8 Equation 5.36 represents the emf induced per phase in a three phase MHD synchronous generator. Compare this expression with that of a conventional three phase alternator of cylindrical rotor. Obtain an expression for the fundamental frequency and a set of harmonics up to the fifth order.

5.9 Equation 5.37 refers to a multiplying factor, k, for the incremental fuel cost curve to keep the [B] matrix, known as the power linkage matrix, for a centralized power system invariant. A and C have been expressed in Chapter 4 by Equations 4.91 and 4.92. The planning in this problem is to replace all nuclear generators in conventional plan A described in Chapters 1 and 2 by MHD generators. Calculate the value of (k) for a new MHD generator. Use the incremental fuel cost curves given in Chapter 2.

5.10 Repeat Problem 5.9, with respect to the other multiplying factor ($k_2$) expressed in Equation 5.49. Parameters $a'$ and $b'$ have been given by Chapter 4, Equations 4.92 and 4.93. Use the incremental fuel cost curves in Chapter 2.

5.11 Repeat Problem 5.9, with respect to alternative power system B described in Chapters 1 and 2, with MHD generators replacing the fossil-steam power plants as new power sources.

5.12 Repeat Problem 5.10, with respect to alternative power system C described in Chapters 1 and 2 with MHD generators replacing gas–turbine generators as new power sources.

5.13 Repeat Problem 5.9, with respect to alternative power system H described in Chapters 1 and 2, with MHD generators replacing storage batteries as new power sources.

5.14 Repeat Problem 5.10, with respect to alternative power system G, with MHD generators replacing fuel cells as new power sources.

5.15 The incremental fuel cost multiplying factor $k_{1\text{-MHD}}$ expressed by Equation 5.48 is a function of $P_i$, $P_j$, $F_i$, $L_j$, $F_{ii}$, $F_{jj}$ and $\lambda$. Consider that $P_j = G(P_i)$, then find an optimal solution for $k_{1\text{-MHD}}$ when both $P_i$ and $P_j$ are subject to change within their range and capacity.

5.16 Repeat Problem 5.15, with respect to $k_{1\text{-MHD}}$ expressed by Equation 5.49. Find the value of $\lambda$ in terms of $P_i$, $P_j$, $F_{ii}$.

5.17 The incremental fuel cost multiplying factor $k'_{1\text{-MHD}}$ given by Equation 5.40 is a function of $P_i$, $P_j$, $\lambda$, $F_i$, $f_j$, $f_i$, $F_{ii}$ and $F_{jj}$. Consider $P_j = G(P_i, \lambda)$, then secure an optimal solution for $k_{1\text{-MHD}}$.

5.18 Repeat Problem 5.17 with respect to $k'_{2\text{-MHD}}$ expressed by Equation 5.41.

5.19 Example 2 in Chapter 1 dealt with an eight plant dispersed system with tie power flow among all plants. Use Equation 5.48 to complete the calculations of $\alpha_5$ - $\alpha_8$.

5.20 Supplemental to the requirements in Problem 5.19 above, proceed to calculate $\beta_1 - \beta_8$.

5.21 Supplemental to data obtained in Problems 5.19 and 5.20, proceed to calculate $\gamma_1 - \gamma_8$.

5.22 Using results secured in Problems 5.19, 5.20, and 5.21, establish a table for the MHD fuel cost multiplying factor, k, expressed by Equation 5.48.

5.23 Equations 5.40, 5.41, and Chapter 4, Equation 4.102 identifies $k_{MHD}$ in terms of $P_i$, $P_j$, $f_i$, $f_j$, $F_{ii}$, $F_{jj}$ and $\lambda$. With only $P_i$ as the independent variable, find condition of $\lambda$ for the optimal value of $k_{MHD}$. Use the data of Example 2 of Chapter 2 for optimal $\lambda$. Consider 67% loading.

5.24 Repeat Problem 5.23 under the conditions that $P_i = G(P_j)$. Also obtain the optimal $\lambda$ for the system of Example 2 of Chapter 2. Loading = 41%.

5.25 Repeat Problem 5.24 for 100% loading.

5.26 In Chapter 1, an eight plant dispersed power system with information for the incremental fuel curves, maximum capacities, and their calculated [B] matrices at 100, 67, and 41% of generation was given. For a new MHD generating plant, if $f_i$ remains constant as given and each $F_{ii}$ is multiplied by the following factors, establish a new optimal scheduling of generation at 100% generation.

| Given $F_{ii}$ | Multiplying factor |
|---|---|
| 0.0082 | 2 |
| 0.0044 | 2 |
| 0.0019 | 5 |
| 0.00429 | 5 |
| 0.00222 | 10 |
| 0.0120 | 10 |
| 0.0208 | 4 |
| 0.0127 | 4 |

Use Equation 5.48 for k.

5.27 Repeat Problem 5.26 for 67% generation.

5.28 Repeat Problem 5.26 for 41% generation.

5.29 Repeat Problem 5.26, but when $F_{ii}$ remains constant and each $L_i$ has the following multiplying factor:

| Given $f_i$ | Multiplying factor |
|---|---|
| 1.28 | 1 |
| 0.795 | 2 |
| 1.809 | 3 |
| 0.657 | 4 |
| 0.889 | 5 |
| 0.300 | 6 |
| 0.635 | 7 |
| 0.572 | 8 |

Use Equation 5.51 for k.

5.30 Repeat Problem 5.29 for 67% generation.

5.31 Repeat Problem 5.29 for 41% generation.

5.32 Repeat Problem 5.26, using Equation 5.49.

5.33 Repeat Problem 5.32 for 67% generation.

5.34 Repeat Problem 5.32 for 41% generation.

5.35 Repeat Problem 5.35 at 67% generation.

5.36 Repeat Problem 5.35 at 41% generation.

## REFERENCES

1. **Carter, C. and Heywood, J. B.,** Optimization studies on open-cycle MHD generators, *AIAA J.*, 6, 1703—1711, 1968.
2. **Deen, J. L. and Schoepel, R. J.,** Hydrogen and the electric economy, *Proc. Frontiers Power Tech. Conf.*, Vol. 4, Oklahoma State University, Stillwater, 1971.

3. **Denno, K.** Auxiliary control of the magnetic field system of the fusion reactor divertor, IEEE Proc. 6th Symp. Eng. Prob. Fusion Res., San Diego, CA, 1975.
4. **Denno, K.,** Dynamic modeling of a hydrogen generating system using fusion reactor exhaust plasma interconnected to a fuel cell, IEEE Proc. 6th Symp. Eng. Prob. of Fusion Res., San Diego, CA, 1975.
5. **Denno, K.,** Pulsed acceleration of exhaust plasma in a fusion-MHD power plant, IEEE Proc. 7th Symp. Eng. Prob. Fusion Res., Knoxville, TN, 1977.
6. **Denno, K.,** Direct energy conversion of exhaust plasma by magnetic deflection, IEEE Proc. 7th Symp. Eng. Prob. Fusion Res., Knoxville, TN, 1977.
7. **Denno, K.,** Generation of electric A.C. power through magnetic piston action of divertor plasma, IEEE Proc. 8th Symp. Eng. Prob. Fusion Res., San Francisco, CA, 1979.
8. **Denno, K.,** Generation aspects of weakened fusion plasma in MHD channel, *J. Appl. Sci. Eng. A,* 213, 1978.
9. **Denno, K. and Fouad, A. A.,** Effects of the induced magnetic fields on the MHD channel flow, *IEEE Trans. of Electron Devices*, 19, 322—331, 1972.
10. **Denno, K.,** Magnetohydrodynamic perturbations for a finite magnetic reynolds number, *J. App. Sci. Eng. A,* 3, 261, 1979.
11. **Denno, K.,** Computerized Solutions of Induced Magnetic Field in MHD Channel, presented at the 3rd Reno Conf. Magn. Fields, University of Nevada, Reno, September 1971.
12. **Denno, K.,** The Global Nuclear Energy Equation, Symp. World Lett. Found., St. Louis, Missouri, 1984.
13. **Denno, K.,** Realities of nuclear fusion reactor and modes of energy conversion, *Int. J. Energy Systems*, 7, No. 1, 24, 1981.
14. **Elliot, D. G.,** Variable velocity MHD induction generator with rotating machine internal electrical efficiency, *AIAA J.*, 6, 1968.
15. **Fish, J. D. and Axtmann, R. C.,** Utilization of plasma exhaust energy for fuel production, *IEEE Proc. 5th Symp. Eng. Probl. Fusion Res.,* Princeton University, NJ, 1973, 146—151.
16. **Hals, F. A.,** *MHD Power Generation,* Am. Soc. Mechan. Eng., AMP 249, 1967.
17. **Hals, F. A.,** Environmental pollution control through MHD power generation, *Combustion,* May 1970 and Report issued by AVCO; Everett Research Lab, Everett, MA.
18. **Panel on MHD,** MHD for Central Station Power Generation, prepared for the Executive Office of the President, June 1969.
19. **Sherman, A. and Sutton, C. W.,** *Engineering MHD*, McGraw-Hill, New York, 1965.
20. **Tenney, F. H.,** A 2000 MW, fusion reactor, an overview, *IEEE Proc. 5th Symp. Eng. Probl. Fusion Res.,* Princeton University, NJ, 1973, 65—74.

Chapter 6

# THE ECONOMICS OF BULK SOLAR ENERGY CONVERSION SYSTEMS (SEC)

## I. PROBLEMS OF SYSTEM OPTIMIZATION[2,3,6,8]

Harnessing the ever present power of solar energy could be realized through the operation of thermoelectric and photovoltaic power generating systems. Recent developments in the manufacturing technology of crystalline silicon reducing its cost (as core material for a solar array) have been conducted at Tyco-Harvard Labs in Japan. These developments are quite encouraging because an efficiency as high as 10% is predicted.

Also, the problem is directly connected with the continuous development and capacity optimization of the production, design, and manufacturing of an adequate solar heat collector-concentrator and storage system.

The development of streamlined processes for manufacturing crystalline silicon at low cost, processing a high temperature gradient with a relatively low temperature at the die, is important to the plans of developing solar bulk power system for effective utilization.

Questions concerning an efficient solar power generating system depend on the identification of optimum parametric criteria for the heat collector–concentrator and storage mechanism, together with the parameters which are integral parts of the thermoelectric and photovoltaic generating devices and the storage batteries which may store energy during off-peak load periods.

### A. STATEMENT OF THE PROBLEM

Given:

1. A power system comprised of (n) photovoltaic generators and (m) thermoelectric steam generators distributed randomly to supply peak and base load and obeying more than a single constraint.
2. Each of the generator types mentioned above or a group of them, the same or of different types, coupled to a solar heat energy system comprising a heat collector- concentrator and a storing mechanism.
3. Parametric identification for the collector-concentrator and heat energy storing system.

Required:

1. The determination of an optimum mode of solar thermoelectric-photovoltaic, interconnected power system. This will require determining the optimum capacity, geographical location, and range of groupings for the thermoelectric and photovoltaic elements, and whether the total system is to be centralized, dispersed, or centralized-dispersed.
2. Determination of the electric generator's optimum parametric components.

   **Solar-steam AC-generator** — Thermoelectric power per degrees celsius, electric resistivity of thermoelectric materials, and specific heat conductivity of thermoelectric material.

   **Photovoltaic cell and solar matrix generator** — Optimum equivalent cell resistance, junction recombination factor, load current, open circuit and short circuit voltampere characteristics, optimum cell output, optimum number of solar cells in an interconnected solar matrix, and solar matrix output power.

   **Solar energy system** — Includes the combined collector-concentrator and storage system.

**Parametric Identification** — This includes operating temperature of the solar collector, optimum number of collector plates, optimum heat removal efficiency, optimum fixed charge on the collector and associated piping per unit area, optimum operating temperature, aperture and focal length of the concentrator, and any specific type of the heat storing system, optimum capacity, efficiency of the solar heat supply system, mode of optimum grouping, and distribution of the solar supply system.

**B. SCOPE OF STUDY**

(1) The economic optimization of the entire solar photovoltaic-thermoelectric interconnected power system could be obtained from the solution of a set of partial differential equations coordinating the cost of plant, n or m, with respect to total losses.

(2) The solution of the coordination equation will result in establishing power matrices of network interconnections describing the degree of interaction among each of the photovoltaic and/or thermoelectric generator or group. Each of those resulting matrices will identify one mode of a system.

The general form of the coordinating equation is

$$\frac{\partial H_n}{\partial P_n} + \lambda \frac{\partial W_2}{\partial P_n} = \lambda \tag{6.1}$$

where $\lambda$ = Lagrange multiplier, $H_n$ = cost of plant (n) in dollars per hour, $W_1$ = total losses in megawatts, and $P_n$ = capacity of plant (n) in megawatts.

Solutions of a spectrum of optimum systems along with the coordinating equation and subject to several imposed constraints are based on variable values of plant outputs $P_n$ or $P_m$.

(3) Output power (P) is to be assumed an arbitrary function of the solar heat supply energy components (the collector–concentrator and storage) and also the internal integral components of the photovoltaic solar matrix and/or the thermoelectric generating cascade. The functional relation between the overall plant output, the solar energy supply, and the electric generator components can establish a criterion for the minimum limitations and optimum design of the entire interconnected power system.

(4) The optimum design interconnection of optimum solar power system, to be identified in Step 2, could be represented in an actual reference frame through a process of series matrix transformations according to the method determined by Kron.[6]

## II. FEASIBILITY OF SOLAR ELECTROCHEMICAL ENERGY[2,3]

Effective feasibility of solar power systems is based on indirect means, such as the production of hydrogen and oxygen, which can be utilized as basic fuel to feed the operation of electrochemical power systems comprised of fuel cell generating units and storage batteries.

Production of hydrogen and oxygen as basic fuel could be physically accomplished by thermal electrolysis of water, through a system of effective solar concentrators and collectors focusing solar energy and directing it to a high temperature boiler that would attain a temperature of the order of 1500°C at which temperature water can be decomposed into hydrogen and oxygen.

The outlook for actual feasibility of fuel cell power systems is encouraging, and actual results have been obtained through two years of intensive research. A criterion is emerging for an optimum power system that is based on the size and capacity of a fuel cell module, and its pattern of fuel consumption has been established and verified (as shown in Reference 3).

Steady state investigation has indicated that economic evaluation of a spectrum of integrated power systems comprised of electromechanical generators (conventional fossil fuel operated)

coupled with electrochemical modules, such as fuel cells for base loading and storage batteries for peaking demand, is progressing in the right channel, especially an integrated system where the fuel cells and storage batteries are patterned on a dispersed large-scale mode.

As a first step toward selecting the most optimum integrated power system, an analytical approach has been obtained based on expressing the power system transmission loss coefficients matrix in terms of optimum scheduling of generating sources and their fuel cost data. Such a criterion can be used very successfully in the determination of the appropriate pattern of solar energy conversion for supplying the basic fuel for fuel cells. The conversion pattern includes the solar collector-concentrator system, nature and type of heat storage system, high temperature boiler, and the optimum temperature of thermal electrolysis.

In the dynamic area, modeling of a solar electrochemical generating bus comprised of a solar and/or chemical fuel reformer, fuel cells module, solid-state inverter, and a suitable transformer is progressing smoothly.

Due to the uniqueness of the basic fuel for the hydrogen-oxygen fuel cell, its dynamic model, based on a thermodynamic approach, has been accomplished successfully in the (s) domain, and on the same line, the dynamic modeling for various types of solid-state inverters, under different modes of commutation, have been obtained also. Development of a unified dynamic model of a solar electrochemical generator, first independent, and then coupled to an electromechanical generator, industrial load, static load, and combined load, has been established in the current research and indicated in Reference 3.

It is anticipated that individual modeling of generating buses will be followed by a simulation of a small-scale integrated power system where dynamic responses will be studied subject to various types of electrical, chemical, and mechanical disturbances.

Steady state and dynamic analysis of integrated power systems will reveal the most optimum system of solar energy conversion as for fuel cost data of hydrogen and oxygen generation, and the mode of allocation for feeding fuel cells under all conditions of loading, stability, economy, reliability, and environmental aspects.

An electrochemical-electromechanical interconnected power system, fueled by hydrogen and oxygen generated by solar energy through thermal electrolysis, offer a real and promising feasibility in the near future.

## III. SYSTEM OPTIMIZATION FOR SOLAR HEATING AND COOLING[3-5,10,11]

This section undertakes system simulation and economic analysis for heating, cooling, and hot water services for buildings. Two major systems will be studied, one involving collector systems (comprised of a collector-concentrator thermal boiler and a heat storage and cooling absorption cycle) and the other involving noncollector systems (special building features contributing to effective maintenance of comfortable temperature through a heat storage and absorption cooling cycle). Physical, mathematical, and computer models will be developed for a spectrum of collector and noncollector systems followed by establishment of criteria for optimum systems. The optimization procedure will be followed by a study of economic comparison among varieties of collector and noncollector systems dealing with various types of buildings, communities, and regions.

Solar energy can contribute effectively toward relieving the energy shortage by providing the primary fuel necessary to a number of systems used to heat and cool buildings. Utilization of solar energy directly for heating and cooling applications is also economically feasible, especially in view of the rising cost of fossil fuels as the supply diminishes.

A solar system comprised of a group of mirrors and lenses as sunlight collectors, a heat storage system, and a fluid circulating system, can effectively heat buildings. The same solar system can be expanded to serve an absorption cooling system where vapor or hot water can

serve as the refrigerant and a simple salt as the absorber. Another heating-cooling system may be established through a combination of operations utilizing a heat pump and a conventional solar system comprised of collectors.

## A. STATEMENT OF THE PROBLEM

Development of preliminary criteria: Requirements for combined heating-cooling systems for building establishments, including lighting and hot water services are based on

1. Optimum economic feasibility of each system.
2. Optimum reliability and total security.
3. Social and environmental impacts.
4. Suitability of each system with respect to type of building (single family, multifamily, commercial, institutional, and public buildings).
5. Physical size of energy-supplied buildings.
6. Determination of requirements for the most optimum system from a spectrum of systems.
7. Specifications of components for each system and subsystem to be established under criteria developed.

## B. PHASES OF ANALYSIS

### 1. Phase 1

At the end of phase 1, the following could be accomplished:

a. Mathematical and physical modeling of the general (heating and hot water services) collector system comprised of the collector-concentrator, solar boiler, storage system, and cooling system (absorption cycle).
b. Development of economic optimization criteria for a spectrum of collector systems, resulting in information about the optimum plant and size of corresponding service region and nature of community.
c. Basic selection of building models with architectural features offering positive contributions in providing effective adequate temperatures in the interior of buildings in summer and winter in addition to providing hot water services. Tests could be conducted for effective contribution of architectural innovations to collector, as well as to noncollector systems, for varieties of regional conditions.

### 2. Phase 2

At the end of phase 2, the following could be accomplished:

a. Spectrum of noncollector systems, based on the architectural contributions for several types of buildings including a basic one family house model, an institutional building, a public building, and an industrial building. A model of group buildings also will be presented.
b. Mathematical and physical modeling of the noncollector system indicated before for several types of buildings.
c. Development of optimization criteria for a spectrum of noncollector systems, resulting in information about the optimum size of a system or subsystem coupled with social, environmental, and economical grounds.
d. Economic analysis among optimum spectrum of collector and noncollector systems and subsystems, setting clear system requirements for their effective establishment under varieties of regional conditions.

## C. SCOPE OF DESIGN STUDY

To accomplish the goals indicated in Section III. A., Statement of the Problem, the following major channels of research could be conducted.

Systematic simulation of each plan of heating, cooling, and hot water services including development of physical, mathematical, and computer models (collector and noncollector systems).

Economic optimization analysis among a spectrum of systems (collector and noncollector systems).

Each system implies a certain arrangement of providing combined services for heating, cooling, and hot water services as indicated below for an integrated collector system.

### 1. An Integrated Collector System

1. Collectors and concentrator system
2. High temperature boiler and piping system
3. Storage system which may be based on solid, liquid, or gaseous for the absorbing storing medium
4. Cooling is through absorption refrigerant cycle machine
5. Contribution to the condition of heating, cooling, and hot water services that will be provided by architectural contribution will be through innovations in building design

Collection and concentration of solar energy and its application of a high temperature boiler can serve two purposes: hot water supply for domestic use and hot water, hot air heating.

Selection of solar collectors and heat storage systems will be weighed on economic factors since it had been established that efficiencies of several designs ranging from water coil, and air heated types do not differ significantly.

However, practical feasibility and matching factors with respect to weather, type of region, and space, will be considered in the selection of the following types of heat storage apparatus.

- Heat of fusion type of heat storage.
- Specific heat type of heat storage.

Their design and selection in an established system will be based on values of heat of fusion and specific heat of the storing medium and a specified temperature rise.

The above system could be the following:

- Totally centralized system
- Totally dispersed system
- Centralized-dispersed system

This will reveal the optimum size of system or subsystem. Also suitability usually will be established as to any of the following consuming regions:

1. Residential area (specific region will be selected).
2. Industrial areas (specific region will be selected).
3. Residential-industrial regional combination (specific region will be selected).

The optimum system or systems, including requirements of all components, will be determined on the principles of minimum dollars input for annual cost in that system, plus the reliability of that system as indicated in preceding steps.

**2. General Parameters of Collector System**

The general equation of the solar collector, interrelating the various parameters is

$$M / A = N_r \left[ H \gamma \tau - M_L / A \right] \tag{6.2}$$

where M/A = total hourly net useful heat transferred through steam per unit area of tilted collector, H = total incidence per hour of solar energy on unit area of a horizontal surface (it is an arbitrary function of temperature), $\gamma$ = a geometrical conversion factor for consideration of tilted surface, taking into consideration the collector as an integral part of roof or spandrel structure, $\tau$ = mean value factor of effective transmittance of the glass cover plates and absorptivity of the receiver, $M_L/A$ = total heat loss per unit area of tilted collectors, and $N_r$ = heat removal efficiency in consideration of the kind of fluid steam and its flow rate.

**3. Concentrator Parameters**

Concentrator (solar furnace) could be a complex of parabolic mirrors and lenses with optimum aperture ratio, focusing solar energy on a boiler. The concentrating system also could be a group of plastic lenses with suitable aperture ratios.

The solar intensity at the boiler can be varied by a reflecting cylinder at the target and by proper focusing. A high concentration of solar energy at the target could be affected by the following:

1. Constant aperture and focal length.
2. Variable apparent aperture.
3. Variable focal length.

**4. Cooling System Parameters**

Absorption system using steam or hot water as refrigerant and salt as absorbent, i.e., lithium bromade. The main system components are evaporator, absorber, generator, condenser, evaporator pump, solution pump, and the heat exchanger.

**5. Heating System Parameters**

This includes air or water circulation system, system control, storage, and contribution from architectural innovations in both collector and noncollector systems.

**6. Heat Storage System**

This may involve the special mode of storage, whether heat type or fusion type, as well as the natural, thermal, mechanical, and physical properties of the storing medium.

Comparison of the merit of each system for total heating and cooling is based on minimum total annual fixed cost plus operating cost. The optimization procedure could be conducted among several systems to determine the most optimum.

## IV. INTEGRATED NONCOLLECTOR SYSTEM[4,5,8,9]

This system has thermal solar energy storage which could be heat of fusion type of heat storage and/or specific heat storage, and an absorption refrigerant cycle.

Architectural considerations in the type of building structure which affect cooling and heating are

1. Shading glass.
2. Evaporative cooling by means of roof ponds and roof sprays, shades over the windows and sprayed with water, contributes effective cooling in dry climate of low humidity.

3. Effective insulation in the building structure contributing to effective heating coupled with partial heat flow from storage thermal basin.
4. Building form to orientation.

Simulation of the noncollector system will follow the pattern of:

1. Selection of a typical housing unit which may start with one family houses, an apartment complex, public institutions, and industrial buildings, and possessing special design features contributing to heating and cooling.
2. Determination of total solar thermal load required for heating, cooling, and hot water service for each sample of building and then for a model region.
3. Simulation of the physical parameters with a mathematical model for each system and subsystem.
4. Conduction of optimization procedure based on coordination between cost of load requirements and losses.

## V. INTEGRATED COLLECTOR-NONCOLLECTOR SYSTEM[4,5,7-9]

A concentrated study will be directed for the possibility of providing heating, cooling, and hot water services through a combination of collector and noncollector solar systems.

### A. OPTIMIZATION PROCEDURE

Determination of a system mode and load suitability will follow the procedure of economic optimization indicated below, based on the principles of coordination between incremental production cost and incremental losses.

Determination of power output generated by solar energy is

$$\frac{dF_n}{dP_n} + \lambda \frac{\partial P_L}{\partial P_n} = \lambda \tag{6.3}$$

where $F_n$ = total cost of solar power input to plant n in dollars per hour, $P_n$ = heating or cooling power output in megawatts of plant n, $P_L$ = total system losses, $\lambda$ = incremental production cost of plant n in dollars per megawatt hour, $F_n$, $P_n$, $\lambda$, $P_L$, are all functions of the following: collector-concentrator parameters, high temperature boiler and piping system, heat storage structure, and cooling cycle performance parameters.

Equation 6.3 is based on minimum total dollars input into the entire system to be determined such that:

$$F_t = \sum_{1}^{N} F_n \tag{6.4}$$

and with the constraint that:

$$\sum_{1}^{N} P_n - P_r = 0 \tag{6.5}$$

where $dF_n$ = incremental solar power input rate in British thermal units per kilowatt hour.

$F_n$, $P_n$, $P_L$, $F_t$ and $\lambda$ are arbitrary functions of the following system and subsystem performance components. An important objective of this presentation is the determination of the above-mentioned functional forms.

Subsystem components include

1. **Collector** — Total incidence per hour per unit area on a horizontal and tilted collector, conversion factor for tilted collectors, mean value factor of effective transmittance of glass cover plates, and heat removal efficiency.
2. **Concentrator** — System lenses, optimum aperture ratio, focusing parameters, boiler design elements, and intensity of solar concentration at the target.
3. **Storage system** — Type of heat storage, whether fusion or specific, solid, liquid, or gaseous medium. Their specific heat, latent heat capacity, entropy and enthalpy.
4. **Heating system** — Air or water circulation system, system control, and cost of architectural contributions (noncollector system).
5. **Cooling system** — Components of absorption cyclic machine listed earlier, circulation system, system control and cost of architectural contributions (noncollector system).

However, $\partial F_n/\partial P_n$ involves most probably an unknown relationship between heat rate of the solar system involving the solar furnace, heat storage high temperature boiler, this combination is expressed in British thermal units per kilowatt hour against power output of the plant in megawatts or determination of incremental power input rate in British thermal units per kilowatt hour against power output of the plant generator.

Following the preceding presentation (Section V.A.), it is felt that it would be a great contribution to this subject matter to reproduce from a paper by Dr. Jack M. Cherne[1] important impact data and illustrations of solar energy conversion systems. These systems include heating and cooling of buildings, solar thermal electric power, photovoltaic power, ocean thermal-gradient power, bioconversion, and wind energy conversion. These are shown in Figures 6.1 to 6.6. Also Table 6.1 lists information for the potential impacts of solar energy technologies while Table 6.2 shows an informational base for market capture.

## VI. SOLAR PHOTOVOLTAIC GENERATOR[3,10-13] *

Figure 6.7 illustrates principle components for the solar thermoelectric or solar photovoltaic generator.

The design basis for the solar thermoelectric generator is characterized by

1. Relatively small thermal conductivity.
2. Relatively large electrical conductivity.
3. Variation of material properties with temperature neglected, implying no Thompson effect.
4. Junction electrical resistance → zero.
5. Temperature of the top parts of the P and n material are those for the source and sink.
6. Area of thermoelectric element is constant.
7. Heat loss to the surroundings → zero.
8. The circuit parameters of the thermoelectric generator are
   $T_l$ = Temperature of the source
   $T_o$ = Temperature of the sink
   $L_p, L_n$ = Length of the thermoelectric elements
   $A_p, A_n$ = Cross-sectional area of the thermoelectric element
   $k_p, k_n$ = Specific thermal conductivity of the thermoelectric element
   $P_p, P_n$ = Specific electrical resistivity (1/6) of the thermoelectric element

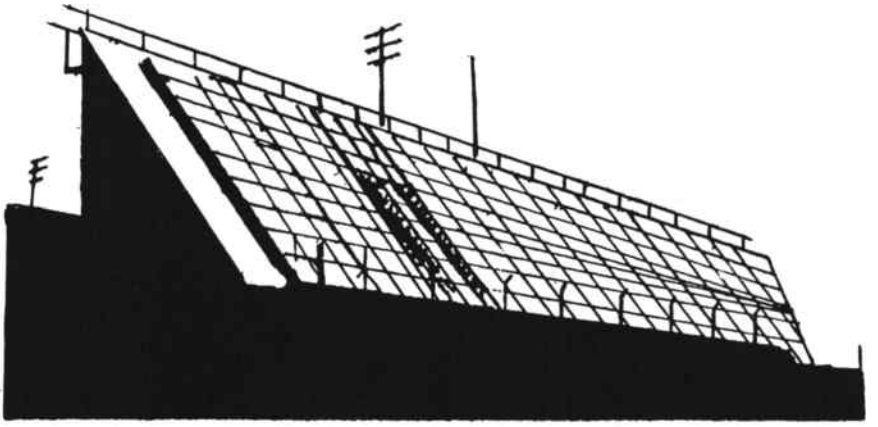

FIGURE 6.1 Solar collectors on Fauquier High School to heat classrooms. Designed by InterTechnology Corporation. (From Cherne, J.M., Solar energy — an overview, *Proc. Symp. Films Sol. Energy*, The American Vaccum Society, 1975, 975—983. With permission.)

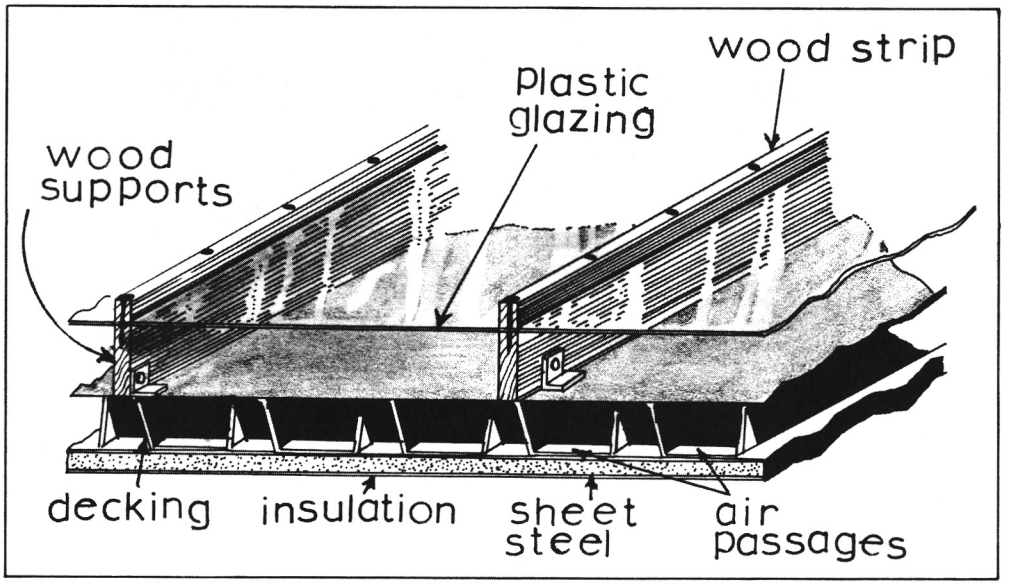


FIGURE 6.2 Solar collector for air. (From Cherne, J.M., Solar energy — an overview, *Proc. Symp. Films Sol. Energy*, The American Vaccum Society, 1975, 975—983. With permission.)

$K_p, K_n$ = The total thermal conductance of an element = kA/L
$R_p, R_n$ = The total electrical resistance of an element = pL/A
$\alpha_{pn}$ = The relative Seebeck coefficient
$\pi_{pn}$ = The relative Peltier coefficient

We would like to note also that $\Delta T$ of $(T_1 - T_o)$ will generate a Seebeck voltage of $\alpha_{p\text{-}n}$ $(T_1 - T_o)$ and a resultant current I to flow to $R_L$.

With respect to energy balance and the first law of thermodynamics, the following physical conditions have been assumed[14] — heat flow into the junction = $H_1$, heat conducted into Dutwokgs = $H_k$, Peltier Heat $H_p$ due to current flow I, and heat flowing into the junction due to joule effect = $^1/_2$ $H_j$.

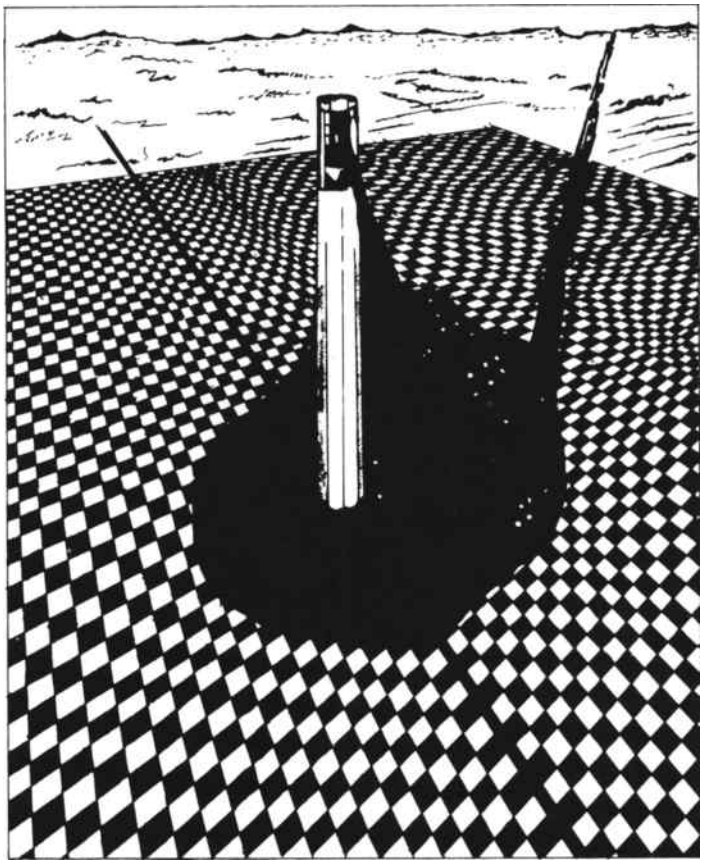

FIGURE 6.3 Central receiver of solar energy. (From Cherne, J.M., Solar energy — an overview, *Proc. Symp. Films Sol. Energy*, The American Vaccum Society, 1975, 975—983. With permission.)

$$H_1 + \frac{1}{2}H_j = H_p + H_k \tag{6.6}$$

$$H_p = \pi_{p-n} I = \alpha_{p-n} I T_1 \tag{6.7}$$

$$H_j = \left(R_p + R_n\right) I^2 \tag{6.8}$$

$$H_k = \left(K_p + K_n\right)\left(T_1 - T_0\right) \tag{6.9}$$

Useful power generated $= P_{i\text{-}2} = I^2 R_L$

$$= \frac{V_L^2}{R_L} \tag{6.10}$$

where

$$V_L = \alpha_{p-n}(T_1 - T_0) - (R_n + R_p) I \tag{6.11}$$

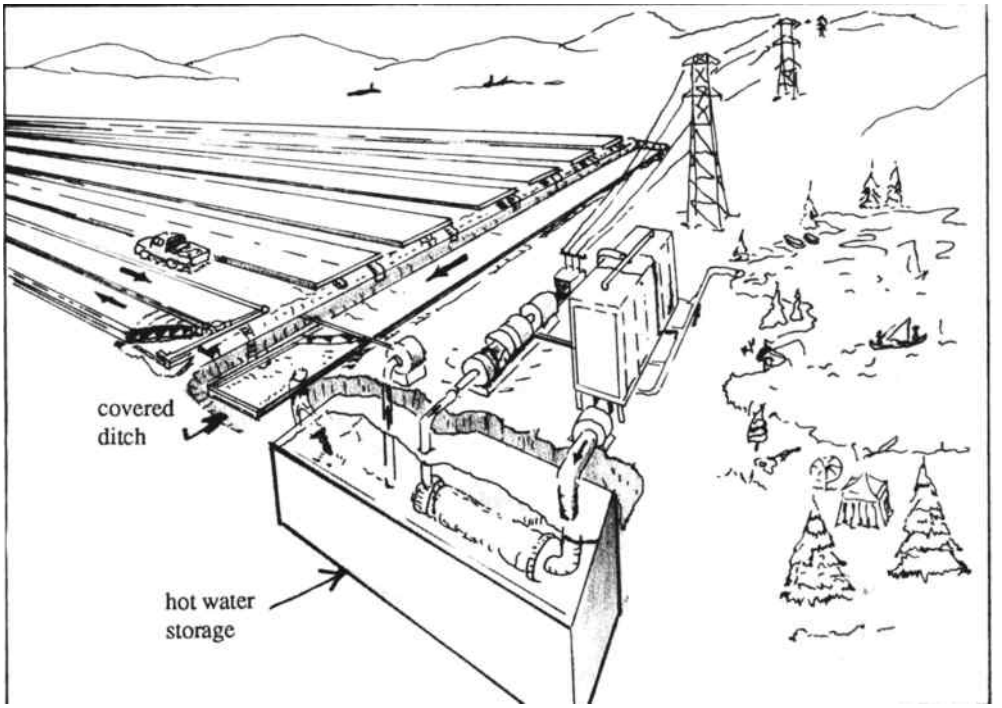


FIGURE 6.4 Solar pond. (From Cherne, J.M., Solar energy — an overview, *Proc. Symp. Films Sol. Energy*, The American Vaccum Society, 1975, 975—983. With permission.)

Then the efficiency η becomes:

$$\eta_{i-2} = \frac{P_{i-2}}{H_1} \tag{6.12}$$

$$= \frac{\left(T_1 - T_0\right)}{T_1} \; m \left[ (1+m) - \frac{1}{2} \; \frac{T_1 - T_0}{T_1} + \frac{\left(k_n + k_p\right)\left(R_n + R_p\right)(1+m)^2}{\alpha_{p-n}^2 \; T_1} \right]^{-1} \tag{6.13}$$

where,

$$m = \frac{R_L}{R_n + R_p} \tag{6.14}$$

and

$$\eta_{carnot} = \frac{T_1 - T_0}{T_1} \tag{6.15}$$

The figure of merit and material efficiency are expressed by first expressing the figure of merit Z.

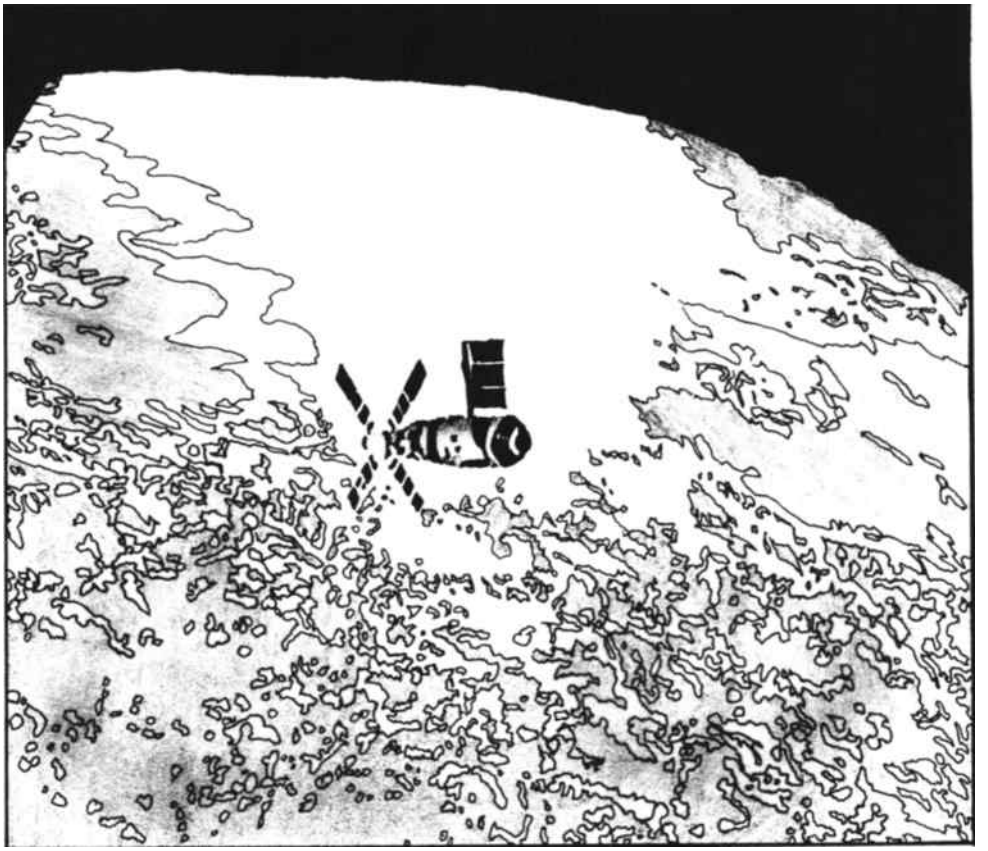

FIGURE 6.5 Solar sky laboratory. (From Cherne, J.M., Solar energy — an overview, *Proc. Symp. Films Sol. Energy*, The American Vaccum Society, 1975, 975—983. With permission.)

$$Z = \left( \frac{\alpha_p - \alpha_n}{\sqrt{P_p K_p} + \sqrt{P_n K_n}} \right)^2 \tag{6.16}$$

$$= \frac{\alpha_{p\text{-}n}^2}{\left(k_n + k_p\right)\left(R_n + R_p\right)}$$

Second the material efficiency $M_G$ which combines properties of materials and geometrical dimensions, is expressed by

$$M_G = m \left[ (m+1) - \frac{1}{2} \frac{T_1 - T_0}{T_1} + \frac{(m+1)^2 (y+x)\left(y+ax^2\right)}{(1+a)^2 x\, y\, Z\, T_1} \right]^{-1} \tag{6.17}$$

where,

$$x = \frac{A_n}{A_p}, \qquad y = \frac{\rho_n L_n}{\rho_p L_p} \tag{6.18}$$

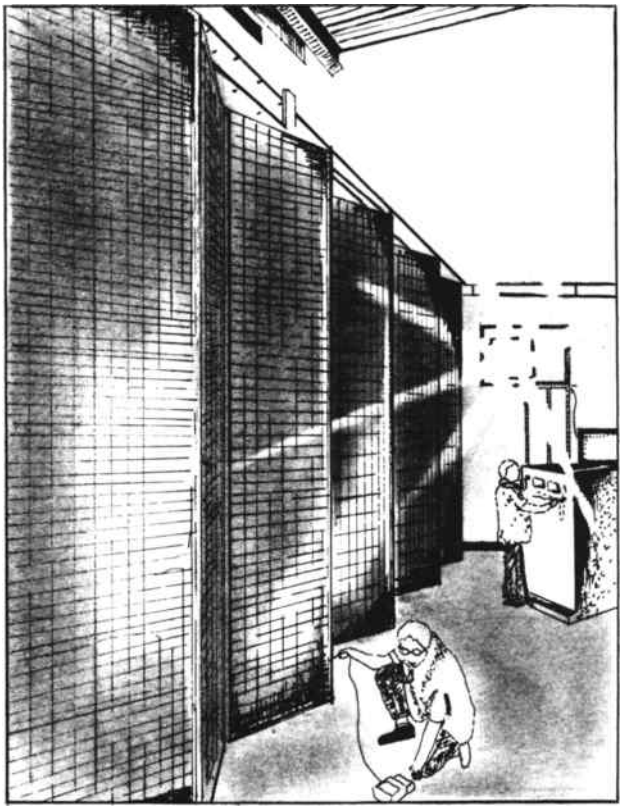

FIGURE 6.6 Sky laboratory solar array. (From Cherne, J.M., Solar energy — an overview, *Proc. Symp. Films Sol. Energy,* The American Vaccum Society, 1975, 975—983. With permission.)

$$a = \sqrt{\frac{\rho_n K_n}{\rho_p K_p}} \tag{6.19}$$

## VII. OPTIMIZATION OF GENERATOR GEOMETRY[3,10-13] *

This process includes optimizing m or optimizing the relations between material properties and geometrical dimensions, and differentiating the material efficiency $M_G$ with respect to $X = A_n/A_p$ and setting the result = 0 obtaining

$$X_{opt} = \frac{y}{a} \tag{6.20}$$

or

$$\left(\frac{A_n L_p}{A_p L_n}\right)_{opt} = \sqrt{\frac{\rho_n K_p}{\rho_p K_n}} \tag{6.21}$$

* © 1968. Reprinted with permission from Soo, S.L., *Direct Energy Conversion,* Prentice-Hall, Englewood Cliffs, NJ, 1968.

**TABLE 6.1**
**Solar Energy[1]**

| | 1980 | 1985 | 1990 | 1995 | 2000 |
|---|---|---|---|---|---|
| Heating and cooling | 0.5 | 0.8 | 2.5 | 3.8 | 5.5 |
| | (0.01) | (0.5) | (0.8) | (1.9) | (3.6) |
| Solar thermal | 0.0 | 0.003 | 0.03 | 0.3 | 1.9 |
| | (0.0) | (0.003) | (0.03) | (0.2) | (0.8) |
| Wind conversion | 0.2 | 0.8 | 3.0 | 5.2 | 7.9 |
| | (0.01) | (0.6) | (2.5) | (4.1) | (6.3) |
| Bioconversion | 0.03 | 0.14 | 0.4 | 1.6 | 7.1 |
| | (0.03) | (0.05) | (0.1) | (0.2) | (0.3) |
| Ocean thermal | 0 | 0.05 | 0.3 | 1.6 | 11.0 |
| | (0) | (0.05) | (0.2) | (0.5) | (2.7) |
| Photovoltaic conversion | Negative | 0.02 | 0.5 | 3.8 | 11.0 |
| | (Negative) | (0.005) | (0.1) | (0.5) | (2.5) |
| Potential total oil imports replaced | 0.5 | 1.8 | 7.0 | 16.0 | 44.0 |
| | (0.05) | (1.2) | (3.7) | (7.0) | (16.0) |

*Note:* Estimates of potential impacts of solar energy technologies (units of equivalent millions of barrels per day of fuel oil saved). Numbers shown without parentheses are for the "Accelerated" implementation scenario; those shown in parentheses are for the "Business-as-Usual" implementation scenario.

FEA Project Independence blueprint, Solar Energy Task Force Report. From Cherne, J.M., Solar energy — an overview, *Proc. Symp. Films Sol. Energy,* The American Vaccum Society, 1975, 975—983. With permission.

**TABLE 6.2**
**Market Capture — Fuel Prices More Important Than Climatic Factors**

| | New York | Los Angeles | Las Vegas |
|---|---|---|---|
| Solar system Btu/$ | Low | Medium | High |
| Solar system cost ($/million Btu) | $9.00 | $7.00 | $5.00 |
| Actual electricity price ($/million Btu) | $9.40 | $7.80 | $3.75 |
| Market viability | Yes | Yes | Yes |

From Cherne, J.M., Solar energy — an overview, *Proc. Symp. Films Sol. Energy,* The American Vaccum Society, 1975, 975—983. With permission.

and that optimum m is expressed by

$$m_{opt} = \sqrt{1 + \frac{Z}{2}\left(T_1 + T_0\right)} \tag{6.22}$$

while optimum efficiency is given by

$$\eta_{opt} = \left(\frac{T_1 - T_0}{T_1}\right)\left(\frac{M_0 - 1}{M_0 + \frac{T_0}{T_1}}\right) \tag{6.23}$$

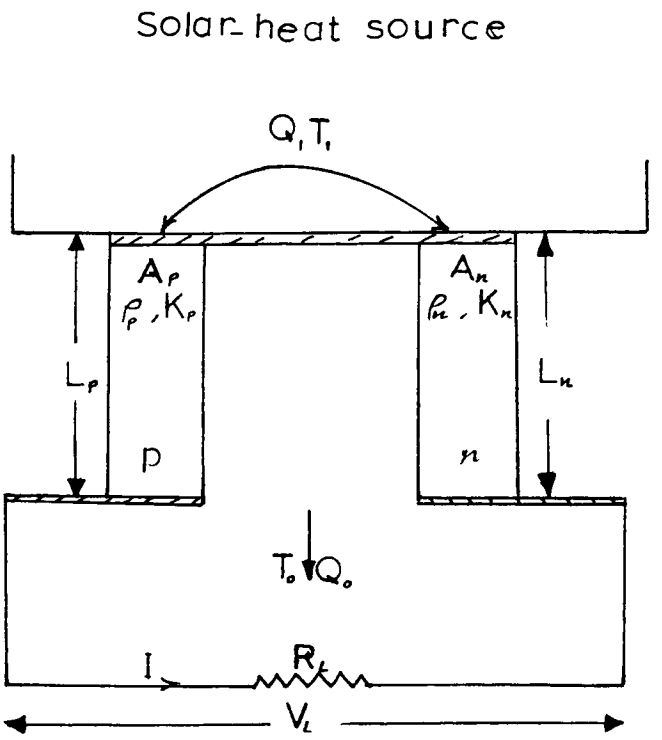


FIGURE 6.7 Schematic for the photovoltaic generator. (From Soo S.L., *Direct Energy Conversion*, Prentice-Hall, Englewood Cliffs, NJ, 1968. With permission.)

Now to develop bulk capacity for the solar photovoltaic generator, we are proceeding to talk about the multistage thermoelectric generators.

Because $\Delta T = T_i - T_o$ for a single stage generator cannot exceed a certain relatively modest level, cascading will enhance the overall efficiency of stages interconnected, whereby:

$$\eta_{total} = 1 - \prod_{i=1}^{n} \left(1 - \eta_i\right) \tag{6.24}$$

where n is the number of thermoelectrics cascaded.

For AC output, the photovoltaic solar generating set has to be connected to a power inverter associated with an efficiency of

$$\eta_{overall} = \eta_{total}\eta' \tag{6.24a}$$

## VIII. INCREMENTAL ENERGY COST[4-6,8]

### A. INCREMENTAL FUEL COST FOR SOLAR THERMOELECTRIC SYSTEM

British thermal units per hour transferred to steam flow:

$$M = N_r A\left[H\gamma\tau - \frac{M_L}{A}\right] \tag{6.25}$$

Incremental fuel cost curve could be represented in terms of British thermal units per megawatt hour will follow an expression of the following form:

$$M' = N_r A \left[ H\gamma\tau - \frac{M_L}{A} \right] \frac{1}{h_i \eta_{i-1}} \tag{6.26}$$

where $\eta_{i-1}$ is the efficiency of $i^{th}$ collector, $h_i$ = conversion factor in terms of mega British thermal units per megawatt, and fuel cost = $k_{i-1}$ in dollars per mega British thermal units.

Therefore,

$$\frac{dF_i}{dP_{i-1}} = N_r A \; k_{i-1} \left[ H\gamma\tau - \frac{M_L}{A} \right] \frac{1}{h_i \eta_{i-1}} \tag{6.27}$$

where $k_{i-1}$ is the cost of fueling in dollars per mega British thermal unit.

## B. INCREMENTAL FUEL COST FOR SOLAR PHOTOVOLTAIC SYSTEM

Now, if $H_1$ represents heat flow into the p-n junction in mega British thermal units per hour, and $k_{i-2}$ is the cost of fueling in dollars per mega British thermal units, the incremental fuel cost for the $i^{th}$ generator becomes

$$\frac{dF_{i-2}}{dP_{i-2}} = P_{i-2} k_{i-2} / \eta_{i-2} \tag{6.28}$$

$$= \frac{k_{i-2} \left[ \alpha_{p-n} T_i - T_o - I \left( R_n - R_p \right)^2 \right]}{R_L}$$

$$\Big/ \left[ \left( \frac{T_i - T_o}{T_1} \right) m \left\{ (1+m) - \frac{1}{2} \frac{T_i - T_o}{T_1} + \frac{\left( K_n + k_p \right) \left( R_n + R_p \right) (1+m)^2}{\alpha_{p-n}^2 T_1} \right\}^{-1} \right] \tag{6.29}$$

where $k_{i-2}$ is the cost of fueling for the $i^{th}$ generator in dollars per mega British thermal unit, $P_{i-2}$ is the power output for the $i^{th}$ generator, and $\eta_{i-2}$ is the efficiency for the $i^{th}$ generator.

Considering a cascaded system of solar photovoltaic generators, the incremental fuel cost becomes

$$\frac{dF_{i-2}}{dP_{i-2}} = n \, k_{i-2} \, P_{i-2} / \eta_{total} \tag{6.30}$$

$$= k_{i-2} \, P_{i-2} / \left( 1 - \prod_{i=1}^{n} \left( 1 - \eta_i \right) \right) \tag{6.31}$$

where n is the number of cascaded solar photovoltaic generators.

Then, from Equations 6.22 and 6.23, the optimal level for $dF_{i-2}/dP_{i-2}$ becomes

$$\left. \frac{dF_{i-2}}{dP_{i-2}} \right|_{opt.} = P_{i-2-opt.} k_{i-2} / \eta_{i-opt.} \tag{6.32}$$

where, opt. is expressed in Equation 6.23, and the optimal power output for $i^{th}$ generator from Equations 6.11 and 6.22 becomes

$$P_{i-2-opt.} = \frac{m_{opt.}}{\left(1+m_{opt.}\right)^2} \quad \frac{\left(T_i - T_o\right)^2 \alpha_{p-n^2}}{\left(R_n + R_p\right)} \tag{6.33}$$

## IX. FORCED OPTIMIZATION ON SOLAR THERMOELECTRIC GENERATOR[3,4,6,8]

This could be secured by the interconnection of thermoelectric and photovoltaic solar generators. The thermoelectric generator is in effect a solar-steam generator and the photovoltaic is coupled to a power inverter.

Equations 6.27 and 6.28 for a single generator will get the following:

$$\frac{P_{i-2}\, K_{i-2}}{\eta_{i-2}} = \frac{N_r A\, k_{i-1}}{h_i \eta_{i-1}} \left( H\gamma\tau - \frac{M_L}{A} \right) \tag{6.34}$$

From Equations 6.2 and 6.34 we arrive at a relationship linking efficiencies of the two generators:

$$\frac{\eta_{i-1}}{\eta_{i-2}} = \frac{N_r\, A\, k_{i-1}}{h_i\, P_{i-2}\, k_{i-2}} \left( H\gamma\tau - \frac{M_L}{A} \right) \tag{6.35}$$

Or under optimal constraint on the photovoltaic generator Equation 6.35 could be rewritten as:

$$\frac{\eta_{i-1}}{\eta_{i-2}} = \frac{N_r\, A\, k_{i-1}}{h_i\, P_{i-2\text{-opt.}}\, k_{i-2}} \left( H\gamma\tau - \frac{M_L}{A} \right) \tag{6.36}$$

where $\eta_{i-1}$ is the efficiency of the thermoelectric solar generator, and $\eta_{i-2}$ is the efficiency of the photovoltaic solar generator.

Also, for a cascaded photovoltaic solar system linked to a large thermoelectric generating system, the relative efficiency relationship becomes

$$\frac{\eta_{i-1}}{1 - \prod_{i=1} \left(1 - \eta_{i-2}\right)} = \frac{N_r\, A\, k_{i-1}}{h_i\, P_{i-2}\, k_{i-2}} \left( H\gamma\tau - \frac{M_L}{A} \right) \tag{6.37}$$

In the scope of forced optimization, we can proceed to use the principle of the power coordination equation, to be applied on a large single isolated system with losses containing the interconnection of solar thermoelectric and solar photovoltaic generators as follows.

For solar thermoelectric generator:

$$\frac{\partial F_{i-1}}{\partial P_{i-1}} + \lambda_1 \frac{\partial P_{L-i-1}}{\partial P_{i-1}} = \lambda_1 \tag{6.38}$$

and for photovoltaic generator:

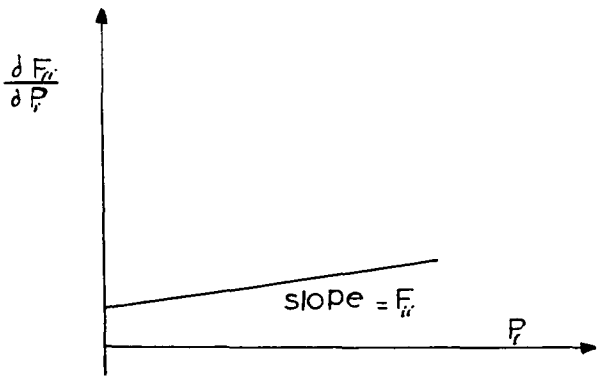


FIGURE 6.8 Incremental fuel cost curve.

$$\frac{\partial F_{i-2}}{\partial P_{i-2}} + \lambda_2 \frac{\partial P_{L-i-2}}{\partial P_{i-2}} = \lambda_2 \tag{6.39}$$

Forced optimization implies $\lambda_1 = \lambda_2$

$$\frac{\partial F_{i-1}}{\partial P_{i-1}} - \frac{\partial F_{L-i-2}}{\partial P_{i-2}} + \lambda\left(\frac{\partial P_{L-i-1}}{\partial P_{i-1}} - \frac{\partial P_{L-i-2}}{\partial P_{i-2}}\right) = 0 \tag{6.40}$$

or

$$\frac{\Delta F_{i-1}}{\Delta P_{i-1}} - \frac{\Delta F_{i-2}}{\Delta P_{i-2}} = \lambda\left(\frac{\Delta P_{L-i-2}}{\Delta P_{i-2}} - \frac{\Delta P_{L-i-1}}{\Delta P_{i-1}}\right) \tag{6.41}$$

where, $\lambda$ is the cost of received power in dollars per megawatt hour.

## X. INCREMENTAL ENERGY COST CURVE AS STRAIGHT LINE[4,6,8,12]

### A. SOLAR THERMOELECTRIC GENERATOR

From Equation 6.27, we have

$$\frac{\partial F_{i-1}}{\partial P_{i-1}} = \frac{N_r A k_{i-1}}{h_i \eta_i}\left(H\gamma\tau - \frac{M_L}{A}\right) \tag{6.42}$$

$$= F_{ii\text{-}1} P_{i-1} + f_{i-1}$$

where $F_{ii\text{-}1}$ is the slope of the straight line, and $f_{i\text{-}1}$ is the vertical intercept of the straight line.

Also, $F_{ii\text{-}1}$ and $f_{i\text{-}1}$ are shown in Figure 6.8.Therefore, from Equations 6.27 and 6.42 (in dollars per megawatt hour per megawatt):

$$F_{ii-1} = \gamma\tau N_r K_{i\text{-}1} \tag{6.43}$$

$$f_{i-1} = -\frac{N_r M_L k_{i-1}}{h_i \eta_i} \tag{6.44}$$

**B. SOLAR PHOTOVOLTAIC GENERATOR**

From Equation 6.28,

$$\frac{\partial F_{i-2}}{\partial P_{i-2}} = n k_{i-2} P_{i-2} / \eta_{i-2} \tag{6.45}$$

where $P_{i-2}$ has been expressed by Equation 6.10.

Also,

$$\frac{\partial F_{i-2}}{\partial P_{i-2}} = F_{ii-2} P_{i-2} + f_{i-2} \tag{6.46}$$

From Equations 6.45 and 6.23, we can write, under optimal efficiency:

$$\frac{\partial F_{i-2}}{\partial P_{i-2}} = \left(n k_{i-2} P_{i-2}\right) \frac{M_o + \frac{T_o}{T_l}}{M_o - 1} \tag{6.47}$$

Therefore,

$$F_{ii-2} = \frac{n k_{i-2}}{\eta_{i-2}} \tag{6.48}$$

or

$$F_{ii-2} = \frac{M_o + \frac{T_o}{\pi}}{M_o - 1} \left(n k_{i-2}\right) \tag{6.49}$$

and

$$f_{i-2} = 0 \tag{6.50}$$

Consequently, the incremental fuel cost curve for the solar photovoltaic generator looks as a straight line passing into the origin. Therefore,

$$\frac{\partial F_{i-2}}{\partial P_i}$$

has no vertical intercept.

**C. INTERCONNECTION OF SOLAR THERMOELECTRIC AND CASCADED PHOTOVOLTAIC GENERATOR**

From Equations 6.42 and 6.45 we can write the following:

$$\frac{\partial F_{i-1}}{\partial P_{i-1}} + \frac{\partial F_{i-2}}{\partial P_{i-2}} = F_{ii-1} P_{i-1} + f_{i-1} + F_{ii-2} P_{i-2} + f_{i-2} \tag{6.51}$$

$$= \gamma\tau N_r\, k_{i-1}\, P_{i-1} - \frac{N_r\, M_L\, k_{i-1}}{h_i \eta_i} + \frac{n\, k_{i-2}}{\mu_{i-2}}\, P_{i-2} \tag{6.52}$$

Let,

$$\frac{\partial F_{i-1}}{\partial P_{i-1}} + \frac{\partial F_{i-2}}{\partial P_{i-2}} = \frac{\partial F_i}{\partial P_i} \tag{6.53}$$

Therefore, from Equations 6.51, 6.52, and 6.53, we can express

$$\frac{\partial F_i}{\partial P_i} = F_{ii} P_i + f_i \tag{6.54}$$

and,

$$P_{i-1} = P_{i-2} = P_i$$

Therefore,

$$F_{ii} = \left(\gamma\, \tau\, N_r\, k_{i-1}\right) + \frac{k_{i-2n}}{\eta_{i-2}} \tag{6.55}$$

and

$$f_i = -\frac{N_r\, M_L\, k_{i-1}}{h_i\, \eta_i} \tag{6.56}$$

## XI. ENERGY COST MULTIPLYING FACTOR FOR INVARIANT [B] MATRIX[4,6,9]

### A. CENTRALIZED SOLAR POWER SYSTEM

For the case where $F_{ii\text{-new}} = k\, F_{ii\text{-old}}$, three criteria (optimal case) on k for optimal power allocation have been expressed in Chapter 4, Equations 4.99, 4.101, and 4.102.

Invariance of the [B] matrix, means that it is permissible to use tables of those matrices given in Chapters 1 and 2 for any new system for similar optimum scheduling of generation, but with new and different incremental fuel cost curves having multiplying factors expressed by equations multiplying factors expressed by Equations 6.57 to 6.62. These multiplying factors have direct linkage to the process of optimum economic scheduling of generation.

However, the cost multiplying factor (nonoptimal) for the case of solar power sources could be expressed according to Equations 6.43, 6.44, 6.48, 6.50, 6.55, and 6.56.

For solar thermoelectric generator:

$$ks_1 = \gamma\tau N_r\, k_{i-1} / F_{ii-old} \tag{6.57}$$

$$ks_2 = -\frac{N_r\, M_2\, k_{i-1}}{h_i\, \eta_i\, f_{i\text{-old}}} \tag{6.58}$$

For solar photovoltaic generator:

$$ks_3 = \frac{n\, k_{i-2}}{\eta_{i-2}\, F_{ii\text{-old}}} \tag{6.59}$$

$$ks_4 = 0 \tag{6.60}$$

For combined solar thermoelectric, photovoltaic generators:

$$ks_5 = \gamma\tau N_r\, k_{i-1} + \frac{n\, k_{i-2}}{\eta_{i-2}} / F_{ii-old} \tag{6.61}$$

$$ks_6 = \frac{N_r\, M_L\, k_{i-1}}{h_i \eta_i f_{i-old}} \tag{6.62}$$

where values for $F_{ii-old}$ and $f_{i-old}$ are those associated with the incremental fuel cost curves given in Chapter 2.

## B. CENTRALIZED-DISPERSED SOLAR POWER SYSTEM

It had been shown in Section V. that the incremental fuel cost curve for a solar thermoelectric generator has the two straight line components $F_{ii}$ and $f_i$, the photovoltaic generator has only the $F_{ii}$ component, and of course the interconnected solar thermoelectric-photovoltaic generator has both $F_{ii}$ and $f_i$ components.

We will consider the case of the solar photovoltaic generator where $f_i = 0$ and $F_{ii}$ is finite.

$$F_{ii-new} = k_{pL}\, F_{ii-old} \tag{6.63}$$

Now referring the [B] matrix for an interconnected dispersed power system expressed by Chapter 5, Equations 5.53 to 5.55, then inserting $f_i = 0$ and $F_{ii-new} = K_{pL}\, F_{ii-old}$.

$$H_{1-new} = \frac{k\, F_{ii}}{F_{jj}} - \frac{\lambda - k\, F_{ii}\, P_i}{F_{jj}\, P_j}$$

$$H_{2-new} = \frac{\lambda - F_{jj}\, P_j}{\lambda - k\, F_{ii} P_i} - \frac{F_{jj}}{k\, F_{ii}} \tag{6.64}$$

Rewriting $[B]^{-1}$ from Chapter 5, Equation 5.53:

$$[B]^{-1}_{old} = \frac{H_1\, P_i\, F_{jj}\lambda}{H_2\, F_{ii}(\lambda - F_{ii}P_i - f_i)} + \frac{H_2\, P_j\, F_{ii}\, \lambda}{H_2\, F_{ii}(\lambda - F_{ii}P_i - f_i)}$$

$$= \frac{H_1}{H_2}\ \frac{P_i F_{jj}\, \lambda}{F_{ii}(\lambda - F_{ii}P_i - f_i)} + \frac{P_j F_{ii}\lambda}{F_{ii}(\lambda - F_{ii}P_i - f_i)} \tag{6.65}$$

Then for $F_{ii-new} = k_p\, F_{ii-old}$, we can write $[B']^{-1}{}_{new}$ as follows:

$$[B']^{-1} = \frac{\lambda\, F_{jj}P_i\left[\dfrac{k_p F_{ii}}{F_{jj}} - \dfrac{\lambda - kF_{ii}P_i}{\lambda - F_{jj}P_j}\right]}{F_{ii}(\lambda - kF_{ii}P_i)\left[\dfrac{\lambda - F_{jj}P_j - F_{jj}}{\lambda - k_pF_{ii}P_i - k_pF_{ii}}\right]} + \frac{\lambda P_j kF_{ii}\left[\dfrac{\lambda - F_{jj}P_j}{\lambda - k_pF_{ii}P_i} - \dfrac{F_{jj}}{k_pF_{ii}}\right]}{F_{ii}(\lambda - kF_{ii}P_i)\left[\dfrac{\lambda - F_{jj}P_j}{\lambda - k_pF_{ii}P_i} - \dfrac{F_{jj}}{kF_{ii}}\right]} \tag{6.66}$$

For [B′] to remain invariant, so that an already established matrix can be used directly as that calculated for a dispersed system shown in Chapter 1 for an eight plant system. The multiplying factor $k_p$ can be calculated by equating $[B']^{-1}$ from Equations 6.65 and 6.66, which will be left as a problem for the student to solve.

Turning to the case of calculating a multiplying factor that is not necessarily optimal, we use the data of case study 2 presented in Chapter 1, where $F_{ii}$ and $f_i$ are given and [B′] matrices have been calculated for 41, 67, and 100% generation.

Multiplying factors for the incremental fuel cost curve of solar electric power generators under nonoptimal situations for any centrallized-dispersed system, could have been indicated whereby using Equations 6.43 to 6.56, the incremental fuel cost multiplying factors are those listed in Equations 6.57 to 6.62. We should remember that $f_{i\text{-old}}$ and $F_{ii\text{-old}}$ refers to an incremental fuel cost curve representing an area having its own central power plant.

## XII. CASE STUDY

Given a centralized power system of 32 bus-bars having total generation of about 10,000 MW, whereby base loading is being supplied by fossil-steam generators, nuclear fueled generators and peak demand is intended to be supplied by solar fueled generators replacing gas turbines. This system has been described in detail in Chapters 2 and 5. In Chapter 1, the [B] matrix has been identified in Table 1.6 and the symmetric [R] matrix has been identified in Chapter 2, Table 2.15 for 70% loading.

Consider that the incremental fuel cost curve for the solar fueled generators has been intended to ensure optimal scheduling of power generation among all sources. Present systematic procedure for the design of the entire power system, i.e., to calculate the bus-bar voltage magnitudes, their phase angles, and reactive and real power flows.

### A. SOLUTION

1. Peak loads supplied by solar thermoelectric generators from Equations 6.43 and 6.44.
2. Peak loads to be supplied by photovoltaic solar generator where $F_{ii\text{-}1}$ is finite and $f_{i\text{-}1}$ = zero.
3. Peak loads to be supplied by an interconnection of solar thermoelectric-photovoltaic combined generators where $F_{ii} = F_{ii}$ (thermoelectric) + $F_{ii}$ (photovoltaic).

However, those three conditions for $F_{ii}$ and $f_i$ specified in Equations 6.43 and 6.44 are under a nonoptimal system for power scheduling of generation. Now, since fuel cell generators used in Chapters 1 and 2 have $F_{ii} = 0$ and $f_i$ = a constant which is 7.35 ¢/kWhr, therefore, for optimal power allocations among all generating sources, we are to consider optimal fuel cost multiplying factors as those expressed in Chapter 4, Equations 4.109 and 4.110, whereby

$$k_1 = 1 - \frac{A_1}{C_1 f_{i\text{-old}}} \tag{a}$$

and

$$k_2 = 1 + \frac{D_1}{E_1 - f_{i-\text{old}}} \tag{b}$$

where, $A_i$, $C_1$, $D_1$ and $E_1$ have been expressed in Chapter 4, Equations 4.104 through 4.106a with $F_{ii} = 0$, because $F_{ii}$ for the fuel cell is also zero.

Hence, we can realize that either a solar thermoelectric generator or a combination of thermoelectric-photovoltaic generators can fit in the system design of the 32 bus-bar centralized

system to meet the demand of peak loading replacing the gas turbines and fuel cells generators, which were selected in the system described in Chapters 1 and 2.

The optimal fuel cost multiplying factors are $k_1$ and $k_2$, which can be used one at a time so that we can use the optimal [B] matrix tabulated in Chapter 1, Table 1.7 for a total 70% loading, i.e., we used the principle of invariant [B] matrix for an optimal change in the incremental fuel cost curve imposed by the bulk solar power generators.

Having identified the applicable [B] matrix for the new interconnected power system, now we can identify the corresponding [R] matrix which represents the mode of power system interconnection in the power flow reference frame where everything is expressed in terms of power sources.

Then from the following equation:

$$[R] = [B]\,[K]^{-1} \tag{c}$$

or

$$[K] = \frac{[B]}{[R]} \tag{d}$$

All elements of the [K] matrix could be identified numerically from data of Chapter 1, Table 1.7 and Chapter 2, Table 2.15.

We can see from Chapter 1, Equation 1.12 that the [K] matrix for any bus-bar is of the following form:

$$K_{ij} = \frac{1}{V_i V_j}\left[\left(1 + S_i S_j\right)\cos\phi_{ij} + \left(S_i - S_j\right)\sin\phi_{ij}\right] \tag{e}$$

From Equation e and with data from the [K] matrix systematic solution could be obtained for all bus-bar voltage magnitudes and their phase angles as well as their reactive powers. Real powers are already known from the process of economic scheduling of generation. In Equation e, S is the ratio of real to reactive power at that bus-bar, V is the voltage magnitude and $\phi$ is the phase angle between any two bus-bars.

Commenting again on the procedure to secure information about every bus-bar in a power system using Equation e, we present the following example on a $4 \times 4$ [K] matrix to show clearly that bus-bar data on voltage magnitude phase angle and reactive power could be secured from elements of the [K] matrix.

A $4 \times 4$ [K] matrix for a 4 bus-bar power system is formed as follows:

$$[K] = \begin{bmatrix} k_{11} & k_{12} & k_{13} & k_{14} \\ k_{21} & k_{22} & k_{23} & k_{24} \\ k_{31} & k_{32} & k_{33} & k_{34} \\ k_{41} & k_{42} & k_{43} & k_{44} \end{bmatrix} \tag{f}$$

For the slack bus, its voltage magnitude, phase angle, and real power are known.

We are left with the remaining three bus-bars for which each is required to calculate three variables, namely, V, $\phi$, and Q. For the three bus-bars, we are looking to find nine unknowns plus the reactive power of the slack bus, for a total of ten variables.

$$K_{11} = \frac{1}{V_1^2}\left[\left(1 + S^2\right)\cos\phi_{11} + 0\right]$$

$$K_{12} = \frac{1}{V_1 V_2}\left[\left(1 + S_1 S_2\right)\cos\phi_{12} + \left(S_1 - S_2\right)\sin\phi_{12}\right]$$

$$K_{13} = \frac{1}{V_1 V_3}\left[\left(1 + S_1 S_3\right)\cos\phi_{13} + \left(S_1 - S_3\right)\sin\phi_{13}\right]$$

$$K_{14} = \frac{1}{V_1 V_4}\left[\left(1 + S_1 S_4\right)\cos\phi_{14} + \left(S_1 - S_4\right)\sin\phi_{14}\right]$$

$$K_{21} = \frac{1}{V_2 V_1}\left[\left(1 + S_1 S_2\right)\cos\phi_{21} + \left(S_2 - S_1\right)\sin\phi_{21}\right]$$

$$K_{22} = \frac{1}{V_2^2}\left[\left(1 + S_2^2\right)\cos\phi_{22} + 0\right]$$

$$K_{23} = \frac{1}{V_2 V_3}\left[\left(1 + S_2 S_3\right)\cos\phi_{23} + \left(S_2 - S_3\right)\sin\phi_{23}\right]$$

$$K_{24} = \frac{1}{V_2 V_4}\left[\left(1 + S_2 S_4\right)\cos\phi_{24} + \left(S_2 - S_4\right)\sin\phi_{24}\right]$$

$$K_{31} = \frac{1}{V_1 V_3}\left[\left(1 + S_3 S_1\right)\cos\phi_{31} + \left(S_3 - S_1\right)\sin\phi_{31}\right]$$

$$K_{32} = \frac{1}{V_2 V_3}\left[\left(1 + S_3 S_2\right)\cos\phi_{32} + \left(S_3 - S_2\right)\sin\phi_{32}\right]$$

$$K_{33} = \frac{1}{V_3^2}\left[\left(1 + S_3^2\right)\cos\phi_{33} + 0\right]$$

$$K_{34} = \frac{1}{V_3 V_4}\left[\left(1 + S_3 S_4\right)\cos\phi_{34} + \left(S_3 - S_4\right)\sin\phi_{34}\right]$$

$$K_{41} = \frac{1}{V_4 V_1}\left[\left(1 + S_4 S_1\right)\cos\phi_{42} + \left(S_4 - S_2\right)\sin\phi_{42}\right]$$

$$K_{42} = \frac{1}{V_4 V_2}\left[\left(1 + S_4 S_2\right)\cos\phi_{42} + \left(S_4 - S_2\right)\sin\phi_{42}\right]$$

$$K_{43} = \frac{1}{V_4 V_3}\left[\left(1 + S_4 S_3\right)\cos\phi_{43} + \left(S_4 - S_3\right)\sin\phi_{43}\right]$$

$$K_{44} = \frac{1}{V_4^2}\left[\left(1 + S_4^2\right)\cos^{-1}\phi_{44} + 0\right] \qquad \text{(g)}$$

The set of Equation g indicates 16 equations, whereby there are 16 unknowns to find.

Voltage magnitude, phase angle, and reactive power for each of bus-bars 2, 3, and 4, plus the

reactive power for the slack bus for a total of 10 unknowns, i.e., $V_2$, $V_3$, $V_4$, $\phi_{22}$, $\phi_{33}$, $\phi_{44}$, $S_2$, $S_3$, $S_4$, and $S_1$ (only reactive) can be secured from load flow calculations program. Then from the set of Equation g, we can list the six additional unknowns:

$$\phi_{12} = -\phi_{21}$$

$$\phi_{13} = -\phi_{31}$$

$$\phi_{23} = -\phi_{32}$$

$$\phi_{24} = -\phi_{42}$$

$$\phi_{32} = -\phi_{23}$$

$$\phi_{34} = -\phi_{43} \qquad \text{(h)}$$

Regarding our present case study, we are having $32 \times 32$ [K] matrix involving 1024 knowns to identify fully all information for the system bus-bars. Hence the feasibility of solution is positive.

Frankly speaking, to solve for all the 1024 unknowns requires a special computer program to develop and my belief is to leave this as a problem for the student to solve.

## XIII. SUMMARY

This chapter covers comprehensive scope for the economics of solar integrated power systems on engineering basis, parametric representation of solar power systems includes the direct solar thermoelectrics, the photovoltaics and their combination. Also discussed is the utilization of direct solar systems for building complexes with their parametric components.

The optimal design of solar energy system centers on the development of optimal [B] matrix which represents transmission linkage among generating centers or sources, and the [K] matrix which could be calculated from load flow data, followed by setting up the [R] symmetric matrix which represents the system design in the power flow reference frame.

Other topics presented in Section I include the identification of basic characterization for the incremental fuel cost curves for the three solar power systems discussed, namely, the direct thermoelectric system, the photovoltaic system, and then for the interconnected thermoelectric-photovoltaic system.

Incremental fuel cost multiplying factors on a nonoptimal basis have been discussed in Section X and the basis for their calculation presented.

## XIV. PROBLEMS

6.1 Express in terms of design parameters the difference between the solar thermoelectric generator and the photovoltaic solar generator. Also identify aspects of compatibility between the two kinds of energy systems.

6.2 In terms of a block diagram similar to that of Figure 6.1, assemble another diagram for the alternating current conventional power fueled by fossil-steam prime movers.

6.3 Verify the relationships established in Equations 6.20, 6.21, and 6.22 by differentiating $M_G$ with respect to x and setting that derivative to zero.

6.4 Derive Equation 6.24 for the cascading of n photovoltaic solar generators connected in series.

6.5 Equation 6.12 represents the efficiency of a photovoltaic solar generator with m as the independent variable, find the condition for maximum efficiency. Compare that with the Carnot cycle efficiency, and express reasoning for that.

6.6 Consider M as the number of solar collector-concentrator systems supplying hot water to groups of building clusters in close proximity such that an interchange from one system to another is operational. Using Equation 6.2, develop criterion for the total power loss calculation resulting from supplying hot water to the M building clusters. Hint: the sought criterion could be similar to that for calculating transmission losses in electric power network, i.e.,

$$P_L = \sum_{i=1}^{M} P_i B_{ij} P_j$$

6.7 Consider a solar collector-concentrator system patterned according to Equation 6.2 supplying steam to a steam turbine operating a cylindrical rotor alternator. Develop a relationship for the overall system efficiency taking into account losses in the collector-concentrator, the steam turbine, and the AC alternator.

6.8 For the efficiency of the system in Problem 6.7, develop the condition for maximum efficiency when $\tau$, the factor of geometrical transmittance, and $\delta$, the torque angle of the alternator, are the two independent variables.$\eta_{total}$ is the main dependent variable.

6.9 Consider a solar steam AC generator linked to a solar photovoltaic generator and coupled to a solid-state power inverter to produce an AC output (with efficiency $\eta$). Solve for the temperature difference between the source and sink for the solar photovoltaic generator and optimum value for (m).

6.10 For equality of incremental fuel cost for both the solar thermoelectric and photovoltaic generators, obtain an expression for the maximum incidence of solar energy per unit area of collector when the temperature gradient in the photovoltaic generator acts as the sole independent variable.

6.11 Repeat Problem 6.10 when $A_n/A_p$ is the sole independent variable.

6.12 Repeat Problem 6.10 when both the temperature gradient and (m) are the independent variables.

6.13 One problem in the performance of the solar photovoltaic generator is the limited range of $(T_1 - T_o)$. Through Equation 6.17 for material efficiency, show possible design avenues where possible such that $(T_1 - T_o)$ is maximum. Express the resulting form of $M_{opt}$.

6.14 Find the average of two incremental fuel cost curves, one representing the solar thermoelectric generator and the other for the solar photovoltaic generator. The solution sought is for a new incremental fuel cost curve to be obtained on an averaged range of total power capacity of $P_i$.

6.15 Repeat Problem 6.14 by seeking a new incremental cost curve averaged over a range of optimum power output for the solar photovoltaic generator (Equation 6.33). Hint: Insert $P_{i\text{-}2\text{-}opt}$ of Equation 6.33 for $P_{i\text{-}2}$ in Equation 6.28 to first represent $dF_{i\text{-}2}/dP_{i\text{-}2}$. Then perform averaging process of $dF_{i\text{-}1}/dP_{i\text{-}1}$ and $dF_{i\text{-}2}/dP_{i\text{-}2}$ over $P_{i\text{-}2\text{-}opt}$.

6.16 Refer to Equations 6.66 and 6.65 each expressing the [B] matrix for centralized-dispersed solar power system pertaining to a change in the slope of the incremental fuel cost curve. Under an invariant [B] matrix, obtain an approximate solution for the fuel multiplying factor $k_p$. You may end up with more than one solution.

6.17 Using the fuel cost multiplying factor of Chapter 4, Equation 4.109 and following the procedure of calculating elements of the [K] matrix presented in the case study in Section XII of Chapter 1, proceed using information of the [B] matrix given in Table 1.7 and the [R] matrix in Chapter 2, Table 2.15 at 70%. Calculate elements of the $32 \times 32$, [kp] matrix.

6.18 From elements of the [K] matrix secured in Problem 6.17, develop an effective comprehensive computer format for the solution of voltage magnitude, phase angles, and reactive power of the 31 bus-bars plus the reactive power for the slack bus.

6.19 Employing data secured in Problem 6.17 and the computer format established in Problem 6.18, solve for the numerical values of $|V_i|$, $\phi_i$, $Q_i$ for every bus-bar as well as $Q_1$ for the slack bus. In effect, we are after designing a new power system where peak loading is to be supplied by solar electric generators. This design is still a reflection in the power flow reference frame, whereby no identification of line impedances and leakage flows are established or identified.

6.20 Repeat Problem 6.17 through the application of the fuel cost multiplying factor expressed by Equation 4.110.

6.21 Repeat Problem 6.18 based on the utilization of the fuel cost multiplying factor of Chapter 4, Equation 4.110.

6.22 Repeat Problem 6.19 based on the utilization of the fuel cost multiplying factor of Chapter 4, Equation 4.110.

6.23 Consider an alternative power system (B) described in the case study of Chapter 2 which is based on the assumption that solar fueled electric generators replace all steam-fossil and gas-turbine powered AC generators, while the remaining generators are pumped-hydro and nuclear powered generators. Using the optimal fuel cost multiplying factor of Chapter 4, Equation 4.109 and its invariant [B] matrix given in Chapter 1, Table 1.5 and the corresponding [R] matrix giiven in Chapter 2, Table 2.16, calculate the new $32 \times 32$, [K] matrix.

6.24 Using the computer format developed in Problem 6.18, calculate numerical values for $V_i$, $\phi_1$, and $Q_i$ for every bus-bar besides $Q_i$ the reactive power of the slack bus.

6.25 Consider an alternative power system (D) described in the case study of Chapter 2, which is based on the assumption that solar fueled electric generators replace all fossil-steam powered generators planned to supply off-peak loading, whereby the remaining type of generators are nuclear, pumped-hydro, and gas-turbine powered generators. Using the optimal fuel cost multiplying factor of Chapter 4, Equation 4.109, the invariant [B] matrix given in Chapter 1, Table 1.8, and the corresponding [R] matrix given in Chapter 2, Table 2.18, calculate the new $32 \times 32$ [K] matrix.

6.26 Using the computer format developed in Problem 6.18, calculate numerical values for $V_i$, $\phi_i$ and $Q_i$ for all bus-bars, as well as $Q_i$ the reactive power of the slack bus.

6.27 Solve Problem 6.23 using the optimal fuel cost multiplying factor of Chapter 4, Equation 4.110.

6.28 Solve Problem 6.24 using the optimal fuel cost multiplying factor of Chapter 4, Equation 4.110.

6.29 Solve Problem 6.25 using the optimal fuel cost multiplying factor of Chapter 4, Equation 4.110.

6.30. Solve Problem 6.26 using the optimal fuel cost multiplying factor of Chapter 4, Equation 4.110.

6.31 In reference to Figure 6.1, establish a systematic process of energy transformation from solar heat input, and moving step by step through each block in DAYTIME LOOP and then the FULL TIME LOOP, passing across storage processes, the steam turbine, and finally the development of AC electric power by the generator. Hint: consider that each box in Figure 6.1 is in effect a transform function in the (s) domain linked by an input to the box and output. The overall transform function sought relates the ratio of $H_{solar}(S)/P_{gen}(S)$, where $H_{solar}(S)$ is the transform function in the complex frequency domain of the total solar energy input, and $P_G(S)$ is the transform function of energy output provided by the AC generator.

6.32 From the multiconnected transform functions obtained in Problem 6.31, secure the time response of the DAYTIME output under zero initial conditions.

6.33 Repeat Problem 6.32 for the FULLTIME LOOP output response.

## REFERENCES


1. **Cherne, J. M.,** Solar energy — an overview, *Proc. Symp. Films Sol. Energy*, The American Vacuum Society, 1975, 975.
2. **Denno, K.,** Feasibility of solar — electrochemical power system, *Conf. Dig., Eur. Conf. Electrotech.*, 1974, A4-2(1) A4-2(2).
3. **Denno, K.,** *Power System Design and Applications for Alternative Energy Sources*, Prentice-Hall, Englewood Cliffs, NJ, 1989.
4. **Hu, C. and White, R. M.,** *Solar Cells — From Basics to Advances Systems*, McGraw-Hill, New York, 1983.
5. **Herwig, L. O.,** Solar Energy System for Electricity Production, Paper C75-014-6 presented at IEEE Power Eng. Soc., Winter 1975.
6. **Kirchmayer, L. K.,** *Economic Operation of Power Systems*, John Wiley & Sons, New York, 1956.
7. **Meinel, A. B. and Petit, M.,** Solar energy — the possible dream, *AWARE*, Optical Science Center, University of Arizona, February 1972.
8. **Mickle, M. H.,** *Optimization in Systems Engineering*, Intext Education Publishers, 1972.
9. **Meinel, A. B. and Petit, M.,** Is it time for a new look at solar energy, *Bull. At. Sci.*, 32, 1971.
10. **Raag, V. and Berlin, R. E.,** Asilicon-germanium solar thermoelectric generator, *Energy Conversion*, Vol. 8, Pergamon Press, Oxford, 1968, 161.
11. **Raag, V.,** Design and performance analysis of panel- type solar thermoelectric generators, *Energy Conversion*, Vol. 8, Pergamon Press, Oxford, 1968, 169.
12. **Stoecker, W. F.,** *Design of Thermal Systems*, McGraw Hill, New York, 1971.
13. New promise for photovoltaics — economy and efficiency will decide the market success of solar cells for bulk power generation, *EPRI J.*, 6, July/August 1983.
14. **Soo, S.L.,** *Direct Energy Conversion*, Prentice-Hall, Englewood Cliffs, NJ, 1968.
15. **Walsh, E.M.,** *Energy Conversion*, The Ronald Press Co., New York, 1967.

Chapter 7

# THE ECONOMICS OF WIND ENERGY CONVERSION SYSTEMS (WEC)

## I. INTRODUCTION*

Wind energy conversion is one of those abundant resources that can provide bulk power generation. Knowledge about quantitative wind energy falls within the area of meteorology; understanding how a wind turbine operates falls within the field of aerodynamics; wind turbine design involves the areas of structural mechanics, control, electrical machinery, and aspects of civil engineering. Integration of wind turbine into a power system involves the tools of interconnection, environmental acceptability, and safety and engineering economics.

Current data indicate that medium sized wind-turbine generators of 20 to 40 m diameter, with power generating capacities ranging from 50 to 500 kW, offer the most economical aspects for land based applications.

Offshore wind energy systems, to be economically competitive, need to use multimegawatt wind turbines with a diameter of 100 m and larger.

Wind energy is considered reliable on the basis of year to year duration. Also, the annual wind energy at a given location depends on the wind velocity duration distribution which can be expressed mathematically as a Weibull function involving two parameters, namely, a shape parameter and a characteristic speed.

The Rayleigh distribution model provides reliable approximation to the wind velocity duration distribution over flat terrain which states that the probability, P, that the wind speed exceeds a certain limit,V, is given by

$$P(V) = \exp\left[-\frac{\pi}{4}\frac{V}{V_m}\right]^2 \tag{7.1}$$

where $V_m$ is the annual average wind speed.

Equation 7.1 indicates that wind speed in excess of $V_m$ can be expected over 46% of the year, whereas wind speed above 2 to 4 $V_m$ occurs for less than 1% of the year.

Wind power density W is expressed by

$$W = \frac{1}{2} M_a V^2 \text{ (watts / m}^2\text{)} \tag{7.2}$$

where $m_a$ is the air density. (Usually $m_a \approx 1.225$ kg/m$^3$.) Using Rayleigh distribution model of wind speeds, it can be shown that the annual average power in the wind is equal to 0.95 $V_m$.

At a typical European site near a coastal location, with $V_m = 5.5$ m/s at a height of 10 m, the annual average power density would be about 190 W/m$^2$, corresponding to 170 kWh/m$^2$ annually.

Due to the Earth's surface, retarding effect variation of wind speed with height h is expressed by the following rule:

$$\frac{V_h}{V_{10}} = \frac{[h]^n}{10} \tag{7.3}$$

* · © 1983, IEE. Reprinted with permission from Musgrove, P.J., Wind energy conversion — an introduction, *IEE Proc.*, 130 (A, No. 9), 506—516, 1988.

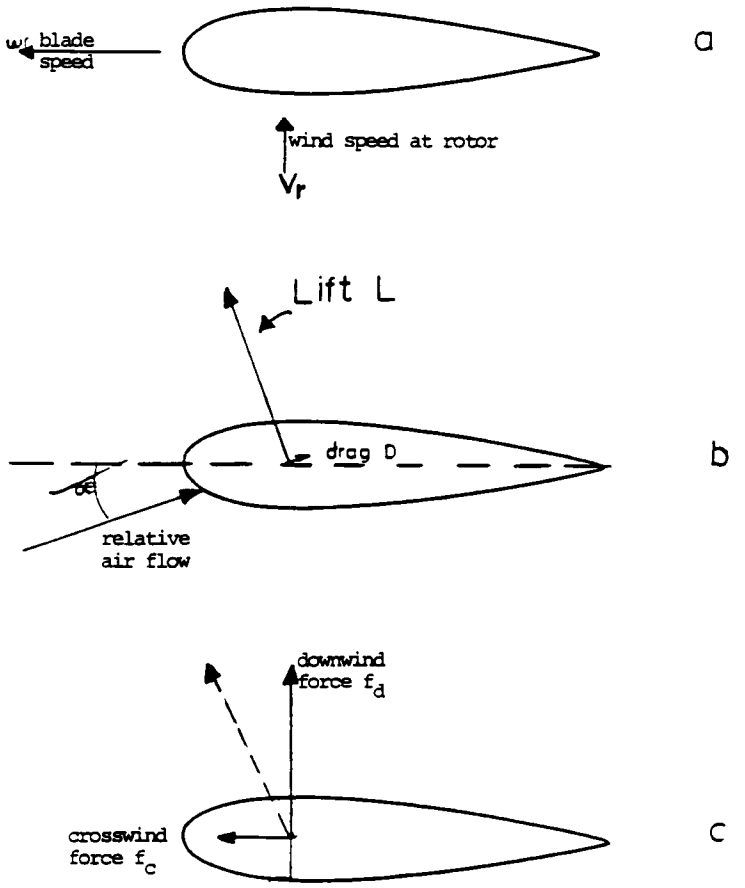


FIGURE 7.1 Aerodynamic forces on wind turbine blade. (From Musgrove, P. J., Wind energy conversion — an introduction, *IEE Proc.*, 130 (A, No. 9), 506 — 516, 1988. With permission.)

where $V_h$ = the wind velocity at height h, $V_{10}$ = the wind velocity at 10 m height, n depends on the terrain roughness, and 1 n = $^1/_7$ for flat terrain.

Large wind turbines usually have a hub height of about 60 m and wind speed is consequently about 30% higher than at h = 10 m, and with wind power proportional to the cube of wind speed this implies that wind power density at this hub height is more than double the wind power density at 10 m height.

For a site where the annual average wind speed $V_{10} \simeq 6$ m/s and where hub height annual average wind speed $V_m = 8$ m/s, the annual average wind speed power density is about 600 W/m$^2$ corresponding to 5200 kWh/m$^2$ annually.

## II. WIND TURBINE CHARACTERISTICS*

On a wind turbine or aerogenerator, the blades are designed to produce a transverse force to rotate them around a central shaft delivering a shaft power output. This is shown in Figure 7.1 (a, b, and c) where $\alpha$ = angle between the relative air flow and blade central axis, $\omega$ = wind

* © 1983, IEE. Reprinted with permission from Musgrove, P.J., Wind energy conversion — an introduction, *IEE Proc.*, 130 (A, No. 9), 506—516, 1988.

turbine rotational velocity in radians per second, r = radial distance from the hub to the section of blade being considered, $V_r$ = wind speed at the rotor, L = transverse lift force, and D = drag force parallel to airflow.

The crosswind force $f_e = L\sin\alpha - D\cos\alpha$, provides a torque $f_e r$ about the hub delivering a shaft power output of $f_e rw$ for blade rotation integration along the entire blade length, from hub to tip, and multiplication by the number of blades gives the total shaft power output.

The downward force $f_d = L\cos\alpha - D\sin\alpha$, imposes loads on the blades and tower of the wind turbine, hence the designer must ensure that the structure can stand these loads even under severe storm conditions.

Associated with $f_d$ on the blades, there is an equal and opposite force experienced by the approaching air flow which reduces its momentum and velocity as it approaches the wind turbine rotor.

Therefore, for maximum output power, $f_d$ should be just sufficient to reduce the approaching air speed to $V_r \simeq 2\ ^2/_3\ V$ (V is the wind speed).

The two parameters most widely used to describe the performance of wind turbines are the tip speed ratio $\gamma$ and the power coefficient $C_p$. Thus,

$$\gamma = \frac{\omega R}{V} \tag{7.4}$$

where R is the rotor radius, measured to the tip of the blade, $\omega$ is the rotational speed, and V is the wind speed upstream.

The power coefficient $C_p$ is given by:

$$C_p = \frac{\omega}{\frac{1}{2} m_a A V^3} \tag{7.5}$$

A is the rotor swept area.

$C_p$ gives a measure of the power output of the wind turbine relative to the power in the wind passing without obstruction, through an area equal to the rotor area.

For good design the average power output from modern wind turbines is given by

$$P_m = 0.25 m_a V_m^2 \tag{7.6}$$

For $V_m$ = 5.5 m/s, $P_m$ = 50 W/m$^2$ which is equivalent to 450 kWh/m$^2$ annually.*

The environmental impact of using wind turbines has to be carefully examined. Areas of concern are noise, electromagnetic interference, and visual intrusion. Well designed machines will be inaudible above the background noise level beyond distances of 100 to 200 m, whereby electromagnetic interference for wind turbines should not be in close proximity to TV and radio transmitting stations.

## III. BASIC ECONOMICS OF WIND TURBINE*

An effective economic measure for wind driven turbines with a diameter in excess of 10 m is expressed in terms of normalized cost per unit rotor area rather than the cost per rates in kilowatts, and indeed the latter could be very misleading. For example, as the rate power is proportional to the cube of the rated wind speed, a relatively slight increase in the latter will significantly increase the rated power and give a corresponding reduction in the nominal cost per kilowatt, but without giving any significant increase in the energy output of the wind

* © 1983, IEE. Reprinted with permission from Musgrove, P.J., Wind energy conversion — an introduction, *IEE Proc.*, 130 (A, No. 9), 506—516, 1988.

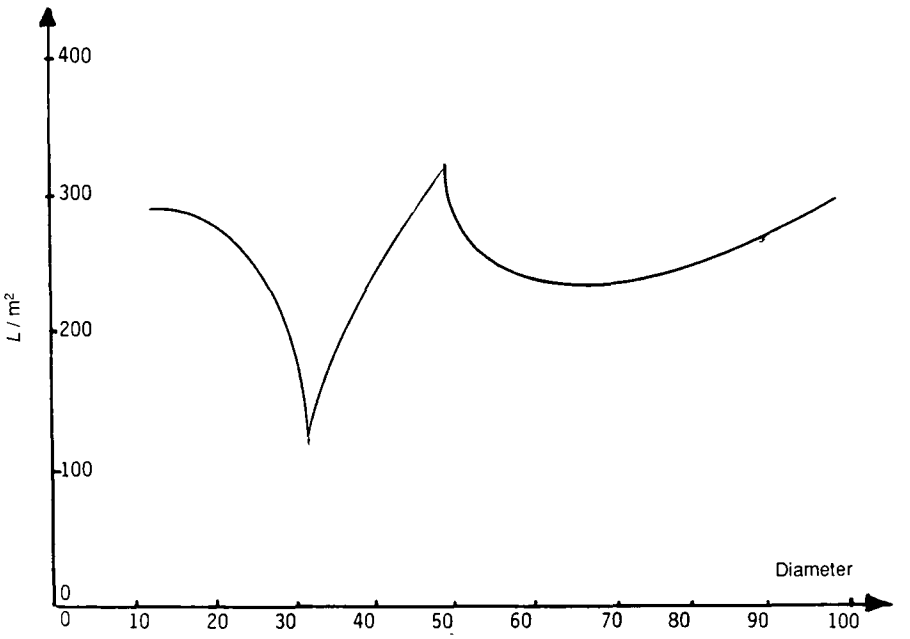


FIGURE 7.2 Normalized cost area, variation with wind turbine diameter.

turbine. Figure 7.2 illustrates reliable information regarding the normalized cost per unit area of turbines rotor.

Given the usual assumption that velocity variation with height can be represented by a one seventh power law, the power in the wind will be proportional to $(H^{1}/_{7})^3 = H^{0.43}$, where H is the hub height of the rotor.

Variation of wind power density with height may be allowed by the simple expedient of defining a normalized cost per unit area of the rotor $C_{10}$ as follows:

$$C_{10} = (\text{cost per unit area})\frac{(10)^{0.43}}{H} \tag{7.7}$$

The parameter $C_{10}$ can be interpreted as the equivalent cost per unit rotor area, relative to the wind speed experienced at a height of 10 m. The cost data in Figure 7.2 has been normalized this way.

Cost information indicated by Figure 7.2 includes those for tower and on site erection, but excludes foundation and power grid connection as well as operation and maintenance costs.

The delivered cost of energy from a wind turbine generator includes, besides the capital cost, the operation and maintenance costs, its lifetime, and the required rate of return on capital investment.

The concept of an annual charge rate C is a very useful and meaningful one, where C is related to r by the following equation:

$$C = \frac{r}{1-(1+r)} - y \tag{7.8}$$

where r is the required real estate of return after allowing for inflation and y is the lifetime in years.

Also y is the annual repayments of an initial investment I and provide a real rate of return r on the capital invested.

In terms of data in the U.K., a 5% rate of return together with a lifetime of 20 years, i.e., r = 0.05, y = 20 corresponds to an annual charge rate of 8%, to this must be added the annual costs associated with operating and maintenance costs.

It had been reported that wind turbines with rotor diameter of about 50 m are more competitive than those with 100 m. Also of high importance is the applicational roles for wind turbines which include operating in parallel with the conventional power grid systems and along side diesel engines in remote places.*

## IV. WINDS BOUNDARY LAYERS**

Bennett et al.[2] developed formulation for wind conditions in upper atmospheric layers based on data collected in lower layers. His formulation identifies that wind main stream velocity is a dependent function on height expressed as a power law, taking into account the state of roughness for land and sea coupled with some interpolation in transition from one air boundary layer to another.

The formulations of Bennett et al.[2] include the following: the overland wind structure is described by the 10 m speed $U_1$, where

$$U_i = 0.41U_f \tag{7.9}$$

and the boundary depth is expressed by

$$H = tU_f \tag{7.10}$$

where $U_f$ is the free stream speed, and t = 60 s.

At the offshore, the formula for 20 m speed has been deduced from weathership data and given by:

$$U_2 = U_f\left[3.8/U_f\right]^{0.2} \tag{7.11}$$

and the boundary layer depth is

$$H = 0.0005\left[U_1^{2.5}/U_f\right]/f\sin\alpha \tag{7.12}$$

where $\alpha$ is the mean sea surface angle, with typical value of $\alpha = \sin^{-1} = 0.17$ and f is the Coriolis parameter and approximately = 0.0001 $s^{-1}$.

Equations 7.9 to 7.12 apply to average terrain and to average onshore and offshore stability conditions.

Interpolation due to imbalance between land and sea is proportional to the difference between the shear stress and its asymptotic value. The recovery equations are

$$U^2 = U_\infty^2 - \left(U_\infty^2 - U_o^2\right)\exp\left(-2xU_fR_f/U^2\right) \tag{7.13}$$

$$R = \left(U^2\sin\alpha_o - U_o^2\sin\alpha_\infty\right)/\left(U^2 - U_o^2\right) \tag{7.14}$$

* © 1983, IEE. Reprinted with permission from Musgrove, P.J., Wind energy conversion — an introduction, *IEE Proc.*, 130 (A, No. 9), 506—516, 1988.

** © 1983, IEE. Reprinted with permission from Bennett, M., Hamilton, P.M., and Moore, D.J., Estimation of low-level winds from upper-air data, *IEE Proc.*, 130 (A), 517, 1983.

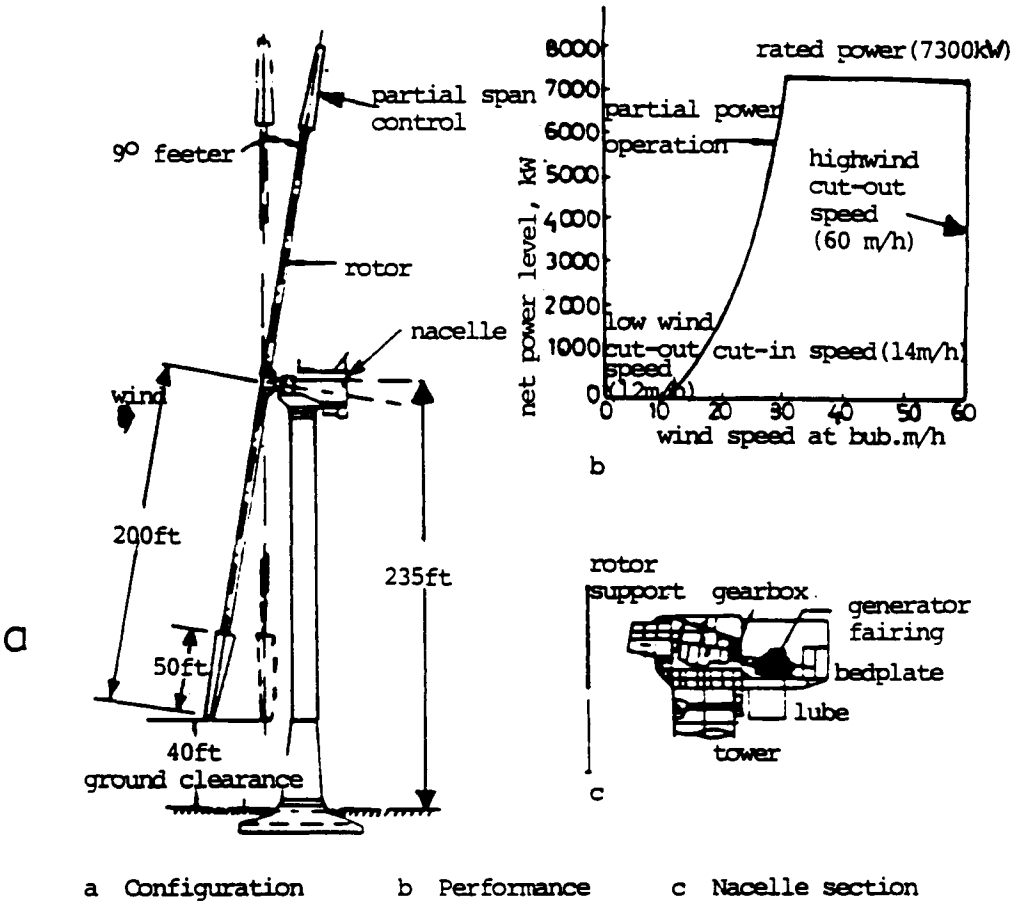


FIGURE 7.3 MOD-5A system. (From Barton, R. S. and Lucas, W. C., Development of the 7.3 MW MOD-5A wind-turbine generator system, *IEE Proc.*, 130 (A, No. 9), 537—541, 1983. With permission.)

where the o subindex refers to the speed U and direction at the discontinuity and the ∞ subindex refers to the asymptotic speed over the new surface after a fetch of distance x. A fetch of 100 km is required for the development of a new asymptotic boundary layer.

## V. MODELING OF WIND TURBINE*

Research has advanced the concept that dynamic modeling of wind turbine systems is the fact that gross movement of any component of the structure occurs relative to another part. This precludes the application of standard finite element packages that usually consider structures in which motion occurs about a mean undisplaced position.

In this section, it is of interest to consider a highly idealized model to show general aspects of wind turbine dynamics based on a three degrees of freedom system shown in Figure 7.3. In this system the blades will perform in a plan lead-lag motion while the tower is permitted to move laterally in a rotational plane.

If $\zeta$ represents the lead-lag angle of the blade, $\psi$ represents the azimuth and the linear motion of tower head, then the kinetic energy of the system can be expressed by:

* © 1983, IEE. Reprinted with permission from Garrad, A. D., Dynamics of wind turbines, *IEE Proc.*, 130 (A, No. 9), 523—530, 1983.

$$T = \frac{1}{2}\left[ I\sum_{i-1}^{2}(\psi_i + \zeta_i)^2 + 2M\dot{\theta}^2 + 2\theta\sum_{i-1}^{2}(\psi_i + \zeta_i)\cos(\psi_i + \zeta_i) + M_e\dot{\theta}^2 \right] \tag{7.15}$$

where

$$\psi_i = R^{+(i-1)}$$

$$\psi_i = \psi + (i-1)\pi$$

$$I = \int_o^R mr^2\, dr$$

$$S = \int_o^R mr\, dr \tag{7.16}$$

$$M_e = \int_o^R m dr$$

where $M_e$ is the mass of tower, R is the blades radius, and m is the blades mass per unit length.

Also, based on the analogy that tower and blades resemble a simple spring, the potential energy of the wind turbine is expressed by:

$$U = \frac{1}{2}K_\zeta \sum_{i-1}^{2}\zeta_i^2 + \frac{1}{2}K_t\theta^2 \tag{7.17}$$

where $K\zeta$ = an equivalent spring for the blades and $K_t$ = tower spring parameter.

The set of equations of motion for the three degrees of freedom model are

$$M_t\ddot{\theta} + S\frac{d^2}{dt^2}\left[(\zeta_1 - \zeta_2)\cos\zeta\right] + K_t = 0 \tag{7.18}$$

$$I\zeta_1 + S\ddot{\theta}\cos(\psi + \zeta_1) + K_\zeta\zeta_1 = 0 \tag{7.19}$$

$$I\zeta_2 + S\ddot{\theta}\cos(\psi + \zeta_2) + K_\zeta\zeta_2 = 0 \tag{7.20}$$

where $M_t = M_e + 2M$ is the total linear mass moving at the top of the tower.

## VI. 7.3 MW MOD WIND TURBINE GENERATOR*

This section presents economic perspective for a prototype design of a 7.3 MW wind turbine generating system designed by General Electric Advanced Energy program under DOE/NASA sponsorship, that will generate electricity at about 3.75 ¢/kWh.

Figure 7.3a shows the system configuration and Figure 7.3b a pattern of net power level speed of the wind turbine.

* © 1983, IEE. Reprinted with permission from Barton, R. S. and Lucas, W. C., Development of the 7.3 MW MOD-5A wind-turbine generator system, *IEE Proc.*, 130 (A, No. 9), 537—541, 1983.

**TABLE 7.1**
**Major Parameters Model 304.0**

| | |
|---|---|
| Tower | |
| Height to rotor CL (feet) | 240 |
| Cylinder diameter (feet) | 14.5 |
| Base diameter (feet) | 22.5 |
| Weight (tons) | 332.5 |
| Nacelle (structure and drive train) | |
| Height (feet) | 20 |
| Width (feet) | 12 |
| Length (feet) | 44 |
| Weight (tons) | 271 |
| Rotor (blade and yoke) | |
| Diameter (feet) | 400 |
| Maximum chord (feet) | 25 |
| Control tips (feet) | 50 |
| Weight (tons) | 224 |

*Note:* 1 ft = 0.3048 m

From Barton, R. S. and Lucas, W. C., Development of the 7.3 MW MOD-5A wind-turbine generator system, *IEE Proc.*, 130 (A, No. 9), 537—541, 1983. With permission.

**TABLE 7.2**
**Operational Characteristics**

| | |
|---|---|
| Rated power (kilowatt) | 7300 |
| Rated wind speed at 240 ft (meters per hour) | 32 |
| Cut-in/cut-out wind speed at 240 ft (meters per hour) | 14/60 |
| Survival wind speed at 240 ft (meters per hour) | 130 |
| Rotor speeds, (RPM, revolutions per minute) | 13/16.8 (nominal) |
| Energy capture/year | |
| (100% availability), million kilowatt hour | |
| (14 m/h average wind speed at 32 ft) | 21.3 |

From Barton, R. S. and Lucas, W.C., Development of the 7.3 MW MOD-5A wind-turbine generator system, *IEE Proc.*, 130 (A, No. 9), 537—541, 1983. With permission.

The MOD-5A system has been developed for a wind regime having a mean wind speed of 14 mph at 10 m height.

Table 7.1 shows major parameters of model 304.0 while Table 7.2 shows operational characteristics of the wind-turbine system. Also this system design has a high cut-out of 60 m/h.

Optimization design procedure that was carried out on model 304.0 resulted in the development of a cost effectiveness of 3.5 ¢/kWh at the 1980 rate. The volume production installed capital cost and cost of energy trends at conceptual design are shown in Figure 7.4. A minimum cost was predicted at a 400 ft rotor diameter for 3.3/kWh for the design of 14 m/h mean wind regime at 32.8 ft with variable sheer.

Table 7.3 and Figure 7.5 show cost of generation data and spider diagram for the relative cost of electricity with respect to design and operation parameters for the wind-driven turbine generator. This information was established by the British Wind Energy Association, London, and published by BWEA professional group S1 in the issue of Part A on Alternative Energy which appeared in May 1987.

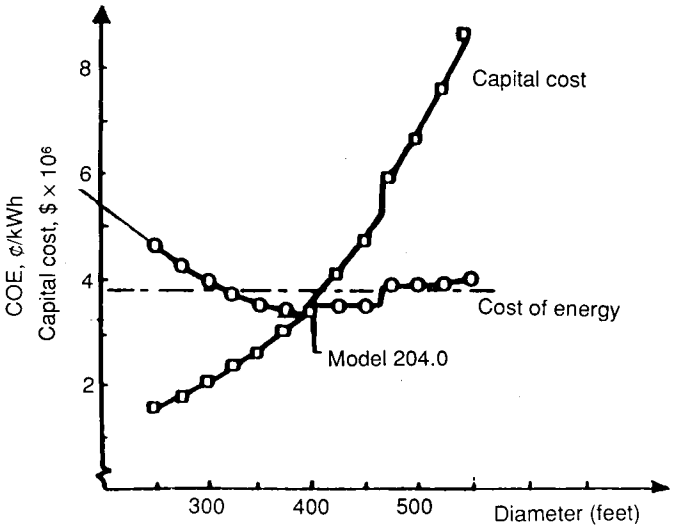


FIGURE 7.4 Cost of wind energy and capital cost. (From Barton, R. S. and Lucas, W. C., Development of the 7.3 MW MOD-5A wind-turbine generator system, *IEE Proc.*, 130 (A, No. 9), 537—541, 1983. With permission.)

**TABLE 7.3**
**Cost of Generation**

| | | |
|---|---|---|
| Capital cost per rated kilowatt | C/W | 880 £/kW |
| Design life expectancy | n | 30 years |
| Required real rate of return | r | 5% |
| Annual charge rate | R | 6.5% |
| Operation and maintenance | M | 2% |
| Hours in a year | h | 8760 h |
| Turbine rated wind speed (hub height) | $v_r$ | 13.3 m/s |
| Site annual mean wind speed (hub height) | $v_m$ | 9.4 m/s |
| Mean as fraction of rated wind speed | $v_m/v_r$ | 0.71 |
| Nominal load factor | F | 0.46 |
| Machine availability | A | 95% |
| Factor for other losses | a | 90% |
| Generation costs | G | 2.1 p/kWh |

From Swift-Hook, D. T., Wind energy — it's the cheapest, *IEEE Rev.*, 34 (No. 1), 30, 1988. With permission.

The brief summary then appeared in the issue of IEE Review, January 1988 through article by Donald T. Swift-Hook.[6]

Next in this chapter to consider is the economic and operational implications arising from the integration of a complex of wind-driven generators on a power system. The purpose is to identify technical and economic problems connected with the dynamic behavior of the interconnected system, the aspects of planning and operation, as well as coordination of the new interconnected system involving the integration of aerogenerators with an existing large grid power system.

Aspects of capital cost, structural integrity, the variable and uncertain nature of the wind, and the remoteness of suitable generation sites from main load centers, will play major roles in the process of economic optimization for the entire system.

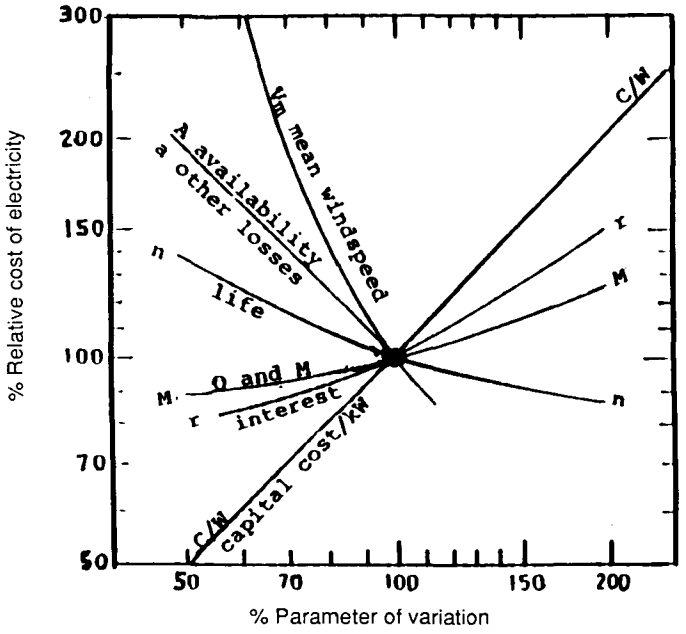


FIGURE 7.5 Cost sensitivities of wind turbine. (From Swift-Hook, D. T., Wind energy — it's the cheapest, *IEEE Rev.*, 34 (No. 1), 30, 1988. With permission.)

Roles for the utilization of pumped-storage generation and gas-turbine plants in servicing the unpredictable changes in wind power output, over the scheduling period, are evaluated by means of meteorological forecasts of wind speed.

## VII. DYNAMIC RESPONSE OF WIND TURBINE*

This involves the steady state and transient behavior of aerogenerators in connection with synchronous and induction generators in an integrated power system. For relatively slow changes in power generation, power output for the aerogenerator is given by

$$P = \frac{1}{2}\pi\rho\, a^2 U^3 \omega T\left(\frac{\omega a}{U}\right) \tag{7.21}$$

where a is the radius of rotor, ω is the angular velocity, and U is the wind velocity.

T is the dimensionless, normalized, torque-speed characteristic that depends on the solidity and blade design, and whose argument is the ratio of the tip to wind speed. A typical characteristic is shown in Figure 7.6.

For induction machines, there has to be a total match between maximum electromagnetic torque at wind speed and maximum operating torque of the generating system.

At the same time, synchronous torques developed and synchronism by alternators must be in perfect conformity and synchronized with that for aerogenerators and induction generators.

## VIII. SYSTEM REGULATION OF INTEGRATED SYSTEM*

Fluctuations in the power output of aerogenerators would place additional regulation demands on the remaining power sources and increase the requirement for short-term reserve

* © 1980, IEE. Reprinted with permission from Farmer, E. D., Newman, V. G., and Ashmole, P. H., Economic and operational implications of a complex of wind-driven generators on a power system, *IEE Proc.*, 127 (A, No. 5), 289—295, 1980.

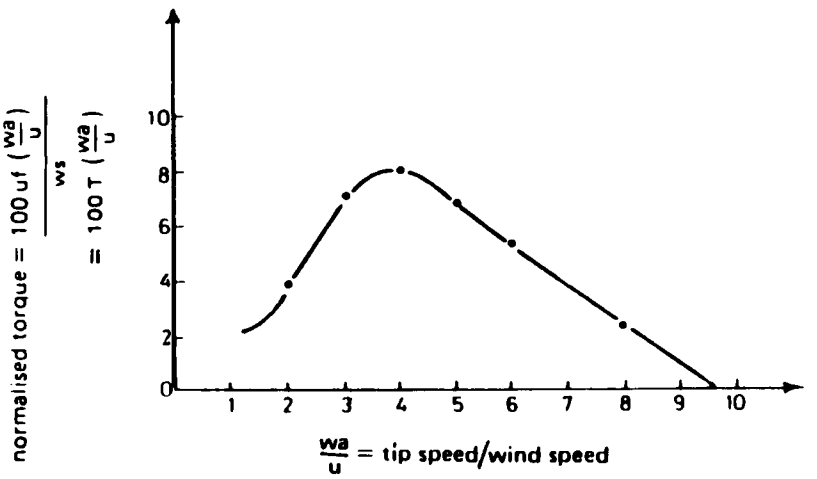


FIGURE 7.6 Torque-speed characteristics of wind driven generator. (From Farmer, E. D., Newman, V. G., and Ashmole, P. H., Economic and operational implications of a complex of wind-driven generators on a power system, IEE Proc., 127 (A, No. 5), 289—295, 1980. With permission.)

capacity. Consequently, it is expected that provisional governing gains by thermal and hydro plants to control frequency changes will produce significant economic penalties to tackle and contain.

Regarding the spectrum of wind turbulence, according to Taylor's hypothesis, the time constant of the associated function is represented by the ratio of L/U, where L is the integral length scale and U is the mean wind speed.

Power output variations for aerogenerators, resulting from changes in wind speed, may be estimated from the machine characteristic given by Equation 7.21, rewritten as follows:

$$P = \frac{1}{2}\pi\rho\, a^2 U^3 f\left(\frac{\omega a}{U}\right) \tag{7.22}$$

where f is a dimensionless form factor function given in terms of torque-speed correlation and given by

$$f = \frac{W_a}{U} = \frac{\omega a}{U} T\left(\frac{\omega a}{U}\right) \tag{7.23}$$

Figure 7.7 illustrates idealized windmill characteristics. For the machine represented by this figure, the power per speed sensitivity between the cut-in and rate speed, takes the form $2/v_r$, where $v_y$ is the rated wind velocity.

Incoherency in wind fluctuations will produce fast variations in individual machines power outputs. In an array of aerogenerators, if the separation between nearest machines exceeds the integral length scale L, variations in machine outputs becomes almost independent.

According to the Markoff model which identifies power system response due to load fluctuations, two aerogenerators with a separation of $X_s$ would experience fluctuations with a cross-spectral density given by

$$2\bar{U} / L \exp\left(jw\, x_s\, \bar{U}\right)\omega^2 + \bar{U}^2 / L^2 \tag{7.24}$$

It had been reported that independence of spectral variations occurs beyond a frequency of U/3L, and for a typical value of U = 10 m/s and L = 500 m, U/3L becomes equal to 1 c/2.5 min.

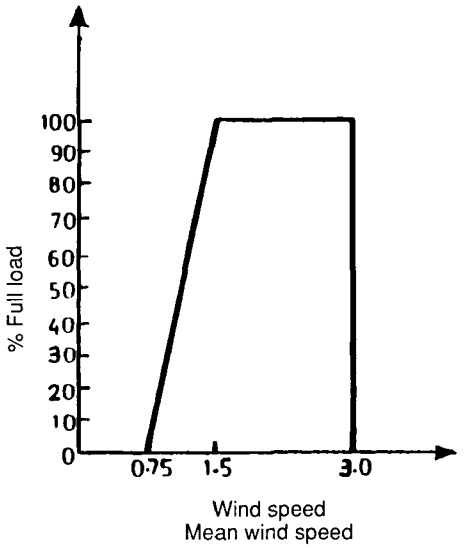


FIGURE 7.7 Idealized windmill characteristics. (From Farmer, E. D., Newman, V. G., and Ashmole, P. H., Economic and operational implications of a complex of wind-driven generators on a power system, *IEE Proc.*, 127 (A, No. 5), 289—295, 1980. With permission.)

Now for an array of N aerogenerators, equally spaced with $X_s$, individual outputs of $P_1$, $P_2$ ... $P_N$ would supply a total generation of

$$P_{tot} = P_1 + P_2 + P_3 + \ldots + P_N \tag{7.25}$$

and the total variance of output fluctuations takes the form:

$$\sigma^2 = P_o^2 \sum_{i=1}^{N} \sum_{j=1}^{N} \exp\left( -x_s |i - j| / L \right) \tag{7.26}$$

where $P_o^2$ is the variance of an individual aerogenerator output.
When $N \geq L/X_s$, $\sigma^2$ becomes

$$\delta^2 = N P_o^2 \coth\left(\frac{x_s}{2L}\right) \tag{7.27}$$

Also percentage and fractional rms (root mean square) variations in total output is reduced in relation to that of an individual aerogenerator by the diversity factor (D) given by

$$D = N \tanh\sqrt{x_s / 2L} \tag{7.28}$$

For a system of aerogenerators with separation $x_s \gg L$, $D = N$

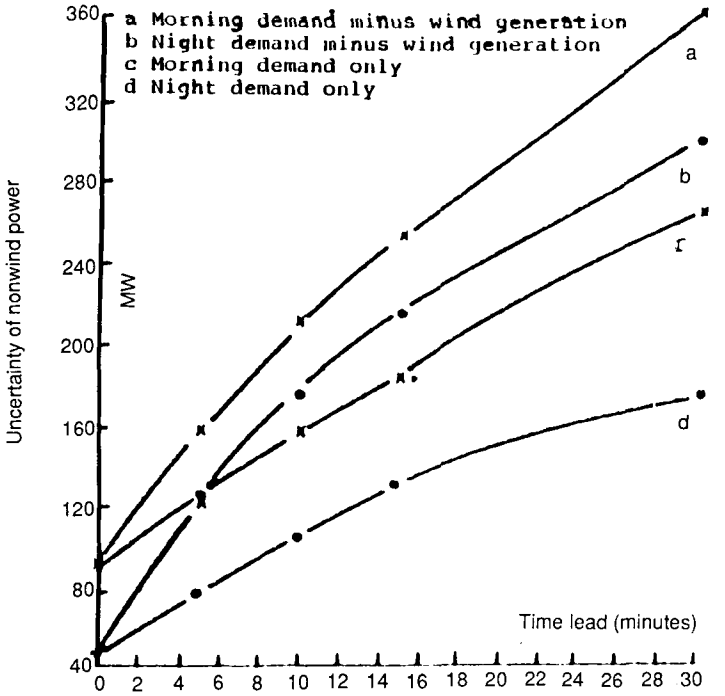


FIGURE 7.8 Uncertainty of nonwind generation due to demand and wind fluctuation. (From Farmer, E. D., Newman, V. G., and Ashmole, P. H., Economic and operational implications of a complex of wind-driven generators on a power system, *IEE Proc.*, 127 (A, No. 5), 289—295, 1980. With permission.)

## IX. PLANT SCHEDULING AND RESERVE ALLOCATION*

If a substantial number of aerogenerators are to be integrated into an existing power system, the variable output of the whole system on a span of a time duration from minutes to several hours would require an increase in the allocated spare capacity and in load meeting capability of the remaining power generators.

Effect of wind fluctuations on the uncertainty of the required nonwind generation as shown in Figure 7.8 as a function of lead time.

In Figure 7.8 a gigawatt wind generation is assumed and rms variation in the remaining plant is compared with that due to demand uncertainty over the same time scale, where it is shown that the assumed wind power component has significant, but not a dominant effect on the system reserve requirements.

Now we'll examine in some detail the aspect of influence of a substantial array of aerogenerators on the scheduling and reserve allocations of a predominantly thermal power system, in particular to pumped storage and gas turbines or other standby plants.

Consider an integrated power system comprised of five basic categories of power plants, namely, thermal-nuclear, wind-driven, thermal-steam, pumped-storage, and gas-turbine generators.

The scheduled capacity ($P_{reg}$) of regulating steam-driven generation at any time is expressed by

$$P_{reg} = P_L + S_g - P_B - P_W \tag{7.29}$$

* © 1980, IEE. Reprinted with permission from Farmer, E. D., Newman, V. G., and Ashmole, P. H., Economic and operational implications of a complex of wind-driven generators on a power system, *IEE Proc.*, 127 (A, No. 5), 289—295, 1980.

where $P_L$ represents predicted demand, $S_g$ is the scheduled reserve, $P_B$ is the expected base load generation, and $P_W$ is the estimated wind power output.

The scheduling error is the sum of load prediction error, thermal plant shortfall, and the deficit in wind-driven generation.

Consequently, the probability density of the scheduling error may be written in the form:

$$Z(P_e) = \int_{-\infty}^{\infty} Z_L(P - x)\, Z_w(x)\, dx \tag{7.30}$$

where $Z_L$ is the combined density function of the demand and thermal steam plant shortfall, and $Z_w$ is the deviation of wind power output from its expected value.

Equation 7.30 is associated with the practical assumption that errors in forecasting demand and wind are independent, and that correlation between unpredictable wind and temperature changes and cooling of buildings by the wind are negligible.

Variances $\sigma_s^2$ and $\sigma_w^2$ of the demand and wind output can add to give the total scheduling dispersion:

$$\sigma_e^2 = \sigma_s^2 + \sigma_w^2 \tag{7.31}$$

To assess the economics of the allocation of thermal reserve, the following costs may be defined. The total cost, per unit, of generation at the rated output on marginal steam plant is denoted by $C_A$, similarly, $C_B$, $C_P$, and $C_G$ represent the incremental cost on marginal steam plant, the effective cost of generation on pumped-storage units and gas-turbine generation cost, respectively.

If $S_p$ denotes the pumped-storage generation capacity that is available to meet unpredictable load and wind power variations, it may be shown that the cost of holding and utilizing spare capacity takes the form:

$$C_{spare} = S_s(C_A - C_B) + \theta_e(C_p - C_B)\, G\left(\frac{S_s}{\theta_e}\right) + \theta_e(C_G - C_P)\, G\left(\frac{S_s + S_p}{\theta_e}\right) \tag{7.32}$$

$$G(y) = \int_{y}^{\infty} (x - y)\, Z(x)\, dx \tag{7.33}$$

Next in this presentation is the calculation of steam reserve as a function of wind power dispersion shown in Figure 7.9. Dependence of steam reserve level on wind power dispersion indicates the accelerating value of pumped storage as in merit standby reserve as the proportion of wind energy increases.

The principal impact of wind-driven generation on the scheduling of steam plants is determined by the dispersion of the unpredictable wind power output over the period of several hours that is required to bring additional steam up to load.

Table 7.4 shows wind output dispersion against time.

Also Figure 7.10 presents a pattern for optimum steam reserve against rated wind power output.

From the preceding presentation, integration of aerogenerators into the grid of a power system requires the following evaluations:

1. Dynamical response of aerogenerating system.
2. Conservative response and effect of diversity of fluctuations on every machine.
3. Characteristics of aerogenerators and associated equipment.

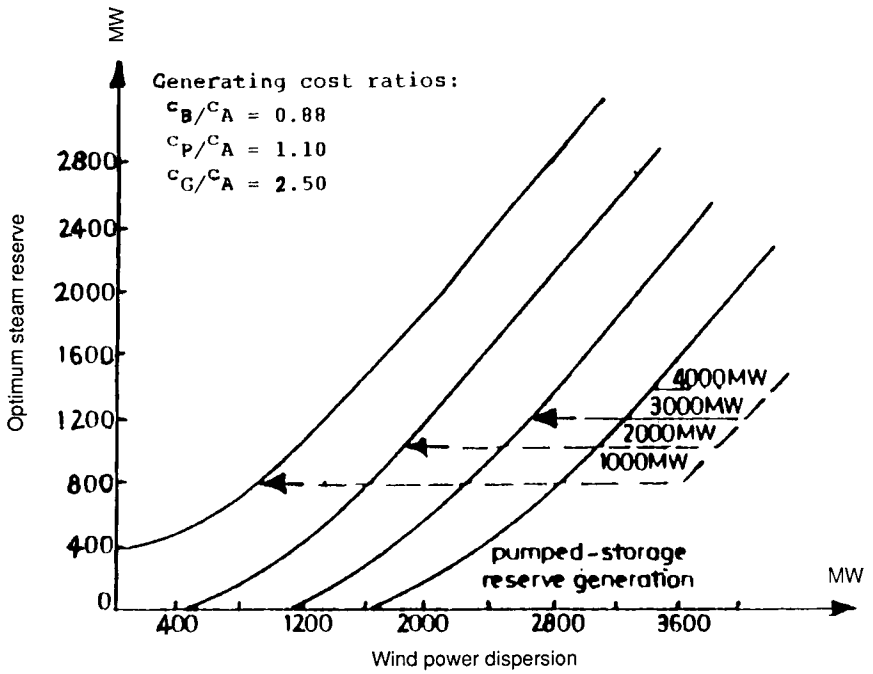


FIGURE 7.9 Showing optimum level of steam spare capacity against wind power dispersion. (From Farmer, E. D., Newman, V. G., and Ashmole, P. H., Economic and operational implications of a complex of wind-driven generators on a power system, *IEE Proc.*, 127 (A, No. 5), 289—295, 1980. With permission.)

**TABLE 7.4**
**Wind Output Dispersion Against Lead Time**

| Lead time | 0.5 | 1.0 | 2.0 | 3.0 | 6.0 | 12 | 18 |
|---|---|---|---|---|---|---|---|
| Dispersion/ rating ratio | 0.067 | 0.094 | 0.13 | 0.16 | 0.21 | 0.26 | 0.29 |

From Farmer, E. D., Newman, V. G., and Ashmole, P. H., Economic and operational implications of a complex of wind-driven generators on a power system, *IEE Proc.*, 127 (A, No. 5), 289—295, 1980. With permission.

4. Impacts of power output fluctuations of aerogenerators on the remaining power plants, including the economic worth of storage units, especially in light of increased dispersion of the generating uncertainty over the economic scheduling duration.
5. Economic impacts of wind energy production taking into account the need to increase reserve requirements.

## X. INCREMENTAL WIND ENERGY COST

To develop an approximate relationship for the incremental energy cost for aerogenerators, in terms of dollars per megawatt hour, we may use the pattern established in Figure 7.11 for model 204.0.

The cost of energy (COE) shown in Figure 7.3 could be piece-wisely linearized into two straight line functions as shown in Figure 7.11, expressing cents per kilowatt hour per unit length of rotor radius.

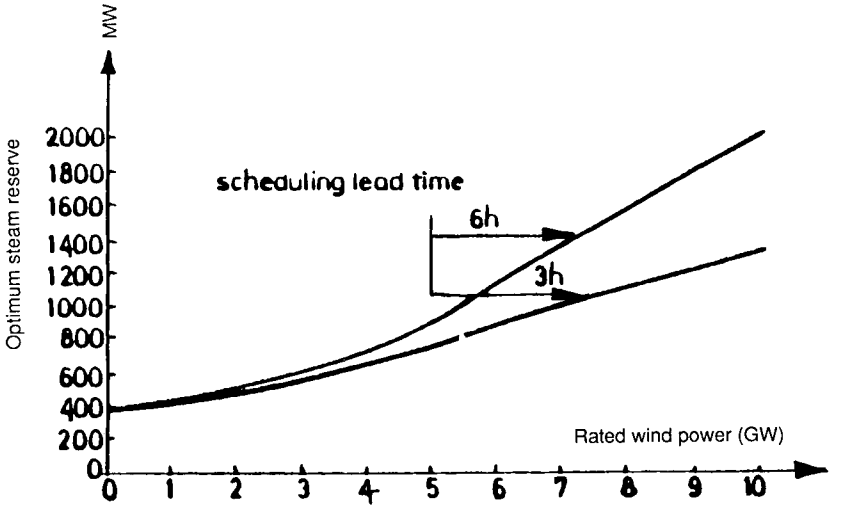


FIGURE 7.10 Optimum steam reserve against rated wind generation. (From Farmer, E. D., Newman, V. G., and Ashmole, P. H., Economic and operational implications of a complex of wind-driven generators on a power system, *IEE Proc.*, 127 (A, No. 5), 289—295, 1980. With permission.)

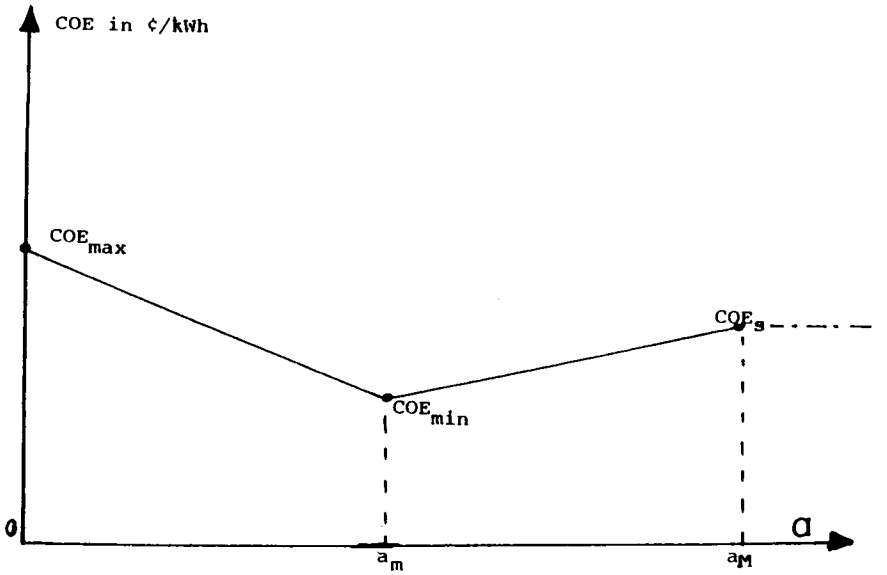


FIGURE 7.11 Incremental wind energy cost.

$$COE = k_1 a + K_2 \tag{7.34}$$

where $k_1$ and $k_2$ are constants. From Figure 7.11, and for $0 \leq a \leq a_m$:

when $a = 0, \quad COE = COE_{max}$

when $a = a_{m,} \quad COE = COE_{min}$ (7.35)

Hence, from Equations 7.35, we have $COE_{max} = k_2$, $COE_{min} = k_1 a_m + COE_{max} a_m$.

For $0 \le a \le a_m$:

$$COE = \frac{COE_{min} - COE_{max}}{a_m} a + COE_{max} \tag{7.36}$$

The other (COE) $\upsilon_s$, (a) function is for $a > a_m$ where for $a = a_m$, $COE = COE_{min}$ and when $a = a_M$, $COE = COE_s$, where $COE_s$ is the steady COE value.

If $COE = k_1 a + k'_2$, then

$$COE_{min} = k'_1 a_m + k'_2$$

$$COE_s = k'_1 a_M + k'_2 \tag{7.37}$$

Therefore, from Equation 7.37 we have

$$k'_1 = \left(COE_{min} - COE_s\right) \Big/ \left(a_m - a_M\right) \tag{7.38}$$

and

$$k'_2 = COE_s - \frac{COE_{min} - COE_s}{a_m - a_M} a_M \tag{7.39}$$

The second COE (a) function for $a > a_m$ by the following linear function is

$$COE = \left(\frac{COE_{min} - COE_s}{a_m - a_M}\right) a + \left(COE_s - \frac{COE_{min} - COE_s}{a_m - a_M}\right) a_M \tag{7.40}$$

Equations 7.36 and 7.40 represent the functional correlation between the COE and wind turbine radius in terms of two straight line functions.

The next step is to develop a functional form for the COE $\upsilon_s$ aerogenerator output power.

From Equation 7.21:

$$a = \left[\frac{2P}{\rho \pi \omega U^3 T\left(\frac{\omega a}{U}\right)}\right]^{\frac{1}{2}} \tag{7.41}$$

To simplify the mathematical correlation, let Equation 7.36 be written as

$$COE_1 = S_1 a + COE_{max} \tag{7.42}$$

and Equation 7.40 be written as

$$COE_2 = S_2 a + S_3 \tag{7.43}$$

Now from Equations 7.36, 7.40, and 7.41, the COE function $\upsilon_s P$ becomes

$$F_1 = COE_1 = S_1 \sqrt{\frac{2P}{\rho \pi \omega U^3 T\left(\frac{\omega a_m}{U}\right)}} + COE_{max} \tag{7.44}$$

$$F_2 = COE_2 = S_2 \sqrt{\frac{2P}{\rho \pi \omega U^3 T\left(\frac{\omega a_m}{U}\right)}} + S_3 \tag{7.45}$$

Therefore,

$$\frac{\partial F_1}{\partial P} = \frac{1}{2S_1}\left[\frac{2P}{\rho \pi \omega U^3 T\left(\frac{\omega a_m}{U}\right)}\right]^{-\frac{1}{2}}\left[\frac{2}{\rho \pi \omega U^2 T\left(\frac{\omega a_m}{U}\right)}\right]$$

$$\frac{1}{\sqrt{2}\, S_1} \frac{P^{-\frac{1}{2}}}{\sqrt[3]{\rho \pi \omega U^3 T\left(\frac{\omega a_m}{U}\right)}} = F_{11} \tag{7.46}$$

and

$$\frac{\partial F_2}{\partial P} = \frac{1}{\sqrt{2}\, S_2} \frac{P^{-\frac{1}{2}}}{\sqrt[3]{\rho \pi \omega U^3 T\left(\frac{\omega a_m}{U}\right)}} = F_{22} \tag{7.47}$$

In both Equations 7.46 and 7.47, the function

$$T\left(\frac{\omega a}{U}\right)$$

is assumed to be constant where $a \simeq a_m$, the mean radius.

A more simple expression for $(\partial F_1)/(\partial P)$ and $(\partial F_2)/(\partial P)$ could be obtained in reference to Equation 7.6 for $P_m = 0.25\ MaV_m$.

From Equation 7.4:

$$V = \frac{\omega R}{\alpha} \tag{7.48}$$

$$V_m = V_r \frac{2}{3} V \tag{7.49}$$

Therefore,

$$V_m = \frac{2}{3}\frac{\omega R}{\alpha}$$

where R = a in the preceding equations.

Hence

$$V_m = \frac{2}{3}\frac{\omega a}{\alpha} \tag{7.50}$$

and now

$$P_{i-w} = 0.25\ Ma\left(\frac{2}{3}\frac{\omega a}{\alpha}\right)^2$$

or

$$P_{i-w} = \frac{1}{9}m\left(\frac{\omega^2 a^2}{\gamma^2}\right) \tag{7.51}$$

and

$$a = \frac{3\gamma}{\omega}\sqrt{\frac{P}{Ma}} \tag{7.52}$$

Turning to Equations 7.42 and 7.43, we can state now:

$$F_1 = S_1\ \frac{3\gamma}{\omega}\sqrt{\frac{P}{ma}} + COE_{max} \tag{7.53}$$

$$F_2 = S_2\ \frac{3\gamma}{\omega}\sqrt{\frac{P}{ma}} + S_3 \tag{7.54}$$

and then:

$$\frac{\partial F_1}{\partial P} = \frac{3S_1\gamma}{2\omega}\sqrt{\frac{Ma}{P_{i-w}}} = F_{11} \tag{7.55}$$

$$\frac{\partial F_2}{\partial P} = \frac{3S_2\gamma}{2\omega}\sqrt{\frac{Ma}{P_{i-w}}} = F_{22} \tag{7.56}$$

It is interesting to observe the compatibility of the incremental energy cost between the set of Equations 7.46, 7.47 and 7.55, 7.56 where in both cases $\partial F/\partial P$ is proportional to $\sqrt{P}$.

## XI. INCREMENTAL ENERGY COST MULTIPLYING FACTORS

In order to use the tables of [B] matrices already given and calculated in Chapter 1, as invariant formations, and the corresponding [R] matrices given in Chapter 2, for various alternative energy systems, certain multiplying factors for the original incremental fuel cost curve must be identified.

Chapter 4, Equations 4.99 and 4.101 give the multiplying factor, k, for the slope of the incremental fuel cost curves which are $F_{11}$ and $F_{22}$ given by Equations 7.46, 7.47, and 7.55.

From Chapter 4, Equation 4.99:

$$k_1 = 1 - \frac{C}{A} \tag{7.57}$$

where A and C have been expressed in Chapter 4, Equations 4.90 and 4.91.

The second multiplying factor, $k_2$, is

$$k_2 = 1 + \frac{b'}{a'x} \tag{7.58}$$

where

$$x = F_{11} \quad \text{for} \quad 0 \le a \le a_m$$

and

$$x = F_{22} \quad \text{for} \quad a \ge a_m$$

Using the [B] matrices in Chapter 1, with the multiplying factor, $k_1$ or $k_2$, will set the stage for using the symmetric [R] matrices given in Chapter 2, leading to establishment of the corresponding [K] matrix for the particular integrated power system.

Elements of the [K] matrix form sequential equations from which the integrated system information for bus-bar voltage magnitudes, phase angles, real, and reactive powers could be calculated.

## XII. INTEGRATION OF AEROGENERATORS FARM IN DISPERSED SYSTEM

From Section 1.8 of Chapter 1, regarding a multiarea power system associated with tie power flow $P_T$ and network losses of $P_L$ where from Equation 1.32:

$$P_T = \frac{\sqrt{P_L}}{P_r} \tag{7.59}$$

and $P_r$ is the given received load.

In a linear array of N aerogenerators equally spaced with $x_s$ and having individual outputs of $P_1, P_2 \ldots P_n$ coupled with variance of outputs $\sigma^2$, the total contribution from the wind driven generators is expressed by:

$$P_{w-total} = \sum_{i=1}^{N} P_i + P_o^2 \sum_{i=1}^{N} \sum_{j=1}^{N} \exp\left(-x_s \left| i - j \right| / L\right) \tag{7.60}$$

In Chapter 1, Sections VIII and IX characteristic formulations had been presented with respect to the coordination Chapter 1, Equation 1.29 with the stipulation that $P_L = F(P_i, B_{ij}, P_j)$ and of course $P_T = G(P_i, B_{ij}, P_j)$.

Solution of the $[B_{ij}]$ matrix for the interconnected multiarea power system as presented in Chapter 1, Equation 1.50 is repeated as follows:

$$B'_{ij} = B_{ij}\left[1 + \frac{k}{2\sqrt{P_L}}\right] \tag{7.61}$$

where $B_{ij}$ is that for one area system given by Chapter 1, Equation 1.4 in this section. The specific function for $P_L$ to be supplied by the array of aerogenerators having a total variance output of:

$$\sigma^2 = P_o^2 \sum_{i=1}^{N} \sum_{j=1}^{N} \exp\left(-x_s |i-j| / L\right) \tag{7.62}$$

was given by Equation 7.60 which represents total power output from the aerogenerators array.

As indicated in Equation 7.27, for a large number of aerogenerators, $N \geq (L/X_s)$, where L is the integral length scale.

Equation 7.60 becomes

$$P_{w-total} = \sum_{i=1}^{N} P_i + N P_o^2 \coth \frac{x_s}{2L} \tag{7.63}$$

$$= P_L$$

Of course,

$$P_T = \left[ \sum_{i=1}^{N} P_i + N P_o^2 \coth \frac{x_s}{2L} \right]^{\frac{1}{2}} / P_r \tag{7.64}$$

From Equation 7.60, $B_{ij}$ becomes

$$B'_{ij} = B_{ij} \left[ 1 + \frac{k}{2 \sum_{i=1}^{N} P_i + N P_o^2 \coth \frac{x_s}{2L}} \right] \tag{7.65}$$

Also based on Chapter 1, Equation 1.31:

$$P_L = \sum_{i}^{N} \sum_{j}^{N} P_{w-i} B_{w-ij} P_{w-j} \tag{7.66}$$

where $P_{w-i}$ is the power output of the $i^{th}$ aerogenerator.

From Equations 7.62, 7.63, and 7.66:

$$\sum_{i=1}^{N} \sum_{j=1}^{N} P_{w-i} B_{w-ij} P_{w-j} = P_o^2 \sum_{i=1}^{N} \sum_{j=1}^{N} \exp\left(-x_s |i-j| / 2\right) + \sum_{i=1}^{N} P_{w-i} \tag{7.67}$$

And for a large N, Equation 7.67 becomes

$$= \sum_{i=1}^{N} P_{w-i} + N P_o^2 \coth \frac{x_s}{2L} \tag{7.68}$$

From either Equation 7.67 or Equation 7.68, knowledge of $P_L$ for a certain power system and total sum of power output from an array of N aerogenerators, we can set the basis of calculating the variance of a single aerogenerator, i.e., $P^2$.

Turning to the general coordination equation for multiarea power system, namely,

$$\frac{\partial F_i}{\partial P_i} + \lambda \frac{\partial P_L}{\partial P_i} + \lambda \frac{\partial P_T}{\partial P_i} = \lambda \tag{7.69}$$

and since

$$P_T = \frac{\sqrt{P_L}}{P_r} \tag{7.69}$$

Equation 7.69 becomes

$$\frac{\partial F_i}{\partial P_i} + \lambda \frac{\partial}{\partial P_i}\left(P_L + \frac{\sqrt{P_L}}{P_r}\right) = \lambda \tag{7.70}$$

In Equation 7.70, we proceed to substitute for

$$\frac{\partial F_i}{\partial P_i}$$

according to the set of Equations 7.46 and 7.47, and then Equations 7.55 and 7.56, and then for $P_L$ expression of Equations 7.67 and 7.68, whereby the solution for $\lambda$ would be secured.

## A. COORDINATION CONFINED TO AEROGENERATORS FARM

In the case of Equations 7.46 and 7.47 for

$$\frac{\partial F_i}{\partial P_i}$$

and Equation 7.67 with $P_L$ = total output variance:

$$\frac{1}{\sqrt{2}\, S_{1,2}} \frac{1}{\sqrt{P_{i-w}}} \frac{1}{\sqrt{\pi \rho \omega U^3 T\left(\frac{\omega a_m}{U}\right)}} + \lambda \frac{\partial}{\partial P_i}\left[P_o^2 \sum_{i=1}^{N} \sum_{j=1}^{N} \exp\left(-x_s \left|i - j\right| / L\right)\right] = \lambda \tag{7.71}$$

In the case of Equations 7.55 and 7.56 for

$$\frac{\partial F_i}{\partial P_i}$$

and Equation 7.68 with $P_L$ = total power variance:

$$\frac{3}{2} \frac{S_{1,2}\gamma}{\omega} \sqrt{\frac{M a}{P_{i-w}}} + \lambda \frac{\partial}{\partial P_i}\left[N P_o^2 \coth \frac{x_s}{2L}\right] = \lambda \tag{7.72}$$

Equations 7.70 and 7.71, rewritten as follows:

$$\frac{1}{\sqrt{2}\,S_{1,2}}\;\frac{1}{\sqrt{P_{i-w}}}\;\frac{1}{\sqrt[3]{\pi\rho\omega U^3 T\left(\frac{\omega a_m}{U}\right)}}+\lambda\frac{\partial P_o^2}{\partial P_i}\left[\sum_{i=1}^{N}\sum_{j=1}^{N}\exp\frac{\left(-x_s\,|i-j|/L\right)}{L}\right]=\lambda \tag{7.73}$$

or

$$\frac{3}{2}\;\frac{S_{1,2}\gamma}{\omega}\sqrt{\frac{M\,a}{P_{i-w}}}+\lambda N\coth\frac{x_s}{2L}\frac{\partial P_o^2}{\partial P_i}=\lambda \tag{7.74}$$

where $P_o^2$ is the output variance for a single wind driven or aerogenerator.

Of course, Equation 7.73 is valid for any value of $X_s$ and Equation 7.74 for a relatively large $X_s$. $X_s$ is the separation among aerogenerators.

## B. COORDINATION COVERS ENTIRE INTEGRATED SYSTEM

$F_i$ is the cost in dollars per hour for any generating plant and $P_i$ is the megawatt capacity of any generating plant.

In this case, we are letting $P_L$ = total power variance of the aerogenerating farm. Therefore, using Equation 7.70, with

$$P_L = P_o\sum_{i=1}^{N}\sum_{j=1}^{N}\exp\left(-x\,|i-j|/L\right)$$

and

$$\frac{\partial F_i}{\partial P_i}+\lambda\frac{\partial P_o^2}{\partial P_i}\sum_{i=1}^{N}\sum_{j=1}^{N}\exp\left(-x_s\,|i-j|/L\right)=\lambda \tag{7.75}$$

Equation 7.75 is valid for any $X_s$, or

$$\frac{\partial F_i}{\partial P_i}+\lambda\frac{\partial P_o^2}{\partial P_i}\coth\frac{x_s}{2L}=\lambda \tag{7.76}$$

Equation 7.76 is valid for large $X_s$.

Also both Equations 7.75 and 7.76 are based on the expression for total wind turbine generated power, $P_{i\text{-}w}$, given by Equation 7.60.

Or if we turn to use Equation 7.51 for the output power of a single aerogenerator, i.e.,

$$P_{i-w}+\frac{1}{9}\,Ma\frac{\omega^2a^2}{\gamma^2}$$

there is a certain variance power of $P^2$, Equations 7.75 and 7.76 become

$$\frac{\partial F_i}{\partial P_i}+\lambda\frac{\partial}{\partial P_i}\left[N\,P_o^2+\frac{N}{9}m_a\frac{\omega^2a^2}{\alpha^2}\right]=\lambda \tag{7.77}$$

Equation 7.77 reflects on the simplest form for the coordination of an integrated power grid system, where total transmission loss is being taken care of by an aerogenerator farm having a total power variance of N $P^2$ and no role for the separation among the aerogenerators.

We may conclude from Equations 7.74 and 7.75, two criteria for the cost of received power $\lambda$ in a system farm of aerogenerators, also known as Lagrange multiplier, a $-\lambda$ as any value of X:

$$\lambda = \frac{P_{i-w}^{-\frac{1}{2}} \left[ \pi \rho \omega U^3 T\left( \frac{\omega a_m}{U} \right) \right]^{\frac{1}{3}}}{\sqrt{2}\, S_{1,2} \left[ 1 - \frac{\partial P_o^2}{\partial P_i} \left( \sum_{i=1}^{N} \sum_{j=1}^{N} \bar{e}\, \frac{x_s |i-j|}{L} \right) \right]} \tag{7.78}$$

for large $X_s$:

$$\lambda = \frac{3}{2} \frac{S_{1,2} \gamma \sqrt{\frac{Ma}{P_{i-w}}}}{\left[ 1 - N \coth \frac{x_s}{2L} \frac{\partial P_o^2}{\partial P_i} \right]} \tag{7.79}$$

From Equation 7.79 $\lambda$ could attain minimum value under the condition:

$$\frac{\partial P_o^2}{\partial P_i} \left[ \coth \frac{x_s}{2L} \right] = 0 \tag{7.80}$$

which implies only the condition:

$$\frac{\partial P_o^2}{\partial P_i} = 0 \tag{7.81}$$

The condition stated in Equation 7.81 indicates first that when an aerogenerator is perfect in performance, meeting completely the expected generation at all loadings within the maximum capacity and hence having no variance,

$$P_o^2 = 0$$

The second implication from Equation 7.81 is that the variance of an individual aerogenerator is independent of any power source capacity within the integrated power system. Of course the second implication is more realistic and practical than the first one, and it represents a clear and beneficial economic reality, especially in the process of economic coordination for the scheduling of source power allocation. The same conclusion, could be drawn by inspecting Equation 7.78, where $\lambda$ is at its minimum when:

$$\frac{\partial P_o^2}{\partial P_i} \left[ \sum_{i=1}^{N} \sum_{j=1}^{N} \bar{e}\, \frac{x_s |i-j|}{L} \right] = 0 \tag{7.82}$$

Therefore, either,

$$\frac{\partial P_o^2}{\partial P_i} = 0$$

or

$$\sum_{i=1}^{N} \sum_{j=1}^{N} \bar{e} \frac{x_s|i-j|}{L} = 0 \tag{7.83}$$

Criterion in Equation 7.83 implies that $x_s >>> L$ ideally,

$$x_s/L \rightarrow \infty \tag{7.84}$$

Equation 7.83 points to a situation where aerogenerators scattered over very large distances, $X_s$, are much greater than the integral length, L.

## XIII. CASE STUDY

It is of real interest and an important contribution to the subject of WEC to obtain a solution of the parameters representing the three degrees of freedom of the wind-turbine generator.

This will be secured by solving the equations of motion given by Equations 7.18, 7.19, and 7.20 for $\theta$ in terms of $\zeta$, $\zeta$, and $\psi$, $\psi$.

### A. LINKAGE SOLUTION

The three parameters are $\theta$, $(\zeta_1 - \zeta_2)$, and $(\psi_1 - \psi_2)$. Or $\theta$, $\zeta$, and $\psi$ where $\zeta = \zeta_1 - \zeta_2$ and $\psi = (\psi_1 - \psi_2)$. The physical facts are that all of $\theta$, $(\zeta_1 - \zeta_2)$, and $(\psi_1 - \psi_2)$ are relatively small arguments and hence their sine and cosine can be approximated in terms of the argument itself by using the following approximations:

$$\sin x \approx x - \frac{x^3}{3!} + \frac{x^5}{5!} + \ldots \tag{a}$$

$$\cos x \approx 1 - \frac{x^2}{2!} + \frac{x^4}{4!} + \ldots \tag{b}$$

Now from Equation 7.18 with $\zeta_1 - \zeta_2 = \zeta$, we can write

$$M_t\ddot{\theta} - k_t\theta = -S \cos\psi\ddot{\zeta}$$

where

$$\cos\psi = 1 - \frac{\psi^2}{2} \tag{c}$$

Therefore, Equation c becomes

$$M_t\ddot{\theta} - K_t\theta = -\frac{S}{2} \psi^2\ddot{\zeta} \tag{d}$$

From Equations 7.19 and 7.20:

$$\cos\left(\psi+\zeta_1\right)-\frac{I+k_\zeta}{S\ddot{\theta}}\zeta_1\approx 1-\frac{1}{2}\left(\psi+\zeta_1\right)^2 \tag{e}$$

and

$$\cos\left(\psi+\zeta_2\right)1-\frac{1}{2}\left(\psi+\zeta_2\right)^2=\frac{I+k_1}{S\ddot{\theta}}\zeta_2 \tag{f}$$

where $\psi=\psi_1-\psi_2$.

Therefore, from Equations e and f:

$$\psi=\sqrt{2}\left[1-\frac{1}{2}\zeta_2\left(I+k_\zeta\right)-\zeta_2\right] \tag{g}$$

$$=\sqrt{2}\left[1-\frac{1}{2}\zeta_1\left(I+k_\zeta\right)-\zeta_1\right] \tag{h}$$

From Equations g and h:

$$\zeta=\zeta_1-\zeta_2=\frac{1}{2}\ \frac{I+k_\zeta}{\theta}\ \left(\zeta_2+\zeta_1\right) \tag{i}$$

Therefore,

$$\psi=\zeta\left[\frac{I+k_\zeta}{2\ddot{\theta}}-\frac{2\ddot{\theta}}{I+k_\zeta}\right]\frac{1}{\sqrt{2}} \tag{j}$$

Returning to the Equation e:

$$M_t\ddot{\theta}-k_\zeta\theta\approx-\frac{1}{8}S\left(I+k_\zeta\right)\left[\frac{1}{\ddot{\theta}}-\frac{(2)^2}{I+k_\zeta}\ddot{\theta}\right]\dot{\zeta}\zeta^2 \tag{k}$$

or

$$\ddot{\zeta}\zeta^2=-\frac{8}{S}\ \frac{1}{I+k_\zeta}\left[\frac{M_{t\theta}-k_{\zeta\theta}}{\ddot{\theta}^2-\left(\frac{2}{I+k_\zeta}\right)^2\ddot{\theta}}\right] \tag{l}$$

$$=-\frac{8}{S}\frac{1}{I+k_\zeta}\left[M_{t\ddot{\theta}}{}^3+\frac{2^2}{\left(I+k_\zeta\right)^2}\ddot{\theta}^6\right] \tag{m}$$

From Equation m:

$$\frac{\partial^2\theta}{\partial t^2} \approx k_1 \pm \frac{k_2}{2A}\left[B^2 M_t^2 + 4A_\zeta^3 - 24A\zeta\dot{\zeta}\right] \tag{n}$$

where

$$A = \left(\frac{2}{I+k}\right)^2, \qquad B = -\frac{8}{S}\,\frac{1}{I+k_\zeta} \tag{o}$$

$$k_1 = -\left(\frac{BM_t}{2A}\right)^{-\frac{1}{3}}$$

$$k_2 = \frac{1}{3}\left(\frac{BM_t}{2A}\right)^{-\frac{2}{3}} \tag{p}$$

Equation n provides correlation between $\partial^2\theta/\partial t^2$ with respect to $\zeta$ and $\partial\zeta/\partial t$, while Equation j provides linkage between $\psi$ with respect to $\zeta$,

$$\frac{\partial\zeta}{\partial t} \quad \text{and} \quad \frac{\partial^2\theta}{\partial t^2}$$

Therefore the linkage solution presented interconnection between,

$$\frac{\partial^2\theta}{\partial t^2} \rightarrow \zeta, \qquad \frac{\partial\zeta}{\partial t}$$

$$\text{and} \quad \frac{\partial^2\theta}{\partial t^2} \rightarrow \psi, \qquad \frac{\partial\psi}{\partial t}$$

Absolute solutions for $\theta$ in terms of $\zeta$ and $\psi$ will be left as problems to be solved by the student.

## XIV. SUMMARY

In this chapter, the concept of a wind-driven turbine generator has been presented systematically and gradually from the basic character of wind velocity, the annual turbine rotor speed, rotor orientation, and height, as well as the annual average wind speed. Expressions have been presented for the wind power density as well as wind speed at any rotor height with respect to a reference speed at 10 m height. Conceptual introduction has been given for the tip speed ratio and the power output of the turbine relative to a case of unimpeded flow of wind.

Also, mathematical modeling for sequential wind boundary layers has been presented in terms of speed at 10 and 20 m, the free stream airflow, as well as limitation of wind speed at layers of discontinuity and asymptotic orientations.

Dynamic modeling of wind-driven turbines is also introduced in terms of lead-lag angle, a zimuthial orientation, and linear motion of tower head. Expressions for the turbine kinetic

and potential energies have been presented in a set for the equations of motion for a model of three degrees of freedom.

Characterization of a wind-driven turbine that had been designed by the General Electric Advanced Energy Program under DOE/NASA sponsorship identified economical based information for the capital cost and cost of energy with respect to rotor diameter which set a reliable tool to develop the corresponding mathematic model.

Aspects for the dynamic response of aerogenerator in conjunction with induction and synchronous machines have been presented with the formulation of power output in terms of rotor radius, wind speed, angular velocity of rotor, air density, and an implicit function characteristic of those parameters.

The Introduction (Section I) in this chapter proceeded to cover total power output of aerogenerators farm comprising a number of wind turbines separated by a certain distance, with each aerogenerator associated with a certain power output variance as well as a total variance for the entire farm system.

Further subject matter covered is the energy cost multiplying factor for the purpose of invariant [B] matrices which already had been calculated in Chapter 1 and their corresponding [R] matrices also presented in Chapter 2. Using the conventional coordination equation for a multiarea power system and the developed incremental energy cost for aerogenerators in a farm system, useful correlations have been established whereby a wind-turbine farm output will supply the expected losses in an integrated large power system. And finally, useful implication has been derived whereby the cost of received power in an aerogenerator farm could be minimized.

## XV. PROBLEMS

7.1 The case study in this chapter presented a simplified linkage solution for $\theta$ in terms of $\zeta$ and $\dot{\zeta}$. Obtain a similar solution in terms of $\psi$ and $\dot{\psi}$.

7.2 Convert the linkage solution for $\ddot{\theta}$ to that for $\dot{\theta}$, and then for $\theta$ in terms of $\zeta$, and $\dot{\zeta}$, and then in terms of $\psi$ and $\dot{\psi}$.

7.3 Based on the linkage solution for $\theta$ established in Problem 7.2, express new forms for the total kinetic energy and potential energy of the wind-turbine generator in three degrees of freedom.

7.4 The set of equations of motion for the wind-turbine generator given in Equations 7.18, 7.19, and 7.20 represents partial differential equations with variable coefficients. Establish from this set a new canonical set of equations as the first step to obtain absolute solution for $\theta$ in terms of $\zeta$ and $\psi$. Hint: the procedure for forming the canonical set of partial differential equations and eventual solution can be found in Chapter 2 of the book entitled *Partial Differential Equations* by P. R. Garabedian, John Wiley & Sons, New York, 1964.

7.5 From the set of canonical equations established in Problem 7.4, secure a solution for $\theta$ as a function of $\zeta$ and $\psi$. All initial conditions assumed equal to zero.

7.6 The increment cost of energy multiplying factors for aerogenerators for the purpose of using invariant [B] matrices that are given in Chapter 1 have been expressed in generalized form in Equations 7.57 and 7.58. Using Equation 7.21, and then 7.51, obtain expressions for the multiplying factor in terms of aerogenerators output power.

7.7 Equation 7.67 relates to a wind-driven turbine generator where the entire output of an aerogenerators farm supplies transmission loss for a larger power grid system. Obtain an expression for $B_{w\text{-}ij}$ matrix in terms of aerogenerators separation and their output power.

7.8 Using the results of the [B] matrix secured in Problem 7.7, then using Equation 7.65, obtain an expression for $[B_{ij}]$ for a multiarea power system with tie power flow and transmission loss.

7.9 An aerogenerator farm contains eight units having total peak generation of 2000 MW and specified optimal scheduling of generation given below in megawatts.

| $P_1$ | $P_2$ | $P_3$ | $P_4$ | $P_5$ | $P_6$ | $P_7$ | $P_8$ |
|---|---|---|---|---|---|---|---|
| 260 | 210 | 270 | 420 | 310 | 240 | 110 | 180 |

Incremental energy cost is expressed by Equation 7.55 where $a \leq a_m$, $a_m = 60$ m, $S_1 = -0.036$, $S_2 = 0.29$, $= 6$, and $V_m = 5.5$ m/s. Using Chapter 1, Equation 1.4, calculate all elements of the [B] matrix for the aerogenerators farm.

7.10 Repeat Problem 7.9 for $a \geq a_m$ and $a_m = 84$ m, i.e., $60 \leq a \leq 84$.

7.11 Repeat Problem 7.9 for 67% total generation and specified optimal scheduling of generation given as follows in megawatts:

| $P_1$ | $P_2$ | $P_3$ | $P_4$ | $P_5$ | $P_6$ | $P_7$ | $P_8$ |
|---|---|---|---|---|---|---|---|
| 145 | 210 | 75 | 285 | 310 | 150 | 75 | 85 |

Let $a \leq a_m$.

7.12 Repeat Problem 7.10 for 67% of total peak generation and specified optimal scheduling of generation given as follows in megawatts:

| $P_1$ | $P_2$ | $P_3$ | $P_4$ | $P_5$ | $P_6$ | $P_7$ | $P_8$ |
|---|---|---|---|---|---|---|---|
| 145 | 210 | 75 | 285 | 310 | 150 | 75 | 85 |

Let $a \geq a_m$.

7.13 Repeat Problem 7.9 for 41% of peak generation and specified optimal scheduling of generation given as follows in megawatts:

| $P_1$ | $P_2$ | $P_3$ | $P_4$ | $P_5$ | $P_6$ | $P_7$ | $P_8$ |
|---|---|---|---|---|---|---|---|
| 45 | 210 | −100 | 160 | 310 | 80 | 45 | 60 |

Let $a \geq a_m$.

7.14 Repeat Problem 7.10 for 41% of peak generation and specified optimal scheduling of generation given as follows in megawatts:

| $P_1$ | $P_2$ | $P_3$ | $P_4$ | $P_5$ | $P_6$ | $P_7$ | $P_8$ |
|---|---|---|---|---|---|---|---|
| 45 | 210 | −100 | 100 | 310 | 80 | 45 | 60 |

Let $a \geq a_m$.

7.15 Assume an aerogenerator farm of eight units having individual peak capacities as indicated below. The aerogenerator system supplies load complexes in close proximity to it such that $P_L = 0$. Having energy cost data as those presented in Problem 7.9, find out the optimal scheduling of generation for each aerogenerator using Chapter 1, Equation 1.4. $B_{ij} = 0$.

**Peak Capacity in megawatts (MW)**

| $P_1$ | $P_2$ | $P_3$ | $P_4$ | $P_5$ | $P_6$ | $P_7$ | $P_8$ |
|---|---|---|---|---|---|---|---|
| 260 | 210 | 270 | 420 | 310 | 240 | 110 | 180 |

Use iteration procedure to secure optimal scheduling of generation.

7.16 Repeat Problem 7.15, but for a total generation of 1340 MW which is 67% of a total system capacity of 2000 MW.

7.17 Repeat Problem 7.15, but for a total generation of 820 MW which is 41% of a system of 2000 MW.

7.18 Obtain two forms for incremental cost of energy for an aerogenerator based on a wind speed probabilistic measure above $V_m$. Hint: use Equation 7.1 in connection with Equations 7.21 and 7.50.

7.19 Obtain the incremental cost of energy for a wind-driven turbine at a wind boundary laser of 10 m, and then at 20 m height.

7.20 Obtain the incremental cost of energy for a wind-driven turbine based on the transition situation between land and sea. Hint: use Equations 7.13 and 7.14 in connection with the appropriate power output equations expressed in this chapter.

7.21 Using the expression for the incremental cost of energy obtained in Problem 7.18, secure a solution for the cost of received power in dollars per megawatt hour when the total output of the aerogenerator farm is used to meet total transmission loss for a grid power system. Show the possibility of minimum condition for $\lambda$.

7.22 Apply the statement of Problem 7.21 with respect to the incremental cost of energy expression established in Problem 7.19.

7.23 Apply the statement of Problem 7.21 with respect to the incremental cost of energy expression established in Problem 7.20.

7.24 Revise expressions for the incremental cost of energy for aerogenerators shown in Equations 7.45 and 7.46 as functions of rotor height.

7.25 Repeat Problem 7.24 with respect to Equations 7.54 and 7.55. Show probabilistic basis for minimizing the incremental cost of energy refer to Figure 7.1 showing a spider diagram for relative cost of electricity produced by a wind-driven turbine generator with respect to parameter variation that was published by the BWFA. Approximate each graph into a piecewise linearized function and then develop the following relationships:

a. RCOE vs. C/W
b. RCOE vs. r
c. RCOE vs. M
d. RCOE vs. n
e. RCOE vs. a
f. RCOE vs. A
g. RCOE vs. $V_m$

where RCOE = relative cost of electricity.

7.26 Using the mathematical functions developed in Problem 7.26, establish a generalized function for RCOE vs. C/W, r, M, n, a, A, and $V_m$.

7.27 Carry out a successive optimization procedure on RCOE = C/W, r, M, n, a, A, and $V_m$ to obtain the optimal condition of RCOE for the following cases:

a. C/W r, M, n, and a are all constants and A and $V_m$ are the two independent variables.
b. C/W, r, M, a, and $V_m$ are all constants and a,n are the two independent variables.

7.28 Continue Problem 7.28 for the following cases:

c. C/W n, a, A, and $V_m$ are all constants and r and M, the two independent variables.
d. r, m, N, A, and a, are all constants and C/W ard r, the two independent variables.

7.29 For the function RCOE of C/W r, M, n, a, A, $V_m$, carry out the total optimization process on RCOE with respect to every one of the seven independent variables. Then assuming that the

$$\frac{\partial^2 \text{RCOE}}{\partial \dfrac{C}{W},\ r,\ M,\ n,\ a,\ A,\ V_m}$$

is linearly independent, establish a set of functional conditions for the optimal cost of a wind-driven turbine generator.

## REFERENCES


1. **Barton, R. S. and Lucas, W. C.,** Development of the 7.3 MW MOD-5A wind-turbine generator system, *IEE Proc.*, 130 (A, No. 9), 537, 1983.
2. **Bennett, M., Hamilton, P. M., and Moore, D. J.,** Estimation of low-level winds from upper-air data, *IEE Proc.*, 130 (A), 517, 1983.
3. **Farmer, E. D., Newman, V. G., and Ashmole, P. H.,** Economic and operational implications of a complex of wind-driven generators on a power system, *IEE Proc.*, 127 (A, No. 5), 289, 1980.
4. **Garrad, A. D.,** Dynamics of wind turbines, *IEE Proc.*, 130 (A, No. 9), 523, 1983.
5. **Musgrove, P. J.,** Wind energy conversion — an introduction, *IEE Proc.*, 130 (A, No. 9), 506, 1983.
6. **Swift-Hook, D. T.,** Wind energy — it's the cheapest, *IEE Rev.*, 34 (No. 1), 30, 1988.

Chapter 8

# THE ECONOMICS OF TIDAL WAVE ENERGY CONVERSION SYSTEMS (TWEC)

## I. INTRODUCTION

This source of energy, generated by the ebb and crest motion of seawater on shorelines, is produced by the combination of gravitation forces of earth, the moon, and the sun, together with the associative effects of water viscosity, nature of shorelines, as well as secondary contributions from big rivers flowing in major sea lanes. Major tidal waves occur twice daily due to the influence of the moon rotation around the Earth every 24 h and 50 min. Coordination between tidal wave phenomenon at a certain potential location and hydroelectric power generation could produce a highly competitive cost of electricity. During tidal crest period, a substantial water head could be built and operate a hydroelectric power plant in the same area.

In the U.K., research and development work[1-3] indicates that tidal wave energy conversion could produce up to 90 kW/m of wave front such that total generation over 1000 km and at 25% efficiency, total production may approach 20 GWe.

Major efforts in research and development in the area of tidal power are being carried out in the U.K., Norway, Sweden, Finland, U.S., and Japan. Data being sought covers wave analysis, structural design loading, moorings, generation and transmission, environmental effects, and wave energy stability, as well as control and dynamics. During stormy conditions, wave power may reach a level of 25 times that of mean annual level, while on a normal, quiet day that may extend up to 10 d, virtually no significant wave power will be available.

Harnessing wave energy could be feasibly secured through either device installation on or near shorelines or partially or totally submerged installations at the bottom of oceanic regions.

On the shore-based system, studies in the U.K.[1-3] reviewed the structure of the hydraulic research station "rectifier", where the cyclic flow of water level variation leads to a steady difference of water level in two reservoirs that can drive a low-head turbine located between them. This is shown in Figure 8.1.

The deep water system is categorized in operation through large rocking structural members or by relying on moving columns of water within the main submerged system.

Other deep water systems mentioned in the paper by Glendenning[2] are the salter duck shown in Figure 8.2 and the Rafts shown in Figure 8.3.

## II. TWEC ECONOMICS*

Costs of generation reported in the paper by Glendenning[2] ranges from 4 to 30 ¢/kWh. These costs are based on the expected capital costs of each system, lifespan, and allowance for repair and maintenance, divided by the expected energy output.

Factors affecting the production cost of TWEC are summarized as follows:

1. Directionality factor ($W_d$) of 0.5 to 0.8 based on the fact that wave energy arrives from different directions.
2. Device efficiency factor ($W_e$) of 0.3 to 0.6 which accounts for the random wave energy distribution over wide range of frequencies.
3. Power conversion and distribution factor ($W_p$) of 0.4 to 0.6 which accounts for the effects of off-design operation as well as component losses and secondary power requirements.

* 

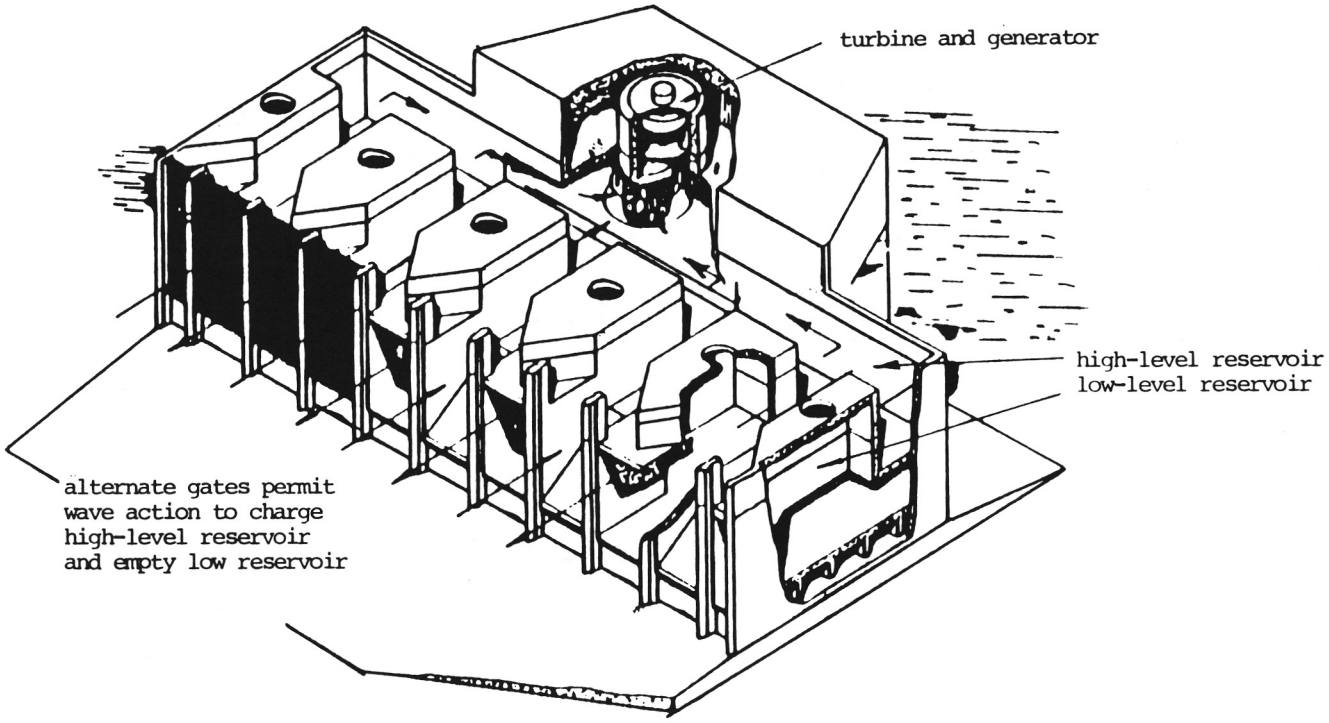


FIGURE 8.1 Hydraulics research station "rectifier". (From Glendenning, I., Wave energy, *IEE Proc.*, 127 (A, No. 5), 301—307, 1980. With permission.

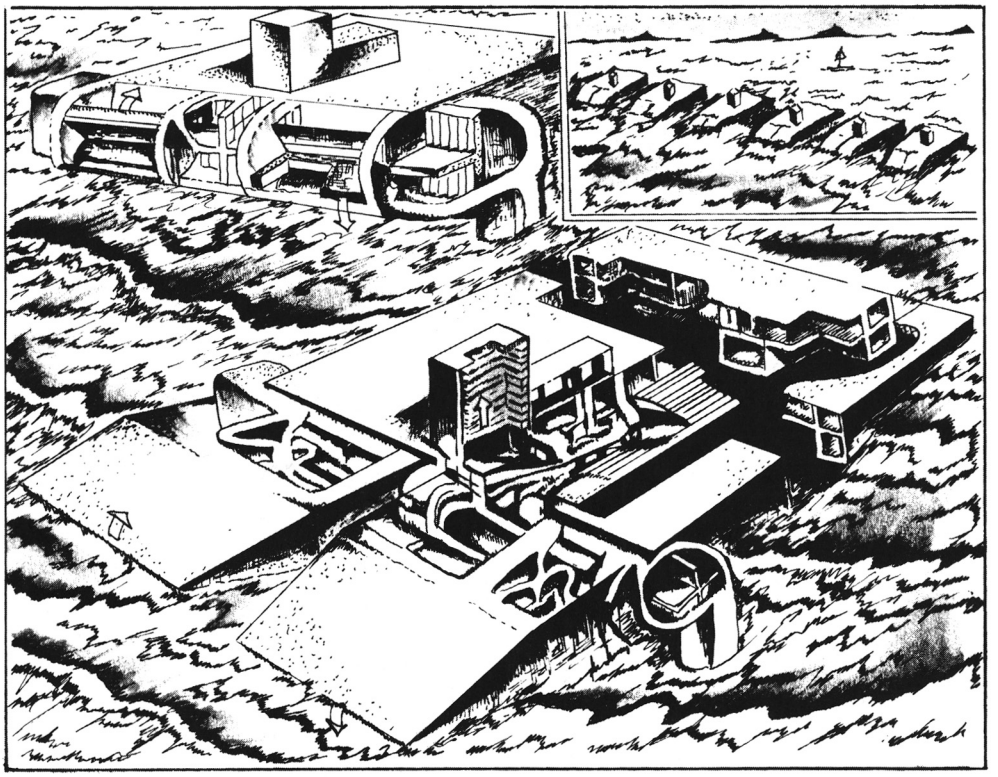

FIGURE 8.2 Wave contouring raft. (From Glendenning, I., Wave energy, *IEE Proc.*, 127 (A, No. 5), 301—307, 1980. With permission.)

4. Annual average availability factor ($W_a$) of 0.1 to 0.25 which accounts for output availability of wave energy.
5. Practical site availability factor ($W_s$) of 0.5 to 0.8 which accounts for effects of shipping and mooring.

The Glendenning paper reported that on a base of 50 kW/m average wave energy measured at 1000 km of U.K. coastline, wave energy expected output is ≤ 60 to 70 trillion Wh/year. Hence the overall efficiency factor

$$W_o = W_d W_e W_a W_s W_p \tag{8.1}$$

The Glendenning paper[2] presented the following future prospects for TWEC systems:

1. All device types are potentially equally efficient; they are distinguished by cost and engineering feasibility.
2. Access for maintenance and simple systems are essential; maintenance and loss of output can more than double the energy cost in the extreme case.
3. The most credible devices are those which employ air turbine power take off. These also tend to be very bulky though not especially expensive to build.
4. Device size and cost may be reduced by employing the spine principle to achieve stability. Gains in efficiency usually also result, and on the evidence of the Loch Ness trials, mooring loads are substantially reduced.
5. The resource size is greatest for offshore devices working in deep water and for devices which are aligned across the waves with a minimum of spacing.

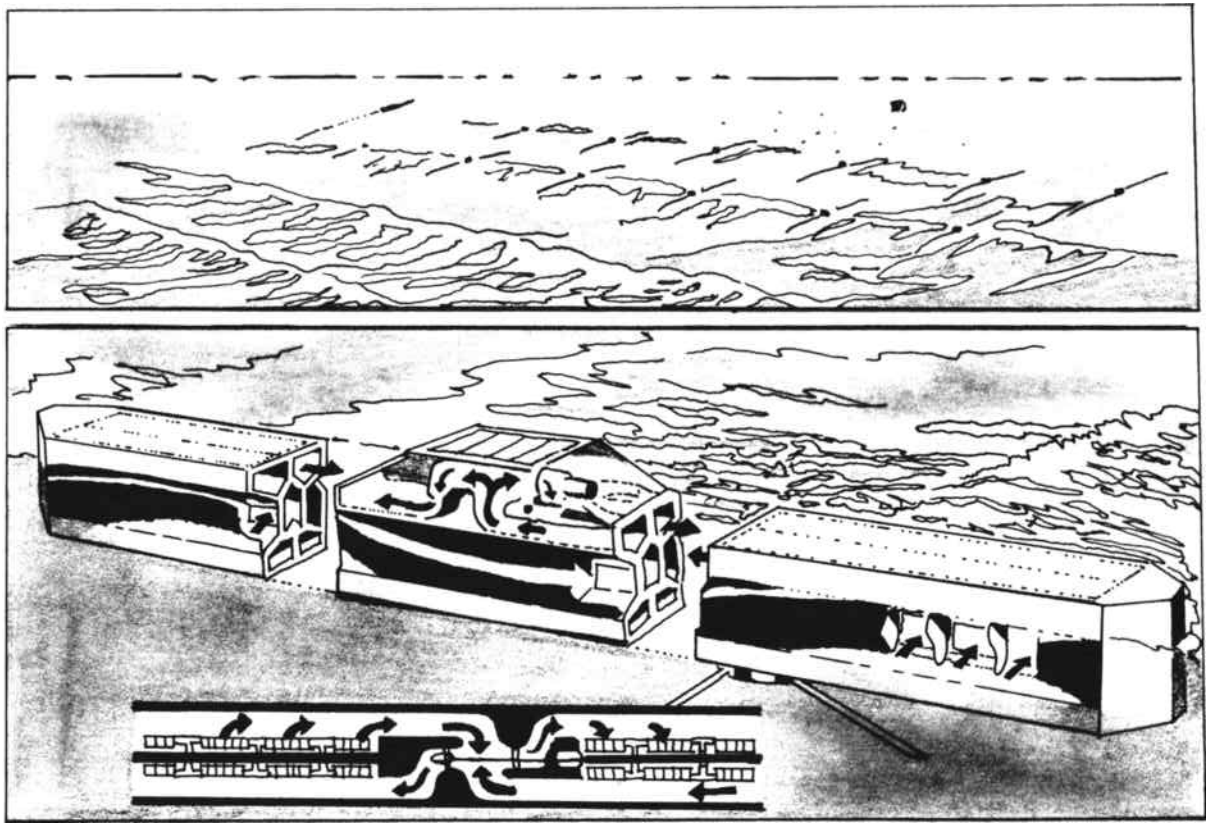

FIGURE 8.3 French floating air bag developed by Lancaster University, France. (From Glendenning, I., Wave energy, *IEE Proc.*, 127 (A, No. 5), 301—307, 1980. With permission.)

**TABLE 8.1**
**Failure Rates and Repair Times for Components of a Typical Wave Energy System**

| Group | Location | Component | Average failure rate (fails/year) | Average repair time (h) |
|---|---|---|---|---|
| 1 | Wave energy device | All mechanical components up to generator shaft | 0.25 | 144 |
| | | generator | 0.20 | 144 |
| | | switchboard | 0.01 | 144 |
| | | transformer | 0.02 | 144 |
| 2 | Seabed | AC flexible cables (unburied) | 2/100 km/year | 1000 |
| 3 | Off shore platform | Rectiformer unit | 0.02 | 48 |
| | | vital auxiliary equipment affecting complete platform output | 0.05 | 240 |
| 4 | Seabed | DC cables/set | | |
| | | buried | 0.3/100 km/year | 2000 |
| | | unburied | 2/100 km/year | 1000 |
| 5 | Mainland | High voltage DC transmission line | 1/100 km/year | 48 |
| 6 | Inverter station | Inverter pole | 6 | 30 |

From Dawson, J. M., Mytton, N. L., Shore, N. L., and Stansfield, H. B., System-reliability studies for wave energy generation, *IEE Proc.*, 127 (A, No. 5), 296—300, 1980. With permission.

## III. RELIABILITY MODEL OF TWEC*

This model as presented in a paper by Dawson, et al.,[1] and considers that TWEC components reside in a regime of operation and in another through a state of failure, whereby the system output depends on the input and the reliable condition of its components.

Let $\lambda$ represent the rate of failure, $\mu$ represent the rate of repair, Q represent the probability of a component being in service, and $\rho$ represent the probability of a component being failed.

Under steady state conditions:

$$Q = \frac{\mu}{\lambda + \mu} \tag{8.2}$$

$$P = \frac{\lambda}{\lambda + \mu} \tag{8.3}$$

Table 1 illustrates failure rates and repair times for components of a typical wave energy system.

Figures 8.4, 8.5, and 8.6, also from the same source mentioned in Reference 1, illustrate useful information for reliability aspects of a TWEC system.

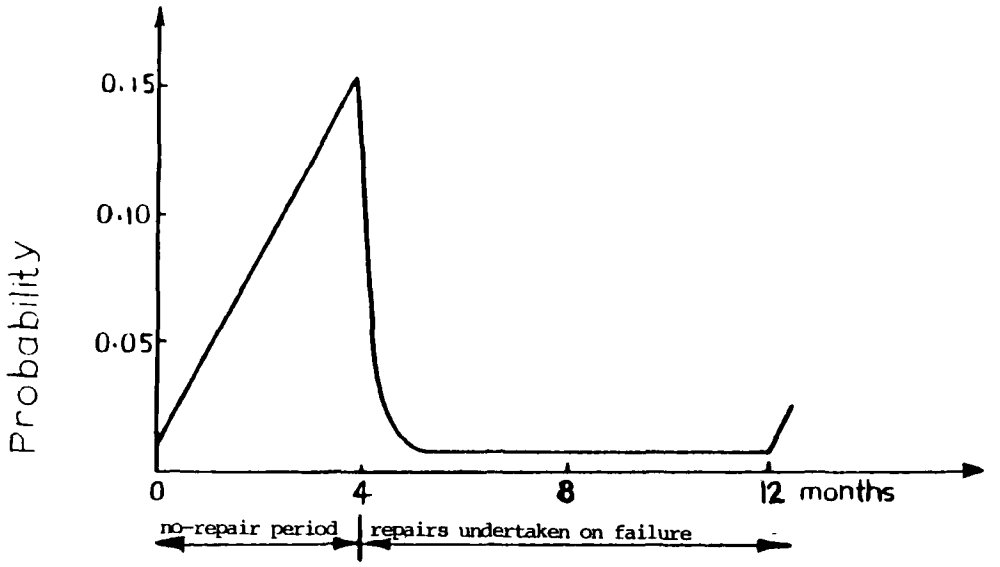


FIGURE 8.4 Probability that a device is not functioning. (From Dawson, J. M., Mytton, N. L., Shore, N. L., and Stansfield, H. B., System-reliability studies for wave energy generation, *IEE Proc.*, 127 (A, No. 5), 296—300, 1980. With permission.)

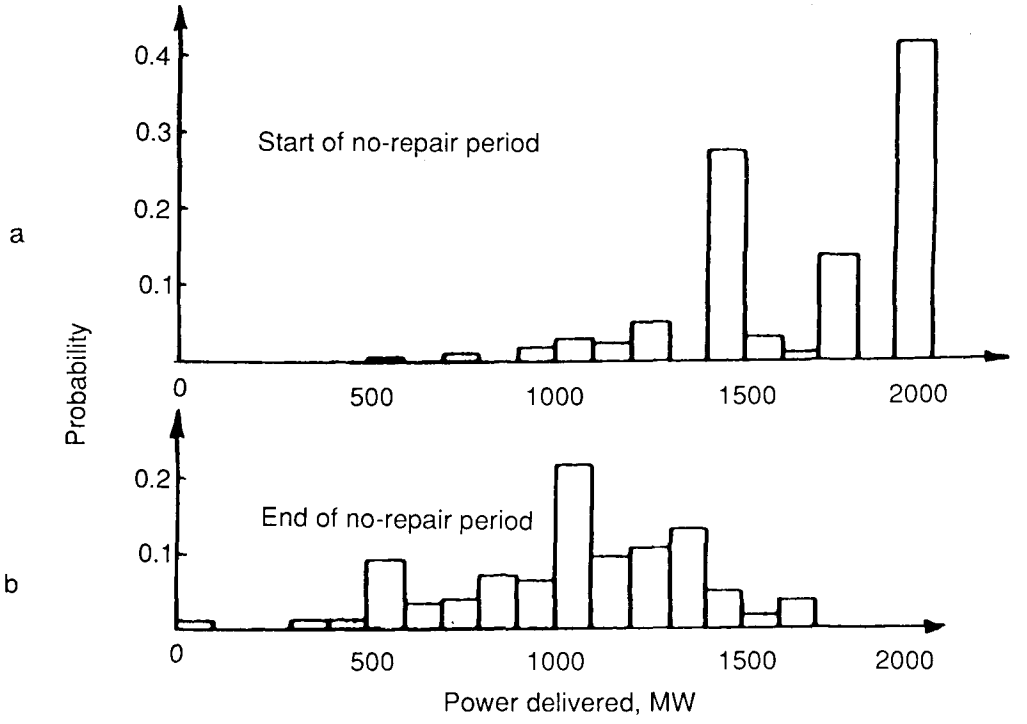


FIGURE 8.5 Probability distribution of power delivered assuming that 2 GW would be available if all components in the system were functioning. (From Dawson, J. M., Mytton, N. L., Shore, N. L., and Stansfield, H. B., System-reliability studies for wave energy generation, *IEE Proc.*, 127 (A, No. 5), 296—300, 1980. With permission.)

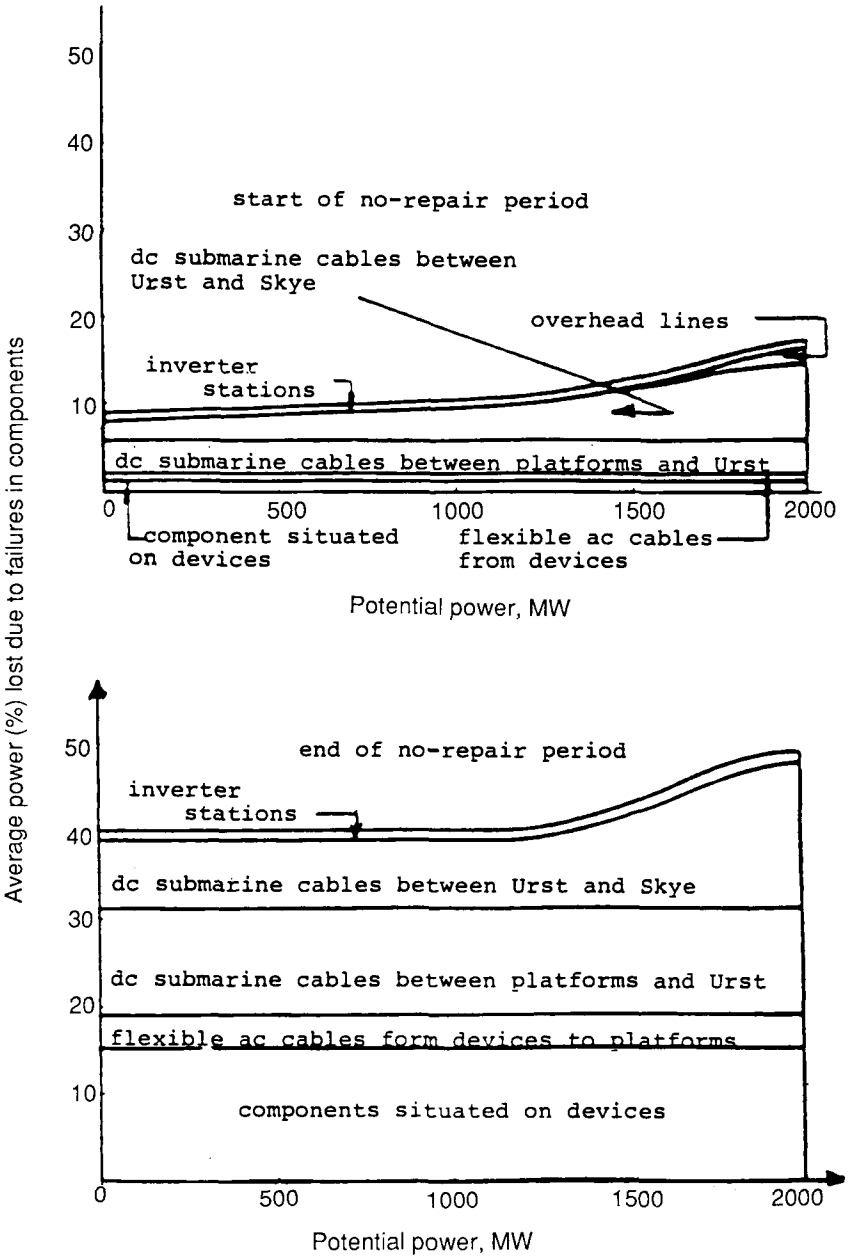


FIGURE 8.6 Average power lost in various components of the system under different load conditions. (From Dawson, J. M., Mytton, N. L., Shore, N. L., and Stansfield, H. B., System-reliability studies for wave energy generation, *IEE Proc.*, 127 (A, No. 5), 296—300, 1980. With permission.)

## IV. ENERGY OF TIDAL WAVE*

In one-dimension along the shoreline let x represent variable along the shoreline and y represent the variable perpendicular to shoreline.

* © 1980, IEE. Reprinted with permission from Dawson, J. M., Mytton, N. L., Shore, N. L., and Stansfield, H. B., System-reliability studies for wave energy generation, *IEE Proc.*, 127 (A, No. 5), 296—300, 1980.

At a free surface, let point x at time t be denoted by $Y_o + \eta$ where $Y_o$ is the ordinate in the undisturbed state.

Neglecting acceleration of ocean water particles, the pressure differential at any point (x,y) is expressed by:

$$\Delta P = g\rho(Y_o + \eta - Y) \tag{8.4}$$

Now we define

$$\xi = \int U\, dt \tag{8.5}$$

where u is the wave velocity parallel to shoreline and g is the gravitational factor.

The potential energy of tidal wave due to elevation or depression above or below the mean level is expressed by:

$$W_p = \frac{1}{2} g\rho \int \eta^2 dx \tag{8.6}$$

While the kinetic energy $W_p$ is expressed by:

$$W_k = \frac{1}{2} \rho h \int \xi^2 dx \tag{8.7}$$

A tidal wave assumed to be advancing toward the shoreline according to a simple harmonic motion has the solutions given by:

$$\zeta = \frac{2f}{\sigma^2 \cos\left(\frac{\sigma l}{2c}\right)} \sin\frac{\sigma X}{2c} \sin\frac{\sigma(l-x)}{2c} \cos(\sigma l + \varepsilon) \tag{8.8}$$

$$\eta = \frac{hf}{\sigma C \cos\left(\frac{\sigma l}{2C}\right)} \sin\frac{\sigma X - \frac{l}{2}}{C} \cos(\sigma l + \varepsilon) \tag{8.9}$$

where

$$C = \sqrt{gh}$$

$$X = f\cos(\sigma l + E) \tag{8.10}$$

X is the sinusoidal force attributed to the presumed wave simple harmonic motion, where $\sigma$ is the wave angular velocity, $\varepsilon$ is a constant phase angle, l is a finite length of frontal shoreline, and f is the tidal force in Newtons.

According to Equations 8.6, 8.7, 8.8, and 8.9, the tidal wave potential and kinetic energy at a point along the shoreline are expressed as follows (derived in the book by Sir Horace Lamb[5]).

$$W_p = \frac{1}{2} g\rho \int \left[ \frac{hf}{\sigma C \cos\left(\frac{\sigma l}{2c}\right)} \sin\frac{\sigma\left(X - \frac{l}{2}\right)}{C} \cos(\sigma l + \varepsilon) \right]^2 dx \tag{8.11}$$

$$W_k = \frac{1}{2}\rho h \int \left[ \frac{2f}{\sigma^2 \cos\frac{(\sigma l)}{2c}} \sin\frac{\sigma X}{2C} \sin\frac{\sigma(1-x)}{2C} \cos(\sigma l + \varepsilon) \right]^2 dx \tag{8.12}$$

Therefore, total energy carried out by a tidal wave over a coastal line of meters is equal to the sum of $W_p$ and $W_k$.

$$W_{tid} = \left(W_p + W_k\right) \text{ in joules} \tag{8.13}$$

Therefore,

$$W_{tid} = G(X, f, h) \tag{8.14}$$

Consider a total mean time span of tidal wave impact as equal to T seconds.

Hence, tidal wave power

$$P_{tid} = \frac{W_{tid}}{T} \text{ in watts} \tag{8.15}$$

Power extraction from $P_{tid}$ will be represented by multiplication of $P_{tid}$ with the overall efficiency factor $W_o$ of Equation 8.1.

$$P_{ext-tid} = W_o P_{tid} 10^{-6} \text{ MW}$$

$$= 10^{-6} W_d W_e W_a W_s W_p P_{tid} \text{ MW} \tag{8.16}$$

## V. INCREMENTAL ENERGY COST FOR TWEC SYSTEM

Let f and h be constants whereby over a finite length of coastal line their fluctuation is considered negligible.

$$P_{ext-tid} \simeq kG(x) \tag{8.17}$$

where

$$k = 10^{-6} W_o \tag{8.18}$$

Let the total cost involving capital operation and maintenance for securing $P_{ext}$ = m$.

Therefore,

$$\text{Incremental energy cost} = \frac{m}{P_{ext}} \$/\text{MW}$$

$$= \frac{m}{W_{ext-tid}} \$/\text{MWh} \tag{8.19}$$

where

$$W_{ext-tid} = 0.0036 W_o W_{tid} \text{ MW} \tag{8.20}$$

From Equations 8.19 and 8.20,

$$\frac{\Delta F_i}{\Delta P_i} = \frac{m}{0.0036 W_o W_{tid}} \approx \frac{\partial F_i}{\partial P_i} \tag{8.21}$$

$$= 277.777 \frac{m}{W_o W_{tid}} \quad \$ / \text{MWh} \tag{8.22}$$

$$\frac{\partial F_i}{\partial P_i} = 277.777 \frac{m}{W_o} \Bigg/ \left[ \frac{1}{2} gp \int \left[ \frac{hf}{\sigma C \cos \frac{l\sigma}{2C}} \sin \frac{\left(x - \frac{1}{2}\right)}{C} \cos(\sigma l + \varepsilon) \right]^2 dx + \frac{1}{2} \rho h \right]$$

$$\int \left[ \frac{2f}{\sigma^2 \cos \frac{l\sigma}{2C}} \sin \frac{\sigma X}{2C} \sin \frac{\sigma(l-x)}{2C} \cos(\sigma l + C) \right]^2 dx \quad \$ / \text{MWh} \tag{8.23}$$

The solution for $\partial F_i / \partial P_i$ is left as a problem for the student to solve.

Also we can write,

$$\frac{\partial F_i}{\partial P_i} = \left. \frac{\frac{\partial F_i}{\partial X}}{\frac{\partial P_i}{\partial X}} \right|_{X = l} \tag{8.24}$$

where $P_i = P_{ext\text{-}tid}$.

Now to obtain $\partial P_i / \sqrt{\partial X}$, we go to Equation 8.16 where

$$P_{ext-tid} = P_i = 10^{-6} W_e P_{tid} = 10^{-6} W_o \frac{W_{p(x)} + W_{k(x)}}{T} \tag{8.25}$$

Therefore,

$$\frac{\partial P_i}{\partial X} = \frac{10^{-6} W_o}{T} \frac{\partial}{\partial X} \left[ W_p(x) + W_k(x) \right] = \frac{10^{-6} W_o}{T} \left[ \frac{1}{2} gp \left[ \frac{hf}{\sigma C \cos \frac{\sigma l}{2C}} \sin \frac{\sigma X}{2C} \sin \frac{\sigma(l-x)}{2C} \cos(\sigma l + \varepsilon) \right] \right] \tag{8.26}$$

From Equations 8.23 and 8.26, we can secure the expression for $\partial F_i / \partial X$ and eventually $F_i$ which represents the functional form for the cost in dollars per hour of extracted energy from tidal wave per unit length along the shoreline. The extracted energy could be used to drive the turbines of conventional AC generators.

$$\frac{\partial F_i}{\partial X} = \frac{\partial F_i}{\partial P_i} \frac{\partial P_i}{\partial X} \tag{8.27}$$

and

$$F_i \quad (\text{in } \$ / h) = \int_{\partial} \frac{\partial F_i}{P_i} \frac{\partial P_i}{\partial X} dx \tag{8.28}$$

Securing a solution for $F_i$ (X) is left as a problem for the student to solve.

## VI. SECURING SOLUTION OF $\Delta F_i/\Delta P_i$ AS FUNCTION OF $P_i$

Our goal is to have

$$\frac{\partial F_i}{\partial P_i} = G_1(P_i)$$

so that it can be compared with respect to any other incremental energy cost of any mode of energy conversion during the process of optimal scheduling of generation. We observe that Equation 8.23 will establish a solution for $\partial F_i/\partial P_i$ in terms of coastline l length in meters, as well as Equations 8.26 and 8.27. Then from Equation 8.25 where $P_i$ is a function of X, and of course, of l. Solutions for $\partial F_i/\partial P_i$ as well as for $\partial F_i/\partial X$, $\partial P_i/\partial X$, and $F_i$ could be converted into explicit functions in terms of $P_i$, which is the individual plant energy that can be extracted from a tidal wave energy system.

From Equations 8.11 and 8.12, an approximate solution for $W_p$ and $W_k$ in terms of X could be secured by replacing

$$\sin\frac{(1-x)\sigma}{2C},\ \sin\frac{\sigma x}{2C},\ \text{and}\ \sin\frac{\sigma(1-x)}{2C}$$

in terms of their argument using binomial expansion. This process, as well as obtaining an expression for $\partial F_i/\partial P_i$ in terms of $P_i$ is left as homework problems for the student to solve.

## VII. CASE STUDY

From Equations 8.11 and 8.12, identify coastal spans at which $W_p$ and $W_k$ may attain maximum levels.

### A. SOLUTION

From Equation 8.11,

$$\frac{\partial W_p}{\partial X} = 0$$

$$= gp\frac{hf}{\sigma C\cos\frac{\sigma l}{2C}}\sin\frac{\sigma\left(x-\frac{1}{2}\right)}{C}\cos(\sigma l+\varepsilon)\frac{\sigma}{C}\cos\frac{\left(\frac{l}{X-2}\right)}{C} \qquad (a)$$

Therefore,

$$\cos\frac{\sigma}{C}\left(x-\tfrac{1}{2}\right)=0 \qquad (b)$$

Equation b implies,

$$\frac{\sigma}{C}\left(X-\tfrac{1}{2}\right)=\left(n+\tfrac{1}{2}\right)\Pi$$

and

$$X=\frac{\Pi C}{\sigma}\left(n+\tfrac{1}{2}\right)+\frac{1}{2} \qquad (c)$$

$$\sin\frac{\sigma}{C}\left(x-\tfrac{1}{2}\right)=0 \tag{d}$$

Therefore,

$$\frac{\sigma}{C}\left(X-\tfrac{1}{2}\right)=n\Pi$$

and

$$X=\frac{n\Pi C}{\sigma}+\frac{1}{2} \tag{e}$$

From Equation 8.12

$$\frac{\partial W_k}{\partial X}=0=\rho h\left[\frac{2f}{\sigma^2\cos\frac{l\sigma}{2C}}\sin\frac{\sigma X}{2C}\sin\sigma\frac{(1-X)}{2C}\cos(\sigma l+\varepsilon)\right]\left[\frac{2f}{\sigma^2\cos\frac{\sigma l}{2C}}\cos(\sigma l+\varepsilon)\right]$$

$$\left[\frac{\partial}{2C}\cos\sigma\frac{X}{2C}\sin\frac{(1-X)\sigma}{2C}\right]\left[\sin\frac{\sigma X}{2C}\cos\frac{(1-X)\sigma}{2C}\frac{(-\sigma)}{2C}\right] \tag{f}$$

From Equation f,

$$\sin\frac{\sigma X}{2C}=0$$

or

$$\frac{\sigma X}{2C}=n\Pi$$

and,

$$X=\frac{2n\Pi C}{\sigma} \tag{g}$$

$$\sin\frac{\sigma(1-X)}{2C}=0 \tag{h}$$

or

$$\frac{\sigma}{2C}(1-X)=n\Pi \tag{h}$$

$$X=\left[\frac{2n\Pi C}{\sigma}+1\right]$$

$$\cos\frac{(\sigma X)}{2C}=0$$

or

$$\frac{\sigma X}{2C}=\left(n+\tfrac{1}{2}\right)\Pi$$

and

$$X = \frac{2C\Pi}{\sigma}\left(n + \tfrac{1}{2}\right) \tag{i}$$

$$\sin\frac{\sigma}{2C}(1 - X) = 0$$

or

$$\frac{\sigma}{2C}(1 - X) = n\Pi$$

$$X = \left(1 - \frac{2nC\Pi}{\sigma}\right) \tag{j}$$

$$\cos\frac{\sigma(1 - X)}{2C} = 0$$

or

$$\frac{\sigma}{2C}(1 - X) = \left(n + \tfrac{1}{2}\right)\Pi$$

and

$$X = 1 - \frac{2C\Pi}{\sigma}\left(n + \tfrac{1}{2}\right) \tag{k}$$

Summarizing for

$$W_{p-max}:\ X_1 = \frac{\Pi C}{\sigma}\left(n + \tfrac{1}{2}\right) + \frac{1}{2}$$

$$W_{p-max}:\ X_2 = \frac{n\Pi C}{\sigma} + \frac{1}{2} \tag{l}$$

for $W_{k\text{-}max}$:

$$X_1 = \frac{2n\Pi C}{\sigma}$$

$$X_2 = \frac{2n\Pi C}{\sigma} + 1 = 2\left[\frac{n\Pi C}{\sigma} + \tfrac{1}{2}\right]$$

$$X_3 = \frac{2\Pi C}{\sigma}\left(n + \tfrac{1}{2}\right) \tag{m}$$

$$X_4 = 1 - \frac{2nC\Pi}{\sigma}$$

$$X_5 = 1 - \frac{2\Pi C}{\sigma}\left(n + \tfrac{1}{2}\right)$$

It is obvious that there is no certain point (X) at which both $W_p$ and $W_k$ attain maximum level.

## VIII. SUMMARY

This chapter introduced factual information and data for the phenomenon of tidal wave occurrence, its geographical impacts, as well as multiphase factors leading to net extraction of developed energy from tidal waves along coastal lines, floating vessels oscillating water column devices, and completely submerged turbines.

Glendenning[2] pointed out in his paper potential prospects for TWEC systems that stress the elements of cost, engineering feasibility, and access to maintenance. His paper also indicated that the most credible system is that based on the utilization of air turbine power take off which is, even though big in size, also relatively economical.

Glendenning also identified that bulky size of TWEC resource is the offshore system working in deep water and also those aligned across a spectrum of tidal waves with minimum spacing.

Reliability aspects of TWEC system that have been presented are based on a paper authored by Dawson, et al.[1] Information from this paper identified measured data pertaining to the rate of system failure and rate of repair for various components at site locations. The next item included in this chapter is the potential and kinetic energy of a typical tidal wave impacting a coastal line of span l.

Solutions for the total energy content along the coast have been presented, as well as the net power extraction.

Then, expressions for the incremental cost of energy extraction from TWEC system in terms of any point along the shore, and with respect to any individual source, have been identified with a procedural pattern.

The central element for meaningful realization of a tidal energy system is based on practicality aspects, efficiency, economic feasibility, and the stressed continuous need for substantial research and development.

## IX. PROBLEMS

8.1 Using the graph shown in Figure 8.5 for the probability of no function, obtain a multifunction representation for the probability against time in months.

8.2 Repeat for the statement of Problem 8.1 for the graph shown in Figure 8.6a for the probability function.

8.3 Repeat for the statement of Problem 8.1 for the graph shown in Figure 8.6b for the probability function.

8.4 Equation 8.16 gave an expression for the net power extraction from a tidal wave confronting a shoreline of length l. Find out a spectrum of points along the cost of impact at which $P_{ext\text{-}tid}$ is maximum.

8.5 Complete the solution for the expression of $\partial F_i/\partial P_i$ shown in Equation 8.23 by carrying out the steps of integrations shown.

8.6 Using expressions for $\partial F_i/\partial P_i$ obtained in Problem 8.5 and for $\partial P_i/\partial X$ given by Equation 8.28, establish a final solution for $F_i(x)$ in dollars per hour.

8.7 Carry out the process of integration for $W_p$ given by Equation 8.11, preceded by replacement of

$$\sin\left[\left(\frac{\sigma}{C}\right)\left(x - \frac{l}{2}\right)\right]$$

by a number of terms (three terms only) from the binomial theorem expansion.

8.8 Carry out the process of integration for $W_k$ given by Equation 8.12, preceded by replacement of

$$\sin\left(\frac{\sigma X}{2C}\right) \text{ and } \sin\frac{\sigma}{2C}(1-X)$$

each by three terms by using the binomial expansion theorem for each function.

8.9 From solutions of $W_p(x)$ obtained in Problem 8.7 and of $W_k(x)$ secured in Problem 8.8 write down the total solution for $P_i(s)$ and then proceed to obtain a final expression for $\partial F_i/\partial P_i$ in terms of $P_i$ and other constant parameters of the tidal wave phenomenon.

8.10 Repeat Problem 8.9 to establish a complete solution for the function of $\partial F_i/\partial X$ in terms of $\partial P_i$.

8.11 Repeat Problem 8.10 to establish a complete solution for $F_i$ in dollars per hour in terms of $P_i$.

8.12 Examine the possibility of approximating the $\partial F_i/\partial P_i$ expression obtained in Problem 8.9 in the form of a single straight function or a set of piece-wise straight line functions, i.e., of the forms:

$$\frac{\partial F_i}{\partial P_i} = \left[F_{ii-1}P_i + f_{i1}\right] + \left[F_{ii-2}P_i + f_{i2}\right] + \left[F_{ii-3}P_i + f_{i3}\right] + \ldots +$$

$$\left[F_{ii-n}P_i + f_{in}\right] = \left[F_{ii-1} + F_{ii-2} + F_{ii-3} + \ldots + F_{i-n}\right]P_i + \left[f_{ii} + L_{i2} + f_{i3} + \ldots + f_{in}\right]$$

8.13 To use the [B] matrices given in Chapter 1 for a centralized power grid system, we have to use one or more multiplying factors so that those matrices remain invariant. Using Chapter 4, Equations 4.99 and 4.101, and using the piece-wise straight line functions for $\partial F_i/\partial P_i$ obtained in Problem 8.12, calculate the required multiplying factors.

8.14 Consider a TWEC plant in close proximity to a conventional power grid system such that its output has been allocated to take care of the conventional system transmission loss. Using the regular economic power coordination, obtain a solution for $\lambda$ (the cost of received power in dollars per megawatt hour) in terms of parameters of the TWEC system.

8.15 From the correlation that $P_L$ (the transmission power loss) is equal to

$$P_{ext-tid} = \sum_i \sum_j P_i B_{ij} P_j$$

write a closed form solution for $B_{ij}$ if $P_i$ and $P_j$ are TWEC power plants where i, j = 1, 2, 3, ... .

8.16 A TWEC interconnected grid power system whereby $\partial F_i/\partial P_i$ is that secured in Problem 8.5, using the regular coordination equation, solve for $P_L$ for any value of $\lambda$.

8.17 Taking into consideration that net power extraction from TWEC power plant is subject to reliability expectation, obtain a mathematical model for power delivery at any point along the coastline in association of the probability function of Figure 8.6a, i.e., to develop a solution for probabilistic $P_{ext}(x)$ against (x).

8.18 Repeat Problem 8.17 for the association of Figure 8.6b.

8.19 Repeat Problem 8.17 for the cost of TWEC in dollars per hour along the coastline in association with Figure 8.6a.

8.20 Repeat Problem 8.17 for the association of the cost of TWEC in dollars per hour along the coastline with Figure 8.6b.

## REFERENCES

1. **Dawson, J. M., Mytton, M. G., Shore, N. L., and Stansfield, H. B.,** System-reliability studies for wave-energy generation, *IEE Proc.*, 127 (A, No. 5), 296, 1980.
2. **Glendenning, I.,** Wave energy, *IEE Proc.*, 127 (A, No. 5), 301, 1980.
3. **Harrison, R., Smith, K. G., and Varley, J. S.,** Energy analysis of wave and tidal power, *IEE Proc.*, 127 (A, No. 5), 274, 1980.
4. **Warnock, J. G. and Wilson, J. A. M.,** Tidal Power: The Relentless, Clean and Predictable Energy Source, Paper 2C, presented to the 68th Natl. Meet. Am. Inst. Chem. Eng., Houston, Texas, February 28—March 1971.
5. **Lamb, Sir H.,** *Hydrodynamics*, 6th ed., Dover Publications, New York, 1932.

Chapter 9

# THE ECONOMICS OF GEOTHERMAL ENERGY CONVERSION SYSTEMS (GTEC)

## I. INTRODUCTION*

Geothermal energy involves capturing the natural heat that lies under the Earth's crust, which could be used in space and process heating and in the generation of bulk electric power. A current estimate of world geothermal power is in the order of 2.5 GW.

Geothermal power resources include: hydrothermal, geopressured, and petrothermal systems.

A hydrothermal system is characterized as the generation of hot water or steam through contact with hot rocks. In geopressured systems hot water occupies a deep reservoir under intense pressure from multilayers of rocks, shale, and sands. This geopressured water sometimes is saturated with natural gas resulting from the decomposition of organic materials.

In petrothermal systems, magna lying close to the Earth's surface heats overlying rocks to a very high temperature. Infection of water or any other fluid in petrothermal layers and then pumping it out will release a huge amount of thermal energy by driving a steam or hot water turbine.

Current U.S. geothermal energy capacity is of the order of 12 GW and is expected to reach the level of 20 GW by the year 2000.

Another mode of utilizing geothermal energy resources is known as the direct-flash steam cycle plant where hot geothermal water at a temperature of 210°C is drawn from a reservoir, allowing its pressure to fall which leads to water vaporization and, of course, the release of steam which can be used to drive steam turbines.

Reported by the Electric Power Research Institute (EPRI),[1] the concept of the Rotary Separator Turbine (RST) which accounts for a reduction of cost of energy in the direct-flash geothermal system is based on using energy that otherwise would be lost in this system. In this system, an RST is linked to a steam turbine, and where a mixture of water and steam develops in the geothermal well, the mixture is allowed to expand in a nozzle such that more water will evaporate and the remaining water is collected by a rotating drum by centrifugal acceleration. The process of water vaporization could be repeated on the remaining water as long as feasible.

Another aspect is the indirect use of geothermal water in the binary cycle system. In this system, the hot water will run through a closed loop that is in close proximity to another loop carrying low boiling temperature fluid such as isobutane or isopentane. The heat from the geothermal water will heat the low boiling point gas and then will be used to drive a gas turbine.

EPRI reports that the binary cycle system will be very effective and more economical than either the direct flash system or the natural steam system, especially at moderate temperatures (150 to 210°C) where it has been shown that it needs two thirds of the geothermal fluids that either the direct flash or natural steam system needs. Also, another benefit for the binary system is that it can operate in a closed cycle system while the direct flash and the natural steam cycle have to operate in an open cycle.

Also, according to an EPRI report,[1] the three geothermal systems namely, the natural steam, the binary cycle, and the direct flash cycle systems, share the problem of mineral accumulation usually dissolved in geothermal water which lead to a reduction in both fluid flow and the smoothness of heat exchange. To counter this problem, EPRI reported a resort to system scaling

* © 1981, EPRI. Reprinted with permission from Charlson, M., *EPRI J.*, December, 19—25, 1981. Michael Charlson, communication specialist; technical information provided by Vasel Roberts, Advanced Power Systems Division, EPRI, Palo Alto, CA.

whereby computer simulation will monitor scale formation by using input data on brine chemistry and operating temperature pressure as well as working fluid flow. The monitoring results will identify optimal design by watching changing operational characteristics and pilot designs parameters, all will set efficient system scale for the geothermal plant.

Another problem requiring a solution in geothermal systems is the presence of noncondensable gases found dissolved in geothermal fluids, which can reduce thermal efficiency, accelerate equipment wear, and cause environmental problems. The EPRI report also stressed an effective solution of this problem along real feasibility of geothermal energy production.

A problem which exists at the geysers is the presence of $H_2S$ dissolved in geothermal fluid at a concentration around 200 ppm. Removing $H_2S$ is very essential for effective plant operation and environmental conditions. The approach tested by EPRI on a small scale proved effective and involves the initial condensation of geothermal steam from which $H_2S$ and other undesirables will be removed and water revaporized by heat from incoming steam.

Due to the relatively high cost of using geothermal fluids, from the mode of geopressured system, a combustion energy system using gas dissolved in the fluid such as methane seems feasible according to the EPRI study.

The thrust of research in geothermal energy system has to concentrate more on the mode of petrothermal resources which accounts for 85% of the geothermal resource base in the U.S. as reported by EPRI.

## II. INCORPORATION OF GEOTHERMAL RESOURCE INTO FOSSIL-STEAM ALTERNATORS*

### A. DIRECT CONVERSION

Figure 9.1a shows a direct energy conversion system for a geothermal well operating at temperature $T_2$ from the well and $T_1$ of return to the well. Figure 9.1b shows temperature per entropy diagram with a sink temperature of T .

The amount of electricity obtained by an ideal conversion system per unit of mass flow is

$$W_e = \int_{T_1}^{T_2} C_p \mu_c(T)\, dt \tag{9.1}$$

where $\mu_c$ is the efficiency of a Carnot cycle engine.

$$\mu_c = 1 - \frac{T}{T_o} \tag{9.2}$$

$$W_e = C_p \int_{T_1}^{T_2} \left(1 - \frac{T_o}{T}\right) dT \tag{9.3}$$

$C_p$ is the specific heat at constant pressure and considered here as independent of T.

By integrating Equation 9.3 and dividing by the heat input, we come to the conversion efficiency expressed by

$$\eta = 1 - \frac{T_o \ln \frac{T_2}{T_1}}{T_2 - T_1} \tag{9.4}$$

* © 1980, IEE. Reprinted with permission from White, A. A. L. and Phil, D., Advantage of incorporating geothermal energy into power-station cycles, *IEE Proc.*, 127 (A, No. 5), 330—335. 1980.

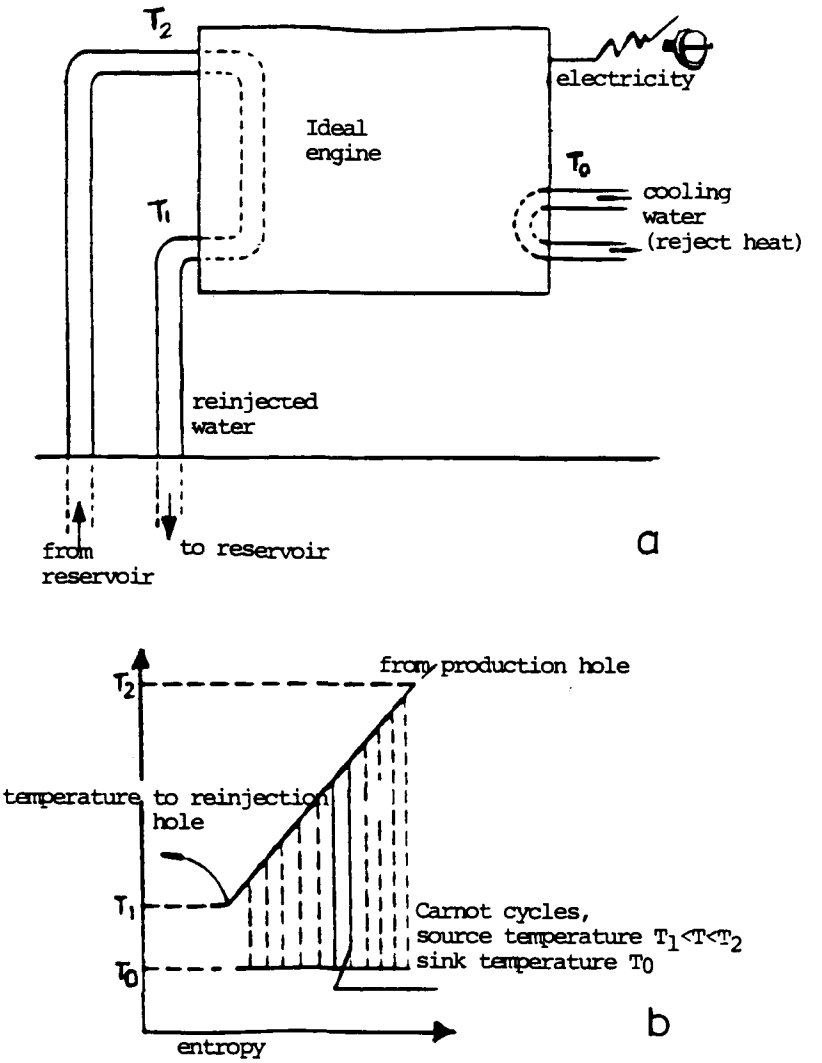


FIGURE 9.1. Direct conversion. a) Energy conversion system. b) Temperature/entropy diagram. (From White, A. A. L. and Phil, D., Advantage of incorporating geothermal energy into power-station cycles, *IEE Proc.*, 127 (A, No. 5), 330—335. 1980. With permission.)

and that

$$\eta < \eta_e \tag{9.5}$$

All information reported on the direct conversion of geothermal energy indicates that $\mu$ is relatively low (of the order of 7 to 8%). Therefore, an alternative of direct conversion is the indirect utilization through the integration of geothermal heat into the fossil-steam cycle of alternators. This is expected to be done by using the geothermal heat in raising the temperature of some sections of feed water into the turbine system and hence allowing more steam flow in the turbine to produce more electricity.

Figure 9.2 shows a plot for efficiency of direct conversion of geothermal system against well temperature.

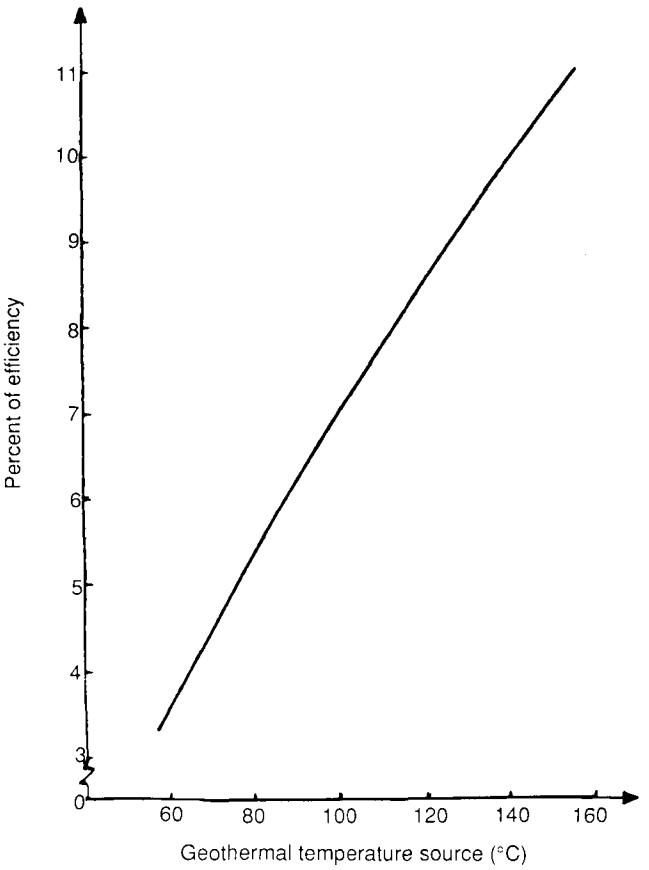


FIGURE 9.2 Efficiency-response temperature. (From White, A. A. L. and Phil, D., Advantage of incorporating geothermal energy into power-station cycles, *IEE Proc.*, 127 (A, No. 5), 330—335. 1980. With permission.)

## III. GEOTHERMAL FEED WATER HEATING*

Most utilities use steam bled from the turbines to preheat the boiler feed water as shown in Figure 9.3.

The geothermal heat is to be supplied to the steam cycle by replacing some sections of the feed water heaters, thereby allowing more steam to remain in the turbine thus generating more electricity. Figure 9.3 illustrates the integration of geothermal power into the steam cycle.

In Figure 9.3, $M_i$ is the amount of steam flow between the $i^{th}$ and the $(i\text{-}1)^{th}$ bled points, $b_i$ is the rate of steam flow at the $i^{th}$ bleed point, $h_i$ is the enthalpy at the $i^{th}$ bleed point, and $T_i$ is the temperature after the $i^{th}$ feed water heater.

Work performed by the turbine $P_i$:

$$P_i = \sum_{i=1}^{n} \dot{M}_i [h_i - h_{i-1}] \eta_i \tag{9.6}$$

where $M_i$ is the net amount of steam in turbine feed water heating system, n is the number of turbine stages, and $\eta_i$ is the efficiency of $i^{th}$ stage.

* © 1980, IEE. Reprinted with permission from White, A. A. L. and Phil, D., Advantage of incorporating geothermal energy into power-station cycles, *IEE Proc.*, 127 (A, No. 5), 330—335. 1980.

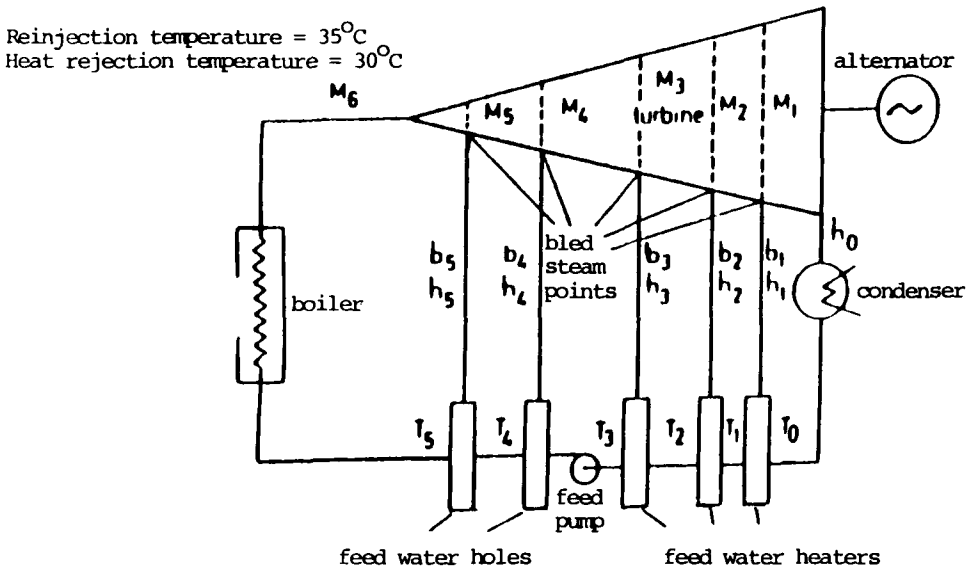


FIGURE 9.3 Modified Rankine cycle system for conversion. (From White, A. A. L. and Phil, D., Advantage of incorporating geothermal energy into power-station cycles, *IEE Proc.*, 127 (A, No. 5), 330—335. 1980. With permission.)

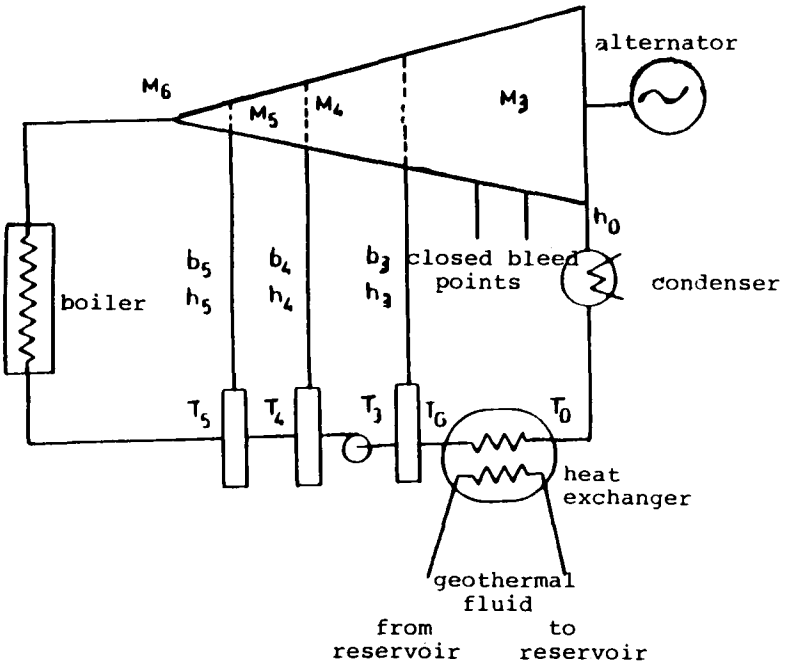


FIGURE 9.4 Geothermal feed water heating. (From White, A. A. L. and Phil, D., Advantage of incorporating geothermal energy into power-station cycles, *IEE Proc.*, 127 (A, No. 5), 330—335. 1980. With permission.)

To integrate geothermal heat into the turbine steam cycle, we may proceed to replace the first and second feed water heaters by a heat exchanger whose primary is connected to the geothermal doublet as shown in Figure 9.4.

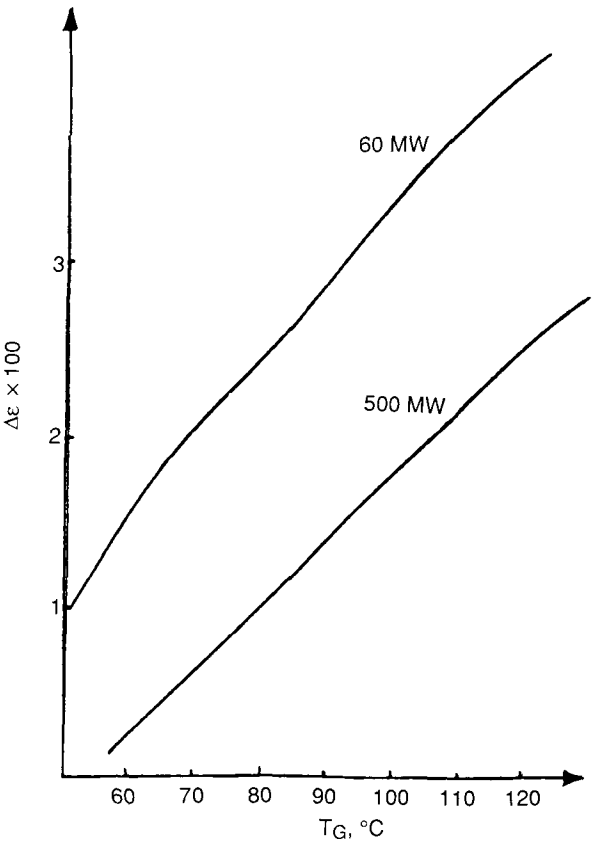


FIGURE 9.5 Percentage increase in fuel efficiency with geothermal heating temperature $T_G$. (From White, A. A. L. and Phil, D., Advantage of incorporating geothermal energy into power-station cycles, *IEE Proc.*, 127 (A, No. 5), 330—335. 1980. With permission.)

In Figure 9.4, we would like to indicate that $b_4$ and $b_5$ as the new steam bleed rates are to remain unchanged, while $b_2$ and $b_1$ are zero and $b_3$ depends on the geothermal temperature $T_o$.

Also that if $T_G = T_2$, then $b_2' = b_3'$ and can adjust to make $T_3 = T_3'$. The work performed by the turbine is written as follows (in watts):

$$P_i = \sum_{i=4}^{n} \dot{M}_i' [h_i - h_{i-1}]\eta_i' + \dot{M}_3' (h_i - h_o)\eta_3' \tag{9.7}$$

and the new cycle's fuel efficiency $\psi$ is given below,

$$\psi_{new} = \psi_{old}(1 + \Delta\varepsilon) \tag{9.8}$$

where

$$\Delta\varepsilon = (P_i - P_i)/P_i \tag{9.9}$$

where $\Delta\varepsilon$ represents the fractional increase in output for given values of $M_6$, and $h_6$.

Figure 9.5 illustrates a plot for $\Delta\varepsilon$ against the geothermal temperature $T_G$. The significant difference in $\Delta\varepsilon$ for the two plants as reported in a paper by White and Phil[2] is due to steam generation and distribution for the two plants.

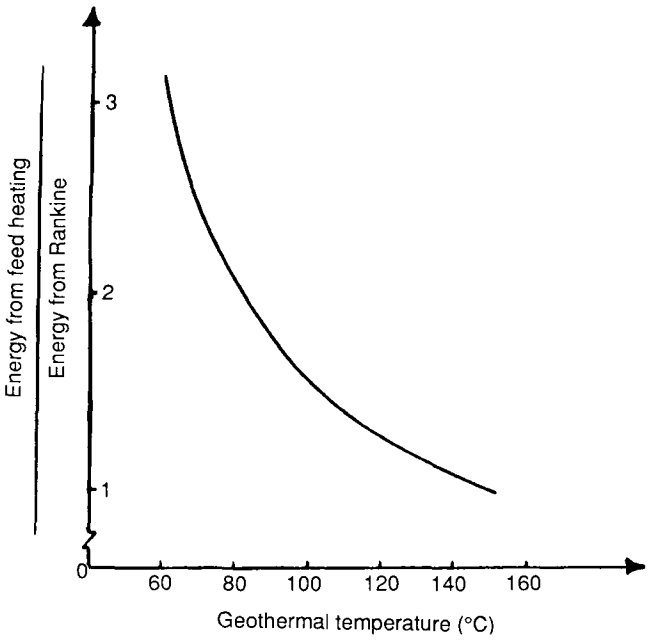


FIGURE 9.6 Comparison of outputs from feed water heating and Rankine cycle conversion system from same geothermal source. (From White, A. A. L. and Phil, D., Advantage of incorporating geothermal energy into power-station cycles, *IEE Proc.*, 127 (A, No. 5), 330—335. 1980. With permission.)

The efficiency of conversion for geothermal energy in the form of increased output from the AC alternator is given as follows:

$$\psi_g = E\ \Delta\varepsilon \Big/ \left(T_G - T_o\right) \dot{m}\, C_p \tag{9.10}$$

where e is the efficiency of heat exchanger, m is the condensate flow rate, and P is the normal power output of the system.

Now since the curve of $\Delta\varepsilon$ against $T_G$ is approximately linear, the functional relationship is

$$\Delta\varepsilon = A\left(T_G - T_o\right) \tag{9.11}$$

Figure 9.6 shows a ratio of geothermal feed water heating contribution for an increase in alternator output to direct conversion on the basis of the Rankine cycle. It is obvious that this ratio is larger than unit x whenever $T_G$ exceeds 150°C.

## IV. FEED WATER HEATING GEOTHERMAL POWER OUTPUT[2] *

The net generation of electric power produced by the effect of feed water heating (fwh) is expressed below by returning to Equations 9.6 and 9.7,

$$P_{fwh} = W' - W$$

$$= \sum_{i=4}^{n} \dot{M}_i'\left(h_i - h_{i-1}\right)\eta_i + \dot{M}_3'\left(h_i - h_o\right)\eta_3 - \sum_{i=1}^{n} \dot{M}_i\left(h_i - H_{i=1}\right)\eta_i \tag{9.12}$$

* © 1980, IEE. Reprinted with permission from White, A. A. L. and Phil, D., Advantage of incorporating geothermal energy into power-station cycles, *IEE Proc.*, 127 (A, No. 5), 330—335. 1980.

Also, from Equations 9.6 and 9.11, we can write,

$$P_{i-fwh} = A\left(T_G - T_o\right)\sum_{i=1}^{n} \dot{M}_i\left(h_i - h_i\right)\eta_i \quad \text{in watts} \tag{9.13}$$

Now from Equation 9.3 without temperature limit we can write for the power output of Rankine cycle geothermal system:

$$P_R = C_p \int \dot{m}\left(1 - \frac{T_o}{T}\right) dT$$

$$= C_p \dot{m} \int \left[dT - T_o \frac{T}{dT}\right]$$

$$= C_p \dot{m}\left[T - T_o \ln T\right] \tag{9.14}$$

where $P_R$ is the Rankine cycle geothermal power output, $\dot{m}$ is the flow rate of steam in Rankine cycle system, and $\dot{M}$ is the amount of steam in bled water heating geothermal turbine system.

## V. INCREMENTAL GEOTHERMAL ENERGY COST

### A. DIRECT RANKINE CYCLE CONVERSION SYSTEM

Let $F_R$ represent the total cost in dollars of geothermal plant (i) and is a function of T.
An approximate expression for the incremental energy cost could be written as,

$$F_R/P_R = \frac{F_R\ 10^{-6}}{C_p \dot{m}\left(T - T_o \ln T\right)} \quad \$/\text{MWh} \tag{9.15}$$

or more rigorously,

$$\frac{\partial F_R}{\partial P_R} = \frac{\partial F_R}{\partial T} \Big/ \frac{\partial P_R}{\partial T} \tag{9.16}$$

From Equation 9.14,

$$\frac{\partial P_R}{\partial T} = C_p \dot{m}\left[1 - \frac{T_o}{T}\right] \tag{9.17}$$

$$\frac{\partial F_R}{\partial P_R} = \frac{\dfrac{\partial F_R}{\partial T}}{C_p \dot{m}\left(1 - \dfrac{T_o}{T}\right)} \tag{9.18}$$

But since $F_R$ is proportional to the plant efficiency $\mu_i$,

$$\mu_i = 1 - \frac{T_o}{T} = \frac{T - T_o}{T} \tag{9.19}$$

Therefore,

$$\frac{\partial F_R}{\partial T} = \frac{\partial F_R}{\partial \mu}\,\frac{\partial \mu}{\partial T}$$

$$= \frac{T_o}{T^2}\,\frac{\partial F_R}{\partial \mu} \tag{9.20}$$

Then we can write,

$$F_R = K_R \mu \tag{9.21}$$

where $K_R$ is a plant constant.

$$\frac{\partial F_R}{\partial \mu} = K_R \tag{9.22}$$

and hence from Equation 9.20 and 9.22,

$$\frac{\partial F_R}{\partial T} = K_R \frac{T_o}{T^2} \tag{9.23}$$

Then back to Equation 9.18,

$$\frac{\partial F_R}{\partial P_R} \approx \frac{K \dfrac{T_o}{T^2}}{C_P \dot{m}\left(1 - \dfrac{T_o}{T}\right)} \tag{9.24}$$

To obtain a solution for $\partial F_R/\partial P_R$, we now return to Equation 9.14, where

$$P_R = C_p \dot{m}\left(T - T_o \ln T\right)$$

since

$$\ln T \cong \frac{T-1}{T} + \frac{(T-1)^2}{{}^2T^2} + \frac{(T-1)^3}{{}^3T^3} + \cdots \tag{9.25}$$

where,

$$T > \frac{1}{2}$$

As a first approximation, we will take $\ln T \cong T - 1/T$, other terms will be considered through homework problems.

Therefore,

$$P_R \approx C_p \dot{m}\left[T - T_o\left(\frac{T-1}{T}\right)\right] \tag{9.26}$$

From Equation 9.26, a solution for T in terms of $P_R$ gives,

$$T \simeq \left[T_o + \frac{P_R}{C_p \dot{m}}\right] \pm \sqrt{\left(T_o + \frac{P_R}{C_p \dot{m}}\right)^2 - 4T_o} \Big/ 2 \tag{9.27}$$

And from Equation 9.24,

$$\frac{\partial F_R}{\partial P_R} \simeq \frac{-K}{C_p \dot{m}} \frac{T_o}{T(T_o - T)} 10^{-6} \tag{9.28}$$

We can see the picture of $\partial F_R/\partial P_R$ more clearly by setting $T_o = 0$ in Equation 9.27 only. (Although it is a controversial assumption.) Therefore,

$$T \simeq \frac{1}{2}\left[\frac{P_R}{C_p \dot{m}} \pm \frac{P_R}{C_p \dot{m}}\right]$$

We have to disregard the (–) sign above, therefore,

$$T \simeq \frac{P_R}{C_p \dot{m}} K_R \tag{9.29}$$

Hence back to Equation 9.28, we obtain

$$\frac{\partial F_R}{\partial P_R} = \frac{-K\, T_o}{C_p \dot{m}} \frac{10^6}{\frac{P_R}{C_p \dot{m}}\left[T_o - \frac{P_R}{C_p \dot{m}}\right]}$$

$$\simeq -\frac{K_R T_o C_p \dot{m}\, 10^{-6}}{P_R\left(T_o C_p \dot{m} - P_R\right)} \$/\text{MWh} \tag{9.30}$$

However the close to exact solution for $\partial F_R/\partial P_R$ in terms of $P_R$ can be expressed by substituting T from Equation 9.27 into Equation 9.28.

The author's comment with respect to Equation 9.30 is that the incremental energy cost for a direct Rankine cycle geothermal plant will become less as the plant operating power generating capacity increases within its maximum range.

**B. FEED WATER HEATING SYSTEM**

First we can write a very approximate expression for $\partial F_{fwh}/\partial P_{fwh}$ in reference to Equation 9.12,

$$\frac{F_{fwh}}{P_{fwh}} = F_{fwh} 10^{-6} \Big/ \left[\sum_{i=4}^{n} \dot{M}_i'(h_i - H_{i-1})\eta_i + \dot{M}_3'(h_i - h_o)\eta_3 - \sum_{i=1}^{n} \dot{M}_i(h_i - h_{i-1})\eta_i\right] \$/\text{MWh} \tag{9.31}$$

Of course, the subscript fwh implies feed water heating mode utilization of geothermal power.

$$i = \frac{e\,\Delta\varepsilon\,P_{fwh}}{(T - T_o)\dot{m}C_p} \tag{9.32}$$

where T in Equation 9.32 is the operational $T_G$, and e is the efficiency of the heat exchanger. Again,

$$\frac{\partial F_{fwh}}{\partial P_{fwh}} = \frac{\partial F_{fwh}}{\partial \mu}\frac{\partial \mu}{\partial P_{fwh}} \tag{9.33}$$

Therefore at a certain $T_{G,}$

$$\frac{\partial \mu_i}{\partial P_{fwh}} = \frac{e\,\Delta\varepsilon}{(T - T_o)\dot{m}C_p} \tag{9.34}$$

Also,

$$F_{fwh} = K_{fwh}\mu \tag{9.35}$$

where K is plant constant, and

$$\frac{\partial F_{fwh}}{\partial \mu} = K_{fwh}$$

Hence from Equations 9.33 and 9.35,

$$\frac{\partial F_{fwh}}{\partial P_{fwh}} = \frac{K_{fwh}e\,\Delta\,\varepsilon}{(T - T_o)\dot{m}C_p} \tag{9.36}$$

$$= \frac{K_{fwh}eA(T - T_o)}{\dot{m}C_p(T - T_o)}$$

$$= \frac{A\,e\,K_{fwh}}{\dot{m}C_p} \tag{9.37}$$

We can see from the result of Equation 9.37 that $\partial F_{fwh}/\partial P_{fwh}$ is constant if m is constant. This is very significant because it is compatible with that of the conventional system as well as major modes of other renewable energy sources.

Therefore, the incremental energy cost for a geothermal feed water heating power plant is expressed in the usual form as follows,

$$\frac{\partial F_{fwh}}{\partial P_{fwh}} = F_{ii}P_i + f_{i-new} \tag{9.38}$$

where,

$$F_{ii} = 0$$

and

$$L_{i-new} = \frac{A\,K'e}{C_p \dot{m}} \tag{9.39}$$

On the other hand, we notice that for a direct geothermal Rankine cycle system, the $\partial F_R/\partial P_R$ in its simplest form is given by Equation 9.30, which shows a quite different mathematical mode, where it is inversely changing with respect to the first and second order of plant power loading.

## VI. MULTIPLYING FACTOR FOR INVARIANT [B]²

We have established in the previous section that incremental energy cost in dollars per megawatt hour for geothermal feed water heating mode operating adjacent or in close proximity to a fossil steam cycle power plant is constant but depending on the efficiency of heat exchanges, specific heat at constant pressure for geothermal fluid, plant constant, and mathematical constant related to the straight line function of $\Delta\varepsilon$ against $T_G$.

As mentioned in previous chapters, a set of [B] matrices for a centralized power system having 32 bus-bars at different loadings and a dispersed one at 70% loading were established and given in Chapter 1 and some in Chapter 2.

We have also derived a set of multiplying factors for those [B] matrices to remain unchanged or invariant. Those multiplying factors are of two kinds.

First, where the incremental fuel or energy cost curve is in the form:

$$\frac{\partial F_i}{\partial P_i} = F_{ii} P_i \tag{9.40}$$

However, for the new system $F_{ii}$ is different than that for which a [B] matrix has been already calculated and established, i.e.,

$$F_{ii-new} \neq F_{ii-old}$$

Second, where the incremental fuel or energy cost curve is of the form,

$$\frac{\partial F_i}{\partial P_i} = f_i \tag{9.40a}$$

Again, if $f_{i\text{-}new} \neq f_{i\text{-}old}$, a multiplying factor or factors have been derived for the calculated [B] matrix or matrices to remain invariant.

For our case regarding the geothermal feed water heating coupled to fossil-steam cycle system, the second form is the one to be considered now.

From Chapter 4, two multiplying factors have been established by Chapter 4, Equations 4.109 and 4.10.

$$K = 1 - \frac{A_1}{C_1 f_{i-old}} \tag{9.41}$$

where

$$f_{i-new} = K f_{i-old}$$

$A_1$ and $C_1$ are given by Chapter 4, Equations 4.104 and 4.105. It is noticed that $A_1$ and $C_1$ are each a function of power plant capacities, cost of received power in dollars per megawatt hour and $f_{i\text{-}old}$.

Another multiplying factor has been given by Chapter 4, Equation 4.110 is expressed by,

$$K = 1 + \frac{D_1}{E_1 f_{i-old}} \tag{9.42}$$

where $D_1$ and $E_1$ have been given by Chapter 4, Equations 4.106 and 4.106a

In our case,

$$K = \frac{A K_{fwh} e}{C_p \dot{m} f_{i-old}} \tag{9.43}$$

## VII. STANDARDIZING GEOTHERMAL RANKINE CYCLE SYSTEM

Restating Equation 9.30 which represents a workable form for the incremental energy cost of a geothermal plant working on the basis of direct Rankine cycle system,

$$\frac{\partial F_R}{\partial P_R} = \frac{K_R T_o C_p \dot{m}\, 10^{-6}}{P_R\left(P_R - T_o C_p \dot{m}\right)} \tag{9.44}$$

Let a new power plant rating $P_i$ where,

$$P_i = 1/P_R \tag{9.45}$$

Now substitute in Equation 9.44,

$$A_1 = K_R T_o C_p \dot{m}\, 10^{-6} \tag{9.46}$$

$$A_2 = T_o C_p \dot{m} \tag{9.47}$$

Therefore,

$$\frac{A_1}{P_R\left(P_R - A_2\right)} = \frac{A_1 P_i^2}{A_2 P_{i-1}} = \frac{\partial F_i}{\partial P_i} \tag{9.48}$$

We can return to the standard form for $\partial F_{i/}\partial P_i$, i.e.,

$$\frac{\partial F_i}{\partial P_i} = F_{ii} P_i + f_i \tag{9.49}$$

From Equation 9.48

$$\frac{A_1 P_i^2}{A_2 P_{i-1}} \approx \frac{A_1}{A_2^2} + \frac{A_1}{A_2} P_i + \frac{A_1}{A_2^2 P_i} + \cdots \tag{9.50}$$

Since $P_R$ is mainly in the order of megawatt capacity, we can discard the third term in Equation 9.50.

Hence,

$$\frac{\partial F_i}{\partial P_i} = F_{ii} P_i + f_1$$

$$\approx \frac{A_1}{A_2} P_i + \frac{A_1}{A_2^2} \tag{9.51}$$

Therefore,

$$\frac{A_1}{A_2} = F_{ii} \tag{9.52}$$

$$\frac{A_1}{A_2^2} = f_i \tag{9.53}$$

where

$$F_{ii} = \frac{A_1}{A_2} = 10^{-6}\ K \tag{9.54}$$

$$f_1 = \frac{A_1}{A_2^2} = 10^{-6} K / T_o C_p \dot{m} \tag{9.55}$$

It is very interesting to note how the replacement of geothermal Rankine cycle plants with their inverse capacity, resulted into a standard incremental energy cost curve compatible with the normal form of such a curve. It may imply that direct geothermal energy conversion follows the inverse mode of the ideal Rankine cycle, however such implication is only a guess.

Now, rewriting the final standardized form of the incremental energy cost for geothermal plant operating on the basis of inverted Rankine cycle is given as follows:

$$\frac{\partial F_{i\text{-}R}}{\partial P_{i-R}} = 10^{-6} K P_{i-R} + \frac{10^{-6} K}{T_o C_p \dot{m}} \tag{9.56}$$

where the subscript (i-R) refers to inverted Rankine cycle system.

## VIII. CASE STUDY

To determine an almost exact form for the incremental energy cost of direct conversion of geothermal energy on the basis of ideal Rankine cycle.

The form required for $\partial F_R/\partial P_R$ must be in terms of $P_R$.

An almost exact form for $F_R/P_R$ could be determined by the linkage of Equations 9.27 and 9.28, and then proceed to have the form compatible to the standard form of $F_{ii}\, P_i + f_i$

Now we can write,

$$\frac{\partial F_R}{\partial P_R} = \frac{K_R T_o 10^{-6}}{C_p \dot{m}} \left[ \frac{2}{\left[ T_o + \frac{P_R}{C_p \dot{m}} \right] \pm \sqrt{\left( T_o + \frac{P_R}{C_p \dot{m}} \right)^2 - 4\, T_o}} \right.$$

$$\left. \frac{1}{\left[ T_o - \frac{1}{2} \left( T_o + \frac{P_R}{C_p m} \pm \sqrt{\left( T_o + \frac{P_R}{C_p m} \right)^2 - 4\, T_o} \right] \right]} \right. \tag{a}$$

Now expand

$$\sqrt{\left( T_o + \frac{P_R}{C_p m} \right)^2 - 4\, T_o}$$

using the binomial theorem:

$$\approx \left( T_o + \frac{P_R}{C_p \dot{m}} \right) \sqrt{1 - \frac{4\, T_o}{\left[ T_o + \frac{P_R}{C_p \dot{m}} \right]^2}} \tag{b}$$

$$\simeq \left( T_o + \frac{P_R}{C_p \dot{m}} \right) \left[ 1 - \frac{2\, T_o}{\left( T_o + \frac{P_R}{C_p m} \right)^2} - \frac{1}{8} \frac{16\, T_o^{\,2}}{\left( T_o + \frac{P_R}{C_p m} \right)^4} + \cdots \right] \tag{c}$$

To simplify the proceeding work, drop the third term in Equation c, therefore,

$$\sqrt{\left(T_o + \frac{P_R}{C_p \dot{m}}\right)^2 - 4\,T_o} \simeq \left(T_o + \frac{P_R}{C_p \dot{m}}\right)\left[1 - \frac{2\,T_o}{\left(T_o + \frac{P_R}{C_p \dot{m}}\right)^2}\right] \tag{d}$$

$$\simeq \left(T_o + \frac{P_R}{C_p \dot{m}}\right) - \frac{2\,T_o}{T_o + \frac{P_R}{C_p \dot{m}}} \tag{e}$$

Back to Equation a,

$$\frac{\partial F_R}{\partial P_R} \cong -\frac{2\,K_R\,T_o 10^{-6}}{C_p \dot{m}}\left[\frac{1}{\left(T_o + \frac{P_R}{C_p \dot{m}}\right) \pm \left(T_o + \frac{P_R}{C_p \dot{m}} - \frac{2\,T_o}{T_o + \frac{P_R}{C_p \dot{m}}}\right)}\right]$$

$$\left[\frac{1}{T_o - \frac{1}{2}\left(T_o + \frac{P_R}{C_p \dot{m}}\right) \pm \left(T_o + \frac{P_R}{C_p \dot{m}}\right) - \frac{2\,T_o}{T_o + \frac{P_R}{C_p \dot{m}}}}\right] \tag{f}$$

Consider the (–) sign in the denominator of Equation f. Therefore,

$$\frac{\partial F_R}{\partial P_R} = -\frac{2\,K_R\,T_o 10^{-6}}{C_p \dot{m}} \frac{1}{\frac{2\,T_o C_p \dot{m}}{T_o C_p \dot{m} + P_R}\left(T_o - \frac{T_o C_p \dot{m}}{T_o C_p \dot{m} + P_R}\right)} \tag{g}$$

or

$$\frac{\partial F_R}{\partial P_R} \simeq A' \frac{\left(P_R + T_o C_p \dot{m}\right)^2}{2\,T_o C_p \dot{m}\,T_o\left(P_R + C_p \dot{m} T_o\right) - T_o C_p \dot{m}} \tag{h}$$

where

$$A' = -\frac{2\,K_R T_o 10^{-6}}{C_p \dot{m}}$$

or

$$\frac{\partial F_R}{\partial P_R} = \frac{10^{-6} K_R}{T_o\left(C_p \dot{m}\right)^2} \frac{\left(P_R + T_o C_p \dot{m}\right)^2}{\left(P_R + C_p \dot{m}\, T_o - C_p \dot{m}\right)} \tag{i}$$

We can neglect the term $C_p \dot{m}$ in the denominator of Equation i since it is

$$\langle\langle \left(P_R + C_p \dot{m}\, T_o\right)$$

$$\frac{\partial F_R}{\partial P_R} = -\frac{10^{-6} K_R}{T_o^2\left(C_p m\right)^2}\left(P_R + T_o\, C_p m\right) \tag{j}$$

The (–) sign could be discarded since it could refer to the direction of flow.

$$\frac{\partial F_R}{\partial P_R} \cong F_{ii}\, P_R + f_i \tag{k}$$

where

$$F_{ii} = \frac{10^{-6} K_R}{T_o^2\left(C_p \dot{m}\right)^{-2}} \tag{k'}$$

and

$$f_i = \frac{10^{-6} K_R}{C_p \dot{m}}$$

We have accomplished an important criterion for the incremental energy cost for geothermal direct conversion on the basis of Rankine cycle (which is expressed in Equation j) that is much more realistic than that of Equation 9.30. The slope of this curve is $F_{ii}$ and its vertical intercept is $F_i$.

Deriving a new incremental energy cost solution for $\partial F_R/\partial P_R$ could be obtained by considering the (+) sign in the denominator of Equation (f). This is left as a homework problem for the student.

## IX. SUMMARY

Resources of geothermal energy have been characterized into three categories, namely, hydrothermal, geopressured, and petrothermal modes. The hydrothermal system is the flow of

hot water or steam generated by direct contact with hot rocks, while geopressured systems are categorized in a mode where hot water or steam occupying a deep reservoir under an intense pressure of rock and heavy soil layers, and the petrothermal system is where magma close to the Earth surface heats up overlying rocks to a very high temperature, such that infection of water and then pumping it out carries a tremendous flow of thermal energy.

Effective utilization of geopressured systems is through a mode known as the direct flash steam cycle operation where a flow of a high temperature, beyond 200°C, released with depressurization will generate a huge amount of steam that can be used directly on steam turbines. An EPRI report[1] mentioned the clear advantage of using the rotary separator turbine in conjunction with the main steam turbine for more effectively leading to the release of mixed water and steam from geothermal wells. Another mode of geothermal energy extraction reported by EPRI is the binary cycle system which is based on producing high temperature gas through an interfacing process of low boiling temperature fluid with a closed loop carrying geothermal water and steam.

Systematic operational uses of geothermal power are based on two channels or principles. The first is the direct Rankine cycle and the second is the integration of geothermal system with steam cycle generating station. The main problem with the Rankine cycle system is the low efficiency that is about 7%, while that for the integrating system as reported in a paper by White and Phil[2] could be as high as 11%.

The integrating system employs geothermal hot water or steam to raise the temperature of the initial number of sections of the turbine feed water heater thereby allowing more steam within the turbine to remain internally and hence generating more electric power output. This second mode of utilizing geothermal power is also known as the feed water heating system.

This chapter proceeded to develop relationships for the incremental energy cost for both the direct Rankine cycle system and the feed water heating system. Compatible forms for the incremental energy cost similar to those of the conventional system have been developed and coupled with working multiplying factors applicable for an invariant [B] matrices that can be used in the design of power system networks and calculating transmission loss.

Also important aspects developed in this chapter are that the slope and vertical intercept of the standard incremental energy cost curve (the standard curve is a straight line that may or may not pass into the origin) which could be numerically calculated from the geothermal system parameters, namely, the specific heat at constant pressure and the rate of flow of hot water or steam, the sink temperature, and the plant constant.

## X. PROBLEMS

9.1 Integrate geothermal heat into the turbine steam cycle shown in Figure 9.4 by replacing the first, second, and third feed water heaters by a heat exchanger whose primary is connected to geothermal triplet. Write an expression for the work done by the turbine in terms of enthalpies, rate of steam bleed, and efficiency of stage in the turbine geothermal feed water heating system. Also write an expression for the combined system new efficiency.

9.2 Generalize Problem 9.1 for a geothermal feed water heating outlets connected to the turbine m feeders while the remaining turbine stages are M.

9.3 Using Equations 9.6 and 9.7, write an expression for the net geothermal turbine power, and then secure a solution for the enthalpy differential in the steam bled turbine to the corresponding case in which m stages have been fed by geothermal feed water heaters.

9.4 Repeat Problem 9.1 for a system in which all the feed water heaters have to be supplied by geothermal outlets.

9.5 The case study considered a solution for the incremental energy cost curve through linkage

of Equations 9.27 and 9.28. However for Equation f, the author dealt only with the (–) sign shown in the expression, whereby a compatible solution for $\partial F_R/\partial P_R$ was eventually obtained in Equation j. Now in this problem, strive to obtain another closed form solution for $\partial F_R/\partial P_R$ considering the (+) sign in Equation f. Compare the new solution with that of Equation j.

9.6 The solution for T in terms of geothermal power plant capacity as given by Equation 9.14 was based on expansion of lnT, where only the first term (T – 1/T) was considered, whereby solution for (T) was T established in Equation 9.27. Obtain another solution for T as a function of $P_R$ where

$$\ln T = \frac{T-1}{T} + \frac{(T-1)^2}{{}^2T^2}$$

9.7 From solution of $T = G(P_R)$ obtained in Problem 9.6 and linking with Equation 9.28, obtain a new solution for $\partial F_R/\partial P_R$ in terms of $P_R$. Simplify the solution to the standard form of:

$$\frac{\partial F_R}{\partial P_R} \simeq F_{ii}\, P_{R-i} + f_{i-R}$$

9.8 Repeat Problem 9.7, where,

$$\ln T \simeq \frac{T-1}{T} + \frac{(T-1)^2}{{}^2T^2} + \frac{(T-1)^3}{{}^3T^3}$$

9.9 Repeat Problem 9.7 for the solution of $T = G_i(P_R)$ obtained in Problem 9.8. Also simplify the expression for $F_R/P_R$ to the standard form of:

$$\frac{\partial F_R}{\partial P_R} \simeq F_{ii-R} + f_{i-R}$$

9.10 Equation 9.30 was obtained on the basis of setting $T_o = 0$ in Equation 9.27. Show with mathematical and physical arguments the controversy of this assumption and its validity or otherwise.

9.11 Equation 9.39 gives the incremental energy cost for geothermal feed water heating power which is constant and given by

$$f_i = A\,K'\frac{e}{C_p \dot{m}}$$

Consider that geothermal feed water heating replaces all fuel cell systems whose [B] matrices are given in Chapter 1. If $f_i$ is numerically equal to $f_i$ for the fuel cell, calculate elements of the [K] matrix at 60% loading for the 32 bus-bars. Hint: Use only diagonal elements of the [B] matrix in conjunction with the [R] matrices given in Chapter 2.

9.12 Repeat Problem 9.11 for the case of 100% loading.

9.13 Four geothermal direct Rankine cycle plants have their incremental energy cost curves specified by:

| Plant | $C_p$ | $F_{ii}$ | $f_i$ | $\dot{m}$ |
|---|---|---|---|---|
| 1 | 10 | 0.008 | 1.2 | 1 kg/s |
| 2 | 10 | 0.004 | 0.8 | 1 kg/s |
| 3 | 10 | 0.002 | 1.4 | 1 kg/s |
| 4 | 10 | 0.001 | 0.7 | 1 kg/s |

Using Equations k given in the case study, solve for each plant constant k and $T_o$.

9.14 If the plant capacities of the four plant system specified in Problem 9.13 have optimal power limits given by:

| Plant | MW |
|---|---|
| 1 | 260 |
| 2 | 210 |
| 3 | 270 |
| 4 | 420 |

Use Equation j in the case study to establish the incremental energy cost curve for each plant.

9.15 Repeat Problem 9.13 for the following four plants:

| Plant | $F_{ii}$ | $f_i$ | $C_p$ | $\dot{m}$ |
|---|---|---|---|---|
| 1 | 0.0024 | 0.9 | 10 | 10 kg/s |
| 2 | 0.014 | 0.3 | 10 | 10 kg/s |
| 3 | 0.018 | 0.6 | 10 | 10 kg/s |
| 4 | 0.020 | 0.5 | 10 | 10 kg/s |

9.16 Repeat Problem 9.14 if optimal power limits of the four plants in Problem 9.15 are

| Plant | MW |
|---|---|
| 1 | 140 |
| 2 | 210 |
| 3 | 80 |
| 4 | 250 |

9.17 Four geothermal power plants operate with linkage to fossil-steam cycle stations through feed water heating, each has the following parameters:

| Plant | Optimal (MW) | m | $C_p$ | $T_o$ | k |
|---|---|---|---|---|---|
| 1 | 150 | 10 kg/s | 10 | 60 | $0.5 \times 10^4$ |
| 2 | 250 | 10 kg/s | 10 | 60 | $10^5$ |
| 3 | 300 | 10 kg/s | 10 | 60 | $2 \times 10^5$ |
| 4 | 400 | 10 kg/s | 10 | 60 | $0.8 \times 10^5$ |

Establish, using Equation 1.4 of Chapter 1 the optimal [B] matrix.

9.18 For the Problem of 9.17, using the incremental energy cost for each plant, calculate the change of total transmission loss $P_L$ with respect to each plant capacity in terms of $\lambda$ (the cost of received power).

# REFERENCES

1. **Charlson, M.,** Geothermal: new potential underground, *EPRI J.*, December, 18, 1981. Written by Michael Charlson, communication specialist. Technical background information was provided by Vasel Roberts, Advanced Power Systems Division, EPRI, Palo Alto, CA.
2. **White, A. A. L. and Phil, D.,** Advantage of incorporating geothermal energy into power-station cycles, *IEE Proc.*, 127 ( A, No. 5), 330, 1980.

Chapter 10

# OCEAN THERMAL ENERGY CONVERSION SYSTEMS (OTEC)

## I. INTRODUCTION

Ocean thermal energy represents the huge amount of solar energy transformed to the vast volume of ocean water creating a clear temperature gradient of the order of 20°C across an ocean depth of about 1 km. Current research on OTEC in tropical zones such as near Puerto Rico, Hawaii, and in Southwest Asia points to clear economic feasibility for extracting thermal energy from ocean water through various systems such as floating platform and deep cold water pipe system. Thermal energy extracted consequently could be used in a conventional steam cycle power plant, istentropic decomposition of water into hydrogen and oxygen followed by using both $H_2$ and $O_2$ as fuel in conventional $H_2$-$O_2$ fuel cell. Another area where OTEC thermal output could be used is in the processed air liquification and eventual extraction of $NH_3$ (ammonia).

However, economic feasibility of OTEC systems are still along the road of continuous research which seeks reliable data and information about ocean water in tropical zones including conditions of salinity, temperature contours, pressure distribution, thermal and electrical conductivities, specific heats, and most importantly the operating efficiency.

In this chapter, the author will present thermal characterizations of ocean water and methods of calculating actual values for ocean water specific heat capacities, and then presentation of OTEC-CWP systems which is now in the forefront from the standpoint of operation and economic feasibility as a promising OTEC plant.

Indirect modes for utilizing OTEC thermal output include linkage to magnetohydrodynamic (MHD) power generation system whereby ocean thermal energy could be used to preheat the MHD working fluid to an operational temperature, and the application of OTEC thermal energy in the isentropic decomposition of water into $H_2$ and $O_2$ where $O_2$ which can be used in the process of oxidation of prepared refuse into synthetic fuel. As mentioned earlier both $H_2$ and $O_2$ could be used in the electrochemical process of the conventional fuel cell.

Another mode of using OTEC output involves its utilization in floating agricultural farms, which is in effect a process of oxidation for ultimate production of food.

## II. THERMAL CHARACTERIZATION OF OCEAN WATER*

The purpose of this section is to present polynomial modelling for thermal properties of ocean water that are relevant to OTEC processes. These properties include salinity, electrical conductivity, temperature and pressure. In the paper published by Poisson[2] identified standard seawater as having 35% salinity and with temperature ranging from –1 to 30°C. A polynomial linking salinity to seawater electrical resistance that was verified experimentally for the standard salinity of 35% is expressed as follows:

$$S = A_o + A_1\sqrt{R} + A_2 R + A_3 R\sqrt{R} \tag{10.1}$$

Salinity is also expressed in a power series in terms of seawater resistance at 15°C.

$$S = \sum_{n=1}^{\infty} A_n R_{15}^n \tag{10.2}$$

* © 1980, IEEE. Reprinted with permission from Poisson, A., Conductivity/salinity/temperature relationship of diluted and concentrated standard seawater, *IEEE J. Oceanic Eng.*, OE-5, No. 1, 41—50, 1980.

where $A_1 = 26.6963$, $A_2 = 26.7686$, $A_3 = 67.2337$, $A_4 = 132.149$, $A_5 = 168.1207$, $A_6 = 130.8093$, $A_7 = -56.3388$, and $A_8 = 10.2700$.

Another form for salinity (S) has been indicated by Poisson in his paper[2] that contains only three coefficients,

$$S = 35\left[A_1\left(R_{15}\frac{5}{2} - R_{15}\right) + A_2\left(R_{15}^2 - R_{15}\right) + \right. \tag{10.3}$$

$$\left. A3\left(R_{15}\frac{3}{2} - R_{15}\right) + R_{15}\right] \tag{10.4}$$

where $A_1 = 0.08887$, $A_2 = 0.2368$, and $A_3 = 0.44499$.

$R_{15}$ is given by:

$$R_{15} = R_T + 10^{-5}\, R_T\left(R_T - 1\right)(T - 15)\left[96.7 - 72\, R_T + 37.3\, R_T^2 - \left(0.63 + 0.21\, R_T^2\right)(T - 15)\right] \tag{10.5}$$

where

$$R_T = \frac{G_{\text{measured}}\ (T)}{G_{\text{at S}} = 35\%} \text{ at temperature T} \tag{10.6}$$

In Equation 10.6, $G_{\text{measured}}$ = measured electrical conductance in $1/\cup$ - cm at temperature T°C. $G_{\text{at S}} = 35Y$ = electrical conductance of seawater at 35% salinity.

Another more general form for S as a function of $R_T$, T is given by Poisson's paper[2] as follows:

$$S = 35\left[A_1\left(R_T\frac{5}{2} - R_T\right) + A_2\left(R_T{}^2 - R_T\right) + A_3\right.$$

$$\left.\left(R_T\frac{3}{2} - R_T\right) + R_T\right] + R_T\left(R_T - 1\right)(T - 15) +$$

$$\left[B_o + R_T^{\frac{1}{2}}\left(B_1 R_T + B_2\, T\right) + TR_T^{\frac{1}{2}}\left(B_3 T + B_4 R_T^{\frac{1}{2}}\right)\right] \tag{10.7}$$

where $A_1$, $A_2$, and $A_3$ are the same constants listed in Equation 10.4 and,

$$\begin{aligned} B_0 &= 3.57944 \times 10^{-2} \\ B_1 &= -1.52869 \times 10^{-3} \\ B_2 &= -1.43951 \times 10^{-4} \\ B_3 &= 8.31276 \times 10^{-6} \\ B_4 &= 7.25836 \times 10^{-4} \end{aligned} \tag{10.8}$$

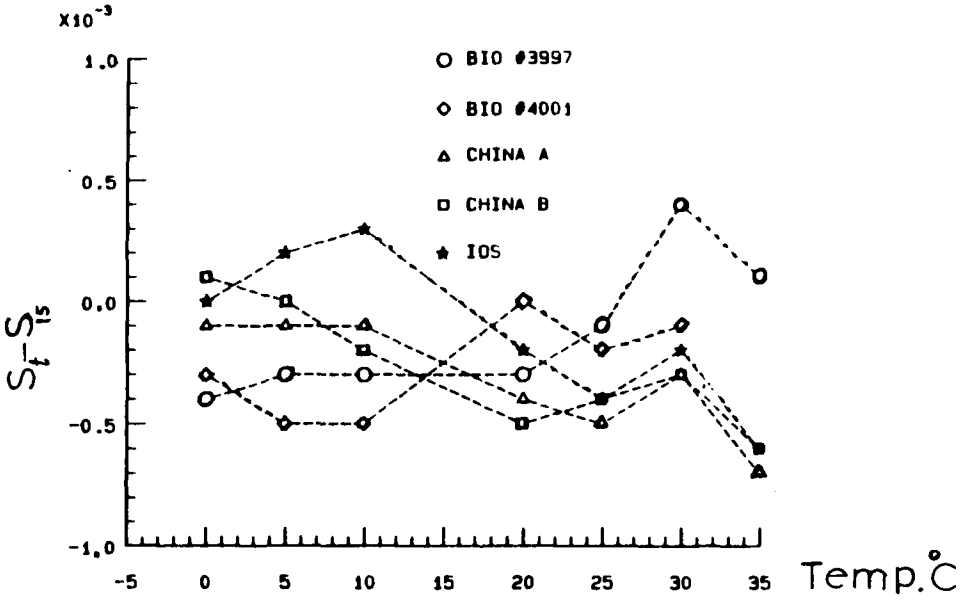


FIGURE 10.1 Difference between salinity measured at various temperatures w.r.t 15°C for Atlantic and Pacific oceans. (From Hill, K. D., Dauphinee, T. M., and Woods, D. J., A comparison of the temperature coefficients of electrical conductivity of Atlantic and Pacific seawaters, *IEEE J. Oceanic Eng.*, OE-11, No. 4, 485—486, 1986. With permission.)

Poisson also pointed out in his paper that Dauphinee and Klein[1] presented a ratio for the electrical conductivity of standard seawater at salinity of 35% and at a temperature T°C to that of the same salinity and at temperature of 15°C. The conductivity ratio $R_D$ is given by:

$$R_D = \frac{\sigma_{T,35}}{\sigma_{15,35}} = 0.6765836 + 2.005284 \times 10^{-2} T$$

$$= 1.110990 \times 10^{-4}\ T^2 - 7.266\overset{-2}{8}4 \times 10^{-7}\ T^3 + 1.3587 \times 10^{-9}\ T^4 \qquad (10.9)$$

For diluted and evaporated seawater, an expression given by the Poisson paper[2] for the specific conductance is written below:

$$G = R_T\ G_{T,35} \qquad (10.10)$$

where G is the conductance at any S and T and $R_T$ is given by Equation 10.6.

$$G_{T,35} = 0.042933\ R_D \qquad (10.11)$$

In another published work by Hill, Dauphinee, and Woods[7] in Oceanic Engineering, a state of comparison for the electrical conductivities and water salinity at the Atlantic and Pacific oceans are indicated in Figure 10.1 and Table 10.1. Table 10.2 gives data for salinity and ratio of conductivities at a range of temperature between –1 and 35°C.

## TABLE 10.1
## Conductivity of Water Salinity

| Sample designation | Location (latitude, longitude) | Depth (m) | Salinity (at 15°C) |
|---|---|---|---|
| BIO #3997 | 28°57.26′N,23°21.34′W | 1800 | 35.18 |
| BIO #4001 | 28°57.26′N,23°21.34′W | 100 | 36.67 |
| CHINA A | 8°40′N,154°E | — | 34.42 |
| CHINA B | 28°N,126°E | — | 34.39 |
| IOS | 49°58.5′N,145°3.1′W | 75 | 32.65 |

From Hill, K. D., Dauphinee, T. M., and Woods, D. J., A comparison of the temperature coefficients of electrical conductivity of Atlantic and Pacific seawaters, *IEEE J. Oceanic Eng.*, OE-11, No. 4, 485—486, 1986. With permission.

## TABLE 10.2
## Measured Data of Temperature (°C), Salinity (‰), and Conductivity Ratio of Different Samples Investigated

| Temperature (°C) | Salinity (‰) | Conductivity Ratio | Temperature (°C) | Salinity (‰) | Conductivity Ratio |
|---|---|---|---|---|---|
| 30.0017 | 30.0478 | 0.873012 | 15.0012 | 12.3669 | 0.388364 |
| 30.0017 | 25.0230 | 0.740915 | 15.0012 | 10.0021 | 0.319347 |
| 30.0017 | 20.1911 | 0.610507 | 15.0012 | 7.5159 | 0.245126 |
| 30.0017 | 14.9670 | 0.465019 | 15.0012 | 6.0375 | 0.199987 |
| 30.0017 | 10.0215 | 0.322045 | 15.0012 | 4.3603 | 0.147642 |
| 30.0017 | 6.1719 | 0.205843 | 15.0012 | 34.9884 | 0.999258 |
| 30.0017 | 4.0684 | 0.139738 | 15.0012 | 34.9710 | 0.999258 |
| 30.0017 | 30.0095 | 0.872024 | 15.0012 | 37.5027 | 1.063534 |
| 30.0017 | 25.0074 | 0.740521 | 15.0012 | 38.9517 | 1.100069 |
| 30.0017 | 19.9995 | 0.605248 | 15.0012 | 40.5259 | 1.139422 |
| 30.0017 | 15.0141 | 0.466387 | 15.0012 | 41.7295 | 1.169348 |
| 30.0017 | 9.9930 | 0.321209 | 15.0012 | 34.9942 | 0.999864 |
| 30.0017 | -5.0260 | 0.170125 | 15.0012 | 34.9969 | 0.999925 |
| 30.0017 | 34.9954 | 0.999876 | 15.0012 | 37.3845 | 1.060587 |
| 30.0017 | 34.9849 | 0.999625 | 15.0012 | 38.9584 | 1.100185 |
| 30.0017 | 37.4448 | 1.061587 | 15.0012 | 39.8064 | 1.121439 |
| 30.0017 | 37.5256 | 1.063599 | 15.0012 | 41.0265 | 1.151893 |
| 30.0017 | 39.0172 | 1.100815 | 9.9994 | 29.9844 | 0.870033 |
| 30.0017 | 40.5543 | 1.138933 | 9.9994 | 25.0037 | 0.738059 |
| 30.0017 | 41.0051 | 1.150048 | 9.9994 | 20.0230 | 0.602831 |
| 24.9976 | 30.0202 | 0.872045 | 9.9994 | 15.0673 | 0.464577 |
| 24.9976 | 24.9990 | 0.739864 | 9.9994 | 10.0138 | 0.318723 |
| 24.9976 | 19.9902 | 0.6044512 | 9.9994 | 5.0944 | 0.170074 |
| 24.9976 | 14.9934 | 0.465126 | 9.9994 | 4.1130 | 0.139213 |
| 24.9976 | 10.0465 | 0.322145 | 9.9994 | 30.0178 | 0.870909 |
| 24.9976 | 5.9969 | 0.199964 | 9.9994 | 25.0006 | 0.737996 |
| 24.9976 | 4.0410 | 0.138453 | 9.9994 | 20.0137 | 0.602577 |
| 24.9976 | 29.9628 | 0.870587 | 9.9994 | 15.0762 | 0.464809 |
| 24.9976 | 24.9772 | 0.739284 | 9.9994 | 9.9956 | 0.318181 |
| 24.9976 | 19.9844 | 0.604258 | 9.9994 | 5.9490 | 0.196547 |
| 24.9976 | 14.9842 | 0.464863 | 9.9994 | 4.0995 | 0.138805 |
| 24.9976 | 10.0350 | 0.321843 | 10.0006 | 41.4145 | 1.162192 |
| 24.9976 | 5.0759 | 0.171246 | 10.0006 | 40.1035 | 1.129397 |
| 24.9984 | 41.5858 | 1.164815 | 10.0006 | 38.5247 | 1.089653 |
| 24.9984 | 39.6100 | 1.115869 | 10.0006 | 36.4773 | 1.037740 |
| 24.9984 | 38.4337 | 1.086534 | 10.0006 | 35.0089 | 1.000228 |
| 24.9984 | 36.4373 | 1.036385 | 5.0019 | 30.0242 | 0.870578 |
| 24.9984 | 34.9875 | 0.999682 | 5.0019 | 24.9280 | 0.735139 |
| 20.0035 | 29.9938 | 0.871051 | 5.0019 | 22.5201 | 0.670066 |

**TABLE 10.2 (continued)**
**Measured Data of Temperature (°C), Salinity (‰), and Conductivity Ratio of Different Samples Investigated**

| Temperature (°C) | Salinity (‰) | Conductivity Ratio | Temperature (°C) | Salinity (‰) | Conductivity Ratio |
|---|---|---|---|---|---|
| 20.0035 | 24.8679 | 0.735824 | 5.0019 | 20.0431 | 0.602291 |
| 20.0035 | 20.0005 | 0.603925 | 5.0019 | 17.3937 | 0.528774 |
| 20.0035 | 15.0120 | 0.464928 | 5.0019 | 15.0916 | 0.464053 |
| 20.0035 | 9.9426 | 0.318437 | 5.0019 | 12.1025 | 0.378521 |
| 20.0035 | 6.0127 | 0.199874 | 5.0019 | 10.0373 | 0.318303 |
| 20.0035 | 4.0634 | 0.138753 | 5.0019 | 5.9987 | 0.197184 |
| 20.0035 | 30.0012 | 0.871256 | 5.0019 | 4.1290 | 0.139058 |
| 20.0035 | 24.9075 | 0.736879 | 5.0019 | 30.0074 | 0.870125 |
| 20.0035 | 20.0053 | 0.604123 | 5.0019 | 24.9541 | 0.735834 |
| 20.0035 | 15.0048 | 0.464724 | 5.0019 | 22.5741 | 0.671528 |
| 20.0035 | 9.9607 | 0.318929 | 5.0019 | 20.0358 | 0.602051 |
| 20.0035 | 5.0602 | 0.170258 | 5.0019 | 17.4056 | 0.529126 |
| 20.0021 | 41.4313 | 1.161483 | 5.0019 | 15.0998 | 0.464254 |
| 20.0021 | 40.0680 | 1.127621 | 5.0019 | 10.0264 | 0.318003 |
| 20.0021 | 38.6639 | 1.092554 | 5.0019 | 5.1327 | 0.170452 |
| 20.0021 | 37.0106 | 1.050973 | 4.9987 | 40.7558 | 1.146415 |
| 20.0021 | 34.9778 | 0.999435 | 4.9987 | 39.1240 | 1.105247 |
| 15.0012 | 32.4731 | 0.935127 | 4.9987 | 37.2700 | 1.058142 |
| 15.0012 | 29.9881 | 0.870591 | 4.9987 | 34.9938 | 0.999841 |
| 15.0012 | 28.0543 | 0.819853 | 0.0027 | 30.2748 | 0.876584 |
| 15.0012 | 25.0932 | 0.741224 | 0.0027 | 24.9904 | 0.735759 |
| 15.0012 | 22.4491 | 0.670037 | 0.0027 | 19.8961 | 0.596834 |
| 15.0012 | 20.3120 | 0.611742 | 0.0027 | 14.9730 | 0.459203 |
| 15.0012 | 17.4156 | 0.531649 | 0.0027 | 10.0068 | 0.316054 |
| 15.0012 | 14.8162 | 0.458511 | 0.0027 | 6.1337 | 0.200299 |
| 15.0012 | 12.4784 | 0.391586 | 0.0027 | 4.1697 | 0.139515 |
| 15.0012 | 9.9905 | 0.318987 | 0.0012 | 40.7391 | 1.146852 |
| 15.0012 | 7.5308 | 0.245582 | 0.0012 | 39.1867 | 1.107453 |
| 15.0012 | 6.0565 | 0.200581 | 0.0012 | 36.9453 | 1.050127 |
| 15.0012 | 4.5068 | 0.152250 | 0.0012 | 34.9707 | 0.999241 |
| 15.0012 | 32.2967 | 0.930563 | −1.1047 | 30.0120 | 0.869544 |
| 15.0012 | 30.0339 | 0.870789 | −1.1047 | 24.9921 | 0.735548 |
| 15.0012 | 27.9890 | 0.818125 | −1.1047 | 20.0851 | 0.601747 |
| 15.0012 | 25.2659 | 0.745856 | −1.1047 | 14.9814 | 0.459095 |
| 15.0012 | 22.4431 | 0.669874 | −1.1047 | 10.0052 | 0.315716 |
| 15.0012 | 20.2692 | 0.610584 | −1.1047 | 6.0268 | 0.196808 |
| 15.0012 | 17.5994 | 0.536771 | −1.1047 | 4.2584 | 0.142138 |
| 15.0012 | 15.1242 | 0.467218 | | | |

From Poisson, A., Conductivity/salinity/temperature relationship of diluted and concentrated standard seawater, *IEEE J. Oceanic Eng.*, OE-5, No. 1, 41—50, 1980. With permission.

## III. SPECIFIC HEAT OF SEAWATER

According to the laws of Dulong and Petit and Neumann, there exists a number of elements and compounds that have in their liquid state the same molar heats as those in solid state, namely 6 cal/mol/atom.

Figure 10.2 illustrates variation of the specific heat of water at any pressure for every parametric temperature in °C. $C_p$ represents the practical parameter for calculating the quantity of heat transfer in OTEC systems whereby the amount of heat transferred Q is given by:

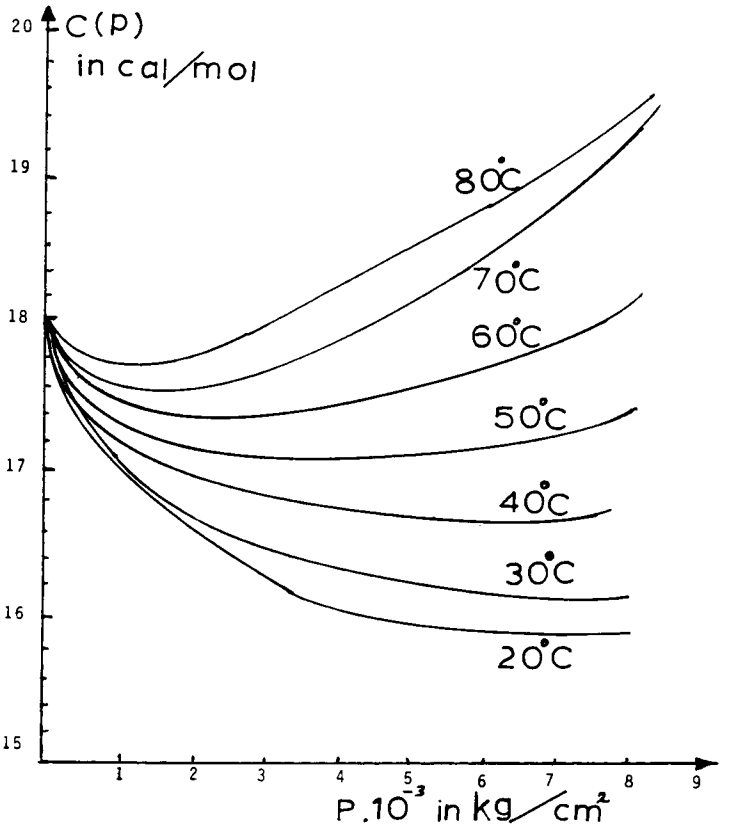


FIGURE 10.2 Specific heat of water as function of pressure.[5]

$$Q = m\,C_p(T_2 - T_1) \tag{10.12}$$

where $T_2 - T_1 = \Delta T$ the temperature gradient, m = quantity of water in kilograms, Q = heat transfer in calories.

C can be calculated from the following equation:

$$C_p - C_v = R \tag{10.13}$$

where R = 1.9864 in cal 1°C/mol which is the universal constant.

Now, from Figure 10.1, we can present a piecewise linearized expression for the salinity of seawater against temperature T in °C. There are five samples of seawater represented in Figure 10.1, however in the following, only China A seawater has been selected.

Functional polynomial representation of $S - S_{15}$ against temperature T is given as follows with respect to several temperature ranges:

$$A_i\ 0 \le T \le 10°C$$

$$S - S_{15} = -0.1 \tag{10.14}$$

$$B_i\ 10 \le T \le 25°C$$

$$S - S_{15} = -0.026\,T + 0.16 \tag{10.15}$$

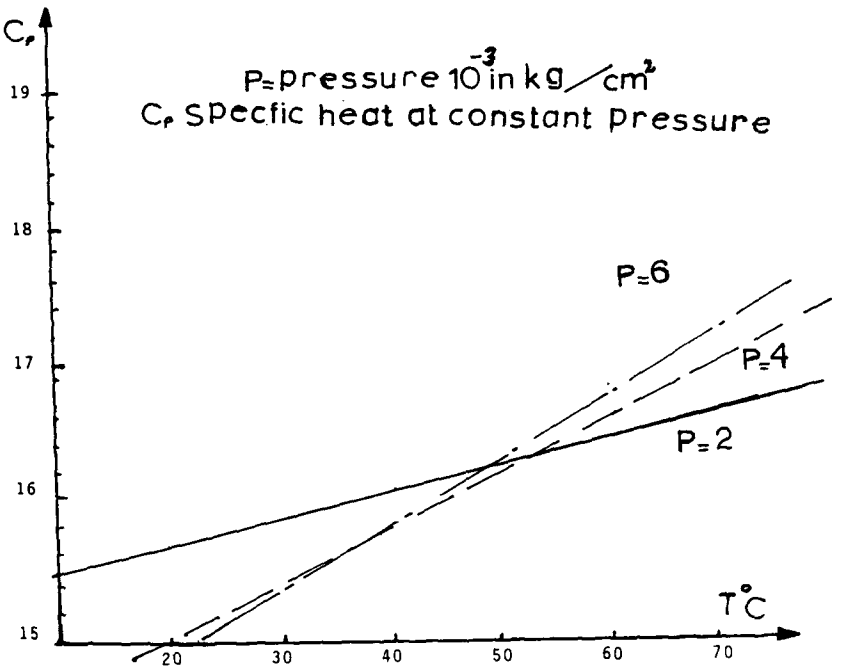


FIGURE 10.3 $C_p$ V, T.

$C_1 25 \le T \le 30°C$

$$S - S_{15} = 0.04\ T + 0.5 \tag{10.16}$$

$D_1 30 \le T \le 35$

$$S - S_{15} = -0.06\ T + 1.2 \tag{10.17}$$

where $S_{15}$ for China A = 34.42 as seen in Table 10.1.

From Figure 10.2 and Figure 10.3, functional representations for $C_p$ against T have been established under four seawater pressure conditions as shown:

$A_2$ $\quad P = 2 \times 10^{-3}\ kg/cm^2$

$$C_p = 0.066T + 16.5 \tag{10.18}$$

or

$$T = 7.5\ C_p - 247.5 \tag{10.19}$$

$B_2$ $\quad P = 4 \times 10^{-3}\ kg/cm^2$

$$C_p = 0.0366T + 15.268 \tag{10.20}$$

or

$$T = 27.27\ C_p - 471.8 \tag{10.21}$$

$C_2$ $\quad P = 6 \times 10^{-3}\ kg/cm^2$

$$C_p = 0.045T + 15 \tag{10.22}$$

or

$$T = 22.22\ C_p - 333.33 \tag{10.23}$$

$D_2$ $\quad P = 8 \times 10^{-3}\ kg/cm^2$

$$C_p = 0.046T + 15.07 \tag{10.24}$$

or

$$T = 21.42\ C_p - 327.6 \tag{10.25}$$

Since OTEC thermal transfer is generally expressed by:

$$Q = m\ C_p \Delta T \tag{10.26}$$

where m is the mass of ocean water, $\Delta T$ is the temperature gradient, and $C_p$ is the specific heat at a specific pressure.

Therefore, it is extremely important to provide information for the functional form of ocean water salinity (S) against $C_p$.

For CHINA A seawater, we would like to write functional expressions for $S - S_{15}$ at various pressure conditions.

From the set of Equations 10.14 to 10.17 and 10.18 to 10.25, the following expressions of ($S - S_{15}$) against $C_p$ have been derived:

$A_3$ $\quad$ at $P = 2 \times 10^{-3}\ kg/cm^2$

$$1)\ 0 \le T \le 10°C \tag{10.27}$$

$$S - S_{15} = -0.1$$

$$2)\ 10 \le T \le 25°C \tag{10.28}$$

$$S - S_{15} = -0.175\ C_p + 6.595$$

$$3)\ 25 \le T \le 30°C \tag{10.29}$$

$$S - S_{15} = -0.3\ C_p - 9.40$$

$$4)\ 30 \le T \le 35°C \tag{10.30}$$

$$S - S_{15} = -0.45\ C_p + 16.15$$

$B_3$ $\quad P = 4 \times 10^{-3}\ kg/cm^2$

$$1)\ 0 \le T \le 10°C \tag{10.31}$$

$$S - S_{15} = -0.1$$

2) $10 \le T \le 25°C$ (10.32)

$$S - S_{15} = -0.709\ C_p + 12.42$$

3) $25 \le T \le 30°C$ (10.33)

$$S - S_{15} = -1.09\ C_p - 18.372$$

4) $30 \le T \le 35°C$ (10.34)

$$S - S_{15} = -1.636\ C_p + 29.508$$

$C_3$ $P = 6 \times 10^{-3}\ kg/cm^2$

1) $0 \le T \le 10°C$ (10.35)

$$S - S_{15} = -0.1$$

2) $10 \le T \le 25°C$ (10.36)

$$S - S_{15} = -0.5777\ C_p + 8.826$$

3) $25 \le T \le 30°C$ (10.37)

$$S - S_{15} = -0.8888\ C_p - 12.833$$

4) $30 \le T \le 35°C$ (10.34)

$$S - S_{15} = -1.333\ C_p + 21.1998$$ (10.38)

$D_3$ $P = 8 \times 10^{-3}\ kg/cm^2$

1) $0 \le T \le 10°C$ (10.39)

$$S - S_{15} = -0.1$$

2) $10 \le T \le 25°C$ (10.40)

$$S - S_{15} = -0.55092\ C_p + 1.01176$$

3) $25 \le T \le 30°C$ (10.41)

$$S - S_{15} = -0.8568\ C_p - 12.60$$

4) $30 \le T \le 35°C$ (10.42)

$$S - S_{15} = -1.2852\ C_p + 20.856$$

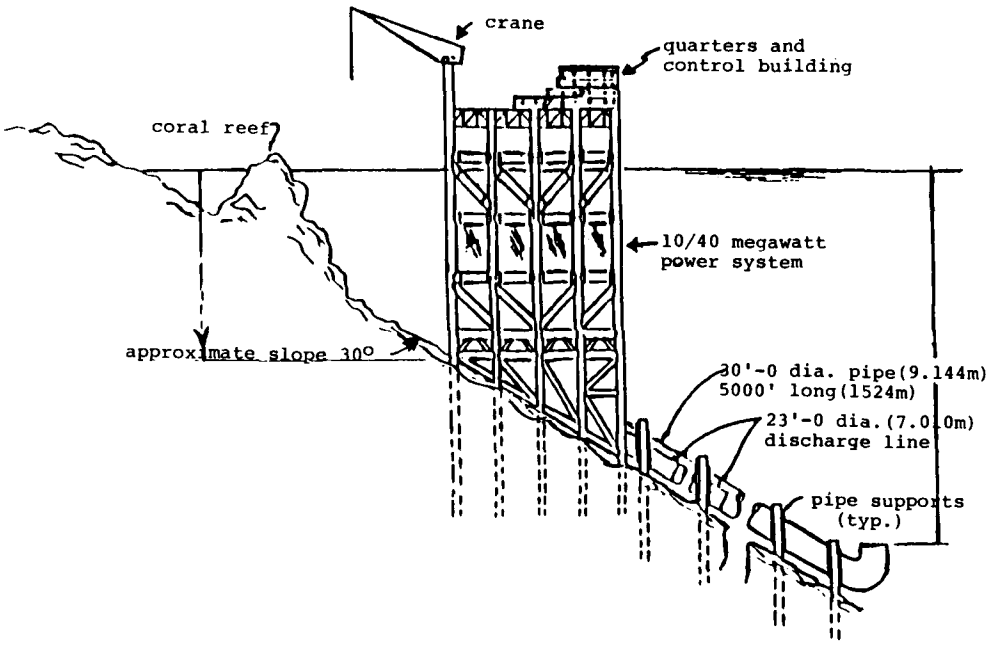


FIGURE 10.4 An early conceptual design for a shelf based OTEC power plant. (From Vadus, J. R. and Taylor, B. J., OTEC — cold-water pipe research, *IEEE J. Oceanic Eng.*, OE-10, No. 2, 114—122, 1985. With permission.)

## IV. OTEC COLD WATER PIPE SYSTEM*

Current research being conducted by National Oceanic and Atmospheric Administration (NOAA) in cooperation with the U.S. Department of Energy (DOE) has been directed toward the development of OTEC computer models for land based, shelf mounted, and fixed systems. The models objective is to set practical procedure for the design, deployment, inspection, maintenance, and repair for feasible operational OTEC systems. The shelf mounted OTEC plant is currently receiving the most attention due to its easy access to warm and cold water as well as it is more economical and practical to house the mechanical system in close proximity to ocean waters having the required $\Delta T$.

Operation of OTEC-CWP (cold water pipe) system is being considered in research work as a challenge due to the tremendous installation work needed which involves slope pipe of the order of 1 km length in a system of water flow around 227,000 l/min/MW. A land based 40 MW power plant requires a pipe of 10 m diameter and 900 m long. A shelf mounted OTEC-CWP system may need as much as 3 km length of pipe with a downward slope on the order of 45°. The main concern of this system is in its ability to withstand cyclic change of loading, especially the flexibility of the coupling joints.

Figure 10.4 shows a shelf-based OTEC power plant from a published work by Vadus and Taylor[3] in IEEE Journal of Oceanic Engineering.

Figure 10.5 illustrates eight conceptual designs for OTEC platform models. NOAA undertook a comparative study for the models shown in Figure 10.5 with regard to design, construction, deployment, installation, operation, maintenance, repair, and survivability.

Also of interest is the foundations of several models for the OTEC-CWP system as shown in Figure 10.6.

* © 1985, IEEE. Reprinted with permission from Vadus, J. R. and Taylor, B. J., OTEC — cold-water pipe research, *IEEE J. Oceanic Eng.*, OE-10, No. 2, 114—122, 1985.

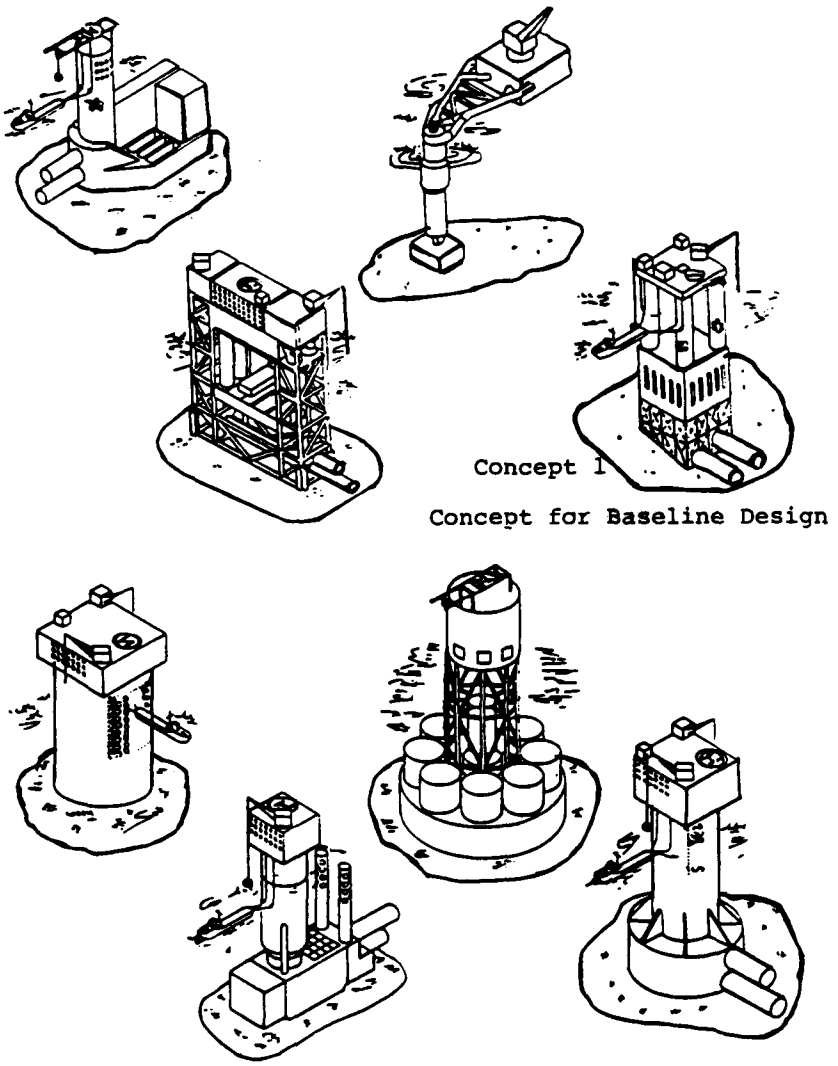


FIGURE 10.5 Eight conceptual OTEC designs. (From Vadus, J. R. and Taylor, B. J., OTEC—cold-water pipe research, *IEEE J. Oceanic Eng.*, OE-10, No. 2, 114—122, 1985. With permission.)

Information from the paper by Vadus and Taylor[3] pointed out to testing on a shelf mounted CWP system for hydrodynamic forces due to ocean water waves and currents. Environmental and test article design conditions for the testing experiment are reproduced as follows:

| Parameter | Design Condition |
|---|---|
| Pipe diameter | 2.4 m |
| Clearance, bottom of pipe to seabed | 1.7 m |
| Roughness (fouled) | 6.44 |
| Slope | 35 to 40° |
| Wave height (significant) | 6.1 m |
| Period (significant) | 10.6 s |
| Maximum current | 1.52 m/s |
| Reynolds number, Re | $2.3 \times 10^6$ |
| Keulegan-Carpenter number | 4.0 |

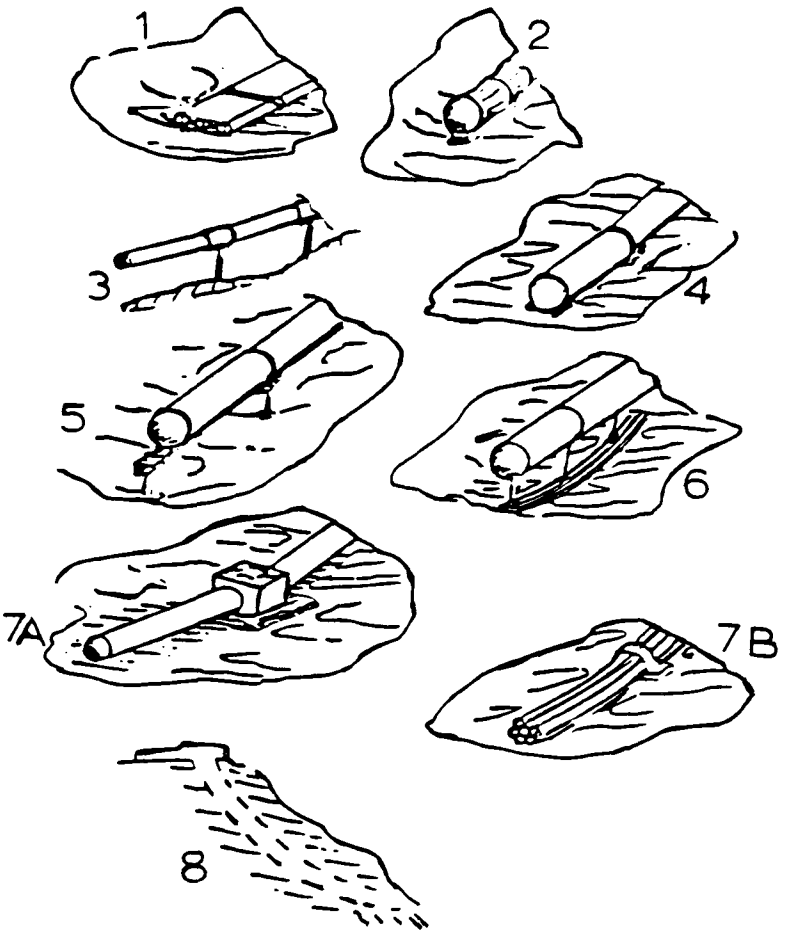


FIGURE 10.6 Various slope mounted cold water pipe concepts. (From Vadus, J. R. and Taylor, B. J., OTEC — cold-water pipe research, *IEEE J. Oceanic Eng.*, OE-10, No. 2, 114—122, 1985. With permission.)

The following measurements are being made during the experiment:

| Parameter | Design Condition |
|---|---|
| Sea surface elevation | Waverider buoy |
| Pressure at fixed depth | Digiquartz pressure transducers |
| Velocity magnitude in x and y directions | Neil Brown and Marsh McBirney current meters |
| Pipe loads | Metrox load-cell system |
| Pipe torsion | Metrox load-cell system |

As reported in the paper by Vadus and Taylor[3] and reproduced as follows, analysis of data from the experiment include:

1. Determining relationships between pressure at the pipe, wave heights, and periods.
2. Determining the relationship between offshore wave heights and periods and those measured at the test site.

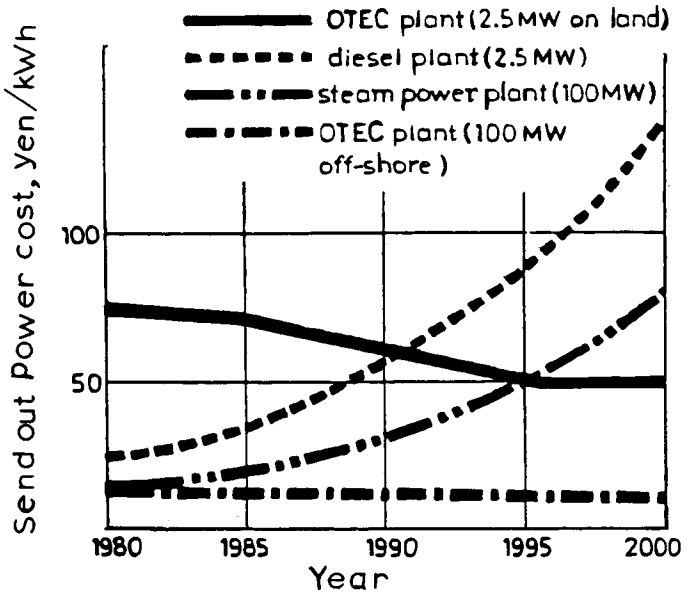


FIGURE 10.7 Send out power generation cost of OTEC plant and diesel steam power plant. (From Ford, G., Niblett, C., and Walker, L., Ocean-thermal energy conversion, *IEE Proc.*, 130 (A, No. 2), 93—100, 1983. With permission.)

3. Determining correlation between loading on the floating test ring and parameters derived from corresponding time history record of velocity magnitudes.
4. Deriving time histories of acceleration.
5. Obtaining pure inertial model force transfer coefficients by least square fit analysis.
6. Obtaining Morison equation coefficients by least square fit analysis.
7. Conducting spectral analysis of data.

Some of the remaining research objectives for the OTEC-CWP system to be operational include the following:

1. Construction and deployment techniques for cold water pipes and foundations.
2. Geotechnical measurement techniques and instrumentation to measure engineering properties associated with soil structure interaction of slope mounted systems.
3. Operational safety, inspection, maintenance, repair, and retrieval of submerged components.
4. Long term materials characteristics for cold water pipes.
5. Hydrodynamic loads on CWP caused by vortex shedding.
6. Piling and anchoring for both steep slopes and rock conditions.
7. Slope and foundation stability for shelf mounted platform and cold water pipe installations.

## V. COST OF OTEC POWER

From a published work by Ford, et al.,[4] a picture of comparative cost estimates at 1977 to 1978 prices indicates that an average cost is around 2.6 ¢/kWh compared to 3 ¢/kWh for coal fired and nuclear pressure water reactors. The same paper reported a comparative picture for the send out power generation cost with respect to a diesel steam power plant as shown reproduced in Figure 10.7. In this figure, we observe that a land based OTEC system of 2.5 mW has its yearly cost declining after 1985 with eventual levelling by 1995.

For a shelf mounted off shore OTEC system, the observation from Figure 10.7 for a 100 mW plant is that the annual cost is relatively the least and will continue along the same pattern up to the year 2000. The observed cost in yen per kilowatthour for OTC is about 15 yen/kWh which is about 12 ¢/kWh.

Therefore, we can conclude that the incremental cost curve for an off shore OTEC plant is of the form:

$$\frac{\partial F_i}{\partial P_i} = f_i \tag{10.43}$$

and

$$f_i = 6 \times 10^{-3} \times 10^{-2} = 60 \ \$ / \text{MWh}$$

Now, since we have determined that the form of the energy cost curve is a straight line with only vertical intercept ($L_i$) and zero slope ($F_{ii} = 0$), it is time for the next step to identify multiplying factors for invariant [B] matrices already established for centralized power systems. Those [B] matrices as have been indicated in all the preceding chapters, already established in Chapter 1 for the 32 centralized bus-bars, each for a total loading of 13,000 MW, and at loading ranging from 60 to 100%, could be used in the process of design.

These multiplying factors for an incremental energy cost curve of the form similar to Equation 10.14 have been derived in Equations 4.109 and 4.110 which are as follows.

For the sake of completeness and convenience for the reader, the parameters $A_1$, $C_1$, $D_1$, and $E_1$ are rewritten with $F_{ii} = 0$.

$$K_1 = 1 - \frac{A_1}{C_1 f_{i-old}} \tag{10.44}$$

$$K_2 = 1 + \frac{D_1}{E_1 f_{i-old}} \tag{10.45}$$

$$F_{ii} = 0$$

$$A_1 = f_{j-old} - \lambda^2 \tag{10.46}$$

$$C_1 = \lambda - f_{j-old} \tag{10.47}$$

$$D_1 = 2\lambda - P_j f_{j-old} - 2\lambda^2 \left(P_i - P_j\right) \tag{10.48}$$

$$E_1 = 2\lambda P_i \tag{10.49}$$

Also to indicate that:

$$L_{i-new} = K_1 f_{i-old} \quad \text{or} \tag{10.50}$$

$$= K_2 f_{i-old} \tag{10.51}$$

and

$$L_{j-new} = K_1 f_{j-old} \quad \text{or} \tag{10.52}$$

$$= K_2 f_{j-old} \tag{10.53}$$

From Equations 10.17 to 10.20, the parameters $A_1$, $C_1$, $D_1$, and $E_1$ are functions of $\lambda$, $P_i$, and $P_j$ as well as the old cost in dollars per megawatt hour.

Now substituting $A_1$, $C_1$, $D_1$, and $E_1$ into Equations 10.15 and 10.16, $K_1$ and $K_2$ are given as follows:

$$K_1 = 1 - \frac{f_{j-old} - \lambda^2}{\left(\lambda - _{j-old}\right) f_{i-old}} \tag{10.54}$$

$$K_2 = 1 + \frac{2\lambda P_j f_{j-old} - 2\lambda^2 \left(P_i - P_j\right)}{2\lambda P_i f_{i-old}}$$

$$= 1 + \frac{P_j f_{j-old} - \lambda \left(P_i - P_j\right)}{P_i f_{i-old}} \tag{10.55}$$

$K_1$ and $K_2$ have direct link to the process of optimal allocation of power among all generating bus-bars in the power flow frame, where $\lambda$ represents the cost of received power in dollars per megawatt hour (also known as Lagrange multiplier).

As we have been doing in the preceding chapters for other modes of renewable energy sources, knowledge of the [B] matrix and a corresponding [R] matrix (the symmetric resistance matrix) can set the stage of calculating the [K] matrix. The [K] matrix is a function of the original power network design parameters including the bus-bar voltage magnitude, phase angle, and real and reactive powers.

The [K] matrix equation is rewritten as follows:

$$[K] = [B]\,[R]^{-1} \tag{10.56}$$

Calculating elements of the [K] matrix will set enough number of equations that can be solved for $V_i$, $\theta_i$, $S_i$ and $S_j$, which in effect established foundations for the design of the power grid network.

Equation 10.56 can set basic identification of elements of the [K] matrix at every percentage loading usually ranging from 60 to 100%. Therefore, from the values for V, θ, S, and S solutions could be used to calculate the transmission or distribution lines parameters which include resistance, leakage inductive reactance, and leakage capacitive reactance.

The [K] functional matrix is rewritten as helpful to the reader:[6]

$$K_{ij} = \frac{1}{V_i V_j}\left[\left(1 + S_i S_j\right)\cos Q_{ij} + \left(S_i - S_j\right)\sin Q_{ij}\right] \tag{10.57}$$

The new [B] matrix for the OTEC-CWP plants arranged centrally in a region interconnected through a transmission network is given by the following expression:

$$B_{ij} = \left[\lambda f_i + \lambda f_j - f_i f_j - \lambda^2\right] \Big/ \left[P_i\left(2\lambda f_i - 2_\lambda{}^2\right) + P_j\left(2\lambda f_j - 2\lambda^2\right)\right] \tag{10.58}$$

Equation 10.58 is obtained from Equation 1.4 by setting $F_{ii} = F_{jj} = 0$.

For the process of optimal scheduling of power generation by a set of OTEC plants, Equation 10.58 is directly linked to the well known economic coordination equation, namely,

$$\frac{\partial F_i}{\partial P_i} + \lambda \frac{\partial P_L}{\partial P_i} = \lambda \tag{10.59}$$

where $P_L$ = total transmission power loss.

$$P_L = \sum_i \sum_j P_i B_{ij} P_j \tag{10.60}$$

And as we have shown earlier in Equation 10.14 that $F_i / P_i = f_i$ and

$$\partial F_j / \partial P_j = f_j$$

## VI. CASE STUDY

### A. CASE 1

Referring to Equation 10.58, find solution for $\lambda$ under which total transmission loss $P_L = 0$, which implies that the assembly of OTEC plants are in close proximity.

Setting $B_{ij} = 0$ in Equation 10.58 implies the numerator = 0, therefore,

$$\lambda f_i + \lambda f_j - f_i f_j - \lambda^2 = 0 \tag{a}$$

or

$$\lambda^2 - \lambda\left(f_i - f_j\right) + f_i f_j = 0 \tag{b}$$

$$\lambda = \frac{1}{2}\left[\left(f_i + f_j\right) \pm \sqrt{\left(f_i + f_j\right)^2 - 4 f_i f_j}\right] \tag{c}$$

For $L_i = L_j = 60$ \$/MWh

$$\lambda = \frac{1}{2}\left[120 \pm \sqrt{120^2 - 4 \times 3600}\right] \tag{d}$$

$$= 60 \text{ \$ MWh}$$

Of course, it is not surprising that $L_i = L_j = \lambda$ since the solution for optimal [B] was obtained from the solution of the power coordination Equation 10.59, where:

$$\frac{\partial F_i}{\partial P_i} = f_i \ \$/MW \qquad (e)$$

**B. CASE 2**

An OTEC plant operating at peak capacity of 100 MW over a duration of 1000 hours, at an ocean site and a pressure of $6 \times 10^{-3}$ kg/cm$^2$.

If the total temperature gradient is at 20°C ($T_2 = 20°C$, $T_1 = 0°C$), calculate the weight of ocean water confined across the contour of the indicated $\Delta T$. Consider plant efficiency to be 20%.

OTEC Energy Output

$$= 100 \times 1000 = 10^5 \text{ MWh}$$

$$= 10^5 \times 8.5 \times 10^6$$

$$= 8.5 \times 10^{11} \text{ Btu} \qquad (a)$$

where

$$1 \text{ MWh} = 8.5 \times 10^6 \text{ Btu}$$

since

$$1 \text{ Btu} = 0.252 \text{ kg} - \text{cal} \qquad (b)$$

Therefore, OTEC Energy Output = $8.5 \times 10^{11} \times 0.252$ g –cal.

From Table 2.1, for $p = 6 \times 10^{-3}$ kg/cm$^2$ and T = 20°C, $C_p$ = 15.8 cal/mol.

Now to find m which is the total weight of ocean water, where

$$Q = m C_p \Delta T \qquad (c)$$

$$Q = 0.252 \times 8.5 \times 10^{11} \text{ kg} - \text{cal}$$

$$C_p = 15.8$$

$$\Delta T = 20°C$$

$$m = \frac{0.252 \times 8.5 \times 10^{11}}{20 \times 15.8}$$

$$= 6.85 \times 10^8 \text{ kg}$$

$$= 6.85 \times 10^8 \text{ meter}^3$$

**C. CASE 3**

For the data of part B, determine the ocean water salinity at temperature of 20°C and for $C_p$ = 15.8

From Equation 10.15:

$$S - S_{15} = -0.0026\ T + 0.16 \qquad \text{(a)}$$

$$= -0.026 \times 20 + 0.16$$

$$= -0.36$$

then from Equation 10.35:

$$S - S_{15} = 0.5777\ C_p + 8.826$$

$$= 0.5777 \times 15.8 + 8.826$$

$$= -0.3$$

where $S_{15}$ is the salinity at 15°C which is from Table 10.1 = 34.42.

## VII. SUMMARY

In this chapter, the author presented a fair coverage of subject matter on the nature and mode of ocean thermal energy conversion (OTEC). This important resource involves harnessing seawater absorption of solar heat creating a huge volume of warm ocean water with a temperature gradient 20°C. The process of extraction of absorbed thermal energy could be used in a variety of ways, ultimately to the generation of electric power through conventional means as well as other modes of energy and food production presentation covered basic properties of seawater such as temperature distribution scope of hydrodynamic pressure, specific heat, and salinity. Ocean waters who represent favorable candidates for the process of OTEC plants are mostly located at 20° north and south latitudes, close to tropical zones.

Characterizations of water salinity against temperature specific heat against hydrodynamic pressure and salinity against ocean water specific heat at any pressure have been established graphically and in the form of algebraic polynomials.

Modes of OTEC systems have been presented briefly, but with some emphasis on cold water piping system since research conducted by NOAA and the DOE identified several positive features regarding a shelf mounted CWP system. Some aspects for the energy cost of OTEC has been discussed which indicate an incremental cost of the order of 12 ¢/kWh.

Material presented in this chapter established important and applicable correlations for ocean salinity with respect to temperature and specific heat at constant pressure. Also criteria for using an already established [B] and [R] matrices have been identified through appropriate multiplying factors which are functions of optimal power allocation and incremental cost of OTEC energy that recognize the invariancy of those [B] and [R] matrices in Chapters 1 and 2.

Appropriate utilization of invariant [B] and [R] matrices can lead to calculation of the corresponding [K] matrix which in effect gives elements of design for the OTEC energy system.

## VIII. PROBLEMS

10.1 Similar to the procedure followed in this chapter to derive functional relationships of

$(S - S_{15})$ against $C_p$ for CHINA A seawater, repeat the process for BIO #3997 seawater, identified in Table 10.1.

10.2 Repeat Problem 10.1 for BIO #4001 seawater identified in Table 10.1.

10.3 Repeat Problem 10.1 for CHINA B seawater identified in Table 10.1.

10.4 Repeat Problem 10.1 for IOS identified in Table 10.1.

10.5 Calculate $R_{15}$ of seawater according to Equation 10.5 if the conductivity ratio was measured at a temperature of 10°C. Use Table 10.2.

10.6 Repeat Problem 10.5 when seawater conductivity ratio was measured at T = – 1°C.

10.7 Repeat Problem 10.5 when seawater conductivity ratio was measured at T = 20°C.

10.8 Use Equation 10.7 to calculate seawater salinity at T = – 1°C. Use Table 10.2.

10.9 Repeat Problem 10.8 when T = 28°C.

10.10 At T = 20°C, compare values of S calculated from Equation 10.15 with that from Equation 10.7. Use Table 10.2.

10.11 Repeat Problem 10.10 when T = 5°C and using Equations 10.14, 10.7, and Table 10.2.

10.12 An OTEC plant is operating at peak capacity of 80 MW over a duration of 2000 hours, at a shelf mounted CWP system under operating pressure of $2 \times 10^{-3}$ kg/cm$^2$, $T_2 = 30$°C, and $T_1 = 8$°C. If plant efficiency is 35%, estimate the volume of ocean water involved in the process.

10.13 Repeat Problem 10.12 if OTEC plant capacity is 500 MW and operating water pressure is at $4 \times 10^{-3}$ kg/cm$^2$, $T_2 = 32$°C, and $T_1 = 0$°C.

10.14 Repeat Problem 10.12 if OTEC plant capacity is 1000 MW and operating water pressure is at $8 \times 10^{-3}$ kg/cm$^2$, $T_2 = 18$°C, and $T_1 = -1$°C.

10.15 Calculate the salinity of seawater for $T_2$ and $T_1$ indicated in Problems 10.12, 10.13, and 10.14. Compare calculated values with those in Table 10.2.

10.16 List ratios of seawater conductivities at $T_2$ and $T_1$ indicated in Problems 10.12, 10.13, and 10.14. Use Table 10.2.

## REFERENCES


1. **Dauphinee, T. M.,** Deep ocean temperature profile measurements, *IEEE J. Oceanic Eng.*, OE-8, No. 3, 184, 1983.
2. **Poisson, A.,** Conductivity/salinity/temperature relationship of diluted and concentrated standard seawater, *IEEE J. Oceanic Eng.*, OE-5, No. 1, 41, 1980.
3. **Vadus, J. R. and Taylor, B. J.,** OTEC — cold-water pipe research, *IEEE J. Oceanic Eng.*, OE-10, No. 2, 114, 1985.
4. **Ford, G., Niblett, C., and Walker, L.,** Ocean-thermal energy conversion, *IEE Proc.*, 130 (A, No. 2), 93, 1983.
5. **Epstein, P. S.,** *Textbook of Thermodynamics,* 5th ed., John Wiley & Sons, New York, 1949.
6. **Kirchmayer, L. K.,** *Economic Operation of Power Systems,* John Wiley & Sons, New York, 1958.
7. **Hill, K. D., Dauphinee, T. M., and Woods, D. J.,** A comparison of the temperature coefficients of electrical conductivity of Atlantic and Pacific seawaters, *IEEE J. Oceanic Eng.*, OE-11, No. 4, 1988.

# INDEX

## A



## B



## C



## D



## E

## F



## G



## H



## I

## K



## L



## M



## N



## O



## P

## R



## S



## T

## V



## W